

# Sheffield Hallam University

*The performance of polymer modified bituminous mixtures.*

WIDYATMOKO, Iswandar.

Available from the Sheffield Hallam University Research Archive (SHURA) at:

<http://shura.shu.ac.uk/20533/>

## A Sheffield Hallam University thesis

This thesis is protected by copyright which belongs to the author.

The content must not be changed in any way or sold commercially in any format or medium without the formal permission of the author.

When referring to this work, full bibliographic details including the author, title, awarding institution and date of the thesis must be given.

Please visit <http://shura.shu.ac.uk/20533/> and <http://shura.shu.ac.uk/information.html> for further details about copyright and re-use permissions.

LEARNING CENTRE  
CITY CAMPUS, POND STREET,  
SHEFFIELD. S1 1WB.

101 585 625 X



**REFERENCE**

**Fines are charged at 50p per hour**

- 1 APR 2008

4pm

ProQuest Number: 10701180

All rights reserved

INFORMATION TO ALL USERS

The quality of this reproduction is dependent upon the quality of the copy submitted.

In the unlikely event that the author did not send a complete manuscript and there are missing pages, these will be noted. Also, if material had to be removed, a note will indicate the deletion.



ProQuest 10701180

Published by ProQuest LLC (2017). Copyright of the Dissertation is held by the Author.

All rights reserved.

This work is protected against unauthorized copying under Title 17, United States Code  
Microform Edition © ProQuest LLC.

ProQuest LLC.  
789 East Eisenhower Parkway  
P.O. Box 1346  
Ann Arbor, MI 48106 – 1346

**The Performance of  
Polymer Modified Bituminous Mixtures**

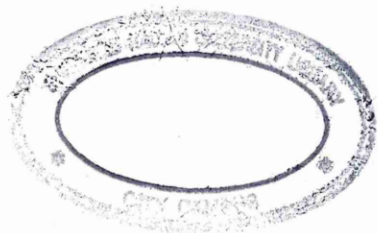
**Iswandaru Widyatmoko**

**Ir. (*Bandung Institute of Technology, Indonesia*)**

**MSc. (*University of Birmingham, England*)**

**A thesis submitted to Sheffield Hallam University in  
partial fulfilment of the requirements for the Degree of  
Doctor of Philosophy**

**August 1998**

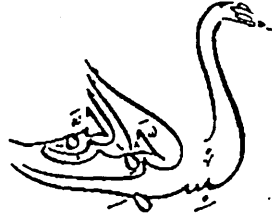


**Allah (Himself) bears witness that  
*Laa ilaaha illa Huwa* (none has the right to be worshiped but He),  
and the angels and those having knowledge also give this witness;**

**He is always maintaining His creation in justice.  
*Laa ilaaha illa Huwa* (none has the right to be worshiped but He),  
the All-Mighty, the All-Wise.**

**(The Holy Qur'an 3:18)**

## ACKNOWLEDGEMENTS AND DECLARATION



In the Name of Allah the Most Gracious and the Most Merciful.

All the praise and thanks be to Allah the Lord of the universe for permitting me to complete this thesis after going through a long struggling period. There were many people who have supported and assisted me in developing my knowledge and understanding on the subject that I was researching on, to whom I would like to express my gratitude.

I always be indebted to my Director of Studies, **Mr C. Ellis**, and my supervisor, **Dr.J.M. Read** for providing extensive guidance, supports, and constructive criticism, whenever required. I would also like to thanks to **Professor P.S. Mangat** for offering the place and support within the School of Construction at Sheffield Hallam University.

Thanks to **Professor A.F. Stock** for introducing me into this research and supervising me during my first year of this work before he left the university, and to **Dr. I.F. Taylor** for his supervisions, discussions and helps in focusing my research program during my second year before he retired. I would also like to extend my gratitude to **Dr.P.C.Hopman** of Delft University of Technology, The Netherlands and **Professor M.F.C. Van de Ven** of University of Stellenbosch, South Africa for the interesting discussions through Email.

The experimental work would have never been possible without the big help of **Mr.S.Linskill** at the Bituminous Materials Laboratory and technical staffs of Concrete Structure Laboratory. Thanks also to all research staffs and everyone at the School of Construction for their support over these three and a half years.

I would like to express my gratitude to the School of Construction Sheffield Hallam University for funding this work. Thanks also to Croda Bitumen Ltd., especially to

**Mr.K. Maw and Mr.L.Cowley**, for the support in providing materials, equipment, and technical advice.

Thanks also to my wife **Bety** and my children **Qonita** and **Saif** for always being there and being patient in spending so many lonely moments while I was writing up this thesis. Very special thanks to my parents for always being supportive and for encouraging me to finish this research, and I love you all.

Finally, I would like to thank all who have assisted me in some way but have not been specially mentioned above.

The work described in this thesis was carried out at Sheffield Hallam University, School of Construction between October 1994 and May 1998. This thesis is the result of my own work, except where specific reference has been made to the work of others. No part of the work has been, or currently being, submitted for any degree, diploma or other qualification.

May Allah grant this work to be a valuable piece of knowledge which can be beneficial for those who are searching for His knowledge and believe in His Greatness.

Sheffield, August 1998

**Ir. Iswandaru Widyatmoko, MSc MIHT**

## ABSTRACT

The use of polymers in bituminous materials has been gaining popularity over the last decade. Despite their superiority in enhancing the performance of bituminous mixtures, problems have been experienced due to limitations on the applicability of currently available assessment techniques.

This thesis is concerned with the mechanical behaviour of polymer modified bitumens and the performance of polymer modified bituminous mixtures. The first part of the thesis presents different pavement distresses and the importance of using polymer modified binders to improve the performance of bituminous mixtures. The second part deals with identification of properties of polymer modified binders and their mixtures by using dynamic mechanical analysis. The third part attempts to develop a novel technique for assessing resistance to permanent deformation of HRA mixtures using a dissipated energy method.

Some polymer modified binders are susceptible to storage instability. However, this work has demonstrated that certain empirical tests are unsuitable for assessing the temperature susceptibility and storage stability of polymer modified binders. Viscoelastic behaviour of bituminous materials is better presented by dynamic mechanical analysis. The dynamic mechanical analysis provides a basis for explaining the unsuitability of some empirical tests on polymer modified binders.

Determination of dissipated energy during creep testing enables more comprehensive and accurate assessment of the resistance to permanent deformation of Hot Rolled Asphalt (HRA) mixtures. This study reveals that assessment of the resistance to permanent deformation based upon permanent strain rate in the linear region is in good agreement with the dissipated energy method. The end of the linear region,  $N_1$ , can be accurately determined by the dissipated energy method and provides a confidence that analysis will always be conducted in the linear region. As expected, polymer modified mixtures are superior to the unmodified ones in their resistance to permanent deformation which confirm by the wheeltracking test, but was not evident from the Marshall tests.

# TABLE OF CONTENTS

<b>ACKNOWLEDGEMENTS.....</b>	<b>ii</b>
<b>ABSTRACT.....</b>	<b>iv</b>
<b>TABLE OF CONTENTS.....</b>	<b>v</b>
<b>LIST OF FIGURES.....</b>	<b>x</b>
<b>LIST OF TABLES.....</b>	<b>xix</b>
<b>LIST OF PLATES.....</b>	<b>xxii</b>
<b>LIST OF ABBREVIATIONS.....</b>	<b>xxiii</b>
<b>LIST OF SYMBOLS.....</b>	<b>xxvi</b>
<b>LIST OF PUBLICATIONS.....</b>	<b>xxviii</b>
<b>GLOSSARY.....</b>	<b>xxix</b>
<b>1. INTRODUCTION .....</b>	<b>1</b>
1.1 Definitions .....	1
1.2 Bitumen Usage.....	2
1.3 The Reasons for Bitumen Modification.....	4
1.4 Statement of Problems .....	11
1.5 Research Aims and Objectives .....	12
1.5.1 Aims.....	12
1.5.2 Objectives .....	12
1.6 Organisation of Thesis .....	13
1.7 References.....	15
<b>2. PAVEMENT PERFORMANCE .....</b>	<b>18</b>
2.1 Introduction.....	18
2.2 Serviceability .....	22
2.3 Damage Mechanisms .....	25
2.3.1 Cracking.....	26
2.3.2 Moisture Damage.....	31
2.3.3 Age Hardening .....	35
2.3.4 Permanent Deformation .....	36

2.4 Concluding Remarks.....	45
2.5 References.....	45
<b>3. MATERIAL PERFORMANCE.....</b>	<b>46</b>
3.1 Introduction.....	46
3.1.1 Composition of Bitumen.....	47
3.1.2 Bitumen Structure .....	50
3.2 Viscoelastic Behaviour of Bitumen .....	51
3.2.1 Tools for Determining Viscoelasticity .....	53
3.2.2 Dynamic Mechanical Analyses.....	56
3.2.3 Time-temperature Superposition .....	60
3.3 Properties of Polymer Modifier Binders.....	64
3.3.1 Molecular Weight Distributions .....	65
3.3.2 Phase Structure of Polymer-Bitumen Blends.....	67
3.3.3 Classification on Polymer Modified Bituminous Binders .....	68
3.3.4 Blending Polymer Modified Bitumens .....	88
3.4 Material Performance.....	92
3.4.1 Tolerance to Application under Adverse Conditions.....	93
3.4.2 Resistance to Cracking.....	94
3.4.3 Resistance to Degradation with Time and High Temperatures .....	99
3.4.4 Resistance to the Effect of Water at Binder/Aggregate Interface .....	105
3.4.5 Resistance to Permanent Deformation.....	110
3.5 General Discussions.....	116
3.5.1 Properties of Polymer Modified Binders .....	116
3.5.2 Performance of Polymer Modified Mixtures.....	121
3.6 References.....	124
<b>4. PERMANENT DEFORMATION.....</b>	<b>134</b>
4.1 Introduction.....	134
4.2 Behaviour of Bituminous Materials Under Various Conditions.....	135
4.2.1 Temperature Dependency .....	135
4.2.2 Mode of Loading.....	136
4.2.3 Boundary Condition.....	146
4.2.4 Remarks .....	155
4.3 Modelling Material Response.....	156

4.3.1 Elastic Model .....	157
4.3.2 Viscoelastic Model .....	161
4.3.3 Viscoplastic and Plastic Model.....	165
4.3.4 Remarks .....	167
4.4 Development of Dissipated Energy Approach.....	167
4.4.1 Theoretical Background.....	167
4.4.2 Practical Applications .....	170
4.4.3 Hypothesis.....	177
4.5 References.....	189
<b>5. EXPERIMENTAL WORKS .....</b>	<b>190</b>
5.1 Introduction.....	190
5.2 Materials investigated .....	191
5.2.1 Aggregates .....	192
5.2.2 Binders .....	194
5.3 Manufacturing of Specimens .....	195
5.4 Tests for the Assessments on the Behaviour of Polymer Modified Materials....	197
5.4.1 Conventional Tests on Bituminous Binders .....	197
5.4.2 Viscosity Measurement.....	199
5.4.3 Storage Stability Test.....	201
5.4.4 Dispersion of Polymer .....	205
5.4.5 Indirect Tensile Stiffness Modulus (ITSM) Test .....	206
5.4.6 Dynamic Mechanical Tests.....	210
5.5 Tests for the Assessments of Permanent Deformation Resistance of Bituminous Mixtures.....	217
5.5.1 Laboratory Wheel-tracking Test .....	217
5.5.2 Dynamic Creep Test.....	219
5.6 References.....	223
<b>6. MECHANISM-INTERACTION OF POLYMER MODIFIED MATERIALS</b>	<b>225</b>
6.1 Binder characterisation and evaluation.....	225
6.1.1 Temperature Susceptibility .....	225
6.1.2 Workability .....	230
6.1.3 Storage Stability.....	231

6.2 Dynamic Mechanical (Rheological) Analyses on Properties of Bituminous Binders .....	237
6.2.1 Storage Stability of Polymer Modified Binders.....	240
6.2.2 Bituminous binders from different manufactures .....	243
6.2.3 Addition of EVA into 50 Pen bitumen from different manufactures .....	243
6.2.4 Addition of polymer modifiers into bitumen with different penetration grades.....	245
6.2.5 Repeatability .....	248
6.3 Dynamic Mechanical Analyses on Properties of Bituminous Mixtures .....	250
6.3.1 High Temperature Properties.....	251
6.3.2 Medium Temperature Properties .....	252
6.3.3 Low Temperature Properties.....	252
6.3.4 Repeatability .....	257
6.3.5 Effect of Binder-Aggregate Interactions to the Viscoelastic Properties of Bituminous Mixtures .....	260
6.3.5 Correlation Between DMA of Binders and HRA Mixtures.....	257
6.4 Concluding Remarks.....	263
6.5 References.....	267
<b>7. ANALYSES ON THE RESISTANCE TO PERMANENT DEFORMATION OF BITUMINOUS MIXTURES.....</b>	<b>270</b>
7.1 Introduction.....	270
7.2 Effect of Mixture Variables on the Resistance to Permanent Deformation.....	271
7.2.1 Aggregate.....	272
7.2.2 Compaction.....	273
7.2.3 Volumetric Properties .....	276
7.2.4 Binder.....	281
7.3 Laboratory Wheel-tracking Test .....	291
7.4 Marshall Test .....	300
7.5 Dynamic Creep Test.....	302
7.5.1 Effect of the applied stress level and the repetitive loading .....	302
7.5.2 Repeatability of Dynamic Creep.....	306
7.5.3 Dissipated energy and the resistance to permanent deformation .....	309
7.5.4 Dissipated energy and the wheel-tracking test.....	312
7.6 Concluding remarks.....	320

7.7 References.....	321
<b>8. DISCUSSIONS.....</b>	<b>325</b>
8.1 Problems With Binder Characterisation .....	325
8.1.1 Limitations of Empirical Tests.....	325
8.1.2 Dynamic Mechanical Analysis .....	327
8.2 Mechanism Interaction of Polymer-Bitumen Blends.....	328
8.2.1 Molecular Entanglements .....	328
8.2.2 Role of the Base Binder .....	329
8.2.3 Viscoelastic Behaviour of Modified Binders.....	329
8.3 Performance of Polymer Modified Mixtures .....	333
8.3.1 Stiffness Modulus of Modified HRA Mixtures .....	333
8.3.2 Performance of Polymer Modified Mixtures .....	336
8.4 Application of Dissipated Energy Method.....	337
8.5 Reference .....	341
<b>9. CONCLUSIONS.....</b>	<b>343</b>
9.1 Binder characterisation .....	343
9.2 Mixture Characteristics.....	344
9.3 Effect of Binder Properties to Mixture Performance .....	345
9.4 Resistance to Permanent Deformation.....	346
<b>10. RECOMMENDATIONS AND FUTURE WORKS .....</b>	<b>347</b>
10.1 Recommendations.....	347
10.2 Future Works .....	348

**APPENDIX A. STORAGE STABILITY**

**APPENDIX B. DYNAMIC MECHANICAL ANALYSES**

**APPENDIX C. DYNAMIC CREEP**

**APPENDIX D. INDIRECT TENSILE STIFFNESS MODULUS**

**APPENDIX E. ANALYSES ON THE REPEATABILITY OF DYNAMIC  
MECHANICAL TESTING ON BITUMINOUS MIXTURES**

## LIST OF FIGURES

Figure 1.1 Constituency of a bituminous mixture as its volumetric proportions. $V_v$ , $V_b$ , and $V_a$ are volumetric proportion of air voids, bituminous binder, and aggregate respectively (in percentage). VMA is volumetric proportion of voids in mineral aggregate ( $V_v+V_b$ ), also in percentage. ....	3
Figure 1.2 Typical cross-sectional views of a bituminous macadam or an asphaltic concrete (upper left), a rolled asphalt (upper right), a stone mastic asphalt (lower left), and a porous asphalt (lower right) mixtures. ....	3
Figure 1.3 A Typical Road Pavement Structure .....	4
Figure 1.4 Effect of traffic loading (axle load) to the damage level of a road pavement in term of equivalent standard axles. After Croney and Croney [15]. ....	6
Figure 1.5. Time/temperature behaviour of "ideal" bitumen. After Van Beem and Brassler [18]. ....	8
Figure 1.6 Schematic Organisation of the Thesis .....	14
Figure 2.1 Illustration of the distribution of traffic loading at various depths of road pavements showing reduction of stress level( $\sigma$ ) at each layer. ....	19
Figure 2.2 An example of an empirical approach: California Bearing Ratio design curve After Whiteoak [1]. ....	20
Figure 2.3 The principal critical strains in the analytical design methods. ....	21
Figure 2.4 Typical relationship between PSI and cumulative traffic, after Roberts et al [8]. ....	24
Figure 2.5 Schematic illustration on the effect of temperature on fatigue life for controlled stress testing. ....	28
Figure 2.6 Effect of different roller compactors to fatigue life [13] .....	28
Figure 2.7 Reflection cracking in road pavement .....	30
Figure 2.8 Different components of an overlay system, after Francken [16]. ....	31
Figure 2.9 Air void content versus retained mixture strength. After Terrel and Shute [20]	34

Figure 2.10 Air void content versus extent of ravelling, after Kandhal and Woehler[23]. Specimens were cored samples of Pennsylvania ID-2 wearing course consisting of dense graded aggregate and AC-20 binder from different sites of similar in-service ageing. ....	35
Figure 2.11 Types of permanent deformation.....	37
Figure 2.12 Example of the Marshall design technique.....	39
Figure 3.1 Make-up of Crude Oil. Reproduced from Roberts et al.[2] after Corbett [5]47	
Figure 3.2 Type of molecular structure of a bitumen [8].....	50
Figure 3.3 Rate of shear of different types of liquids under a constant shearing stress as a function of time [6]. Type I is a very viscous non-colloidal liquid or a sol with non- or slightly elastic particles. Type II is a sol type colloid. Type III is a gel type colloid.....	51
Figure 3.4 Representation of viscoelastic response of asphalt cement under static loading, showing elastic (e), delayed elastic (de), and viscous (v) strain components. ....	52
Figure 3.5 Schematic master curve of creep stiffness as a function of loading time [10]54	
Figure 3.6 Poisson's ratio .....	54
Figure 3.7 Parallel Plate Geometry and Torsional Rectangular Bar .....	56
Figure 3.8 Vectorial resolution of complex modulus and shear compliance in sinusoidal shear deformations (after Ferry,1990) .....	57
Figure 3.9 Modelling of the temperature shift factor mastercurve by Equation 3.12 and Equation 3.13. After Cheung [23]. ....	63
Figure 3.10 Phase angle ( $\delta$ ) as a function of frequency and temperature, with the mastercurve at reference temperature of 25°C, and also the temperature- frequency shift factor ( $a_t$ ).Binder : 50 Pen (Type C50).....	63
Figure 3.11 Dynamic complex modulus ( $G^*$ ) as a function of frequency and temperature, with the mastercurve at Reference Temperature of 25°C, and also the temperature-frequency shift factor ( $a_T$ ). Binder: 50 Pen (Type C50).....	64
Figure 3.12 HP-GPC Profiles of Parent AC-20 and Ethylene Vinyl Acetate Modified Bitumens [30] .....	66
Figure 3.13 Illustration of different polymer structures [37]. ....	69
Figure 3.14 Inter-relation between MFI, molecular weight, viscosity, and penetration. 70	
Figure 3.15 Relations between polymer content, phase structure and softening point of ethylene copolymer blended with AC-20. After Nahas et al [45] .....	73

Figure 3.16 Packing of Polyethylene in EVA. After Gilby [41].....	75
Figure 3.17 Typical relationship between applied force and elongation from the toughness and tenacity test.....	78
Figure 3.18 Different processes and technologies in application of rubbers in bituminous mixtures [59].....	81
Figure 3.19 Thermoplastic block copolymers. After Collins and Mikols [65]. $T_g$ is the glass transition temperature. ....	85
Figure 3.20 Effect of asphaltenes content on the $pen_{top}/pen_{bottom}$ ratio after hot storage of bitumen/TR blends. Bitumen blended from three base bitumens and non-volatile flux oil. After Morgan and Mulder [4]. ....	87
Figure 3.21 Influence of bitumen constitution on bitumen/TR blends. After Von Gooswilligen and Bull [65] .....	87
Figure 3.22 Relationship between the colloidal instability index (CI) and the critical polymer concentration (CPC). After Loeber et al [67]. ....	89
Figure 3.23 The effect of temperature on tensile strength and thermally induced stress, showing the maximum tensile strength reserve ( $\Delta\beta_{max}$ ) and the fracture temperature ( $T_{fr}$ ). After Stock and Arand [54]. ....	97
Figure 3.24 A model of polymer-bitumen interaction where polymer particles fill the gaps within bitumen solvent. ....	117
Figure 3.25 Storage modulus and phase angle of base and 6% linear SBS polymer modified Bitumen C at $1 \text{ rad}\cdot\text{s}^{-1}$ as a function of temperature. After Lu and Isacson [111]. ....	118
Figure 3.26 Illustration of molecular movement due to heat application within the bitumen's microstructure.....	118
Figure 3.27 A model of polymer-bitumen interaction showing interparticle distance between polymer particles within bitumen. ....	120
Figure 4.1 Dynamic mechanical analysis on different bituminous mixtures showing the effect of temperature on the rheological properties of bituminous mixtures. After Goodrich [3] .....	136
Figure 4.2 In situ stress generated by a moving wheel load. After Brown [6].....	137
Figure 4.3 Shear stress variation in a typical pavement element as a wheel passes overhead. After Bell [7]. ....	137
Figure 4.4 Typical Marshall test data plot .....	139
Figure 4.5 Typical NAT creep test data plot.....	139

Figure 4.6 Typical stress and strain history in repetitive loading test, showing the applied stress duration ( $t_o$ ) and the relaxation time ( $t_r$ ).....	141
Figure 4.7 Idealised permanent deformation curves under repetitive loading.....	142
Figure 4.8 Stress and strain of incremental static test [reproduced after Huang] .....	144
Figure 4.9 Log-log plot of incremental static test [after Huang] .....	144
Figure 4.10 Basic types of stress. The arrows indicate the directions of loading (forces per unit area). .....	147
Figure 4.11 Typical deformation results in a simple tensile test. ....	148
Figure 4.12 Mohr-Coulomb failure line and some stress conditions.....	149
Figure 4.13 SHRP Shear test device.....	153
Figure 4.14 Illustration of a hollow cylindrical apparatus for testing bituminous mixtures. ....	154
Figure 4.15 Procedures to predict cumulative loading from results of simple loading test. After Monismith [25].....	161
Figure 4.16 Maxwell element model .....	162
Figure 4.17 Voigt (Kelvin)'s element model.....	163
Figure 4.18 Burger's model .....	163
Figure 4.19 Bingham model and plastic deformation.....	166
Figure 4.20 Idealised hysteretic loops.....	169
Figure 4.21 Typical plot of a hysteric loop from a fatigue test.....	171
Figure 4.22 Variation of Dissipated Energy per Load Cycle during Controlled Stress and Strain Fatigue Test. After Rowe [37].....	172
Figure 4.23 Stiffness Ratio versus Energy Ratio, controlled-stress flexural beam fatigue test at 20°C. After Tayebali, Rowe, and Sousa [38]. ....	174
Figure 4.24 Schematic of cumulative dissipated energy versus number of cycles showing the effect of mode of loading. After Tayebali, Rowe and Sousa [38]176	
Figure 4.25 Typical plot of data captured at each load cycle (interval) from a dynamic creep testing. Reference mixture no. E3045. ....	179
Figure 4.26 A Typical plot of a hysteretic loop at one cycle load application obtained from NAT dynamic creep. Reference mixture no. E3045. ....	180
Figure 4.27 Cumulative Dissipated Energy $W_N$ as the area under the $w_i$ energy line ..	181
Figure 4.28 Plot of permanent strain curve from mixture no.BP502, as produced by the dynamic creep test from NAT.....	183

Figure 4.29 Plot of dissipated energy per cycle [ $J/m^3$ ] against the number of load repetitions N from mixture no.BP502. ....	183
Figure 4.30 Plot of dissipated energy ratio [ $W_N/w_i$ ] against the number of cycles from mixture no.BP502. ....	184
Figure 5.1 Aggregate gradation adopted for this study .....	192
Figure 5.2 Schematic presentation of laboratory frameworks .....	193
Figure 5.3 Effect of blending duration on softening points .....	196
Figure 5.4 Rotational viscosity by measurement (135-190°C) and data extrapolation (90-135°C) .....	200
Figure 5.5 Typical side view of ITSM loading arrangement .....	207
Figure 5.6 ITSM results for mixtures with 50 pen based binders and a 100 pen bitumen, showing variations between samples of the same mixture. Dashed lines represent the average ITSM values of the corresponding mixtures.....	209
Figure 5.7 ITSM results for mixtures with 100 pen based binders, showing variations between samples of the same mixture. Dashed lines represent the average ITSM values of the corresponding mixtures.....	210
Figure 5.8 Dimensions (in millimetres) of the compaction mould and the finished specimen. ....	213
Figure 5.9 Compaction arrangement.....	214
Figure 5.10 Loading configuration (the length dimensions are in millimetres). ....	218
Figure 5.11 Configuration for dynamic creep test. LVDT <sub>R</sub> and LVDT <sub>V</sub> are the radial and the vertical LVDTs, respectively. ....	220
Figure 6.1 Penetrations indices as determined by three different procedures (a, b, and c). Detail description is presented in Table 6.1.....	227
Figure 6.2 Viscosity-frequency relationships, showing thixotropy (shear-thinning) on 50Pen+5%EVA and 50Pen+5%SBS binders. The measurements were carried out by a dynamic shear rheometer. ....	230
Figure 6.3 Deformation failure in a ring and ball softening point test.....	234
Figure 6.4 Penetration values of polymer modified binders during the storage stability test at top and bottom sections.....	234
Figure 6.5 Schematic representation of unstable specimen after storage stability test. ....	237
Figure 6.6 Dependency of the binder's dynamic viscosity on temperature and frequency (shear rate). Binder reference number: A50.....	240

Figure 6.7 Black curves showing comparison of SBR modified binder (50 pen + 5%SBR), before and after seven day-storage stability test. ....	242
Figure 6.8 Black curves showing comparison of SBS modified binder (50 pen + 5%SBS), before and after seven day-storage stability test. ....	242
Figure 6.9 Dynamic viscosity before and after stability test as measured by a dynamic shear rheometer at several service temperatures. Temperature sweeps from 0°C to 80°C at a frequency of 1 Hz.....	243
Figure 6.10 Black curves of 50 pen bitumens from different suppliers.....	244
Figure 6.11 Black curves of EVA modified 50 pen binders with the base binder from different suppliers .....	244
Figure 6.12 Master curves of complex modulus and phase angle. (Temperature : -5 to 80°C and frequency: 0.1 to 20 Hz. WLF time-temperature superimposition.)	246
Figure 6.13 Black curves of polymer modified binders (50 pen based). ....	246
Figure 6.14 Dynamic mechanical tests on 100 pen based binders. Frequency sweeps of 1 Hz at temperatures 0 to 80 <sup>0</sup> c .....	248
Figure 6.15 The effect of temperatures on the measured complex modulus in DSR ...	250
Figure 6.16 Black curves of bituminous mixtures obtained from the dynamic bending tests (T=-15 to 45°C and frequency = 0.2 to 30 Hz).....	253
Figure 6.17 Master curves of bituminous mixtures (T=-15 to 45°C and frequency = 0.2 to 30 Hz). ....	254
Figure 6.18 DMA of HRA mixtures at 45°C showing relationships between complex stiffness modulus and test frequency. ....	254
Figure 6.19 DMA of HRA mixtures at 45°C showing relationships between phase angle and test frequency. ....	255
Figure 6.20 DMA of HRA mixtures at 20°C showing relationships between complex stiffness modulus and test frequency. ....	255
Figure 6.21 DMA of HRA mixtures at 20°C showing relationships between phase angle and test frequency. ....	256
Figure 6.22 DMA of HRA mixtures at -10°C showing relationships between complex stiffness modulus and test frequency. ....	256
Figure 6.23 DMA of HRA mixtures at -10°C showing relationships between phase angle and test frequency. ....	257
Figure 6.24 Test variability for mixture E50 .....	258
Figure 6.25 Test variability for mixture EP50 .....	259

Figure 6.26 Test variability for mixture ER50.....	259
Figure 6.27 Test variability for mixture ES50 .....	260
Figure 6.28 Master curves of the phase angle of mixture E50 and binder E50 versus the reduced frequency.....	261
Figure 6.29 Master curves of the phase angle of mixture EP50 and binder EP50 versus the reduced frequency.....	261
Figure 6.30 Master curves of the phase angle of mixture ER50 and binder ER50 versus the reduced frequency.....	262
Figure 6.31 Master curves of the phase angle of mixture ES50 and binder ES50 versus the reduced frequency.....	262
Figure 6.32 Correlations between the stiffness of binders and their mixtures.....	263
Figure 7.1 Constituents of a rolled asphalt .....	272
Figure 7.2 Effect of binder content on resistance to deformation. After Szatkowski [5].	273
Figure 7.3 Deflection of Bituminous Pavement Under Traffic Loading and Binder Rheology. Reproduced after Phillips and Robertus [16] .....	282
Figure 7.4 The effect of softening point of binders to the resistance to permanent deformation of hot rolled asphalt. Data for regression analysis were obtained from Szatkowski [5]. .....	284
Figure 7.5 Effect of the softening point of binder on wheel-tracking rate at 45°C showing Jacobs' work [17] and this study.....	284
Figure 7.6 Effect of the softening point of binder on the wheel-tracking rate at 60°C. After Claxton, Lesage, and Planque [13]. Mixture type: 0/10 continuously graded asphaltic concrete. Binder content: 5.3%.....	285
Figure 7.7 Effect of the softening point of the studied binders on the wheel-tracking rate at 60°C. ....	285
Figure 7.8 Shear stress versus shear rate for a Newtonian liquid, a pseudoplastic liquid, and a Bingham plastic. After Sybilski [20].....	287
Figure 7.9 Viscosity test results and calculated zero-shear viscosity of different polymer-bitumen systems. After Sybilsky [15].....	288
Figure 7.10 Comparison between the SHRP permanent deformation parameter ( $G/\sin\delta$ ) and the zero shear viscosity ( $\eta_0$ ). After Phillips [23].....	290
Figure 7.11 Wheel-tracking results at 45°C and 60°C for 50 pen HRA mixtures. ....	292
Figure 7.12 Wheel-tracking results at 45°C and 60°C for EVA modified HRA mixtures with 50 pen bitumen as the base binder.....	292

Figure 7.13 Wheel-tracking results at 45°C and 60°C for SBR modified HRA mixtures with 50 pen bitumen as the base binder.....	293
Figure 7.14 Wheel-tracking results at 45°C and 60°C for SBS modified HRA mixtures with 50 pen bitumen as the base binder.....	293
Figure 7.15 Wheel-tracking results at 45°C and 60°C for 100 Pen HRA mixtures. ....	294
Figure 7.16 Wheel-tracking results at 45°C and 60°C for SBR modified HRA mixtures with 100 pen bitumen as the base binder.....	294
Figure 7.17 Wheel-tracking results at 45°C and 60°C for SBS modified HRA mixtures with 100 pen bitumen as the base binder.....	295
Figure 7.18 Results of wheel-tracking test at 45°C on different mixtures. These results shown are the average values from a number of replicates (see Table 7.6)...	296
Figure 7.19 Results of wheel-tracking test at 60°C on different mixtures. These results shown are the average values from a number of replicates (see Table 7.6)...	297
Figure 7.20 Phase Angle versus temperature for 50 pen and 100 pen bitumens (dynamic mechanical test by using temperature sweeps from 0 to 80°C at frequency 1 Hz). ....	300
Figure 7.21 Typical relationship between dissipated energy per cycle and the number of load repetitions for SBS modified HRA (FS100) mixtures.....	302
Figure 7.22 The effect of stress level upon the dissipated energy per cycle of the mixtures at test temperature of 45°C. ....	303
Figure 7.23 The effect of stress level upon the dissipated energy per cycle of the mixtures at test temperature of 60°C .....	304
Figure 7.24 Typical relationships between dissipated energy per cycle and the number of cycles to $N_1$ . Mixtures 50 Pen and EVA Modified 50 Pen HRA. Test temperature 60°C. ....	304
Figure 7.25 Relationship between the normalised dissipated energy and the stress level at a test temperature of 45°C.....	305
Figure 7.26 Relationship between the normalised dissipated energy and the stress level at a test temperature of 60°C.....	305
Figure 7.27 Variability of the normalised dissipated energy for mix FS100.....	308
Figure 7.28 Variability of the normalised dissipated energy for mix EP50.....	308
Figure 7.29 Correlation between normalised dissipated energy and strain rate in dynamic creep tests for all mixtures at two test temperatures.....	310

Figure 7.30 Effect of air void content on the strain rate in dynamic creep tests for mixtures with 50 pen bitumen as the base binder.....	311
Figure 7.31 Effect of air void content on the normalised dissipated energy on dynamic creep testing for mixtures with 50 pen bitumen as the base binder.....	311
Figure 7.32 Relationship between the normalised dissipated energy from the dynamic creep test and the wheel-tracking rate for all mixtures. Test temperature 45°C .....	314
Figure 7.33 Relationship between the normalised dissipated energy from the dynamic creep test and the wheel-tracking rate for all mixtures. Test temperature 60°C.. .....	314
Figure 7.34 Relationship between the normalised dissipated energy from the dynamic creep test and the wheel-tracking rut depth for all mixtures. Test temperature 45°C. ....	315
Figure 7.35 Relationship between the normalised dissipated energy from the dynamic creep test and the wheel-tracking rut depth for all mixtures. Test temperature 60°C. ....	315
Figure 7.36 Relationship between the normalised dissipated energy from the dynamic creep test and the wheel-tracking rate, showing the effect of test temperature and applied stress.....	316
Figure 7.37 Relationship between the normalised dissipated energy from the dynamic creep test and the wheel-tracking rut depth for all mixtures, showing the effect of test temperature and the applied stress. ....	316
Figure 7.38 The normalised dissipated energy against the normalised dilatational stress at different bitumen film ratio.....	318
Figure 7.39 The normalised deviatoric stress against the normalised stress at different bitumen film ratio .....	318
Figure 7.40 Dissipated energy versus transversal distance for several depth .....	320
Figure 8.1 Black curves showing three zones of viscoelastic regimes.....	330
Figure 8.2 Black curves of binders with similar PI values. ....	332
Figure 8.3 Relationship between strain rate and wheel-tracking rate at stress level of 196 kPa. Test temperatures are 45 and 60 °C. ....	338
Figure 8.4 Flowchart for the analysis of permanent deformation.....	339

## LIST OF TABLES

Table 1.1 Typical Characteristics of Various Bituminous Mixtures. ....	4
Table 1.2 Draft Clause 943 Wheel-tracking Requirements for Site Classification [17] ..	7
Table 2.1 Classification of the condition of the road surface used by TRL[10].....	25
Table 2.2 Typical distress in bituminous pavements. After Huang [11] .....	25
Table 2.3 BS 594: 1992 Design criteria for stability of laboratory design asphalt [27] .	38
Table 2.4 Classification of sites by traffic and stress condition, Notes for Guidance NG 943 [29].....	40
Table 3.1 The API gravity indices .....	47
Table 3.2 The chemical composition of bitumen showing the major elements. After Whiteoak [1]. .....	48
Table 3.3 Characteristics of S.A.R.A.....	49
Table 3.4 Configurations for dynamic mechanical tests adopted by Goodrich [19].....	59
Table 3.5 Configurations for dynamic mechanical tests adopted by SHRP [10].....	59
Table 3.6 Forms of rubber modifiers .....	80
Table 3.7 Relative increase in mixing temperature (in centigrade) as the polymer content increased. After King et al. [61] .....	84
Table 3.8. Evaluation of water sensitivity test methodologists [93].....	107
Table 3.9 Summary of the ECS test procedure [87] .....	108
Table 3.10 Variables addressed during development of the ECS [71] .....	108
Table 3.11 Several factors to be assessed in this research .....	123
Table 3.1 The API gravity indices .....	3.2
Table 3.2 The chemical composition of bitumen showing the major elements. After Whiteoak [1]. .....	3.3
Table 3.3 Characteristics of S.A.R.A.....	3.4
Table 3.4 Configurations for dynamic mechanical tests adopted by Goodrich [19]....	3.14
Table 3.5 Configurations for dynamic mechanical tests adopted by SHRP [10].....	3.14
Table 3.6 Forms of rubber modifiers .....	3.35

Table 3.7 Relative increase in mixing temperature (in centigrade) as the polymer content increased. After King et al. [61] .....	3.39
Table 3.8. Evaluation of water sensitivity test methodologies [93].....	3.62
Table 3.9 Summary of the ECS test procedure [87] .....	3.63
Table 3.10 Variables addressed during development of the ECS [71] .....	3.63
Table 3.11 Several factors to be assessed in this research .....	3.78
Table 4.1 Effects of axial test configuration. After Gibb [1].....	151
Table 4.2 Correction factor for dynamic effects, $C_m$ (after Van de Loo).....	158
Table 4.3 Comparison between Maxwell, Voigt, and Burger models.....	164
Table 5.1 Binders studied .....	195
Table 5.2 Estimated shear rates for various testing and service condition [14].....	199
Table 5.3 Equiviscous temperatures recommended for mixing and compaction of polymer modified mixtures.....	201
Table 5.4 Advantages and disadvantages of using ITSM. After Scholz [19].....	208
Table 5.5 Testing parameters for dynamic mechanical test.....	211
Table 5.6 Comparison of Single and Double-tracking. Methods of calculations: BS 598:Part 110:1996. After Broadhurst [20].....	219
Table 5.7 Comparisons of specimen types in the wheel-tracking tests. Methods of calculations: BS 598:Part 110:1996. After Broadhurst [20].....	219
Table 5.8 Configuration for dynamic creep test.....	222
Table 6.1 Theoretical penetration at softening point temperature ( $1/10^{\text{th}}$ mm). .....	228
Table 6.2 Relationship between PI and properties of bitumen .....	229
Table 6.3 Penetrations and Softening Points of Binders before (Original) and after storage stability (Top & Bottom). These results are after 7 days of storage..	233
Table 6.4 Penetration Indices(PIs) and Stability Indices (SSs) calculated from Penetration values and Softening Points of Binders before (Original) and after storage stability (Top & Bottom) by using Equations 5.3 and 5.4 Chapter Five. The penetration indices calculated were based on Equation 5.2. These results are after 7 days of storage. ....	236
Table 6.5 Regression coefficients for Black curves of studied binders .....	247
Table 6.6 DSR compliance to ensure linearity of 50 pen bitumen .....	249
Table 6.7 Accuracy measurement of DSR.....	249
Table 6.8 Volumetric measurements for bending beam specimens.....	251
Table 6.9 Repeatability of the DSR for all temperatures and frequencies.....	258

Table 6.10 Constants k and n obtained from the dynamic mechanical tests. ....	264
Table 7.1 Comparison between three compaction techniques. Summarised from Sousa, Deacon, and Monismith [8]. ....	274
Table 7.2 The Asphalt Institute design criteria for roads [11] .....	275
Table 7.3 Volumetric measurements on Marshall size specimens for dynamic creep test. Names designated to the mixture types refer to the binder types as presented in Table 5.2 (Chapter Five).....	278
Table 7.4 Volumetric measurements of specimens with different Marshall compaction efforts. Names designated to the mixture types refer to the binder types as presented in Table 5.2 (Chapter Five). ....	280
Table 7.5 Volumetric measurements of wheel-tracking specimens.. ....	281
Table 7.6 Results from wheel-tracking tests. Rut depth at 45°C. ....	297
Table 7.7 Results from wheel-tracking tests. Wheeltracking rate at 45°C. ....	298
Table 7.8 Results from wheel-tracking tests. Rut depth at 60°C. ....	298
Table 7.9 Results from wheel-tracking tests. Wheeltracking rate at 60°C. ....	301
Table 7.10 Marshall test results. Names designated to the mixture types refer to the binder types as presented in Table 5.2 (Chapter Five).....	301
Table 7.11 Individual data of mixtures EP50(EVA), ER50(SBR), and ES50(SBS)...	301
Table 7.12 Analyses of variance for testing whether there is a difference at 5 per cent level of significant ( $\alpha=5\%$ ) between mixtures EP50(EVA), ER50(SBR), and ES50(SBS).....	301
Table 7.13 Repeatability of dynamic creep testing at 45°C .....	306
Table 7.14 Repeatability of dynamic creep testing at 60°C .....	307
Table 7.15 Ranking performance to the resistance to permanent deformation of the dynamic creep and the wheel-tracking specimens. ....	331
Table 8.1 Properties of the viscoelastic zones. ....	333
Table 8.2 Comparison between the ranking performance obtained from the maximum phase angle and the resistance to permanent deformation of the binders and the mixtures. ....	336
Table 8.3 Summary of improvements by the addition of polymer modifiers obtained from ITSM test. ....	336
Table 8.4 Comparisons between ITSM results and the estimated elastic modulus ( $E'_{estimate}$ ).....	320

## LIST OF PLATES

Plate 3.1 Three dimensional phase structure of thermoplastic rubber [reproduced by kind permission of Shell International Ltd.].....	91
Plate 3.2 The Weissenberg effect during stirring of a polymeric liquid [ reproduced by kind permission of Shell International Ltd.].....	91
Plate 5.1 Forms of polymer modifiers used in this study.....	194
Plate 5.2 Testing arrangement for ITSM in the NAT machine.....	207
Plate 5.3 A Mand dynamic three-point bending machine for testing bituminous mixture.....	216

## LIST OF ABBREVIATIONS

i.e.	that is
e.g.	for example
<i>et al.</i>	and co workers
<i>etc.</i>	<i>et cetera</i> (and so on)
AAPA	Australian Asphalt Paving Association
AAPT	Association of Asphalt Paving Technologists
AASHO	American Association for Soil and Highway Officials
API	American Petroleum Institute
ARRB	Australian Road Research Board
ASTM	American Society for Soil and Testing Materials
BBR	Bending Beam Rheometer
BRF	British Road Federation
C	Carbon
CHRSST	Constant Height Repeated Simple Shear Test
CTAA	Canadian Technical Asphalt Association
CTOT	California Tilt Oven Test
DBM	Dense Bitumen Macadam
DSR	Dynamic Shear Rheometer
EAPA	European Asphalt Paving Association
Ed(s).	Editor (s)
EPDM	Ethylene Propylene Diene Rubber
ESA(L)	Equivalent Standard Axle (Loading)
EVA	Ethylene Vinyl Acetate
FHWA	Federal Highways Agency
H	Hydrogen
HA	Highways Agency
HRA	Hot Rolled Asphalt
IR	Infra Red
KSLA	<i>Koninklijke/Shell-Laboratorium Amsterdam</i>
LDPE	Low Density Polyethylene
LCPC	<i>Laboratoire des Pont et Chaussées</i>

LPO	Low Pressure Oxidation
LR	Laboratory Report
LST	Limiting Stiffness Temperature
LTD	Long Term Durability
LTOA	Long-term Oven Ageing
NAPA	National Asphalt Pavement Association
NAT	Nottingham Asphalt Tester
NCHRP	National Council for Highway Research Program
No.	Number
OSU	Oregon State University
Pen	Penetration
PAV	Pressure Ageing Vessel
PI	Penetration Index
POV	Pressure Oxygen Vessel
RBA	Refined Bitumen Association
RN	Road Note
RR	Research Report
RTFOT	Rolling Thin Film Oven Test
SB	Styrene Butadiene
SBR	Styrene Butadiene Rubber
SBS	Styrene Butadiene Styrene
SPDM	Shell Pavement Design Manual
SS	Storage Stability
SHRP	Strategic Highway Research Program
SHU	Sheffield Hallam University
SMA	Stone Mastic Asphalt
STOA	Short Term Oven Ageing
TFOT	Thin Film Oven Test
TR	Thermoplastic Rubber
TRB	Transportation Research Board
TRL	Transport Research Laboratory, formerly Transportation and Road Research Laboratory (TRRL)
TRR	Transportation Research Record
TSRST	Thermal Stress Restrain Specimen Test

UK	United Kingdom
US(A)	United States (of America)
UV	Ultra Violet
VMA	Voids in Mixture Aggregate
VFB	Voids Filled with Bitumen
Vol.	Volume
WLF	Williams, Landel, and Ferry

## LIST OF SYMBOLS

$a_T, \alpha_T$	Temperature shift factor
$\delta$	Phase angle
$\Delta$	Difference in values
$\epsilon$	Strain
cSt	centi-Stoke
C	Celsius (unit temperature), $C = (F - 32) * 5/9$
$C_1, C_2$	Constants of WLF Equation
E	Tensile modulus
$E^*$	Complex tensile (flexural) modulus
g	Gram
F	Fahrenheit (unit temperature), $F = (C * 9/5) + 32$
G	Shear modulus
$G^*$	Complex shear modulus
$G'$	Elastic modulus
$G''$	Loss modulus
H	Activation energy
Hz	Hertz
J	Shear compliance
$J'$	Elastic compliance
$J''$	Loss shear compliance
kg	Kilogram
K	Kelvin (unit temperature), the absolute temperature. $K = C + 273.2$
lb.	Pound-force
l	litre
h	Hour
$\mu$	Micron (meter x $10^{-6}$ )
$\mu\text{strain}$	Strain x $10^{-6}$
$\nu$	Poisson's ratio
m	Meter

mm	millimetre ( $10^{-3}$ m)
ml	millilitre ( $10^{-3}$ l)
$M_w$	Molecular weight
MFI	Melt Flow Index
MPa	Mega Pascal ( $10^6$ Pascal)
$\eta$	Viscosity
$\eta_0$	Zero shear viscosity
$\eta^*$	Complex viscosity
N	Newton
Pa	Pascal
psi	pounds per square inches
R	Universal gas constant, 8.31 joules per Kelvin per mole
s	Seconds
S	Tensile stiffness modulus (bending test)
$\sigma$	Tensile stress
$\Sigma$	Sum of values
$\tau$	Shear Stress
t	Time
T	Temperature
$T_{REF}$	Reference Temperature
%	Percent
$V_v$	Air void content, by percentage of volume
$V_b$	Binder content, by percentage of volume
$\omega$	Reduced frequency

## LIST OF PUBLICATIONS

### Conference Paper

- \* C. Ellis, I. Widyatmoko and J.M. Read, “*The Storage Stability and Behaviour of Polymer Modified Bituminous Binders*”, A paper presented at the Second European Symposium on The Performance and Durability of Bituminous Materials, Leeds, April 1997.  
(The paper was presented by I. Widyatmoko)

### Pending Refereed Publications and Workshop

1. I. Widyatmoko, C. Ellis, and J.M. Read, “*Energy Dissipation and The Deformation Resistance of Bituminous Mixtures*”, a scientific paper - accepted for publication in Materials and Structures, RILEM, 1998.
2. I. Widyatmoko, C. Ellis, and J.M. Read, “*The Application of The Dissipated Energy For Assessing The Performance of Polymer Modified Bituminous Mixtures*”, accepted for publication in Materials and Structures, RILEM, 1998.
3. I. Widyatmoko and C. Ellis, “*New Relationships Between Polymer Modified Binders and Their Mixtures as Measured by Dynamic Loading*”, A paper submitted for the Eurobitume Workshop on the Performance Related Properties for Bituminous Binders, Luxemburg, 1999.
4. C.Ellis and I. Widyatmoko, “*Performance and Durability Aspects of Asphalts Incorporating Steelslag Aggregates Proposed for Use in Thin Pavement Surfacing*”, A paper submitted for presentation at the 3<sup>rd</sup> European Symposium on Performance and Durability of Bituminous Materials & Hydraulic Stabilised Composites, Leeds 8/9 April 1999.

**Amorphous polymers** are materials which have polymer chains which either cannot crystallise due to chain irregularity (e.g. atactic chain) or have been cooled from the melt so quickly as to inhibit crystallisation.

**Complex (shear) compliance  $J^*$  (for shear)  $\text{Pa}^{-1}$ :** the mathematical representation of a (shear) compliance as the sum of a real and an imaginary part. The real part is sometimes called storage compliance and the imaginary part loss compliance. It is usually adopted for analysis at the same stress level.

**Complex (shear) modulus  $G^*$  (for shear)  $\text{Pa}$ :** the mathematical representation of a (shear) modulus as the sum of a real and an imaginary part. The real part is sometimes called storage modulus and the imaginary part loss modulus. It is also called dynamic modulus and is used for comparison of different materials at the same strain amplitude.

**Deformation Characteristics [1, 2], see also Figure 1:**

1. **Elastic deformation** is a condition where deformation is instantaneous upon application but reversible on the removal of load. Elastic deformation in solids, such as steel, can be determined either by static or dynamic tests.
2. **Viscous deformation** is a condition where deformation upon removal of load is not reversible then a viscous or permanent deformation occurs as a function of loading time.
3. **Plastic deformation** is one type of permanent deformation when the applied stress exceeds the yield stress value of the material, resulting in the loss of structural cohesiveness. Hence, the permanent deformation occurs as independent of loading time. The yield stress is the value of stress measured at the yield point, at which the an application of load (or strain) above this point causes the irrecoverable (plastic) deformation.
4. **Dilatancy** is the tendency of a mix to change in volume as aggregate particles are forced to slide past each other during shear deformation. This condition may be found when the Poisson's ratio exceeds 0.5.

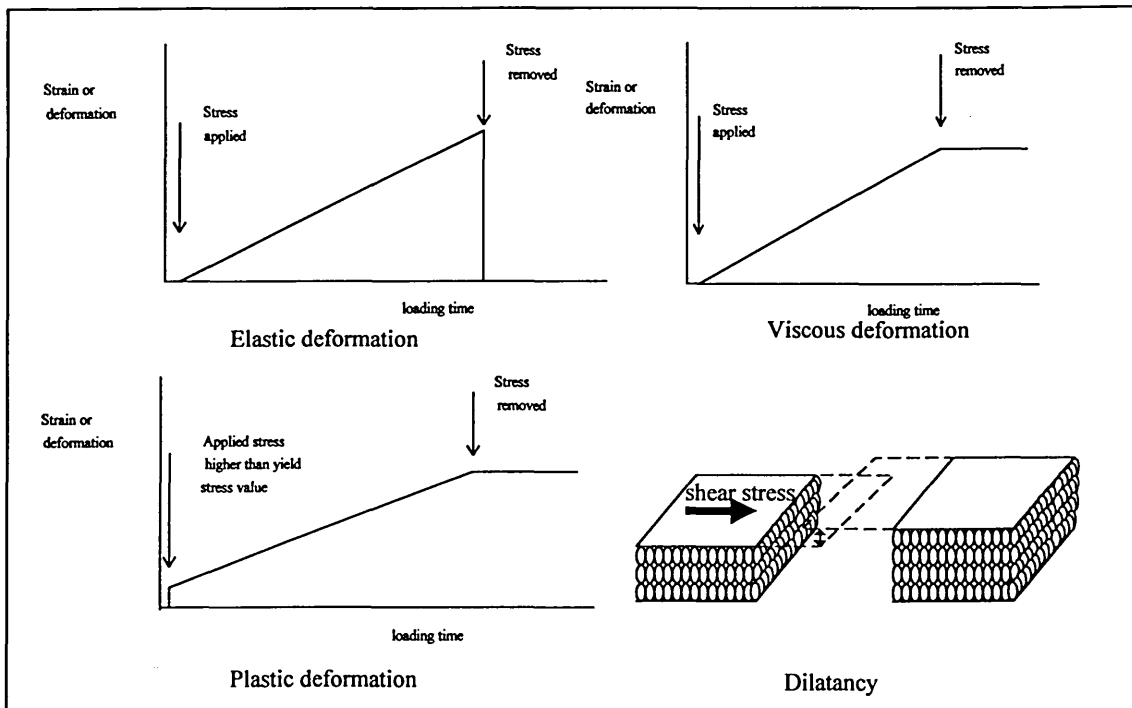


Figure 1 Deformation characteristics

**Delta ( $\delta$ )** is the phase of angle, that is the difference phase between strain input and stress response of the bitumen.

**Dynamic mechanical test** is a type of test which seeks to measure mechanical properties, .e.g. complex shear modulus  $G^*$ , under dynamic conditions, such as regular vibration.

**Isotherm curve** is a curve on a graph representing the behaviour of a system at a constant temperature. This will incorporate the use of a time-temperature superposition technique.

**Loss compliance  $J''$**  is defined as the strain  $90^\circ$  out of phase with the stress divided by stress in a sinusoidal shear deformation. When different materials are compared at the same stress level, the viscous effect as a measure of energy dissipated per cycle of sinusoidal deformation is associated with this loss compliance.

**Loss modulus  $G''$**  is defined as the stress  $90^\circ$  out of phase with the strain divided by strain in a sinusoidal shear deformation. When different materials are compared at the same strain level, the viscous effect as a measure of energy dissipated per cycle of sinusoidal deformation is associated with this loss modulus.

**Loss tangent ( $\tan \delta$ )** is a measure of the viscoelastic characteristics of the materials. This parameter ( $\tan \delta$ ) is dimensionless [3] and independent of temperature [4].

**Relaxation time:** the time taken for the shear stress of a fluid that obeys the Maxwell model to reduce to  $1/e$  of its original equilibrium value on the cessation of steady shear flow.

**Retardation time:** the time taken for the strain in a material that obeys the Kelvin model to reduce to  $1/e$  of its original equilibrium value after the removal of the stress.

**Storage compliance  $J'$**  is defined as the strain in phase with the stress divided by stress in a sinusoidal shear deformation. This storage compliance is associated with elastic effects and is a measure of the energy stored and recovered per cycle when different materials are compared at the same stress level.

**Storage modulus  $G'$**  is defined as the stress in phase with the strain divided by strain in a sinusoidal shear deformation. This storage modulus is associated with elastic effects and is a measure of the energy stored and recovered per cycle when different materials are compared at the same strain level.

**Volumetric properties** is variables in the composition of mixture which expressed as percentages of the total volume of the compacted specimen. and has influence to the performance of the mixture:

1. Air voids ( $V_v$ ) is the total volume of air between coated aggregate particles of the compacted mixture, expressed as percentages of the total volume of the compacted specimen.
2. Voids in mixture aggregate (VMA) is the volume occupied by the air voids and the amount of binder not absorbed into the pores of the aggregate, expressed as percentages of the total volume of the compacted specimen.

3. Voids filled with binder (VFB) is the percentage of the VMA filled with binder.

## REFERENCES

- 1 Eurobitume, "Glossary of Rheological Terms. A Practical Summary of The Most Common Concepts", European Bitumen Association, Brussel, 1996
- 2 "Bituminous Materials in Road Construction", Road Research Laboratory, HMSO, London, 1962
- 3 Ferry, J.D., "Viscoelastic Properties of Polymers", 3<sup>rd</sup> Edition, John Wiley & Sons, 1980
- 4 Dobson, G.R., "The Dynamic Mechanical Properties of Bitumen", Proceedings of AAPT, Vol. 38, 1969, pp. 123-139.

# *Chapter One*

## **1. Introduction**

### *1.1 Definitions*

Bitumen has been defined as “A viscous liquid, or a solid, consisting essentially of hydrocarbons and their derivatives, which is soluble in trichloroethylene and is substantially non-volatile and soften gradually when heated. It is black or brown in colour and possesses waterproofing and adhesive properties. It is obtained by refinery processes from petroleum, and is also found as a natural deposit or as a component of naturally occurring asphalt, in which it is associated with mineral matter” [1]. The American term for bitumen is “asphalt”<sup>a</sup>[2], or, it is called “asphalt cement (AC)” when the bitumen is refined to meet specifications for paving, industrial, and special purposes [3]. In the rest of this thesis, the word “bitumen” is used instead of the other terms.

The word “polymer” is originally from Greek words *polus* which means many, and *meros* which means part [4]. It has been described as long chain molecules built up by multiple repetitions of group atoms known as repeat units or parts [5].

Comprehensive discussion on the properties and performance of bitumens and polymer modified bituminous binders are presented in *Chapter Three*.

---

<sup>a</sup> In the UK practice, asphalt is a type of bituminous mixture e.g. a rolled asphalt. See next section.

## 1.2 Bitumen Usage

The first known usage of bitumen was as a waterproofing agent. The ancient civilisation in the Indus Valley (north-western India) used bitumen in the construction of large public baths or tanks back to the year of 3000 BC. The Egyptians (2600 BC) used the naturally occurring bitumens as a mortar binder for building and paving blocks, mummifications, and numerous waterproofing applications [6]. The use of bitumen has been extended to a huge variety of applications such as: industrial, civil engineering, and agriculture [7].

Bitumen plays an essential role in the construction and reinforcement of road pavements where it has been predominantly used as the binder. There are about 2.2 million miles of paved roads in the United States (US) of which 94% are surfaced with bituminous materials [8] whereas in the United Kingdom (UK) this figure is about 90% [9].

A bituminous mixture is normally made up from combinations of aggregates, filler, and bituminous binder<sup>b</sup>, as illustrated in Figure 1.1. The quantity of the bituminous binder in the mixture should be sufficient enough to coat the aggregates and filler, and also to provide good workability during mixing, laying, and compaction of bituminous mixtures, with exception that some particular types of bituminous mixture may require higher binder contents to meet specification criteria for design and performance.

---

<sup>b</sup> The term “bituminous binder” used in the rest of this thesis will have meaning as both unmodified and polymer modified bituminous binders whereas the word “bitumen” will solely mean an unmodified bituminous binder.

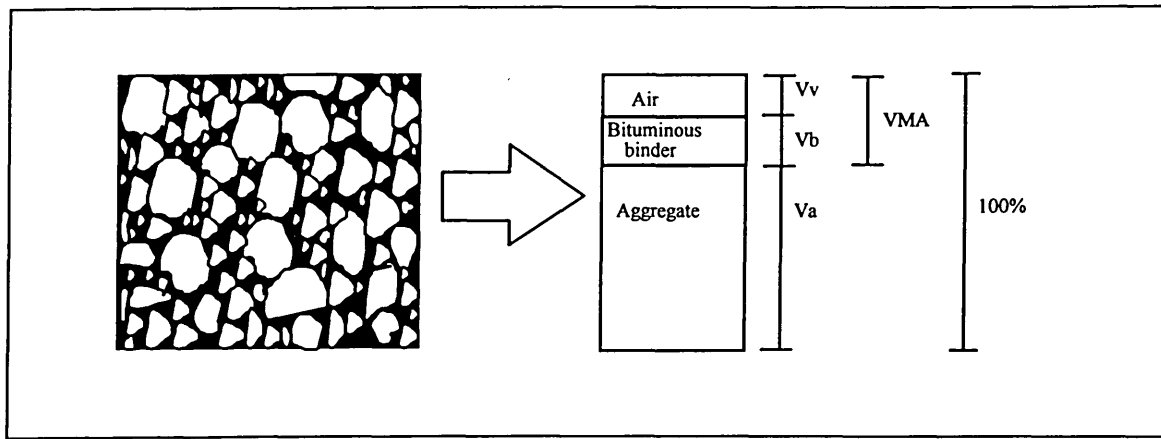


Figure 1.1 Constituency of a bituminous mixture as its volumetric proportions.  $V_v$ ,  $V_b$ , and  $V_a$  are volumetric proportion of air voids, bituminous binder, and aggregate respectively (in percentage).  $VMA$  is volumetric proportion of voids in mineral aggregate ( $V_v+V_b$ ), also in percentage.

In the UK, bituminous macadam and rolled asphalt mixtures are the most common types of bituminous mixtures. Other types of bituminous mixtures, such as: asphaltic concrete, porous asphalt, and stone mastic asphalt, can also be found in Europe (see Figure 1.2). The main properties of these mixtures are summarised in Table 1.1.

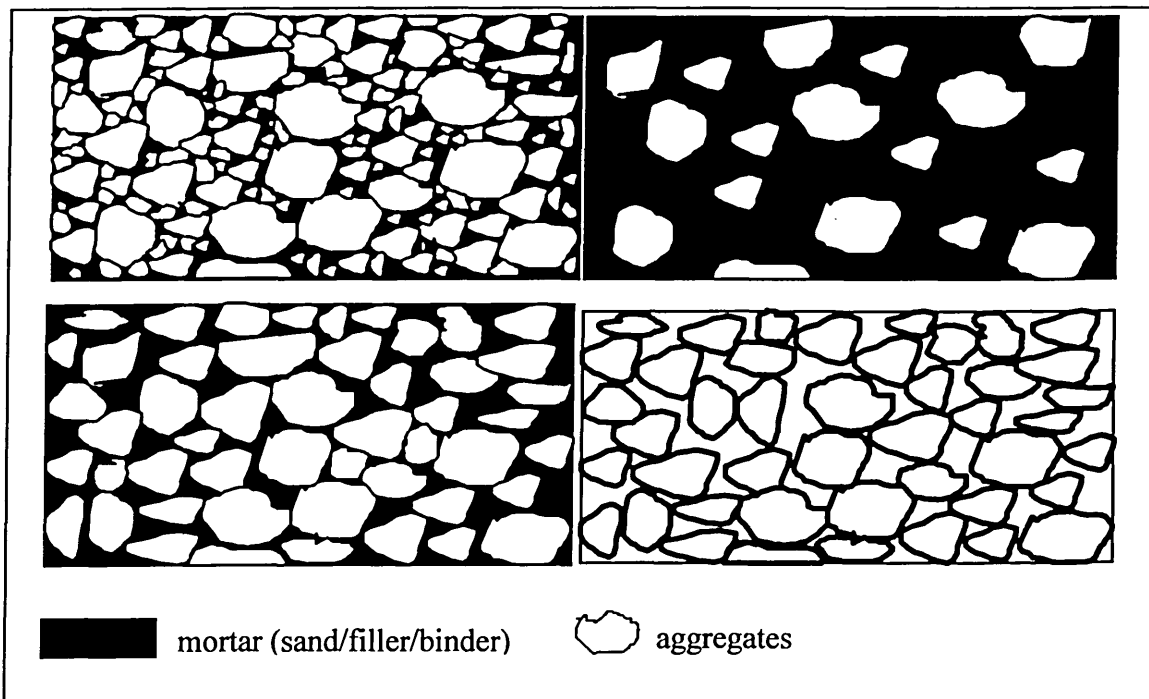
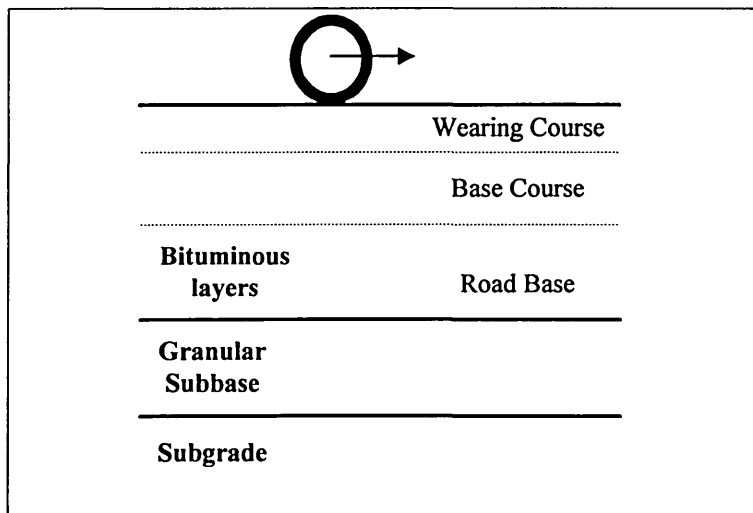


Figure 1.2 Typical cross-sectional views of a bituminous macadam or an asphaltic concrete (upper left), a rolled asphalt (upper right), a stone mastic asphalt (lower left), and a porous asphalt (lower right) mixtures.

*Table 1.1 Typical Characteristics of Various Bituminous Mixtures.*

	Stone Mastic Asphalt (SMA)	Hot Rolled Asphalt (HRA)	Asphaltic Concrete	Bituminous Macadam	Porous Asphalt
Aggregate grading	gap (open), single size	gap (open)	continuous	continuous	continuous
Primary source for the strength of the mixture	aggregate interlock and stiffness of mortar <sup>c</sup>	stiffness of mortar	aggregate interlock	aggregate interlock	aggregate interlock

These types of mixtures are normally placed as the surfacing materials in the road pavement, and some particular mixtures are also used as the base course and road base materials. A typical flexible road pavement structure is shown in Figure 1.3.



*Figure 1.3 A Typical Road Pavement Structure*

### ***1.3 The Reasons for Bitumen Modification***

In the late twentieth century, a rapid increase in the demands placed on highways (i.e., traffic levels, higher tyre pressures, new axle designs, and heavier trucks) has been recognised to significantly increase pavement distress [10]. The Federal Highway Administration (FHWA) of the United States has reported an increase in heavy vehicle traffic by twofold within the last 15 years [11]. Heavy vehicles typically make up about

---

<sup>c</sup> Mortar is a mixture of sand, filler, and binder

Chapter 1: Introduction

10% to 15% of traffic, but cause about 80% to 90% of pavement distress, including permanent deformation, fatigue cracking and surface wear [12].

Car traffic in the UK is expected to rise by 14% to 23% and up to 18% for heavy vehicle traffic by the year 2000, where 90 out of every 100 tonne of inland freight will be moved by road [13]. Data from the British Road Federation (BRF) also shows that the increase of heavy vehicle traffic between 1983 and 1993 is up to 38% and 67% on rural areas and motorways, respectively [13]. The Refined Bitumen Association (RBA) reported that the defects that can be seen in the road structure including cracking, deterioration, patching, and potholes<sup>d</sup>, have increased by an average of 42.2% over the past 10 years [14].

These distresses have raised awareness of the serious problems faced in road paving technology, from the material design to the related application techniques. Furthermore, the damage level caused by the increase of traffic loading is very significant with regard to the service life of the road pavement. The damage level is a condition where the road is at minimum level of serviceability to support traffic, e.g. roads can be designed at the minimum present serviceability indices (see *Chapter Two*) of 2.5. and 2.0 for major highways and highways at lower traffic, respectively [8]. Figure 1.4 shows the damage level, in term of equivalent standard axles (ESA), increases in accordance to a 4<sup>th</sup> power law, as the axle load increases. From the AASHO road test, an axle carrying load of 8.16 tonnes (18000 lb.) has been adopted as being the standard axle [15], or this means that 1 ESA is equivalent to an axle load of 8.16 tonnes. An axle carrying a load of 16.32 tonnes would do as much damage as 16 passes of a standard axle (8.16 tonnes). This condition shows that even a small increase of axle loads can cause a huge increase in the damage level, and hence leads to the reduced service life of a road pavement. Additionally, the recently adopted super single tyres can escalate up to twice as much damage to pavements as dual tyres [16]. The Author needs to emphasise here that the AASHO road test used a static axle load for the formulation of pavement damage due to the simulated traffic loading (i.e. dynamic loading). Pavement damage, however, can

---

<sup>d</sup> Further information on the damage mechanisms of road pavement is presented in *Chapter Two*.

also be attributed to the interactions between traffic (dynamic) loading with the road pavement, such as: spatial repeatability, speed and frequency of traffic loading, dynamic tyre force, *etc.* An extensive reviews and analysis on the effect of dynamic loading on the development of pavement damage has been reported by Collop [17], Cebon [18] and Potter *et al* [19].

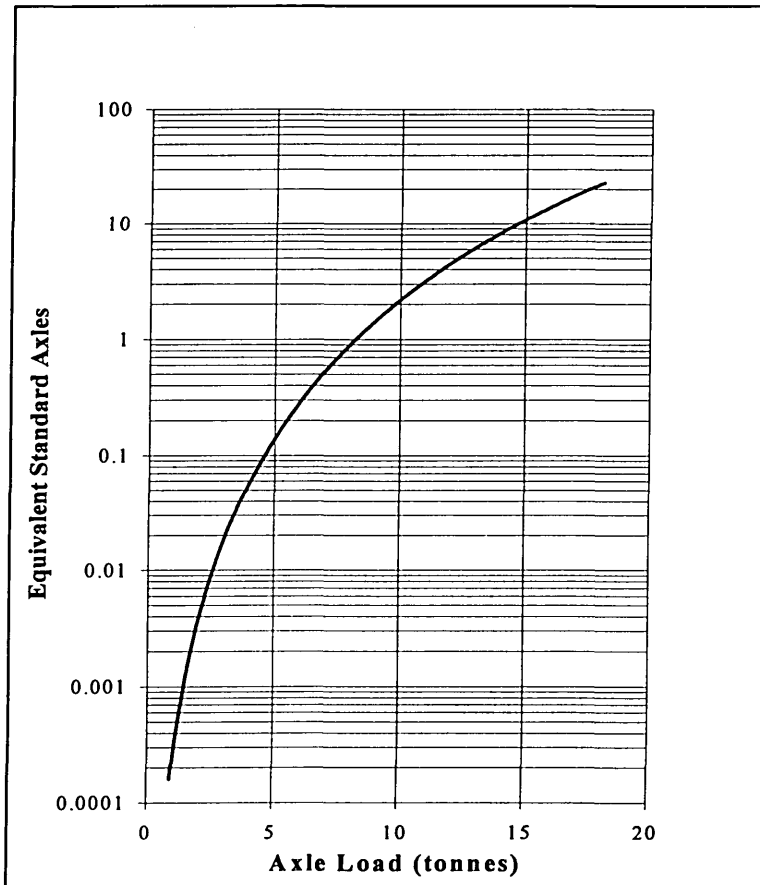


Figure 1.4 Effect of traffic loading (axle load) to the damage level of a road pavement in term of equivalent standard axles. After Croney and Croney [15].

Hot Rolled Asphalt (HRA) has been used as the primary road surfacing material in the UK. This material has performed well in most major sites, even under extreme loading conditions. However, this scenario will change with the increase of traffic volumes of heavy good vehicles, in particular with the rapid adoption of super-single truck tyres in recent years, that results in the need to develop more deformation resistance HRA [20]. The UK Highway Agency has released a draft clause (Clause 943) of the UK Highway Agency's Specification for Highway Works containing the performance based specification for HRA mixtures (see Table 1.2) [21].

Table 1.2 Draft Clause 943 Wheel-tracking Requirements for Site Classification [21]

Classification	Description of Site	Test Temperature [°C]	Rut Rate [mm/h], max.	Total Rut Depth [mm], max.
0	Lightly stressed, not requiring specific design for permanent deformation resistance	Should comply with the requirements of BS594: Part 1 Not Required.		
1	Moderate to heavily stressed, requiring high permanent deformation resistance	45	2.0	4.0
2	Very heavily stressed, requiring very high permanent deformation resistance	60	5.0	7.0

The resistance to deformation of HRA mixtures is predominantly obtained from the properties of the mortar of sand, filler, and binder, in which most of the strength of the mortar are from the properties of the sand and the binder. However, bitumen as a viscoelastic material will undergo changes in properties with changes in temperature and loading conditions. The use of hard bitumens, such as a 35 pen grade bitumen, may not be sufficient to overcome the increased distress experienced by the World's Highways as hard bitumens tend to be brittle at low temperatures and hence susceptible to cracking. On the other hand, soft bitumens can be superior to prevent cracking at low temperatures but cannot sustain heavy loading at high temperatures. Therefore, a modification of bitumen can be an alternative and economical solution. Furthermore, Clause 943 allows the use of an approved polymer modified binder, if a combination of a particular sand and a normal paving grade bitumen (unmodified binder) cannot meet the permanent deformation requirements of Clause 943.

Van Beem and Bresser proposed an "ideal" performance of road bitumens, as illustrated in Figure 1.5, and steps towards this performance can be achieved by addition of polymer modifier [22].

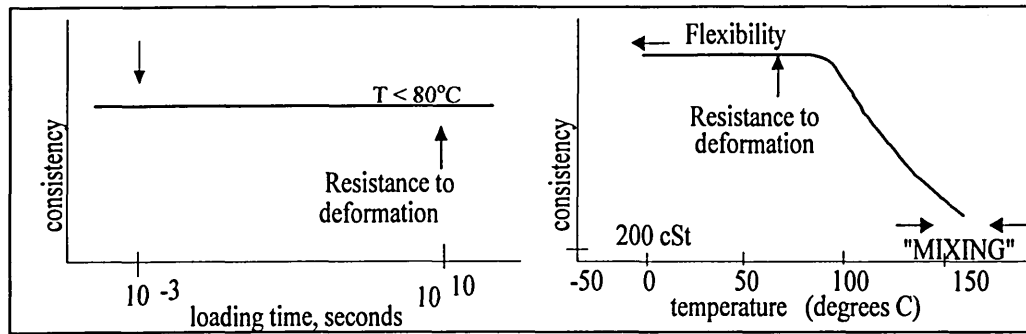


Figure 1.5. Time/temperature behaviour of "ideal" bitumen. After Van Beem and Bresser [22]

There are some common reasons for modifying bituminous binders and mixtures with a polymer, such as:

1. To obtain softer mixtures at low service temperatures to reduce cracking and to increase flexibility and for the mixtures to become stiffer at high temperatures to reduce permanent deformation.

This is the condition that has been proposed by Van Beem and Bresser [22], that the service temperature range can be extended by using polymer modified mixtures (see *Sections 3.3 and 3.4*).

2. To increase structural strength.

For road pavements treated as a multilayer structural system, the strength of the whole structure is interdependent on the strength of the constituent layers. Therefore, an increase in the strength of a particular layer can also increase the strength of the whole pavement structure. Some particular bituminous mixtures, such as HRA, where the strength of the mixtures relies on the stiffness of mortar binder may gain the most benefit from the polymer modification.

3. To improve workability and compaction.

Adverse weather conditions, such as strong winds and low temperatures, is one of the major problems in road construction. Addition of polymers in bituminous mixtures can extend the temperature range for mixing, laying, and compaction [23]. Hence, it improves the workability (see also *Section 3.4.1*).

4. To improve marginal asphalt binders.

The addition of polymers generally reduces the penetration of the binder by one grade, for example: the addition of 5% EVA into 200 pen bitumen can produce a

mixture with performance better than/or similar to a mixture with 100 pen bitumen [24].

5. To allow thicker binder films on aggregate.

As the addition of polymers can also increase the stiffness and viscosity of the binder (see *Section 3.3*), it is also possible to apply thicker binder films, i.e. as a binder-rich mixture, to gain a better workability and a better fatigue resistant mixture without sacrificing the resistance to permanent deformation. A typical binder-rich mixture that can gain potential benefits from polymer modification is the SMA mixture.

6. To improve bonding and to reduce stripping of bitumen and aggregate.

Loss of adhesion between binder and aggregates, especially in the presence of moisture, leads to serious problems in terms of stripping and other moisture damage mechanisms (see *Section 2.3.2*) that happens regularly in surfacing materials [25]. The addition of polymers has shown a significant improvement in reducing moisture damage potential (see *Section 3.4*).

7. To reduce bleeding (high temperature)

It has been stated in *points one and five* that the addition of polymers improves the service temperature range and increases the stiffness at high temperatures, consequently the bleeding potential can also be reduced.

8. To improve resistance to ageing or oxidation.

Durability of bituminous mixtures in term of resistance to ageing or oxidation has been reported to be significantly improved by the addition of polymers (see *Section 3.4.2*). The improvement is even higher than the addition of antioxidant into the mixtures. This property can be beneficial for porous asphalts where binder exposure to oxidation and salt is greater.

9. To reduce structural thickness of road pavement layers.

Some pavement design methods, such as The Shell Method [30], use the thickness of individual pavement layers and their stiffness values as the parameters for designing the pavement structure to meet the strength criteria (see *Section 2.1*) and it has been pointed out previously that the addition of polymers can increase the structural strength (see *point two*). Therefore, structural thickness may be reduced by addition of polymers to meet the same strength criteria as the road pavement structure without polymer modification in its bituminous layers.

However, there are some arguments in opposition to the use of polymers as bitumen modifiers, such as:

1. Polymer modified binders are more expensive than the unmodified bitumen, the cost might be up to seven times of the unmodified one [26], but normally in the range of two to three times more expensive. In order to achieve effectiveness, practicability, and economical use of modified bitumen, it has been suggested that the modifier: should be readily available, have good solubility when blending with bitumen, should resist degradation at asphalt mixing temperatures, should improve resistance to flow at high road temperatures without increasing viscosity of bitumen at mixing and laying temperature or making it too stiff or brittle at low road temperature and the polymer-bitumen blends can be applied with the conventional techniques used in bitumen industry [27,28].
2. The improvement of the performance of modified binders should offset the additional cost of using the polymer. Additionally, in order to optimise the cost effectiveness, the modified binders are best applied in combination with high quality aggregate, in uncommon mixtures such as porous asphalt, in regions which need exceptional resistance to permanent deformation.
3. Current design methods and specifications are mostly based on an empirical approach that is only valid for materials based on unmodified bitumens or those with characteristics similar to unmodified bitumens. Consequently, other design techniques such as analytical designs or mechanistic-analytical designs can be more suitable for polymer modified materials (see *Section 2.1*).

Further discussions on polymer modified binders are presented in *Chapter Three*.

#### ***1.4 Statement of Problems***

In the analysis and design of a new pavement structure or an overlay, engineers used to focus on the issue of fatigue as the main damage mechanism in the bituminous layers [29, 30, 31], rather than looking at the importance of the plastic flow that leads to deformation at higher service temperatures [31]. The increases in the severity of road

traffic have caused permanent deformation to become a more important issue for thick structurally sound pavements [32]. Furthermore, the “global warming situation”<sup>e</sup> that the Earth’s atmospheric temperature is increasing gradually will worsen this problem. Even though, fatigue is still important especially for thin pavements which constitute the majority of the road networks [31].

It was reported that the permanent deformation on the M11 was rapidly increasing during the hot Summer in 1995. With the traffic flows exceeding 32000 vehicles over a 16-hour period on an average week day of which about 20% were heavy goods vehicles, the average permanent deformation of 0 to 10 mm at the end of 1994 was found to have accelerated to be more than double, i.e. the worst permanent deformations observed by October 1995 were 25 to 30 mm [34]. The use of hard binders may accommodate the increasing demands on highway networks. However, the use of hard binders may also bring other problems due to thermal cracking occur at low pavement temperatures. Therefore, there is a need to develop new materials and designs that can cope with the new conditions.

The use of additives to improve the performance of bituminous mixtures has increased in recent years. Polymeric additives have been proposed as a potential source of improvement of the performance of bituminous road pavements especially under adverse loading and climatic conditions. For example, rubbers have been implemented in the USA and Canada since the 1970's. In the UK, polymer modified mixtures for construction and maintenance of some main roads, such as the use of polymer modified mixtures on motorways (e.g. on the M11 between junctions 9 and 10, on the M25 between junction 23 and 24) and other major routes (e.g. on the A14, on the A21, on the A346, and on the A38) [33, 34, 35 ,36].

The increased use of polymer modified binders has been followed by some problems related to properties of the base binder (i.e. the bitumen) and the polymer modifier. The

---

<sup>e</sup> Scientists from the United Nations (UN) sponsored Intergovernmental Panel on Climatic Change (IPCC) predicted that the Earth’s average temperature could rise by about 2.8°C during the next century. Source: “Earth Week : a Diary of the Planet”, The Observer 17 December 1995.

bitumen may be manufactured from one or more crude oils which can lead to a large variety in the properties and end performance of the mixtures. The addition of polymer may add to this complexity. In previous conferences [37, 38], researchers have also reported that some conventional tests are not valid if applied to polymer modified mixtures [31] as they tend to undermine the enhanced performance of the polymer modified mixtures (see also *Sections 3.3 and 3.4.* for further information). Therefore, a better understanding on the properties of the bitumen (e.g. physical and chemical properties) which relates to the end performance of the mixture is very important [39], and the understanding should lead to developments of test methods and specifications that accommodate the use of polymer modified binders.

## ***1.5 Research Aims and Objectives***

### **1.5.1 Aims**

To investigate the characteristics of polymer - bitumen blends and to develop a better understanding of the relationship between the interaction mechanism within polymer-bitumen blends and their effect on the performance of bituminous mixtures.

### **1.5.2 Objectives**

- a) To develop an understanding of the properties of bituminous binders, both unmodified and polymer modified ones, by using more fundamental tests (e.g. using a dynamic shear rheometer and a viscometer) as opposed to empirical tests (e.g. the penetration, and the ring and ball softening point tests), and also the fundamental properties of bituminous mixtures over a range of test frequencies and temperatures by using a dynamic mechanical test.
- b) To study the performance of bituminous mixtures in relation to their permanent deformation characteristics.
- c) To develop a new approach using dissipated energy as a performance indicator of the resistance to permanent deformation.

## ***1.6 Organisation of Thesis***

This thesis is divided into ten chapters, which has been arranged and presented by the following orders: the introduction (*Chapter One*), literature review (*Chapters Two and Three*), hypothesis (*Chapter Four*), testing arrangements and data collection (*Chapter Five*), analyses (*Chapters Six and Seven*), general discussions (*Chapter Eight*), conclusion (*Chapter Nine*) and recommendations (*Chapter Ten*), as demonstrated in Figure 1.6. This arrangement is found useful when distinguishing each objective set in this thesis. The first three chapters are to present the level of understanding acquired by the Author during this research work whereas the rest of the thesis is to explore this understanding further, i.e. to develop a novel contribution to knowledge.

### **Descriptions of each chapter are as follows:**

General views of the development of bituminous materials with regards to their historical facts, material performance, and current demands, which have led to the use of polymer modified bitumens to overcome the increase in severity and damage level experienced by today's highways, is presented in *Chapter One*. The importance of having a good understanding of damage mechanisms for the analysis and design of road pavements is highlighted in *Chapter Two*, together with a presentation of various approaches in the pavement design. The study is then focused in *Chapter Three* on the identification on behaviour and properties of polymer modified bituminous mixtures. Their performances with particular reference to resistance to permanent deformation are presented more comprehensively in *Chapter Four*. The discussions on the resistance to permanent deformation lead to the development of a novel approach for assessing the performance of bituminous mixtures, i.e. by using the dissipated energy method. Research methodology and procedure for conducting these tests are presented in *Chapter Five*. Reviews on the limitations of some conventional test procedures, in comparison to the dynamic mechanical test, when using polymer modified materials are also presented. The analysis and discussions on the interaction mechanisms of polymer modified mixtures and the applicability of the use of the dissipated energy method for assessing the mixture performance are presented in the *Chapters Six, Seven and Eight*. The last chapters (*Chapters Nine and Ten*) present findings of this research, and some suggestions and recommendations for further works.

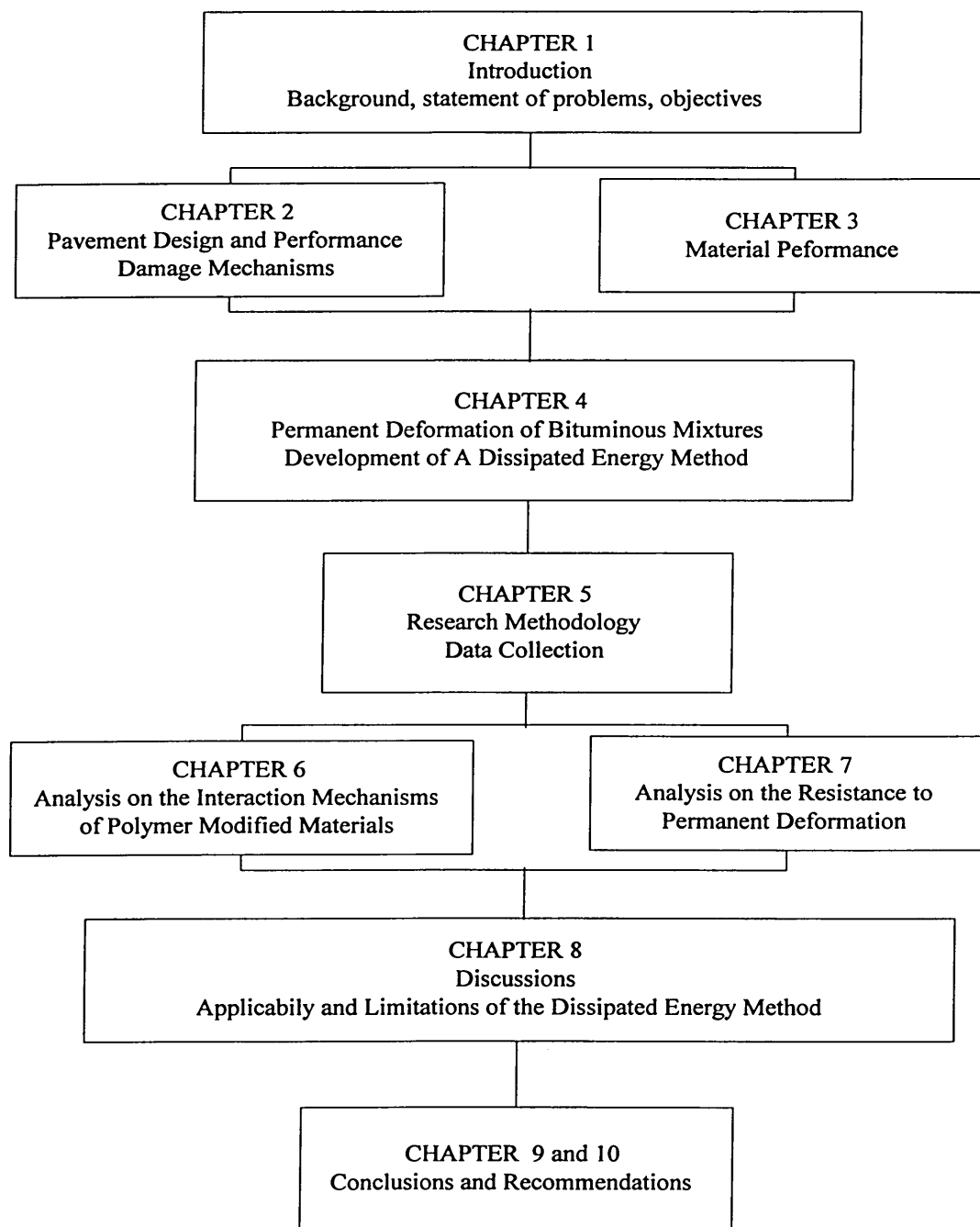


Figure 1.6 Schematic Organisation of the Thesis

## 1.7 References

- 1 Anon, "Bitumen for Building and Civil Engineering. Part-1. Specification for Bitumens for Road Purposes", British Standard 3690:Part 1: 1989.
- 2 Anon, American Society for Testing and Materials Designation D8.
- 3 Anon, American Society for Testing and Materials Designation D946 and D3381.
- 4 Anon, "Network's Guide to Polymers in Bitumen" The Nynas Digest of Bitumen, Issue No. 3 Summer 1996.
- 5 Walker, P.M.B., "Chambers Materials Science and Technology Dictionary", Chambers Harrap Publishers Ltd., 1993.
- 6 Roberts, F.R., Brown, E.R., Kandhal, P.S., Lee, D.Y., and Kennedy, T.W., "Hot Mix Asphalt Materials, Mixture design, Construction", NAPA Research and Education Foundation.
- 7 Anon, The Asphalt Institute, "The Asphalt Handbook", Manual Series No.4, 1989.
- 8 Huang, Y.H., "Pavement Analysis and Design", Prentice Hall, 1993.
- 9 Shell, "Bituminous Materials for Road and Airfield" (Audio Visual).
- 10 Brown, S.F., Rowlett, R.D., and Boucher, J.L., "Asphalt Modification", Highway Research: Sharing The Benefits, London, 1990, pp. 181-204.
- 11 Liang, Z., Hesp, S.A.M., "In Situ Steric Stabilization of Polyethylene Emulsions in Asphalt Binders for Hot-Mix Pavement Applications", Colloids and Surfaces A: Physicochemical and Engineering Aspects, 81,1993, pp. 239-250.
- 12 Anon, Focus on Hot Mix Asphalt Technology, Summer 1996, Vol. 1, No. 2.
- 13 Anon, "Road Facts 95", British Road Federation
- 14 *Private Communication*, Refined Bitumen Association, "Key Findings of RBA 1996 Local Authority Survey".
- 15 Croney, D, and Croney, P., "The Design and Performance of Road Pavements. Second Edition", McGraw-Hill, 1991.

- 16 Anon, "Heavy Duty Pavements. The Arguments for Asphalt", European Asphalt Pavement Association, The Netherlands, 1995.
- 17 Collop, A.C., "Effects of Traffic and Temperature on Flexible Pavement Wear", PhD Thesis, University of Cambridge, June 1994.
- 18 Cebon, D., "Interaction Between Heavy Vehicles and Roads", L. Ray Buckendale Lecture, SAE 1993, SP-951, SAE Trans 930001.
- 19 Potter, T.E.C., Cebon, D., and Cole, D.J., "Using Parameter Estimation to Assess Road Damage", Proceedings of 14<sup>th</sup> IAVSD Symposium on the dynamics of vehicles on roads and tracks, Ann Arbor, Michigan, 1995, Swets & Zeitlinger.
- 20 Fabb, T, "Bitumen Breakthrough", Highways, January/February 1997, pp. 16-21.
- 21 Anon, "Hot Rolled Asphalt Wearing Course (Performance Related Design Mix)". UK-Highway Agency's Specification for Highway's Works: Clause 943, Draft No 4.0, 5th July 1996.
- 22 VanBeem, E.J. and Brassler, P., "Bituminous binders of improved quality containing Cariflex thermoplastic rubbers", Journal Institute of Petroleum, Vol 59, No 556, pp. 91-97.
- 23 Masterman, J., "Polymers Prove Their Worth", Highways, May 1996.
- 24 Giavarini, C., "Polymer Modified Bitumen", Asphaltenes and Asphalts Vol. 1, Developments in Petroleum Science, Series 40, Edited by T.F. Yen and G.V. Chilingarian, Elsevier, 1994.
- 25 Ruth, E., "Evaluation and Prevention of Water Damage to Asphalt Pavement Materials", ASTM STP 899, 1984.
- 26 Denning, J.H., and Carswell, J., "Improvement in Rolled Asphalt Surfacing by The Addition of Sulphur", TRRL, LR 963, 1981.
- 27 Denning, J.H., and Carswell, J., "Improvements in Rolled Asphalt Surfacing by The Addition of Organic Polymers", TRRL, LR 989, 1981.
- 28 Hoban, T., "Modified Bitumen Binders for Surface Dressing", Chemistry and Industry, 1990, pp. 538-542.

- 29 Van Dijk, W., "Practical Fatigue Characterization of Bituminous Mixes", Proceedings of the Association of Asphalt Paving Technologists, Vol. 44, 1975, pp. 38-74.
- 30 Claessen, A.I.M, Edwards, J.M., Somme, P., and Uge, P., "Asphalt Pavement Design. The Shell Method", Proceedings of the Fourth International Conference on Structural Design of Asphalt Pavements, 1977, pp. 37-74.
- 31 Francken, L., "RILEM TC-152-PBM-Performance of Bituminous Materials. Progress Report 1992-1996", Materials and Structures, Supplement March 1997, pp. 33-42.
- 32 Emery, J., "Asphalt Pavement Rutting Experience in Canada", Proceeding Canadian Asphalt Paving Technology, Vol XXXV, November 1990, pp.80-91.
- 33 Anon, "Bitumen Products Technical Data Sheets", Nynas UK.
- 34 Anon, "Modified Mixes Used to Combat Rutting", Highways & Transportation, December 1996.
- 35 Anon, "Olexobit 100", British Petroleum (BP) Bitumen, 1997.
- 36 Anon, "ESSO Flexipave", ESSO Petroleum Company Limited.
- 37 ASTM Symposium on Polymer Modified Asphalt Binders, San Antonio, Texas, 4 December 1990.
- 38 Euroasphalt & Eurobitume Congress, Strasbourg, 1-10 May 1996.
- 39 Jones, D.R., and Kennedy, T.W., "Asphalt Chemistry and Its Effect on Roadway Surface Conditions", ASTM Standardisation News, February 1991.

## Chapter Two

### 2. Pavement Performance

#### 2.1 Introduction

In bituminous (flexible) pavements, the tensile and compressive stresses induced by heavy vehicle loads decrease with increasing depth. This condition allows the use of a gradation of materials, where the relatively strong and expensive materials are used for the surfacing and the less strong and cheaper ones for base and subbase. The whole structure of pavement must limit the stresses in the subgrade to an acceptable level, and the upper layers must in a similar manner protect the layers below. Figure 2.1 shows that, in a multilayer pavement system, normal stresses become smaller ( $\sigma_n < \sigma_2 < \sigma_1$ ) with the increase in depth of the pavement structure, due to the distribution of wheel loads throughout the pavement layers.

The main objective of pavement design is to economically build road pavements with good performance which meet criteria on both structural and functional conditions during the design life. The functional condition is the riding quality which is primarily related to the roughness of the pavement, and sometimes termed the serviceability of the pavement. The structural condition is concerned with the bearing capacity, e.g. how long the pavement will maintain its structural integrity and continue to protect the subgrade, *etc.*

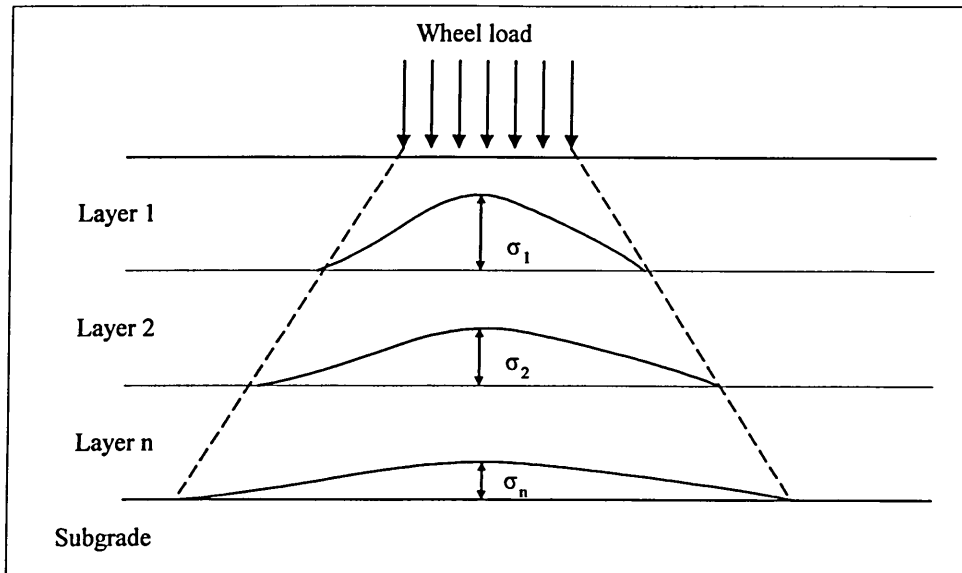


Figure 2.1 Illustration of the distribution of traffic loading at various depths of road pavements showing reduction of stress level( $\sigma$ ) at each layer.

In general there are three approaches that have been used for the analysis and design of bituminous pavement; empirical, analytical (mechanistic), and semi-empirical (analytical-empirical or mechanistic-empirical) methods.

Traditionally, most road pavements are designed using an empirical approach which is based on experience accumulated from practice and from specially constructed test sections, as this kind of approach is simple and generally suitable for certain materials under certain environmental and loading conditions. The most commonly used method in this category is the California Bearing Ratio (CBR) method, in which the strength of the subgrade and granular materials is measured by the CBR test (Figure 2.2) [1]. Road Note 29 [2] and Road Note 31 [3] are empirical design procedures which were produced by the Transport and Road Research Laboratory (TRRL) - UK. This approach, however, cannot any longer accommodate the current changes and the development of new road materials and the increased demand in road traffic. Therefore, an analytical approach is used instead.

In the analytical approach, theoretical analysis of the mechanical properties of bituminous materials is used to assess a designed pavement structure. This approach

offers the flexibility to accommodate new materials and changes in traffic and environmental conditions.

Two of the well-known analytical methods are reviewed here, i.e. the Shell Pavement Design Manual (SPDM) [4] and the Nottingham method [5]. Both methods apply a similar principal criterion, i.e. by limiting the critical strains (Figure 2.3), e.g.:

- horizontal tensile strain at the bottom of the bound layer which measures the pavement's resistance to fatigue,
- the vertical compressive strain at the top of the subgrade which measures the pavement's resistance to permanent deformation.

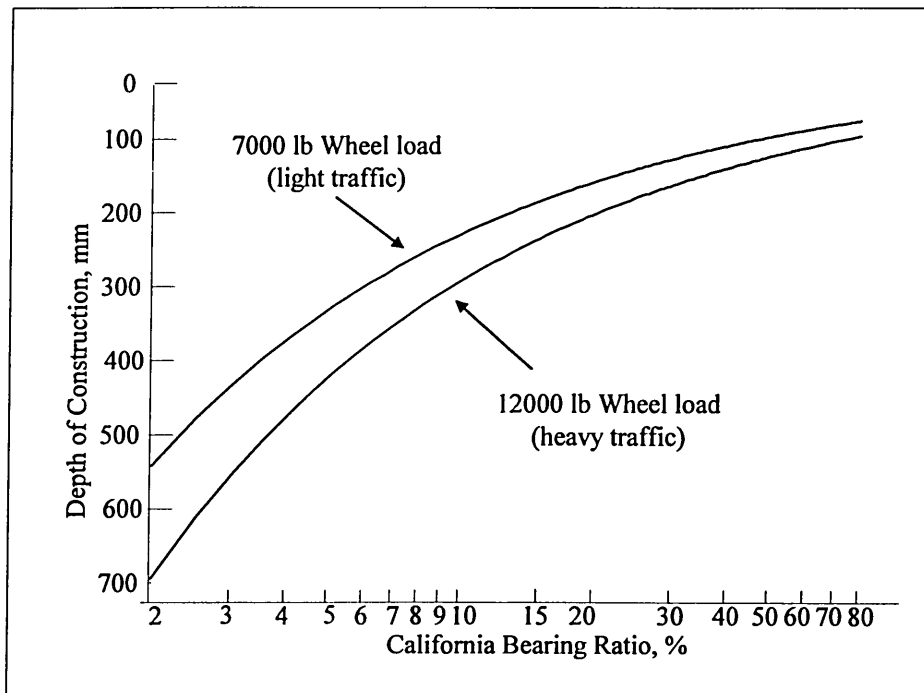


Figure 2.2 An example of an empirical approach: California Bearing Ratio design curve. After Whiteoak [1]

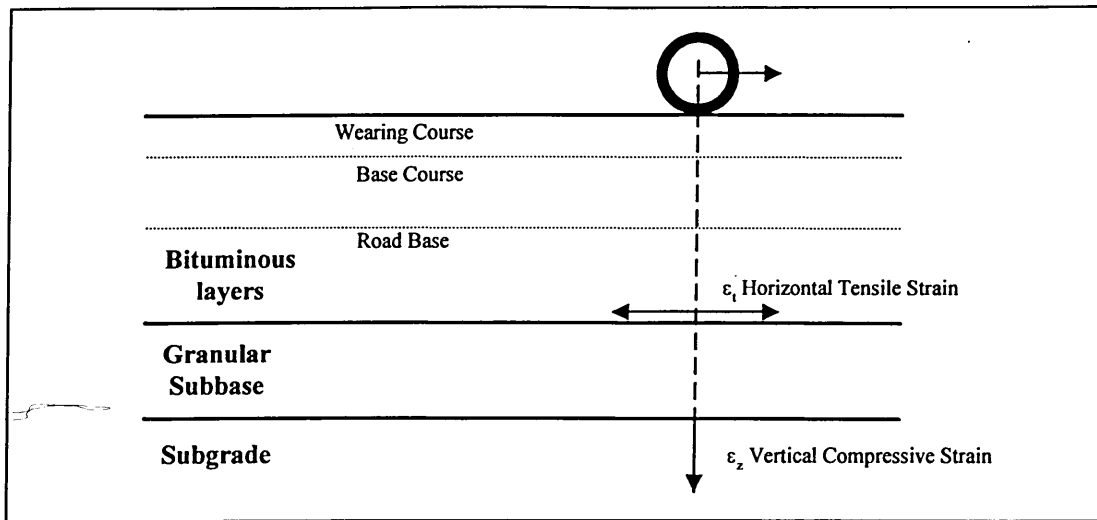


Figure 2.3 The principal critical strains in the analytical design methods

The mechanistic-empirical approach has generally been adopted by highway agencies following the vast development in bituminous materials, e.g. UK started adopting this approach when TRRL proposed a design recommendation in LR 1132 [6] to replace the previous recommendation in Road Note 29 [2]. Road Note 29 does not deal with the resurfacing<sup>a</sup> and maintenance of existing roads, but merely with the construction of new roads. The design life recommended by Road Note 29 is of 20 years to cater traffic of up to 40 million standard axles (msa), of which the pavement is considered to be at a failed state<sup>b</sup> and a major overlay or partial reconstruction<sup>c</sup> would be necessary at the end of the service life of the pavement. However, this condition is not beneficial in terms of the pavement's performance after overlaying or reconstruction (as severe damage has already developed). Therefore, LR 1132 recommends that a design should be based on the structural deterioration associated with 10 mm rut in the wheel path rather than a 20 mm rut, to give a substantially longer service life. The pavement condition at a 10 mm rut is considered to be at the "critical" condition where an overlay should take place (*see next section*).

<sup>a</sup> Resurfacing is replacing the old surface layer with a new layer.

<sup>b</sup> This condition is associated with a rut depth of 20 mm or more, in accordance to LR1132 recommendation.

<sup>c</sup> Reconstruction is replacing the old pavement structure with a new structure, usually a new pavement design is applied.

This mechanistic-empirical approach is simple and is robust enough to be used on a regular basis [7], which deals with two main components: response and performance. The pavement response is normally calculated by an analytical method, such as the theory of linear elasticity, to determine the critical stresses and strains in each of the pavement layers for any combination of loading and environmental conditions. A rough estimate of the pavement performance can be obtained by developing an empirical relationship between the response and the rate of deterioration as measured by the serviceability, and then the damage caused by different combinations of loading and environmental conditions can be determined.

## ***2.2 Serviceability***

Serviceability is the ability of a specific pavement section to serve traffic in its existing condition [7]. The serviceability can be quantified either using pavement roughness alone, or using both roughness and distress condition (e.g. cracking or permanent deformation in the wheel path, *etc. -see next section-*)

Pavement roughness is the main factor which represents the level of serviceability of the pavement with regard to user benefits, such as:

1. Riding comfort: the rougher the pavement, the lower the riding comfort.
2. Road user costs: the rougher the pavement, the higher the user costs (e.g. due to the increase in vehicle maintenance costs, the increase in fuel and oil consumption and the longer journey time).
3. Safety, which is affected by skid resistance, permanent deformation, pavement colour and light reflection characteristics.
4. Surface characteristics related to splash and spray.
5. Noise emission can be amplified by regularity of the pavement.
6. Tyre wear and rolling resistance, which are affected by the surface regularity of the pavement.

During the AASHO road test, as described by Ullidtz [7], Present Serviceability Index (PSI) is introduced as an index to be used to quantify the level of serviceability of road pavement. This index is developed based on both pavement roughness as well as

distress condition, i.e. the PSI is determined from the riding quality (SV), the rut depth (RD), and the extend of cracking and patching (C+P). An empirical relationship was derived for bituminous (flexible) pavements:

$$PSI = 5.03 - 1.91 \log(1 + \overline{SV}) - 1.38 \overline{RD}^2 - 0.01 \sqrt{C + P}$$

*Equation 2.1*

where,

PSI = present serviceability index

$\overline{SV}$  = slope variance, the variance of slopes measured over a 6-inch wheel base using a profilometer

$\overline{RD}$  = average rut depth

C = pavement cracking in feet/1000 square feet of pavement surface; and

P = patching in square feet/1000 square feet of pavement surface

Generally, new pavements have a PSI between 4 and 5, and repair is usually needed when PSI falls to between 1.5 and 2.5 (Figure 2.4) [8]. Furthermore, decisions on the maintenance strategy for when work, for example: new overlay, should take place is critical as the cost increases as the structural integrity decreases [9]. However, the decision of when this “critical condition” will be reached is a rather complicated matter because pavement deterioration involves various types of distress which may be functional or structural in nature and other factors which contributes to the deterioration such as traffic, environment and material properties. Therefore, accurate identification of distress mechanisms and their levels of severity is important.

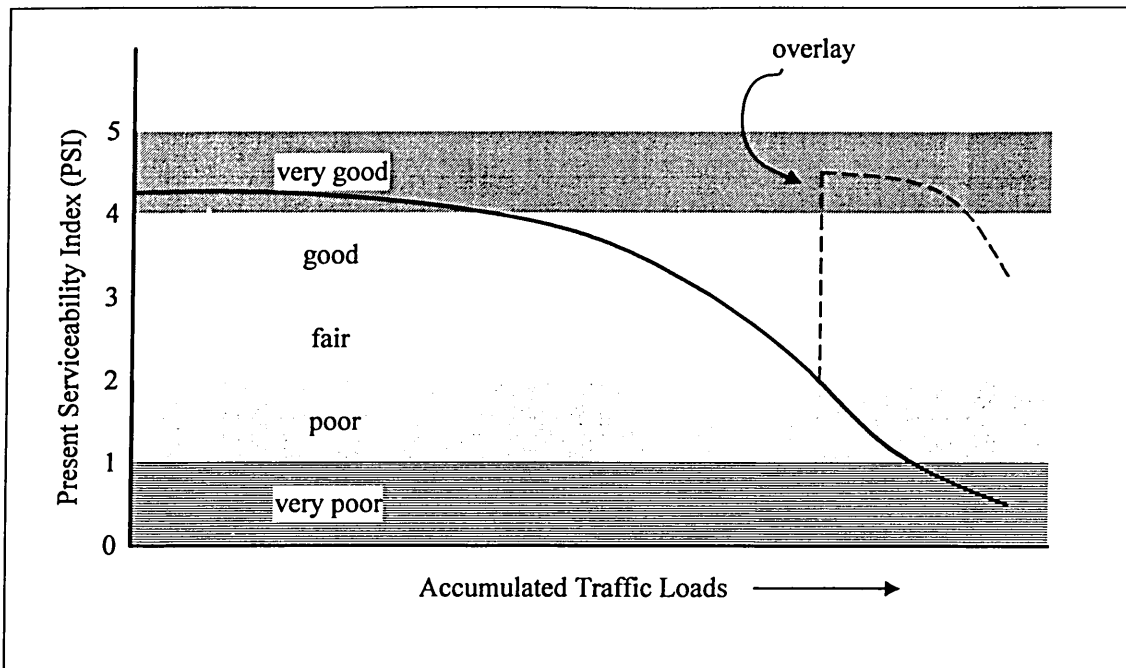


Figure 2.4 Typical relationship between PSI and cumulative traffic, after Roberts et al [8]

In the UK, the design criteria to determine terminal serviceability of a pavement includes a critical distress parameter as determined by permanent deformation<sup>d</sup> [10], e.g. a pavement is regarded as being at critical condition if it has a rut depth of 10 mm. When this condition is reached, maintenance should be carried out without delay (if it has not been already done) before the maintenance cost increases too rapidly. A pavement failure is marked by a terminal rut depth of 20 mm where major maintenance work, such as resurfacing or reconstruction, may be required. The complete classification is presented in Table 2.1.

<sup>d</sup> Permanent deformation, rut, or rutting are of the same meaning and will be used interchangeably in this thesis.

Table 2.1 Classification of the condition of the road surface used by TRL[10]

Classification	Code	Visible evidence
Sound	1	No cracking. Rutting under 2m straightedge less than 5 mm.
	2	No cracking. Rutting from 5mm to 9mm.
Critical	3	No Cracking. Rutting from 10mm to 19mm.
	4	Cracking confined to a single crack or extending over less than half of the width of the wheel path. Rutting 19mm or less
Failed	5	Interconnected multiple cracking extending over the greater part of the width of the wheel path. Rutting 19mm or less.
	6	No Cracking. Rutting 20mm or greater.
	7	Cracking confined to a single crack or extending over less than half of the width of the wheel path. Rutting 20mm or greater.
	8	Interconnected multiple cracking extending over the greater part of the width of the wheel path. Rutting 20mm or greater.

### 2.3 Damage Mechanisms

Identification of distress is important in pavement design and maintenance. In the mechanistic-empirical approach, each failure criterion is developed separately to take care of each specific damage mechanisms [11]. One of the important steps in identifying pavement distress is studying the damage mechanisms that occur in bituminous pavements, then the level of severity can be quantified and a measurement criterion developed. Table 2.2 presents different types of pavement distress. They can be classified into four major damage mechanisms: cracking, rutting, moisture damage, and age hardening.

Table 2.2 Typical distress in bituminous pavements. After Huang [11]

Type of Distress	Structural	Functional	Load-associated	Non load-associated
Alligator or fatigue cracking	x		x	
Bleeding		x		x
Block cracking	x			x
Corrugation		x		x
Depression		x		x
Joint reflection cracking	x			x
Lane/shoulder drop-off or heave		x		x
Lane/shoulder separation		x		x
Longitudinal and transverse cracking	x			x
Path deterioration	x	x	x	
Polished aggregate		x	x <sup>a</sup>	
Potholes	x	x	x	
Pumping and water bleeding	x	x	x	x
Ravelling and weathering		x		x
Rutting		x	x	
Slippage cracking	x		x	
Swell	x	x		x

<sup>a</sup>Tyre abrasion

### 2.3.1 Cracking

Cracking in bituminous pavements can be caused by thermal contraction under severe climatic conditions, by fatigue under repeated loading, or by construction practices, e.g. roller cracks. In terms of road performance, the existence of cracks at the road surface must be avoided as they cause numerous problems, such as: discomfort for the users, reduction of safety, intrusion of water and subsequent reduction of the bearing capacity of the soil, and progressive degradation of the pavement structure in the presence of the cracks due to localised excessive stresses.

#### 2.3.1.1 Thermal Cracking

Thermal cracking, or low temperature cracking, is caused by the exposure of asphalt to a single thermal cycle at which the temperature reaches a critical low temperature, or from thermal cycling (relatively small number of large strain movements) above the critical low temperature. At the critical temperature, a bituminous binder can no longer flow quickly enough to relieve the stress as it attempts to accommodate the large tensile strains developed due to expansion and contraction caused by variation in temperatures.

Failure occurs when the thermally induced stress exceeds the tensile strength. Usually, this kind of mechanism can be observed as :

- transverse cracking, as the main phenomenon, across the full width of bituminous pavements at regular intervals,
- longitudinal cracking parallel to the centre line of bituminous pavements, and usually occurring at the joint between adjacent lanes,
- block cracking in the transverse and longitudinal direction of road pavement, which is usually caused by embrittlement of the binder, generally on low traffic roads (due to less traffic densification) which leaves high voids allowing oxidation of the bituminous surface.

A liquid bitumen or other type of sealing material can be used for repairing thermal cracking in order to prevent moisture from penetrating the base course and subgrade and helps to minimise ravelling near to the cracks. However, if cracking becomes too severe, all cracked layers may have to be removed and replaced with an overlay, otherwise it is

likely that the underlying cracks will reflect through the overlay during the first or second winter.

### **2.3.1.2 Fatigue Cracking**

Fatigue in bituminous pavements has been defined as the phenomenon of cracking which consists of two main phases, i.e. crack initiation and crack propagation, and is caused by tensile strains generated in the pavement by traffic loading, temperature variations, and construction practices [12].

Read [12] reported that “*cracks always propagate around the coarse aggregate passing as close to the aggregate as possible*”, and they also travel the shortest route between the point of crack initiation and the point of applied load. The cracks propagate to the surface initially as one or more longitudinal parallel cracks but then under repeated traffic loading, the cracks connect and develop a pattern like the skin of alligator, therefore it is sometimes also termed alligator cracking.

Alligator cracking occurs only in areas that are subjected to repeated traffic loading, and usually measured in square meters of surface area. The typical relationship between the initial stress and the fatigue life of a pavement due to repetitive loading at different temperatures is schematically illustrated in Figure 2.5. Construction induced cracking (roller cracking), e.g. cracks due to wheel roller compactor, has also been reported to have a detrimental effect upon fatigue life of bituminous pavements, in that the cracks allow moisture to penetrate the subsequent layers resulting in stripping and loss of tensile strength of up to 30%, which leads to a reduction in fatigue life of up to 50% [13]. The use of soft plate compactors eliminates the possibility of roller cracking that is generally found with conventional vibratory or steel wheeled rollers, and hence, to longer fatigue lives (Figure 2.6).

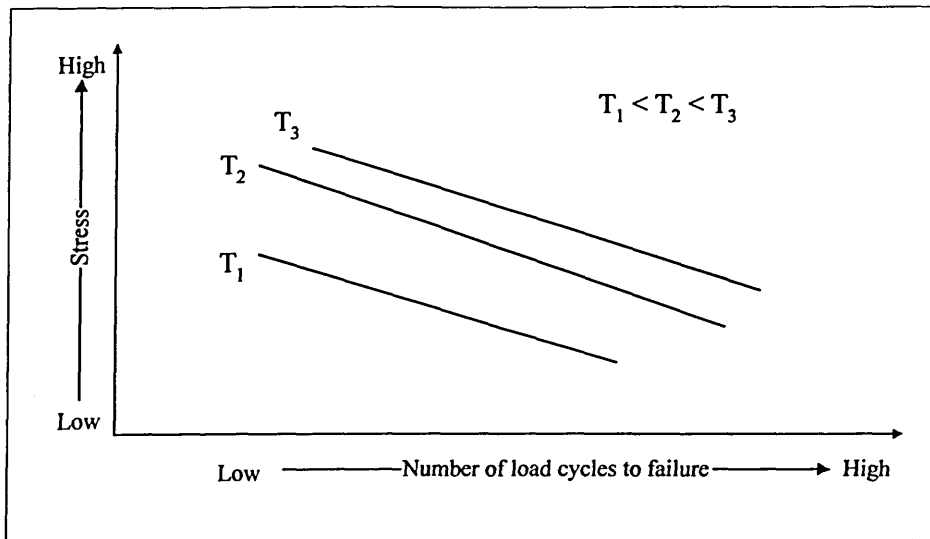


Figure 2.5 Schematic illustration on the effect of temperature on fatigue life for controlled stress testing.

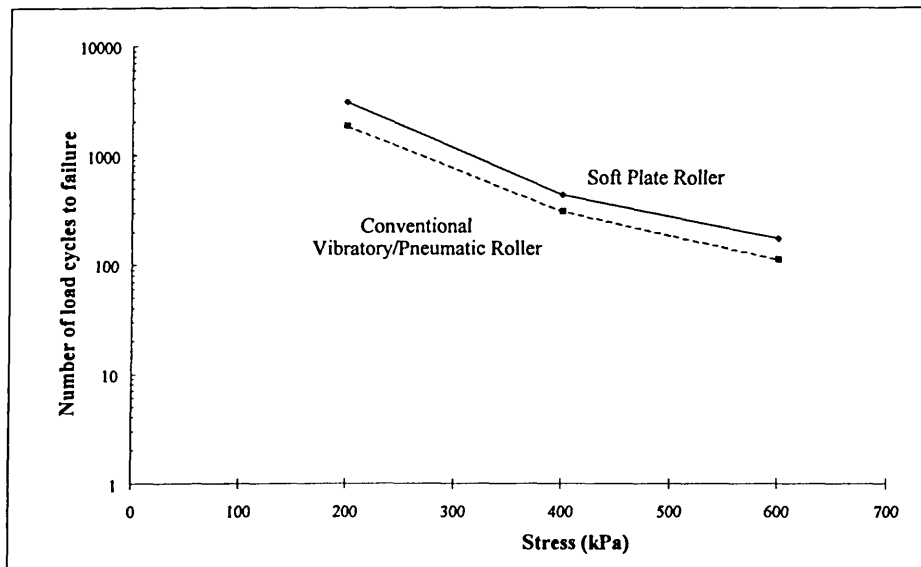


Figure 2.6 Effect of different roller compactors to fatigue life [13]

In bituminous pavement design, a damage model originally developed by Miner is often used for analysis and prediction of fatigue life due to repeated loading imposed onto a pavement. A damage factor  $D_i$  is defined as the number of load repetitions  $n_i$  at condition  $i$  divided by the number of load repetitions  $N_i$  to failure at condition  $i$ , and  $D_k$  is the accumulation of fatigue damage. The fatigue failure is reached when  $D_k$  exceeds 1 ( $D_k = 0$  if no damage,  $D_k = 1$  at failure), see Equation 2.2 [14].

$$D_k = \sum_{i=1}^{i=k} D_i = \sum_{i=1}^{i=k} \frac{n_i}{N_i} \leq 1$$

Equation 2.2

Wu [9] suggests that the Miner equation can be modified if fatigue life is considered to be influenced by temperature and physical state (e.g. age and stiffness) of a pavement as well as traffic loading, and hence:

$$D_k = \sum \frac{n_{ij}}{N_{ji}}$$

Equation 2.3

where  $i$  = different levels of critical strain

$j$  = different levels of combinations of temperature and physical state.

Fatigue cracking is also often associated with loads which are too heavy for the pavement structure or more repetitions of a given load than provided for in the design. Inadequate pavement drainage can exacerbate this problem by allowing the pavement layers to become saturated and lose strength, which causes layers to experience high strain and subsequently leads to premature fatigue failure [8]. This distress can lead to the development of potholes when the individual pieces of bituminous material physically separate from adjacent material and are dislodged from the pavement surface by the action of traffic.

### 2.3.1.3 Reflection Cracking

Reflective cracking through a pavement structure is one of the main causes of premature pavement deterioration. This phenomenon which frequently occurs when a layer of bituminous material is placed on top of a discontinuous base, can represent many different aspects related to the large number of factors governing the mechanism of crack initiation and its propagation through a road structure. Reflection cracking is produced by either traffic or thermally induced stresses (Figure 2.7) [8, 15] which may be initiated from:

- cracks or joints in an underlying concrete pavement,

- cracks already existing in old bituminous surfaces before overlaying, e.g. low temperature cracks, longitudinal cracks or fatigue cracks,
- block cracks induced by the old bituminous surface, or those induced by subgrade soil cracking due to shrinkage.

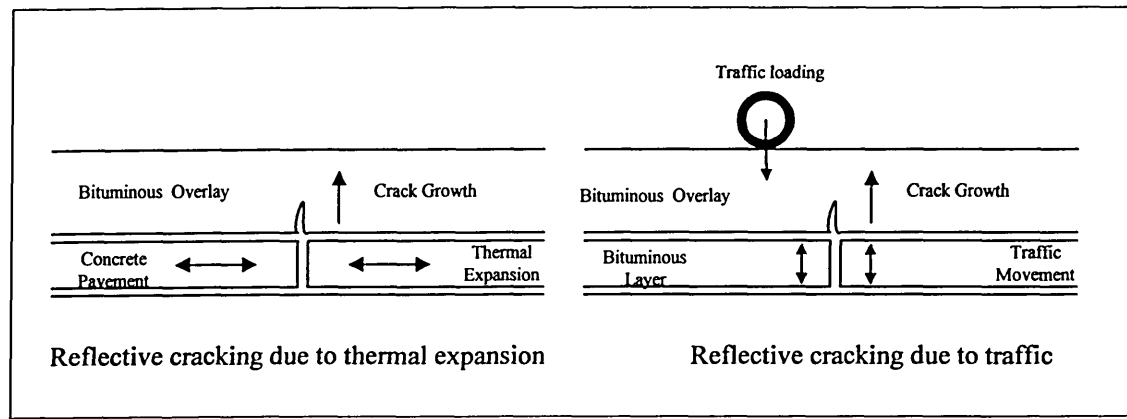


Figure 2.7 Reflection cracking in road pavement

Roberts *et al.* [8] stated that “if the new surface is bonded to the old surface using a standard tack coat, cracks in the underlaying layer almost always propagate through the new surface within 1-2 years”, by considering that the crack is initiated by the action of the underlaying layers to produce stresses in the bituminous surface which exceed the strength of the material. Therefore, Francken [16] suggested two methods that can be applied to reduce appearance of cracks at the road surface:

1. Interventions on cracks themselves to eliminate them or to limit their activity.
2. The use of an appropriate overlay system (Figure 2.8), which includes:
  - ♦ assessment of the site
  - ♦ preventive measures
  - ♦ preparatory work
  - ♦ choice and possible laying of an interlayer
  - ♦ choice, design and laying of a wearing course

The development of efficient system involves innovative materials and products, e.g.:

1. Soft interlayer products (saturated geofabrics, rubber-bitumen)
2. Reinforcing interlayer products (polymer grids, metallic grids)
3. Composite materials (asphalt mixtures containing additives, fiber, *etc.*)

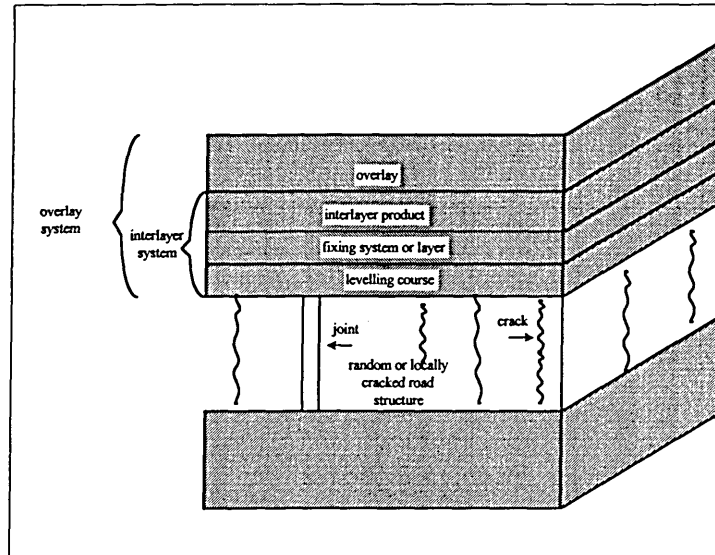


Figure 2.8 Different components of an overlay system, after Francken [16].

### 2.3.2 Moisture Damage

Moisture damage usually involves the displacement of the binder film from the aggregate surface in the presence of water. Loss of cohesion<sup>6</sup>, adhesion failure in binder-aggregate bond and related moisture-induced damage have costly consequences as they reduce both pavement durability and serviceability. Durability here has been defined as *“the ability of the materials comprising the mixture to resist the effects of water, ageing and temperature variations, in the context of a given amount of traffic loading”* [17]. Failure of the adhesive bond between binder-aggregate (e.g. stripping) and/or reduction of cohesion in the bituminous mixture results in a reduction of the strength and stiffness of the mixture and, therefore, a reduction in the ability of the pavement to withstand traffic induced stresses and strains. Two of the most popular moisture damages, e.g. stripping and ravelling, are presented.

<sup>6</sup> Cohesion, as used here, is defined as the overall attraction by which particles of bodies stick together to make up a compatible mixture. After Scholz [17].

### 2.3.2.1 Stripping

Stripping is generally related to the presence of moisture and is characterised by the loss of adhesion between the aggregates and the binder which typically begins at the bottom of the bituminous layer and progresses upwards (i.e. flushing or bleeding) and resulting in reduction of cohesion in the lower part of stripped layer as well as instability in the upper part of the layer due to excessive bitumen [17]. Once stripping is developed, it can manifest in several forms (such as ravelling, cracking, and permanent deformation), which makes identification of stripping difficult [8], and consequently it is also difficult to select appropriate remedies.

Stripping is more prevalent in moist pavements than in dry pavements. Before 1974, stripping in bituminous pavements was considered to be a relatively minor problem [18]. However, severe problems related to stripping have been noted in the period from 1974 to 1977 which caused research in this field to become extremely active to overcome the problems [18, 19]. One of the findings indicated that bituminous mixtures are more susceptible to stripping when exposed to severe traffic and climatic conditions.

The amount and ease with which moisture can enter a bituminous mixture are dependent on the binder content and aggregate gradation. Dense, continuously graded mixtures with the optimum binder content will prevent moisture ingress effectively. Adequate compaction will reduce the air voids and the continuity of the air void system, which prevents moisture ingress into the mixture.

Terrel and Shute [20] introduced the concept of “pessimum voids” content for stripping (Figure 2.9). There are four regions as shown in Figure 2.9. Region A for mixtures with air void content less than 5%, here the mixtures are virtually impermeable and, hence, have good resistance to stripping. Mixtures with air void contents between regions B and C, which are often found in construction practice, are most susceptible to stripping. This region is termed “pessimum voids” because voids in this range are the opposite of optimum. The mixture strength becomes less affected by moisture at air void contents beyond region D, as the mixtures are free draining.

The presence of water within a bituminous mixture can create a potential stripping problem due to the build up of hydraulic pore water pressure under traffic loading, this condition is often found in base courses [22].

Moisture, in the form of vapour or liquid, can also penetrate through the binder film to reach the aggregate surface, especially where the binder film is very thin such as at the sharp edges of aggregates. This movement may then produce a detached film of binder which leads to film rupture in the presence of stresses imposed by traffic [1].

Reduction in stripping can be achieved by [18, 21, 22]:

1. Controlling the moisture in mixture by:
  - preventing moisture ingress, e.g. creating an impermeable pavement layer
  - discharging moisture as soon as possible, e.g. by providing adequate pavement drainage
2. Controlling the quality of the aggregates:
  - avoid excessive dust coating on the aggregate
  - adequate drying of aggregate
  - eliminate the use of moisture-susceptible aggregate
3. Adequate binder film thickness
4. Construction techniques:
  - minimise mixture segregation
  - provide adequate compaction to achieve an adequate air void level
5. Using some additives or anti-stripping agents
6. Sealing layers beneath a permeable layer (e.g. a porous asphalt surface)

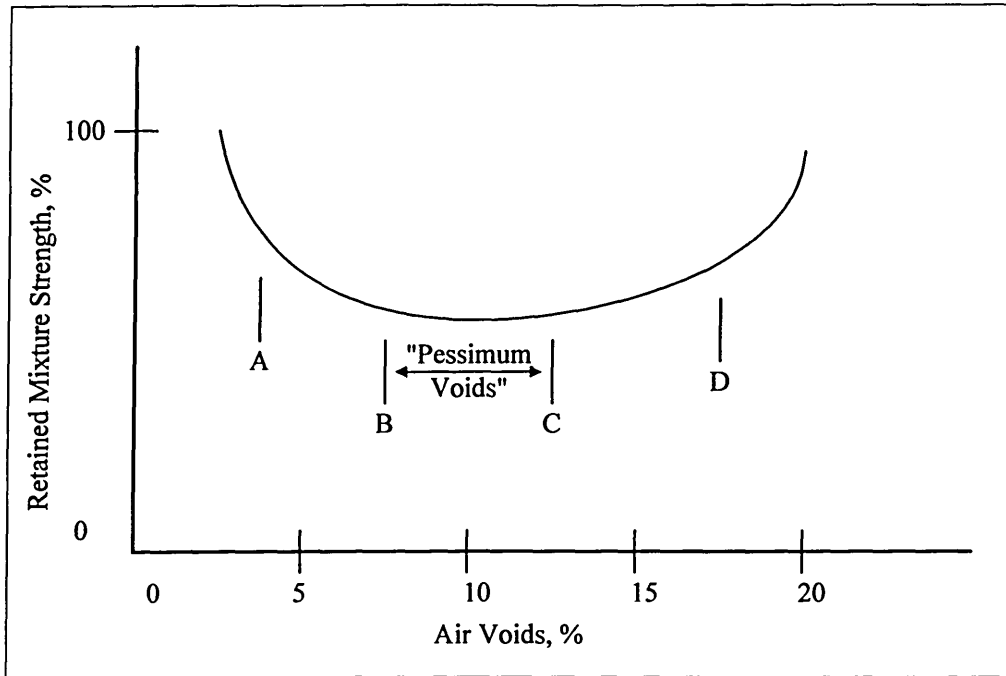


Figure 2.9 Air void content versus retained mixture strength. After Terrel and Shute [20]

### 2.3.2.2 Ravelling

Ravelling is the wearing away of the pavement surface which progresses downward through the pavement layers. Ravelling is usually caused by one or a combination of the following factors [8, 11, 23]:

1. Deficient binder content that causes poorly coated aggregate and reduces adhesion between binder and aggregate. By increasing binder film thickness, the rate of ageing can be reduced and also offset the effects of high air voids [8].
2. Insufficient amount of fine aggregate matrix to hold coarse aggregate particles together this causes a condition where coarse aggregate are in contact with each other over only a few contact points where the binder bonds the aggregate matrix
3. Insufficient compaction that can lead to:
  - high void content which leads to acceleration of age hardening and results in premature ravelling [23]. Figure 2.10 presents the effect of air void content to the extent of ravelling.
  - low in-place density which causes lack of the cohesion in the mixture
4. Loss of binder adhesion due to excessive age hardening.

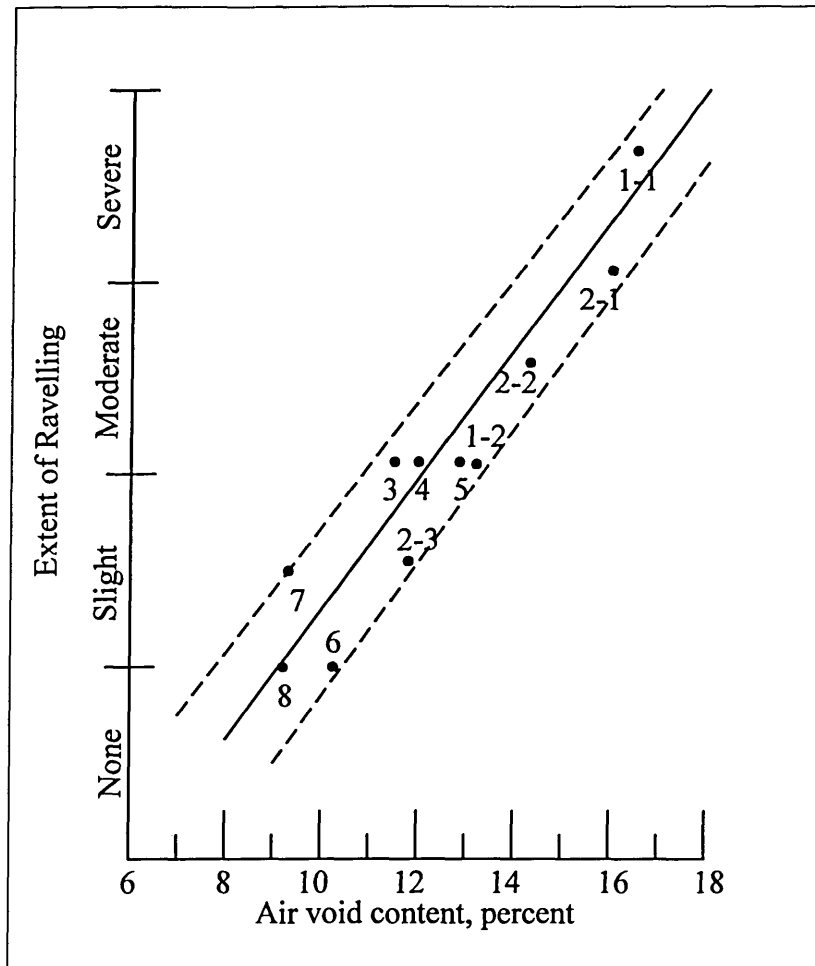


Figure 2.10 Air void content versus extent of ravelling, after Kandhal and Woehler[23]. Specimens were cored samples of Pennsylvania ID-2 wearing course consisting of dense graded aggregate and AC-20 binder from different sites of similar in-service ageing.

### 2.3.3 Age Hardening

This mechanism usually constitutes the change of chemical and physical properties of bituminous materials during road construction, i.e. mixing and paving, or under exposure to the in-service condition. There are several factors identified for causing age hardening of bitumen, i.e.:

1. Loss of the oily components of bitumen by volatility or absorption by porous aggregates,
2. Changes in chemical composition of bitumen molecules from reaction with atmospheric oxygen (oxidation),
3. Molecular structuring that produces thixotropic effects (steric hardening),

of which oxidation is considered to be the major and best understood cause of age hardening [24].

The age hardening makes the binder film on the surface of pavement become harder and more brittle. In the later stage, this hardening contributes to the development of various forms of cracking in the bituminous layer (see *Section 2.3.1*). The age hardening also contributes to the loss of materials at surface layer due to the decrease in binder-aggregate bond (see *Section 2.3.2.2*).

#### **2.3.4 Permanent Deformation**

Permanent deformation or rutting is a surface depression generally in the wheel path as a result of traffic loading. A very small amount of deformation can occur in bituminous surfaces due to densification under traffic after compaction. In most cases, the densification by traffic loading during the first 2 or 3 years of service leads to a reduction of air void contents of bituminous surfaces. The level of reduction in air void contents is generally from 7% or 8% down to about 4% to 5% [8, 22], which is helpful (Figure 2.9). However, permanent deformation becomes more significant as the cumulative number of traffic loading increases and in a later state leads to major structural failures and the potential for hydroplaning.

There are three main types of permanent deformation, as also shown in Figure 2.11 [25,26]:

1. Wear rutting in the wheel path which is caused by combined environmental and traffic conditions that lead to the progressive loss of coated aggregate particles from the pavement.
2. Structural rutting which is caused by the permanent vertical deformation of pavement structure due to repeated traffic loading and is widely accepted as the reflection of permanent deformation in the subgrade.
3. Instability rutting or plastic deformation which is due to lateral displacement (shear) and/or densification of a single bituminous layer in the wheel path.

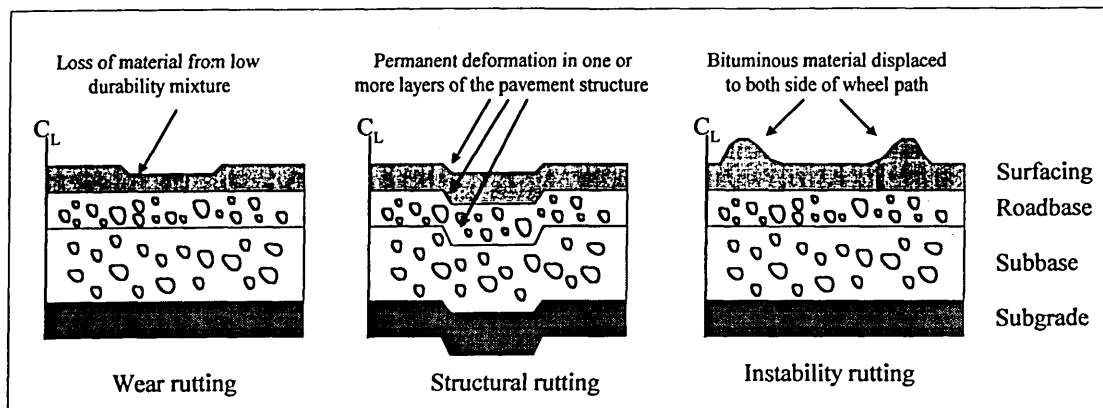


Figure 2.11 Types of permanent deformation

Safety is the most serious problem caused by rutting. Drivers can face loss of control when driving along a rutted surface due to hydroplaning, ice formation in the wheel path, and difficulties in changing lanes with a rutted surface. Any of these may lead to a serious accident. Other problems can be a nuisance to pedestrians when splashed by vehicles and also high maintenance and repair costs (*Section 2.2*).

### 1. Wear rutting

Wear rutting can be caused by:

- a poor mixture, such as: low bitumen content, low durability aggregates, inappropriate mixture design
- inadequate compaction
- studded tyres

Proper material design, restriction on the use of studded tyres, and the use of appropriate aggregates can reduce wear rutting.

Good mixture design can be obtained if the aggregates and the binder used in the mixture are at their optimum composition. The Marshall mixture design procedure has been adopted in the UK for designing the optimum binder content of hot rolled asphalts in the laboratory [27, 28]. The procedure is conducted by testing bituminous mixtures with a minimum of nine different binder contents at 0.5% increments with a Marshall device. The optimum binder content is determined from the average values of the binder contents required to achieve the maximum density of the mixture, the

maximum compacted aggregate density and the maximum stability (Figure 2.12). The design binder content is obtained by adding an empirical factor, e.g. 0.7% for a mixture containing 30% coarse aggregate (to ensure durability), to the value of optimum binder content, and then an unspecified quantity of bitumen may be added to this value and adopted as the target binder content.

For pavement design purposes, the values of Marshall stability and flow at the optimum binder content of hot rolled asphalt should comply with the values presented in Table 2.3.

*Table 2.3 BS 594: 1992 Design criteria for stability of laboratory design asphalt [27]*

Traffic Flow, Commercial vehicle/lane/day	Stability, kN
less than 1500	3.0-8.0
1500-6000	4.0-8.0
over 6000	6.0-10.0

NOTE:

For stabilities up to 8.0 kN the maximum flow is 5.0 mm.

For stabilities greater than 8.0 kN the maximum flow is 7.0 mm.

The stability and flow values are those pertaining to the target binder content

This design method, however, is to be enhanced by the recent Highways Agency development Draft Clause 943 on the performance related design mixture for rolled asphalt wearing courses [29], in which the use of Marshall stability and flow is no longer specified (due to the limitations of their empirical nature) but specification on the performance related properties (wheel-tracking rate, wheel-tracking rut depth, and air voids content) of the mixture are given. The limiting wheel-tracking requirements for different site classifications are presented in Table 1.2 (*Chapter One*) and Table 2.4.

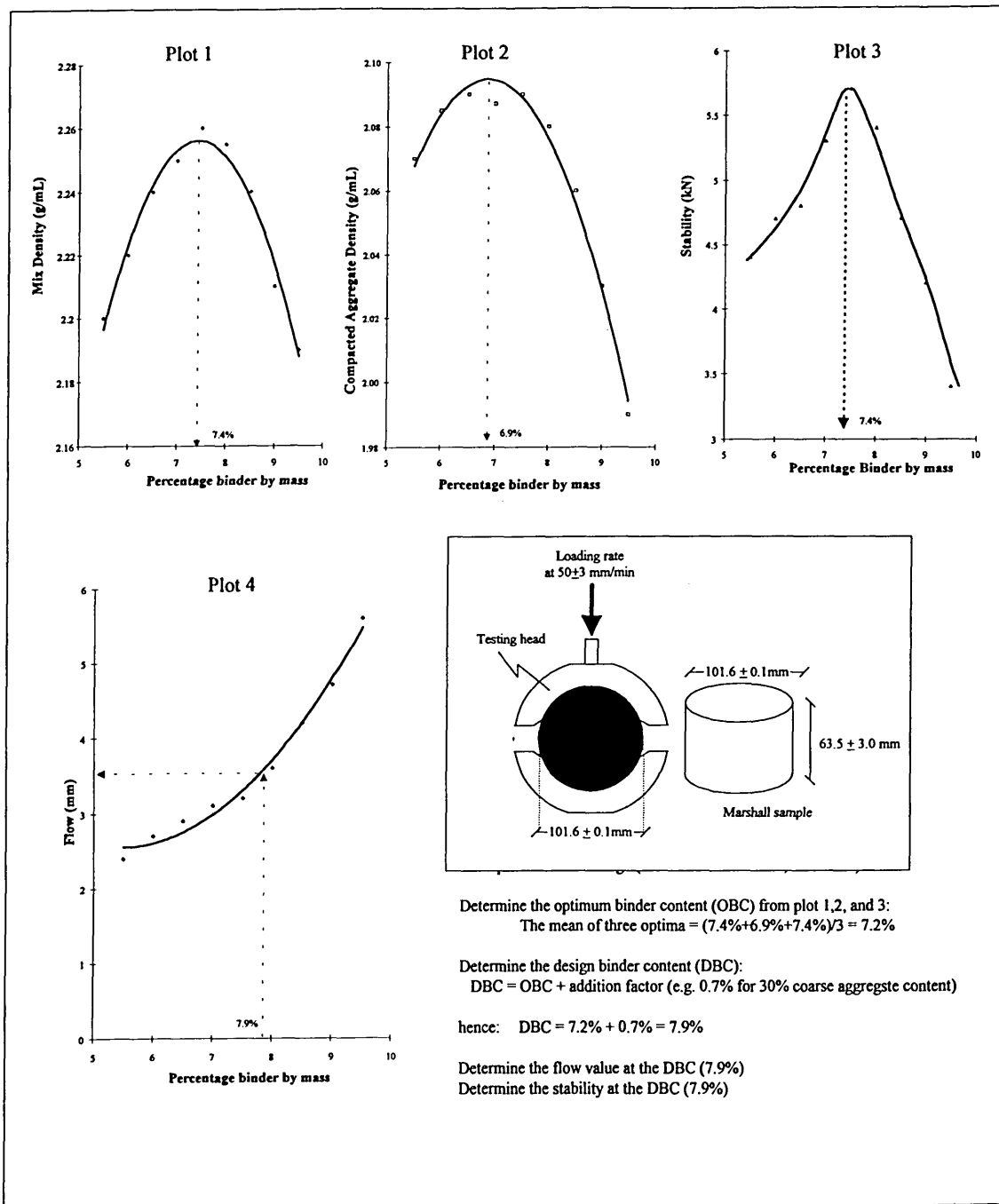


Figure 2.12 Example of the Marshall design technique

Table 2.4 Classification of sites by traffic and stress condition, Notes for Guidance NG 943 [29]

Site Category	Site Definition	Traffic at Design Life (Commercial vehicles per lane per day)													
		up to 250	251 to 500	501 to 1000	1001 to 1500	1501 to 2000	2001 to 2500	2501 to 3000	3001 to 4000	4001 to 5000	5001 to 6000	over 6000			
I & II	A B D C E Motorway (mainline) Dual carriageway (all purpose) non-event sections Dual carriageway (all purpose) minor junctions Single carriageway non-even sections Single carriageway minor junctions		0				1								2
IA & IIA	As I and II above but with contra-flow anticipated during summer months		0			1									2
III	F G1 L Approaches to and across major junctions (all limbs) Gradient 3% to 10%, longer than 50 m: Dual (uphill and downhill) Single (uphill and downhill) Roundabout		0			1									2
IIIA	As III above but with contra-flow anticipated during summer months or in a south-facing curving uphill		0		1										2
IV	G2 Gradient steeper than 10%, longer than 50 m: Dual (uphill and downhill) Single (uphill and downhill)		0		1										2
IVA	As IV above but with contra-flow anticipated during summer months or in a south facing curving uphill		0		1										2
V	J/K Approach to roundabout, traffic signals, pedestrian crossings, railway crossings and similar		0		1										2

## 2. Structural rutting

Structural rutting can be caused by:

- poor drainage
- frost action
- overstressing pavement layers, e.g. due to excessive traffic loading
- poor construction practices, e.g. inadequate compaction
- contribution from other pavement distress, e.g. fatigue cracking, stripping

Structural rutting can be prevented by providing good drainage, adequate pavement design, construction quality control, and selection of good quality materials. However, once permanent deformation due to overstressing pavement layers is developed, overlaying will only solve the problem temporarily, and the only way to resolve the problem is by carrying out a complete structural evaluation followed by a redesign of the structural section and construction of a pavement thick enough to reduce stresses in the subgrade and other pavement layers to a tolerable level [8].

## 3. Instability rutting

Instability rutting can be caused by:

- environment, e.g. hot weather
- traffic loading, e.g. increased traffic loading, increased tyre pressure, high steering axle loading, slow speed vehicles
- material characteristics and design, e.g. aggregate and binder characteristics, air void content in mixture, selection of a suitable mixture design

Instability rutting can be reduced by restrictions on traffic loading, or by improving the quality of the materials. The use of high stiffness bitumens can also help.

This research is specifically focused on the plastic deformation (instability rutting) and research has been carried out to study how polymer modified binders work to resist plastic deformation developed by higher traffic loading. However, reference to both wear and structural rutting will be made where appropriate.

## **2.4 Concluding Remarks**

Different damage mechanisms affect the pavement structure in different manners and to different degrees of severity. Consequently different considerations in selecting appropriate pavement designs and maintenance strategies are required to achieve and maintain the desirable functional and structural condition during the design life. Therefore, the correct identification of these distress mechanisms and their interactions is important before an appropriate maintenance or rehabilitation procedure is implemented. The decision on selecting the right time for action is also important to avoid high maintenance costs at the latter stage of distress.

Alternative distress mitigation techniques, by improving the performance properties of the bituminous mixtures, will be discussed in the next chapter, where the use of polymer additives and the development of laboratory performance related testing are also presented.

## **2.5 References**

- 1 Whiteoak, D., "The Shell Bitumen Handbook", Shell Bitumen UK, 1990.
- 2 Anon, "Road Note 29 - A Guide to the Structural Design of Pavements for New Roads", Department of The Environment-Department Transport, Transport Road and Research Laboratory Third Edition, HMSO, London, 1970.
- 3 Anon, "Road Note 31- A Guide to the Structural Design of Bitumen-Surfaced Roads in Tropical and Sub-tropical Countries", Department of The Environment-Department Transport, Transport Road and Research Laboratory, Third Edition, HMSO, London, 1977.
- 4 Anon, "Shell Pavement Design Manual", Shell International, London, 1978.
- 5 Brown, S.F., and Brunton, J.M., "An Introduction to the Analytical Design of Bituminous Pavements", Second Edition.
- 6 Powell, W.D., Potter, J.F., Mayhew, H.C., and Nunn, M.E., "The Structural Design of Bituminous Roads"., TRRL, LR 1132, 1984.

- 7 Ullidtz, P., "Pavement Analysis", Elsevier, 1987
- 8 Roberts, F.L, Kandhal, P.S., Brown, E.R., Lee, D.Y., Kennedy, T.W., "Hot Mix Asphalt Materials, Mixture Design, Construction", NAPA Research and Education Foundation.
- 9 Wu, F., "Assessment of Residual Life of Bituminous Layers for the Design of Pavement Strengthening", PhD Thesis, The Polytechnic of Wales, 1992.
- 10 Kennedy, C.K., Lister, N.W., "Prediction of Pavement performance and the Design of Overlays", TRRL, LR 833, 1978.
- 11 Huang, Y.H., "Pavement Analysis and Design", Prentice Hall, 1993.
- 12 Read, J.M., "Fatigue Cracking of Bituminous Paving Mixtures", PhD Thesis, University of Nottingham, 1996.
- 13 El Halim, A.O.A., Razaqpur, A.G., and El Kashef, A.H., "Effects of Construction Cracks on the Design of Asphalt Pavements", Canadian Journal of Civil Engineering, Vol 21, 1994, pp.410-418.
- 14 Pronk, A.C., "Evaluation of Dissipated Energy Concept for The Interpretations of Fatigue Measurements in The Crack Initiation Phase", The Road and Hydraulic Engineering Division, Ministry of Transport, Public Work and Water Management, The Kingdom of Netherlands, 1995.
- 15 Woodside, A.R., Clements, H.W., Sikich, J., and Russel, T.E.I, "Reflective Cracking-Retardation and Prevention", Proceedings of 2<sup>nd</sup> European Symposium on the Performance and Durability of Bituminous Materials, J.G. Cabrera, Ed., Leeds, April 1997, pp. 517-528.
- 16 Francken, L., "Rilem TC 157-PRC: Systems to Prevent Reflective Cracking in Pavements, Progress Report 1993-1996", Materials and Structures, Supplement March 1997, pp. 43-46.
- 17 Scholz, T.V., "Durability of Bituminous Paving Mixtures", PhD Thesis, University of Nottingham, 1995.

- 18 Takallou, H., Hicks, R.G., and Wilson, J.E., "Evaluation of Stripping Problems in Oregon", Evaluation and Prevention of Water Damage to Asphalt Pavement Materials, B.E. Ruth, Ed., ASTM STP 899, Philadelphia, 1985.
- 19 Emery, J.J. ,"Properties of Flexible Pavement Materials", ASTM STP 807, Philadelphia, 1981.
- 20 Terrel, R.L., and Shute, J.W., "Summary Report on Water Sensitivity", Report No. SR-050-A-89-3, SHRP, Washington D.C., 1989.
- 21 Brown, S.F., Rowlett, R.D., and Boucher, J.L., "Asphalt Modification", Proceedings of the Conference on the US SHRP: Sharing the Benefits, ICE, London, 1990, pp. 181-203.
- 22 Kandhal, P.S., "Field and Laboratory Investigations of Stripping in Asphalt Pavements: State of the Art Report", TRR 1454, TRB, 1994, pp. 36-47.
- 23 Kandhal, P.S., and Woehler, W.C., "Pennsylvania's Experience in the Compaction of Asphalt Pavements", ASTM, Special Technical Publication 829, 1984.
- 24 Scholtz, T.V., and Brown, S.F., "Factors Affecting Durability of Paving Mixtures", Performance and Durability of Bituminous Materials, J.G. Cabrera and J.R. Dixon, Eds., E&FN Spon, 1996.
- 25 Emery, J., "Asphalt Pavement Rutting Experience inCanada", Proceeding of CTAA, vol. XXXV, November 1990, pp.80-91.
- 26 Dawley, C.B., Hogewiede, B.L., and Anderson, K.O., "Mitigation of Instability Rutting of Asphalt Concrete Pavements in Lethbridge, Alberta, Canada", Journal of APT, Vol. 59,1990, pp.482-509.
- 27 Anon, "Hot Rolled Asphalt for Roads and Other Paved Areas. Part 1. Specification for Constituent Materials and Asphalt Mixtures", British Standard 594: Part 1: 1992, BSI, London.
- 28 Anon, "Sampling and Examination of Bituminous Mixtures for Roads and Other Paved Areas. Part 107. Methods for of Test for Determination the Composition of Design Wearing Course Rolled Asphalt", British Standard 598: Part 107: 1990.

29 Anon, "Hot Rolled Asphalt Wearing Course (Performance Related Design Mix)", UK-Highway Agency's Specification for Highway's Works: Clause 943, Draft No 4.0, 5th July 1996.

## Chapter Three

### 3. Material Performance

#### 3.1 Introduction

Bitumen used in today's road construction is generally manufactured from refining crude oil. Therefore, the world supply of crude oil is significant to the supply of bitumen. Even though there are nearly 1500 different crudes produced world wide only a few of these are considered suitable for the manufacture of bitumen [1]. Crude oils should contain the heavy bitumen-bearing gradient to make good bitumen products [2]. Heavy crudes contain a much smaller proportion of volatile substances, more of the heteroatoms nitrogen, sulphur, oxygen, and metals, and also tend to be more naphthanic and aromatic than the lighter crudes [3].

The main sources of crude oil are the United States, the Middle East, the countries around the Caribbean, and the countries of the former Soviet Union [1]. The North Sea crudes are generally light with very low bitumen yields, therefore, a special processing route is necessary to achieve the required properties [4]. The variation of crudes from source to source yields different amounts of residual bitumen and other distillable fractions [2]. Therefore, variations in composition of bitumens refined from different sources can be expected. An example is presented by Roberts *et al* [2] from Corbett's [5] as shown in Figure 3.1.

	Boscan Venezuelan	Arabian Heavy	Nigeria Light
API Degrees	10.1	28.2	28.1
Specific Gravity	0.999	0.886	0.834
% Sulphur	6.4	2.8	0.2

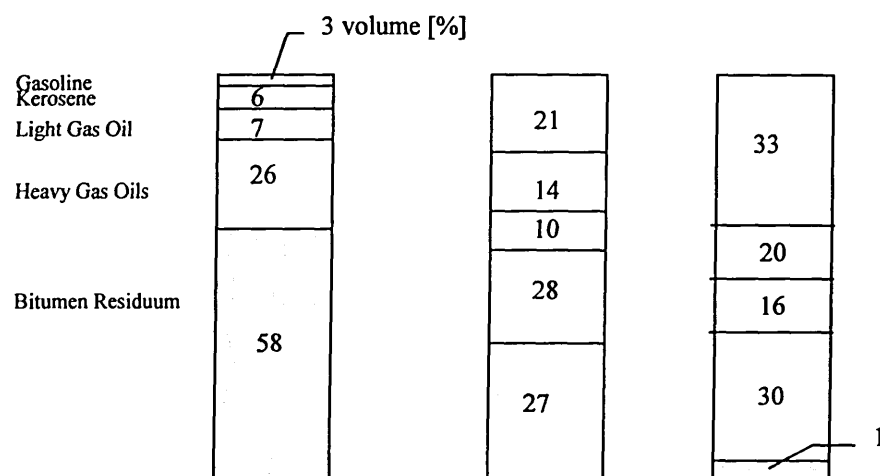


Figure 3.1 Make-up of Crude Oil. Reproduced from Roberts et al.[2] after Corbett [5]

The API (American Petroleum Institute) gravity is an expression of the density of weight of a unit volume of material expressed at 60°F and is determined from the following equation [2]:

$$\text{API Gravity (degrees)} = \frac{141.5}{\text{Specific Gravity}} - 131.5$$

Equation 3.1

Table 3.1 The API gravity indices

Low API gravity crudes	API < 25	Low percentages of distillable overhead fractions High percentages of bitumen
High API gravity crudes	API > 25	High percentages of distillable overhead fractions Low percentages of bitumen

### 3.1.1 Composition of Bitumen

As has been defined in *Chapter One*, bitumen is a complex system that predominantly consists of hydrocarbons and their derivatives. Elementary analysis of bitumen refined from a variety of crude oils has been presented previously [1,4], as shown in Table 3.2.

This composition varies in accordance with the source of the crude oil from where the bitumen is refined.

*Table 3.2 The chemical composition of bitumen showing the major elements. After Whiteoak [1].*

<b>Element</b>	<b>Concentration % by mass</b>
Carbon	82 - 88
Hydrogen	8 - 11
Sulphur	0 - 6
Oxygen	0 - 1.5
Nitrogen	0 - 1

Despite the complexity in the chemical composition of bitumen, a method has been established to separate bitumen into four major chemical groups, namely saturates, aromatics, resins, and asphaltenes (S.A.R.A). The saturates, aromatics, and resins are sometimes classified into one group called maltenes. The asphaltenes are the fraction which is diluted in a large excess quantity of the hydrocarbon solvent where parts of the micelles are precipitated and the maltenes are the fraction which during the separation process remained dissolved [6]. Summary of the main characteristics of these components is presented in Table 3.3.

There are three types of molecular structures of a bitumen [7, 8], as shown Figure 3.2:

1. Aliphatic or parafinic type: carbon atoms are linked to each other in straight or branched chains.
2. Napthenic type : the carbon is linked in simple or complex (condensed) saturated rings, where the highest hydrogen to carbon ratio is present.
3. Aromatic: made up of one or more stable six-atom rings that form the basis compounds such as benzene and toluene.

Components	Main Characteristics
Saturates	<p>Comprise straight and branch-chain aliphatic hydrocarbons, alkyl-naphthenes and some alkyl-aromatics</p> <p>Straw or white, non-polar viscous oils</p> <p>Average molecular weight around 300 to 2000</p> <p>Constitute 5% to 20% of bitumen</p>
Aromatics	<p>Comprise the lowest molecular weight naphthenic aromatic compounds</p> <p>Represent the major proportion of the dispersion medium for the peptised asphaltenes</p> <p>Constitute 40% to 65% of bitumen</p> <p>Dark brown viscous liquids</p> <p>Average molecular weight around 300 to 2000</p> <p>Consist non-polar carbon chains in which the unsaturated ring system dominated</p> <p>Have a high dissolving ability for other high molecular weight hydrocarbons</p>
Resins	<p>Soluble in n-heptane</p> <p>Composed of hydrogen and carbon</p> <p>Contain small amount of oxygen, sulphur and nitrogen</p> <p>Dark brown, solid or semi-solid, and very polar in nature</p> <p>As the dispersing agents or peptisiers for asphaltenes</p> <p>Average molecular weight around 500 to 50000</p> <p>Particle size of 1 nm to 5 nm</p> <p>Hydrogen to carbon (H/C) atomic ratio of 1.3 to 1.4</p>
Asphaltenes	<p>Not soluble in n-heptane</p> <p>Black or brown amorphous solids</p> <p>Contains carbon, hydrogen, nitrogen, sulphur, and oxygen</p> <p>Highly polar and complex aromatic materials</p> <p>Average molecular weight around 1000 to 100000</p> <p>Particle size of 5nm to 30 nm</p> <p>Hydrogen to carbon (H/C) atomic ratio of about 1.1</p> <p>Has a large effect on the rheological characteristics of bitumen: the higher asphaltene content the harder the bitumen.</p> <p>Constitute 5% to 25% of the bitumen</p>

Table 3.3 Characteristics of S.A.R.A.

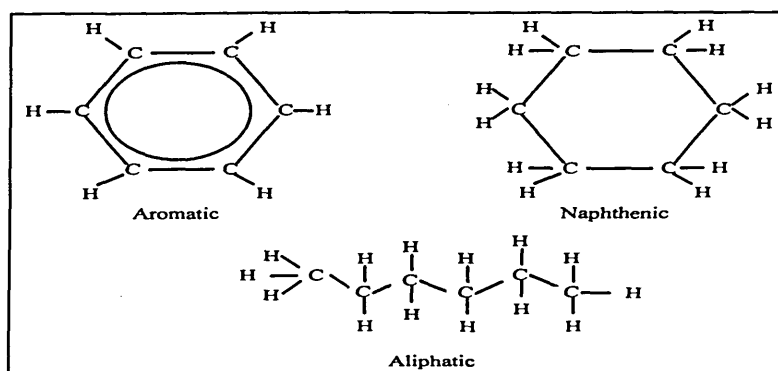


Figure 3.2 Type of molecular structure of a bitumen [8]

### 3.1.2 Bitumen Structure

Bitumen has been long known to be a colloidal system [6]. In this colloidal system, the highest molecular weight components, i.e. the asphaltenes micelles, are dispersed and the lower molecular weight of maltenes (i.e. aromatics, saturates, resins) are dissolved in the saturated hydrocarbon mixture. Depending on the degree of aromaticity of the maltenes and the nature and the concentration of the asphaltenes, the micelles in the bitumen may either move freely with respect to each other (sol type) or by mutual attraction they may form a structure throughout the bituminous mass (gel type). The rheological properties of bitumen can be largely reflected by the colloidal state of the system (Figure 3.3). The rheology itself has been defined as the part of science that is interested in the description of the mechanical properties of different materials under various deformation conditions when they simultaneously perform the capability to flow and accumulate recoverable deformation [9].

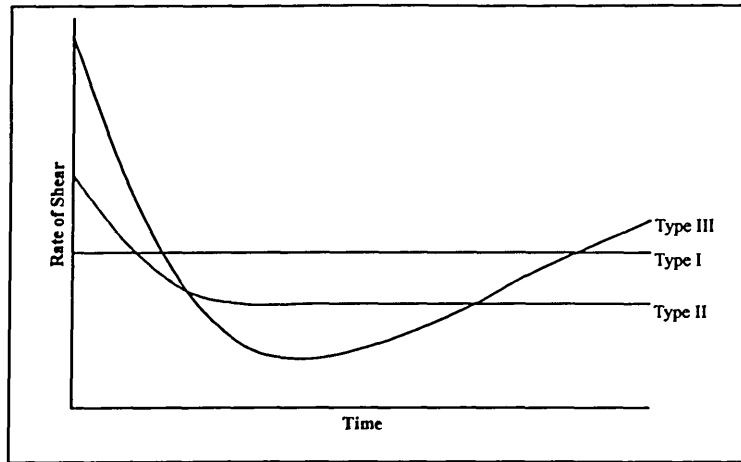


Figure 3.3 Rate of shear of different types of liquids under a constant shearing stress as a function of time [6]. Type I is a very viscous non-colloidal liquid or a sol with non- or slightly elastic particles. Type II is a sol type colloid. Type III is a gel type colloid.

As presented in Figure 3.3, the type I material behaves in accordance with Newton's Law. From the beginning of the deformation, the shear rate is constant and proportional to the applied shearing stress. No recovery occurs upon removal of stress. With the second type (II), the rate of shear decreases at constant shearing stress, however, after some time the rate of shear has become virtually constant, and the value becomes proportional to shearing stress. With the third type (III), the rate of shear also drops at the beginning of deformation, then reaches a minimum value and then starts to increase again when the shearing stress above a certain value. Elastic recovery after release of stress can be expected if the deformation remains within certain limits [6].

### 3.2 Viscoelastic Behaviour of Bitumen

Viscoelasticity is a measure of the transitional behaviour of a material between the elastic-solid state and the viscous-liquid state, under a particular loading arrangement.

In general, the response and performance of bitumen is mainly dependent upon several external factors:

1. Temperature. This is the most critical parameter, as it stiffens bitumen at low temperature but also makes the bitumen less stiff at high temperature allowing it to flow freely.

2. Rate of loading. At short-times of loading the bitumen responds like an elastic solid, however, at long-time of loading it behaves as a viscous liquid. In the intermediate level, the delayed elastic response is dominant.
3. Nature of the bitumen, e.g. the composition or the colloidal state of the bitumen.

It is also broadly accepted that bitumen at a fixed rate of loading, high temperatures will behave viscously whereas at low temperatures the response turns to elastic behaviour. This elastic behaviour indicates high stiffness and brittleness; while the viscous response reflects high ductility and low stiffness. The overall viscoelastic behaviour is represented in Figure 3.4. The viscoelastic behaviour of bitumen, in the linear region, indicates several essential functions: complex modulus as a function of loading frequency, creep modulus as a function of loading time and Newtonian viscosity as a function of temperature. The linear viscoelastic properties are often applied for characterising the bitumen, while the non-linear properties are related to failure characteristics [12].

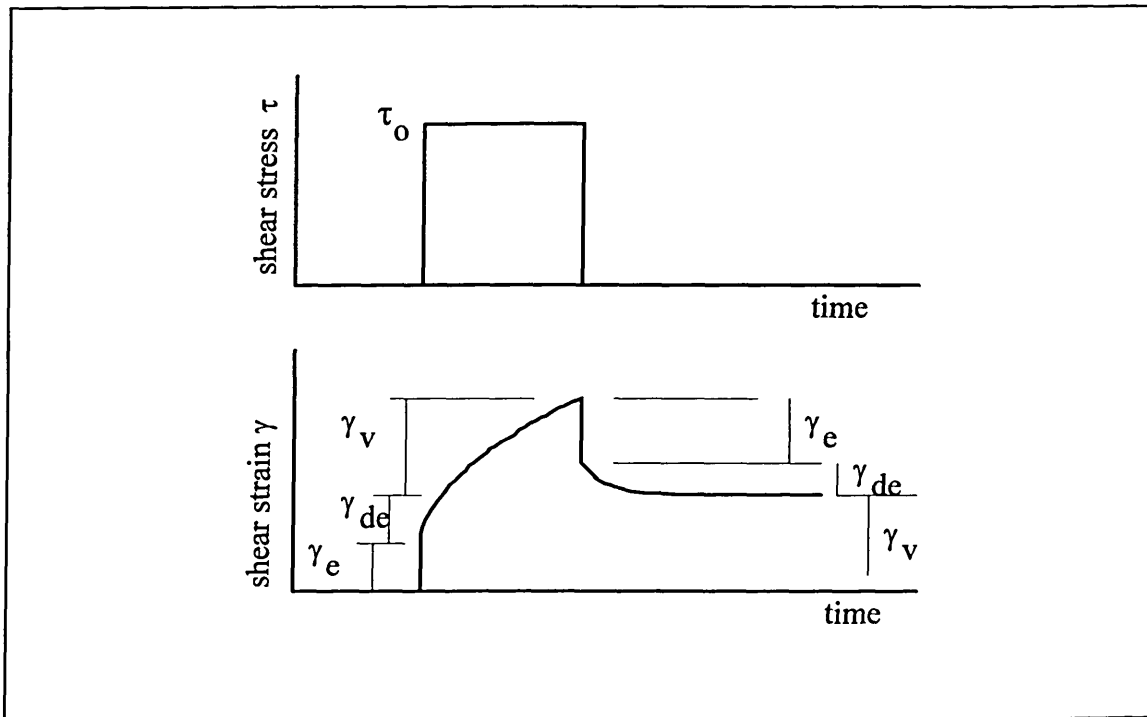


Figure 3.4 Representation of viscoelastic response of asphalt cement under static loading, showing elastic (e), delayed elastic (de), and viscous (v) strain components.

### 3.2.1 Tools for Determining Viscoelasticity

There are different methods for determining the viscoelasticity of materials. These methods can be classified based on direction of load applications (axial or shear loading) and loading arrangements (static or dynamic loading).

#### 3.2.1.1 Static loading arrangements, e.g. creep test.

The test can be conducted by application of a static uniaxial tension or compression loading arrangement on a specimen. The resulting uniaxial strain as a function of time  $\epsilon(t)$  and time dependent stiffness  $S(t)$  can be observed, and the viscoelastic response can be monitored. The time dependent stiffness can be formulated as:

$$S(t) = \frac{\sigma}{\epsilon(t)}$$

*Equation 3.2*

where  $\sigma$  is the applied stress (Pa) and  $t$  is the loading time (seconds) and the stiffness is a uniaxial property.

Christensen and Anderson [10] suggested that the stiffness of the carbon-carbon backbone that compose bitumen molecules makes all bitumens have a constant value of glassy modulus of 3 MPa when subjected to a very short time of loading (Figure 3.5). At a longer loading time, the bitumens behave as Newtonian fluids and exhibit similar viscous asymptotes of minus 0.5 on log-log slope of the creep curve. Van der Poel [11] has previously indicated that at the intermediate stage, the "viscous asymptote" on log-log slope of the creep curve may consequently vary between a horizontal line ( $0^\circ$ ) to  $45^\circ$ , but it will never be steeper. Furthermore, Jongepier and Kuilman [12] reported that the limiting viscous behaviour was strongly temperature-dependent but the elastic behaviour was not. The latter could be explained as at very high frequencies, the modulus curves at the low temperature nearly coming to one horizontal asymptote (Figure 3.5 and also Figure 3.11). Therefore, this exhibited an independency of frequency as well as temperature.

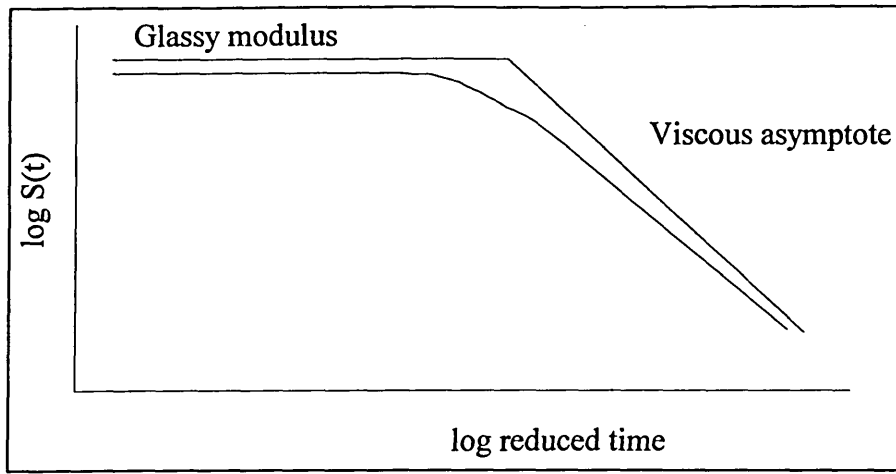


Figure 3.5 Schematic master curve of creep stiffness as a function of loading time [10]

The relationships between the uniaxial creep stiffness  $S(t)$ , the uniaxial creep compliance  $D(t)$  and shear creep compliance  $J(t)$  can be formulated as:

$$D(t) = \frac{1}{S(t)}$$

$$\frac{1}{J(t)} = \frac{S(t)}{2(1 + \nu)}$$

Equation 3.3

whereas  $\nu$  is the Poisson's ratio. Poisson's ratio is the ratio between lateral (x-direction) and longitudinal (y-direction) strains on a material subjected to a stress at y-direction .

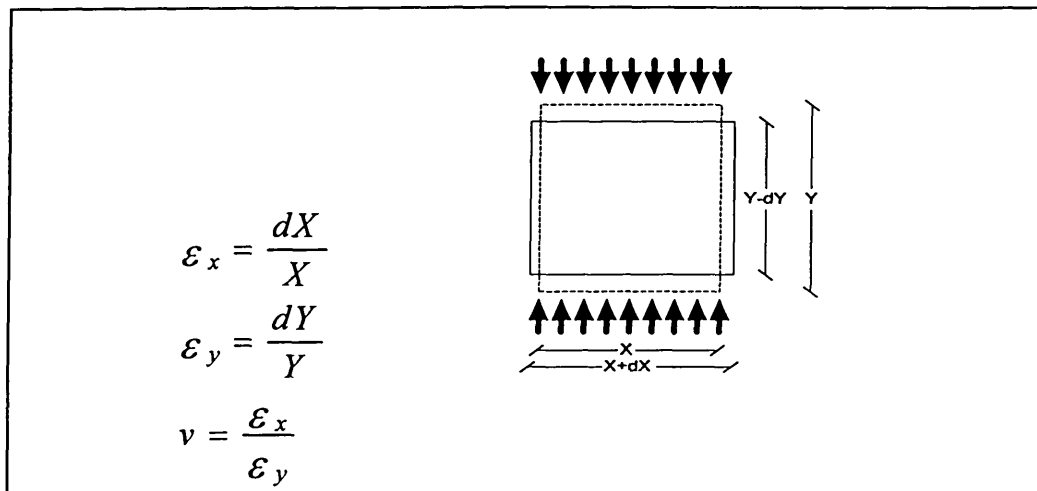


Figure 3.6 Poisson's ratio

If bitumens are regarded as a non-compressible material, then Poisson ratio  $\nu$  of bitumens is equal to 0.5 [11]. Therefore the relationship (Equation 3.3) can be rewritten as:

$$S(t) = \frac{3}{J(t)}$$

*Equation 3.4*

Read [13] reported that variations on the value of Poisson's ratio of bituminous mixtures can be generalised into one value, i.e. 0.35, of which this value should represent the Poisson's ratio of bituminous mixtures tested under wide range of testing condition (0°C to 33°C).

### ***3.2.1.2 Dynamic loading arrangements, e.g. vibrational, bending, and torsional tests***

The test can be carried out by shearing a specimen using sinusoidal waves of loading. By this method the complex dynamic modulus can be determined. Dobson [14] suggested that vibrational techniques are best applied to study short loading times in measuring complex dynamic modulus. The latest developments in research on dynamic mechanical properties of bitumens have adopted torsional bar and parallel plates' geometry techniques [3,8,19].

The parallel plate geometry is commonly used for characterisation of the dynamic mechanical properties of bituminous binders whilst the torsional rectangular bar apparatus can be used for dynamic mechanical analysis of either bituminous mixtures or for low temperature measurement of bituminous binders [19]. A bending beam rheometer can also be used for dynamic mechanical analysis of bituminous binders at low temperatures [3,8]. The one thing that should be noted here is the relationship between shear compliance and the stiffness value for shear loading  $G(t)$  is different from the relationship obtained from the uniaxial loading arrangements (Equation 3.4). Under shear loading at the linear viscoelastic condition, the shear compliance is simply the inverse value of the shear stiffness  $G(t)$ , hence:

$$G(t) = \frac{1}{J(t)} \quad \text{where} \quad J(t) = \frac{\gamma(t)}{\tau_o}$$

Equation 3.5

where  $\tau_o$  is a constant shear stress, and  $\gamma(t)$  is the shear strain.

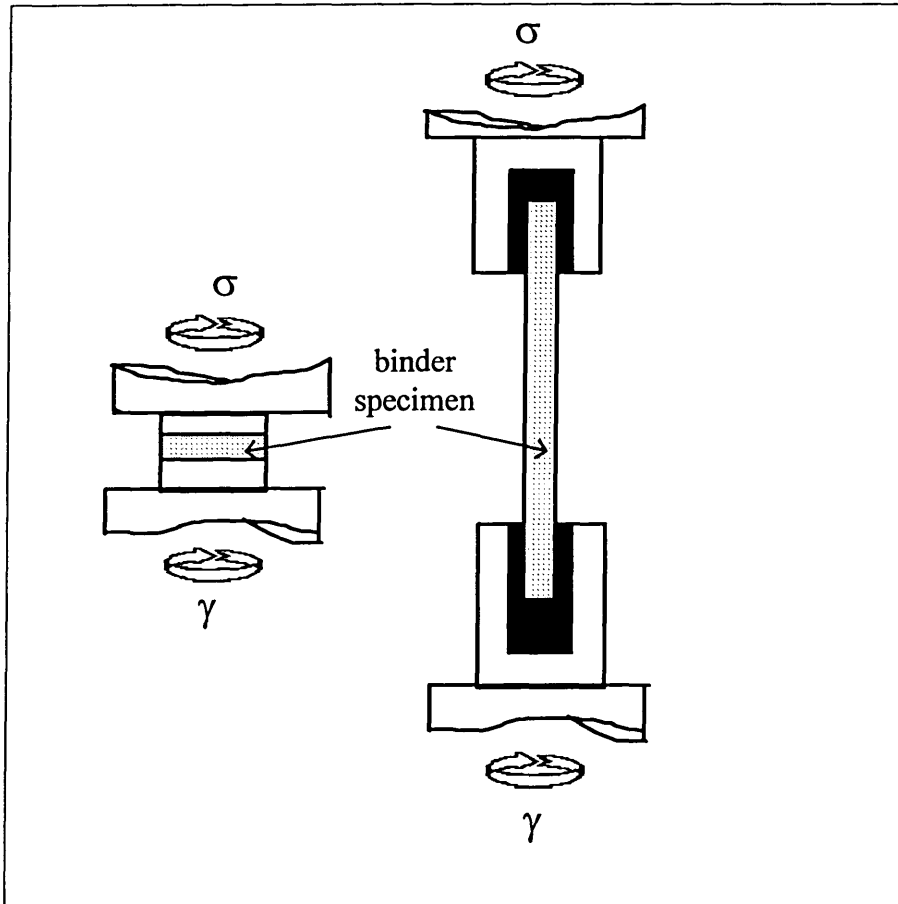


Figure 3.7 Parallel Plate Geometry and Torsional Rectangular Bar

### 3.2.2 Dynamic Mechanical Analyses

Originally, the dynamic mechanical measurement was used for assessing the viscoelastic behaviour of polymeric materials [15]. The early developments in the use of the dynamic mechanical measurement of bituminous materials are reported by Dobson in 1967-1969 [16] and Jongepier and Kuilman in 1969 [12]. In recent development, the Strategic Highway Research Program (SHRP) has undertaken series of test based on dynamic mechanical analysis [17]. The American Standard for Testing and Materials

(ASTM) is proposing a standard practice for rheological measurements of bitumen using dynamic shear rheometers (ASTM D-4 Proposal P 244), in which the proposal refers to the current practice of dynamic mechanical procedures of polymer melts (ASTM D 4440). In the United Kingdom a draft standard specification on performance related design for hot rolled asphalt mixture has been released by the UK's Highway Agency (HA) [18] incorporating the requirements for determination of the rheological properties by using a dynamic mechanical test if a polymer modified binder is used.

### 3.2.2.1 Theory of complex modulus

Complex modulus is a representation of the viscoelastic response of a material under dynamic loading at a given strain level. It comprises loss modulus and storage modulus. Similarly, shear compliance is defined as a representation of the viscoelastic response of a material under dynamic loading at a given stress level. It comprises loss compliance and storage compliance. The complex modulus and complex compliance are vectorial parameters as they have magnitude and direction.

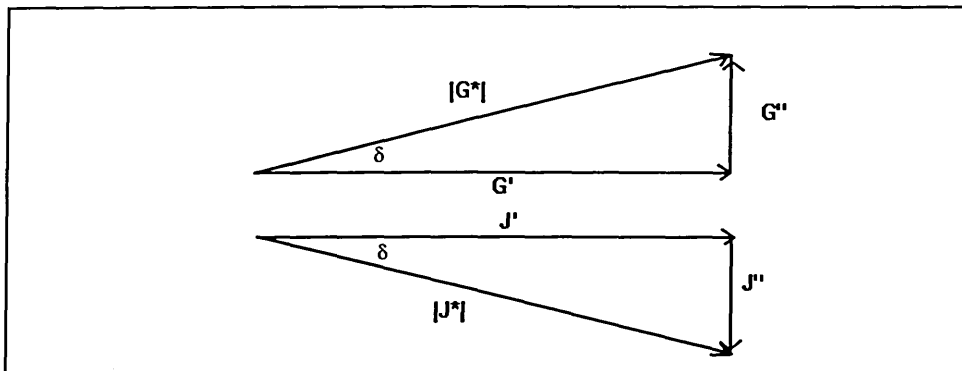


Figure 3.8 Vectorial resolution of complex modulus and shear compliance in sinusoidal shear deformations (after Ferry, 1990)

Hence, the relationship shown in Figure 3.8 can be formulated as:

$$G^* = G' + iG'' \quad \text{or} \quad |G^*| = \sqrt{G'^2 + G''^2}$$

*Equation 3.6*

$$\tan \delta = G'' / G'$$

*Equation 3.7*

where  $|G^*|$  is a ratio of peak stress to peak strain or:

$$|G^*| = \frac{\text{Peak stress}}{\text{Peak strain}} \quad [\text{in Pascal}]$$

*Equation 3.8*

and  $i = \sqrt{-1}$ .

A relationship for the complex compliance can be derived similarly to that for the complex modulus:

$$J^* = J' - iJ'' \quad \text{or} \quad |J^*| = \sqrt{J'^2 + J''^2}$$

*Equation 3.9*

Although  $J^* = \frac{1}{G^*}$ , their individual components are not reciprocally related, however,

they are connected by the following relationships:

$$J' = \frac{G'}{G'^2 + G''^2} = \frac{\cos \delta}{G^*}$$

*Equation 3.10*

$$J'' = \frac{G''}{G'^2 + G''^2} = \frac{\sin \delta}{G^*}$$

*Equation 3.11*

### 3.2.2.2 Parallel Plate Geometry

There are different sizes of disk diameter that can be used: 8, 15, 25 or 40 mm. The size of disk diameter is chosen based on test temperatures. The higher the test temperature the bigger the diameter that is used. The following tables indicate different

configurations adopted by Goodrich [19] and SHRP [10], for dynamic mechanical tests of bituminous binders:

*Table 3.4 Configurations for dynamic mechanical tests adopted by Goodrich [19]*

Disk Diameter	Test Temperature
8 mm	-40°C to +10°C
25 mm	+10°C to +50°C
40 mm	+50°C to +80°C

*Table 3.5 Configurations for dynamic mechanical tests adopted by SHRP [10]*

Apparatus/size	Test Temperature
parallel plate $\varnothing=8$ mm	+5°C to +35°C
parallel plate $\varnothing=25$ mm	higher than 35°C
torsional bar RMS 803	less than +5°C

In general, the experimental procedures for a dynamic mechanical test are as follows:

1. Carry out strain sweeps at selected temperatures to obtain the strain level that can be applied to the test to ensure the sample is still within the linear viscoelastic region, i.e. material functions such as  $G^*$  and  $\eta^*$ , are independent of applied strain levels.
2. Apply frequency sweeps over a range of test temperatures at the related strain level.

The binder specimen thickness between the parallel disks was 1 to 2.5 mm. Strain was maintained small at low temperatures, i.e. less than 0.005, and increased at high temperatures. Care should be taken to maintain the strain values in the linear viscoelastic region as indicated by the strain sweeps. In the case of polymer modified binders, however, this strain sweep technique may fail. Therefore, application of frequency sweeps at two strain levels for polymer modified binders are recommended by Collins *et al* [20] to ensure that the materials give a linear viscoelastic response, i.e. the recorded data are equivalent at both strain levels.

In future UK practice, a contractor shall provide Product Identification Test results for the binder proposed, comprising rheological data for recovered binder in the form of a master curve showing the relationship of complex modulus ( $G^*$ ) in Pascal to frequency in Hertz (Hz), and phase angle to temperature at 0.4 Hz [18]. A master curve is a curve

that is constructed by shifting a series of overlapping isotherm curves<sup>a</sup> at different temperatures.

The HA draft specification [18] requires data collection of at least 5 frequency sweeps at different temperatures at least 10°C apart in the range -10°C to 60°C, of which one shall be 25°C<sup>b</sup>. The difference between the highest and the lowest temperature shall be at least 55°C and the highest temperature shall be at least 50°C. Each frequency sweep shall include at least 5 values covering at least 2 decades, one of which shall be 0.4 Hz as the standard frequency which relates to penetration value.

### 3.2.3 Time-temperature Superposition

The principle of time-temperature superposition is well known and has been described in detail elsewhere [15]. This principle is commonly used to provide a convenient way of extrapolating the data obtained from a dynamic mechanical tests.

The principle is based on the phenomena that occur during the relaxation processes of some polymeric materials, which are thermally activated and that shows the same dependence on temperature. For example if raising the temperature by a given amount halves the relaxation time of one mode, it will halve those of all the other modes [21]. Furthermore, Costello *et al.* [21] explain that the slower processes are only co-operative combinations of the faster processes. Their rates are therefore proportional to those of the faster processes, and exhibit the same temperature dependency. The benefit of this tendency is that increasing or decreasing the test temperature does not change the shapes of the of modulus against frequency curves for the material. It will only stretch or compress them along the frequency axis. Therefore, the shape of each curve will be identical but shifted to higher or lower frequencies, if the frequency is plotted on a log scale.

The procedure for time-temperature superposition is straightforward:

---

<sup>a</sup> See Glossary

<sup>b</sup> The temperature of 25°C is the UK ambient temperature and is also known as the standard temperature.

1. A series of oscillation experiments is performed to produce isotherm curves at several temperatures. The modulus is plotted against angular frequency on logarithmic axes.
2. A particular temperature is selected as a reference, e.g. 25°C.
3. The data for the next highest temperature are then shifted to lower frequencies by a factor  $a_T$  until there is correspondence between the overlapping regions of this and the reference curve. The process is repeated for each higher temperature in turn. Lower temperature data are similarly brought onto the reference curve by shifting to higher frequencies.

The resulting plots of modulus against  $a_T\omega$  are referred to as a master curve, (Figure 3.11),  $a_T\omega$  is known as the reduced frequency. The complex modulus,  $G^*$ , and the phase angle  $\delta$ , can both be shifted, the value of  $a_T$  being the same in each case. This analysis ignores any other influences of temperature on the material. Materials which obey the principle of time-temperature superposition are said to be thermorheologically simple, e.g. almost all amorphous polymer melts and concentrated solutions [15]. It has also been shown that bituminous binders obey this principle many times, and a consideration of their chemical and physical properties suggests that they should do so [21]. The time-temperature superposition fails where the relaxation times do not show the same dependence on temperature; in effect, when they arise from independent mechanisms. This is commonly the case in, for example, liquid crystals or particulate dispersions and for dilute solutions where the strength of the interaction between the polymer and solvent is also affected by temperature.

The Eurobitume Task Force [22] has recommended two equations for determining the shift factors for the temperature-time superposition: the Arrhenius equation and the Williams, Landel, and Ferry (WLF) equation.

### 3.2.3.1 Arrhenius equation

$$\log(a_T) = K\left(\frac{1}{T} - \frac{1}{T_{REF}}\right)$$

Equation 3.12

$K = 0.4347 \Delta H/R$  where  $\Delta H$  = activation energy (a constant, characteristic for the material), and  $R$  = universal gas constant (8.31 joules per Kelvin per mole). Temperatures are in Kelvin.

The Arrhenius equation is a one parameter equation which is suitable for some viscoelastic materials like bitumen [22].

### 3.2.3.2 William, Landel, and Ferry (WLF) equation

$$\log(a_T) = \frac{-C_1(T - T_{REF})}{C_2 + (T - T_{REF})}$$

*Equation 3.13*

The WLF equation describes the relationship between shift factor and temperature. The empirical constants for the WLF equation ( $C_1$  and  $C_2$ ) are obtained from a linear regression  $(T - T_{REF})/\log(a_T)$  versus  $(T - T_{REF})$  [15], as follows:

$$(T - T_{REF}) = s \frac{(T - T_{REF})}{\log(a_T)} + i$$

*Equation 3.14*

From the slope line,  $s$ , and the intercept,  $i$ , the two empirical constants are calculated as follows:  $C_1 = -1/s$  and  $C_2 = i/s$ .

The comparison in modelling the time-temperature shift factor by the two methods to the data obtained from the Van der Poel nomograph is presented in Figure 3.9 [23].

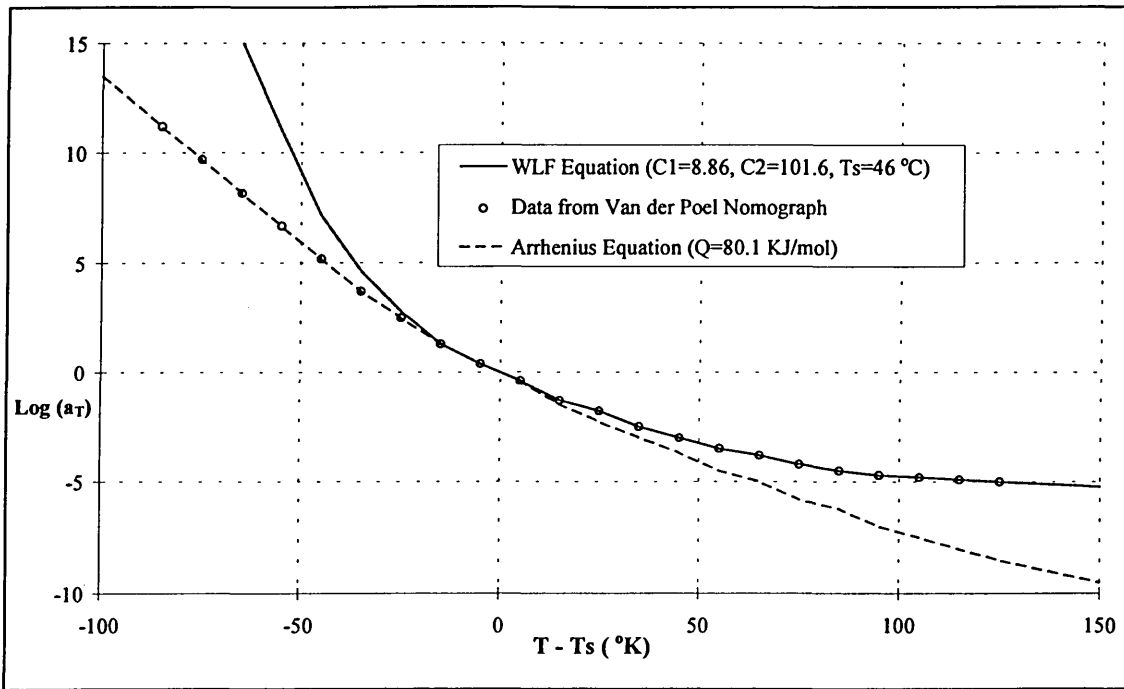


Figure 3.9 Modelling of the temperature shift factor mastercurve by Equation 3.12 and Equation 3.13. After Cheung [23].

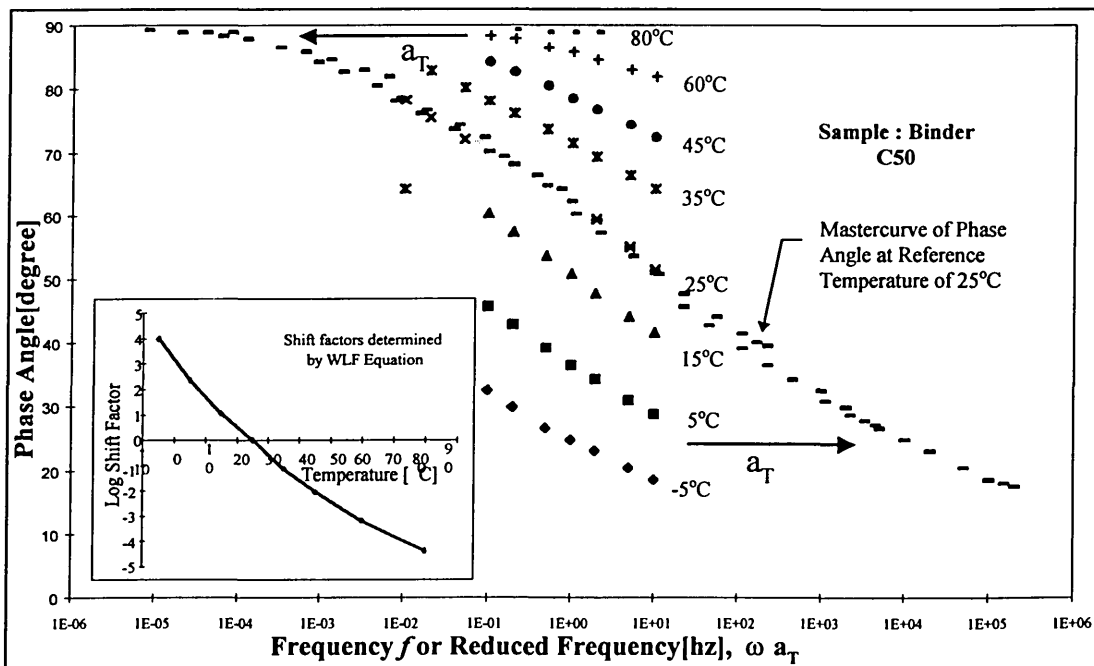


Figure 3.10 Phase angle ( $\delta$ ) as a function of frequency and temperature, with the mastercurve at reference temperature of 25°C, and also the temperature-frequency shift factor ( $a_T$ ). The binder is 50 Pen (Type C50) which is used in this study.

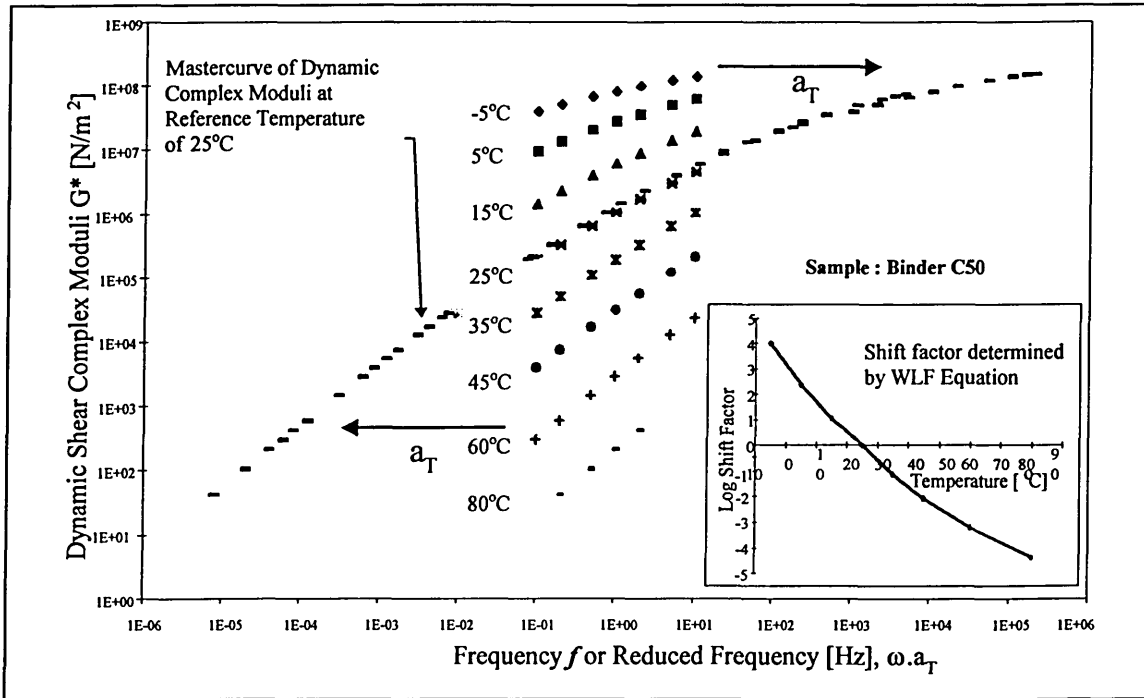


Figure 3.11 Dynamic complex modulus ( $G^*$ ) as a function of frequency and temperature, with the mastercurve at Reference Temperature of 25°C, and also the temperature-frequency shift factor ( $a_T$ ). The binder is 50 Pen (Type C50) which is used in this study.

### 3.3 Properties of Polymer Modifier Binders

Over sixty-five years, many investigations on the utilisation of polymers for bitumen modification have been conducted. Many of them have reported that polymers contribute significant improvement to pavement performance. It has also been observed that certain polymers cannot always easily be blended with a bitumen from a specific source and the response of bitumen from different sources to any given polymer varies. Therefore, a concept of 'compatibility' between the polymer and the base bitumen has been introduced. Researchers [24,25,26,27] consider that the 'compatibility' between the polymer and the base bitumen has a strong link with any improvement to pavement performance.

A polymer is regarded as 'compatible' with a bitumen if the mixture of the two constituents performs the conventional properties of bituminous binders [24], such as: homogeneity, ductility (flexibility), cohesion, and adhesiveness. Further research [25] explained that the homogeneity is a function of a polymeric network that has several

variables such as: polymer concentration, polymer chemical structure, polymer molecular weight, degree of branching, types of interactions between the polymer and asphalt, asphaltene content, and the thermal/mechanical history of the blend. It is also suggested that the criteria of 'compatibility' between bitumen and polymer additives should also include storage stability [26,27].

The storage stability test was initially introduced as a tool for determining the storage stability of bitumen emulsion in a relatively short time period. Developments in bituminous binders, especially with the use of polymer as a bitumen modifier, introduce the possibility of phase separation within a polymer modified bitumen during hot storage. The stability may not be a problem if the blends are manufactured and used immediately, however, changes in properties may be expected if the blends need to be stored for a prolonged period, such as at the weekend or during holiday breaks. Ellis, Widyatmoko, and Read [28] have presented that a blend of polymer and bitumen can experience phase separation between polymer and the bitumen as early as one day storage. Some countries have introduced different types of storage stability test, such as the tube test or beverage can test. These tests are generally conducted in a similar procedure, that samples of a particular binder are normally put into a container (a tube, a beverage can, *etc.*), and stored for a specified duration (e.g. 7 days) at a specified storage temperature (e.g. 180°C). The differences in the properties of top and bottom sections of the container are normally adopted as the parameters of storage stability. In the United Kingdom, a draft of specification for the storage stability test is currently being developed [29].

### 3.3.1 Molecular Weight Distributions

Molecular weight distribution has been considered to be one of the important components of polymer properties. The complete molecular weight distribution differentiates the mole (number) or mass (weight) fraction of molecules at each size level in a sample.

The popular method for conducting the molecular weight distribution of polymeric materials is size exclusion chromatography (SEC) or sometimes called gel permeation

chromatography (GPC). It makes use of a column or series of columns packed with particles of porous substrate. Two of the common substrates are gel, in terms of gel permeation chromatography, and porous glass beads. The gel refers to a crosslinked polymer that is swollen by the solvent used. The column kept at constant temperature, and solvent is passed through it at a constant rate. At the beginning of a test, a small amount of polymer solution is injected just ahead of the column. The solvent flow carries the polymer through the column. The large molecules in the sample can not easily fit into the substrate pores, and are swept more or less directly into the interstices in the packing. The smaller molecules have easy access to the pores and diffuse in and out of the pores, following a circuitous route as they pass through the column. Hence, a separation is obtained, the largest molecules are washed through the column first, followed by gradually smaller ones.

Other types of chromatographic analyses are high pressure liquid chromatography (HPLC), iatroskan chromatography (IC), gas chromatography (GC), thin layer chromatography with flame ionisation detector (TLC FID), differential scanning calorimetry (DSC), and high pressure gel permeation chromatography (HP GPC). Typical results from HP-GPC are shown in Figure 3.12 [30].

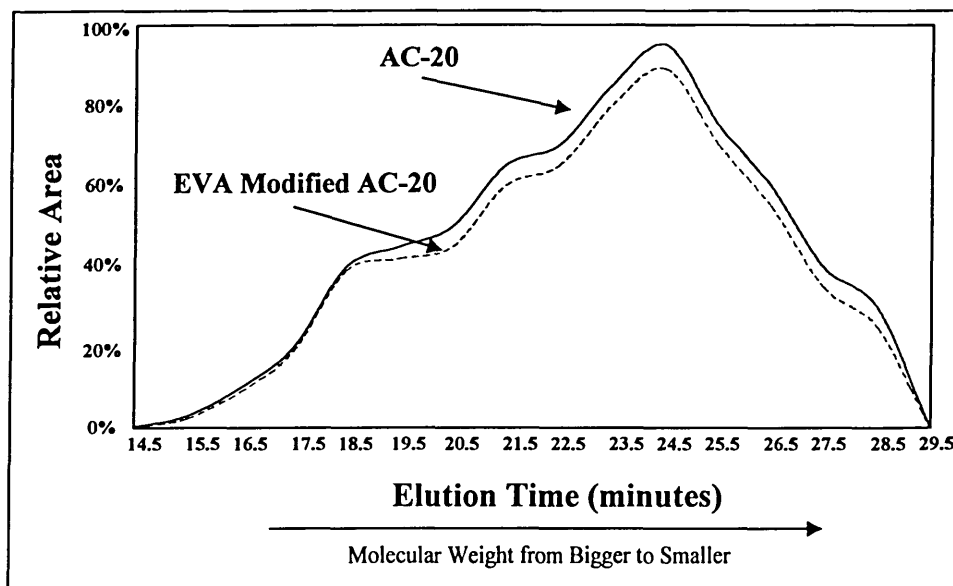


Figure 3.12 HP-GPC Profiles of Parent AC-20 and Ethylene Vinyl Acetate Modified Bitumens [30]

### 3.3.2 Phase Structure of Polymer-Bitumen Blends

It has been well known that bitumen has an irregular chemical structure because of the extremely large variety of chemical compounds. The variation is mainly caused by different crude sources and refining processes used to produce the final product, i.e. bitumen. The main chemical elements found in a bitumen are carbon and hydrogen. The ratio between these two elements is relatively constant for any bitumen regardless of its crude source [25]. However, the concentration of heteroatoms (oxygen, nitrogen, sulphur, *etc.*) and heavy metals, that usually have a major contribution to the properties of the bitumen, tend to vary. On the other hand, polymers usually have a definite chemical structure. This source-dependent condition of bitumens have made the development of a general model for performance prediction of polymer-bitumen blends difficult and complicated. The Strategic Highway Research Program (SHRP) researchers recommend that a better understanding of the chemistry of bitumen and the relationships between chemistry and performance, modification of bitumen to enhance its properties, and performance based specification, should be able to overcome this complexity [31].

The physicochemical phenomena that control the interaction between the added polymer and the bitumen are swelling and solvation of the polymer by maltenes. The maltenes contain the original asphaltenes dissolved. The interaction is governed by the time it needs to reach an equilibrium between the solvated solids (i.e. the polymer) and the solvating maltenes. The time to reach this equilibrium stage is temperature dependent.

Once the swelling equilibrium is reached, it can result in one of the following states [32]:

1. A gel stage will be reached if the total maltenes fraction is taken up by the asphaltenes and the polymer. This stage will not have sufficient fluidity to be a useful bonding agent.
2. A poor dispersion system occurs if one of these solids, asphaltenes and polymer, are present in an excessive amount.
3. If the maltenes are present in a higher amount than necessary to be taken up by the asphaltenes and polymer, those solids will be dispersed in the solvent maltenes.

In the case of modification with elastomers, it is particularly important for the elastomer particles to be swollen sufficiently by bituminous materials [33] and they should be well dispersed in the bitumen. If the elastomer particles are difficult to get swollen, a rubbery blend can still be obtained but the elastomers will be acting as a filler, i.e. not as a bitumen modifier. If the elastomers are fully dissolved, an increase in viscosity can still be found but no improvement in toughness and elasticity will be developed.

Brule, Brion, and Tanguy [24] reported that a relationship can be found between microstructure and physical properties, i.e. tensile strength, of Styrene Butadiene Styrene (SBS) modified binders. Binders with coarser microstructure are more brittle at low temperature. This result is confirmed by Lee, Morrison, and Hesp [34] in a low temperature study of polyethylene-modified binders. They reported that the fracture toughness could be affected significantly by the interparticle distance. Hence, "the larger particle size and the weak interface lower the plastic deformation in the matrix and produce a more brittle modified binder".

### **3.3.3 Classification on Polymer Modified Bituminous Binders**

Materials used as modifiers have been classified into different groups by different researchers or agencies, i.e. the SHRP [35] classified the modifier into six groups that are based on the addition of:

1. Mineral fillers (dust, lime, Portland cement, carbon black, sulphur)
2. Rubbers (random Styrene Butadiene Rubber (SBR), block Styrene Butadiene Styrene (SBS), cross linked Styrene Butadiene (SB))
3. Plastics (polyethylene, polypropylene, Ethylene Vinyl Acetate (EVA))
4. Oxidants (manganese and other metal salts)
5. Antioxidants (lead compounds, carbon, calcium salts)
6. Hydrocarbons(aromatic oils)

However, this study will be focused only on two main groups of modifiers called polymers, i.e. thermoplastics/plastomers/plastics and elastomers/rubbers.

Lancaster [36] stated that there are two stages in classifying various groups of polymeric materials. The first stage is from the overall composition of the polymer. If the polymer contains only one type of unit or monomer then it is termed as a homopolymer, and if more than one unit is present then it is termed as copolymer. The second stage is through structural consideration, i.e. from a knowledge of how the individual components of the polymer fit together. There are three main structures of polymer: linear, branched, and block polymers. The homopolymers can only be found in the form of linear and branched<sup>c</sup> structures, whereas other types of structures, such as linear- random and linear-block, can be found in the copolymers (Figure 3.13) [37].

The linear structure is simply a long chain of repeat units that are linked together along the backbone chain. The random structure is formed by vulcanisation to produce crosslinked or a network structure, whereas the block copolymer is produced by anionic polymerisation instead of by vulcanisation.

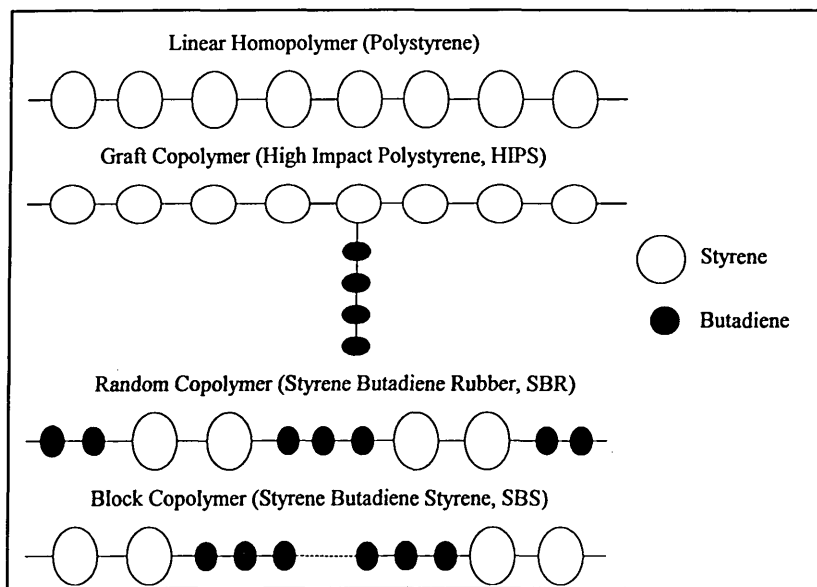


Figure 3.13 Illustration of different polymer structures [37].

<sup>c</sup> The branched structure is usually reserved only for homopolymers. In a case of non-linear or branched copolymers, the term graft structure is usually used instead of branched structure.

### 3.3.3.1 Thermoplastic polymers

The thermoplastic polymers are characterised by softening on heating and hardening on cooling. These characteristics are similar to that of bitumen. One of the advantages offered by thermoplastic polymers is that viscosity and stiffness of the binders modified by the thermoplastic polymers increase at ambient temperature. However, most of thermoplastic polymers have some drawbacks in that they tend to separate in storage, which leads to a coarse dispersion of polymer in the polymer-bitumen blends at the end of the storage period [26,38], and do not improve elastic properties of the binder [38]. Further, thermoplastic polymers were described as being stiff but brittle, i.e., they exhibit high early tensile strength but tend to rupture after small deformation [39]. However, studies [40,41,42] on specific types of thermoplastic polymers, such as polyethylene and ethylene vinyl acetate, reported that plastomers do have good flexibility at low temperature, and hence they are not brittle. The first opinion that stated that plastomers are brittle is in part true when compared with elastomeric polymers. However, the properties of modified binders are strongly influenced by the methods of measurement and analyses, and therefore, care should be taken in correlating the ranking performance of the modified binder to the ranking performance of the modified mixtures.

The Melt Flow Index (MFI) is usually adopted as a measure of viscosity and molecular weight for thermoplastic polymers. The higher the MFI, the lower the viscosity and the molecular weight.

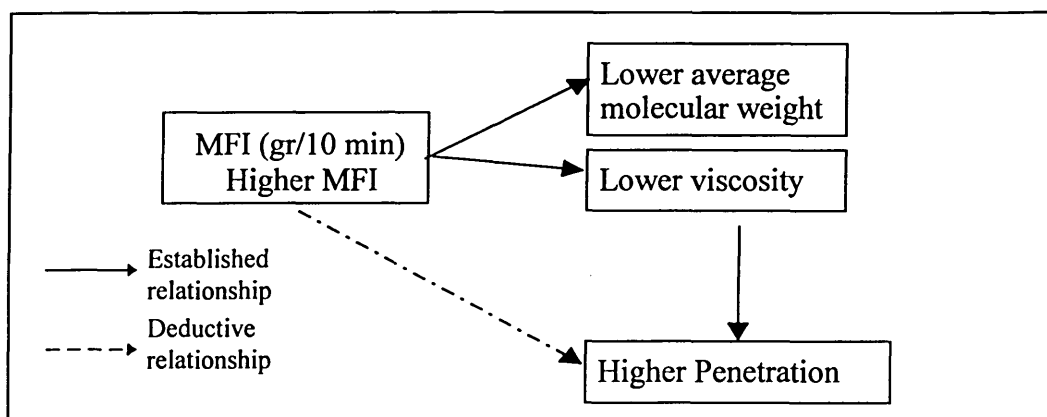


Figure 3.14 Inter-relationship between MFI, molecular weight, viscosity, and penetration.

The commonly used thermoplastic polymers are polyethylene, polypropylene, polyvinyl chloride, polystyrene, and ethylene vinyl acetate.

### **Polyethylene**

Polyethylenes are polymers that principally derive from polymerisation of the ethylene monomer. A linear polyethylene is often expressed as  $-(\text{CH}_2\text{CH}_2)_n-$

Investigations into the use of polyethylene have frequently been encouraged in recent years, especially in Canada and United States [43]. One of the interesting points for using polyethylene as a modifier for bitumen is the cost. A study reported that the cost of polyethylene is not much different from bitumen price [44]. Polyethylene is also widely available as both virgin and recycled materials [40,43].

Some characteristics of polyethylene can be described as follows:

1. The dispersion of polyethylene in bitumen occurs at elevated temperature under high shear conditions, i.e. at mixing temperature above 140°C. The stage of dispersion can be described as: the molten polyethylene particle will gradually absorb the aliphatic maltene components of the bitumen. The process then continues by formation of a highly viscous elastic dispersion as the polyethylene dissolves in the bitumen.
2. Polyethylene is solid and crystalline below its melting transition. Within a polyethylene-bitumen blend, at the temperature when the bitumen matrix becomes soft and deformable, i.e. temperature near 50°C, the dispersed polyethylene particles assume the characteristic of a filler.
3. As with other thermoplastic polymers, polyethylenes are characterised by three main factors: molecular weight, degree of branching, and composition of the homopolymers and copolymers of ethylene. Therefore, polyethylene is classified based on these factors as: High Density Polyethylene (HDPE), Low Density Polyethylene (LDPE), and Linear Low Density Polyethylene (LLDPE). These copolymers usually melt in the temperature range between 100°C and 130°C.
4. Polyethylene has a low glass transition temperature, i.e. near -120°C. This indicates the high flexibility of the polyethylene chain at low temperature that can lead to an improvement in toughness and ductility of the base bitumen at low temperatures.

5. The fully saturated chain of polyethylene has also made the polymer more resistant to oxidative degradation.
6. The Melt Flow Index ranges between 0.6 and 150 g/10 min.
7. The stability and performance of the resulting dispersion are influenced by mixing the condition and the presence of dispersing agents such as the block copolymer. A combination between three components: shearing conditions, dispersion agents, and molecular structure of the polyethylene will influence the minimum attainable particle size and the adhesion between the phases.

Novophalt was used in the study by Jew *et al* [40] which reported some of the disadvantages and advantages for using this product with an 85/100 penetration grade bitumen obtained from a middle eastern crude. The disadvantages are: firstly, higher energy was required to blend the polyethylene modified bitumen with the aggregates, and secondly, there was a tendency for the polyethylene particles to float to the surface of the liquid bitumen where they coalesced into a highly viscous layer which could not be easily redispersed. These problems can be partly resolved by addition of chemical additives such as dispersing agents, viscosity depressants, wetting agents, and emulsion stabilisers. Some advantages: increased resistance to permanent deformation (rutting) at elevated temperature below the melting transition of polyethylene, greater tensile strength, increased impact fracture toughness, greater fatigue resistance, lower brittle temperature, and longer service life, i.e. around 2.7 to 2.9 fold [40].

Nahas *et al* [45] presented a relationship between polymer content, phase structure and softening point of ethylene copolymer as presented in Figure 3.15. The figure explains that, as seen by microscope, the phase structure can be divided into four phases:

**Phase A** : Homogeneous phase, in which the polymer has little effect on softening point.

**Phase B** : Polymer dispersed, a phase separation occurs with a polymer rich phase appearing as a dispersion in the continuous bitumen phase.

**Phase C** : Two continuous phases, volume of polymer swells significantly, i.e., 5 - 10 times its original volume. The polymer absorbs a volume of the solvent from the bitumen. Softening point increases as polymer content increases (note: the polymer content applied was never exceeded 10% by mass of bitumen).

**Phase D** : Polymer phase continuous, the bitumen phase become discontinuous and dispersed within a continuous polymer rich phase. The rate of increase in softening point starts to decrease.

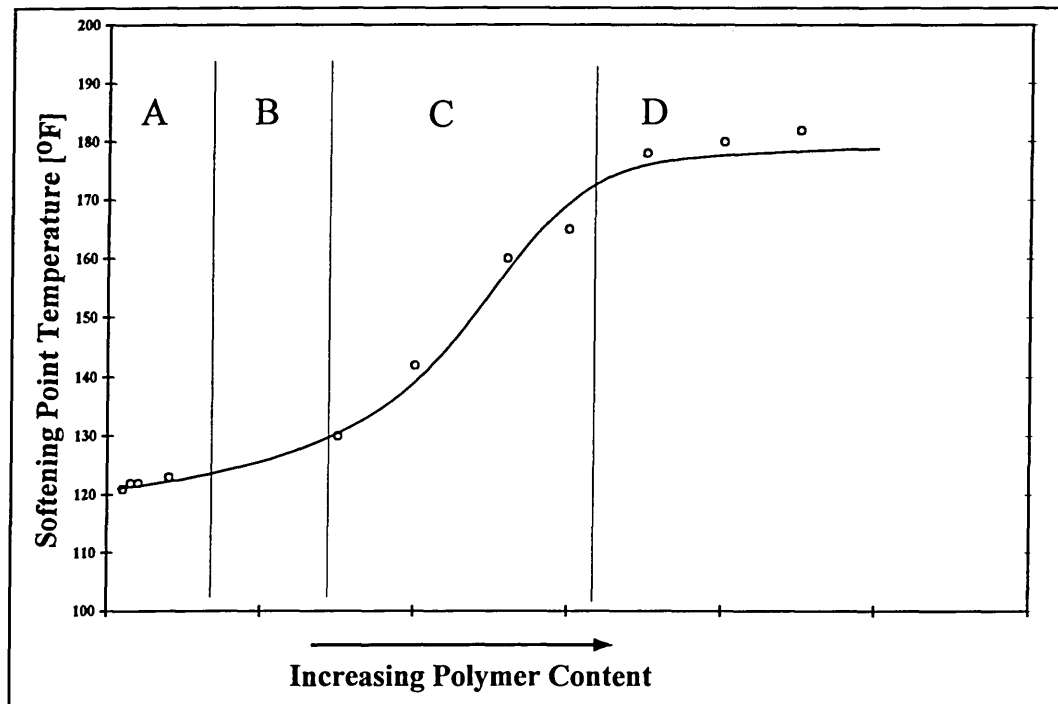


Figure 3.15 Relations between polymer content, phase structure and softening point of ethylene copolymer blended with AC-20. After Nahas et al [45]. (note: unfortunately the actual numbers on the x-axis were not reported by the Authors).

### Ethylene vinyl acetate (EVA)

EVA has been widely used as a polymer modifier in asphalt in European countries because it significantly improves the performance of modified asphalts. In the UK, EVA modified binder has been used in hot rolled asphalt wearing course mixtures, friction courses, mastic asphalts, and base courses, i.e. for the construction and maintenance of trunk roads, motorways, urban roads, and bridges [46].

The EVA copolymers have a random structure derived from copolymerisation of ethylene and vinyl acetate. The properties of EVA copolymers are mainly governed by molecular weight, in terms of MFI, and vinyl acetate content, e.g. a 150/19 grade EVA copolymer contains 19% vinyl acetate and has an MFI of 150 g/10min. The higher the MFI value indicated the lower the molecular weight.

As described in Figure 3.16, crystalline regions are formed by the polyethylene segments that are packed closely together. It also describes how these massive vinyl acetate groups break this closely packed arrangement to produce non-crystalline or amorphous rubbery regions. The crystalline regions are relatively stiff and provide the strength of EVA. The higher rubbery regions are found at the higher Vinyl Acetate (VA) content hence the higher VA content contributes to the higher flexibility.

However, the high VA content does not necessarily contribute to the enhancement of performance of the modified mixtures, i.e. resistance to permanent deformation of HRA with 70 pen grade base bitumen was improved by addition of EVA copolymer with lower VA content [47]. The improvement to the resistance to permanent deformation of HRA was also found when using EVA copolymers with higher molecular weight (lower MFI value).

The EVA copolymers can be dispersed easily in bitumen and are thermally stable at normal mixing temperature. No storage problem has been found with EVA even for storage for several days at moderate temperature [48]. However, storage at elevated temperature i.e. higher than 180°C, should be avoided to prevent storage instability. Equipment used for the storage of conventional binders can be used for EVA modified binders.

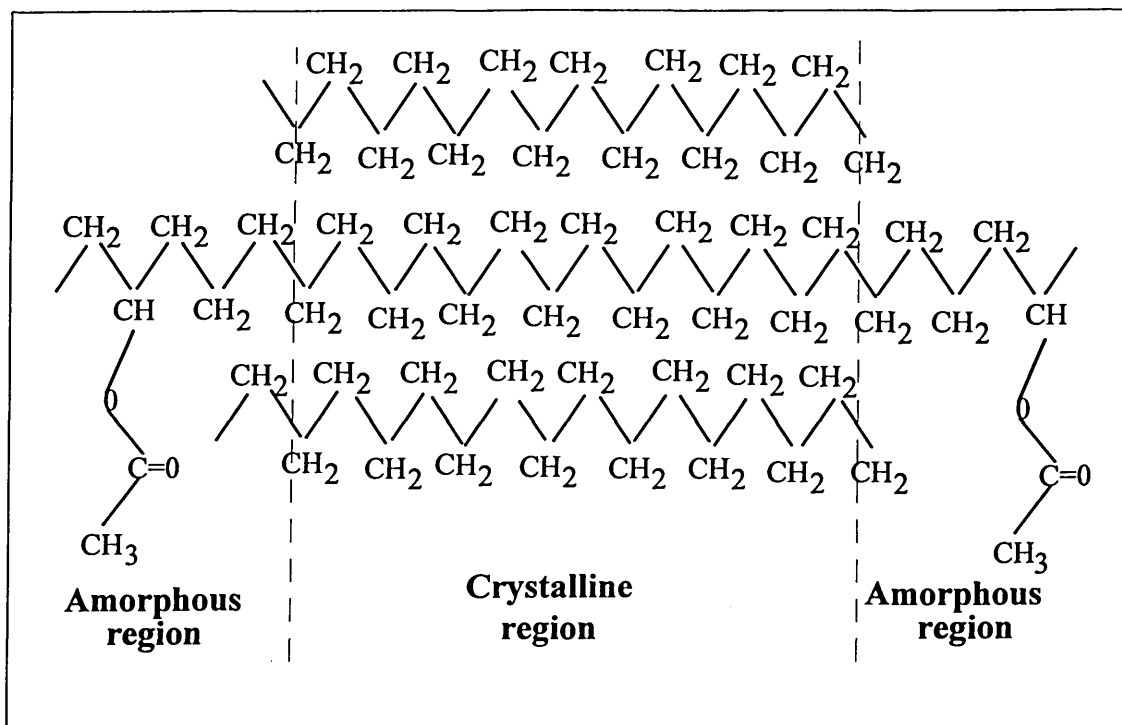
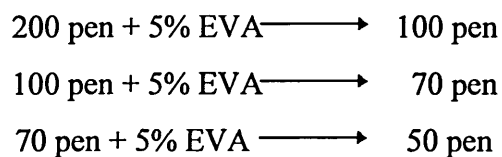


Figure 3.16 Packing of Polyethylene in EVA. After Gilby [41]

Studies on two commercial EVA modified binders [49, 50] have reported that they can be used to replace 50 pen grade bitumen, i.e. the results obtained from controlled stress rheometric tests indicate that the binders had almost identical master curves for the shear modulus. Another study also reported that the addition of EVA at 5% by mass of binder reduces the penetration value up to one grade [51], i.e.:



Additionally, for asphalt mixtures (rolled asphalt wearing course), the modified binders should improve the workability as they have a wider laying temperature range than the two others. Wheel tracking tests at 45°C also reported an improvement for the polymer modified asphalts of up to two folds as compared with the mixtures without polymer modifiers [49, 50].

### 3.3.3.2 Elastomeric polymers (rubbers)

The use of rubbers as bitumen modifiers was first introduced by Henry Austin in 1843 with his UK Patent No 9737 [4]. Since then, numerous research project have been undertaken to investigate the benefits of using rubbers.

Rubber additives have been found to increase softening point and flow behaviour, and also to decrease temperature susceptibility. Rubbers also exhibit a decrease in apparent viscosity under constant shear stress or shear rate, followed by a gradual recovery when the stress or shear rate is removed. This effect is called thixotropy behaviour and is time-dependent. Several techniques have been developed for measuring this behaviour, such as force ductility, toughness and tenacity, elastic recovery, and torsional recovery.

The force ductility test is a modification of a standard ductility test where the specimen has a longer region with consistent cross sectional area. Rate of deformation is usually set at 1 cm/min or 5 cm/min. The higher rate results in a shorter period of rupture and conversely the slower the rate allows greater elongation before rupture.

In a study on the effect of adding a polymer into bitumens with different penetration grades, the force ductility at 4°C was correlated well with field performance for the prediction of resistance fatigue cracking [52]. The test temperature of 4°C for modified binder is also confirmed by Muncy, King, and Prudhome [53]. However this test has some drawbacks:

1. The non-linear behaviour of the rate of deformation may not be found in bituminous pavements.
2. The geometry is poorly defined.
3. The results are material specific, i.e. synthetic and thermoplastic rubbers such as SBS modified binders tends to behave differently than EVA, LDPE, and SBR modified binders [25,54].

Tensile strength test (ASTM D 412-80) has been widely used especially for rubbery materials. An instron tension tester is generally used for this purpose. A sample of 3 by 0.3 by 0.3 cm is pulled to 24 cm or 800% of its original length at speeds of 1 to 50 cm/min, and at temperature from -20°C to 20°C. Muncy, King, and Prudhome [53]

recommended the use of this test on modified binders because this test has already been standardised and the apparatus needed for this test is already available. The test also meets the criteria of uniform cross-sectional area, temperature control, and constant strain. The only thing needs to be standardised is the interpretation of results.

The toughness and tenacity test is a test method that has been used for characterising elastomer modified binders, but the ASTM proposal extends the use of this test for any type of polymer modified and non-modified binder [55]. The test is conducted by embedding a hemispherical head in molten asphalt and allows the sample to cool to 25°C. The head is then pulled at a rate of 50 cm/min or 20 in/min to produce a load deformation curve as shown in Figure 3.17. Toughness is calculated from area under the main curve (A+B) and tenacity is the area (B).

Despite the simplicity in conducting the test, there some difficulties with regard to the data collection and analysis :

1. It is difficult to define the area B on some polymer systems, especially for styrene-butadiene copolymer (see Figure 3.17). There is subjective judgement in deciding where the tenacity begins [53, 54].
2. Stress-strain curves cannot be reproduced due to lack of well defined cross-sectional area [25,53, 54].
3. The test has a poor reproducibility, i.e. it tends to give different results for the same blends with the same level of loading [53].
4. This test is usually run at ambient temperature. Small temperature changes affect the viscosity of bituminous binders and the toughness and tenacity are also affected by the temperature changes [53].

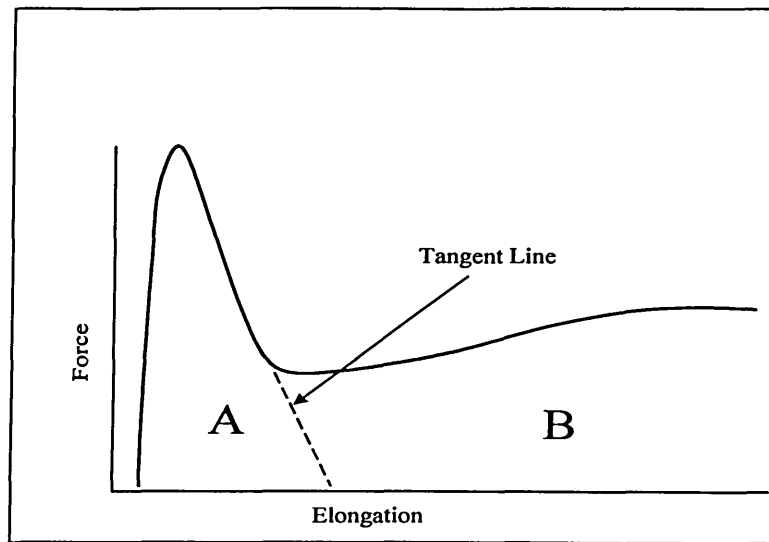


Figure 3.17 Typical relationship between applied force and elongation from the toughness and tenacity test.

Elastic recovery (also termed modified ductility or ductility recovery) test is another modification from a standard ductility test that was designed to measure the ability of a binder to elastically recover from deformation. The simplest procedure of this test is by adopting the standard ductility apparatus. The test is conducted by pulling a specimen to a defined length (i.e. 20 cm), cut in the middle, and then the recovery time is measured as an indication of elasticity. Rate of loading is usually set at 5 cm/min. Some other devices have been developed for this test, such as the Australian Road Research Board's (ARRB) Elastic Recovery Rheometer, and the Dekker Elastic Recovery Device.

This test also has poor repeatability and is material specific, i.e. it is best applied only for elastomeric polymers. This test cannot explain the relative benefits of the presence of different polymers to mixture performance, i.e. elastomeric modified binder has a tendency to have better elastic recovery than other types of modified binder. Lenoble and Nahas [56] reported that modified binders, except those modified by elastomers, that have good resistance to permanent deformation did not perform well in the elastic recovery test. Therefore, it should be noted here that resistance to permanent deformation is not necessarily solely reflected by this test as each modified binder resists permanent deformation with different mechanisms.

In spite of these disadvantages, the ductilometer has been regarded to be the best test for modified binders in comparison to other devices, because it is fast and easy to run, uses readily available apparatus, offers good temperature control, and has good precision [53].

The torsional recovery test was originally developed to test the recovery of a latex modified bitumen emulsion residue. This procedure offers an excellent, fast, and inexpensive field screening tool for monitoring elastic recovery. However, there are also some limitations such as a lack of precise temperature control, the inability to apply a constant strain, a large specimen size requiring multiple emulsion evaporations, and the exclusion of the instantaneous elastic recovery occurring in the first 30 seconds after release [53]. This method can only be used on rubbers, it should not be used for comparing different polymers. Some other factors that should be considered in conjunction with this test are: the molecular weight of polymer, the styrene-butadiene ratio, the crosslinking structure, the styrene block size, the bitumen compatibility and the viscosity of the bitumen.

The addition of rubbers into bituminous materials, as reported by Thompson [33], can be in various forms such as : massive forms (such as sheets, chunks, slabs), crumbs or granules, fluxes in low melting bitumens, solutions in liquid hydrocarbons, powders, masterbatches in pitches, lattices, and dispersion in nonaqueous media (see Table 3.6).

<b>Rubber Forms</b>	<b>Characteristics</b>
Massive forms (slabs, sheets, chunks)	Difficult to be dissolved in bitumen, therefore require a heavy duty mixer High ductility and elasticity
Crumbs or Granules	More readily blended than the massive forms Generally produce inhomogeneous blends with bitumen Forming a visible skeleton network in the bitumen matrix
Fluxes	Require a low viscosity and low melting bitumen and high temperature and long blending times Susceptible to polymer degradation on stirring
Solutions	Produced by dissolving raw rubbers into organic solvents, e.g. naphtha, kerosene, or toluene Easy to be blended with bitumen
Powders	Fine particle size, highly effective modifying agents Easy to disperse in bitumen solvent
Masterbatches	Produced from blending elastomers and high melting bituminous materials on two-roll mills or in internal mixers. The blend can be granulated on cooling, and the product can be added as a masterbatch to a bitumen or tar.
Latices	Produced by adding the latex to the molten bitumen at temperature above the boiling point of water, and by controlling the following creation of foam to aids dispersion of the elastomer in the bitumen. The dispersion obtained is generally excellent.
Non-aqueous dispersions	It is a colloidal suspension of an elastomer in an organic fluid which has boiling point beyond the temperature that will be experienced during mixing, processing, and application of the bituminous materials to which it is added. The fluid component is not necessarily miscible but remains in the finish blend. It eliminates the water removal problems and so can be added directly to the bitumen.

*Table 3.6 Forms of rubber modifiers*

Polybutadiene, polyisoprene, natural rubber, butyl rubber, chloroprene, random styrene/butadiene rubber, and Ethylene Propylene Diene Rubber (EPDM) are the principal polymers in this group. These polymers hardly associate when dispersing with bitumens at ambient temperature [26]. Therefore, they need higher mixing temperatures which in some cases will be too high for bitumens or fluxing oils.

### **Natural rubber**

The oldest technique for bitumen modification is by addition of natural rubbers obtained from scrap waste tyres. The preference for using this modifier is because the utilisation

of waste tyre not only solves environmental problems [57] but because it also offers other benefits such as increased skid resistance [35, 58], improved flexibility and crack resistance [35, 57, 58], and reduced traffic noise [57].

There are two methods of modification with rubbers [57, 58, 59] :

- a. Dry process (rubber acts as filler aggregate)
- b. Wet process (rubber acts as binder modifier)

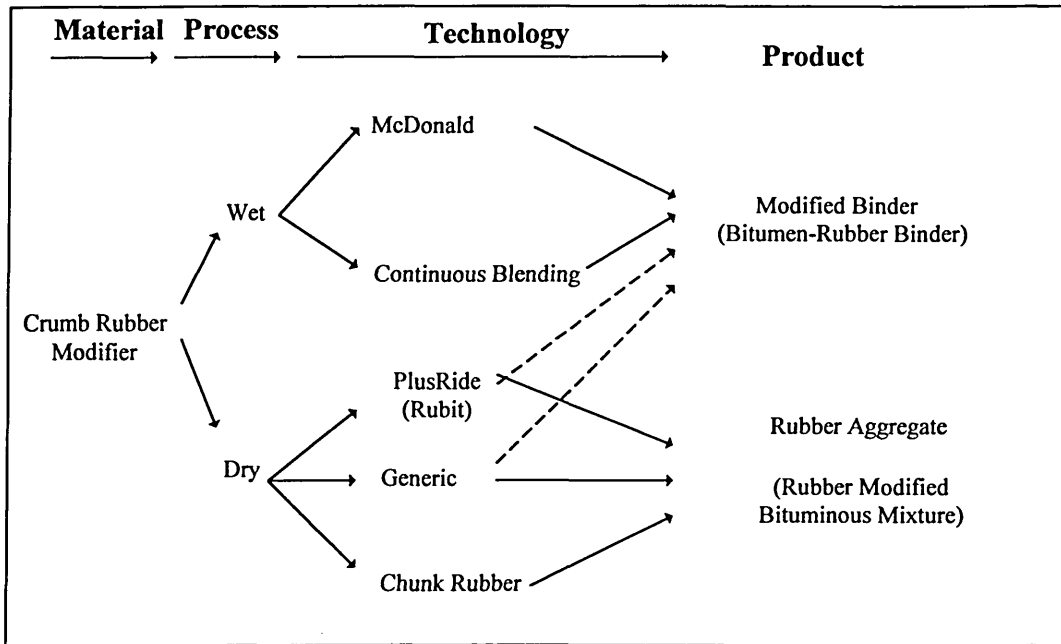


Figure 3.18 Different processes and technologies in application of rubbers in bituminous mixtures [59]

With the first method, rubber is used to replace some aggregate in the mixtures whereas with the second method, rubber is blended with bitumen to create a rubberised bituminous binder. Both methods can provide better pavement performance but with different mechanisms.

Takallou *et. al* [57] reported on the use of ground tyre rubber as a filler aggregate (dry process). In this process, about 3% to 4% by mass of relatively large rubber particles ( $1/16$  inches to  $1/4$  inches) are used to replace some of the aggregate in a bituminous mixture. The rubber particles were produced in roughly cubical forms by grinding waste tyres, which have previously had the steel wires in the tyre bead area removed.

Allowance was given to some tyre cord and steel fibres from tyre belts as long as the gradation complies with the specification [57]. As well as utilisation of rubber tyre waste, this process also provides other benefits such as increased flexibility, increased fatigue life, resistance to studded tyre, reduced noise and crack reflection control. However, difficulties were also encountered due to the increased optimum binder content, i.e. about 7.5% to 9.5% [58, 59], which causes the modified mixtures to be more susceptible to mixture preparation, e.g. it tends to produce smoke during mixing process and the lowest mixing temperature is 325°F (163°C), and compaction, e.g. rutting and pickup problems can occur more easily during compaction, than in conventional mixtures [57, 59].

In the wet process, finely ground crumb rubber is blended with a bitumen at an elevated temperature (200°C) by means of an oil extender [58]. Typically, the proportion of crumb rubber varies from 10% to 30% and the oil extender from 3% to 15% by total mass of the binder. The interaction of bitumen-rubber in the wet process is affected by the blending temperature, the duration of blending, the type and amount of mechanical blending energy, the size and texture of the CRM, and the aromatic component of the bitumen. The absorption of aromatic oils from the bitumen into the polymer chains causes the polymer to swell and soften. The type and amount of aromatic oil in the bitumen also plays a major role in determining the compatibility of bitumen-rubber blends [59]. A bitumen modified with 15% CRM can increase the high temperature viscosity of the blend by a factor of 10 or more [59]. The rate of reaction can be increased by enlarging the surface area of the CRM, i.e. by reducing the size of the polymer. There is also an undesirable side effect, i.e. CRM will require an increase in the binder content, which leads to potential problems of flushing or bleeding, increasing the paving material's cost, and may cause tracking [59]. The other problem was found to be the storage stability of the rubberised bituminous binder. It was reported that "the rubberised binder must be used within hours of its production" [58]. However, the problem may be overcome by addition of a catalyst into the mixture. Hence, cost-effectiveness should also be considered together with the benefits that are being obtained by the use of the modifier.

### **Polybutadienes**

Polybutadienes are linear amorphous polymers<sup>d</sup> having a molecular weight below  $10^6$ , may dissolve at relatively high temperature, and produce a stable dispersion at lower temperatures. Van Beem and Bresser [26] reported on blending an 80/100 pen bitumen with 5% by mass of polybutadiene that the change-over to single phase structure of the heated blend can be reached at temperature about 80 °C for low molecular weight polybutadiene (average molecular weight  $M_w$  of 40000) and at about 135°C for high molecular weight polybutadiene (average  $M_w$  of 200000). The softening point of the blend was reported to be only slightly higher than the base bitumen (80/100 pen), but that the viscosity at 175°C was very high, i.e. 20 poise (2 Pa.s) and 700 (70 Pa.s) poise for binder modification with 5% by mass of polybutadiene with molecular weight of 200000 and 850000, respectively. Therefore, it is impossible to blend the polybutadienes with the bitumen using conventional techniques.

Despite the difficulties in blending, the study [26] also reported that the performance of polybutadiene modified bitumen improved viscosity at high temperature (60°C) and hence improved the resistance to permanent deformation. The flexibility of the binder at low temperature was also improved as shown by the lower value of Fraas breaking temperature, i.e. around -25°C, than the Fraas breaking temperature of the original bitumen, i.e. -15°C.

### **Random styrene/butadiene rubber (SBR)**

Like natural rubber, SBR is an unsaturated hydrocarbon polymer. Therefore, unvulcanised compounds will dissolve most hydrocarbon solvents and other liquids of similar solubility parameters, whilst cured stocks will show extensive swelling. The SBR exhibits good low temperature properties, such as flexibility, due to the lack of crystallisation, the typical glass transition temperature of SBR with a low styrene content (e.g. 18%) is around -75°C [60].

---

<sup>d</sup> See *Glossary*

King *et al.* [61] reported that the mixing temperature for styrene butadiene block copolymer depends upon the polymer concentration and penetration grade of the base bitumen, as shown in Table 3.7. This study also reported that the addition of the polymer into different grades of bitumens always significantly increased the softening point and the absolute viscosity (measured at 60°C) of the binders. However, it was also reported that soft bitumens (e.g. 180/200 pen) with high polymer concentration could exhibit the high softening points, but this did not necessarily make them have resistance to permanent deformation as high as that implied by the increased softening point.

*Table 3.7 Relative increase in mixing temperature (in centigrade) as the polymer content increased. After King et al. [61]*

Penetration Grade	% Polymer			
	0 %	x%	1.5x%	2x%
40/50	165	170	185	200
60/70	160	165	175	190
80/100	150	155	165	175
180/200	145	155	160	165

### **EPDM (Ethylene Propylene Diene Rubber)**

EPDM is a ternary copolymer (terpolymer<sup>6</sup>) that is produced with a double bond in the polymer structure to facilitate a sulphur-based cure. The presence of the double bond in the structure improves the resistance to oxidation and heat-ageing in comparison to normal diene rubbers. The main characteristics of EPDM are that the grade properties depend on the ethylene-propylene ratio, type and amount of third monomer molecular weight and molecular weight distribution, microstructure, and whether or not oil extended. The optimum rubberiness and low temperature flexibility can be achieved at ethylene contents between 50% to 60%.

In road construction, the EPDM modifier has been widely used in Europe as a polymer modifier for asphalt concrete, porous asphalt, stone mastic asphalt, and thin surfacing layer system. It offers greater resistance to permanent deformation and lower

---

<sup>6</sup> Terpolymer is a copolymer that comprised from three different monomers.

temperature susceptibility than conventional bitumen and the polymer can be blended directly into the bitumen at the refinery. Furthermore, it is storage stable at the maximum storage temperature of 160°C. The storage stability can be extended for up to 3 to 4 days without the need to add fresh binder if the storage temperature is controlled between 70°C to 120°C [62].

### 3.3.3.3 Thermoplastic rubbers (TR)

The thermoplastic rubbers, as implied by the name, have the combined properties of thermoplastics, i.e. styrene domains, and rubbers. Polymers in this group are sometimes abbreviated as SBS (styrene-butadiene-styrene), SIS (styrene-isoprene-styrene), SEBS (styrene-ethylene/butadiene-styrene), and SEPS (styrene-ethylene/propylene-styrene). Hence, these TRs can be formulated as presented in Figure 3.19:

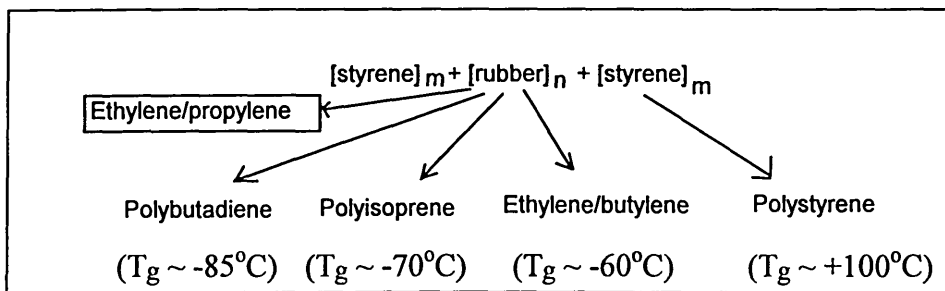


Figure 3.19 Thermoplastic block copolymers. After Collins and Mikols [63].  $T_g$  is the glass transition temperature.

The behaviour of these polymers is predominantly governed by temperature:

1. They behave as thermoplastic polymers at high temperatures, i.e. the polymers disassociate and dissolve in bitumen at mixing temperature.
2. They behave as vulcanised rubber at ambient temperature due to association.

The strong elasticity of TR is provided by the plastic nature of small styrene blocks known as domains which are embedded in the rubbery matrix [4] (Plate 3.1). These styrene blocks have a glass transition temperature of approximately 100°C. Because of their thermoplastic nature, the modified blends will flow under shear at mixing temperatures above the glass transition temperature of the styrene. Conversely, the rubber properties, that are provided by polybutadiene, polyisoprene or ethylene/butylene

blocks, with glass transition temperatures below  $-60^{\circ}\text{C}$ , will produce a high resilience and flexibility at low temperature. Therefore, by varying the ratio of the total molecular weight of these two constituents, polymers can be designed to provide specific mechanical properties for certain applications. For example, a more elastic nature in the designed polymer can be obtained by reducing the percentage of the polystyrene blocks.

Kraus [64] stated that to achieve optimum effectiveness of bitumen modification with SBS copolymers several important structural criteria must be met such as:

1. the block polymer must be rich in butadiene and contain 30%-40% styrene
2. the polymer must have two polystyrene blocks or a suitable branch point giving either a linear (SBS) or radial (SBx) configuration.
3. the molecular weight of the polystyrene must exceed 10,000 to obtain polystyrene rich domain.

Additionally, high aromatic bitumens will be easily blended with SBS copolymer. A study [24] suggested that base bitumens with aromatic oils and resins content around 85% to 89% is preferable. A blending temperature of about  $180^{\circ}\text{C}$  for 30 minutes is suggested [63] in order to get a good dispersion of SBS copolymer within the bitumen.

The storage stability of this polymer is mainly affected by: the amount and molecular weight of the asphaltenes, the aromaticity of the maltene phase, the amount of polymer present, the molecular weight and structure of the polymer, and the storage temperature [4, 65]. Figure 3.20 and Figure 3.21 show some factors that can affect the stability of TR blends.

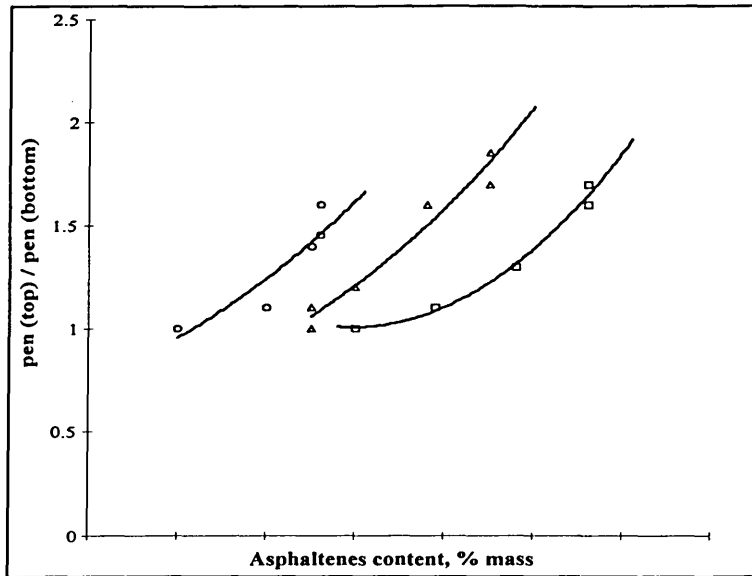


Figure 3.20 Effect of asphaltenes content on the  $pen_{top}/pen_{bottom}$  ratio after hot storage of bitumen/TR blends. Bitumen blended from three base bitumens and non-volatile flux oil. After Morgan and Mulder [4].

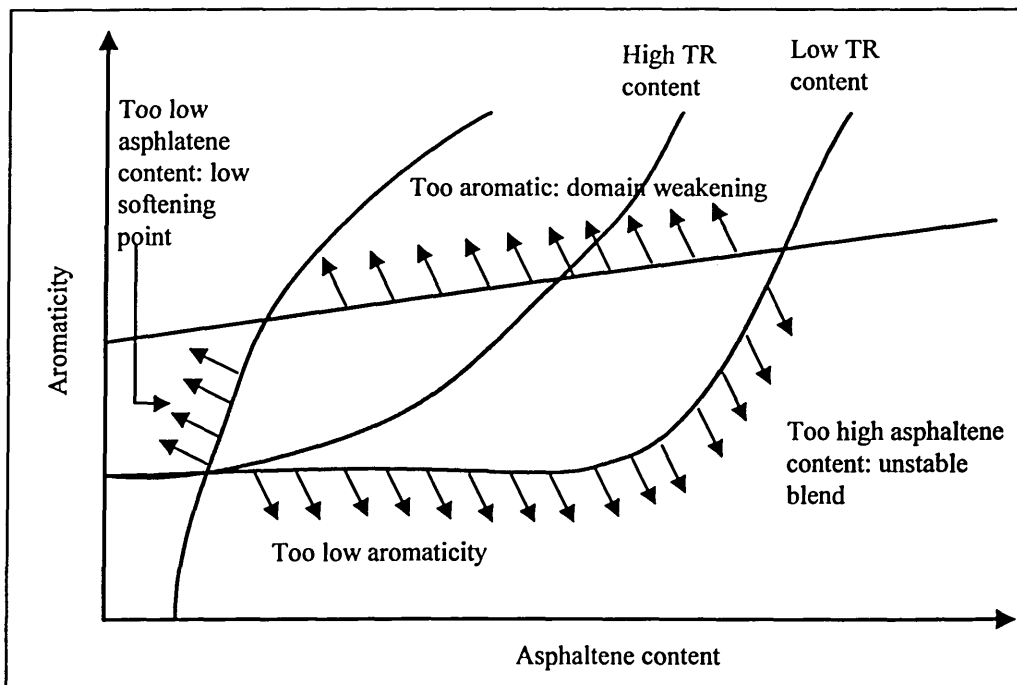


Figure 3.21 Influence of bitumen constitution on bitumen/TR blends. After Von Gooswilligen and Bull [65]

A study on a specific SBS group [26] reported that in order to get a good compatibility between polymer and bitumen several conditions should be met:

1. To avoid phase separation during hot storage, polystyrene blocks should be continuously dispersed during heating. Polystyrene domains should contain only a minimum amount of bitumen to provide good crosslinking bonds for the dispersed butadiene.
2. Polybutadiene blocks should also be well dispersed to avoid the phase separation during cooling, hot storage or if the blend is kept at ambient temperature for a long period of time.

The process of dispersion of the same SBS group was also reported [66]. It started from ingress of hot bitumen into the microstructure of the polymer which is mainly polystyrene blocks. The final stage is reached when the SBS particles are uniformly dispersed throughout the bitumen which will result in a continuous SBS network stabilised in the bitumen.

### 3.3.4 Blending Polymer Modified Bitumens

It is not simple to achieve a good blend between polymer and bitumen. A parameter that is usually adopted for this purpose is the phase of dispersion and a polymer may need a solvent in order to be able to be dispersed properly in a bitumen.

The absorption of bitumen solvent by a polymer can cause the polymer to swell. Brule, Brion, and Tanguy [24] investigated the extent of swelling on five different bitumens modified with SBS copolymer. The extent of swelling was independent of temperature over the 80-160°C range, however the rate decreased as the polymer content increased. They reported a value of polymer content beyond which a polymer is no longer swollen in the modified binder but solubised in bitumen. This value was then termed the Colloidal Instability (CI) index.

The colloidal instability index is a parameter to characterise the fragility of the colloidal equilibrium, i.e. the state of dispersion. The index is defined as follows:

$$\text{Colloidal Instability Index} = \frac{\text{asphaltenes} + \text{saturated oils}}{\text{resins} + \text{aromatic oils}}$$

Loeber *et al* [67] reported a study on the addition of EVA copolymers with different VA contents into several bitumens from different origins that a high colloidal index leads to a low critical polymer concentration (CPC) and a heterogeneous structure, low cohesivity in the tensile strength measurements and low values of the maximum phase angle. Conversely, a low colloidal index gives a high CPC with a finely dispersed structure which exhibits a high cohesion energy and a high maximum phase angle. Figure 3.22 shows that the best rheological performance of the polymer modified binders with a minimum polymer concentration can be obtained at the CI index of 0.3.

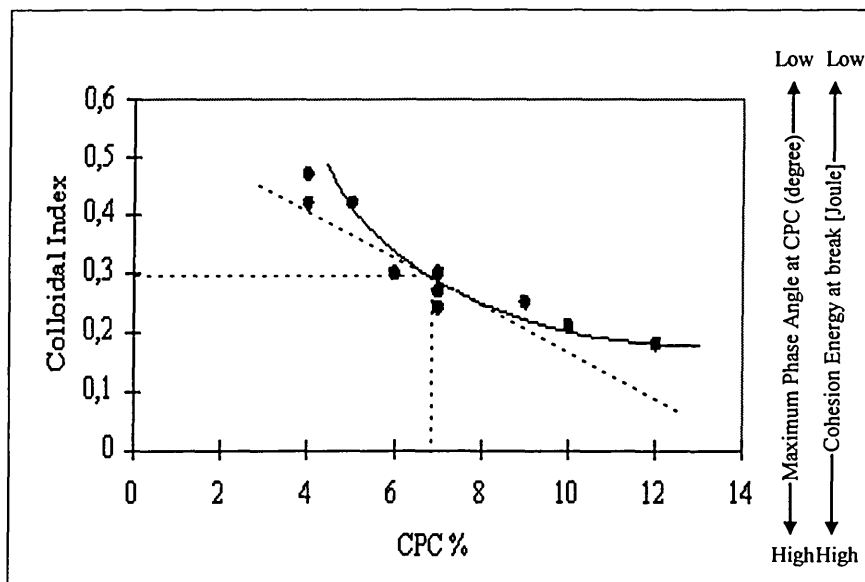


Figure 3.22 Relationship between the colloidal instability index (CI) and the critical polymer concentration (CPC). After Loeber *et al* [67].

A high shear mixer is the commonly used apparatus for making polymer-bitumen blends, especially for modification with SBS and SBR polymers whereas a lower shear mixer can be used for EVA. The high rate of shearing force will have the ability to break down the cohesive bonds within the individual materials (polymer and bitumen) and to generate adhesion between the polymer and bitumen. Care should be taken during the blending as modified binders generally behave as non-Newtonian fluids that can exhibit the Weissenberg effect (Plate 3.2). The Weissenberg effect is an effect shown by elastic liquids during rotary stirring that the melt or solution climbs up the stirring rod, and in some cases winds itself entirely around the rod [68]. This effect is caused by normal

stresses developed in the sheared liquid and is particularly dangerous as the hot liquid can climb up towards the stirrer and may then cause an explosion.

The required degree of mixing is generally affected by the type and grade of the base bitumen. Collins *et al.* [69] reported that blending a polymer with the Shell Martinez AR1000 bitumen required a blending duration of about 30 minutes while at least four hours was required for blending with a Boscan bitumen. Therefore, there is no standard blending time. The blending process is stopped when a homogenous blend is reached.

The simplest way to decide whether a polymer has been well blended is by carrying out a visual observation. This procedure is generally applicable for pelletised polymers. A good blend is reached when the size of polymer pellets in the blends become invisible.

More accurate evaluation can be carried out by observation under a microscope. The common microscopes used are Scanning Electron Microscope (SEM), Scanning Transmission Electron Microscope (STEM), and Fluorescence Optical Microscope (FOM). Under these microscopic observations, phase behaviour of polymer modified asphalt binders can also be studied. Different microscopes may use a different solution as the solvent, for example: a solution containing Osmium Tetroxide ( $\text{OsO}_4$ ) will be needed for SEM analysis as this solution will react with polymer-bitumen blends[25].

The other important parameters are temperature and the stage at which the polymer will be added to the bitumen. Both polymer and bitumen should have a certain viscosity during the mixing process. The stage at which the polymer is added to the bitumen and/or when the blend is mixed with the aggregates should be optimised. For example, mixing temperature in blending polyethylene, especially Novophalt, with bitumen, should be maintained higher than  $140^\circ\text{C}$ , i.e. maintained at between  $150^\circ\text{C}$  -  $170^\circ\text{C}$ , in order to get a good dispersion. The blend then needs to be mixed immediately with the aggregates just prior to compaction to avoid phase separation [34].

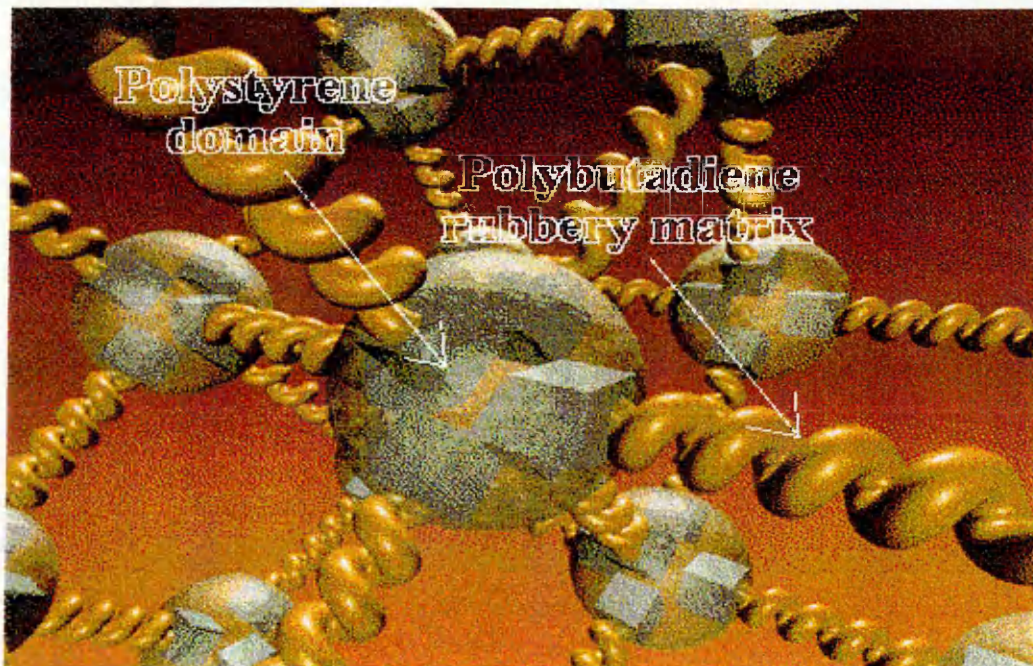


Plate 3.1 Three dimensional phase structure of thermoplastic rubber [extracted from Shell's Homepage and reproduced by kind permission of Shell International Ltd.]

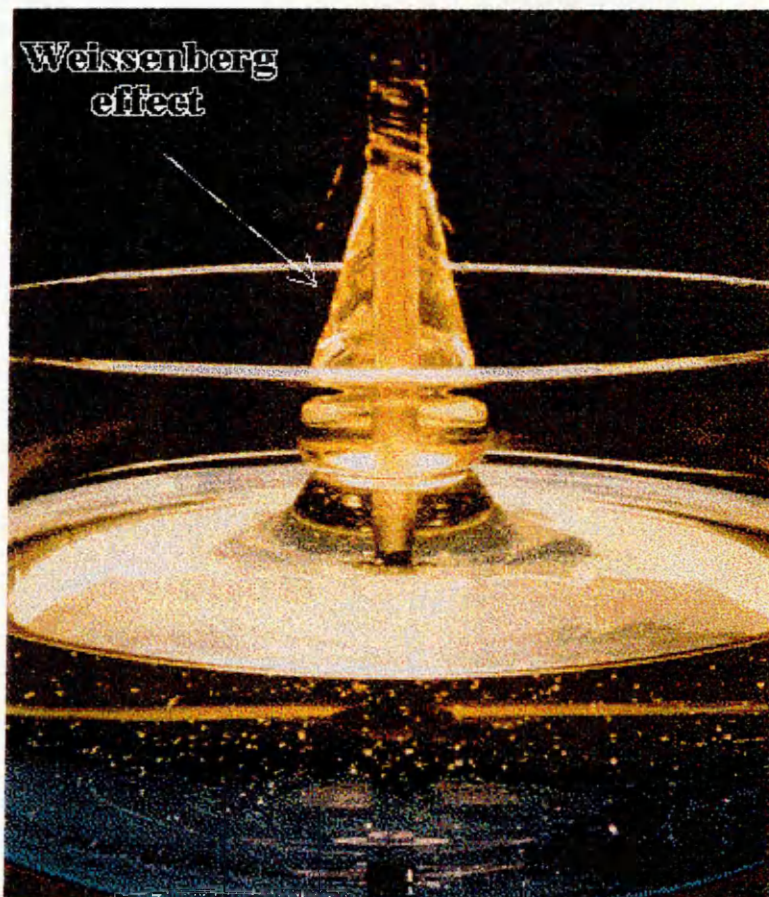


Plate 3.2 The Weissenberg effect during stirring of a polymeric liquid [extracted from Shell's Homepage and reproduced by kind permission of Shell International Ltd.]

### 3.4 Material Performance

Recently, the issue of performance-related tests has been attracting more attention from governmental offices, highway agencies, and researchers, as a method to define binder-aggregate interactions which significantly affect the end performance of bituminous pavements [70, 71]. The methods lead to the development of performance based specifications which are based on the measurement of fundamental engineering properties that reflect the critical failure modes of bituminous binders and their mixtures.

The idea of performance based specification originally arose from the need to have a specification which was simple, practicable, implementable over all environmental conditions, and was based upon fundamental principles applicable to all materials.

Some benefits that can be obtained from a performance-based specification [70] are:

1. Variability in a certain parameter, i.e. elastic stiffness, can be reduced because contractors will have to produce their materials to meet a specified level of quality. It has been reported [72] that a reduction in the variability of roadbase stiffness by 25% can increase pavement life by 7%.
2. Structural properties can be improved, i.e. increase in pavement life up to 40% and reduction in pavement thickness of up to 7%.
3. Manufacturers will have more flexibility to design their own materials to meet the specified requirements in a more economical manner.

The main components, that should be considered in pavement design, are load-deformation or stress-strain characteristics which are required for analysis of the structure and the performance characteristics that determine the mode of failure.

It is widely accepted that the main performance criteria for flexible pavements are resistance to fatigue and to permanent deformation. However, modified bituminous mixtures should offer more advantages than conventional ones in terms of actual field

performance. Therefore, their performance has been assessed to satisfy the following criteria:

1. Good tolerance to application under adverse conditions.
2. Good resistance to cracking.
3. Good resistance to degradation with time and high temperatures.
4. Good resistance to the effects of water at binder/aggregate interface.
5. Good resistance to permanent deformation.

In this section, these criteria are explained further by reference to prominent research work. Discussions of the work are also presented.

### **3.4.1 Tolerance to Application under Adverse Conditions**

Adverse conditions are defined as difficult conditions that might occur during laying and compaction of bituminous mixtures, i.e. cold weather conditions, which could have a deleterious effect on their mechanical performance. Modified binders, as they are assumed to possess superior properties, should offer the ability to withstand these conditions. Flexibility in accommodating varying laying temperatures is usually connected with high shear susceptibility allowing the binder to flow easily. However, the high shear susceptibility generally means a high temperature susceptibility, and, hence lower resistance to rutting. Therefore, modification should also provide a wide temperature range for laying and compaction without sacrificing the mechanical properties. The ability of modified binders to be laid in adverse conditions is predominantly affected by their viscosity.

### **Research on Polymer Modified Mixtures**

EVA copolymers help workability in cold weather construction as they are susceptible to shear [50]. An EVA modified mixture has been tested [49] and it was demonstrated that the workability was improved over 50 pen and 70 pen<sup>f</sup>. However, the workability of EVA modified mixtures can drop rapidly when the laying temperature falls below

---

<sup>f</sup> Unfortunately, there is no information on the base bitumen used for this modification. However, the resistance to permanent deformation of this EVA modified mixture, as shown by the wheel-tracking test, was also improved over the mixture with 50 pen bitumen.

minimum rolling temperature as the EVA modified bitumen stiffens rapidly due to the crystallisation of the polymer.

Denning and Carswell [73] reported an assessment of a polyethylene modified HRA, as a binder for rolled asphalt wearing course. The viscosity of the material, between 100°C and 190°C, was found to be greater than that of the conventional binder, i.e., 50 pen grade bitumen. This indicates that polyethylene modified mixtures require a higher temperature for both mixing and laying. During Marshall testing, both stability and density of the mixtures fell sharply below a compaction temperature of around 120°C. Their findings indicate that polyethylene modified mixtures are more difficult to compact at temperatures towards the lower end of the temperature range recommended for conventional mixtures. Finally, it was suggested that a rolling and compaction temperature of 10°C to 20°C higher and 40°C higher respectively than for a conventional mixture is required.

Thermoplastic rubbers have also shown a good tolerance to varying laying temperatures. An investigation on an SBS modified mixture reported that the modified mixture showed a very good tolerance in laying temperature [74], even though, the tolerance is still slightly lower than for an EVA modified mixture [49].

It has been shown that in most cases, polymer modified binders need higher laying temperatures than conventional mixtures, and that the temperature is critical especially when application takes place during cold weather.

### **3.4.2 Resistance to Cracking**

In general, resistance to cracking can be classified into three categories: fatigue cracking, low temperature cracking and reflective cracking. Research into the addition of polymer modifiers into bitumen has demonstrated that the modification can improve the resistance to cracking, i.e. thermal (low temperature), fatigue and reflective cracking. However, different polymers show significantly different performance with regard to each of the three mechanisms. For example, rubber modifiers have shown better resistance to reflective cracking than other polymer modifiers [75,76,77].

## 1. Thermal Cracking

Thermal cracking occurs when a rapid temperature drop leads to thermal stresses that exceed the tensile strength of the binder. Cracking may result from a single thermal cycle at which the temperature reaches a critical low temperature or repeated thermal cycling above critical temperature. This temperature is also sometimes defined as the temperature at which a bituminous mixture can no longer flow fast enough to relieve the stress (e.g. in a restrained rectangular specimen) as it attempts to contract because of the decreasing temperature.

### Binder tests

Penetration test at 4°C (5°C), low temperature ductility test and the Fraas breaking temperature test are the conventionally adopted tests to measure low temperature properties of bitumen with regard to the prediction of resistance to thermal cracking. These procedures, however, have been found to be no longer appropriate, especially in the use of polymer modified binders [97]. Therefore, more fundamental tests are proposed, such as the dynamic shear rheometer (DSR), bending beam rheometer (BBR) and direct tensile test.

In dynamic mechanical analysis, the loss tangent can be used as an indicator of whether a bitumen behaves as a brittle elastic solid or whether it maintains a viscous component. It has been presented [19] that binder rheology can give an indication of low temperature performance of bituminous mixtures. The rheology of the mixture largely reflects binder rheology, thus, binders with higher loss tangents will give mixtures with higher loss tangents. Hence, resistance to thermal cracking may be improved by selecting a bitumen that can maintain its viscous flow capability at low temperature. This characteristic is mainly found in soft bitumens, and therefore a modification of a soft bitumen with a polymer modifier can maintain low temperature performance without sacrificing high temperature performance. However, resistance to thermally induced cracking cannot be simply deduced from bituminous binder data because it is also strongly affected by the aggregate-binder combination and the presence of air voids.

The SHRP project recommends the use of BBR instead of DSR as binders tend to be too stiff to be reliably measured by DSR at low temperatures [97]. The BBR is used to measure the stiffness of bitumen by applying a constant creep loading at a constant temperature. The stiffness values are normally adopted for estimating the failure or strength properties of bituminous binders, however, the relationship between stiffness and strength properties of some binders especially polymer modified binders is not well known. Therefore, the direct tensile test is also recommended to be conducted to measure strength and the strain at failure [8].

### **Mixture tests**

Thermal Stress Restrained Specimen Test (TSRST) is a test developed for measuring the tensile stress developed in a bituminous mixture when cooled at a constant rate while being restrained from contracting. This test can provide data for stress at fracture and temperature at fracture, and is very reliable for ranking performance of modified mixtures at low temperature from good to poor or from acceptable to unacceptable [54]. Furthermore, the SHRP has proposed this apparatus to be a standard testing device for measuring the low temperature cracking properties of bituminous mixtures [71]. Typical results from the TSRST are demonstrated in Figure 3.23.

Based on this work, they concluded that the addition of polymers always improve the low temperature performance of a binder, however, the effectiveness of the additives can be dependent on the characteristics of the base binder [54].

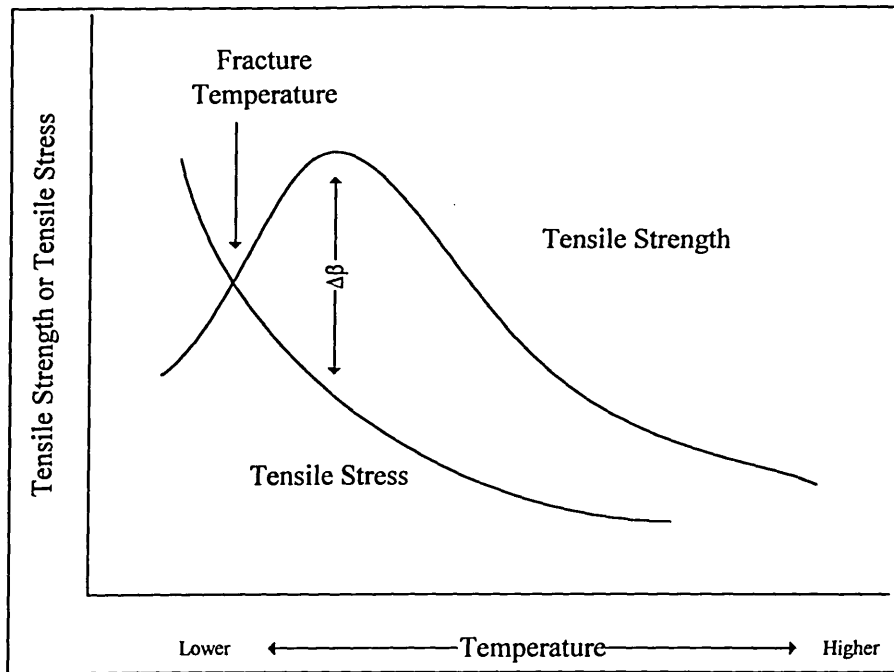


Figure 3.23 The effect of temperature on tensile strength and thermally induced stress, showing the maximum tensile strength reserve ( $\Delta\beta_{max}$ ) and the fracture temperature ( $T_f$ ). After Stock and Arand [54].

Goodrich [52] introduced the use of the limiting stiffness temperature (LST) concept as a parameter to assess the resistance of bituminous materials to thermal cracking. The LST is the temperature at which the bituminous mixture reaches a critical stiffness value, beyond which thermal cracking may occur, as measured by low temperature creep testing. Further, Goodrich stated that bitumen with small molecules has good viscoelastic behaviour at low temperature due to sufficient viscous flow that is needed to resist thermal cracking. This property has also been observed with the addition of two polymers into a soft bitumen and, hence, the addition of polymers improves the low temperature performance of bituminous mixtures.

## 2. Fatigue Cracking

Fatigue failure has been defined as the point at which a specimen no longer performs satisfactorily under application of load. Assessment of the resistance to fatigue cracking can be carried out in three loading arrangements, i.e. controlled stress, controlled strain, and more recently controlled dissipated energy [78]. There are also different varieties of testing apparatus that are used for fatigue testing, such as: three

points bending test, simple flexural test, four points bending test, cantilever with rotational bending test, and repeated load indirect tensile fatigue (RLITF) test. The analysis from these tests is generally focused on the tensile characteristics of the material. Review on these different testing arrangements and approaches has been presented previously [79, 81].

Tensile characteristics of bituminous mixtures are strongly influenced by the tensile characteristics of the binder they contain, of which the characteristics are better represented by the parameter of stiffness than either by stress or strain. Wheel tracking devices can be a good simulator for laboratory investigations into fatigue behaviour [80] as this apparatus can simulate actual loading by developing the dynamic loading action of a rolling wheel. However, the apparatus is rather elaborate and time consuming. Therefore flexural bending tests can be used as an alternative from using wheel tracking devices. The flexural bending tests can also give a good prediction of the fatigue characteristics of bituminous mixtures. The energy dissipation method can be used for explaining the fatigue characteristics of bituminous mixtures which eliminates the apparent inconsistency between fatigue life under controlled stress and similarly under controlled strain [81, 82].

### **Research on Polymer Modified Mixtures**

The addition of additives generally increases the fatigue life of bituminous mixtures. Widyatmoko [79] reported that the modification of a dense bitumen macadam (DBM) by a thermoplastic polymer improved resistance of the mixture against fatigue cracking. The tests were conducted on a four point bending apparatus at temperatures between 21-27 °C and the fatigue life of DBM mixtures were reported doubled up to ten fold by increasing the polymer content from 3.5% to 7% by mass of the total binder. Whereas Brennan and Clancy [83], who studied on the addition of polymer modifiers, also reported that the EVA modified HRA had the best performance in resistance to fatigue in comparison to other type of binders and mixtures, as measured by a uniaxial controlled stress fatigue test. The increase of fatigue resistance on other type of polymer modified binders have also been reported in previous research papers [35,57, 84].

### 3. Reflective Cracking

As has been presented previously in *Chapter Two*, reflective cracking is the propagation of a previously defined crack through subsequent layers of a pavement structure, they may be produced by low temperature cracking or induced traffic cracking. The solution to the reflective cracking is mainly by the application of stress absorbing membrane interlayers (SAMI) (see *Section 2.3.1.3*), however, research also reported that the use of polymers increases the material resistance to reflective cracking.

Rust, Coetser, and Verhaege [77] reported that roads in South Africa are more susceptible to load associated movements, which leads to reflective cracking, than to thermal movements. The observation that was conducted over a 5 year period reported that crumb rubber was the best modification technique with regard to the resistance to reflective cracking, i.e. the addition of 20% crumb rubber into 80/100 pen bitumen doubled the service life of the pavement in comparison to the addition of 2% SBR into the same base binder. The superiority of rubber modifier to prevent reflective cracking was also reported by Jimenez [76] and Strauss, Kleyu, and duPleiss [75] as it can maintain flexibility at low temperature without sacrificing high temperature performance.

#### 3.4.3 Resistance to Degradation with Time and High Temperatures

Degradation means that there are changes in properties during the service life of a pavement that lead to a weakening of the pavement. Laboratory investigations into the resistance to degradation with time, sometimes called resistance to long term ageing, are particularly important for predicting long term performance of a pavement. Excessive ageing can lead to embrittlement of bitumen which then causes further distress in the bituminous mixture in the forms of cracking, e.g. fatigue, thermal, or reflective cracking, and hence can significantly reduce the performance of the bituminous layers in the road pavement to support traffic loading.

The exposure of bituminous materials to high temperature conditions has similar effect as the time-ageing, as the high temperatures also cause oxidation of binders and

Chapter 3. Material Properties

evaporation of volatile fractions that can cause hardening and a resultant increase in stiffness, as well as brittleness making the bituminous mixture more susceptible to low temperatures and fatigue cracking.

Aged samples are usually obtained by manufacturing them in laboratory and applying an accelerated ageing technique or by coring them from observed pavement sections. However, it is very difficult if not impossible, to replicate the ageing shown by cored samples as obtained from pavements, in the laboratory. Some factors which significantly affect in service ageing are reported by Verhasselt and Choquett [85] as follows:

1. Susceptibility of the binder itself to ageing.
2. Porosity of the bituminous pavement.
3. Temperature.
4. Sun radiation particularly UV (ultra violet) and IR (infra red) rays. The UV rays will affect a very thin film layer of the binder at the surface (embrittlement), and the IR rays increase the mean temperature in pavement as they are absorbed (stiffening).
5. The nature of the aggregate.
6. Factors such as moisture, precipitation, aggregate porosity and deicing salts.

Several procedures have been proposed as methods to simulate aged bituminous binders and mixtures, as follows:

### 1. Procedure for bituminous binders

**Thin Film Oven Test (TFOT)** is a procedure that intended to simulate hardening of a bitumen sample, to the same point as occurs in a normal mixing plant. As specified in AASHTO T179 and D1754, the test is carried out by placing a 50 ml sample of bitumen in a weighed, flat bottomed sample with 140 mm inside diameter and 10 mm deep, The bitumen thickness is about 3 mm and heated for 5 hours at 163°C with it rotating at a speed of 5 to 6 revolution per minute. The mass loss is weighed after completion of the test, and sample is then used for further tests, such as the penetration or viscosity test [86].

A variant of TFOT has been developed and is known as the **Rolling Thin Oven Film Test (RTFOT)**, which is also an established test method to assess the durability of

bitumen against ageing as specified on AASHTO T240, ASTM D2872, DIN 52016. The procedure is quite different from the TFOT, that bottle glasses, each containing about 35g of bitumen, are rotated in an oven at 163°C for 75 minutes [86]. Film in thickness of about 1.25 mm can be obtained and at the end of the test, the bitumen is used for further tests [87].

**Pressure Oxygen Vessel (POV)** technique was developed by Lee [88] and uses a 3.18 mm (1/8 inches) thick bitumen film in a TFOT pan exposed to oxygen at 2.07 MPa (300 psi). Pure oxygen and elevated pressure are used to accelerate the rate of ageing [89].

**Thin Film Accelerated Ageing Test (TFAAT)** uses a 160 µm (0.0063 in) bitumen film deposited on the inside of a RTFOT bottle which contains a capillary opening to restrict volatile loss to an amount similar to that of pavement service. The TFAAT causes a similar level of chemical oxidation to the in-service ageing of 11 to 13 years old [87].

**California Tilt Oven Test (CTOT)** is another modification from RTFOT that a 35 g samples are heated at 111°C for 24, 72, and 168 hours with the oven slightly tilted to prevent asphalt build up. After the process, the RTFOT bottles are put into a 160°C oven for 20 minutes to obtain sufficient fluidity to pour the aged residue out of the bottles. This test is meant to simulate 2 years of exposure to a hot desert environment. One drawback of this test is that higher viscosity bitumens tend to roll less during the rolling process in the RTFOT, which may result in lower oxidation rate [90].

**Pressure Ageing Vessel (PAV) Test** is a method proposed by the SHRP researchers to simulate long-term ageing of bituminous binders. The procedure uses a standard TFOT pans that are placed in a PAV at 2 MPa air pressure. The pans are stored for 6 days at 71°C, or alternatively, for 20 hours at 100°C [3]. Oxidation of bitumen can be accelerated by application of a higher oxygen content through increased air pressure, of which this condition is closer to real exposure temperature. In the validation report, Petersen *et al.* [3] recommended to do the tests at several ageing temperatures

to simulate ageing in the desert. Therefore, it can be performed at 90°C, 100°C, or 110°C, depending on bitumen grade.

## 2. Procedure for bituminous mixtures

**Ultra Violet (UV)** chamber is a procedure that has been developed at the University of Florida, it involves the use of an UV chamber maintained at a temperature of 60°C to simulate the effects of heat, UV light, and air on bituminous mixtures. Chiu *et al.* [90] reported that no significant hardening of the bitumen residue was observed on samples exposed for 7 to 28 day in the UV chamber. They explained that this condition might be due to the formation of a thin skin on the surface of the sample during early UV exposure, which might seal the rest of the sample from oxidation.

**Short-term Oven Ageing (STOA)** is a procedure developed at the Oregon State University (OSU) under the SHRP A-003A test development program [92]. The procedure is conducted by curing mixture samples, that are placed loose in a pan at spread rate of approximately 21 kg/m<sup>2</sup>, in a forced-draft oven at 135°C for 4 hour period. During the curing period, the mixture is stirred and turned once an hour to ensure the ageing is uniform throughout the sample. After the curing period, the samples are conditioned to an equiviscous temperature of 665 + 80 cSt and then compacted.

**Long-term Oven Ageing (LTOA)** is also a procedure developed at the OSU to simulate long-term ageing. The procedure is conducted on compacted specimens that have been previously short-term aged by placing the specimens in a force-draft oven either at storage temperature of 85°C for a duration of 5 days or at a temperature of 100°C for a period of 2 days [92]. After the ageing period, the samples are left to cool in the oven to room temperature, and further tests can be done after 24 hours of the sample's removal from the oven.

As an alternative for long-term ageing procedure, the **Low Pressure Oxidation (LPO)** is also proposed by OSU [92]. The procedure also uses specimens after the have been short-term aged, but covered with silicon rubber to ensure the oxygen is flowing through the specimen rather than around the sides, and then the specimen is

put into a triaxial pressure cell and conditioned at a confining pressure of 10 to 30 psi, and then oxygen is passed to the sample at flow rate of 4 ft<sup>3</sup>/h.

**Link Bitutest Procedures** are the standard practices proposed for UK practice by the University of Nottingham for short term and long term oven ageing tests for compacted bituminous mixtures [87]. The short term ageing refers to hardening or embrittlement of the bitumen which may occur during any stage of road construction process. The procedure is simply to place loose bituminous mixture on a preheated metal pan to a depth of approximately 20 mm, and stored them in a force-draft oven at 135°C for 2 hours. After the curing period, the sample is then compacted at the specified compaction temperature. If the compaction temperature is greater than 135°C, then for dense bituminous macadams, the mixtures can be cured at the specified compaction temperature for about 2 hours prior to conditioning the sample to meet the compaction temperature, however, gap graded mixtures can be compacted without subjecting the mixture to the 2 hour cure [87]. The long term ageing is used to simulate the hardening of bitumen in the mixtures of 15 years or more in-service for dense graded mixtures. The procedure is conducted by placing the specimen in the forced-draft oven at temperature of 85°C for 120 hours. After the completion of 120 hours, specimen is left to cool to room temperature for about 24 hours, and then the specimen is ready for further tests [87].

### **Research on Polymer Modified Mixtures**

Excellent performance of polymer modified mixtures to resist ageing has been reported by many researchers. Rust, Coetser, and Verhaege [77] has conducted a series of field tests on trafficked pavements after 4 years of construction. The results obtained from sliding plate viscometer testing indicated that the addition of SBR-modified bitumen into the mixtures reduced the rate of increasing viscosity and increased the elastic recovery, when compared with a conventional binder.

Goodrich [19] has also observed the effect of ageing by using RTFOT and long term durability test (LTD<sup>8</sup>) methods. The results he obtained indicated that the addition of a polymer improves the resistance of ageing. However, he noted that the viscosity still increased but that the rate of increase of the viscosity was considered low. His results are supported by Chui-Te *et. al.* [90]. They conducted several ageing procedures, i.e. TFOT, CTOT, UV chamber, and PAV, and reported the benefits of using polymer modifiers for improving ageing resistance based on standard penetration value (25°C), absolute viscosity (60°C), infrared absorption spectral analyses, and dynamic mechanical analysis on the binders.

Studies at Oregon State University [91,92] suggested that the ageing of asphaltic mixtures was influenced by both the bitumen and the aggregate. Therefore, they suggested that ageing of the bitumen alone would not be sufficient for predicting mixture performance. Three different types of laboratory ageing procedures were conducted: STOA, LPO, and LTOA. The results indicated that the STOA procedure was not able to give a prediction of long term ageing. Dynamic mechanical tests were also conducted on both aged and unaged mixtures. The studies recommended the dynamic mechanical test as an excellent indicator of asphalt-aggregate mixture susceptibility to rutting or cracking before and after ageing, as shown from comparative relationships between complex moduli and phase angle before and after ageing.

Some laboratory studies have reported that the presence of polymers in bituminous binders significantly improves the mixture resistance against ageing. The improvement has been shown by results obtained from dynamic mechanical analyses [19,91,92] and size exclusion chromatography [19]. Furthermore, a field study has also proved that the addition of polymers shows a significant improvement in resistance to degradation with time [77]. The improvement was shown by the lower rate of increasing viscosity.

The use of dynamic mechanical tests to analyse ageing resistance is recommended by the Author. Some benefits of using this type of test are:

---

<sup>8</sup> LTD is a test with a similar procedure as CTOT.

1. It is non-destructive
2. It can generate results for a wide range of temperatures and frequencies
3. It can also provide excellent predictions to the performance of the bituminous mixtures.

The test can be done either on the binders or the mixtures, however, it is recommended to do the test on the mixtures. Scholz [87] stated that “ *although tests on the binders alone have shown a degree of correlation to field performance for a limited number of materials and under specific conditions, the effect of the aggregate is neglected even though the effect of the aggregate has been shown to have significant influence on the ageing characteristics of bituminous mixtures*”.

#### **3.4.4 Resistance to the Effect of Water at Binder/Aggregate Interface**

It has been witnessed that moisture can cause serious damage to the pavement construction [93]. No matter how well a pavement is designed, once moisture has entered the interlayers of the pavement, the pavement will begin to deteriorate, sometimes very rapidly.

Moisture usually enters a pavement through interconnected voids in the bound layers. The current standard specification for mixture design for HRA's allows a nominal void content of 4% whereas in practice it is allowed up to 6%. This value allows traffic to further compact the pavement during service life. However, these voids will also allow moisture to penetrate into the pavements' interlayers and interstices between the bitumen and the aggregate. This may then cause a series of problems such as stripping. In general, the adverse effect of water on bituminous mixtures is caused by two main mechanisms:

1. Reduction or loss of adhesion between the bitumen and the aggregate surface, known as stripping,
2. Reduction or loss of cohesion within the bitumen phase of the mixture, of which the damage can be deteriorated by the increase of permeability or voids in mixture, and environmental conditions such as extreme temperature, high loading, high degree of saturation.

### Test Methods

A Study by Terrel and Shute in 1989 [93] reported that there was no standard specification that was widely accepted for assessing the effect of moisture on asphalt-aggregate interaction. The study presented several methods that were being implemented in different US' States. The methods were summarised as shown in Table 3.8.

**Lottman moisture susceptibility testing** is a standard ASTM test for measuring resistance to stripping under water immersion for bituminous mixtures. Samples are run through the Lottman vacuum saturation freeze-thaw procedure to generate adhesion failure. This procedure relies on measuring the indirect strength before and after conditioning to indicate the potential for adhesion failure of the mixture in service. A study [94] using this test indicated that modified bituminous mixtures did not decrease the moisture sensitivity. Later investigations on modified bituminous mixtures use a modified version of the Lottman test.

The most recent conditioning system to evaluate the performance of bituminous mixture in the presence of water has been developed by Terrel and Al-Swailmi [71], called the **Environmental Conditioning System (ECS)**. The system has three major subsystems: fluid conditioning, environmental conditioning cabinet and loading system. The test procedure is summarised in Table 3.9 with the proposed methods for assessing the performance of the mixture presented in Table 3.10.

Table 3.8. Evaluation of water sensitivity test methodologies [93]

Method (Reference)	Application of Test Results	Advantages	Limitations	Simulation of Field Conditions	Ease of Use
1. Lottman (NCHRP 246, AASHTO T283)	<ul style="list-style-type: none"> <li>Diametral Resilient Modulus (MR) test</li> <li>Diametral Indirect Tensile Strength</li> </ul>	<ul style="list-style-type: none"> <li>Severe test</li> <li>Wide range of mixes and cores</li> <li>Good for lime and liquid additives</li> </ul>	<ul style="list-style-type: none"> <li>Time consuming (3 days/cycle)</li> <li>Equipment is expensive</li> </ul>	<ul style="list-style-type: none"> <li>Good correlation with field performance</li> <li>Simulates freeze thaw condition</li> </ul>	<ul style="list-style-type: none"> <li>Moderately complex</li> </ul>
2. Tunnickliff Root (NCHRP 274)	<ul style="list-style-type: none"> <li>Diametral Tensile Strength</li> <li>Visual rating</li> </ul>	<ul style="list-style-type: none"> <li>Wide range of mixes, cores</li> <li>Good for additives</li> </ul>	<ul style="list-style-type: none"> <li>Requires trial mixes to obtain air void level</li> <li>May not be severe enough</li> </ul>	<ul style="list-style-type: none"> <li>Initial use shows good correlation with field performance</li> </ul>	<ul style="list-style-type: none"> <li>Moderately complex</li> </ul>
3. Boiling Water (ASTM 3625)	<ul style="list-style-type: none"> <li>Stripping potential</li> <li>Visual rating</li> </ul>	<ul style="list-style-type: none"> <li>Initial screening</li> <li>Simple equipment</li> <li>Laboratory or field mix</li> <li>OK for additives</li> </ul>	<ul style="list-style-type: none"> <li>Subjective analysis</li> <li>Loose mix only</li> <li>Water purity has effect</li> </ul>	<ul style="list-style-type: none"> <li>May indicate potential for stripping</li> </ul>	<ul style="list-style-type: none"> <li>Simple</li> </ul>
4. Texas Freeze- Thaw Pedestal (T.W. Kennedy, 1983)	<ul style="list-style-type: none"> <li>Cracking after number of freeze- thaw cycles indicates degree of moisture susceptibility</li> </ul>	<ul style="list-style-type: none"> <li>Measures additives effectiveness</li> <li>Simple</li> </ul>	<ul style="list-style-type: none"> <li>Only fines used</li> <li>Time consuming (1 day/cycle)</li> <li>Measure only cohesion</li> </ul>	<ul style="list-style-type: none"> <li>Only fair correlation with field performance</li> </ul>	<ul style="list-style-type: none"> <li>Simple but special equipment required</li> </ul>
5. Immersion-compression (ASTM D1075, AASHTO T-165)	<ul style="list-style-type: none"> <li>Visual assessment</li> <li>Minimum compressive strength</li> </ul>	<ul style="list-style-type: none"> <li>Uses actual mix</li> <li>Simple</li> </ul>	<ul style="list-style-type: none"> <li>Time consuming</li> <li>Air voids play large role</li> <li>Poor reproducibility</li> </ul>	<ul style="list-style-type: none"> <li>Correlation not known (if any)</li> </ul>	<ul style="list-style-type: none"> <li>Simple</li> <li>Equipment should be readily available</li> </ul>
6. Static Immersion (ASTM D1664, AASHTO T-182)	<ul style="list-style-type: none"> <li>Potential for stripping; &lt;95% coating</li> <li>visual assessment</li> </ul>	<ul style="list-style-type: none"> <li>Simple, quick</li> <li>Low cost</li> </ul>	<ul style="list-style-type: none"> <li>Subjective evaluation</li> <li>Loose mix only</li> <li>Not sufficiently severe</li> </ul>	<ul style="list-style-type: none"> <li>Short term stripping potential only</li> </ul>	<ul style="list-style-type: none"> <li>Simple</li> </ul>
7. Retained Stability (no standard method)	<ul style="list-style-type: none"> <li>Ratio of soaked (wet) to dry of Marshall stability</li> </ul>	<ul style="list-style-type: none"> <li>Uses conventional specimens and equipment</li> </ul>	<ul style="list-style-type: none"> <li>No standard conditioning or criteria</li> </ul>	<ul style="list-style-type: none"> <li>Not known</li> </ul>	<ul style="list-style-type: none"> <li>Simple</li> </ul>

Table 3.9 Summary of the ECS test procedure [87]

Step	Description
1.	Prepare test specimens as per SHRP protocol
2.	Determine the geometric and volumetric properties of the specimen. Determine the triaxial and diametral modulus using the MTS system
3.	Encapsulate specimen in silicon sealant and latex rubber membrane, allow to cure overnight (24 hours)
4.	Place the specimen in the ECS load frame, between two perforated teflon disks, determine air permeability
5.	Determine unconditioned specimen (dry) triaxial resilient modulus
6.	Vacuum condition specimen (subject to vacuum of 51 cm (20 in.) Hg for 10 minutes)
7.	Wet specimen by pulling distilled water through specimen for 30 minutes using 51 cm (20 in.) Hg vacuum
8.	Determine unconditioned water permeability
9.	Heat the specimen to 60°C (140°F) for six hours, under repeated loading. This is a hot cycle
10.	Cool the specimen to 25°C (77°F) for at least four hours. Measure triaxial resilient modulus and water permeability
11.	Repeat steps 9 and 10 for two more hot cycles
12.	Cool the specimen to -18°C (0°F) for 6 hours, without repeated loading. This is a freeze cycle
13.	Heat the specimen to 25°C (77°F) for at least 4 hours and measure the triaxial resilient modulus and the water permeability
14.	Split the specimen and perform a visual evaluation of stripping
15.	Plot the triaxial resilient modulus and water sensitivity

Table 3.10 Variables addressed during development of the ECS [71]

Issue	Proposed	Selected Method	Rational
Strength or stiffness measurement	<ul style="list-style-type: none"> <li>• Diametral modulus</li> <li>• Triaxial modulus</li> <li>• Indirect tensile strength</li> </ul>	<ul style="list-style-type: none"> <li>• Triaxial modulus (ECS-M<sub>R</sub>)</li> </ul>	<ul style="list-style-type: none"> <li>• Compatible with flow system</li> <li>• Non-destructive</li> </ul>
Specimen dimensions	<ul style="list-style-type: none"> <li>• 20 cm (8 in.) height x 10 cm (4 in.) diameter (ASTM D3497)</li> </ul>	<ul style="list-style-type: none"> <li>• 10 cm (4 in.) height x 10 cm (4 in.) diameter</li> </ul>	<ul style="list-style-type: none"> <li>• Typical pavement layer thickness</li> <li>• Reasonable flow path length</li> <li>• Minimise end effects</li> </ul>
Strain measurements	<ul style="list-style-type: none"> <li>• Strain gauges</li> <li>• LVDTs</li> </ul>	<ul style="list-style-type: none"> <li>• LVDTs</li> </ul>	<ul style="list-style-type: none"> <li>• Ease in use</li> <li>• Reusable</li> </ul>
Frictionless interface between specimen and loading platens	<ul style="list-style-type: none"> <li>•</li> </ul>	<ul style="list-style-type: none"> <li>• Perforated teflon disks</li> </ul>	<ul style="list-style-type: none"> <li>• Allows water flow</li> </ul>
Surface perimeter flow	<ul style="list-style-type: none"> <li>• Use latex membrane to seal middle third of specimen</li> <li>• Encase specimen in 15 cm (6 in.) latex membrane</li> </ul>	<ul style="list-style-type: none"> <li>• 15 cm (6 in.) latex membrane</li> </ul>	<ul style="list-style-type: none"> <li>• Simple</li> <li>• Ensures no flow along specimen surface</li> </ul>
Specimen end condition preventing flow	<ul style="list-style-type: none"> <li>• Wet cut ends</li> <li>• Ambient dry cut ends</li> <li>• Use specimens as manufactured by the kneading rolling compactor</li> </ul>	<ul style="list-style-type: none"> <li>• Use specimens as manufactured by the kneading or rolling compactor</li> <li>• Use cooled dry cut for field specimens</li> </ul>	<ul style="list-style-type: none"> <li>• Do not want to introduce water into specimen</li> <li>• Ambient cutting smears asphalt, sealing specimen</li> </ul>

In the recent investigation, Scholz [87] introduces a new approach in assessing aged samples. Modification has been made of a dynamic shear rheometer, that the binders to be sheared are coated on a disc of mineral aggregate plate used in the mixture, rather than only on a steel plate. This arrangement demonstrated that tests conducted on a binder coated on the steel plate may ignore the effects contributed by the mineral aggregate to the binder, which may lead to inappropriate characterisation of the binder with regard to the potential performance of the mixture. However, this test is not recommended for a routine test, therefore, an additional ageing test to see the aggregate susceptibility is recommended in order to support results obtained from the normal arrangement (by using steel plate).

### **Research on Polymer Modified Mixtures**

Schuller and Forsten [95] conducted a series of tests to investigate the performance of modified bituminous mixtures, i.e. by the addition of an SBS copolymer, before and after water immersion. They used three different sets of apparatus to conduct the tests, i.e. Marshall test, indirect tensile test and Troger test. The samples with polymer modified binders were found to be slightly less water sensitive than the samples with normal straight run bitumen. However, this result could be explained by the fact that the modified mixtures had higher initial stiffness than the unmodified ones. The rolling bottle test was also conducted to observe the adhesive properties of the binders. However, this "adhesive" test was found to be unreliable.

King *et al.* [96] presented a paper in the proceedings of Association of Asphalt Paving Technologists (AAPT) that discussed the stripping resistance of mixtures with modified binders. The samples that were tested in both the dry and the water exposed conditions were found to have very different performances. The assessment of performance was based on strength and stability tests such as Marshall, unconfined compression and split tensile test. The results demonstrated that the modified mixtures had wet strengths within ten per cent of the dry conventional asphalt mix with the same design. However, the relative performance of both modified and unmodified when comparing the wet condition to dry condition was found to be similar, i.e., wet strength was 50%-65% of dry strength.

It appears that the addition of polymers improves the adhesion between aggregates and binders in wet conditions. The Modified Lottman test offers better results when compared with the tests shown in Table 3.8, as the specimens have been subjected to the worst conditions likely to be encountered in service.

### **3.4.5 Resistance to Permanent Deformation**

Permanent deformation occurs when bituminous pavements accumulate plastic deformation caused by the repeated application of loads generally at high service temperatures, i.e. greater than 45°C. Permanent deformation is sometimes considered as the most critical failure parameter, especially for heavy duty pavements, as it does not only reduce driver comfort and safety for vehicles passing over areas that are badly rutted, but it structurally damages the pavement and can cause traffic accidents.

#### **Test Methods**

Some pieces of apparatus have been developed and used to measure laboratory permanent deformation in order to predict the permanent deformation which will occur in the field, i.e.: Marshall test, confined (triaxial) creep test, unconfined creep test, repeated load axial tests, Hveem Stabilometer, and wheel tracking tests.

The creep tests have been widely used to check whether a material has adequate resistance to permanent deformation whereas the wheel tracking tests are considered to give a better simulation of the permanent deformation mechanism that takes place in pavement.

Additions of polymer modifiers have provided significant contributions to pavement performance in the resistance to permanent deformation. However, polymer responds in a different way and, hence, gives different results if it is tested by different test configurations.

Laboratory test devices that were originally for conventional binders have been adopted to investigate the performance of modified binders. Some of them have demonstrated a fair correlation with field performance. The devices can be summarised as follows:

### 1. Wheel Tracking apparatus

Amongst the various tests available to evaluate the resistance to permanent deformation, the wheel tracking test is traditionally considered to be the best test in predicting the pavement performance as it simulates traffic loading on the actual pavement. Therefore, it is recommended that the wheel tracking test be used for measurement resistance to permanent deformation of polymer modified mixtures [95,97,98,99].

### 2. Repeated Load Triaxial test

The repeated load triaxial test has been recommended as the best alternative test to the wheel tracking test, as it can provide a confinement to the sample thus allowing the shear mechanism to take place as opposed to compressive failure [98].

### 3. Dynamic Creep Test

Dynamic creep data for polymer modified asphalt mixtures confirms the results found using wheel tracking [100]. Therefore, this mixture test can also be adopted to predict the performance of modified asphalt mixtures with regard to the resistance to permanent deformation.

Repeated load axial (RLA) testing with a NAT machine also gives similar results to the dynamic creep test [99,101]. Further Brown and Cooper [102] explained that the RLA test uses the same principle as the dynamic creep in the sense that the specimen is subjected to repeated application of axial stress.

### 4. Static Creep test

The static creep test does not give a good correlation with the dynamic creep test, the wheel tracking test, or the Laboratory Test Tracks results [69,99,100]. The test can only differentiate between conventional mixtures with a low elastic recovery after removal of the load. Further, it has been previously discussed [103] that there are two fundamental things missing in the static creep test: one is repeated loading, and the other is confining stress. Therefore, it is better not to adopt this test for predicting pavement performance especially in the case of non-conventional mixtures.

The common laboratory test condition for creep testing is conducted under a test temperature of 30°C or 40°C. Test temperatures higher than 60°C are not recommended, as under high temperature conditions the differences between binders are not so obvious. This is considered to be because the mixture performance will be mainly affected by the aggregate in mixture. Therefore, for high temperature performance, a good mixture design is preferred to changes in the binder properties.

#### 5. Marshall test

The use of the Marshall test to predict the resistance to permanent deformation should be avoided as the test is an empirical test that does not measure any fundamental mechanical property and, therefore, cannot give a good prediction of the performance of bituminous mixtures with regard to any property [98,101]. In the case of modified mixtures, the test is not sensitive to the permanent deformation characteristics of the mixture, i.e. the test results were not consistent with observed pavement performance [101], even though Marshall stabilities tend to increase when a polymer is added [104].

#### 6. Hveem Stabilometer

The Hveem test method is sensitive to bitumen content and gives a similar ranking of mixtures to that observed in triaxial (confined) repeated load testing. However, the Hveem Stabilometer cannot rank mixtures according to bitumen types and, therefore, it is unlikely to be applicable for modified mixtures [101].

From these various test methods, there are certain factors that should be considered when determining the permanent deformation characteristics in the laboratory such as: stress level, stress path, temperature, confinement, compaction, binder content, binder type, aggregate type, packing characteristics, *etc.* Further discussions on these factors are presented in *Chapters Four and Seven.*

### Research on Polymer Modified Mixtures

The TRL [49,109,73] has conducted investigations on the use of ethylene vinyl acetate copolymers (EVA) and sulphur as additives to rolled asphalt wearing course in a wheel tracking machine. It was found that EVA gave significant improvement in the resistance to permanent deformation of rolled asphalt. The polymer did not only increase the Marshall stability up to 20% but it also contributed a significant reduction in the wheel tracking rate and furthermore, it made it less sensitive to binder content. The addition of EVA at five percent by mass of binder was found to be more than sufficient to equal or improve the resistance to permanent deformation achieved with heavy duty bitumen having the highest softening point permitted for rolled asphalt wearing courses.

The softening point of modified binder was considered to have a poor correlation with wheel tracking test, especially for binders with highly viscoelastic properties such as SBS copolymer. However, a good correlation was found in the relationship between the apparent viscosity at a shear rate of 0.05 per seconds at a temperature of 45°C and wheel tracking rate at a test temperature of 45°C for all binders studied.

Another piece of work [47] reported that the improvement of resistance to permanent deformation by EVA copolymers was contributed by the molecular weight and the VA content of the EVA copolymers. Wheel tracking tests on HRA samples with 70 pen grade base bitumen at 5% polymer addition was conducted to simulate permanent deformation. The test temperature was set at 45°C. The results indicated that addition of EVA copolymers with higher molecular weight and lower VA content can improve the resistance to permanent deformation. The improvement was reported up to 3 to 5 fold as compared with the unmodified mixture.

Luxemburg and Hanzik [105] investigated the performance of elastomers on the resistance to permanent deformation of bituminous mixtures. The wheel-tracking tests which conducted at test temperature of 40°C and 50°C indicated that the addition of elastomers improve the resistance to permanent deformation. At the test temperature of 40°C, permanent deformation of modified mixtures were lower than the unmodified ones, i.e., approximately 55%-80% of the unmodified mixtures. The longitudinal sections of permanent deformation on the modified mixtures were found to be 55%-

Chapter 5. Material Performance

85% of the unmodified mixtures. The average deformation of the polymer modified mixture was 55%-60% of the unmodified mixtures. At the test temperature of 50°C, the permanent deformation of the unmodified mixtures was found to be double as compared with the rut depth at 40°C whereas the modified mixtures performed much better, i.e. the rut depth was only 35% greater than when tested at 40°C. Therefore, besides increasing the resistance to permanent deformation, these results also indicated that the polymer modified mixtures had less temperature susceptibility than the unmodified mixture.

Collins *et. al.* [69] investigated the influence of the mechanical properties of the binders on the resistance to permanent deformation on the addition of SBS copolymer. They stated that the overall mixture performance, as measured by using a wheeltracking device, could be influenced significantly by the rheological behaviour of the binder. The permanent deformation resistance could also be improved by polymer modification, especially at concentrations at which allowed network structures to be developed. The blend containing 6% SBS by mass of the binder was reported to increase the rutting resistance by a factor of 7.5.

King *et. al.* [97] reported that the present trend of using softening point as a parameter to predict resistance to permanent deformation should be changed. The results from wheel tracking test indicated that it is dangerous to use softening point solely as the parameter for predicting rutting resistance. They explained that the correlation between softening points and permanent deformation can reasonably be used at fairly low level of polymer modifier concentration. They emphasised that at higher level of polymer content, this correlation should not be used as soft bitumen with high polymer content can achieve high softening point while these do not necessarily have a good rut resistance. However, the addition of polymer at a proportional amount can be used effectively to improve high temperature performance. This can be explained from the results obtained from the wheel tracking test that once a binder reached a certain stiffness level, the addition of polymer had only a marginal effect on resistance to permanent deformation. Conclusions drawn from this experiment proved that conventional bitumen tests such as penetration, absolute viscosity, kinematic viscosity, and ring and ball softening point did

not correlate well with the predicted rutting result from laboratory simulator when polymers were added as the modified binders.

Dynamic mechanical analysis results indicated a good correlation with wheel tracking results. When corresponding temperature and frequency parameters were used in the analyses, the viscous modulus  $G''$  and the complex modulus  $G^*$  could predict rut depths on French wheel tracking simulator. However, the loss tangent ( $\tan \delta$ ) at  $60^\circ\text{C}$  did not correlate well with the rut depths. This result was explained as the temperature dropped from  $60^\circ\text{C}$  to  $30^\circ\text{C}$ , a cross-over in the stiffness-temperature relationship of modified asphalt was taking place. Therefore, the selection of the appropriate test temperature and frequency to estimate the high temperature performance of modified mixtures is critical in dynamic mechanical analysis. However, it can be concluded that, from both dynamic mechanical analysis and wheel tracking results at  $60^\circ\text{C}$ , polymer has a tendency to reduce rutting.

The influence of the aggregate on high temperature mixture properties analysed by using a dynamic mechanical analysis was reported by Goodrich [19]. The loss tangent was found to be a good indicator for high temperature properties. This means that the lower the loss tangent at high temperature, the more elastic the mixtures and hence more resistance to creep deformation. The results obtained from dynamic mechanical analysis of mixtures indicated that at middle temperatures ( $10^\circ\text{C}$  to  $50^\circ\text{C}$ ) the asphalt concrete rheology was influenced by both the binder and the aggregate while at high temperature it was predominantly influenced by the aggregate. At high temperatures, the differences in the binders were not so obvious in the dynamic mechanical properties of the mixtures. The rheology of the mixture at test temperatures above  $50^\circ\text{C}$  is only affected by high levels of modification. Therefore, to achieve the best mixture stability at high temperature, a good mixture design was preferred to changes in binder properties.

### 3.5 General Discussions

#### 3.5.1 Properties of Polymer Modified Binders

Bitumen has thermoplastic behaviour, but the behaviour of polymers varies according to their main chemical components, i.e. thermoplastics, rubbers, or combination from both components (such as thermoplastic rubbers). The chemical structure of polymers is usually definite but this is not the case for bitumens. Therefore, a blend of polymer and bitumen can exhibit various behaviours.

Researchers have reported the importance of swelling of polymer in bitumen. However, none of them had explained definitively about what this swelling phenomenon is. Van Beem and Bresser [26] explained the importance of swelling for bitumen modified by crosslinked polymer as being necessary to obtain a good dispersion. Brule, Brion and Tanguy [24] reported that the extent of swelling of SBS modified bitumens decreases as the polymer content increases. However, general opinion says that if a polymer is added at higher amounts, the performance should be higher. Predominantly the swelling phenomenon has been observed and reported for crosslinked elastomers, such as SBS. Hence this would seem to indicate that the swelling phenomenon has little to do with mixture performance as SBS is a proven modifier. Therefore, it may be prudent to state that swelling is only a phenomenon that occurs on blending an elastomer with a bitumen, and this does not necessarily have an effect on the end performance of the mixture.

There are conflicting arguments about the role of polymer, as to whether the polymer is acting solely as a binder or also as a filler [40], and whether there is bridging between the aggregates. The arguments about polymer bitumen interaction that appear during this literature search are:

1. The possibility that the interaction mechanism between polymer and bitumen could be affected by the polymer size and/or interstices or the 'gap' between the particles within the microstructure of bitumen.

Polymers with a size just large enough to fill the 'gap' within the bitumen may produce an enhanced performance of the blend. Therefore, this hypothesis supports the argument that polymers act as a filler to the bitumen (Figure 3.24).

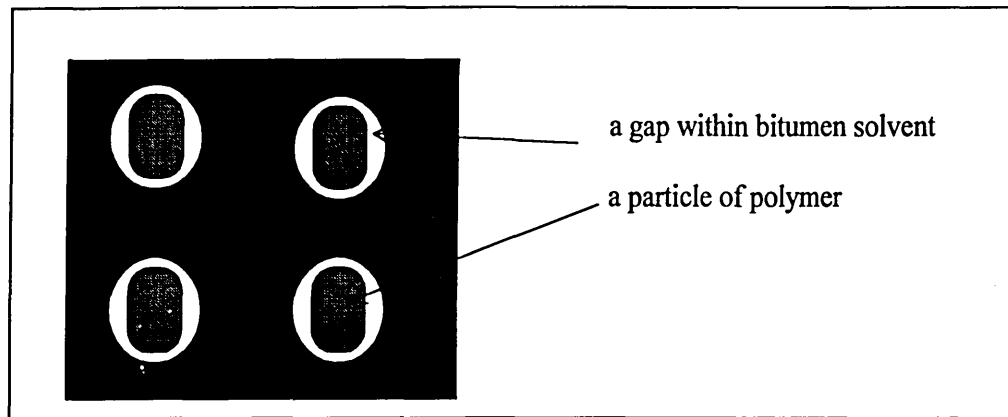


*Figure 3.24 A model of polymer-bitumen interaction where polymer particles fill the gaps within bitumen solvent.*

Anderson, Christensen, and Bahia [106] reported that many polymers have a plateau zone in their microstructure whilst this zone is never found in bitumens. The plateau zone is a zone where the phase angles or moduli recorded in a dynamic mechanical test are not affected by changes in temperature, which means that the material maintains its elasticity, that can be an indication of molecular entanglements in a form of network structure. This behaviour is normally seen in polymeric materials but not in bitumen at intermediate temperatures (or loading times). Therefore, the presence of polymer may create this kind of network structure in the polymer bitumen blends (see Figure 3.25).

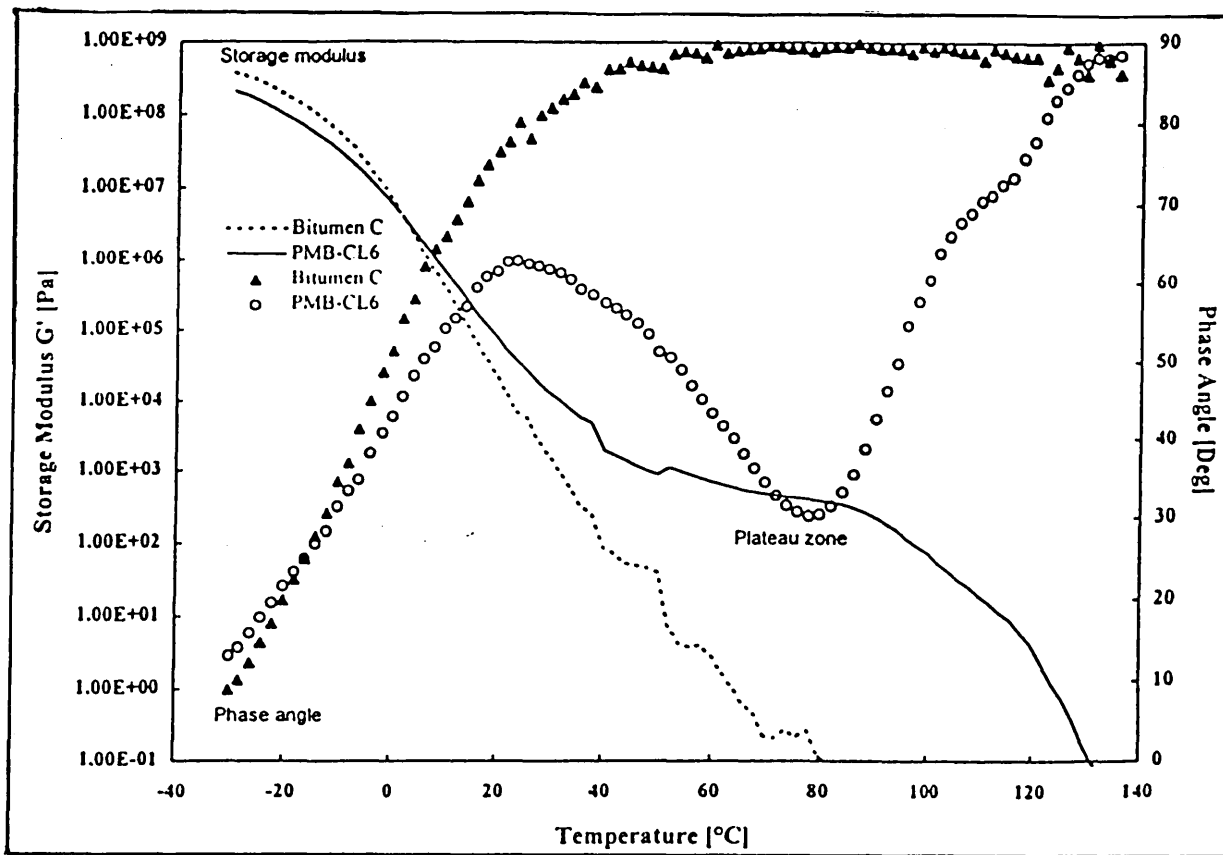


Figure 3.25 Storage modulus and phase angle of base and 6% linear SBS polymer modified Bitumen C at  $1 \text{ rad.s}^{-1}$  as a function of temperature. After Lu and Isacsson [111].

Another theory states that bitumens create porous structures like "holes" when subjected to heat application. The "holes" are created from molecular movements on heating which follows the free space (free volume) concept where spaces arise from thermal expansion of the liquid without changing the phase, as illustrated in the Figure 3.26.

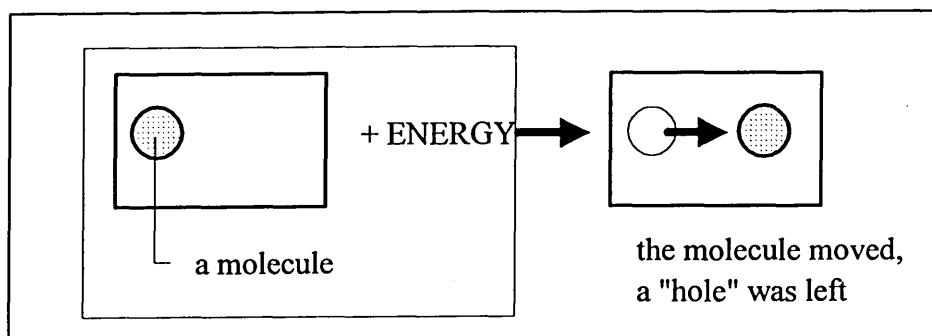


Figure 3.26 Illustration of molecular movement due to heat application within the bitumen's microstructure.

Polyethylene at high service temperature, i.e. at 50 °C, has the tendency to act as a filler in the polyethylene bitumen blend [40]. Van Beem and Bresser [26] explained that hot blends of modified binders with linear crystalline polymers have a very coarse dispersion similar to a bitumen-mineral filler system. This filler system has been witnessed to contribute additional performance for the blends. However, whether or not a network was developed in polymer-bitumen blends still needs further investigation and how these fillers, i.e. the polymers, structure themselves into "this network" also need further investigation.

2. Another way of explaining the polymer-bitumen interaction is if it is assumed that the polymer particles are well dispersed in bitumen solvent then the interparticle distance between two neighbouring polymer particles will have a strong contribution to the performance of the polymer-bitumen blend.

A critical interparticle distance (Figure 3.27) has been proposed as a parameter that determines the tough-brittle transition points of rubber, i.e. in nylon [107]. If the interparticle distance is greater than a critical value, the blend is considered as brittle. Conversely, a blend will be tough if the distance is smaller than the critical value. The rubber volume fractions used in this study were 10%, 15%, and 25%. Therefore, this model may not be economically applicable for polymer-modified bitumen unless a further investigation is conducted for lower polymer contents, i.e. less than 10% of binder content.

Others have reported that the maximum performance of polymer modified bituminous binders is achieved when a polymer is finely dispersed within the bitumen [24,34]. Binders with a coarser microstructure tend to be more brittle at low temperature. This may indicate the importance of interparticle distance on binder performance.

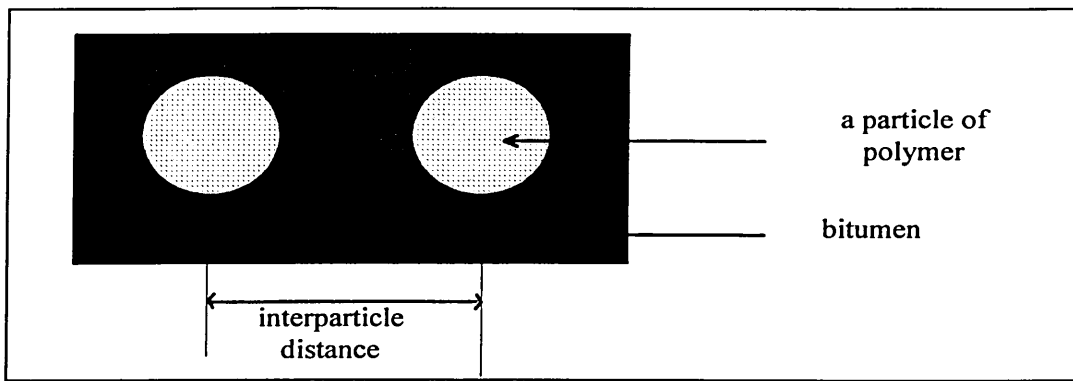


*Figure 3.27 A model of polymer-bitumen interaction showing interparticle distance between polymer particles within bitumen.*

### 3. Glass transition temperature as an indicator of low temperature property.

The importance of the glass transition temperature, as an indicator of the stage of brittleness or flexibility of a material as a function of temperature, has been witnessed in polymeric materials [15]. Further Zanzotto [108] also indicated that "the properties of the material at glass transition temperature of different materials are equal". In the case of polymer modified bitumen, a polymer that has a low glass transition temperature can improve low temperature properties [109].

Anderson et. al. [106] anticipated that there should be a direct relationship between glass transition temperature and molecular weight for bitumens, as is the case for all polymers, while the average molecular weight will control the temperature dependency of bitumens.

However, further investigations and verifications are required to know which, if any, of these three possibilities is valid.

Other parameters that can be considered in analysing modified binders are molecular weight and molecular size. The molecular weight in the terms of the molecular weight distribution or state of dispersion can be important in characterising polymer modified binders in relation to mixture performance.

Some parameters that should be controlled during blending polymer with bitumen are:

1. Type of mixer, high shear mixers are preferred.
2. Blending duration, the blending duration is governed by the stage when the polymer has dispersed properly in bitumen.
3. Blending temperature should be as low as possible but the blend should remain workable (blending temperature greater than 190°C is not recommended)
4. The point when a polymer to be added with a bitumen during blending.

The storage stability test is important to assess the stability of the phase of dispersion of polymer bitumen blends after being stored for prolonged periods. Amongst the various methods, the beverage can method offers more benefits because of the simplicity and cost-effectiveness of the test and also because the quantity of samples recovered after the storage is sufficient for conducting several tests, such as dynamic mechanical test, penetration and softening point, and observations on the phase of dispersion under microscope. The Author recommends stability test to be essential for polymer modified binders.

Problems in conducting and correlating the results obtained from ring and ball softening point tests were identified in several reports [73, 76, 97, 99], that the relative increase in softening point value does not reflect the relative increase in the performance of bituminous mixture especially in the presence of polymer modified binders, e.g. with regard to the resistance to permanent deformation. Dynamic mechanical tests are recommended by the Author as being suitable for the assessment of performance based properties of polymer modified binders.

### **3.5.2 Performance of Polymer Modified Mixtures**

Almost all literature reviews report that polymers significantly improve the performance of bituminous mixtures. The level of improvement on the performance, however, is achieved by the polymer modified binders using different mechanisms and also varies dependent upon the polymers used and the characteristics of the base binder, i.e. the bitumen. 'Compatibility' between a polymer and a bitumen provides the key to producing a high performance binder and, hence, a high performance mixture. The term

'compatibility' here is defined as the ability of a polymer to be dispersed easily into a bitumen and to produce a stable blend.

Some conventional tests have been found to correlated poorly with the field when a polymer is used for binder modification. Based on the literature reviews, the Author recommends certain tests that can provide a good prediction of the performance of modified mixtures, i.e.:

1. Flexural tests on beams which can be used to investigate the resistance to fatigue cracking of modified mixtures. Simple laboratory simulations can also be carried out using wheel-tracking apparatus on a resilient support.
2. Thermal cracking is reflected well by the Thermally Stress Restrained Specimen Test. The test procedure can be referred to that proposed by SHRP.
3. Resistance to degradation with time can be predicted using the tensile characteristics of oxidised specimens. Methods of conditioning for laboratory aged samples can be done by adopting ageing procedures proposed by SHRP methods. Alternatively, the simplified method proposed from the LINK Bitutest study can be adopted to produce reasonable laboratory aged samples.
4. Resistance to degradation from the presence of water at the binder-aggregate interface can be simulated by immersion wheel tracking devices. The environmental conditioning system (ECS) with its related test methods is good as an accelerated test for assessing durability of bituminous mixtures. Alternatively, the modified Lottman test also gives an indication of the performance of modified mixtures under the worst case condition.
5. Wheel-tracking apparatuses can be, in principle, adopted as a laboratory simulation test with regard to the mixture's resistance to permanent deformation. Dynamic creep or repeated load axial testing in a fully confined condition can also provide a good correlation with wheel tracking results and, hence, with in-service performance.

In most cases, the use of dynamic mechanical analysis can give a good reflection of the performance of the modified mixtures. The complex modulus and the phase angle can be used to explain the viscoelastic behaviour of polymer modified mixtures with regard to the end performance of the mixtures, e.g. resistance to fatigue cracking and permanent deformation, under certain conditions. The existence of a plateau in the

complex modulus may indicate some sort of molecular entanglements within the blends, hence, dynamic mechanical analysis are recommended to get a general view on the performance of modified mixtures. Furthermore, this test offers other advantages in that it is non-destructive and can generate results for a wide range of temperatures and frequencies. The test can be carried out on both the binder and the mixture, however, testing on the mixture is recommended to obtain more reliable results with regard to binder-aggregate interaction.

In this research, the laboratory assessment of the performance of bituminous mixtures is focused on the resistance to permanent deformation. The assessment of the resistance to permanent deformation was conducted by the wheel-tracking test and the dynamic creep test (without confinement). The effect of confinement was neglected in the dynamic creep test by considering that the mixture used in this study was a wearing course type HRA, of which the major strength to the resistance to permanent deformation is provided by the mortar binder, and it has been reported previously that the relative performance of bituminous mixtures in which strengths rely on the stiffness of mortar binder is not significantly affected by the confinement [110]. Details of the test configuration is presented in *Chapter Five*. Table 3.11 shows several factors considered in this thesis indicates that some conventional tests were also conducted for comparison.

*Table 3.11 Several factors to be assessed in this research*

<b>Properties Measured</b>	<b>Test Method (Apparatus)</b>
Mixing and Compaction Temperatures	Viscosity Test (Brookfield Viscometer)
Rheological Properties of Binders	Empirical Tests : Penetration and Softening Point Tests Dynamic Mechanical Analysis (DSR)
Storage Stability of Binders	Rheological Properties Before and After Storage Observation under Ultra Violet Fluorescent Microscopy
Stiffness of Bituminous Mixtures	Indirect Tensile Stiffness Test (NAT) Dynamic Mechanical Analysis (Dynamic Bending Machine)
Permanent Deformation	Standard Marshall Test Dynamic Creep Test (NAT) Wheel-tracking Test

### 3.6 References

- 1 Whiteoak, D., "The Shell Bitumen Handbook", 1990.
- 2 Roberts, F.L., Kandhal, P.S., Brown, E.R., Lee, D.Y., and Kennedy, T.W., "Hot Mix Asphalt Materials, Mixture Design and Construction", National Asphalt Paving Association (NAPA) Research and Education Foundation.
- 3 Petersen, J.C., Robertson, R.E., Branthaver, J.F., Harnsberger, P.M., Duvall, J.J., Kim, S.S., Anderson, D.A., Christensen, D.W., and Bahia, H.U., "Binder Characterization and Evaluation, Volume 1", Strategic Highway Research Program, SHRP-A-367, Washington D.C., 1994.
- 4 Morgan, P., and Mulder, A., "The Shell Bitumen Industrial Handbook", 1995.
- 5 Corbett, L.W., "Refining Processing of Asphalt Cement", TRB, TRR 999, 1984.
- 6 Pfeiffer, J.P., "The Properties of Asphaltic Bitumen", Elsevier, 1950.
- 7 Halstead, W.J., "Relation of Asphalt Chemistry to Physical Properties and Specifications", Proceedings of AAPT, Vol. 54, 1985, pp. 91-117.
- 8 Asphalt Institute, "Performance Graded Asphalt Binder Specification and Testing", Superpave Series No. 1 (SP-1).
- 9 Vinogradov, G.V., and Malkin, A. Ya (1980), Rheology of Polymers, Mir Publ., Moscow.
- 10 Christensen, D.W., and Anderson, D.A. (1990), "Interpretation of Dynamic Mechanical Test Data for Paving Grade Asphalt Cements", Proceedings of AAPT, Vol. 61, pp. 67-116.
- 11 Van der Poel, C. (1954), "A General System Describing the Viscoelastic Properties of Its Relationship to Routine Test Data", Journal Applied Chemistry, No. 4, pp. 221.
- 12 Jongepier, R., and Kuilman, B., "Characteristics of The Rheology of Bitumens", Proceedings of AAPT, Vol. 38, 1969, pp. 98-122.

- 13 Read, J.M., "Fatigue Cracking of Bituminous Paving Mixtures", PhD Thesis, University of Nottingham, 1996.
- 14 Dobson, G.R., "An Apparatus for Measuring the Dynamic Elastic Properties of Bitumens", *Journal of Scientific Instrument*, Vol. 44, 1967, pp. 375-378.
- 15 Ferry, J.D., "Viscoelastic Properties of Polymers", John Wiley and Sons, 3rd. Edition, 1980
- 16 Dobson, G.R., "The Dynamic Mechanical Properties of Bitumen", *Proceedings of AAPT*, Vol. 38, 1969, pp. 123-139
- 17 Transportation Research Board, "Conference on SHRP Asphalt Research", TRR 1386, National Research Council, Washington D.C, 1993
- 18 United Kingdom's Highway Agency Clause 943, "Hot Rolled Asphalt Wearing Course (Performance Related Design Mix)", Draft No. 4.0, 5 July 1996.
- 19 Goodrich, J.L., "Asphaltic Binder Rheology, Asphalt Concrete Rheology and Asphalt Concrete Mix Properties", *Proceedings of AAPT*, Vol.60, 1991, pp.80-120.
- 20 Collins, J.H., Bouldin, M.G., Gelles, R., and Berker,A., "Improved Performance of Paving Asphalts By Polymer Modification", *Proceedings of AAPT*, Vol. 60, 1991, pp. 43-79.
- 21 Costello, B.A., Hodder, P.T.,and Saunders, G.L., "Use of Time Temperature Superposition in Conjunction with SHRP Procedures to Evaluate The Mechanism of Energy Dissipation in Bituminous Binders", *Euroasphalt & Eurobitume Congress*, 1996.
- 22 Anon, "Glossary of Rheological Terms", Eurobitume Task Force, Eurobitume, 1996.
- 23 Cheung, C.Y., "Mechanical Behaviour of Bitumens and Bituminous Mixes", PhD Thesis, University of Cambridge, 1995.
- 24 Brule, B., Brion, Y., and Tanguy, A., "Paving Asphalt Polymer Blends: Relationship Between Composition, Structure and Properties", *Proceedings of AAPT*, Vol. 55, 1986, pp. 41-64.

- 25 Lewandowski, L.H., "Polymer Modification of Paving Asphalt Binders", Rubber Chemistry and Technology, Vol. 67, No. 3, 1994, pp. 447-480.
- 26 VanBeem, E.J. and Brassier, P., "Bituminous Binders of Improved Quality Containing Cariflex Thermoplastic Rubbers", Journal Institute of Petroleum, vol 59, no 556, pp. 91-97.
- 27 Collins, J.H. and Shuler, S., Discussion part from the paper: "Block Copolymer Modification of Asphalt Intended for Surface Dressing Applications", Proceedings of AAPT, Vol. 54, 1985, p. 14
- 28 Ellis, C., Widyatmoko, I., and Read, J.M., "The Storage Stability and Behaviour of Polymer Modified Bituminous Binders", Proceedings of the Second European Symposium on Performance and Durability of Bituminous Materials, J.G. Cabrera, Ed., Leeds, April 1997.
- 29 Anon, British Standard Draft of Development (Second Draft) released on 17th November 1995, "DD ABE Method For The Determination Of The Storage Stability Of Modified Binder", BSI London
- 30 Price, R.P., and Burati, J.L., "Predicting Laboratory Results for Modified Asphalts Using HP-GPC", Proceedings of AAPT, Vol. 59, 1990, pp. 1-32.
- 31 Jones, D.R., and Kennedy, T.W., "Asphalt Chemistry and Its Effect on Roadway Surface Conditions", ASTM Standardisation News, February 1991.
- 32 Rostler, F.S., and White, R.M., "Fractional Components of Asphalts - Modification of The Asphaltenes Fraction", Proceedings of AAPT", Vol. 39, 1970, pp. 532-574.
- 33 Thompson, D.C., "Bituminous Materials: Asphalt, Tars, and Pitches", A.J. Hoiberg, Ed., Interscience Publishers, 1964, Vol.1.
- 34 Lee, N.K, Morrison, G.R., and Hesp, S.A.M., "Low Temperature Fracture of Polyethylene-Modified Asphalt Binders and Asphalt Concrete Mixes", A paper presented at the Annual Meeting and Technical Sessions of the Association Asphalt Paving Technologists, March 27-29, 1995

- 35 Terrel, R.L., and Walter, J.L., "Modified Asphalt Materials - The European Experience", Proceedings of AAPT, vol. 55, 1986, pp.482-518.
- 36 Lancaster, I., "Polymer Chemistry and Polymerisation", Nynas Network, Issue No 3, Summer 1996.
- 37 Walker, P.M.B., "Chambers Materials Science and Technology Dictionary", Chambers Harrap Publishers, 1993.
- 38 Hoban, T., "Modified Bitumen Binders for Surface Dressing", Chemistry and Industry, 1990, pp. 538-542
- 39 King, G.N., King, H., Harders, O., Chaverot, P., "Low Temperature Benefits of Polymer Modified Asphalts", Proceedings of CTAA", November, 1988, pp.198-217
- 40 Jew, P., Shimizu, J.A., Svazic, M., and Woodhams, R.T., "Polyethylene-Modified Bitumen for Paving Applications", Journal of Applied Polymer Science, Vol. 31, 2685-2704, 1986
- 41 Gilby, G.W., "Ethylene-Vinyl Acetate (EVA) Copolymers as Modifiers for Bitumen Binders", Journal of the Institute of Asphalt Technology, Vol. 36, 1986, pp. 37-41.
- 42 Jew, P., and Woodhams, R.T., "Polyethylene-Modified Bitumens for Paving Applications", Proceedings of AAPT, Vol. 55, 1986, pp. 541-563
- 43 Liang, Z., Hesp, S.A.M., "In Situ Steric Stabilization of Polyethylene Emulsions in Asphalt Binders for Hot-Mix Pavement Applications", Colloids and Surfaces A: Physicochemical and Engineering Aspects, 81(1993), pp. 239-250
- 44 Svazic, M., and Woodhams, Economic Survey of Low Density Polyethylene Scrap, Ontario Ministry of Transportation and Communications, Contract Report, July, 1983
- 45 Nahas, N.C., Bardet, J., Eckmann, B., and Siano, D.B., "Polymer Modified Asphalts for High Performance Hot Mix Pavement Binders", Proceedings of AAPT, Vol. 59, 1990, pp. 509-525
- 46 Gilby, G.W., "Ethylene-Vinyl Acetate (EVA) Copolymers as Modifiers for Bitumen Binders", Journal Institute of Asphalt Technology, Vol. 36, 1986, pp. 37-41.

- 47 Choyce, P.W., and Wooley, K.G., "EVA Modified Binders", Highways, January, 1988.
- 48 Anon, "EVA Modified Bitumen", Croda Bitumen Ltd.
- 49 Nicholls, J.C., "EVATECH polymer-modified bitumen", T.R.L, P.R.109, 1994
- 50 Woolley, K.G., "Polymer Modified Bitumen for Extra Value Asphalt", Asphalt Technology, No. 38., pp. 45-51, September 1986
- 51 Giavarini, C., "Polymer Modified Bitumen", *Asphaltenes and Asphalts, I., Development in Petroleum Science, 40*, Chapter 16, Eds. T.F. Yen and G.V. Chilingarian, Elsevier Science, B.V., 1994.
- 52 Goodrich, J.L., "Asphalt and Polymer Modified Asphalt Properties Related to the Performance of Asphalt Concrete Mixes", Proceedings of AAPT, Vol. 57, 1988, pp. 116-175
- 53 Muncy, H.W., King, G.N., Prudhomme, J.B., "Improved Rheological Properties of Polymer Modified Asphalts", ASTM Special Technical Publication 1987, pp. 146-165.
- 54 Stock, A.F., and Arand, W., "Low Temperature Cracking in Polymer Modified Binders", Proceedings of AAPT, Vol. 62, 1993, pp 23-55.
- 55 Anon, "Proposed Test Method for Toughness and Tenacity of Bituminous Materials", ASTM D-4 Proposal P 243, 1994.
- 56 Lenoble, C., and Nahas, N.C., "Dynamic Rheology and Hot-Mix Performance of Polymer Modified Asphalt", Proceedings of AAPT, Vol. 63, 1994, pp.450-480
- 57 Takallou, H.B., and Hicks, R.G., "Development of Improved Mix and Construction Guidelines for Rubber-Modified Asphalt Pavements", TRR 1171, pp. 113-120.
- 58 Takallou, H.B., and Sainton, A., "Advances in Technology of Asphalt Paving Materials Containing Used Tire Rubber, TRR 1339, pp. 23-29.
- 59 Heitzman, M., "Design and Construction of Asphalt Paving Materials with Crumb Rubber Modifier", TRR 1339.

- 60 Brydson, J.A., "Rubbery Materials and Their Compounds", Elsevier Applied Science, 1988.
- 61 King, G.N., King, H.W., Harders, O., Chavenot, P., and Planche, J.P., "Influence of Asphalt Grade and Polymer Concentration on The High Temperature Performance of Polymer Modified Asphalt", Proceedings of AAPT, Vol. 61, 1992, pp. 29-66
- 62 Anon, "Olexobit 100", British Petroleum (BP) Bitumen, 1997.
- 63 Collins, J.H. and Mikols, W.J., "Block Copolymer Modification of Asphalt Intended for Surface Dressing Applications", Proceedings of AAPT, Vol. 54, 1985, pp. 1-17.
- 64 Kraus, G., Paper no. 44 presented at a meeting of the Rubber Division, American Chemical Society, Philadelphia, Pennsylvania, May 4-7, 1982
- 65 Von Gooswilligen, G., and Bull, A.L., "The Role of Bitumen in Blends with Thermoplastic Rubbers for Roofing Applications", Presented at Roofing and Waterproofing World-wide, London, April 1986.
- 66 Dinnen, A., "Bitumen-Thermoplastic Rubber Blends in Road Applications", Journal of the Institute of Asphalt Technology 1988, pp. 646-651
- 67 Loeber, L., Durand, A, Muller, G, Morel, J., Sutton, O, Bargiachi, M., "New Investigations On The Mechanism of Polymer-Bitumen Interaction and Their Practical Application for Binder Formulation", Euroasphalt & Eurobitume Congress, 1996.
- 68 Walker, P.M.B, "Chambers Materials Science and Technology Dictionary", Chambers Harrap Ltd., 1993.
- 69 Collins, J.H., Bouldin, M.G., Gelles, R., and Berker, A., "Improved Performance of Paving Asphalts By Polymer Modification", Proceedings of AAPT, Vol. 60, 1991, pp. 43-79
- 70 Nunn, M.E., Bowskill, G., "Towards A Performance Specification for Bituminous Roadbase", The Institute of Asphalt Technology, Asphalt Year Book 1994

- 71 Anon, "Accelerated Performance-Related Tests for Asphalt-Aggregate Mixes and Their Use in Mix Design and Analysis Systems", SHRP-A-417, Strategic Highway Research Program, National Research Council, Washington D.C., 1994.
- 72 Powell, W.D., Potter, J.F., Mayhew, H.C., and Nunn, M.E., "The Structural Design of Bituminous Roads", TRRL, LR 1132, 1984.
- 73 Denning, J.H., and Carswell, J., " Assessment of Novophalt as a binder for Rolled Asphalt wearing course", TRRL, LR 1101, 1983.
- 74 Nicholls, J.C., "Assessment of Multiphalte, the Shell Multigrade Bitumen", TRL, PR 61, 1994.
- 75 Strauss, P.J., Kleyn, E., duPleiss, J.A., "Field Performance, Laboratory Testing and Predictive Models for Modified Binders Used in Reflection Cracking", 7th International Conference on Asphalt Pavements, 1992
- 76 Jimenez, R.A., Morris, G.R., and DeDeppa, D.A., "Tests for a Strain Attenuating Asphaltic Material", Proceedings of AAPT, Vol. 48, 1979, pp. 163-191.
- 77 Rust, F.C., Coetser, K., Verhaege, B.M.J.A., "The Evaluation of Six Modified Binders For Retardation of Crack Reflection Through Laboratory Studies and Field Work", 7th. International Conference on Asphalt Pavements, 1992, pp. 292-306.
- 78 Tayebali, A.A., Deacon, J.A., Coplantz, J.S., and Monismith, C.L., "Modelling Fatigue Response of Asphalt-Aggregate Mixtures", Proceedings of AAPT, Vol. 62, 1993.
- 79 Widyatmoko, I., "Fatigue Testing of Bituminous Mixtures. An Investigation on The Effect of Fines and a Polymer Modified Binder", MSc Thesis, University of Birmingham, 1994.
- 80 Van Dijk, W., "Practical Fatigue Characterization of Bituminous Mixes", Proceedings of AAPT, Vol. 44, 1975, pp. 38-74.
- 81 Van Dijk, W., and Visser, W., "The Energy Approach to Fatigue For Pavement Design", Proceedings of AAPT, Vol. 46, 1977.

- 82 Rowe, G.M., "Application of Dissipated Energy Concept to Fatigue Cracking In Asphalt Pavements", PhD Thesis, University of Nottingham, 1996.
- 83 Brennan, M.J., and Clancy, F., "A New Initiative In Measuring The Fatigue Performance of Bituminous Materials", 7<sup>th</sup> International Conference on Asphalt Pavements, 1992.
- 84 Salter, R.J., and Rafati-Afshar, F., "Effect of Additives on Bituminous Highway Pavements Materials Evaluated by the Indirect Tensile Test", TRR 1115.
- 85 Verhasselt, A.F., and Choquet, F.S., "Comparing Field and Laboratory Aging of Bitumens on a Kinetic Basis", TRR 1391, 1993, pp. 30-38.
- 86 Anon, "The Asphalt Handbook", Asphalt Institute Manual Series No 4, 1989
- 87 Scholz, T.V., "Durability of Bituminous Paving Mixtures", PhD Thesis, University of Nottingham, 1995.
- 88 Lee, D., "Development of Highway Durability Tests for Asphalts", Highway Research Record 231, HRB, National Research Council, Washington D.C., 1968.
- 89 Petersen, J.C., Branthaver, J.F., Robertson, R.E., Harnsberger, P.M, Duval, J.J., and Ensley, E.K., "Effects of Physicochemical Factors on Asphalt Oxidation Kinetics", Transportation Research Record 1391, 1993.
- 90 Chiu, C, Tia, M, Ruth, B.E., and Page, G.C., "Investigations of Laboratory Aging Process of Asphalt Binders Used in Florida", TRR 1436, 1994.
- 91 AbWahab, Y., Sosnovske, D, Bell, C.A., and Ryus, P., "Evaluation of Asphalt-Aggregate Mixture Aging by Dynamic Mechanical Analysis", TRR 1386, 1993.
- 92 Sosnovske, D.A., AbWahab, Y., and Bell, C.A., "Role of Asphalt and Aggregate in the Aging of Bituminous Mixtures", TRR 1386, 1993.
- 93 Terrel, R.L., and Shute, J.W., "Summary Report on Water Sensitivity", Report no. SR-OSO-A-003A-89-3, SHRP, Washington, DC 1989.
- 94 Carpenter, S.H., VanDam, T., "Laboratory Performance Comparisons of Polymer Modified and Unmodified Asphalt Concrete Mixtures", TRR 1115, pp. 62-73.

- 95 Schuller S and Forsten L., "Effect of Binder Properties on Polymer Modified Asphalt Concrete", 5th Eurobitume Congress, 1993.
- 96 King, G.N., Muncy, H.W., and Prudhomme, J.B., " Polymer Modification: Binder's Effect On Mix Properties", Proceedings of AAPT, Vol. 55, 1986.
- 97 King, G.N., King, H.W., Harders, O., Chavenot, P., and Planche, J.P., "Influence of Asphalt Grade and Polymer Concentration on The High Temperature Performance of Polymer Modified Asphalt", Proceedings of AAPT, Vol. 61, 1992, pp. 29-66.
- 98 Brown, S.F., Cooper, K.E., and Pooley, G.R., "Mechanical Properties of Bituminous Materials for Pavement Design", Proc. 2nd Eurobitume Symposium, Cannes, October 1981, pp. 143-147.
- 99 Koole, R.C., Valkering, C.P., and Lancon, D.J.L., "Development of a Multigrade Bitumen to Alleviate Permanent Deformation", 8th AAPA International Asphalt Conference, Sydney, November 10-13, 1991
- 100 Valkering, C.P., Lancon, D.J.L., deHilster, E., and Stoker, D.A., "Rutting Resistance of Asphalt Mixes Containing Non-Conventional and Polymer-Modified Binders", Proceedings of AAPT, Vol. 59, 1990, pp. 590-609.
- 101 Tayebali, A.A., Goodrich, J.L., Sousa, J.B., Monismith, C.L., "Relationship Between Modified Asphalt Binders Rheology and Binder-Aggregate Mixture Permanent Deformation Response", Proceedings of AAPT, Vol. 60, 1991, pp. 121-158.
- 102 Brown, S.F., and Cooper, K.E., "Simplified Methods for Determination of Fundamental Material Properties of Asphalt Mixes", SHRP Conference, The Hague, 1993.
- 103 Discussion part between: Brown and Van Der Heide, "Application of New Concepts in Asphalt Mix Design", Proceedings of AAPT, Vol. 60, 1991, pp. 264-286.
- 104 Shuler, T.S., Hanson, D.I., and McKeen, R.G., "Design and Construction of Asphalt Concrete Using Polymer Modified Asphalt Binders", Polymer Modified Asphalt

- Binders, ASTM STP 1108, Kenneth R. Wardlaw and Scott Shuler, Eds., American Society for Testing and Materials, Philadelphia, 1992.
- 105 Luxemburg, F., Hanzik, V., "Improvement of Asphalt Mixes by Modifying Bitumen Binders", 5<sup>th</sup> Eurobitume Congress, 1993.
- 106 Anderson, D.A., Christensen, D.W., Bahia, H., "Physical Properties of Asphalt Cement and the Development of Performance-Related Specifications", Proceedings of AAPT, Vol. 60, 1991, pp. 437-476.
- 107 Wu, S., "Phase Structure and Adhesion in Polymer Blends: A Criterion for Rubber Toughening", Polymer, Vol. 26, 1985, pp. 1855-1863
- 108 Discussion part of Symposium of SHRP Asphalt Program, Proceedings of AAPT, Vol. 60, 1991
- 109 Carswell, J., "An Assessment of Bitumen Basecourse and Roadbase Material Containing EVA and Sulphur", TRRL, RR 92, 1986
- 110 Gibb, J.M., "Evaluation of Resistance to Permanent Deformation in The Design of Bituminous Paving Mixtures", PhD Thesis, University of Nottingham, 1996.
- 111 Lu, X and Isacson, U., Styrene-Butadiene-Styrene Copolymer Modified Bitumens", Construction and Building Materials, Vol. 11, No. 1, pp.23-32, 1997.

# Chapter Four

## 4. Permanent Deformation

### 4.1 Introduction

Previous chapters have stated that the rapid growth in traffic intensity (traffic density, axle loading, tyre pressure) and the change in axle and wheel configuration on heavy good vehicles with the introduction on the use of super singles tyre, leads to the increase in pavement damage due to permanent deformation. This is a situation that is exacerbated in areas with hot climatic temperatures.

Gibb [1] reported that the resistance to permanent deformation of bituminous mixtures can be improved if the mixture has, either one or a combination, of the following characteristics:

1. Aggregate with coarse surface texture, continuous gradation, angular shape and/or large in size.
2. Binder with high stiffness at high temperature.
3. Mixture with low binder content, low air voids (but not less than 3%<sup>a</sup>), low VMA content (but not less than 10%), and/or proper method of compaction.

However, estimation of the performance of bituminous mixtures based solely on a mixture's composition can be misleading because the environmental conditions may contribute significantly to the resistance to permanent deformation. For example, the deformation resistance can be reduced by increasing temperature, level of loading, load repetition, and/or the presence of water (if the mixture is water sensitive) [1]. Therefore,

---

<sup>a</sup> For dense graded mixes, when air void contents drop below 2-3% the binder acts as a lubricant between the aggregate and reduces point to point contact

some form of mechanical test is required for the assessment of the performance of bituminous mixtures.

This chapter will be focused on the identification of the response of bituminous mixtures to variation of the state of loading and environmental conditions, and analysis techniques that are commonly employed to predict the permanent deformation resistance of bituminous materials. Specific discussions on the effect of different mixture compositions on the resistance to permanent deformation can be found in *Chapter Seven*. A new approach for assessing the resistance of bituminous mixtures to permanent deformation based on dissipated energy is also presented.

## ***4.2 Behaviour of Bituminous Materials Under Various Conditions***

### **4.2.1 Temperature Dependency**

The mechanical behaviour of bituminous materials is highly dependent upon temperature and loading time, of which their effects are interchangeable, i.e. the high temperature behaviour is mirrored by the long loading time behaviour. The dependence of the flow properties of bituminous mixtures on temperature (or loading time) is due to changes in the rheological properties of the binder and these can be shown by the dependency of the viscosity (stiffness) of the binder on temperature.

At temperatures above 20°C, bituminous materials become significantly more susceptible to permanent deformation. Simulative tests on bituminous mixtures, such as wheel-tracking tests, generally confirm that the resistance to deformation decreases rapidly with an increase in temperature [2].

The interaction behaviour of the binder-aggregate mixtures has been observed to be significantly affected by temperature. Goodrich [3] reported that bituminous binder and aggregate interact more effectively at moderate temperatures, between 10°C and 50°C, as indicated by the results of his observations on the changing viscoelastic properties of bituminous mixtures due to temperature changes (Figure 4.1). The loss tangent has been selected as a parameter to represent viscoelastic behaviour of the materials. The higher the loss tangent indicates the more viscous the material, and hence the less resistant to

deformation. The contribution of the binder decreases as the temperature goes up, therefore, at high temperatures (above 50°C) the performance of bituminous mixture is predominantly influenced by the aggregate [3] and *vice versa* the performance at low temperatures (less than 10°C) is predominantly influenced by the binder properties [3,4]. Furthermore, permanent deformation of bituminous mixtures can be ignored at low temperatures (below 10°C) [5].

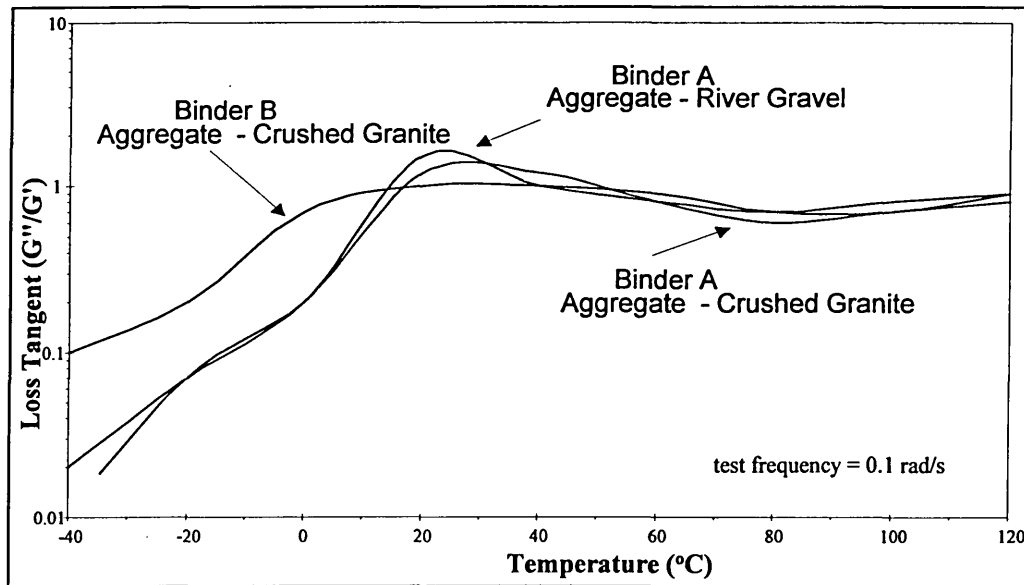


Figure 4.1 Dynamic mechanical analysis on different bituminous mixtures showing the effect of temperature on the rheological properties of bituminous mixtures. After Goodrich [3]

#### 4.2.2 Mode of Loading

Selection of the appropriate mode of loading is very important to obtain test results which represent the actual loading imposed by traffic. Figure 4.2 and 4.3 present typical stress variations within a bituminous pavement generated by traffic [6, 7]. These indicate that traffic direction (one or two way traffic) can significantly alter the stress patterns.

In general, there are three modes of loading, i.e. static (creep), repetitive (dynamic), and incremental static loading. The incremental creep test is applicable only to bituminous mixtures and fine-grained soils that show a predominance for viscous flow, whereas the dynamic and creep tests can be applied to all materials [8].

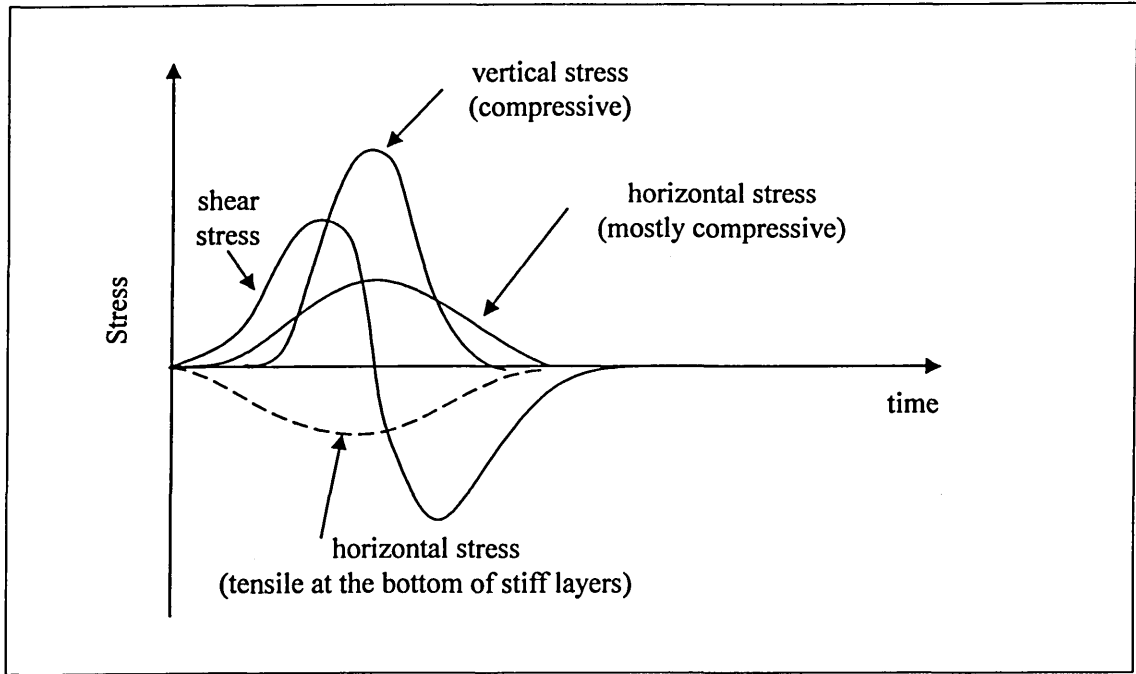


Figure 4.2 In situ stress generated by a moving wheel load. After Brown [6]

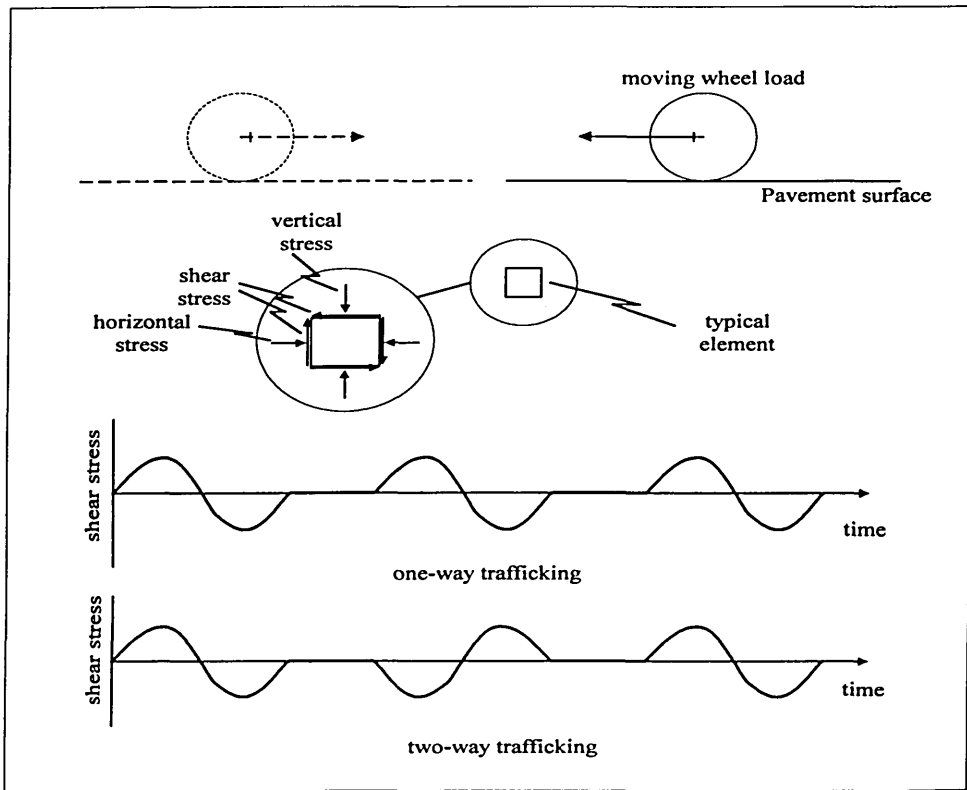


Figure 4.3 Shear stress variation in a typical pavement element as a wheel passes overhead. After Bell [7].

#### **4.2.2.1 Static (Creep) Loading**

A static creep loading is generally conducted by placing a specimen under a static load, and the deformation (flow) with time is measured. This test is generally carried out in two ways:

1. To measure load (stability) and deformation (flow) of bituminous mixture at failure point, e.g. Marshall test (Figure 4.4). However, due to the test configuration and resultant stress condition this cannot be related to any fundamental mechanical properties.
2. To measure the permanent deformation after the bituminous mixture is given a specified time to recover upon load removal, e.g. NAT static creep test (Figure 4.5)

#### **Advantages:**

- Simplicity. Static loading is the simplest way to assess the mechanism of resistance to permanent deformation of bituminous mixtures.
- Robust and proven technique for designing deformation resistance of conventional (unmodified) bituminous mixtures.
- This type of loading represents the traffic loading experience by a pavement under severe conditions, such as on climbing line or parking areas for heavy vehicles.
- For qualitative comparison purposes, this method appears very effective and can reasonably quantify deformation potential [5].

#### **Disadvantages:**

- Material specifics. This type of loading tends to underestimate the strength of some bituminous mixtures. Tests on mixtures whose strengths rely on good aggregate skeleton, such as macadam mixtures, will show better resistance to permanent deformation than mixtures whose strengths rely on the binder or the binder/filler mortar, such as asphalt mixtures [1].
- The lack of repetitive loading means that the material is not given a chance to recover from the deformation under consecutive stress applications, hence the deformation is purely due to the viscous flow of the binder and no consideration is given to the contribution of the elasticity of the binder to the resistance to permanent deformation of the mixture.

- The static creep test was originally developed for unmodified binders and it has been reported to be unsuitable for polymer modified binders (see *Section 3.4*).

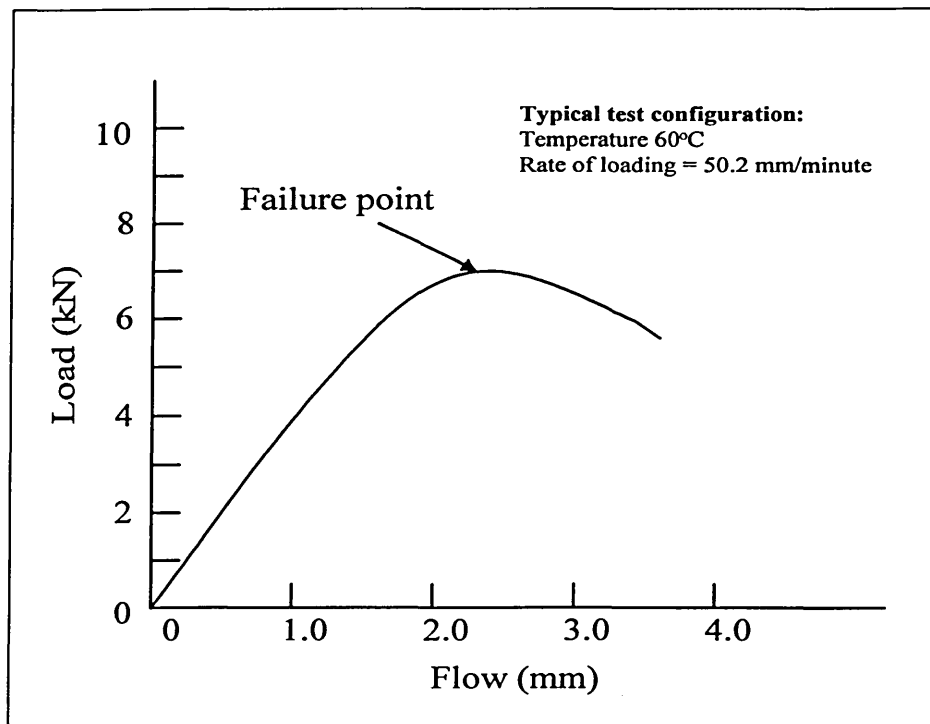


Figure 4.4 Typical Marshall test data plot

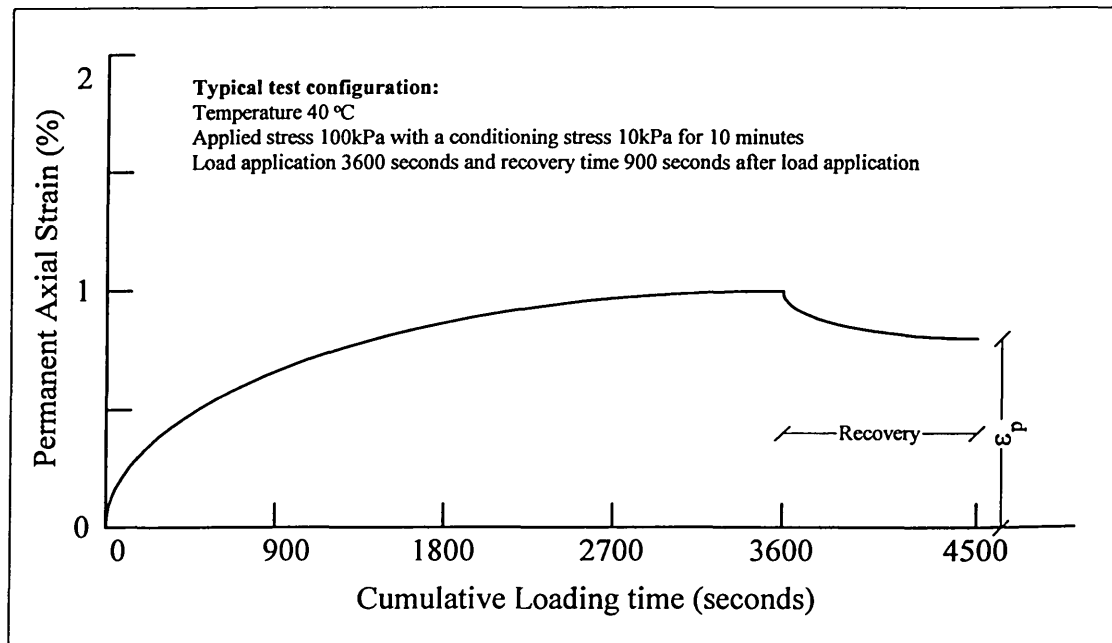


Figure 4.5 Typical NAT creep test data plot

Recent developments in the analysis techniques based on the static creep test have introduced correction factors to cover the limitations of the test, such as the dynamic effect, and also to account for the effect of climate and traffic loading, as reported by Lijzenga [9] on the improvement and extension of the Shell Pavement Design Manual (SPDM)[10]. This is a model for predicting permanent deformation based on the modification of work by Van de Loo [11,12]. Description of this model is presented in *Section 4.3.1*.

#### ***4.2.2.2 Repetitive (Dynamic) Loading***

This type of loading is preferable amongst other type of loading, as it represents more closely the loading pattern of traffic, incorporating the effect of load repetitions and rest periods (loading interval). Some of the shortcomings of static tests for assessing modified binders, which are related to the recovery of the deformation after removal of the load, have been overcome by dynamic loading tests.

The response of bituminous mixtures to repetitive loading is also different to the response from static loading. With repetitive loading, permanent deformation developed after each load application may continue to accumulate as viscous strains are induced in the binder-aggregate skeleton. A typical plot from a repetitive load test is presented in Figure 4.6.

Different types of loading patterns can be applied, such as sinusoidal, haversine, triangular, or square wave patterns. Read [13] recommends the use of the haversine loading pattern as representative of that experienced in the field.

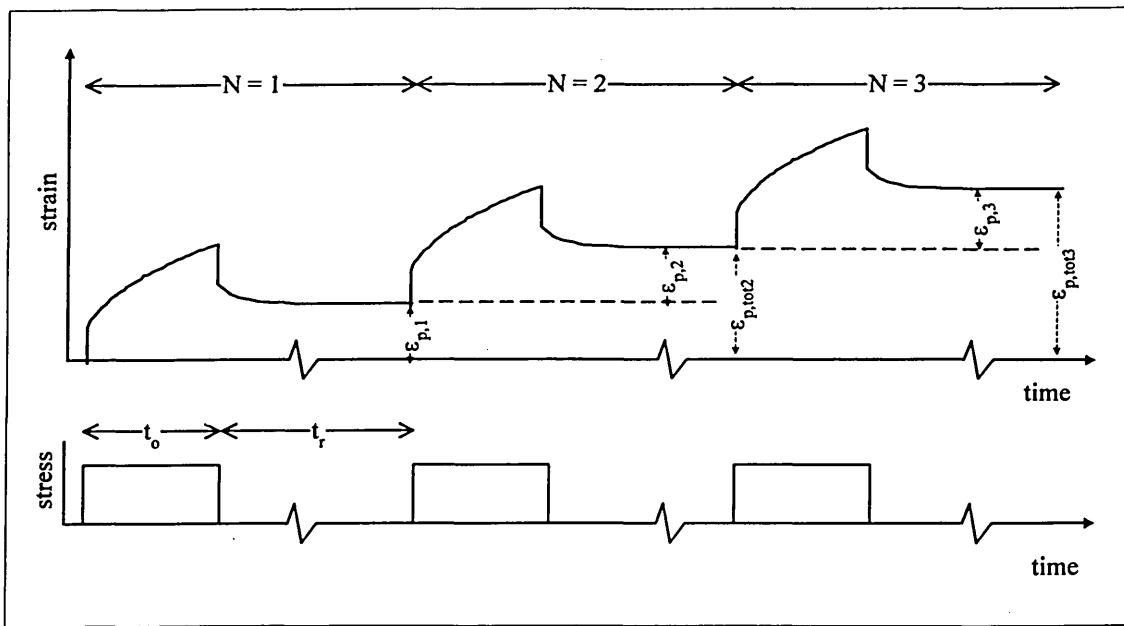


Figure 4.6 Typical stress and strain history in repetitive loading test, showing the applied stress duration ( $t_0$ ) and the relaxation time ( $t_r$ )

The cumulative permanent strain  $\epsilon_p$  can be determined by:

$$\epsilon_p = \sum_{i=1}^N \epsilon_{p,i}$$

Equation 4.1

where  $i$  is the number of loading up to  $N$  load application.

Gibb [1] reviewed the use of three parameters to represent the resistance to permanent deformation from this type of loading:

1. The ultimate strain which is the cumulative (terminal) permanent strain at the end of loading (Equation 4.1)
2. The mean strain rate which is determined from all the data from the start until the end of loading (Equation 4.2).
3. The minimum strain rate which is determined by the strain rate over a particular interval that gives the minimum value.

$$\text{Mean strain rate} = \frac{\sum_{i=1}^N \frac{\Delta \epsilon_i}{\Delta n_i}}{N}$$

Equation 4.2

where:

$\Delta\varepsilon_i = (\varepsilon_{i+1} - \varepsilon_i)$ , and  $\varepsilon_i$  is the permanent strain recorded at increment  $i$

$\Delta n_i = (n_{i+1} - n_i)$ , and  $n_i$  is the number of load cycles elapsed at increment  $i$

$N$  = the number of increments at which the permanent strain is recorded

By quoting all three parameters, the behaviour of materials under repeated loading can be represented more completely, e.g. whether the materials tend to have low strain failure or high strain failure. Figure 4.7 shows that a material may have similar minimum strain rate, but the deformation behaviour may be significantly different.

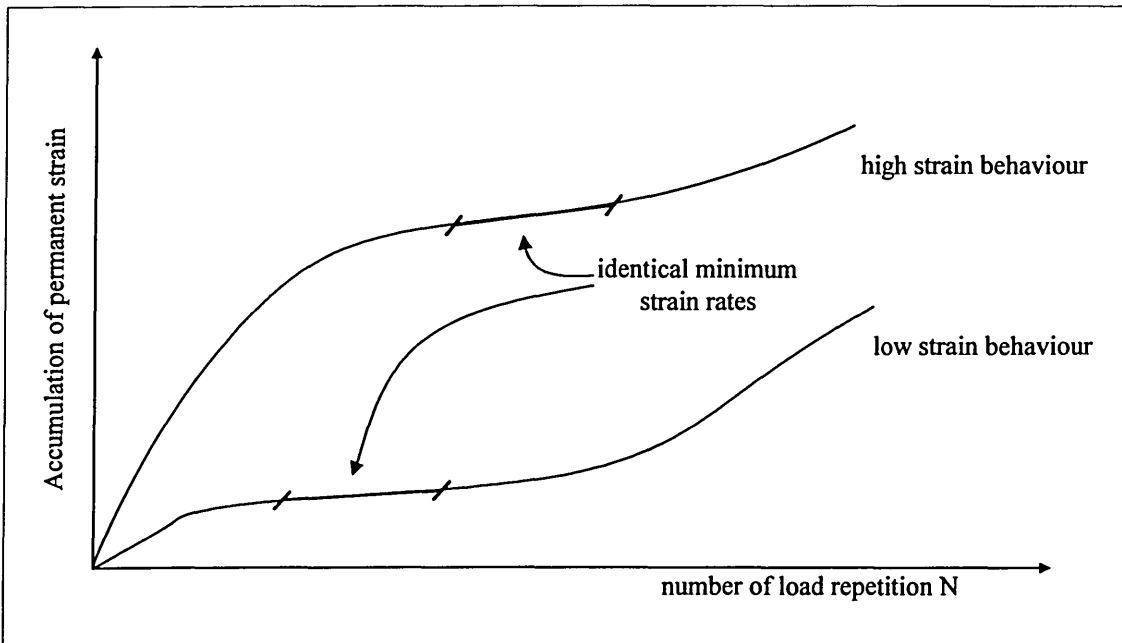


*Figure 4.7 Idealised permanent deformation curves under repetitive loading*

For practical purposes, however, Gibb recommends the use of the minimum strain rate rather than the other parameters (the ultimate strain and the mean strain rate) especially when the state of initial deformation is critical, for example: the initial positioning of load in the wheel-tracking device causes variation in the initial deformation prior to the main testing which can lead to significant error in the ultimate permanent strain.

Several different types of apparatus can be used to generate repetitive or dynamic loading effects, e.g. a repeated (dynamic) load triaxial devices, repeated (dynamic) load axial devices, repeated (dynamic) simple shear devices, and wheel tracking devices.

#### **4.2.2.3 Incremental Static Loading**

Incremental static loading is a simplified testing method that requires shorter test duration to perform than dynamic tests. For example: with a dynamic loading time of 0.1 second duration, a static load of  $t$  seconds is equivalent to  $10t$  load repetitions. Therefore, the permanent deformation of a dynamic test after 10000 repetitions is equivalent to that of the incremental creep test after 1000 seconds. A procedure of this type of loading can be found in the VESYS (viscoelastic analysis system) method as previously presented by Huang [8], as follows:

1. For conditioning, apply two ramp stresses of 20 psi (138 kPa) and hold each peak load for a 10 minute duration, with a minimum of unload time between them. A third load is then applied for 10 minutes, followed by a 10 minute rest period.
2. Five different ramp loads with duration of 0.1, 1, 10, 100, and 1000 seconds and rest periods of 2, 2, 2, 4, and 8 minutes are applied successively, as shown in Figure 4.8. The total permanent strains at the end of each rest period are measured.
3. In the fifth ramp load or 1000 second creep test, measure the magnitude of creep deformations after 0.03, 0.1, 0.3, 1, 3, 10, 30, 100, and 1000 seconds. The 0.03 second creep strain is equivalent to the resilient strain  $\epsilon$  under a dynamic haversine load of 0.1 second duration. The creep data should be extrapolated to obtain the strains at 0.001, 0.003, and 0.01 seconds so that the creep compliance at 11 time increments can be determined, e.g. by VESYS.
4. Plot the total permanent strain  $\epsilon_p$  versus the incremental loading time and fit with a straight line, as shown in Figure 4.9.
5. Determine the slope  $S$  and the intercept  $I$  of the straight line and compute  $\alpha$  and  $\mu$  (refer to VESYS method), in which  $\epsilon$  is the creep strain at 0.03 seconds.

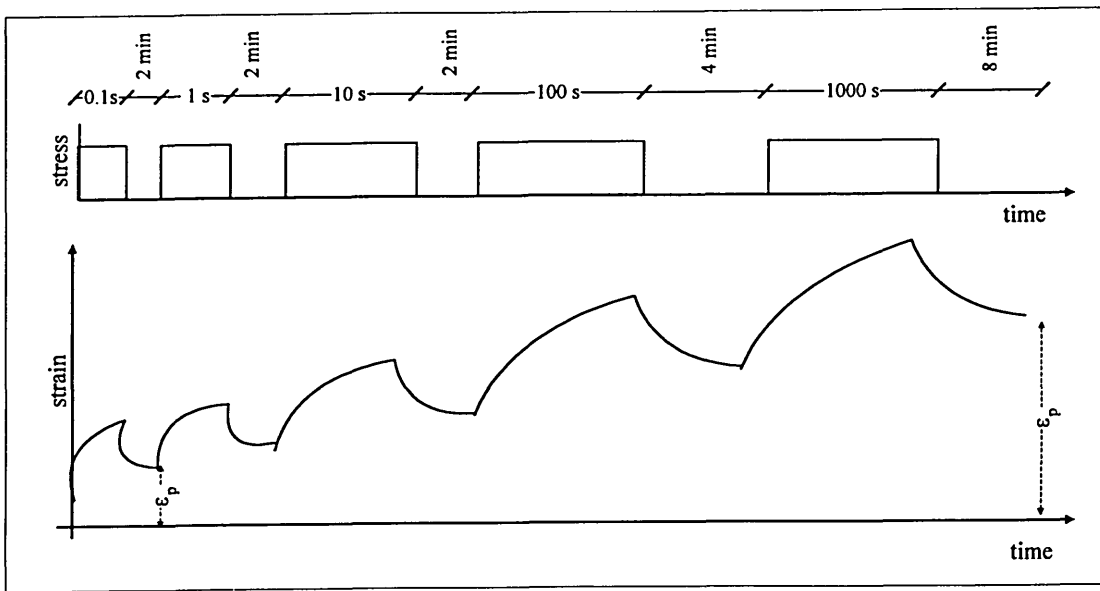


Figure 4.8 Stress and strain of incremental static test [reproduced after Huang]

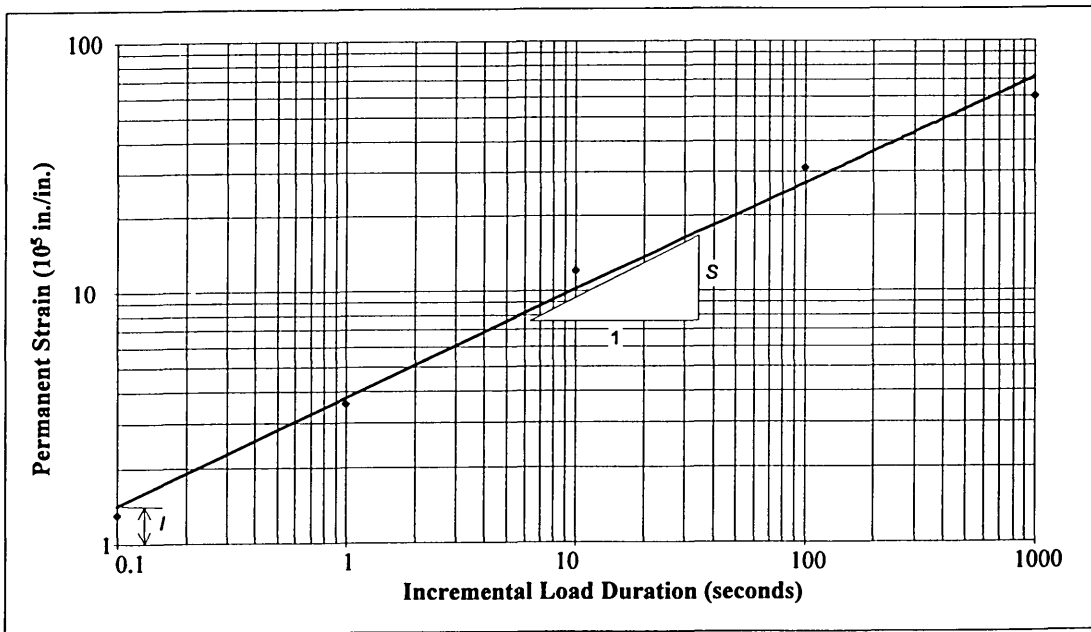


Figure 4.9 Log-log plot of incremental static test [after Huang]

Prediction of rut depth by VESYS method is based on the assumption that the permanent strain is proportional to the resilient strain by:

$$\epsilon_p (N) = \mu \epsilon N^{-\alpha}$$

Equation 4.3

in which:

$\varepsilon_p(N)$  is the permanent strain due to a single load application, i.e. at the Nth application;

$\varepsilon$  is the elastic or resilient strain at the 200<sup>th</sup> repetition;

N is the number of load applications

$\mu$  is the permanent deformation parameter representing the proportionality between permanent and elastic strain

$\alpha$  is a permanent deformation indicating the rate of decrease in permanent deformation as the number of load application increases

The total permanent deformation can be obtained by integrating Equation 4.3:

$$\varepsilon_p = \int_0^N \varepsilon_p(N) dN = \varepsilon\mu \frac{N^{1-\alpha}}{1-\alpha}$$

*Equation 4.4*

Equation 4.4 indicates that a plot of  $\log \varepsilon_p$  versus  $\log N$  results in a straight line, as shown in Figure 4.9, and therefore:

$$\log \varepsilon_p = \log I + S \log N \quad \text{or,} \quad \varepsilon_p = IN^S$$

*Equation 4.5*

$$\log \varepsilon_p = \log\left(\frac{\varepsilon\mu}{1-\alpha}\right) + (1-\alpha) \log N$$

*Equation 4.6*

where :      the slope line  $S = 1-\alpha$ , or       $\alpha = 1-S$   
                  the intercept at  $N = 1$ ,  $I = \varepsilon\mu/(1-\alpha)$ , or       $\mu = IS/\varepsilon$

Development of VESYS method has been enable an integrated design system for flexible pavements covering four major interactive models, i.e. primary response, general response, damage, and pavement performance. A comprehensive information of these models is given by Huang [8] and therefore will not be repeated in detail here.

Despite the advances and simplicity of this method, however, the Author anticipates some of their limitations, i.e.:

- ◆ The basic assumption that the permanent strain is proportional to the resilient strain may only be suitable for low strain or low stress condition, where the response of bituminous materials is predominantly affected by the elastic properties. On the contrary, high stress or high strain condition usually generate non-linearity where viscous behaviour of the material need to be put into account.
- ◆ The condition where the permanent strain changes linearly with loading times or load repetitions is normally found in the second region (see Figure 4.11) and non-linearity can be found in the first region and the third region. However, there is no indication that VESYS identify where the linear region starts or ends.

### **4.2.3 Boundary Condition**

Determination and identification of mechanical properties under different types of stresses are important because the actual stresses that occur in the field are very complex and vary with time. There are different types of stresses that may be experienced by road pavements, such as hydrostatic compression and tension, simple tension, shear, and triaxial compression (as illustrated in Figure 4.10) [2], and a combination of axial and torsional loads, such as in a hollow cylindrical apparatus [14, 15].

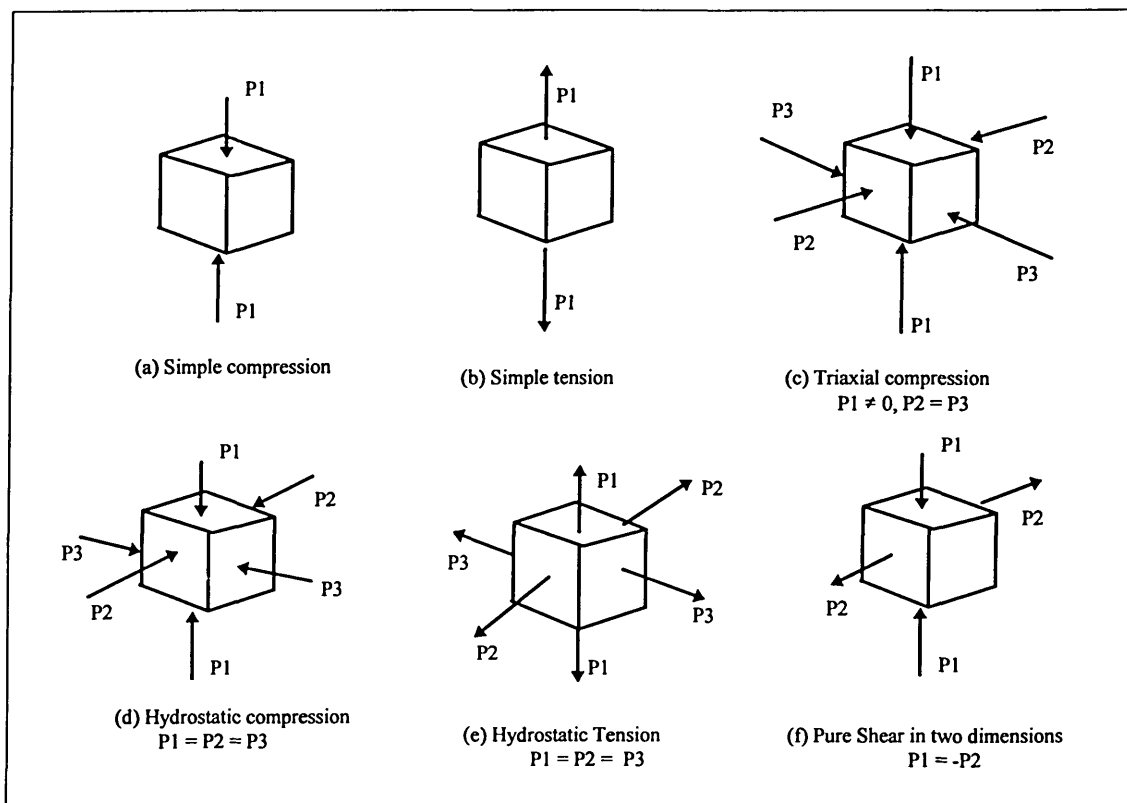


Figure 4.10 Basic types of stress. The arrows indicate the directions of loading (forces per unit area).

#### 4.2.3.1 Simple Tensile Stress

A simple tensile stress can be found as a hydrostatic tensile stress or as two pure shear stresses, which in most the cases tends to produce volumetric expansion or dilation<sup>b</sup> of the material. At temperatures above ambient, this condition will lead to a loosening of the structure, followed by fracture.

There are normally three stages of creep region under these conditions (Figure 4.11); the first is the rapid extension at decreasing rate, the second is the slower extension at steady rate (creep), and the third is an acceleration of creep rate resulting in fracture. The decreasing rate in the first region is due to the strain hardening<sup>c</sup> whereas the second region is where the minimum strain rate occurs due to the cohesive strength of the material which is developed to resist the deformation (viscous flow). In the third region, the material starts losing its stability as the viscous flow exceeds the cohesive strength,

<sup>b</sup> See Glossary

and eventually lead to failure. Analyses are generally focused in the first and second regions due to the unstable nature of the third stage and the associated difficulty in modelling or simulating.

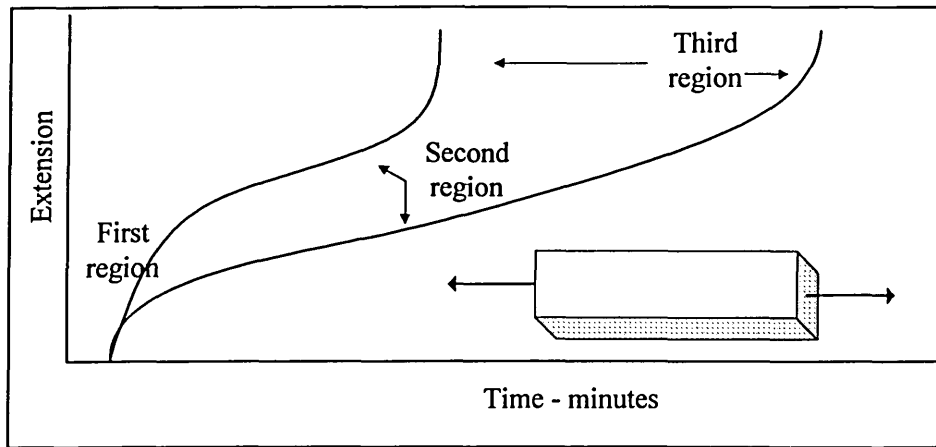


Figure 4.11 Typical deformation results in a simple tensile test.

#### 4.2.3.2 Triaxial Compressive Stress

The stress condition that is normally found in the field is generally well reflected by the triaxial stress condition (Figure 4.10), where, the bituminous material is put into a mechanical equilibrium under a stress that is just below the level needed to cause flow. The failure is usually assumed to have occurred when the axial strain greatly exceeds the rate of increase of axial stress.

The state of stress of the material in the triaxial cell is generally represented by the Mohr-Coulomb curves (Figure 4.12), and formulated as:

$$\tau \geq C + \sigma \tan \phi$$

Equation 4.7

- where  $\tau$  = shear stress  
 $C$  = cohesion  
 $\phi$  = angle of friction

<sup>c</sup> Strain hardening is an increase resistance to plastic deformation, usually indicated by a reduced strain rate.

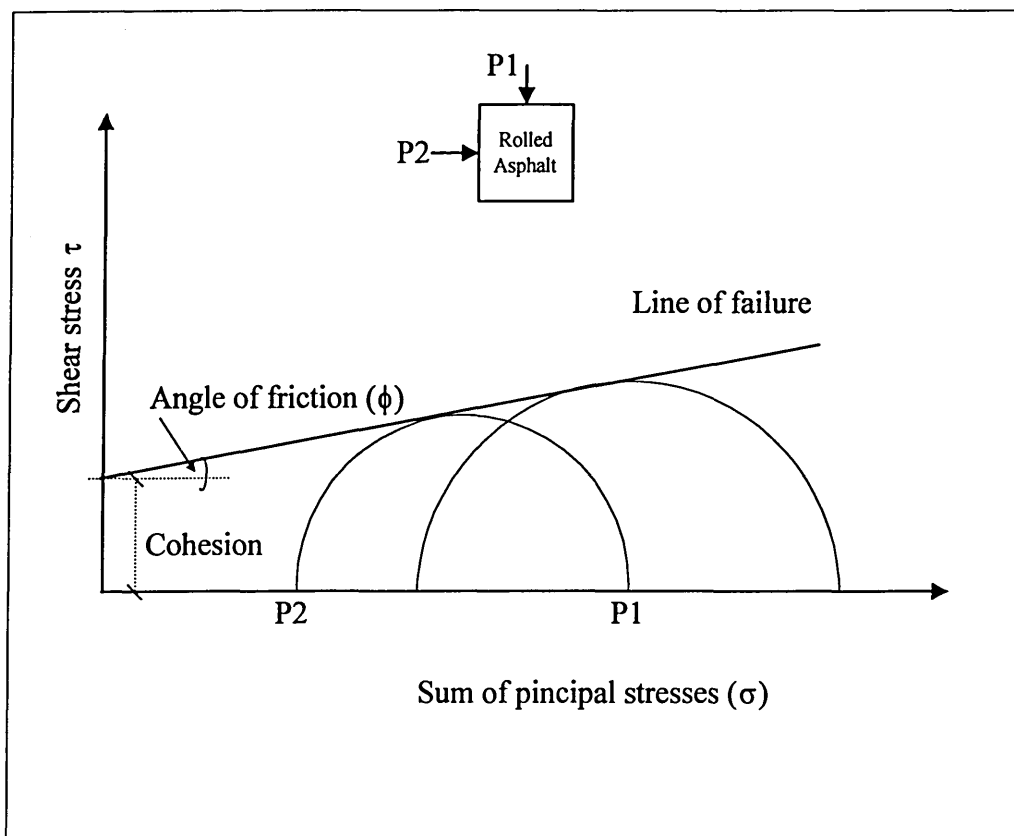


Figure 4.12 Mohr-Coulomb failure line and some stress conditions

Another advantage of the triaxial test, apart from the ability to produce a representative in situ stress-strain conditions, is that the test generates lots of information as the test progresses which are beneficial for further analysis (subject to mode of loading whether it is static, repetitive or dynamic loading) e.g. creep modulus, resilient modulus, permanent deformation, Poisson's ratio, and the damping ratio.

However, there is also a limitation in that the triaxial test can only produce the stress condition occurring on the axis of symmetry of the load where the principal stresses are vertical and horizontal, and the horizontal stresses are equal and compressive. Off the load axis, two of the principal stresses are inclined, all three principal stresses are different, and even if their vertical and horizontal components can be approximated the resulting shear stresses are ignored. The tensile stresses which also exist especially at the bottom part of the bituminous layer (Figure 4.2) cannot be reproduced directly in a conventional triaxial cell, i.e. the conventional triaxial horizontal stresses are

compressive and of the same stress level (Figure 4.10-c) whereas the in situ horizontal stresses are not always compressive and/or the stress levels usually vary.

#### ***4.2.3.3 Uniaxial (Unconfined) Compressive and Simple Shear Stress***

The flow behaviour of bituminous mixtures in unconfined compression and simple shear is qualitatively similar. In general, both tests are rather less sensitive than tensile tests but they have the advantage of allowing more reliable measurements to be made on materials with high coarse aggregate contents. However, the lack of confinement, particularly in the compression test, means that materials are not assessed in the *in situ* stress condition. Furthermore, confinement helps the materials to support the load without deformation or failure.

Previous studies [1] reported that unconfined compressive tests are still suitable for providing information on the relative performance of bituminous mixtures, whose strength relies on the stiffness of mortar binder rather than the aggregates interlock. Furthermore, a recent British Standard [16] recommends the unconfined uniaxial loading arrangement to be used as a method for determination of resistance to permanent deformation of bituminous mixtures “*at temperatures and loads similar to those experienced by these materials in roads*”. The Author should make a note here that the latter statement means that the tests are carried out at selected service temperatures and load levels but does not necessarily mean that the test can generate stresses similar to the in situ stress condition. The complete information on the effects of axial test configuration, as reported by Gibb [1], is presented in Table 4.1.

Table 4.1 Effects of axial test configuration. After Gibb [1].

Test Configuration	Effect of Test Configuration on the Mechanism of Resistance to Permanent Deformation		Remarks
	Contiguous Aggregate Skeleton	Binder or Binder/Filler Mortar	
Static Loading	Beneficial	Adverse	Low binder stiffness Deformation principally due to viscous flow in the binder. Little no plastic strain induced in the aggregate skeleton.
Repeated Loading (short duration)	Adverse	Beneficial	Relatively high binder stiffness. Promote plastic strains in aggregate skeleton.
High Temperature	Adverse	Adverse	Low binder stiffness. Effect likely to be greatest on binder/filler mechanism at very high temperatures.
Confinement	Beneficial	Neutral	Constrains relative displacement of aggregate particles.

The simple shear test is sensitive to the elastic and viscous characteristics of bituminous binders, and it also measures the effect of dilatancy which is the expansion of the specimen measured perpendicular to the applied force ( $\nu > 0.5$ ). The shear response is affected by characteristics of the bitumen/binder, characteristics of the aggregates, the air voids level, and the external (environmental) conditions.

Recent developments by The Strategic Highway Research Program (SHRP) have recommended the use of a constant height repeated simple shear test (CHRSST) (Figure 4.13), with confinement, as a laboratory method to produce representative shear failure as expected in the upper layer of the pavement structure. The study considers that permanent deformation is primarily caused by shear deformation rather than densification (vertical deformation) in properly constructed pavements [17].

The CHRSST method offers several benefits by the ability to capture important mixture characteristics which relate to the resistance to permanent deformation [17], such as:

- dilation under shear loading
- increasing stiffness with increasing confinement at elevated temperatures
- negligible volumetric creep
- residual permanent deformation on removal of load
- temperature and rate of loading dependence

Despite the benefits offered by this method, it may not be suitable for daily practice as the equipment costs in excess of \$350000 US, the length of time required to carry out a design, and the need for staff trained to a higher level than would otherwise be required in a commercial laboratory (from Haydon as reported in [1]). Furthermore, the consideration of shear deformation as the primary cause of failure of wearing courses was argued by Gibb [1]. He stated that the densification (vertical deformation) represents the in situ performance of the materials better than the shear deformation as observed from the phenomena of reduction in air voids in pavements after construction due to the densification by traffic.

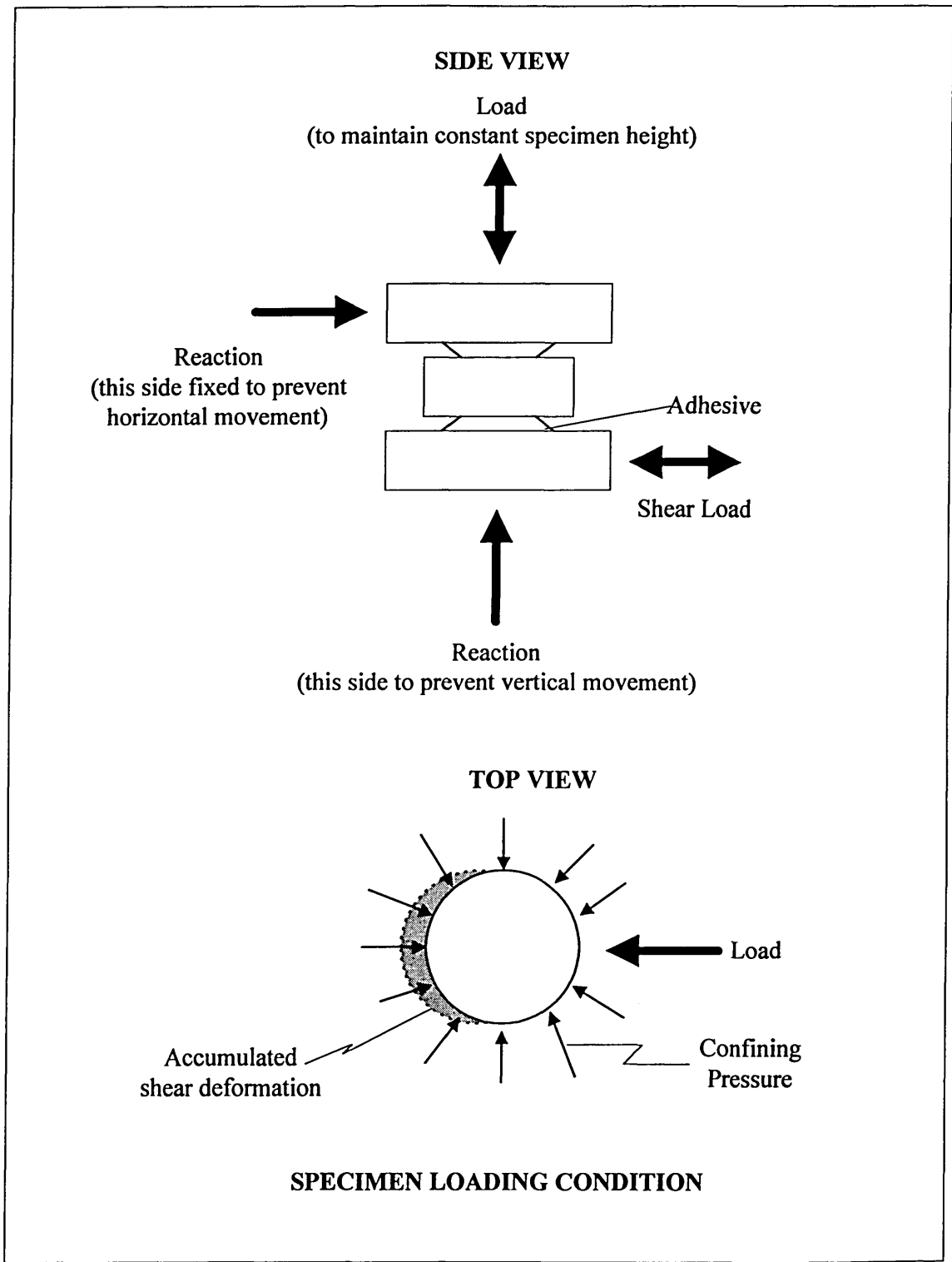


Figure 4.13 SHRP Shear test device

4.2.3.4 Dynamic Axial and Shear Loads in Hollow Cylindrical Apparatus

Recent research undertaken at the University of California at Berkeley has adopted a hollow cylinder apparatus for assessing viscoelastic properties of bituminous mixtures.

The test apparatus was designed to simulate the three dimensional stress state which occur in pavement materials *in situ* when subjected moving dynamic loads. Illustration of the apparatus is presented in Figure 4.14.

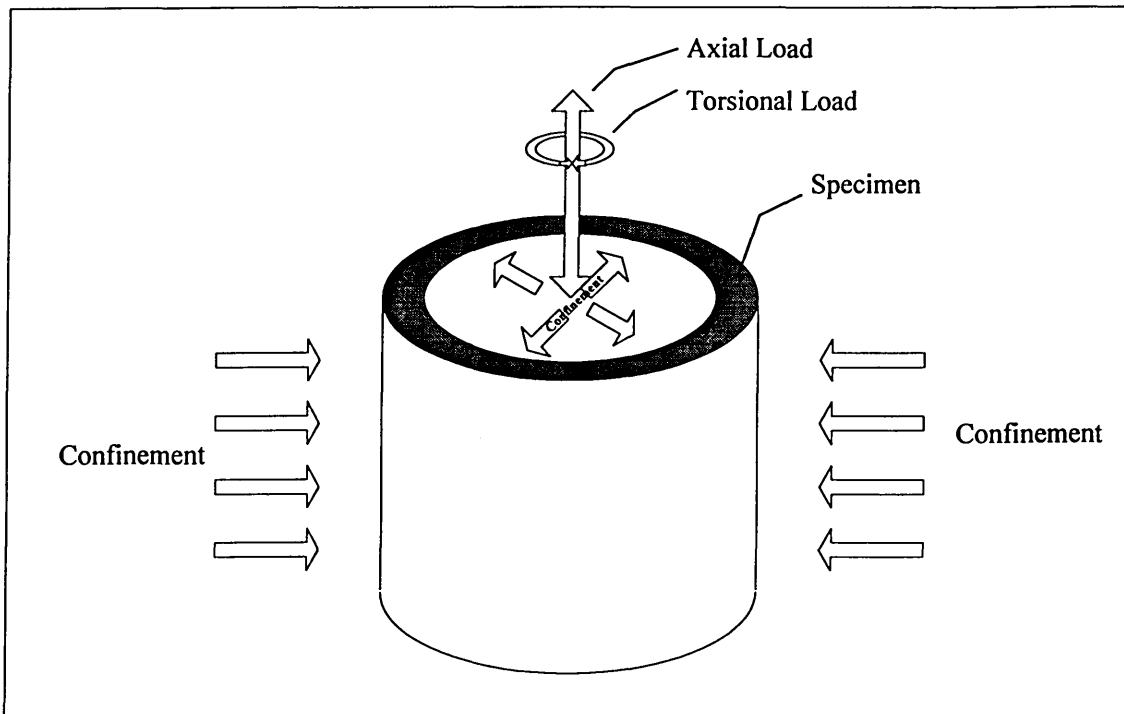


Figure 4.14 Illustration of a hollow cylindrical apparatus for testing bituminous mixtures.

The hollow cylindrical specimen is 45.7 cm (18 in.) high, with a 22.8 mm (9 in.) external diameter and a wall 2.54 mm (1 in.) thick [14, 15]. The loading system generates an axial and shearing (due to torsional load) actions which supposedly simulates the *in situ* traffic loading. Other parameters such as confining pressure, load wave-form, temperature, and rate of loading are controlled by a microcomputer.

The apparatus has some advantages, i.e.:

- ♦ it has the capability of applying three dimensional state of stress e.g. investigating the principle stresses and also the rotation of principle phase angle that occurs *in situ*
- ♦ it has the capability of applying both axial and shear stresses simultaneously through closed-loop control hydraulic system
- ♦ high precision measurements with good repeatability

- ♦ it provides a wide range of information on the viscoelastic properties of the specimens

Despite these advantages, the specimens need to be prepared by a specialised compaction equipment. Sousa and Monismith [14] used a kneading compactor which is specially designed for manufacturing of hollow cylindrical specimens, whereas Alavi and Monismith [15] compacted the specimens using a rolling wheel compactor. This condition causes a complexity during the specimen preparation.

#### 4.2.4 Remarks

The above discussions suggest that perhaps no single laboratory based testing can fully represent the *in situ* permanent deformation behaviour. The hollow cylindrical apparatus may be the best technique for simulating the *in situ* behaviour, but complexity during specimen preparation may make this technique becomes less preferable as a routine test. Nevertheless, for qualitative comparative purposes (for ranking the performance of different materials), any method can be adopted as long as it is supported by an appropriate analytical technique to obtain reasonable results.

The Author feels that some testing devices which are capable of generating repetitive loading, such as NAT or MATTA, are already commonly found in testing laboratories and they offer more advantages than the static loading devices. Therefore, this type of equipment was selected and used in this study.

The use of confinement can be advantageous but its availability is still limited, e.g. the confining device is not currently available in the NAT device at SHU. Furthermore, HRA mixtures have been selected for this study for which a confinement should not significantly affect the relative performance of this type of mixture as the strength of the mixture primarily relies on the stiffness of mortar/binder [1]. Therefore, the Author omits this confining effect with an additional assumption that the materials tested in this study represent a severe *in situ* condition.

### 4.3 Modelling Material Response

The general practice in modelling of pavement response to traffic loading used to be to treat it as a multilayer elastic system, and therefore, the material's behaviour was assumed to be linear elastic. In the linear elastic analyses, the material is characterised mainly by the elastic modulus and Poisson's ratio. The elastic analyses have been found to be reliable for the calculation of stresses, strains, and displacements in the road structure, especially when the pavement is subjected to short loading times. However, problems have been identified that the increase of pavement distress due to today's heavier traffic generates stresses beyond the elastic limit that, consequently, lead to premature failure of the material [18]. Therefore, despite the simplicity of this method, the linear elasticity can only be a rough representation of the real behaviour of the pavement [20].

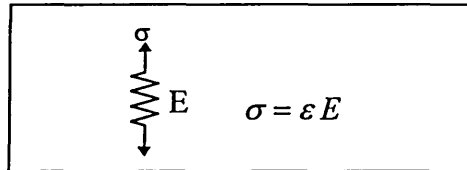
The limitation of the elastic theory leads to further developments in modelling pavement response based on viscoelastic response [19] which can then be analysed by either linear viscoelastic or non-linear non-elastic (e.g. plastic and viscoplastic) analyses [20,21].

The linear viscoelastic analysis has been proposed to be more representative in calculating viscoelastic response of flexible pavements under dynamic loading, particularly for long loading times. In this analysis, doubling the stress as a function of time results in a doubled strain as a function of time, and *vice versa* [22]. The stiffness modulus is independent of stress level and strain level.

The non-linear non-elastic analyses can be carried out by using finite element programs. However, this method is still not capable to "*account for the time dependency of the load, and: as it is traffic, the load moves*" [20]. Additionally, the mathematical models and material testing involved can be too complicated for everyday practice [21], unless a computer based software, which employs the finite element analysis and has a user-friendly design, is developed.

### 4.3.1 Elastic Model

Elastic models are the simplest form of stress/strain relationship and are developed based on the theory of elasticity, e.g. Hooke's Law, that stress is always directly proportional to strain in small deformation but independent of the rate of strain. The relationship between uniaxial stress and strain in the elastic condition can be formulated as:



The diagram shows a rectangular box containing a vertical spring symbol. To the left of the spring is the Greek letter sigma ( $\sigma$ ) with a downward-pointing arrow. To the right of the spring is the letter E. To the right of E is the equation  $\sigma = \epsilon E$ .

*Equation 4.8*

where  $\sigma$ ,  $\epsilon$ , and  $E$  are stress, strain, and elastic stiffness, respectively. As implied by its formulation, there is no energy dissipated during the deformation process since the elastic materials have the ability to store energy and to recover to the original position, without loss, upon the removal of load. This condition is never found in viscoelastic materials, such as bituminous materials at medium and high temperatures. Furthermore, the materials are assumed to be homogeneous, isotropic, and experiencing small deformations. Therefore, these limitations have put the reliability of using this model for simulating the response of bituminous materials into question.

In general, there are two procedures for limiting permanent deformation in the road pavement based upon this elastic model, i.e. by limiting vertical compressive strain at the top of the subgrade and by limiting the total accumulated permanent deformation on the pavement surface based on the permanent deformation properties of each individual layer.

The first procedure is based on a condition that if the maximum compressive vertical strain or stress at the top of the subgrade is less than a critical value, then excessive permanent deformation will not occur for a specified number of load applications to terminal serviceability of the pavement [23]. The critical stress for the relationship between strain and the logarithm of the number of load repetitions, above which the

slope increases until failure, was introduced from the AASHO Road test (as quoted in the Valejo's report [23]). At stresses below the critical stress, the material exhibits a stable condition.

The Shell Pavement Design Manual (SPDM) is a well-known permanent deformation model developed based upon the elastic stress using a static creep device [9, 10, 11, 12]. This model is based on the condition that the accumulation of permanent deformation of individual layers in a multilayer pavement structure must be controlled below a threshold value. The summary of analysis based on this model is as follows:

$$\Delta h = k h \left[ \frac{\sigma_o}{S_{mix,v}} \right] \quad \text{where} \quad k = C_m Z_o$$

Equation 4.9

where:

$C_m$  = a correction factor for dynamic effect with values ranging between 1 and 2 depending on the type of bituminous mixture (Table 4.2).

Table 4.2 Correction factor for dynamic effects,  $C_m$  (after Van de Loo)

Mix Type	$C_m$
Sand sheet and lean sand mixes Lean open asphaltic concrete	1.6 - 2.0
Lean bitumen macadam	1.5 - 1.8
Asphaltic concrete Gravel sand asphalt Dense Bitumen Macadam	1.2 - 1.6
Mastic types Gus-asphalt Hot rolled asphalt	1.0 - 1.3

$\Delta h$  = the resulting rut depth at the observed bituminous layer.

$h$  = the thickness of the observed bituminous layer.

$S_{mix,v}$  = the stiffness modulus of the mixture under long loading time (viscous condition) which is obtained from a static creep test (the subscript-v is to indicate a viscous condition)

$Z_o$  = a configuration factor to account for the absence of confinement pressure, as found in actual pavements, in the uniaxial static creep test, as a measure of stress distribution in the bituminous layer due to loading with standard pressure  $\sigma_o$  (note that the *subscript-o* is to indicate that the SPDM standard wheel is used to calculate the stress distribution in the structure).

$$Z_o = \frac{\sigma_{av,o}}{\sigma_o}$$

*Equation 4.10*

$\sigma_o$  = the standard pressure.

$\sigma_{av}$  = the average vertical stress in the bituminous layer resulting from one standard wheel pass.

Relationship between the stiffness modulus of the mixture,  $S_{mix,v}$ , and the modulus of the binder,  $S_{bit,v}$ , is:

$$\log S_{mix,v} = \log b + q \log S_{bit,v}$$

*Equation 4.11*

where  $b$  and  $q$  are the constants (the intercept and the slope line, respectively) determined from the regression line of Equation 4.11.

The slope value  $q$  varies typically between 0.10 and 0.20, and for the static creep model,  $S_{mix,v}$  can be derived from the deformation curve (permanent deformation  $\epsilon_p$  versus loading time  $t$  under constant load compressive test), and hence:

$$S_{mix,v} = \frac{\sigma}{\epsilon_p}$$

*Equation 4.12*

where  $\sigma$  is the applied stress. For the bituminous binder, the stiffness  $S_{bit,v}$  can be calculated from the shear viscosity  $\eta$  at the test temperature and the loading time  $t$ :

$$S_{bit,v} = \frac{3\eta}{t}$$

*Equation 4.13*

The effect of traffic loading and climatic condition on the parameter  $S_{bit,v}$ , can be assessed from:

$$S_{bit,v} = \frac{3\eta}{W_{eq} t_w}$$

*Equation 4.14*

where  $t_w$  is the wheel loading time as a measure for the traffic speed,  $W_{eq}$  is the number of standard wheel passes obtained from traffic spectrum, and  $\eta$  is the binder viscosity at the average paving temperature.

The binder viscosity ( $\eta$ ) can be empirically determined from [24]:

$$\eta = 1.3 * 10^{\left[3 + \frac{T_{SP} - T}{10}\right]}$$

*Equation 4.15*

where  $T_{SP}$  and  $T$  are ring and ball softening point and test temperatures in centigrade, respectively. The binder viscosity ( $\eta$ ) is in  $N.s/m^2$  (Pa.s).

#### **4.3.1.1 Cumulative Damage in Permanent Deformation**

Monismith [25] stated that the use of layer strain procedure allows application of alternative cumulative damage analysis based on plastic creep studies and termed the “time-hardening” and “strain-hardening” procedures as illustrated in Figure 4.15. This figure can be developed from simple loading tests to predict the cumulative effects of stresses of different intensities.

In the time-hardening procedure, the resulting permanent strain  $\epsilon_1^P(N)$  is developed from stress level  $\sigma_1$  for  $N_1$  repetition. An equivalent number of load repetitions  $N_2'$  which would give the same permanent strain at different stress level, say  $\sigma_2$ , is obtained as shown in Figure 4.15. The same thing applies for  $N_2$  repetitions at stress level  $\sigma_2$ , the resulting permanent strain will be  $\epsilon_2^P(N)$ , and this will give the total strain ( $\epsilon_1^P + \epsilon_2^P$ ) which is obtained from the path shown in Figure 4.15. This approach is included in the Shell pavement design procedure [10].

The strain-hardening procedure requires determination of permanent strain  $\epsilon_1^p(N)$  after  $N_1$  repetitions of stress level  $\sigma_1$ . The number of repetitions at stress level  $\sigma_2$  is then taken equal to  $N_1$ , and additional applications are applied to  $N_2$ . Total permanent strain is then the sum of  $\epsilon_1^p$  and  $\epsilon_2^p$ .

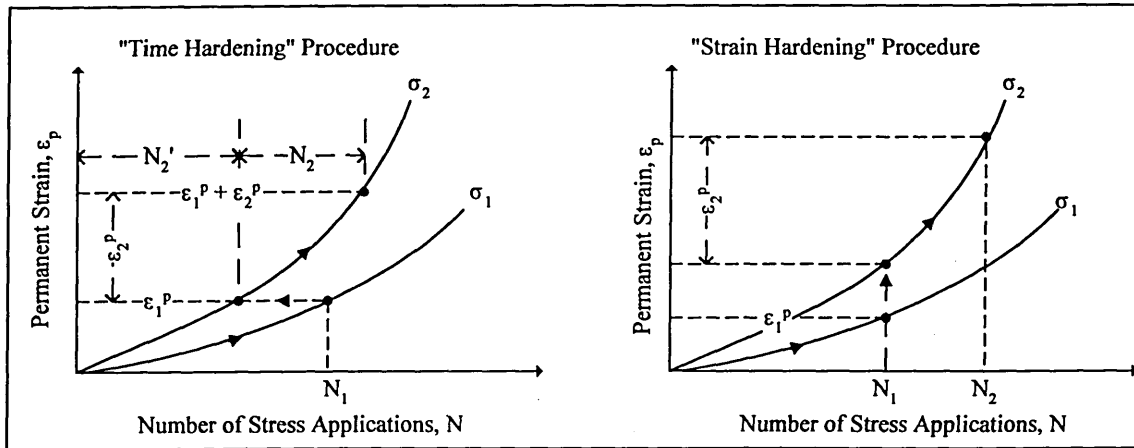


Figure 4.15 Procedures to predict cumulative loading from results of simple loading test. After Monismith [25]

### 4.3.2 Viscoelastic Model

Linear viscoelastic approach has been used to describe the behaviour of polymeric materials. Mechanical behaviour of materials has been commonly modelled as an arrangement of a finite number of linear Hookean springs and Newtonian dashpots. Some configurations have been developed based on Maxwell and Voigt (or Kelvin) elements (Figure 4.16 and Figure 4.17). The dashpots represent viscous properties while the springs represent elastic properties. Pavement responses are time dependent due to the fact that they have a viscous as well as elastic materials. Therefore, a viscoelastic approach offers many advantages over elastic theory for the design or analysis of pavements. However, the assumption that bituminous materials behave linearly in the linear viscoelastic models, is not necessarily true especially at high temperatures at which materials tend to behave in a non-linear manner.

A linear viscoelastic model for pavement materials is suggested by Thrower [26], where in the time limit of unloading the permanent deformations of the structure are obtained from purely viscous parameters, as represented by the Maxwell model (Figure 4.16).

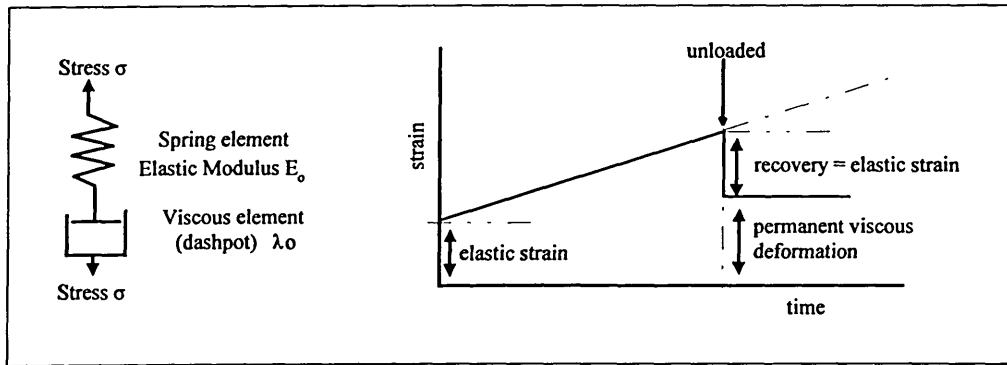


Figure 4.16 Maxwell element model

Under a constant stress, the total strain of the Maxwell element's model is the sum of the strains of both spring and dashpot, and hence:

$$\begin{aligned} \varepsilon_{elastic} &= \frac{\sigma}{E_0} \\ \varepsilon_{viscous} &= \frac{\sigma}{E_0} \left( \frac{t}{T_0} \right) \\ \varepsilon &= \frac{\sigma}{E_0} \left( 1 + \frac{t}{T_0} \right) \end{aligned}$$

Equation 4.16

in which  $T_0 = \lambda_0/E_0 =$  relaxation time.

Under constant stress the recovery (delayed elastic) modelled by the Voigt's element (Figure 4.17) can be calculated as:

$$\varepsilon_{de} = \frac{\sigma}{E_1} \left( 1 - e^{-\frac{t}{T_1}} \right)$$

Equation 4.17

where  $T_1 = \lambda_1/E_1 =$  retardation time.

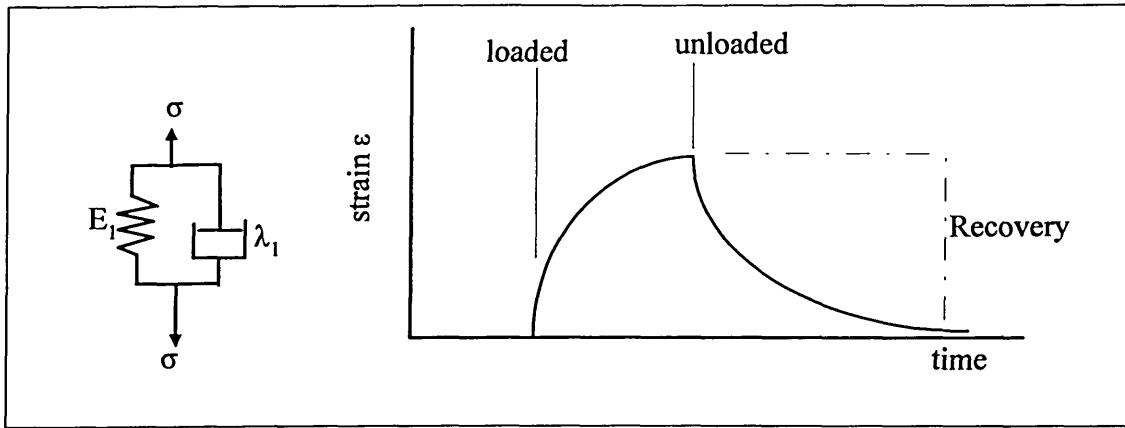


Figure 4.17 Voigt (Kelvin) element model

Another model which widely used to describe the response of a viscoelastic material is reported by Hopman *et al* [21, 27] and Verburg *et al* [28], i.e. a four-element viscoelastic model (Burger's model), which consists of a Maxwell and Kelvin elements in series, as shown in the Figure 4.18.

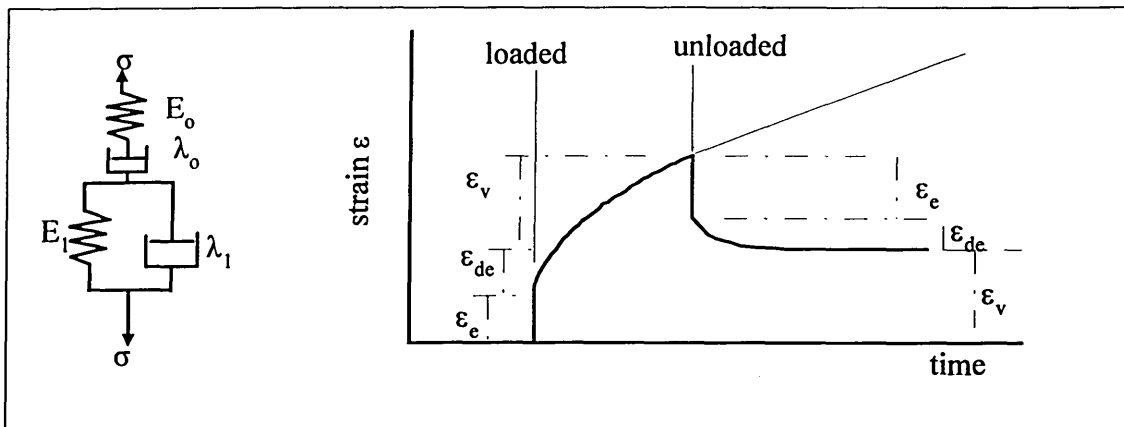


Figure 4.18 Burger's model

In this model, the total deformation consists of an instantaneous elastic deformation ( $\epsilon_e$ ), delayed or retarded elastic deformation ( $\epsilon_{de}$ ), and viscous flow ( $\epsilon_v$ ). The first two are recoverable deformations on the removal of the load and the third results in a permanent deformation in the structure. Therefore, the total deformation for a constant applied stress at the time  $t$  can be formulated as follow:

$$\epsilon_t = \epsilon_e + \epsilon_{de} + \epsilon_v$$

Equation 4.18

Therefore, by replacing the values of strain components with Equation 4.16 and Equation 4.17:

$$\varepsilon = \frac{\sigma}{E_0} \left( 1 + \frac{t}{T_0} \right) + \frac{\sigma}{E_1} \left( 1 - e^{-\frac{t}{\tau_1}} \right)$$

Equation 4.19

This model has shown that the effect of the viscous element  $\lambda_0$  can be seen as the permanent deformation [28]. However, there is a disagreement over this parameter, the first opinion [27] says that the element  $\lambda_0$  is responsible for causing permanent deformation as implied by the philosophy of the model, whereas the second opinion [28] states that the model is not suitable for the calculation of permanent deformation in the dynamic creep test because  $\lambda_0$  is not constant during the test. These different interpretations of these models are summarised in Table 4.3.

The author believes that the viscous element  $\lambda_0$  of the Burger's model is the only element that contributes to the permanent deformation. The inconstant values of determined from a dynamic creep test may be due to the effect of repetitive loading that the viscous response becomes more dominant with the increased number of load repetitions. Therefore, the Burger's model may be more appropriate for static creep test rather than for dynamic creep test.

Table 4.3 Comparison between Maxwell, Voigt, and Burger models.

Represented response	Maxwell element	Voigt (Kelvin) element	Burger model	Reference
Model	viscoelastic liquid	viscoelastic solid	viscoelastic liquid	
Creep	no yes -	yes no -	- yes no	Ferry [29] Hopman <i>et. al</i> [21] Verburg <i>et al</i> [28]
Stress relaxation	yes	no	yes	Ferry [29]
Viscoelastic retardation	no	yes	yes	Hopman <i>et. al</i> [21]

Souse *et al.* [30] proposed a three dimensional Maxwell elements in parallel. The dilatancy effect and the increase in effective shear modulus under hydrostatic pressure

(hardening) are due to the aggregate skeleton and are associated with the spring element whereas the temperature effect and the loading rate are due to the bituminous binder and are associated with the dashpot element. This technique incorporating the use of finite element analysis allows computations of longitudinal and transversal stresses and strains. Their validation report indicates that the model is capable of capturing the important aspects of the permanent deformation response of binder-aggregate mixtures, and it accurately ranks the performance of the materials according to their known permanent deformation resistance. However, more constants need to be determined which makes this approach is time consuming and requires a well-developed finite element program, e.g. testing duration of 5 hours was required to run the simulation for five cycles.

### 4.3.3 Viscoplastic and Plastic Model

Mortazavi [31] reported that bituminous mixture exhibits plastic behaviour under certain conditions where the applied stress results in deformation exceeding a yield value due to inter-connection between particles in the structure of the materials. The Bingham model is widely used to illustrate this behaviour, as represented by the following equation:

$$\tau = \tau_y + \eta_{pl} \left[ \frac{d\gamma}{dt} \right]$$

*Equation 4.20*

where  $\tau$  is the stress,  $\tau_y$  is the yield stress,  $\eta_{pl}$  is the plastic viscosity, and  $d\gamma/dt$  is the strain rate. In this model, flow occurs resulting in continuous deformation only at stresses which exceed the yield stress. The material behaves as an elastic solid up to the yield stress without undertaking permanent deformation. The flow curve of a Bingham body is a straight line indicating that the rate of shear is proportional to the shear stress in excess of the yield stress. However, many of these materials show a non-linearity at the early stage of their deformation, as shown in the Figure 4.19 (dashed line).

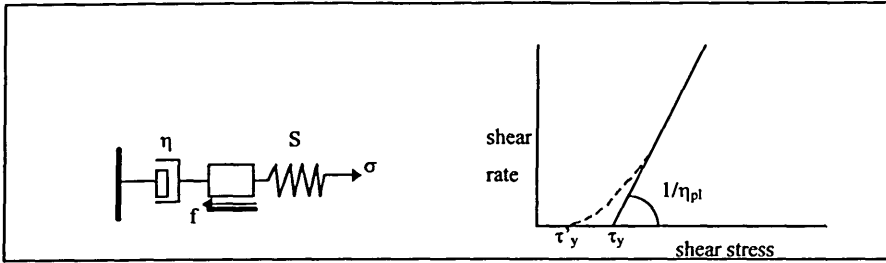


Figure 4.19 Bingham model and plastic deformation

The Bingham model is a combination of a plastic solid and a Newtonian fluid, and exhibits a kind of viscoplastic flow which is impossible to separate into plastic and viscous components.

Other models for the plastic deformation of bituminous materials have been proposed by Hopman and Nilsson [27] using the principal of Mohr-Coulomb (Figure 4.12). The model suggests that the material fails when the stress circle crosses the failure line (also termed the “failure envelope”). Materials will behave linear viscoelastically if the applied stresses generate a condition such that the shortest distance of the circle to the failure line is very large [27]. They used a parameter  $R$  as a measure of stability of the material against plastic flow. The material is in stable condition if  $R$  is small, and hence no plastic flow occurs.

$$R = \frac{\sigma_1 - \sigma_3}{\sigma_{1,f} - \sigma_3}$$

Equation 4.21

$$\sigma_{1,f} = \frac{(1 + \sin \phi)\sigma + 2C \cos \phi}{1 - \sin \phi}$$

Equation 4.22

where  $\sigma_1$  is the first (largest) principal stress

$\sigma_3$  is the third (smallest) principal stress

$\sigma_{1,f}$  is the first principal stress at failure

$C$  is the cohesion in the Mohr-Coulomb failure model

$\phi$  is the angle of friction in the Mohr-Coulomb failure model

#### 4.3.4 Remarks

Amongst different approaches in modelling material response, the linear viscoelastic approach has been gaining more popularity. More and more works have been carried out by conducting repetitive or dynamic loading as opposed to the “traditional” static creep loading. Nevertheless, the role of yield stress which is usually determined from static triaxial creep loading is also important as materials with low yield stress are susceptible to permanent deformation. Different types of loading (static or dynamic) can be selected to fit a particular design purpose, for example: static loading is better used for designing of parking area or airport apron where static wheel loading is dominant and dynamic or repetitive loading may be better for designing of airport runways or road pavement where dynamic wheel loading is dominant.

Selection of an appropriate mechanical model based on the viscoelastic nature of bituminous materials is important to avoid under- or over-estimation of the material performance. More complex approaches, such as non-linear viscoelastic [30] models, may offer better accuracy than the linear viscoelastic model but this model is more complicated and requires more constants to be determined, which makes them not suitable for routine analysis. The Author concludes that the linear viscoelastic model with its limitations is reasonably sufficient for material design purposes.

### 4.4 *Development of Dissipated Energy Approach*

#### 4.4.1 Theoretical Background

During the deformation of a viscoelastic material, part of the total energy required to perform the work is dissipated and the remainder of the deformational energy being stored elastically. The dissipated work can be exhibited by one or more damage mechanisms: fatigue cracking, crack propagation, permanent deformation (plastic flow) and heat. Tschoegl [32] states that “*the rate of absorbed energy per unit volume of a viscoelastic material during deformation is equal to the stress power, i.e. the rate at which the work is performed*” (see Equation 4.23).

$$\frac{dW}{dt} = \sigma(t) \frac{d\varepsilon}{dt}$$

## Equation 4.23

where  $dW/dt$  is the rate of absorbed energy per unit volume,  $\sigma(t)$  is the applied stress as a function of loading time  $t$ , and  $d\varepsilon/dt$  is the strain rate.

The total work of deformation which is the mechanical energy absorbed per unit volume of material in the deformation up to time  $t$ , can be formulated as:

$$W(t) = \int_0^t \frac{dW}{du} du = \int_0^t \sigma(u) \frac{d\varepsilon}{du} du$$

## Equation 4.24

where  $W(t)$  is the total work of deformation and  $u$  is the number of load applications as a function of loading time  $t$ , or,  $u = N(t)$ .

The total energy,  $W(t)$ , is the combination of both the stored (elastic) energy,  $W_e(t)$ , and the dissipated energy,  $W_d(t)$ . How much of the total energy can be stored, and how much can be dissipated depends on the type of deformation and on the properties of the material.

$$W(t) = W_e(t) + W_d(t)$$

## Equation 4.25

Differentiation of the above equation results in:

$$\frac{dW}{dt} = \frac{dW_e}{dt} + \frac{dW_d}{dt}$$

## Equation 4.26

The rate at which energy is absorbed by the material during the deformation at time  $t$  equals the sum of the rates at which energy is stored and dissipated.

In Figure 4.20, a load is applied at O and reaches its peak load value at A, the load is maintained until B and then it is released to allow the corresponding strain to recover

from the deformation. Eventually, if there is no permanent deformation, the strain will return to its original position O (plot I) or otherwise it goes to O' (plot II).

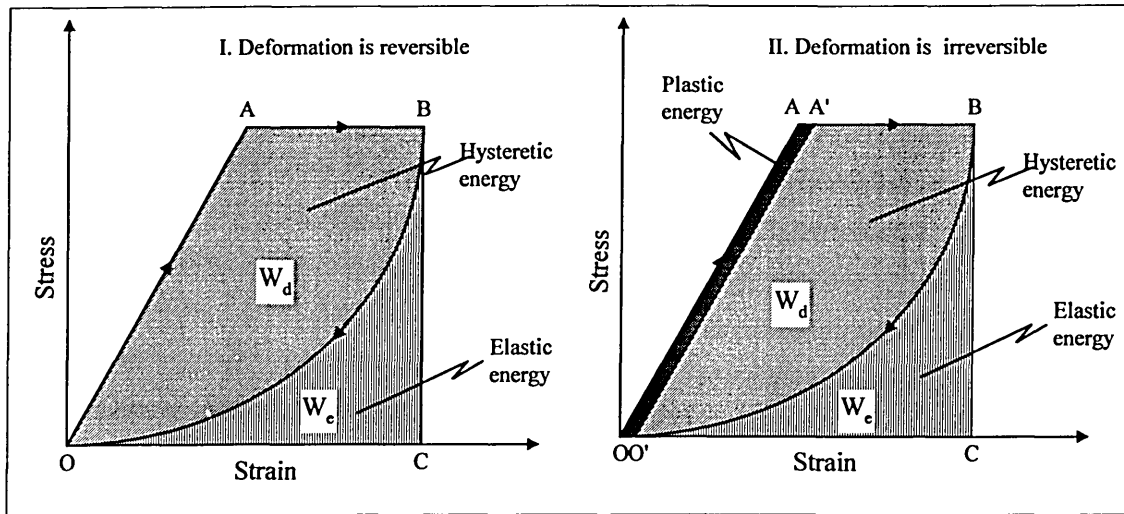


Figure 4.20 Idealised hysteretic loops.

In the case of reversible deformation (plot I), the energy stored during the deformation is completely released during the recovery. The dissipated energy is the area within the hysteretic loop (OAB), and the storage (elastic) energy is the area below the recovery curve (OBC). However, the energy stored in the deformation may not be completely released during the recovery, and hence a permanent (plastic) deformation occurs (plot II). In this case, the dissipated energy is the sum of the area within the hysteretic energy (O'A'B) and the area within the plastic energy section (OAA'O'), and the storage (elastic) energy is the area below the recovery curve (O'BC), where OO' is the irrecoverable strain. Hence the total dissipated energy can be formulated as:

$$W_{dissipated} = W_{hysteretic} + W_{plastic}$$

Equation 4.27

#### 4.4.2 Practical Applications

Studies on metals by Miner, as reported by Cao and Law [33], show that the effect of damage in one cycle of loading is directly proportional to the energy level of the cycle, independent of where in the time history that the particular cycle is applied. Studies by

Chapter 4 Permanent Deformation

these authors [33] also reported that the damage potential of soil under cyclic loading can be described by the energy dissipated by the soils during the loading. Soil deforms under vibrations during which energy is dissipated through hysteretic damping and plastic deformation of the soil.

In the bituminous road pavement, a certain amount of work is done in deforming the surface layer during each cycle of traffic loading. Part of this work is recovered in elastic recovery of the surface layer, while the remaining work is dissipated. The dissipated work is exhibited by one or more damage mechanisms: fatigue cracking, crack propagation, permanent deformation (plastic flow) and heat. However, the Author has never found any previous work that applies dissipated energy concepts to assessing the resistance to permanent deformation of bituminous mixtures. To the contrary, many authors [17, 34, 35,36,37,38,39] have reported the advantages of using the dissipated energy method for predicting fatigue life and crack initiation of bituminous mixtures. Some of the reports on the use of the dissipated energy method in fatigue testing are reviewed in this section, whereas the proposed application of this method for assessing the resistance to permanent deformation is presented in the next section.

Most of the tests in the fatigue testing have been carried out by dynamic bending tests (flexural or trapezoidal specimens) with sinusoidal loading. The conditions under which most of these studies were undertaken were at temperatures ranging from 0°C to 20°C (a few tests at 30°C were also reported) where the response of the bituminous materials were well within the linear viscoelastic region.

A time delay, normally referred to as phase lag, is usually observed between the load and the measured deflection, and an associated amount of energy is dissipated with every loading cycle. The dissipated energy per cycle is determined from the area within the hysteretic loop (Figure 4.21) which can be determined from Equation 4.28 [34]. The dissipated energy is usually associated with viscous flow of the binder which dissipates most of the energy as heat.

$$w_i = \pi \sigma_i \varepsilon_i \sin \phi_i$$

where,

$w_i$  = dissipated energy in cycle  $i$

$\sigma_i$  = stress amplitude in cycle  $i$

$\varepsilon_i$  = strain amplitude cycle  $i$

$\phi_i$  = phase lag in cycle  $i$

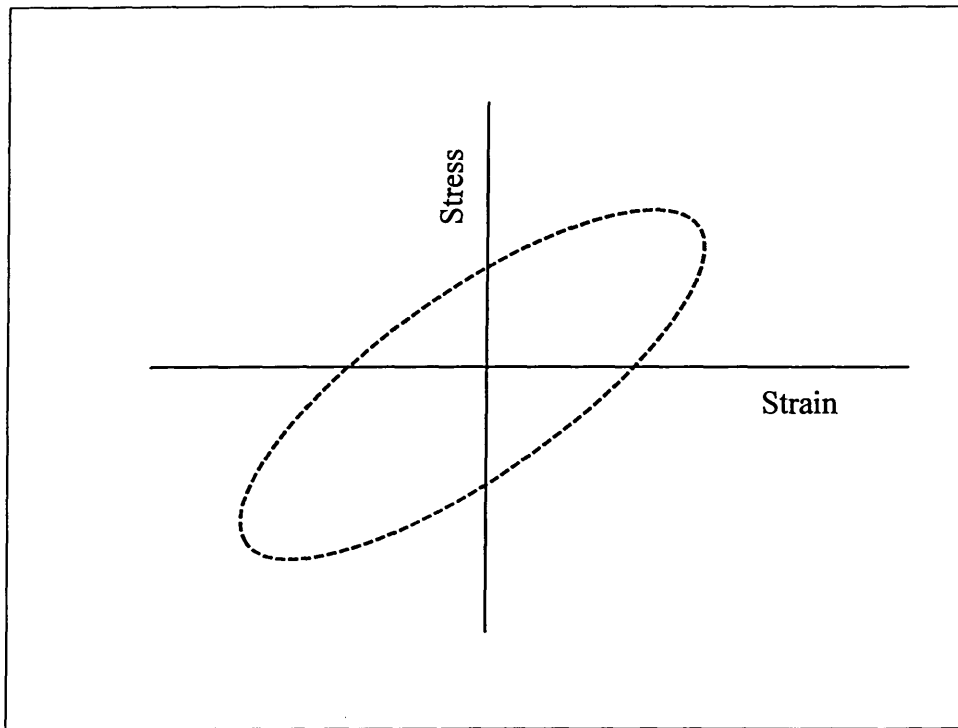


Figure 4.21 Typical plot of a hysteresis loop from a fatigue test

In controlled stress testing, the dissipated energy per cycle increases whereas in a controlled strain test it decreases, which is consistent with the reduction in the stiffness of the material and the change in dimensions of the hysteresis loop [38], as illustrated in Figure 4.22.

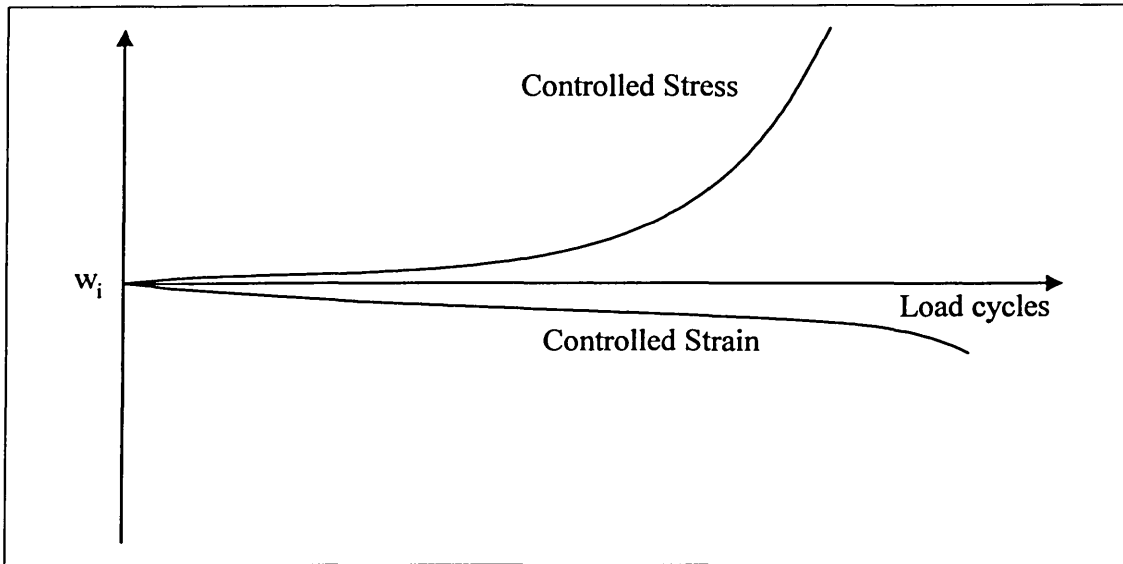


Figure 4.22 Variation of Dissipated Energy per Load Cycle during Controlled Stress and Strain Fatigue Test. After Rowe [38].

The cumulative dissipated energy is calculated by summing up the dissipated energy throughout a fatigue test and a relationship between the cumulative dissipated energy and the number of loading cycles to crack initiation is developed.

$$W = A N^c$$

Equation 4.29

$$W = \pi \sum_{i=1}^{i=N} \sigma_i \varepsilon_i \sin \phi_i$$

Equation 4.30

Previous research reported by Van Dijk and Visser [35] stated that the relationship presented in Equation 4.29 was independent of test method or testing conditions, frequency, temperature, or rest periods. However, a latter investigation by Tayebali, Rowe, and Sousa [39] showed that the energy-fatigue life is dependent on the mode of loading and temperature.

Van Dijk [34] and Van Dijk and Visser [35] introduced an energy ratio parameter  $\psi$  to accommodate the change in dissipated energy during repetitive loading due to change in stress/strain and phase angle during the test. The ratio of initial dissipated energy

( $w_{initial}$ ) to the total dissipated energy ( $W$ ) is represented by  $\psi$  and mainly dependent on the type of test and stiffness of the mixture. The  $\psi$  value ranges between 0.5 and 1.5 where  $0.5 \leq \psi \leq 1$  for controlled stress testing and  $1 \leq \psi \leq 1.5$  for controlled strain testing. The  $\psi$  value was observed to approach a value of unity when the mixture stiffness exceeds 26000 MPa, whereas  $\psi$  is dependent on the type of mixture if the mixture stiffness is between 1000 and 10000 MPa.

$$\psi = \frac{W_{initial}}{W}$$

*Equation 4.31*

$$w_{initial} = \pi N \sigma_o \varepsilon_o \sin \phi_o$$

*Equation 4.32*

where,

- $w_{initial}$  = initial dissipated energy per cycle
- $\sigma_o$  = the initial values of stress
- $\varepsilon_o$  = the initial values of strain
- $\phi_o$  = the initial values of phase lag
- $N$  = the total number of loading cycles

Tayebali, Rowe, and Sousa [39] reported that a linear relationship exists between stiffness ratio and energy ratio with stiffness ratio decreasing as energy ratio increased (Figure 4.23). Stiffness ratio is the ratio of stiffness at a given number of repetitions ( $N_i$ ) to the initial stiffness (stiffness at 200 repetitions,  $N_{200}$ ) and the energy ratio is the normalised dissipated energy, i.e. the ratio of cumulative dissipated energy at  $N_i$  to the cumulative dissipated energy at failure (which is different from the energy ratio  $\psi$  developed by Van Dijk and Visser).

Even though there are two different procedures in expressing the “energy ratio”, i.e. Van Dijk and Visser [35] and Tayebali, Rowe, and Sousa [39], however, there are no contradictions between them. Both procedures are independent of type of mixture and are dealt solely with the corresponding stiffness of the mixture. However, the Tayebali,

Rowe, and Sousa approach has benefits that it provides information of the reduction stiffness at the end of fatigue test, i.e. around 40% and 50% of the initial stiffness respectively for controlled strain and controlled stress fatigue testing [38], and enables estimation of fatigue life without performing fatigue testing up to failure. Similarly, estimation of fatigue life based upon Van Dijk and Visser approach, i.e. by evaluating the dynamic properties ( $S_{mix}$  and  $\psi$ ), without performing fatigue testing is also possible if the dissipated energy per cycle is constant and the database of the material characteristics is available (i.e. constants A and z in Equation 4.29 or by using rheological approach developed by Rowe (38)). The complete procedure can be found in their reports. However, the Author finds the Tayebali, Rowe, and Sousa approach is simpler and less time consuming.

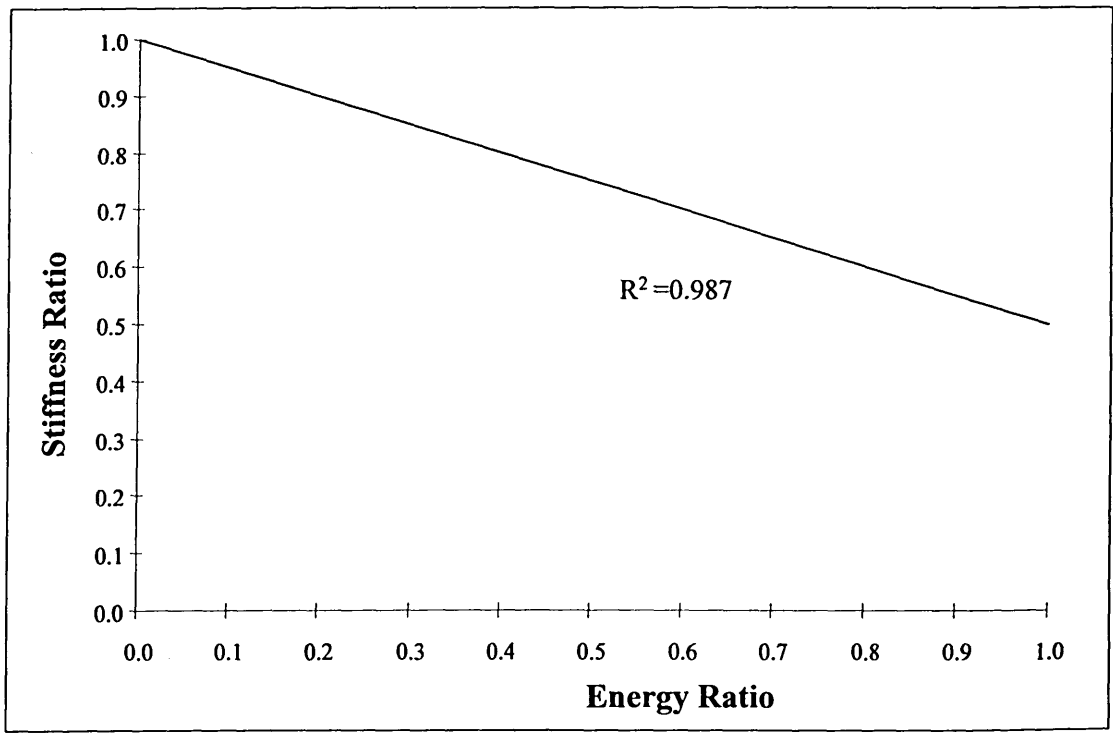


Figure 4.23 Stiffness Ratio versus Energy Ratio, controlled-stress flexural beam fatigue test at 20°C. After Tayebali, Rowe, and Sousa [39].

Some of the advantages of the dissipated energy method reported from the fatigue testing are:

1. A controlled energy fatigue test may provide a suitable solution for the inconsistent fatigue lives resulting from controlled stress or controlled strain fatigue testing (Figure 4.24) [39].

2. Dissipated energy can be used to accurately predict the life to crack initiation [38].  
The dissipated energy ratio ( $\psi$ ) can be used to define  $N_1$  which is the number of load cycles to crack initiation. The complete procedure to determine  $N_1$  can be referred to Rowe's thesis [38]. The point  $N_1$  allows a comparison of materials at equal states of damage and avoids an arbitrary definition of failure.
3. The presentation of fatigue results based on a dissipated energy law equation introduces loss of information for the individual measurements, i.e. the decrease of stiffness modulus during the test and the applied strain/stress amplitude.
4. A strong relationship between the normalised dissipated energy and the stiffness ratio which is independent of mixture type offers practicality and simplicity as a tool for prediction and evaluation of fatigue response of binder-aggregate mixtures [39].
5. Even though the dissipated energy law alone is not suitable for the prediction of the fatigue life in a fatigue test, it is possible to create a prediction procedure valid for all loading conditions based on the dissipated energy approach if the initial dissipated energy per period is known [37, 39].

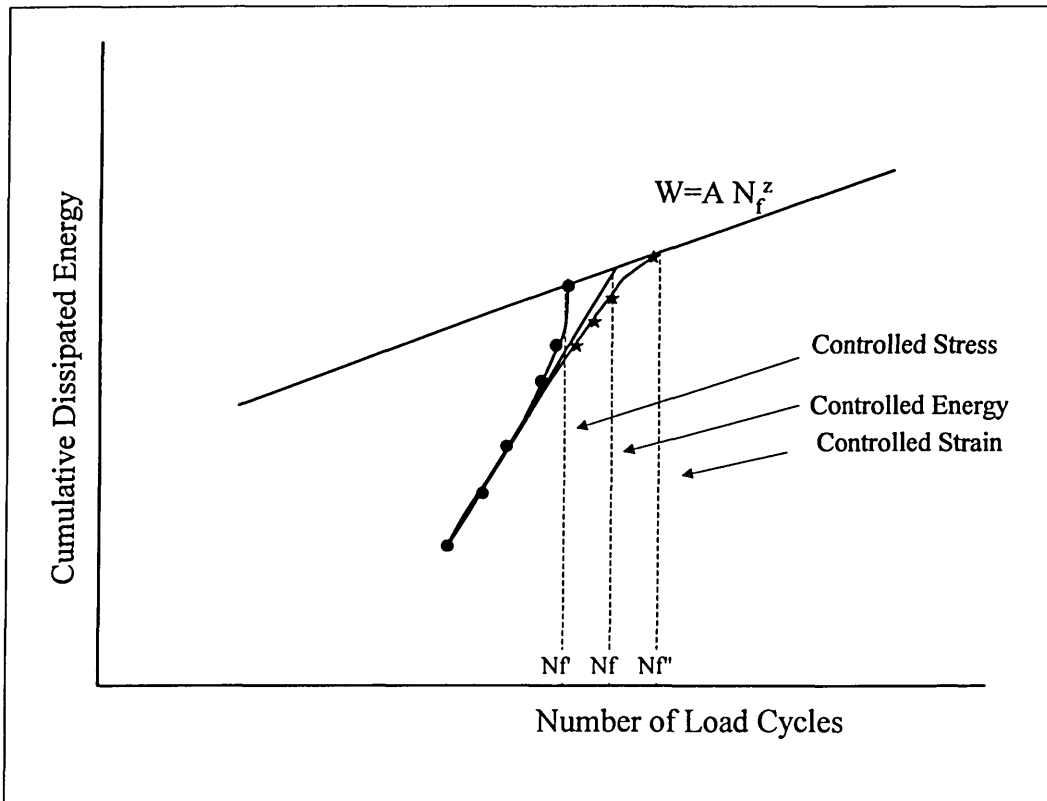


Figure 4.24 Schematic of cumulative dissipated energy versus number of cycles showing the effect of mode of loading. After Tayebali, Rowe and Sousa [39]

Disadvantages:

1. The test requires a data acquisition device which has the ability to capture stress-strain data, e.g. about 100 readings per second per load application (or per selected interval). This leads to a huge amount of data which can make the analysis more difficult.
2. The opinion that the ability of the dissipated energy to eliminate the apparent inconsistency between fatigue lives under controlled stress and controlled strain and that the fatigue lives under controlled stress and controlled strain are equal if the total dissipated energies in both types of tests are equal, appears no longer valid. No unique relationship exists between the cumulative dissipated energy and the number of load repetition to failure as it is now understood that the relationship is affected by the temperature and mode of loading [39].

#### 4.4.3 Hypothesis

Bituminous mixtures can exhibit non-linearity in the viscoelastic region at service temperatures above ambient, where in most cases permanent deformation is the major distress mechanism. In common to that of the fatigue phenomena, energy is also dissipated during the development of plastic deformation. Therefore, in order to minimise rutting, work dissipated by the material during each loading cycle should be minimised.

It is commonly accepted that binders deform and dissipate energy as heat by viscous flow [38] whereas bituminous mixtures predominantly deform by plastic flow of the aggregates [27]. Energy dissipated by viscous flow creates an accumulation of damage which can generate the creation of a plastic zone, which is commonly accepted as the start of crack initiation during fatigue testing.

Plastic flow may not be found in fatigue testing because fatigue testing is usually carried out by which no permanent deformation is allowed to develop<sup>d</sup> and, therefore, the

---

<sup>d</sup> However, permanent deformation can also be developed in controlled stress fatigue testing such as by using the Indirect Tensile Fatigue Testing (ITFT) on cylindrical specimens.

Chapter 4 Permanent Deformation

generated stress-strain curve (hysteretic curve) is generally drawn as a “closed loop” (Figure 4.21) and the calculated dissipated energy is solely due to viscous flow of the binder. However, the potential for permanent deformation increases as the temperature increases due to the onset of plastic flow by aggregate movement (reorientation) in the development of damage and leads to formation of an “open loop” in the stress-strain curve (Figure 4.20). This area has not been extensively explored by researchers in the explanation of the development of permanent deformation by using the dissipated energy method.

Based on these facts, one hypothesis that comes from this research is that there is a possibility for the dissipated energy method to be used to assess the resistance to permanent deformation of bituminous mixtures. The total energy dissipated to produce permanent deformation of bituminous mixtures due to repetitive loading can be calculated in the same manner as Equation 4.27. Therefore, a new definition of dissipated energy is proposed:

*The dissipated (loss) energy is the amount of energy which is dissipated by viscous flow and/or plastic flow, and leads to a potential damage (e.g. fatigue cracking or permanent deformation) when a bituminous material is subjected to repetitive loading.*

The hysteretic energy section represents the amount of energy dissipated due to a part of the viscous flow of the binder which leads to fatigue failure due to repetitive or cyclic loading, whereas the plastic energy section represents the amount of dissipated energy due to a part of the viscous flow of the binder and the plastic flow of the aggregate which leads to permanent deformation (Figure 4.20).

The main advantage of using this method is that energy incorporates both stress and strain, and therefore it can more adequately reflect both the strength and deformational aspects of the performance of bituminous materials.

### **Experimental Study**

Experimental works were carried out by using a dynamic creep test (unconfined) on the Nottingham Asphalt Tester (NAT) apparatus [40] where repetitive loading, using a square waveform, was applied for 200 and 1800 milliseconds of load application and removal, respectively, for every cycle of loading. The main objectives of applying load for 200 milliseconds was to generate a creep effect, e.g. to represent a condition where traffic speed is below 10-15 km/h. At this traffic speed, pavement damage due to the permanent deformation could increase by a factor of 70 compared to the damage at 50 km/h [41]. On the other hand, the 1800 milliseconds should provide sufficient duration for the strain to recover before the next load is applied. A permanent deformation is expected at the end of the recovery time due to the viscoelastic-plastic nature of the tested material.

Stress and strain data occurring during load applications were captured at 4 millisecond intervals and hysteretic loops plotted as the stress-strain curve for every load cycle or every cycle interval. Typical results are presented in Figure 4.25 and Figure 4.26.

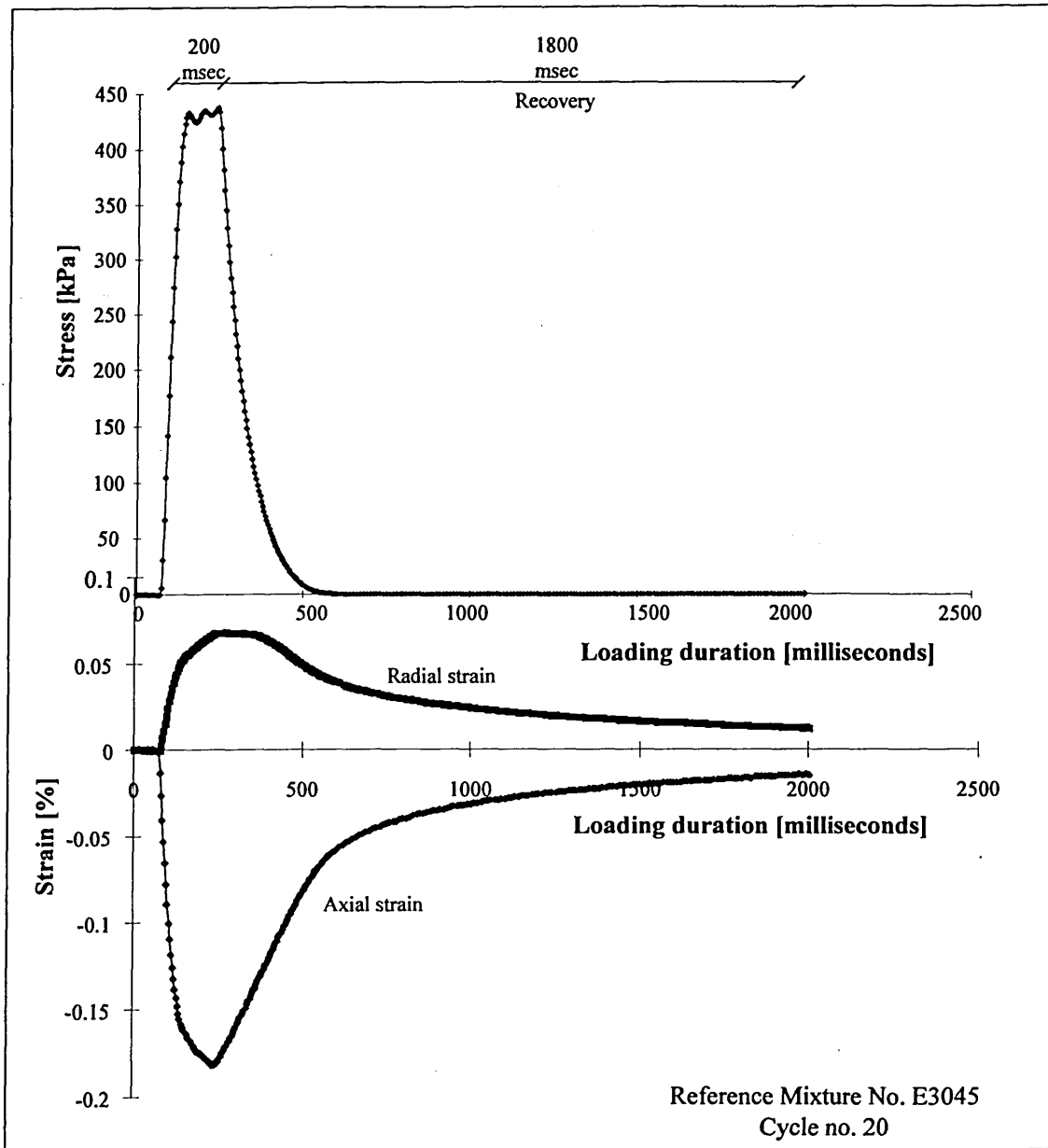


Figure 4.25 Typical plot of data captured at each load cycle (interval) from a dynamic creep testing. Reference mixture no. E3045.

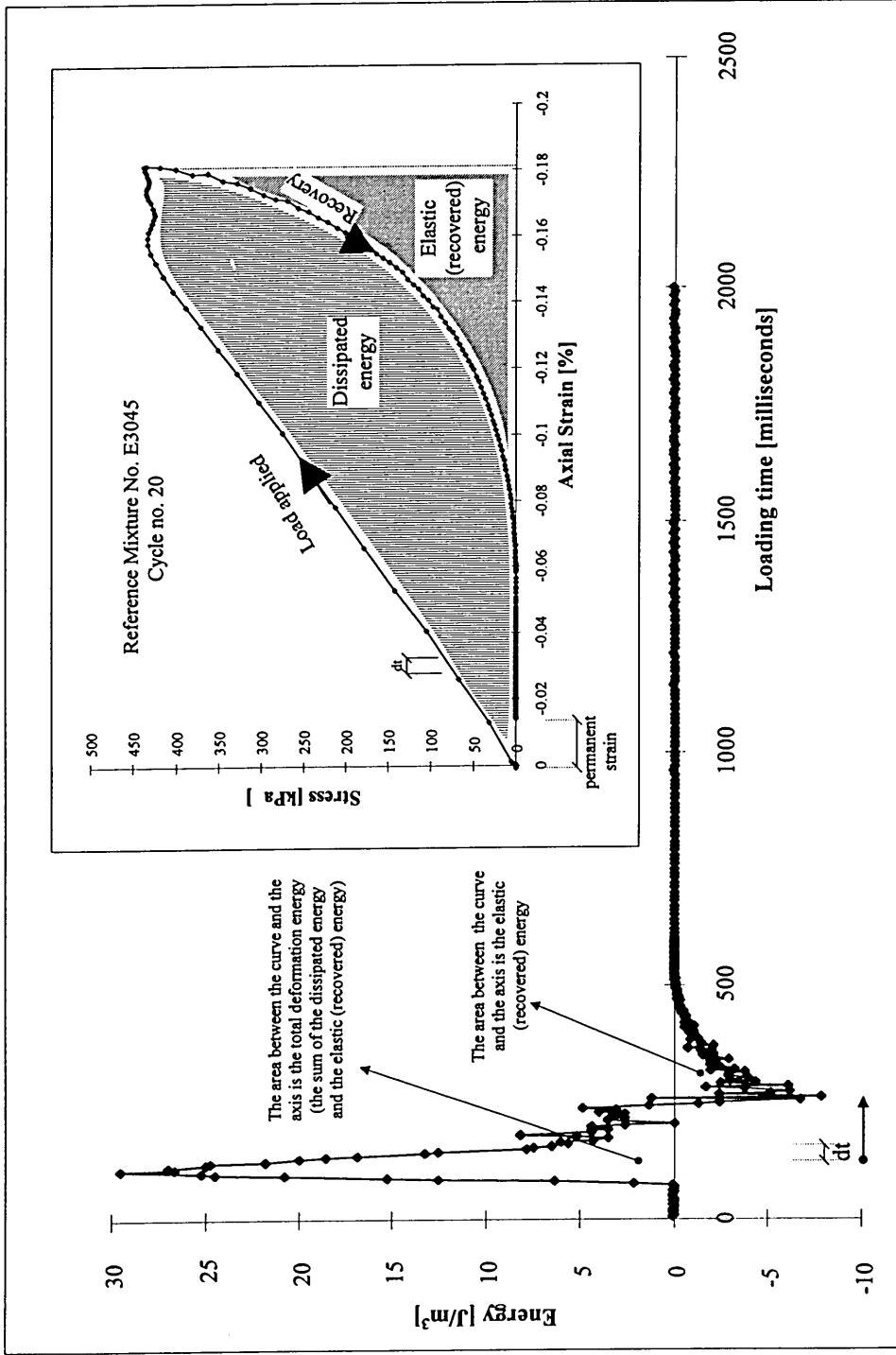


Figure 4.26 A Typical plot of a hysteretic loop at one cycle load application obtained from NAT dynamic creep. Reference mixture no. E3045.

The dissipated energy per cycle at a particular time interval- $i$  ( $w_i$ ) (see Figure 4.26 and Figure 4.27) is determined as the area within the hysteretic loop, or it can be formulated as:

$$w_i = \sum_{t=1}^{2000} \frac{(\sigma_t + \sigma_{t-1})}{2} (|\epsilon_t| - |\epsilon_{t-1}|)$$

Equation 4.33

where :

$t$  = loading/unloading time in milliseconds per cycle (from  $t=0$  seconds to  $t=2000$  milliseconds per cycle).

$\sigma$  = applied stress (recorded every 4 milliseconds)

$\epsilon$  = resultant strain corresponding to the applied stress (recorded every 4 milliseconds)

$w_i$  = the average total dissipated energy per cycle at an interval  $i$

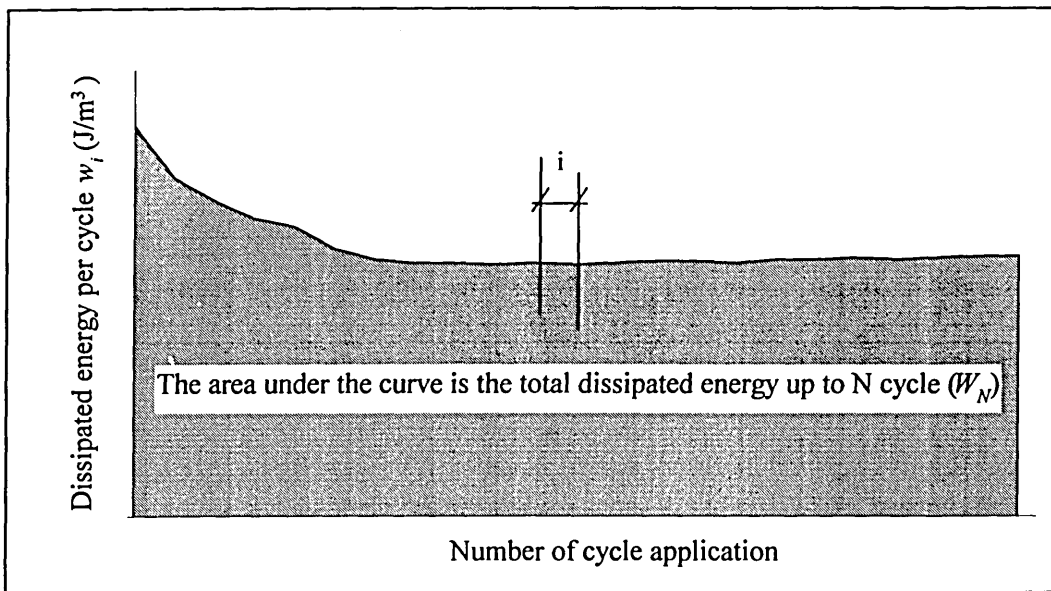


Figure 4.27 Cumulative Dissipated Energy  $W_N$  as the area under the  $w_i$  energy line

The cumulative dissipated energy ( $W_N$ ) is the area below the energy line and can be formulated as:

$$W_N = \sum_{i=1}^N w_i * n_i$$

*Equation 4.34*

where  $N$  = total number of intervals to failure

$n_i$  = number of pulse within time interval  $i$

if the dissipated energy per cycle = constant, then

$$W_{N_f} = N_f * w_o$$

*Equation 4.35*

where  $w_o$  is the “initial” (average) dissipated energy and  $N_f$  is the number of load applications to failure.

Figure 4.28 shows that the curve of permanent strain against number of loading cycle can be divided into three zones, i.e. compaction, stable, and unstable. Similar conditions are also found in the curve of dissipated energy per cycle against the number of loading cycle (Figure 4.29). The reduced strain rate in the compaction zone, as the test progressing, is related to the reduced dissipated energy per cycle. In the linear zone where the dissipated energy per cycle is constant, the strain rate is also constant. In the third (unstable) zone where the dissipated energy per cycle starts to increase towards the failure point is also related to the increased strain rate.

As the energy in the linear zone is constant (see Figure 4.29), the value of  $w_o$  was calculated as the average value of dissipated energy per cycle in this region. A potential benefit deduced from this condition is that the dissipated energy per cycle  $w_o$  can be used as a reliable procedure to determine the end of the linear region of a creep curve and can probably be related to the rate of permanent strain in the linear zone, and hence to explain the resistance to permanent deformation of bituminous mixtures.

#### **Determination of $N_1$**

The end of the linear zone ( $N_1$ ), as indicated in Figure 4.28, is normally determined as an arbitrary point. No available methods have provided a technique to definitively determine this point. The commonly adopted technique is to apply a linear regression

over some points in the curve of permanent strain versus number of load applications and, by doing iterative calculations, a line which gives the highest coefficient of correlation ( $R^2$ ) is selected. However, the application of dissipated energy method provides a solution to this matter, i.e. by using the dissipated energy ratio ( $DER_i$ ) as presented by Equation 4.36.

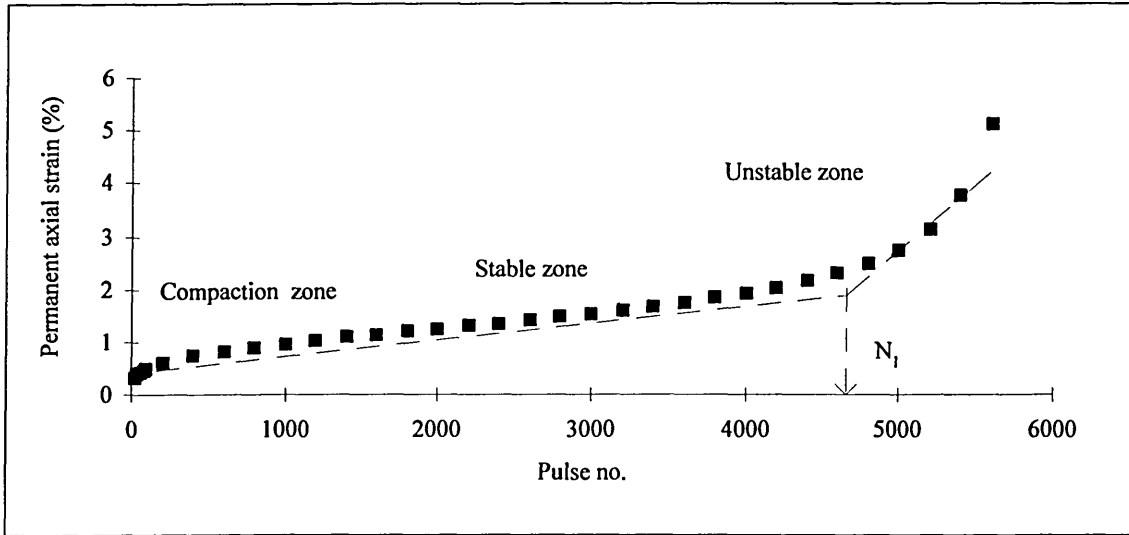


Figure 4.28 Plot of permanent strain curve from mixture no. BP502, as produced by the dynamic creep test from NAT.

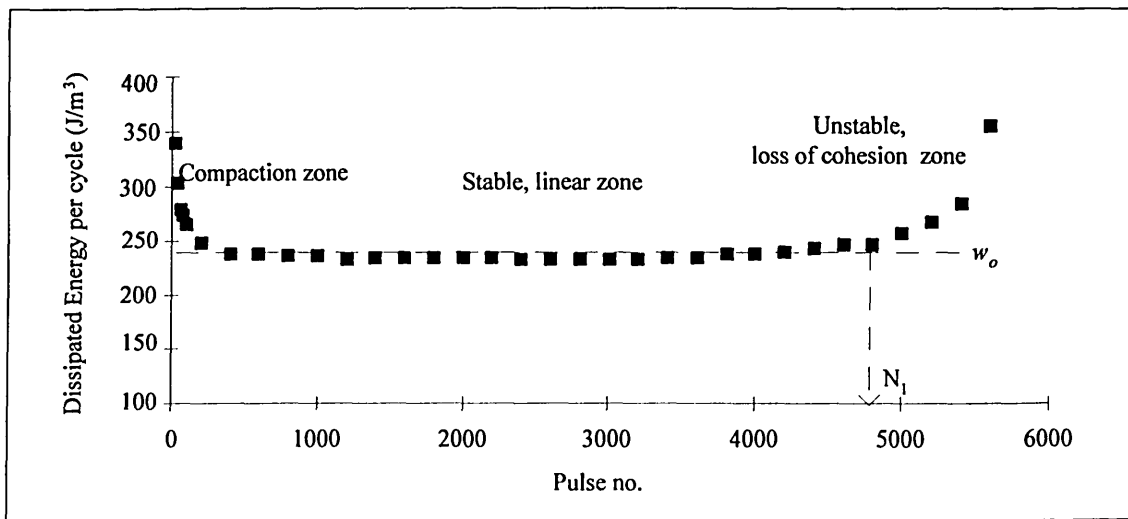


Figure 4.29 Plot of dissipated energy per cycle [ $J/m^3$ ] against the number of load repetitions  $N$  from mixture no. BP502.

The cumulative dissipated energy ( $W_{N_f}$ ) can be defined as the required energy to fail the specimen. The applicability of whether the initial dissipated energy ( $w_o$ ) and the cumulative dissipated energy ( $W_{N_f}$ ) can be used as indicators of the ability of a particular mixture type to resist deformation which lead to failure will be assessed in this thesis.

In this research, the dissipated energy ratio per cycle ( $DER_i$ ) is defined as:

$$DER_i = W_N/w_i$$

Equation 4.36

The curve of  $W_N/w_i$  is a straight line curve up to a value of  $N_l$  at which a significant change occurs in the progression of dissipated energy per period (Figure 4.29). This value can be related to the beginning of the unstable zone (see also Figure 4.28).

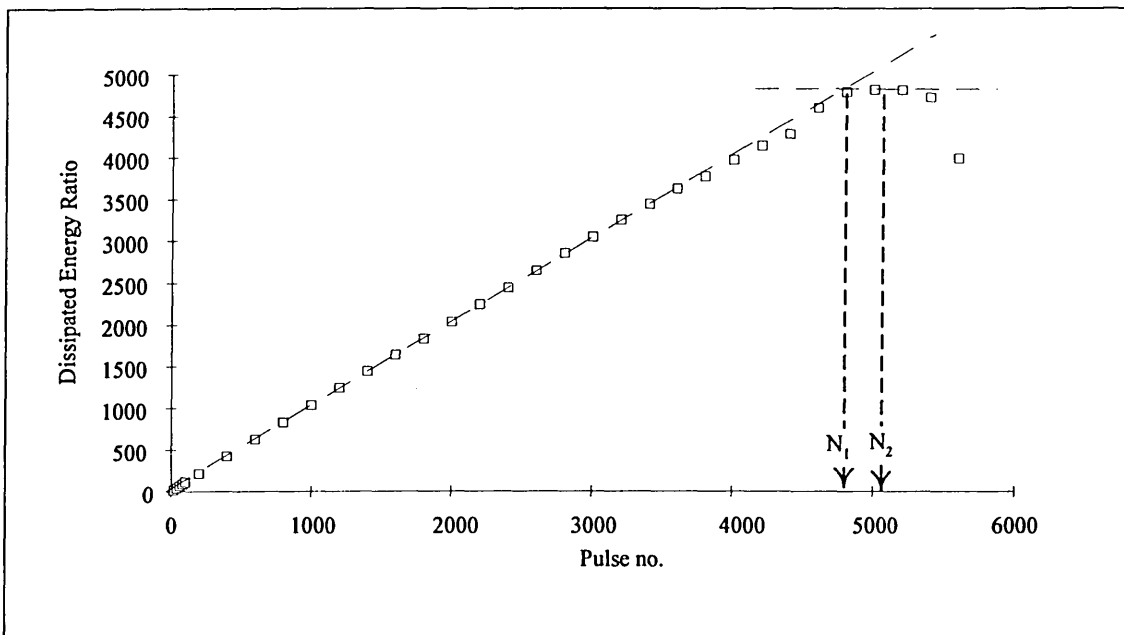


Figure 4.30 Plot of dissipated energy ratio [ $W_N/w_i$ ] against the number of cycles from mixture no. BP502.

As seen in the Figure 4.29,  $N_2$  is the turning point of the curve and  $N_l$  is the projection of  $N_2$  to the straight line curve, i.e. the line of equality where the values of  $W_N/w_i$  equal to  $N_l$ . The accurate identification of  $N_l$  can be beneficial as the analysis on the

performance of bituminous materials is normally undertaken at the linear region. Furthermore, it is also important to identify the point of  $N_I$  for the material design purposes to prevent the material from entering the unstable zone.

A hypothesis can be deduced from this pattern that the cumulative damage will still be below the bearing capacity of the sample if the dissipated energy ratio per cycle ( $DER_i$ ) is less than or equal to  $N_i$ , and hence a damage model based on the dissipated energy can be formulated:

$$\frac{DER_i}{N_i} \leq 1$$

*Equation 4.37*

The hypotheses presented in this section will be examined by a series of tests with the testing arrangement as described in *Chapter Five*, and be discussed in *Chapters Seven and Eight* will include an assessment of the test results for their limitations and applicability for their use in practice.

#### **4.5 References**

- 1 Gibb, J.M., "Evaluation of Resistance to Permanent Deformation In The Design of Bituminous Paving Mixtures", PhD Thesis, University of Nottingham, 1996.
- 2 "Bituminous Materials in Road Construction", Road Research Laboratory, HMSO, London, 1962
- 3 Goodrich, J.L., "Asphaltic Binder Rheology, Asphalt Concrete, and Asphalt Concrete Mix Properties", Proceedings of AAPT, Vol. 60, 1991, pp. 80-120.
- 4 Reese, R.E., "Development of a Physical Property Specification for Asphalt-Rubber Binder", Discussion part, Proceedings of AAPT, Vol. 63, 1994, pp.373-413.
- 5 Mahboub, K., "Rutting Characterisation In an Improved Asphalt Concrete Mix Design Procedure for the State of Texas", PhD Thesis, Texas A&M University, 1988.

- 6 Brown, S.F., "Material Characteristics for Analytical Pavement Design", Development in Highway Engineering-1, Edited by P.S.Pell, Applied Science, 1978.
- 7 Bell, C.A., "The Prediction of Permanent Deformation in Flexible Pavements". PhD Thesis, University of Nottingham, 1979.
- 8 Huang, Y.H., "Pavement Analyses and Design", Prentice Hall, 1993
- 9 Lijzenga, J., "On the Prediction of Pavement Rutting in the Shell Pavement Design Method", Proceedings of the 2<sup>nd</sup> European Symposium on Performance and Durability of Bituminous Materials", Leeds, April 1997, pp. 175-194.
- 10 Shell International, "Shell Pavement Design Manual", London, 1978.
- 11 Van de Loo, P.J., "Creep Testing, a Simple Tool to Judge Asphalt Mix Stability", Proceedings of AAPT, Vol. 43, 1974, pp. 253-281
- 12 Van de Loo, P.J., "The Creep Test: A Key Tool in Asphalt Mix Design and in the Prediction of Pavement Rutting", Proceedings of AAPT, Vol. 47, 1978, pp. 522-554.
- 13 Read, J.M., "Fatigue Cracking of Bituminous Paving Mixtures", PhD Thesis, University of Nottingham, 1996.
- 14 Sousa, J., and Monismith, C.L., "Dynamic Properties of Asphalt Concrete", Journal of Testing and Evaluation, Vol. 16, No. 4, July 1988, pp. 350-363.
- 15 Alavi, S.H., and Monismith, C.L., "Time and Temperature Dependent Properties of Asphalt Concrete Mixes Tested as Hollow Cylinders and Subjected to Dynamic Axial and Shear Loads", Proceedings of AAPT, Vol. 63, 1994, pp. 152-181.
- 16 British Standard 598: Part 111: 1995, "Sampling and Examination of Bituminous Mixtures for Roads and Other Paved Areas. Part 111. Method for Determination of Resistance to Permanent Deformation of Bituminous Mixtures Subject to unconfined Uniaxial Loading".

- 17 SHRP-A-417, "Accelerated Performance-Related Tests for Asphalt-Aggregate Mixes and Their Use in Mix Design and Analysis Systems", Strategic Highway Research Program, National Research Council, Washington D.C., 1994.
- 18 Davis, R.L., "Engineering Properties of Asphalt Mixtures and Their Relationship to Performance", Properties of Asphalt Mixtures and the Relationship to Their Performance, ASTM STP 1265", G.A. Huber and D.S. Decker, Eds., ASTM, Philadelphia, 1995.
- 19 Pagen, C.A., "Rheological Response of Bituminous Concrete", Highway Research Record, No. 67, HRB, 1965, pp. 1-26.
- 20 Hopman, P.C., "Fundamental Research on Asphalt Mixes; Practical Design and Applications", Strategic Highway (SHRP) and Traffic Safety on Two Continents (Preprint), The Hague, The Netherlands, 22-24 September 1993.
- 21 Hopman, P.C., Pronk, A.C., Kunst, P.A.J.C., Molenaar, A.A.A., Molenaar, J.M.M., "Application of The Viscoelastic Properties of Asphalt Concrete", 7th International Conference on Asphalt Pavement, 1992, pp. 73-88.
- 22 Phillips, M.C., "Developments in Specifications for Bitumens and Polymer-Modified Binders, Mainly from a Rheological Point of View", Proceedings of the 2nd European Symposium on the Performance and Durability of Bituminous Materials, J.G. Cabrera, Ed., Leeds, April 1997, pp. 3-18.
- 23 Valejo, J., "Permanent Deformation Characteristics of Asphalt Mixes", Texas University Centre for Highway research, FHWA/TX/RR-183-7, June 1976.
- 24 Ullidz, P., "Pavement Analysis", Developments in Civil Engineering, Vol. 19, Elsevier, 1987.
- 25 Monismith, C.L., "Permanent Deformation Prediction in Asphalt Concrete Pavements: Use of Creep Test Data".
- 26 Thrower, E.N., "Permanent Deformation of Flexible Road Pavements by A Viscoelastic Analysis", PhD Thesis, Department of Civil Engineering, Imperial College of Science and Technology, London, 1985.

- 27 Hopman, P.C., and Nilsson, R.N., "Mix Design Dealing with Mechanical Distress in the Pavement", A paper presented in the RILEM Symposium, Lyon, May 1997.
- 28 Verburg, H.A., Naus, R.W.M, Krans, R.L., and Pronk, A.C., "Burger's Model as A Response Model for the Dynamic Creep Test; Relationships with Mix Composition Parameters", 5<sup>th</sup> Eurobitume Congress, Stockholme, 16-18 June 1993.
- 29 Ferry, J.D., "Viscoelastic Properties of Polymers", John Wiley and Sons, 3rd. Edition, 1980.
- 30 Sousa, J.B., Weissman, S.L., Sackman, J.L., and Monismith, C.L., "Nonlinear Elastic Viscous with Damage Model to Predict Permanent Deformation of Asphalt Concrete Mixes", TRR 1384, 1993.
- 31 Mortazavi, S.H., "Finite Element Analysis of Permanent Deformation in a Flexible Road Pavement", PhD Thesis, Imperial College of Science and Technology, London, 1986.
- 32 Tschoegl, N.W., "The Phenomenological Theory of Linear Viscoelastic Behavior, An Introduction", Springer-Verlag, 1989.
- 33 Cao, Y.L, and Law, K.T., "Energy Dissipation and Dynamic Behaviour of Clay Under Cyclic Loading", Canadian Geotechnics Journal, Vol. 29, 1992, pp. 103-111.
- 34 Van Dijk, "Practical Fatigue Characterisation of Bituminous Mixes", Proceedings of AAPT, Vol. 44, 1975, pp. 38-74.
- 35 Van Dijk, W., and Visser, W, "Energy Approach to Fatigue Pavement Design", Proceedings of AAPT, Vol. 46, pp. 1-40, 1977.
- 36 Pronk, A.C., and Hopman, P.C., "Energy Dissipation: The Leading Factor of Fatigue", Proceedings of Highway Research: Sharing The Benefits, pp. 255-267, 1990.
- 37 Pronk, A.C., "Evaluation of Dissipated Energy Concept for The Interpretations of Fatigue Measurements in The Crack Initiation Phase", The Road and Hydraulic Engineering Division, Ministry of Transport, Public Work and Water Management, The Kingdom of Netherlands, 1995.

- Chapter 11 Environmental Engineering
- 38 Rowe, G.M., "Application of Dissipated Energy Concept to Fatigue Cracking In Asphalt Pavements", PhD Thesis, University of Nottingham, 1996.
  - 39 Tayebali, A.A., Rowe, G.M., and Sousa, J.B., "Fatigue Response of Asphalt-Aggregate Mixtures", Proceedings of AAPT, Vol. 61, 1992, pp. 333-360.
  - 40 Brown, S.F., and Cooper, K.E., "Simplified Methods for Determination of Fundamental Material Properties of Asphalt Mixes", International Conference on Strategic Highway and Traffic Safety on Two Continents (Preprint), The Hague, The Netherlands, 22-24 September 1993.
  - 41 Anon, "Heavy Duty Pavements. The Arguments for Asphalt", European Asphalt Pavement Association, The Netherlands, 1995.

# Chapter Five

## 5. Experimental Works

### 5.1 Introduction

A methodology for this research has been divided into two main sections. The first section is aimed at assessing the mechanisms of polymer-bitumen interactions, and the second is to assess the applicability of dissipated energy as a predictor of mixture resistance to permanent deformation.

The mechanisms of polymer-bitumen interaction were assessed based on:

1. Workability: the blends should be workable, e.g. they can be pumped and handled by a conventional hot mixing facility.
2. Storage stability: the blends should show no phase-separation or at least the phase-separation should be a minimum if stored for a prolonged period.
3. Binder properties: selection of characterisation techniques for measuring the properties of the polymer-bitumen blends, i.e. based on empirical and rheological tests, which relate to enhanced performance of the blends.

Resistance to permanent deformation was assessed based on:

1. Stability and flow: the widely used Marshall test procedure was assessed for its suitability for assessment of the resistance to permanent deformation of polymer modified mixtures. The test procedure was in accordance with BS 598: Part 107:1990 [1].
2. Permanent strain: assessments were carried out by using the dynamic creep test in the NAT device and by using the wheel-tracking device. The wheel-tracking test procedure was conducted in accordance with BS 598: Part 110: 1996 [2].

3. Dissipated energy method: traces of dissipated energy from the dynamic creep test were assessed for their suitability to explain the resistance to permanent deformation of bituminous mixtures.

Data and analyses obtained from these two sections will be inter-related to develop an understanding of which binder mechanisms reflect the enhanced performance of their bituminous mixtures. Figure 5.1 presents the experimental works.

## ***5.2 Materials investigated***

A Hot Rolled Asphalt (HRA) 14 mm wearing course type F with 30% coarse aggregate content was selected and was manufactured in accordance with BS 594 Part 1 : 1992 [3]. The adopted aggregate gradation is demonstrated in Figure 5.2. Binder content was selected to be 7% by mass of the total mixture, in which the selection was based on the optimum binder content of an unmodified 50 pen HRA mixture determined in accordance with BS 598: Part 107:1990 [1]. The unmodified 50 pen HRA mixtures were selected as the reference mixtures in this thesis.

The HRA mixture was selected because the strength of this type of mixture predominantly relies upon the stiffness of mortar binder, therefore, it may gain the most benefit from binder modification as opposed to some mixtures whose strength relies heavily on aggregate interlock. Furthermore, HRA has been used as the primary wearing course mixture in the UK for many years and has performed well in most major sites, even under extreme loading conditions. However, this scenario is changing with the increase of traffic volumes of heavy good vehicles, in particular with the rapid adoption of super-single truck tyres in recent years. This has resulted in the need to develop more deformation resistant HRA [4].

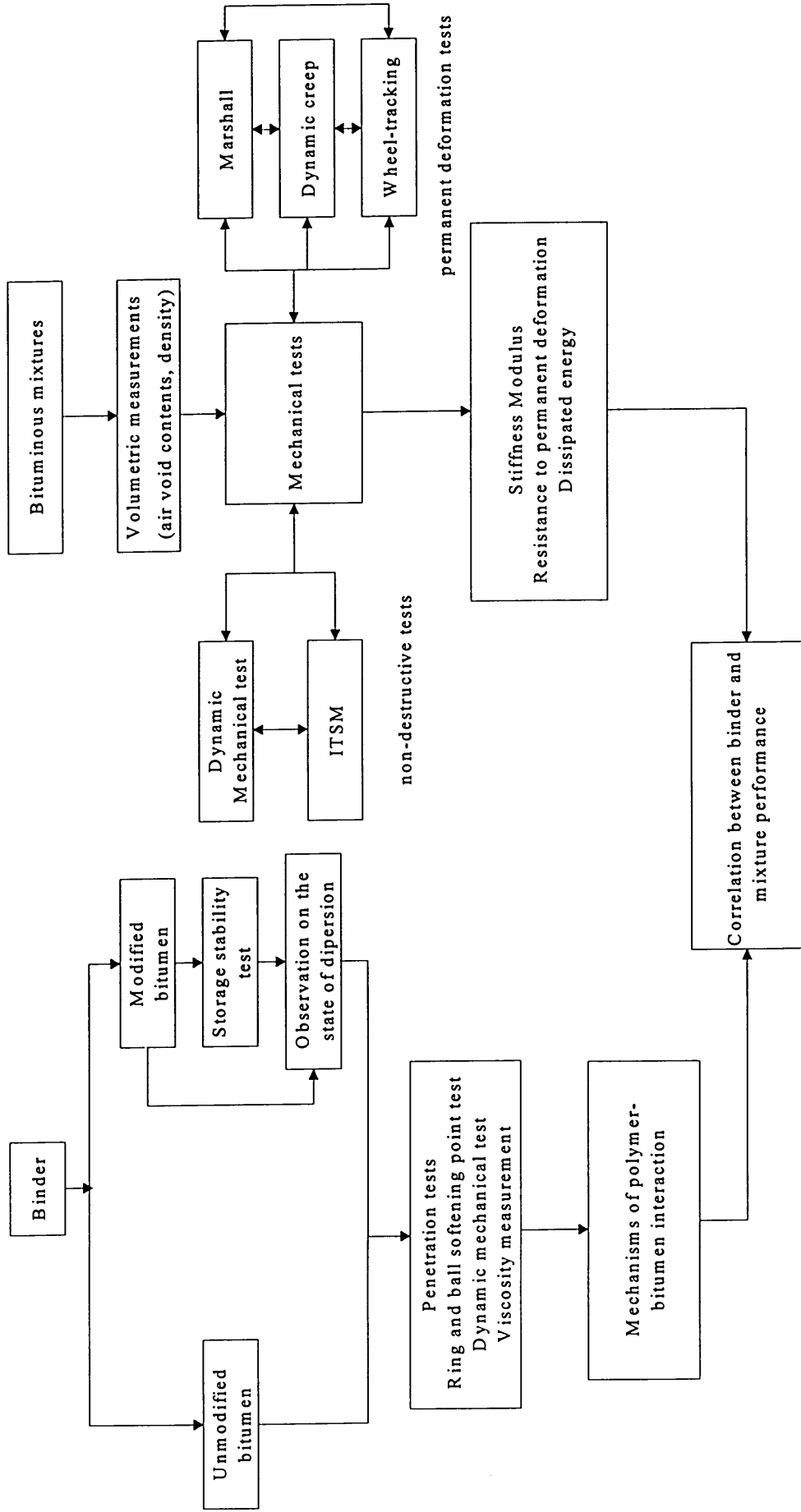


Figure 5.1 Schematic presentation of laboratory frameworks

### 5.2.1 Aggregates

The aggregates used in this study were:

1. Coarse aggregate (30% by mass of total aggregate in the mixture)

Type: crushed rock granite

Location: Leicestershire

Specific gravity: 2.688

Water absorption: 0.5%

2. Fine aggregate (60% by mass of total aggregate in the mixture)

Type: sub-angular rough-surfaced sand

Location: Redford

Specific gravity: 2.607

Water absorption: 2.6%

3. Mineral filler (10% of total aggregate in the mixture)

Type: limestone

Specific gravity: 2.698

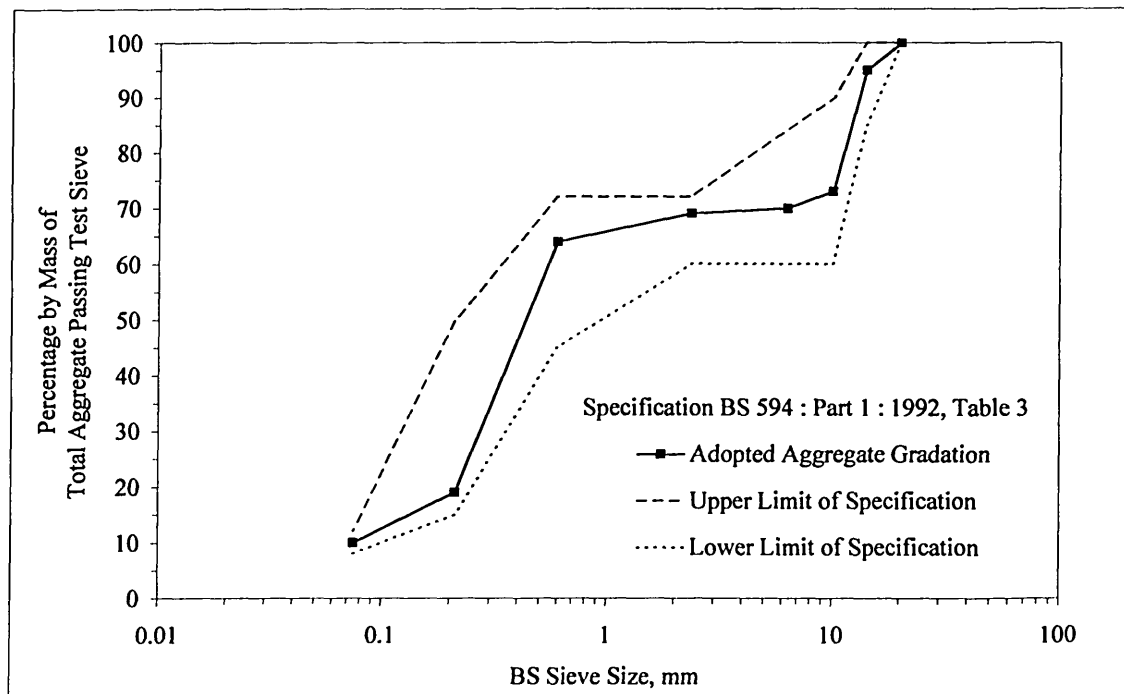


Figure 5.2 Aggregate gradation adopted for this study

### 5.2.2 Binders

The main binders studied were modified binders with 50 pen bitumen as the base binder, however a set of polymer modified binders based on 100 pen bitumen was also assessed for comparison purposes. The bitumens were supplied by a number of different bitumen manufacturers. The designated codes for these bitumens and their modifications are presented in Table 5.1.

Polymers used in this study (Plate 5.1) are:

1. Ethylene Vinyl Acetate (EVA) type 150/19
2. Styrene Butadiene Rubber (SBR)
3. Linear Styrene Butadiene Styrene (SBS)

Polymers were added at 5% by weight of total binder (5% polymer + 95% bitumen), and blending was carried out to a strict protocol (given in *Section 5.3*) by the Author.

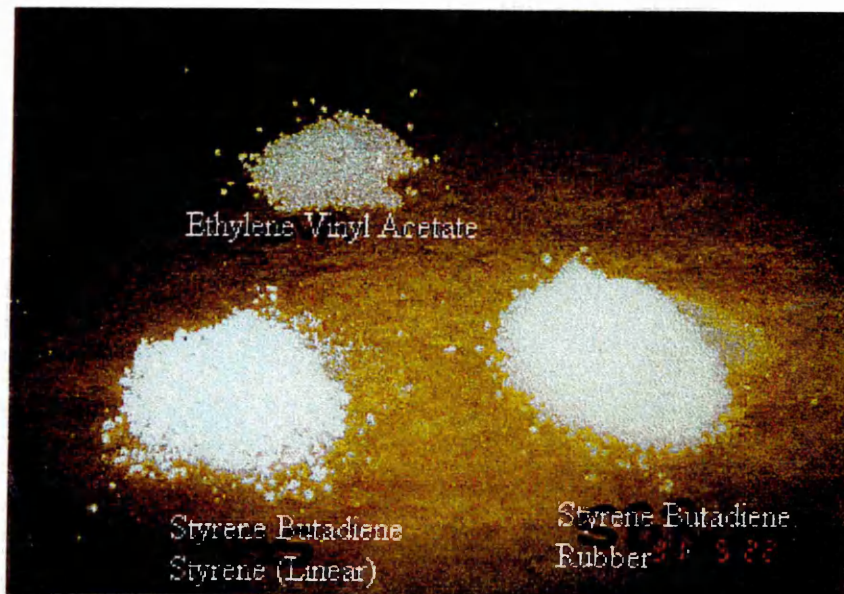


*Plate 5.1 Forms of polymer modifiers used in this study.*

Table 5.1 Binders studied

Binder		Penetration Value* (0.1 mm)			Ring and Ball Softening Points** (°C)
Types	Codes	5°C	25°C	35°C	
50Pen	A50	7	46	122	53
50Pen	B50	7	46	125	54
50Pen	C50	6	42	110	54
50Pen	D50	7	42	111	55
50Pen+ 5% EVA	AP50	5	33	78	65
50Pen + 5% EVA	BP50	5	34	70	65
50Pen + 5% EVA	CP50	5	31	69	66
50Pen + 5% EVA	DP50	5	33	73	67
50Pen	E50	6	47	115	53
50Pen + 5% EVA	EP50	5	36	73	64
50Pen + 5% SBR	ER50	5	33	87	66
50Pen + 5% SBS	ES50	4	34	85	89***
100Pen	F100	9	103	334	42
100Pen + 5% SBR	FR100	11	68	195	52
100Pen + 5% SBS	FS100	8	72	189	86***

Notes: \* BS 200 Part 49 , \*\* BS 2000 Part 58, \*\*\* measured in glycerol

### 5.3 Manufacturing of Specimens

#### Blending Polymer - Bitumen

Polymers used in this study were supplied either in form of pellets (EVA and SBR) or crumbs (SBS). In every case the polymers were pre-blended with the bitumen to make up the polymer modified binders. A Silverson high shear mixer was used for this purpose.

#### Blending procedures:

1. Bitumen of 2000 grams is heated up to about 180°C for about two hours prior to blending.
2. Pour the bitumen into the bending container, switch on the shear mixer and apply low shear rate for about 30 minutes while maintaining the temperature of the bitumen between 170 °C and 190°C.
3. Pour a predetermined mass of polymer crumbs or powder into the bitumen at the rate of 50 grams per minute.

4. Apply a medium shear rate on the mixer, observe the dispersion of polymer in the blend every 10 minutes by using a glass spatula, and take samples for softening point tests (Figure 5.3).
5. Stop the blending after the polymer has been visually dissolved in the blend (usually after an hour blending). Figure 5.3 indicates that softening point temperature increases rapidly as the blending duration increases but after a certain duration of blending, the values become stable. An extended duration of blending should be avoided to prevent the bitumen from hardening and to minimise thermal effects on the polymer.
6. Put the blend into a smaller container for further tests. Take samples for penetration and softening point tests for quality control.

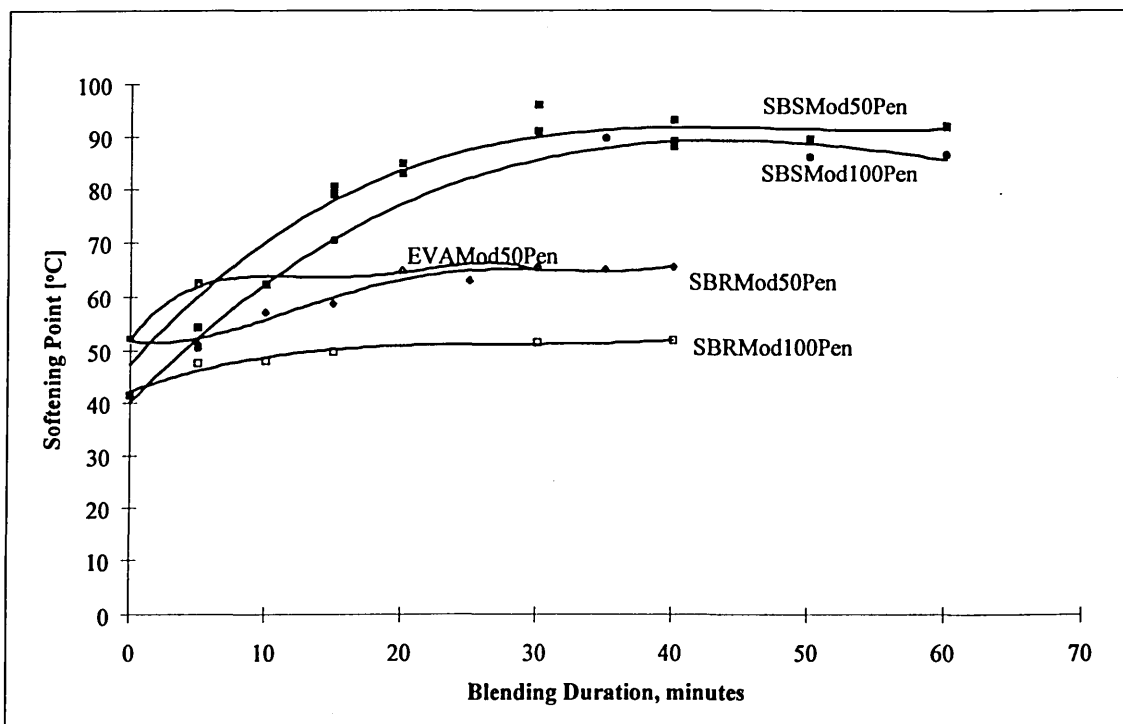


Figure 5.3 Effect of blending duration on softening points

This test procedure was based on the following assumptions:

1. The polymers have been evenly dispersed in the bitumen if the polymer pellets or crumbs have disappeared under visual observation. However, this method can produce significant error as the polymer may be in a coarse dispersion (ideally, the polymer should be finely dispersed). Therefore, observation of the microstructure of

the blend under a microscope is preferable rather than relying solely on the visual observation.

2. The double examination by doing a softening point test at each stage of blending assumes that the softening point temperature reflects the viscosity of the blends. Therefore, the blending duration at which there is no further increase in the softening point temperature assumes that the viscosity is stable.

### **Mixing**

Aggregates and binders were mixed using a Hobart mixer for about 90 to 120 seconds. The mixing temperature refers to the equiviscous temperature of the binder (Table 5.3).

### **Compaction**

Compaction was carried out either by Marshall compactor, laboratory rolling wheel compactor, or static compression. The compaction procedures are presented in the relevant sections of this chapter.

## ***5.4 Tests for the Assessments on the Behaviour of Polymer Modified Materials***

### **5.4.1 Conventional Tests on Bituminous Binders**

Conventional test methods were originally applied to the characterisation of the properties of straight run (unmodified) bituminous binders. However, some of them have also been adopted to characterise properties of polymer modified binders, in which they have sometimes failed to rank the performance of polymer modified binders. Therefore, alternative methods are necessary to accommodate the differing response of modified binders.

Several tests have been especially designed for the assessment of the properties of polymer modified binders, such as ductility-recovery [5], tensile strength test [6], toughness and tenacity test [5, 7], and torsional recovery [8]. These tend to be material specific and have some drawbacks, as described previously in *Chapter Three*. Other

Chapter 5: Experimental Methods

tests that offer more benefits and are suitable for general purpose testing is the “go to basic tests”, i.e. rheological testing such as dynamic shear testing.

In this research two empirical tests, i.e. penetration test and ring and ball softening point test, were carried out by considering that these tests are still widely used in most highway specifications and practices. Furthermore, the recent UK’s Highway Agency draft of specification Clause 943 [9], which requires data from the dynamic mechanical test when using polymer modified binders, still refers to the properties of binders as tested by the penetration test under standard conditions (100 grams, 5 seconds, 25°C) and at 5°C (200 grams, 60 seconds) and the ring and ball softening point temperature, e.g.:

1. The frequency of 0.4 Hz is selected as the standard frequency for the dynamic mechanical test. Gershkoff [10] reported that the log complex modulus at this frequency and the reference temperature of 25 °C correlates well ( $r = 0.933$ ) with the log penetration value at standard condition (100 grams, 5 seconds, 25°C), by the following relationship:

$$\text{Log}|G^*|_{(0.4)} = 8.717 - 1.914 \text{Log}(Pen)$$

2. The calculated penetration at 25°C and the temperature at a penetration of 800 shall also be reported.
3. The storage stability test for polymer modified binders (tooth-paste tube method [11]) requires an average value of the difference in the softening points of top and bottom sections of the specimens shall not exceed 5°C.

It is quite obvious that the temperature at a penetration of 800 refers to the work of Pfeiffer and Van Doormaal [12] where the temperature is an equi-stiffness temperature corresponding to the ring and ball softening point temperature (even though the condition shall not be necessarily true for all types of binder). Therefore, this condition may imply that the so called “performance related specification” has not moved away from the empirical specification but represents the conventional/empirical properties in more engineering terms. For example: a complex stiffness modulus value at a loading frequency of 0.4 Hz and a temperature of 25°C is to represent the penetration at the standard condition (25°C, 100 grams, 5 seconds). Furthermore, Hayton [13] and Heslop and Catt [14] reported that the temperature at which the complex stiffness modulus ( $G^*$ ) is 2000 Pascals at the loading frequency of 0.4 Hz (termed as the equi-stiffness temperature  $T_{2000}$  °C) can be used to determine the highest temperature at which a

surface course could be opened to traffic. This parameter is regarded as an indicator of high temperature properties of polymer modified binders and is used in the same manner as the softening point of unmodified bitumen .

Based on these facts, selected tests were carried out by the following procedures:

1. Penetration test in accordance to BS 2000 Part 49 (25°C, 100 grams, 5 seconds) and at additional test temperatures, i.e. 5°C and 35°C, without changing other procedures.
2. Ring and ball softening point temperature in accordance to BS 2000: Part 58.

#### 5.4.2 Viscosity Measurement

Workability is an important factor especially when considering using polymer modified binders, as the viscosity of the binder, which governs the workability, may increase rapidly as the temperature decreases.

A rotational viscosity test, i.e. a Brookfield rotational viscometer, was used to determine the flow characteristics of the binders to provide some assurance that it can be pumped and handled at the hot mixing facility. Experience from the field indicates that for some modified binders shear thinning occurs during pumping and that capillary viscometers do not give realistic measurements where pumpability is a concern [15]. Because of the close tolerances in most pumps, very high energies are involved and energy transfer may be the main cause of the shear thinning. The shear rate produced by rotational viscometers, e.g. Brookfield viscometer has a shear rate operating range between 0.06 to 750 per seconds, which is much closer to those expected in pumps (Table 5.2).

*Table 5.2 Estimated shear rates for various testing and service condition [15]*

Testing or Service Condition	Estimated Shear Rate, sec <sup>-1</sup>
Settlement	$3 \times 10^{-7}$
Light load (static)	$2 \times 10^{-5}$
Heavy load (static)	$3 \times 10^{-4}$
Penetration test	$2 \times 10^{-1}$
Moving traffic (slow)	$1 \times 10^1$
Moving traffic (fast)	$1 \times 10^3$
Capillary viscometer	$1 \times 10^{-3}$
Sliding plate viscometer	$5 \times 10^{-2}$
Transfer in hot mix plant	$1 \times 10^3$ to $1 \times 10^4$

The Brookfield viscometer is capable of automatically calculating the viscosity at the specified temperature from which a temperature-viscosity relationship for estimating mixing and compaction temperatures for use in mixture design can be developed (Figure 5.4). The Brookfield's viscosity reading is usually in units of centipoise (cP) which is equivalent to 0.001 Pa.s.

Figure 5.4 and Table 5.3 demonstrate that the recommended temperature for mixing and compaction increases with the use of polymer modified binders. The equiviscous temperatures were determined as recommended by Nicholls and Daines for rolled asphalts [16]:

- ♦ at temperatures for which the binder viscosity is 0.2 Pa.s (200 cP); for mixing temperature
- ♦ at temperatures for which the viscosity is between 0.6 Pa.s (600 cP) and 5 Pa.s (5000 cP); for compaction temperature.

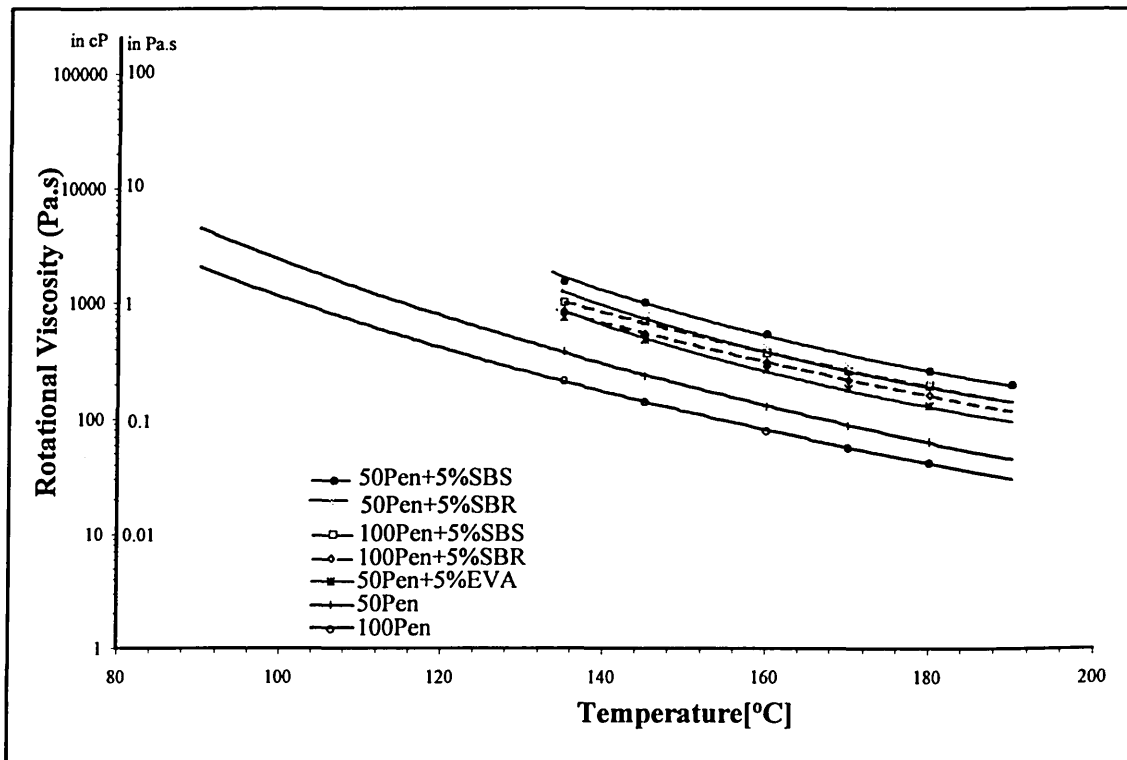


Figure 5.4 Rotational viscosity by measurement (135-190°C) and data extrapolation (90-135°C)

Table 5.3 Equiviscous temperatures recommended for mixing and compaction of polymer modified mixtures.

Binder	E.V.T Mixing <sup>1</sup> (°C) at 0.2Pa.s (200 cP)	E.V.T. Compaction (°C)		Adopted Temperature	
		Maximum <sup>(1)</sup> at 0.6 Pa.s (600 cP)	Minimum <sup>(2)</sup> at 5 Pa.s (5000cP)	Mixing °C	Compaction °C
50 Pen	140	125	90	125-140	120-125
100 Pen	135	115	85	120-135	110-115
50Pen/EVA	165	140	N/A	150-165	130-135
50Pen/SBR	180	150	N/A	165-180	135-140
50Pen/SBS	190	155	N/A	175-190	135-140
100Pen/SBR	175	140	N/A	160-175	120-130
100Pen/SBS	180	150	N/A	165-180	120-130

E.V.T. = Equiviscous Temperature      N/A = No Data Available

<sup>(1)</sup> = as measured by Brookfield rotational viscometer

<sup>(2)</sup> = extrapolated from data points (minimum  $R^2 = 0.998$ )

### 5.4.3 Storage Stability Test

The storage stability test was originally adopted as a tool for assessing the storage stability of bitumen emulsion in a relatively short time period [17]. Developments in bituminous binders, where polymers are used as bitumen modifiers, introduces the possibility of phase separation within a polymer modified bitumen during hot storage. Stability may not be a problem if the blends are manufactured and used immediately, however, changes in properties may be expected if the blends need to be stored for a prolonged period at elevated temperature, such as at the weekend or during holiday breaks.

The procedures and the assessment techniques adopted in this research have been reported by Ellis, Widyatmoko and Read [17], of which they are modifications from a British Standard draft of specification [18]. The draft of the specification allows the use of a beverage-can which meets a specified dimension.

The main advantage of using a beverage-can container, apart from its availability (readily available with no extra cost), is that a sufficient amount of sample is available (after stability test) for conducting further assessments (a penetration, a softening point,

and dynamic mechanical tests, and also an observation under a microscope), can be obtained from just one container. However, one disadvantage is that it requires a large amount of binder to fill up one container (about 500 ml) and it is recommended by the Author to carry out three tests for each type of binder to obtain a representative result. Others may prefer a tooth-paste tube [11] as the container rather than the beverage-can because it requires less binder to make up one sample with the tooth-paste tube, however, the sample's portion after the stability test is only sufficient for conducting a softening point test or a dynamic mechanical test or observation under microscope but not together. Furthermore, the tooth paste-tube needs to be ordered from a special supplier.

### **Testing procedures:**

#### **1. Specimen preparation:**

- ◆ A bulk of bituminous binders were heated up to a temperature at which the viscosity was low enough to allow the binder to be transferred into smaller containers (about 600 ml). Excessive heating was avoided to prevent the binder from hardening, and stirring of the binder prior partitioning was necessary to ensure homogeneity in some cases.
- ◆ A container made of a beverage can with dimensions of  $200 \pm 40$  mm height and  $65 \pm 5$  mm diameter (about 500 ml) with aluminium foil for sealing the container.
- ◆ The binder was then poured into the container and sealed immediately with the aluminium foil.

#### **2. Oven:**

- ◆ A force draft oven was preheated to  $160^{\circ}\text{C}$  for 120 minutes to ensure uniformity.
- ◆ The recorded temperature should be the actual temperature of the specimen. Therefore, a dummy specimen with thermocouples attached to the top and middle sections was used.

#### **3. Storage duration:**

- ◆ The specimen was stored in the oven for durations of 1, 3, and 7 days.
- ◆ The specimen was removed from the oven at the end of each storage duration. Care was taken so that the storage temperature was not disturbed when opening the oven (in case there are still other specimens left in the oven).

- ◆ Specimens (after storage stability test) were left to cool overnight at room temperature ( $21.5 \pm 0.5$  °C) ready to be cut into three sections in the following day. The top and bottom sections were used for further tests and the middle portion was discarded.
4. Preparation prior to further tests
- ◆ The top and bottom sections were placed in separate containers with their lids on and clear marks were put on each container.
  - ◆ The container was placed into an oven, and the temperature raised from ambient up to 160°C or to a minimum temperature at which the viscosity was low enough for pouring.
  - ◆ Prior to pouring, the specimen was stirred to ensure homogeneity.
  - ◆ The specimen was then poured into specified containers for further tests, and marked for further identification.

**Further tests:**

- ◆ Penetration test, in accordance with BS 2000 Part 49 (25°C, 100 grams, 5 seconds)
- ◆ Ring and Ball softening point test, in accordance with BS 2000: Part 58
- ◆ Observation under UV Fluorescent microscopy at 500 times magnification
- ◆ Dynamic mechanical test: temperature sweep from 0°C to 80°C at a frequency of 1 Hz

**Assessment techniques:**

1. Consistency of the binders:

- ◆ Penetration index based on Pfeiffer and Van Doormaal’s method [12] which can be rearranged as:

$$PI = \frac{19515 - 500 \log Pen_{25} - 20SP_{ASTM}}{50 \log Pen_{25} - SP_{ASTM} - 120.1}$$

*Equation 5.1*

It is important to remember when using the Equation 5.1 that the penetration value ( $Pen_{25}$ ) is determined under standard conditions (25°C, 100 grams, 5 seconds) and the softening point value ( $SP_{ASTM}$ ) is determined in accordance to the ASTM procedure (ASTM D36). In the ASTM version of softening point the test bath is not stirred

whereas the water or glycerol is stirred in the British Standard procedure<sup>a</sup>. Consequently, the recorded softening points between these two procedures differ. The British Standard results are generally 1.5°C lower than for the ASTM [19]. Therefore, Equation 5.1 can be modified as:

$$PI = \frac{19215 - 500 \log Pen_{25} - 20SP_{BS}}{50 \log Pen_{25} - SP_{BS} - 121.6}$$

*Equation 5.2*

where  $SP_{BS}$  is the softening point determined in accordance with the British Standard procedure.

- ♦ Penetration stability index ( $SS_{pen}$  mm/10) [18]

$$SS_{pen} = Penetration_{top} - Penetration_{bottom}$$

*Equation 5.3*

- ♦ Softening point stability index ( $SS_{SP}^{\circ C}$ ) [18]

$$SS_{SP} = SP_{top} - SP_{bottom}$$

*Equation 5.4*

- ♦ Dynamic mechanical data:

Data obtained from the dynamic mechanical test were presented as Black curves which are plots of complex modulus versus phase angle. The assessment by using Black curves was selected because this procedure is simple and straightforward, i.e. data of complex modulus are directly plotted against phase angle without a need of further modification or calculation, and it is also beneficial as Hayton [13] stated that “*a series of bitumens differing in penetration but not temperature susceptibility (penetration index) will give a single black curve*”. Deviations from this curve indicate changes in composition or variation in structure caused by processing,

---

<sup>a</sup> The non-stirred version was first introduced by ASTM in 1916 and was designated as D36-26. A modification took place in 1942 where the stirring of the bath was introduced. The methods both survive up to now. (Reference: M.C. Siegmann, 1950)

ageing, or polymer addition, in which these properties need to be monitored during storage of polymer modified binders.

2. Qualitative analyses were carried out by observation on the state of dispersion of the polymer modified binder before and after the storage stability test under a UV Fluorescent microscope.

#### **5.4.4 Dispersion of Polymer**

As has been presented in *Chapter Three*, the state of dispersion is very important as it can affect the properties and performance of polymer modified materials. Therefore, a UV Fluorescent microscope was selected for observation of the macrostructure of the polymer modified binders. The investigated binders, both before and after the stability test, were observed under the UV Fluorescent microscope available at the Bituminous Laboratory of Croda Bitumen Ltd.

The reference binder was an unmodified 50 pen bitumen. Under a UV Fluorescent microscope, the polymer particles were normally shown yellow and the bitumen to be in darker colour (see *Appendix A*).

#### **Specimen preparations:**

1. Specimens were prepared by heating them up to the minimum temperature at which the viscosity becomes low enough for pouring whilst excessive heating was avoided but care was taken to prevent air bubbles in the specimens.
2. The binder was stirred when its viscosity was sufficiently low to ensure homogeneity and then a drop of binder was placed (about 10 mm diameter) on a plastic film. It was left to cool at room temperature.
3. The UV Fluorescent microscope before use was warmed up and set to 500 times magnification.
4. The plastic film with the specimen on was placed in the microscope.
5. The focus and the positioning of the specimen was adjusted to find a representative view of polymer dispersion.

6. The microscopic view on to the video monitor was then adjusted for colour, format, and layout. The image was then transferred onto a screen monitor and captured by a special device.
7. The captured image was then annotated for further reference.

#### 5.4.5 Indirect Tensile Stiffness Modulus (ITSM) Test

The ITSM test was carried out by using the NAT machine. The test runs by application of a vertical load generated by a pneumatic actuator to achieve a desired horizontal deformation (Figure 5.5 and Plate 5.2). The stiffness modulus is a function of vertical load, horizontal deformation, and an assumed Poisson's ratio [20], and can be formulated as follows:

$$S_m = \frac{P(c_5 - \nu \cdot c_6)}{\delta_h \cdot t_h}$$

*Equation 5.5*

where:

$S_m$  = stiffness modulus, in Pascals

$P$  = applied load, Newtons

$\nu$  = resilient Poisson's ratio

$\delta_h$  = resilient total horizontal deformation, metres

$t_h$  = thickness (height) of specimens, metres

$c_5$  and  $c_6$  = constants dependent on the specimen diameter and width of loading strip; e.g. for a 101.6 mm diameter specimen and a 12.7mm width of loading strip,  $c_5 = 0.2692$  and  $c_6 = -0.9974$ .

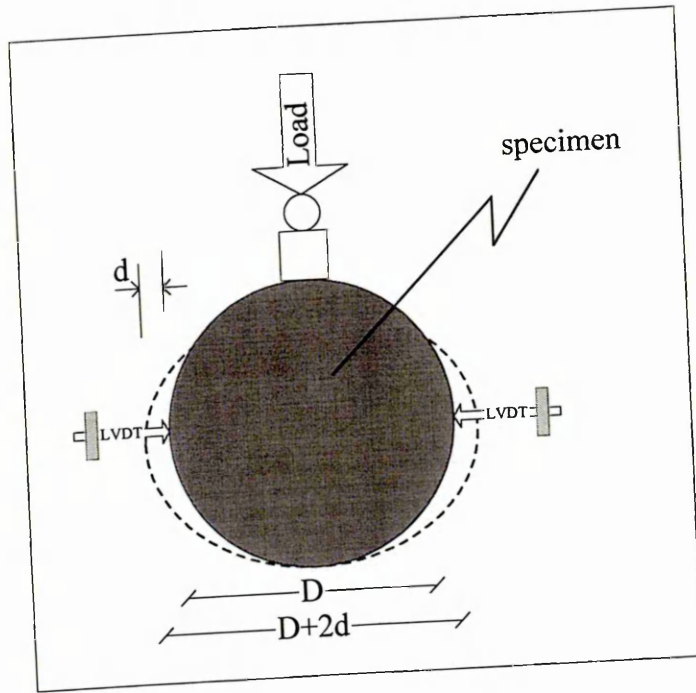


Figure 5.5 Typical side view of ITSM loading arrangement

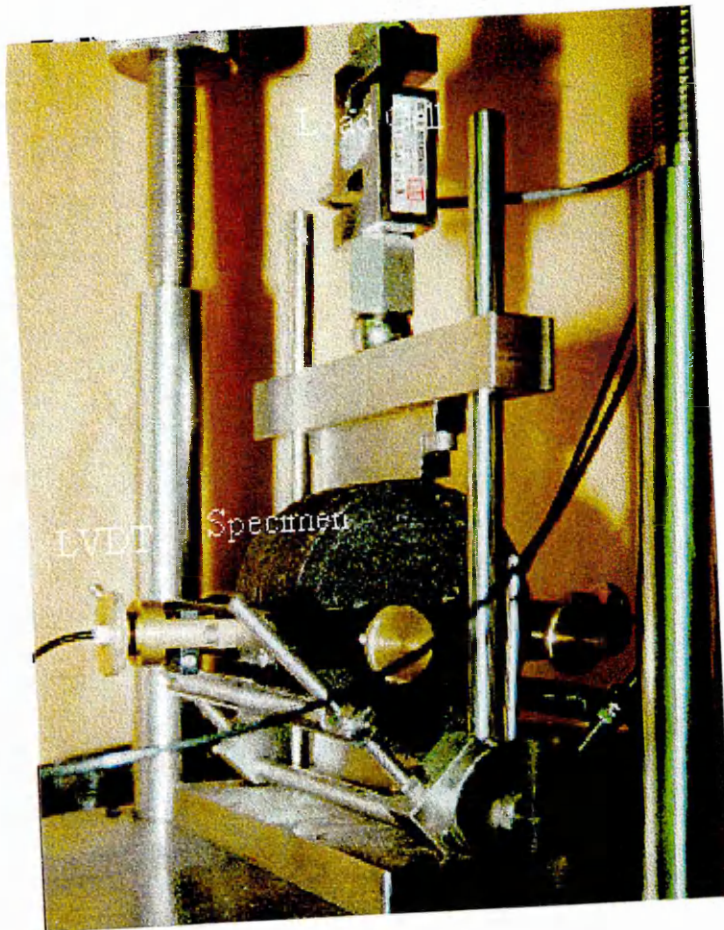


Plate 5.2 Testing arrangement for ITSM in the NAT machine.

In comparison with other methods to determine the stiffness of bituminous materials (e.g. direct tension and/or compression or bending beam), the indirect tensile testing has several advantages and disadvantages (Table 5.4).

Table 5.4 Advantages and disadvantages of using ITSM. After Scholz [20].

Advantages	Disadvantages
<ol style="list-style-type: none"> <li>1. The test is simple, quick to conduct</li> <li>2. Non-destructive if testing conditions ensure elastic response</li> <li>3. Fewer problems with manufacturing specimens, e.g. specimens are moulded or cores</li> <li>4. Thin specimens can be tested as the equipment can accommodate specimens with thickness of between 25-75 mm</li> <li>5. A biaxial stress state exists during the test which better represents field conditions than the stress condition found in flexural testing</li> </ol>	<ol style="list-style-type: none"> <li>1. The method relies on theoretical analysis using elastic theory.</li> <li>2. Using an assumed Poisson's ratio which makes the test less reliable than direct tension/compression or flexural tests</li> <li>3. Susceptible to the development of permanent deformation if tested at high temperature. Temperatures higher than 40°C should be avoided.</li> </ol>

The main reason for conducting the ITSM test in this research was to ensure samples with the same mixture configuration had similar engineering properties prior to further testing, and hence, it was basically used for quality control purposes. The results are presented in Figure 5.6 and Figure 5.7. Variations of results within the same mixture are found in the range of 5-17%. However, most of the results are well within 95% confidence interval. Details of the results are presented in the *Appendix D*. Most of the samples were subjected to ITSM test before being tested for dynamic creep.

The author suspects some factors which may contribute to these variations:

- Specimen preparation and manufacturing:
  - a) Different level of hardening may have taken place on binder during manufacturing of the specimens, e.g. the mixture which was manufactured later may have different properties from the previous one due to binder hardening.
  - b) Variability between specimens during handling, mixing, and compaction. The variations were found to be as high as 9.4% for specimens with the same target volumetric proportions.
  - c) Non-uniformity within a specimen, e.g. voidage and aggregate distributions.

- Effect of test temperature may be minimum as the specimens were well conditioned at the test temperature prior to the ITSM testing and, the temperature was also tightly controlled during the data collection. However, a change of temperature by only 1°C may vary the stiffness modulus by 10%.
- Binder characteristics. Harder binder such as 50 pen and EVA modified 50 pen demonstrated smaller variations than 100 pen and the elastomeric modified binders, i.e. SBS and SBR modified binders.

### **Specimen manufacturing**

Specimens used for the ITSM and dynamic creep tests were all laboratory manufactured by Marshall compaction to achieve an average dimension of 102 mm diameter by 64 mm height. A standard Marshall compactive effort of 50 blows (each side) was applied, but other compactive efforts, i.e. 10, 20, 30, and 75 blows, were also used to assess the effect of variation. Specimens were left overnight and ITSM tested immediately the next day.

### **Testing configurations**

1. Test temperature = 20°C
2. Assumed Poisson's ratio = 0.35
3. Rise time = 120 milliseconds
4. Conditioning pulses = 5
5. Specimen size = diameter 102 mm and height 64 mm

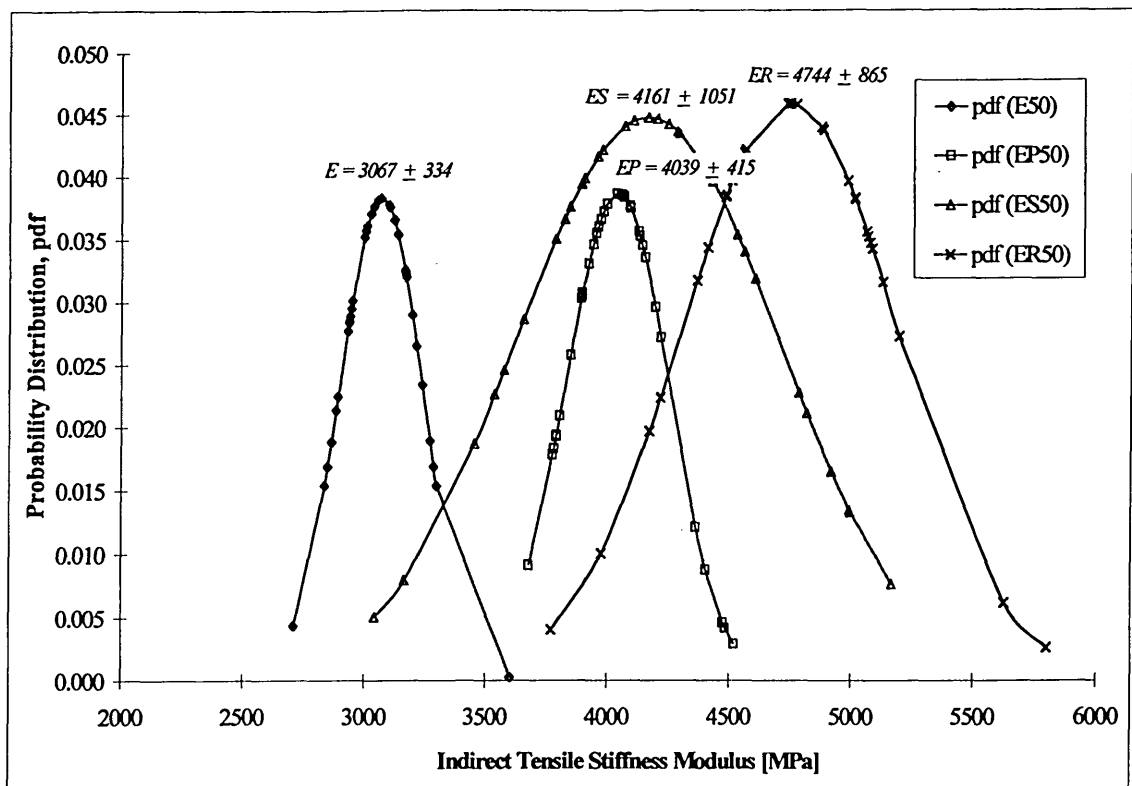


Figure 5.6 Probability distributions of ITSM results for mixtures with 50 pen based binders. E, EP, ER, and ES are the straight run, EVA modified, SBR modified, and SBS modified binders.

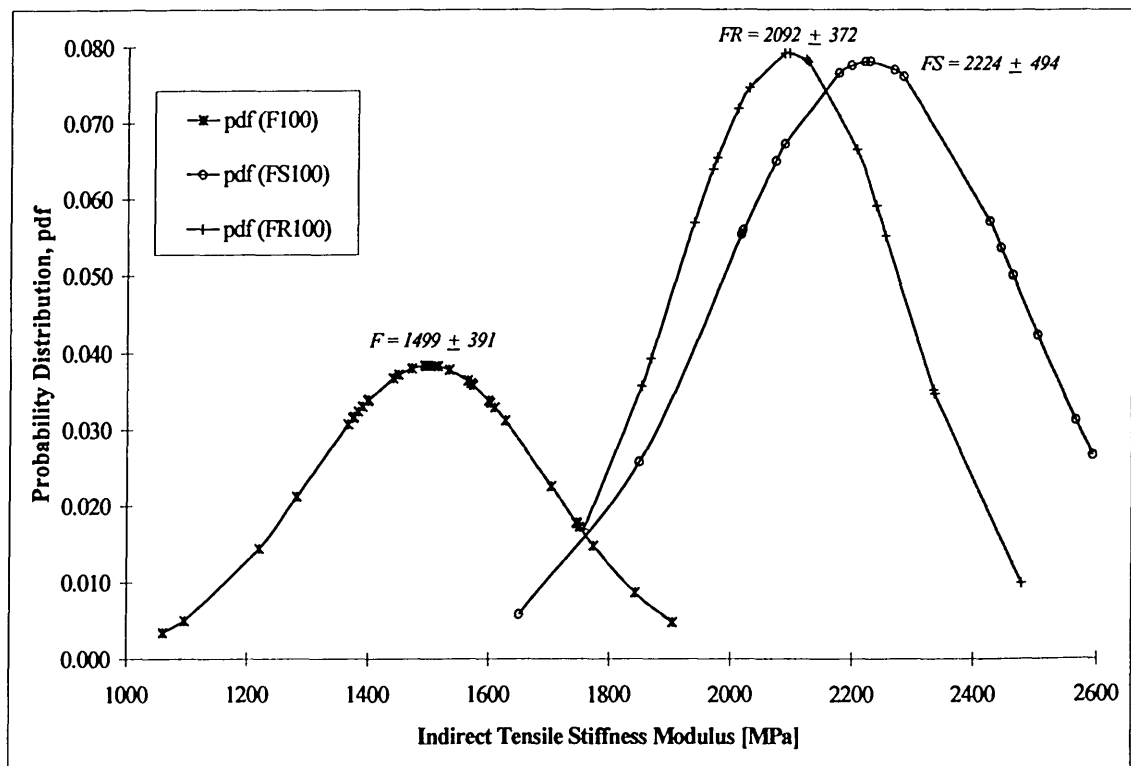


Figure 5.7 Probability distributions of ITSM results for mixtures with 100 pen based binders. F, FR, and FS are the straight run, SBR modified and SBS modified binders.

#### **5.4.6 Dynamic Mechanical Tests**

Dynamic mechanical tests were carried out on binders and mixtures to observe the variation in the viscoelastic response of the materials under different loading and temperature conditions.

This is a very reliable test as it can provide information on fundamental properties over a wide range of testing conditions. The results can be utilised for further analyses and be used in the design of bituminous materials. However, despite this superiority, the test is time consuming and requires specialised equipment and assessment techniques. These conditions make the dynamic mechanical test expensive and potentially unsuitable for daily practice.

##### **5.4.6.1 Binder tests**

Rheological measurements of bituminous binders were conducted on a Bohlin shear rheometer at the Bitumen Laboratory of Croda Bitumen Ltd.

Test preparation:

1. A sample of about 50 grams was heated until it became liquid and workable. Care was taken to prevent overheating.
2. The air compressor of the rheometer was warmed up prior to the test.
3. The base plate was cleaned in order to be free from dirt or oil.
4. The base plate and the top plate were placed on their positions. Selection of plate's size was as shown in Table 5.4.
5. The gap between the base and top plates was adjusted, as shown in Table 5.4.
6. An amount of binder was carefully poured on the base plate just enough to make a sandwich of binder between base and top plates. (The binders were always stirred prior to pouring)
7. The top plate was lowered, checking that there were no air bubbles in the sandwich of binder. The binder was allowed to cool and trimmed to a specified size.
8. The plastic cover was placed to allow the sample to be immersed in the water for conditioning.

9. The software application was run, and the test parameters was set (Table 5.4), the test was conducted within the linear viscoelastic region.

*Table 5.5 Testing parameters for dynamic mechanical test*

Temperature [°C]	-5	5	15	25	35	45	60	80
Plate diameter [mm]	8	8	8	15	15	15	15	15
Gap [mm]	2.5	2.5	2.5	2.0	2.0	2.0	2.0	2.0
Conditioning liquid	IPA* + water	IPA+ water	IPA+ water	water	water	water	water	water
Frequency [Hz]	0.1-20	0.1-20	0.1-20	0.1-20	0.1-20	0.1-20	0.1-20	0.1-20
Strain level-a	0.02%	0.05%	0.5%	1%	1%	1%	2%	5%
Strain level-b	0.1%	0.2%	1%	0.5%	0.5%	0.5%	10%	10%
Thermal equilibrium duration [seconds]	300	300	300	300	300	300	300	300

\*IPA is an anti-freezing agent.

Parallel plates with different diameters (8 and 15 mm) and gaps (2.0 and 2.5 mm) were selected so that the loading device is capable of generating the required shear stress level to produce the target strain level at a given test temperature and frequency. Smaller diameter plates allow higher shear stress to be applied. Larger gaps increase angular displacement for a given strain level, and hence improve sensitivity. The smaller plate (8 mm) with the higher gap between the parallel plates (2.5 mm) was adopted at temperatures lower than or equal to 15 °C where the binder possessed higher stiffness. At temperatures higher than or equal to 25°C where the binder stiffnesses were relatively low, the 15 mm plate with 2.0 mm gap was used.

The frequency sweeps were conducted from the lower range of frequency to a higher frequency in the following steps: 0.1, 0.2, 0.5, 1, 2, 5, 10, 15, 20 Hz. The test temperature started from the lowest temperature to the higher ones, and finally tested again at the initial temperature to ensure that there was no damage developed during the test.

Prior to the main test, strain sweep tests were carried out at each temperature to determine the linear viscoelastic limit. The dynamic mechanical tests were conducted at two strain levels to ensure that the measurements were well within the linear viscoelastic region, i.e. the measurements should give similar results at these two strain levels. This procedure has been previously explained in *Sections 3.2.2 and 3.2.3*.

#### **5.4.6.2 Mixture test**

The test was conducted on a Mand Testing machine which is a three point bending device (Plate 5.3).

#### **Specimen preparation:**

A universal servo-hydraulic testing machine was modified for manufacturing specimens to be used for the complex moduli tests. The loading frame was capable of generating dynamic actions up to 100kN with different shapes of loading patterns. A steel mould with dimension of 400mm x 100mm x 130mm with a collar was specially designed for this purpose and a wooden compaction block for transferring the load from the servo-hydraulic ram onto the loose mixture (Figure 5.8 and Figure 5.9).

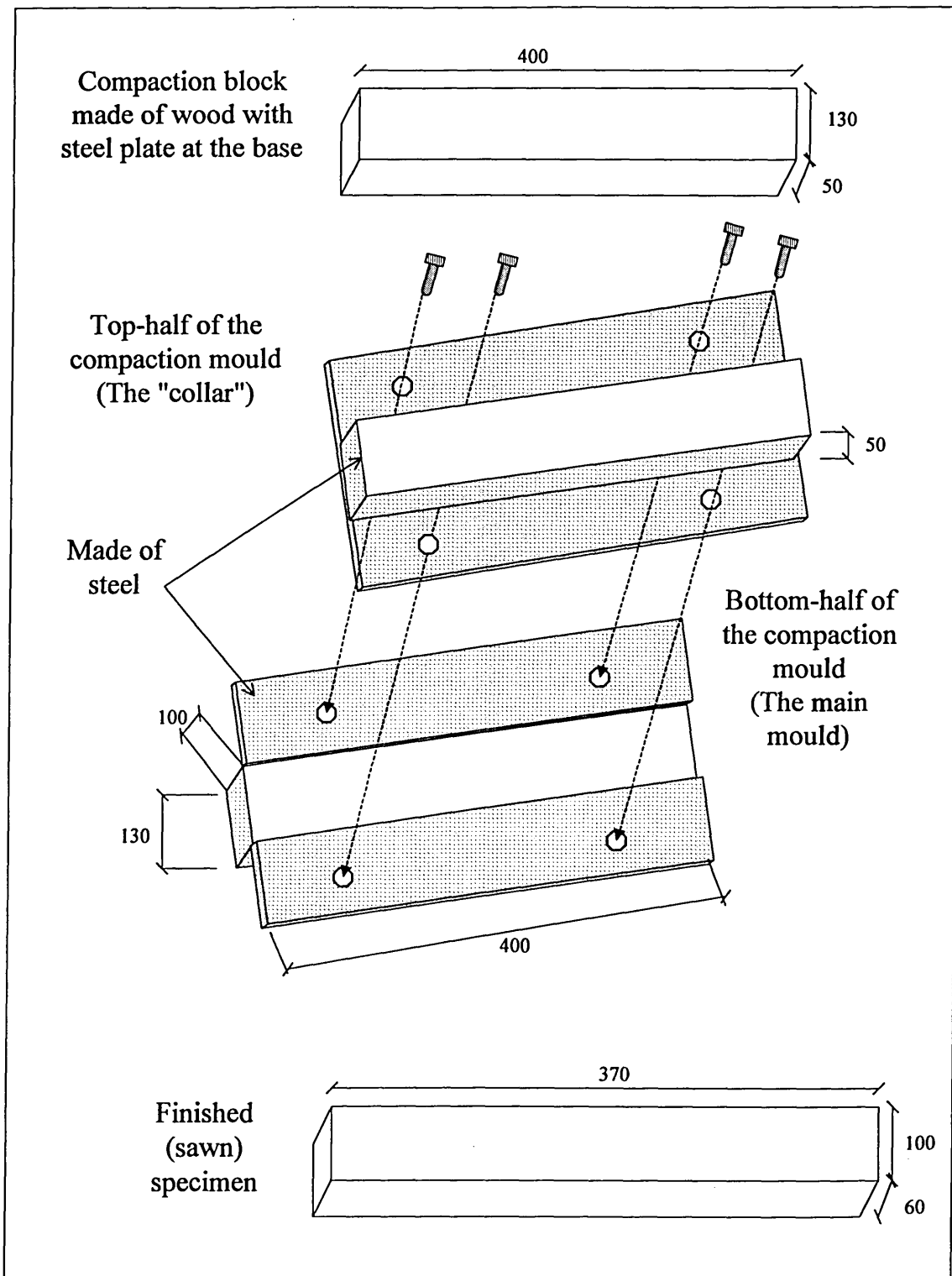
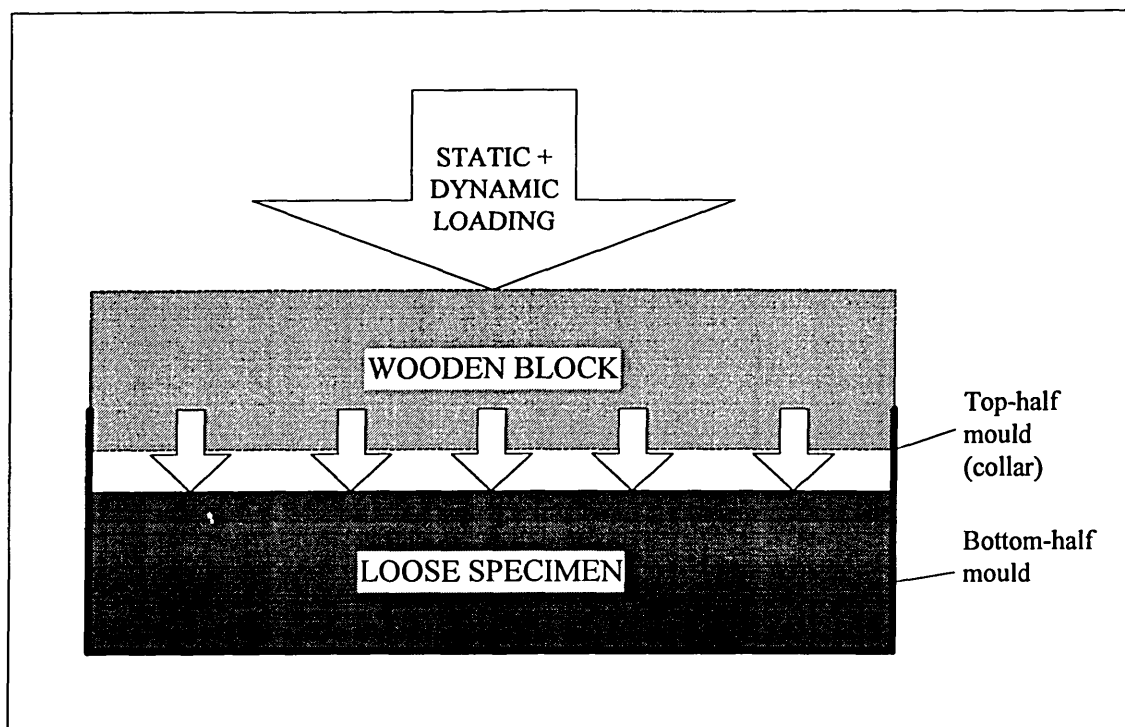


Figure 5.8 Dimensions (in millimetres) of the compaction mould and the finished specimen.



*Figure 5.9 Compaction arrangement*

The blends of binder-aggregate mixture were compacted in this mould by applying an increment of load up to 100kN within 2 seconds. A superimposition of dynamic sinusoidal and static loading was applied in this action. The sinusoidal load has an amplitude of 2 mm and the static load was to achieve 100kN. During loading, the load was maintained for about 30 seconds to achieve the final finish (the target of finished height is 100 mm) The load was then released, and the recovery and swelling of specimens after the load removal were observed.

Difficulties were experienced during the manufacturing of the specimens by this equipment. The equipment failed to produce specimens with final air void levels of 4-6%, even though, the full capacity of the equipment, i.e. 100 kN, and both static and dynamic loading were applied. The air void contents were obtained in the range of 11-14%. It was observed that the volume expansion (swelling) at the end of the compaction process due to recovery/healing was the major contributor to the high air void content of the specimens where recoveries of up to 10 mm were recorded. A static load at the end of the compaction process may be applied to restrain the specimen from

swelling. However, this procedure was not adopted to avoid a pre-stressed condition in the specimen.

After cooling, the specimen was then extracted from the mould to be sawn to a finished dimension of 370mm x 100mm x 60mm, and ready for further tests.

**Dynamic Mechanical Test configuration:**

1. Test temperature: -15, -10, -5, 0, 5, 10, 15, 20, 25, 35, 45 °C with a tolerance of  $\pm 0.5^{\circ}\text{C}$
2. Loading frequency: 0.2, 0.5, 1, 2, 5, 10, 20, 30 Hz
3. Load levels: L, 2L, and 0.5L where L is the load required to achieve a deformation between 5 to 50 micron. The device is capable of generating loads between 5 to 100 N.

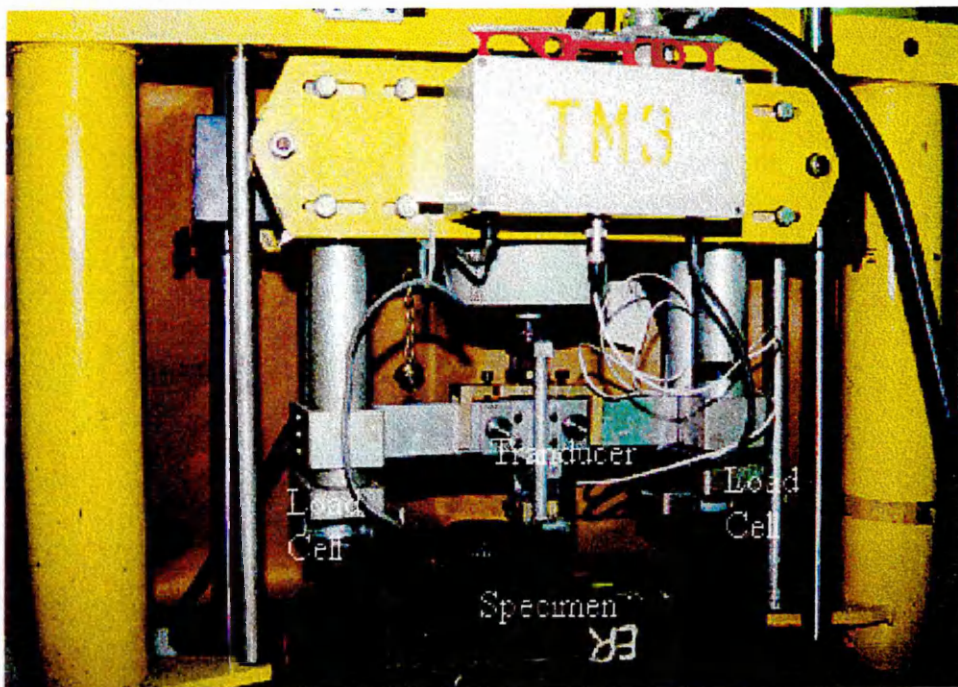


*Plate 5.3 A Mand dynamic three-point bending machine for testing bituminous mixture.*

The test was conducted by applying frequency sweeps from the lowest frequency to the higher ones at each temperature. The test temperature started from the lowest temperature to the higher ones, and finally tested again at the initial temperature to ensure that there was no damage developed during the test.

## ***5.5 Tests for the Assessments of Permanent Deformation Resistance of Bituminous Mixtures***

### **5.5.1 Laboratory Wheel-tracking Test**

#### **Specimen preparation**

Slabs for wheel-tracking tests were manufactured by the laboratory roller compactor. About 16kN of compaction effort was applied for 30 cycles at specified compaction temperatures to achieve a finished specimen dimension of 305mm x 305mm x 50mm. The average air temperature during compaction was maintained at 20°C. After cooling, the slab was extracted from the mould and the density of slab determined.

Prior to wheel-tracking, the slab was stored in an environmental cabinet for a period of 4 hours at the designated test temperature.

#### **Test configurations:**

1. Test temperature : 45°C and 60°C
2. Specimen size: 305 x 305 x 50 mm
3. Wheel-tracking frequency of  $21 \pm 0.2$  load cycles per 60 s and a total distance of travel of  $230 \pm 5$  mm, in accordance with BS 598:Part 110 [2]
4. Type of test: double tracking (Figure 5.10). Tests at 45°C were carried out first.

Assessments were carried out in accordance with BS 598: Part 110 procedure [2], however, each type of mixture had only four replicates instead of six.

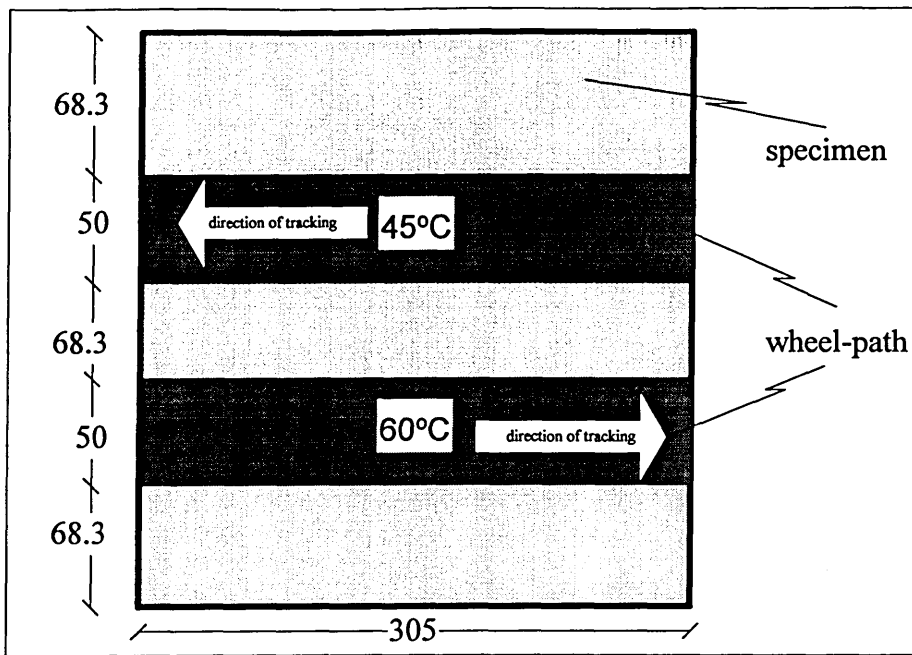


Figure 5.10 Loading configuration (the length dimensions are in millimetres).

The decision of adopting the double-tracking technique as opposed to the single-tracking was based upon the report of another research project carried out at SHU [21]. The project reported that there was no significant difference between the wheel-tracking results based on single-tracking (BS 598: Part 110) and double tracking at temperatures of 45 and 60 °C. Furthermore, the project also reported that the wheel-tracking specimens which were manufactured in laboratory either as slabs (dimensions of 305 x 305 x 50 mm) or cores (diameter 200 mm) give similar performance when tracked at 60°C. The results are demonstrated in Table 5.6 and Table 5.7. Based on these facts, the Author adopted the double-tracking technique and the specimens were manufactured as slabs.

*Table 5.6 Comparison of Single and Double-tracking. Methods of calculations: BS 598:Part 110:1996. After Broadhurst [21].*

Tracking Mode	Test Temperature (°C)	Wheel-tracking rate (mm/h)	Rut Depth (mm)
Double	45	1.1	2.7
Single	45	1.1	2.9
Double	60	10.0	11.3
Single	60	9.9	11.0

*Table 5.7 Comparisons of specimen types in the wheel-tracking tests. Methods of calculations: BS 598:Part 110:1996. After Broadhurst [21].*

Specimen Type	Wheel-tracking rate (mm/h)	Rut Depth (mm)
Slab	3.2	5.3
Core	3.3	4.9

### 5.5.2 Dynamic Creep Test

Dynamic creep testing was carried out in the NAT machine using the same specimens as were previously tested in the ITSM test. The specimen arrangement for the dynamic creep test is illustrated in Figure 5.11.

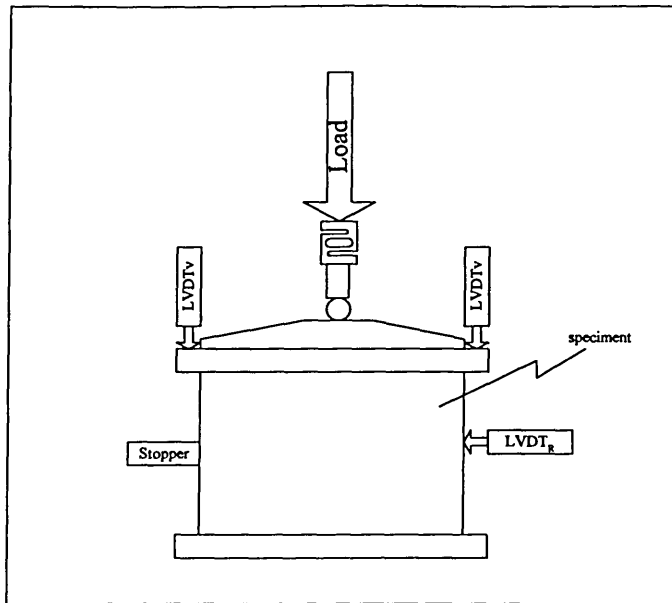


*Figure 5.11 Configuration for dynamic creep test.  $LVDT_R$  and  $LVDT_v$  are the radial and the vertical LVDTs, respectively.*

### **Specimen preparation:**

Prior to the main test, the specimens were coated by silicone grease/graphite powder mixture which was to reduce any friction that may take place between the surface of the specimen and the loading platen. The specimens were then conditioned for at least 3 hours within an environmental cabinet at a selected test temperature. Each set of specimens was tested within three weeks of manufacturing.

### **Test configurations:**

#### 1. Data recording

Measurements of load, axial strain, and radial strain were automatically taken by the software every 4 milliseconds per cycle. Each cycle lasts for about 2 seconds (2000 milliseconds).

#### 2. Terminal strain

The test terminates automatically when the permanent axial strain reaches 7% or after 10000 loading cycles, whichever comes first. The results are then calculated and analysed on a spreadsheet. Dissipated energy per cycle was calculated from the hysteretic loop drawn from compressive stress-axial strain relationship.

#### 3. Test temperatures : 45°C and 60°C

#### 4. Conditioning pulses = 8

5. Stress levels as presented in Table 5.8.

Different stress levels were applied so that:

- ♦ The specimens failed between 200 to 10000 cycles or when the permanent axial strain reached 7%, whichever came first.
- ♦ The effect of stress level upon the resistance to permanent deformation of the specimens can be observed.

As demonstrated in Table 5.8, a higher stress level is required for polymer modified mixtures to fail within the specified load repetitions. However, the maximum stress level that can be applied is 538 kPa. A stress level higher than 538 kPa causes instability in achieving the target peak load so that the load actuator cannot maintain a such high stress level due to the limitation of the actuator. There are also some cases that some of the specimens, particularly the polymer modified mixtures at a test temperature of 45°C, did no failing after the completion of 10000 cycles.

Table 5.8 Configuration for dynamic creep test.

$\sigma$ [kPa]	50 Pen	50 Pen + 5% EVA	50 Pen + 5% SBR	50 Pen + 5% SBS	100 Pen	100 Pen + 5% SBR	100 Pen + 5% SBS
T=45°C	73.5				*		
	98				*		
	147				*		
	196	*			*	*	*
	294	*			*	*	*
	392	*		*	*	*	*
T=60°C	490	*	*	*			*
	538	*	*	*			
	49	*					
	98	*	*	*	*	*	*
	196	*		*	*	*	*
	245		*	*	*		
294		*	*	*		*	*
392		*		*			*

## 5.6 References

- 1 Anon, "Sampling and Examination of Bituminous Mixtures and Other Paved Area".  
British Standard 598: Part 107: 1990, Method of Test for the Determination of the  
Composition of Design Wearing Course Rolled Asphalt. BSI London.
- 2 Anon, "Methods of Test for The Determination of Wheel-tracking Rate" British  
Standard 598: Part 110: 1996, BSI London.
- 3 Anon, "Specification for Rolled Asphalt for Roads and Other Paved Areas -  
Specification for Constituent Materials and Asphalt Mixtures", British Standard  
594:Part 1: 1992, BSI London.
- 4 Fabb, T, "Bitumen Breakthrough", Highways, January/February 1997, pp. 16-21.
- 5 Thompson, D.C., "Rubber Modifiers", Bituminous Materials: Asphalts, Tars, and  
Pitches Vol. 1, Edited by Arnold J. Hoiberg, Interscience Publisher, 1964.
- 6 Anon, ASTM D 412-80
- 7 Anon, ASTM D-4 P243, "Proposed Test Method for Toughness and Tenacity of  
Bituminous Materials", 1994.
- 8 Isacson, U., and Lu, X., "Testing and Appraisal of Polymer Modified Road Bitumens-  
State of the Art", Materials and Structures, Vol. 28, 1995, pp. 139-159.
- 9 Anon, "Hot Rolled Asphalt Wearing Course (Performance Related Design)", United  
Kingdom's Highway Agency Clause 943, Draft No.4.0, 5 July 1996.
- 10 Gershkoff, D.R., "A Study of The Rheological Behaviour of Some Surface Dressing  
Binders", MSc thesis, University Nottingham 1991.
- 11 Anon, "Draft Proposal for Bitumen Test Method for Modified Bitumen.  
Determination of Storage Stability", CEN/TC 19/SC 1 N22 REV.
- 12 Pfeiffer, J. Ph, and Van Doormaal, P.M., Journal Institute of Petroleum Technology,  
Vol. 22, 1936, p.414.
- 13 Hayton, B, Presentation at the Bitumen Rheology Workshop, Bohlin Instruments  
Ltd., Cirencester, 6-7 March 1997.

- 14 Heslop, M.W., and Catt, C.A., "Specifying for Durability for Bituminous Surfacing - The Importance of Binder Rheology", Proceedings of the 2<sup>nd</sup> European Symposium on the Performance and Durability of Bituminous Materials, J.G. Cabrera (Editor), Leeds, April 1997, pp. 19-38.
  - 15 Anon, "Binder Characterisation and Evaluation. Volume 3: Physical Characterization", SHRP-A-369, Strategic Highway Research Program, National Research Council, Washington D.C., 1994.
  - 16 Nicholls, J.C., and Daines, M.E., "Laying Condition for Bituminous Materials", The Asphalt Year Book 1994, The Institute of Asphalt Technology, pp. 94-98.
  - 17 Ellis, C, Widyatmoko, I., and Read, J.M., "The Storage Stability and Behaviour of Polymer Modified Bituminous Binders", Proceedings of the 2<sup>nd</sup> European Symposium on the Performance and Durability of Bituminous Materials, J.G. Cabrera (Editor), Leeds, April 1997, pp. 133-148.
  - 18 Anon, "DD ABE Method For The Determination Of The Storage Stability Of Modified Binder", British Standard Draft of Development (Second Draft) released on 17th November 1995, BSI London
  - 19 Siegmann, M.C., "Methods of Routine Investigation". The Properties of Asphaltic Bitumen, edited by J. Ph. Pfeiffer, Elsevier Publishing Company, Inc., 1950, p. 155-188.
  - 20 Scholz, T.V., "Durability of Bituminous Paving Mixtures", PhD Thesis, University of Nottingham, October 1995.
  - 21 Broadhurst, S.J., *private communication*.
-

## *Chapter Six*

### **6. Mechanism-Interaction of Polymer Modified Materials**

#### ***6.1 Binder characterisation and evaluation***

##### **6.1.1 Temperature Susceptibility**

All bitumens show thermoplastic properties in that they become softer when heated and harder when cooled and hence, they are susceptible to temperature changes. The susceptibility of the bitumens to temperature is ideally expressed by changes in viscosity with temperature. However, in most cases the viscosity is not the simplest way for routine assessment and a penetration based procedure is usually adopted.

Penetration index (PI) as a parameter to assess temperature susceptibility of bitumens, is usually determined from the penetration-temperature relationship which was originally developed by Pfeiffer and Van Doormaal [1]. Basically, the PI value is determined by drawing a best fit line in the plot between the logarithm of penetration and temperature, and the PI value is calculated by:

$$PI = \frac{20(1 - 25A)}{1 + 50A}$$

*Equation 6.1*

where the slope of the line, A, can be determined by two methods:

1. penetration at two temperatures  $T_1$  and  $T_2$ :

$$A = \frac{\log \text{pen at } T_1 - \log \text{pen at } T_2}{T_1 - T_2}$$

*Equation 6.2*

2. penetration at the softening point temperature (pen 800) and at 25°C :

$$A = \frac{\log \text{pen at } T_{25^\circ\text{C}} - \log 800}{25 - SP_{ASTM}}$$

*Equation 6.3*

Equation 6.3 can be rearranged to Equation 5.1 ( $SP_{ASTM}$ ) or Equation 5.2 ( $SP_{BS}$ ) previously presented in *Chapter Five*. For convenience, Equation 5.2. is rewritten here:

$$PI = \frac{1921.5 - 500 \log Pen_{25} - 20SP_{BS}}{50 \log Pen_{25} - SP_{BS} - 121.6}$$

*Equation 6.4*

In this study, the selected temperatures  $T_1$  and  $T_2$  for the Equation 6.2 are 5°C and 25°C. The results shown in Figure 6.1 indicate that calculations based on Equation 6.2 and Equation 6.4 produce different results, and consequently, resulting different rankings of binder in terms of temperature susceptibility. It can be seen that binders A50, B50, C50, D50, and F100 (the unmodified binders) show no significant difference between the two procedures. However, the rest of the binders which are polymer modified binders differ significantly, the highest difference was found to be in SBS-modified binders (ES50 and FS100). This difference may be due to the assumption of a penetration of 800 (1/10<sup>th</sup> mm) at the softening point temperature is not valid for polymer modified binders.

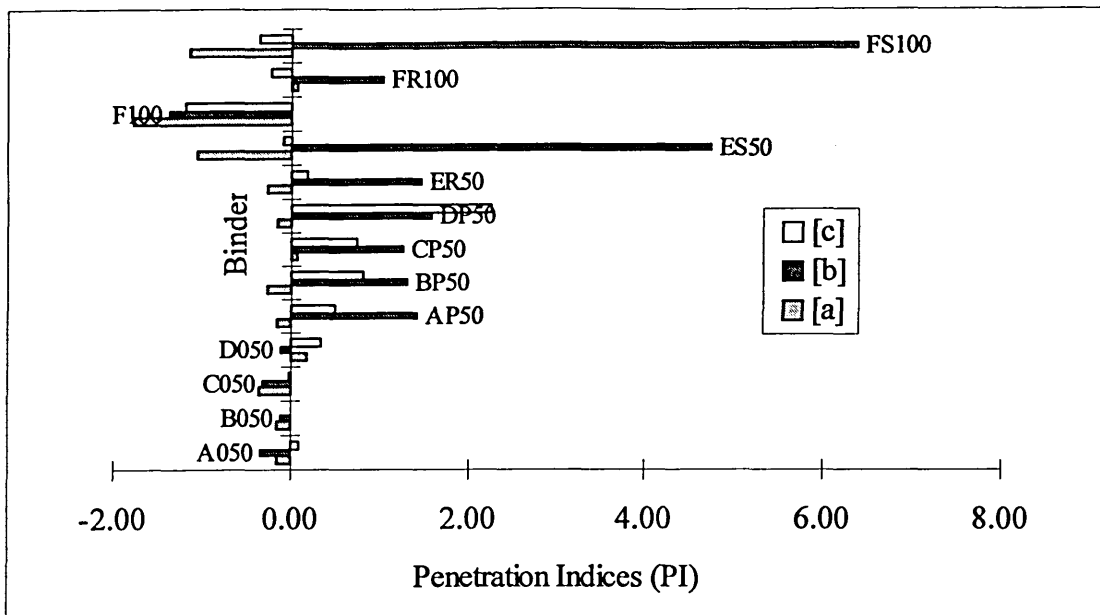


Figure 6.1 Penetrations indices as determined by three different procedures (a, b, and c). Detail description is presented in Table 6.1.

The “theoretical” penetrations at the softening point temperature (PenSPcal) of a particular binder were calculated by applying linear regression to the logarithm values of penetrations determined at temperatures of 5, 10, 25, and 35°C against the corresponding temperatures. The regression curve was then extrapolated to the softening point temperature to obtain the corresponding penetration value. The results are presented in Table 6.1. Most of the binders have “theoretical” penetration values between 600 to 1000 ( $1/10^{\text{th}}$  mm) at their softening point temperatures which are within the range reported by Pfeiffer and Van Doormaal [1]. However, the “theoretical” penetration value of SBS and SBR modified binders (ER50, ES50, FR100, and FS100) at the softening point temperature are higher than the expected range (i.e. higher than 1000 ( $1/10^{\text{th}}$  mm)).

Table 6.1 Comparisons of penetration indices (PIs) based upon the measured data points and the calculated values.

Binder Code	Base Binder	Polymer	Pen 25°C (1/10 mm)	Pen SPcal (1/10 mm)	RBSP °C	SPcal °C	PI25/5 [a]	PI 25/SP [b]	PIcalT [c]	PIcalPen [d]
A050	50 Pen	none	46	659	53	55	-0.15	-0.33	0.11	0.11
B050	50 Pen	none	46	765	54	54.5	-0.15	-0.11	0.00	0.00
C050	50 Pen	none	42	696	54	55.4	-0.36	-0.32	-0.02	-0.02
D050	50 Pen	none	42	657	55	57.2	0.19	-0.10	0.35	0.35
AP50	50 Pen	150/19	33	1256	66	60.8	-0.16	1.41	0.50	0.50
BP50	50 Pen	150/19	34	1026	65	62.1	-0.26	1.31	0.80	0.80
CP50	50 Pen	150/19	31	1042	66	62.9	0.06	1.28	0.75	0.75
DP50	50 Pen	150/19	33	601	67	71.3	-0.16	1.58	2.25	2.25
ER50	50 Pen	SBR	34	1803.3	66	58.8	-0.26	1.48	0.19	0.19
ES50	50 Pen	SBS	35	24310	89	57	-1.06	4.73	-0.09	-0.09
F100	100 Pen	none	103	907.6	41.5	42	-1.77	-1.36	-1.19	-1.19
FR100	100 Pen	SBR	68	1174.4	54.7	49.4	0.07	1.05	-0.22	-0.22
FS100	100 Pen	SBS	72	52450.6	86.3	48.3	-1.14	6.37	-0.35	-0.35

*Pen 25°C = measured penetration at 25 °C*

*Pen SPcal = calculated penetration at softening point temperature*

*RBSP = measured softening point temperature (BS method)*

*SPcal = calculated softening point temperature at penetration 800 (0.1 mm)*

*[a] PI25/5 = PI calculated based upon the measured penetrations at temperatures 5 and 25 °C (Equation 6.2)*

*[b] PI 25/SP = PI calculated based upon the measured penetration at 25 °C and the assumed penetration of 800 (0.1 mm) at RBSP (Equation 6.4)*

*[c] PIcalT = PI calculated based upon Pen 25 °C and SPcal (Equation 6.2)*

*[d] PIcalPen = PI calculated based upon Pen 25 °C and PenSPcal (Equation 6.2)*

The exercise shown in Table 6.1 and Figure 6.1 indicated that the PI methods cannot provide reliable description of the temperature susceptibility of polymer modified binders, in particular those which modified by elastomers. Binder FS100 (SBS modified 100 Pen) was the least temperature susceptible binder based upon procedure [b] but, was the second most temperature susceptible based upon procedure [a]. These contradictions can be due to the non-linearity found in then the relationship between the logarithms of penetration versus temperature, i.e. where penetration at softening point temperatures are far greater than 800 (1/10<sup>th</sup> mm) or outside the range of 600 to 1000 (1/10<sup>th</sup> mm). Therefore, application of Equation 6.4 as a measure of temperature susceptibility of modified bitumens, in particular those which modified by elastomers, is fundamentally not correct. Consequently, assessments of polymer modified binders based upon their fundamental properties as opposed to their empirical ones are highly recommended by the Author and are presented later in this chapter.

It is commonly accepted that there is a close relationship between PI and the type of bituminous materials, as demonstrated in Table 6.2 [2]. It has also been reported previously [3] that PI is not actually a measure of the temperature-susceptibility of viscosity for bitumen, but rather gives a measure of their deviation from Newtonian behaviour as also demonstrated in Table 6.2.

*Table 6.2 Relationship between PI and properties of bitumen*

PI value	Principal properties	Type of bituminous materials
less than -2	Show purely viscous flow Show Newtonian behaviour Characterised by brittleness at low temperatures	Pitch type, e.g. coal tar pitches
between -2 and +2	Show elasticity and a little thixotropy	Sol-type (normal type) bitumen, e.g. road making bitumen
higher than +2	Show marked time-dependent elasticity Show thixotropy to a large extent owing to structure formation	Gel-type (blown type) bitumen, e.g. blown (oxidised) bitumen

The results presented in Figure 6.1 indicate that the binders are well within the normal type category ( $-2 < PI < +2$ ), if the PI values are determined based on Equation 6.2. However, analysis based on Equation 6.4 indicates otherwise, that most of the modified binders have PI values close to +2 and for SBS-modified binders the values are higher than +2. This indicates that the modified binders deviate from the Newtonian behaviour and exhibit thixotropy. The deviations from the Newtonian behaviour are also demonstrated in Figure 6.2.

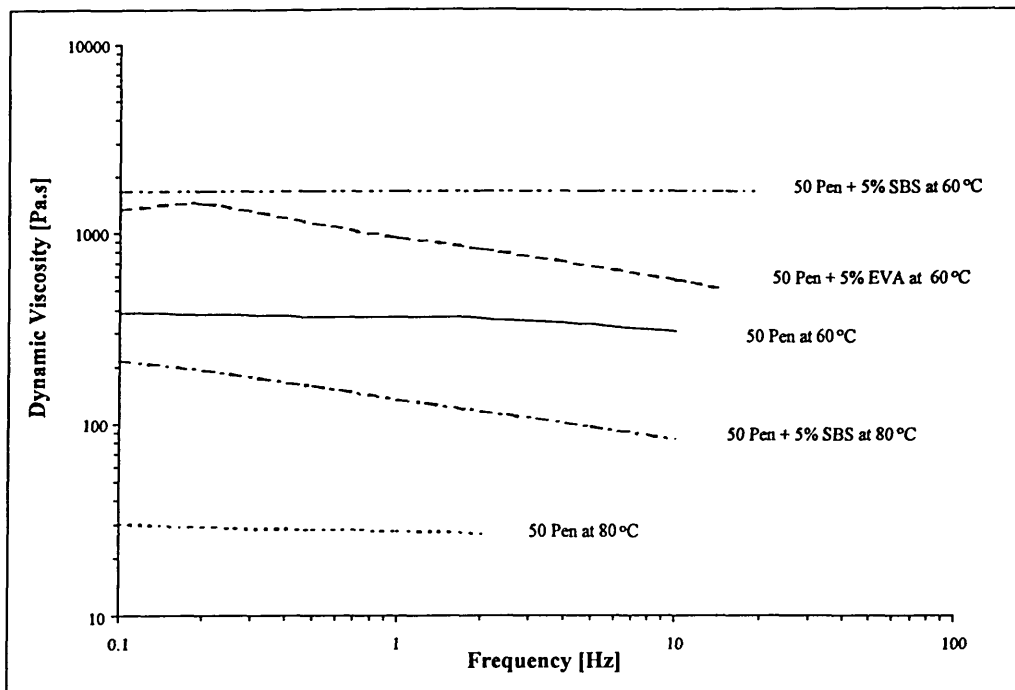


Figure 6.2 Viscosity-frequency relationships, showing thixotropy (shear-thinning) on 50Pen+5%EVA and 50Pen+5%SBS binders. The measurements were carried out by a dynamic shear rheometer.

### 6.1.2 Workability

Assessment of the workability of polymer modified binders is important as modification tends to increase the viscosity of the binder, which may cause a problem in pumping and handling in the hot mixing plant and/or during the construction process. Consequently, higher temperatures may be necessary to obtain adequate workability.

The required viscosity for pumping bitumen in a hot mixing facility is between 1.5-2.0 Pa.s [4] at which the process can be done within a temperature range of between 120-135°C for polymer modified binders used in this study. The results in Figure 5.4. (*Chapter Five*) show that the temperature range of polymer modified binders at which the viscosity is 1.5 Pa.s is between 120-135°C. Therefore, the modified binders should be able to be pumped without any significant problems.

However, results presented in *Chapter Five* indicate that the polymer modified binders, especially those modified by SBS and SBR copolymers, require a mixing temperature, at a viscosity of 0.2 Pa.s, as high as 190°C which means high energy consumption.

Additionally, laying/compaction temperatures for these binders are also very high (up to 150°C) at 0.6 Pa.s, which may cause difficulties if the mixture needs to be laid during cold weather and/or high wind chill conditions. On the other hand, EVA copolymer crystallises rapidly at temperatures below its minimum rolling temperature and makes EVA modified binder stiffen considerably. Therefore, these polymer modified mixtures need to be applied and compacted as quickly as possible to keep the temperatures within the permissible range. Nevertheless, overall results based upon the effects of mixing-laying-compaction temperatures and rate of cooling towards the level of workability indicate that EVA modified binders are better in comparison to the other modifiers and, furthermore, previous findings presented in *Section 3.4.1.* reported that EVA modified binders improved workability in cold weather over unmodified 50 pen and 70 pen bitumens.

### **6.1.3 Storage Stability**

Polymer modified binders should remain stable if stored for a prolonged period. Therefore, the storage stability test is as essential test for polymer modified binders. Table 6.3 presents results from stability tests carried out in accordance with the procedure presented in *Chapter Five.* From these results, the binders can be classified into three categories:

#### **1. Very stable binders:**

As shown in Table 6.3, the ER50 (SBR) binder shows very good stability as the recorded penetration and softening point values were similar. Additionally, the blend has similar penetration and softening point values after stability testing when compared to the original binder, i.e. before the stability test. Hence, it is not only very stable but it is also not significantly susceptible to oxidative hardening. These results (Table 6.3) also indicate that the FR100 (SBR) and FS100 (SBS) binders are very stable as the penetration and softening point values of the top and bottom sections remained similar. The penetration values suggest that these binders tend to be harder after the stability test. However, different trends were found in the softening point values. The softening point of FR100 (SBR) tends to be higher after stability testing, hence, consistent with the drop in penetration values. Contrary to this, the softening point of FS100 was lower after the stability test which was not consistent with the

drop in penetration values after stability testing. The drop in penetration values after stability test was confirmed with the increase of complex stiffness modulus after stability test. The unique case that softening point of FS100 (SBS) was lower after stability test, unfortunately, cannot be understood from the dynamic mechanical analyses alone. There might be some changes in the chemical properties or microstructure of the blends, such as de-polymerisation or polymer degradation due to excessive heating. Therefore, further assessments to study the effect of heating to the microstructure or chemical properties need to be conducted.

## 2. Moderately stable binders:

The EP50 (EVA) shows a big difference between the top and bottom sections for penetration values but retained the softening point values in both sections. Similarly, it is also showed that the penetration values of top and bottom sections changed but their softening points did not, when compared with the original binder.

## 3. Unstable binders:

Results from ES50 (SBS) indicate inconsistent behaviour as it has both high penetration and softening point values. The discrepancy found in the ES50 binder was probably due to the nature of the SBS copolymer domain in that it may not be compatible with the conventional 50 pen bitumen. The SBS copolymer as a crosslinking type of copolymer has the ability to resist flow when subjected to gradual heating which leads to the huge increase in softening point. During the ring and ball softening point test, the original ES50 (before stability test) and the top section of ES50 (SBS) after stability test, showed an unusual state of failure (Figure 6.3). Unlike conventional bitumen, this did not deform uniformly until it reached the base plate, but failure was found on the binder-brass ring interface where the binder was separated from the brass ring. This can be due to the cohesion bond being stronger than the adhesion. Our experiment recorded the softening point of ES50 binders as the point when the steel ball touched the lower steel plate, even though in each case the steel ball was not necessarily coated with, or did not deform together with, the binder.

Figure 6.4 shows that the penetration value on storage may increase significantly even though the binder is stored only for a one day period. The rate of change in the penetration value decreases as the storage duration increases. The BS draft of specification [5] only required assessment of the stability indices at a seven-day storage. This procedure is good to obtain reasonable stability indices as, from this study, the rate of change in the binders' properties was found constant (stable) when they are stored for more than three days (Figure 6.4). However, this information can be misleading that, for example in the case of SBS modified binder, a significant change of penetration values was developed just within one day storage which means that a special treatment to prevent instability is required even though the polymer modified binder is only stored for a short period (e.g. while the binder is: being transported from the supplier to the construction site, waiting to be mixed with the aggregates or waiting to be applied for surface dressing). Therefore, assessments on storage stability of polymer modified binders at different storage duration from as early as one-day storage is necessary.

*Table 6.3 Penetrations and Softening Points of Binders before (Original) and after storage stability (Top & Bottom). These results are after 7 days of storage.*

Binder	Penetration [0.1 mm]			Softening Points [°C]		
	Original	After Stability Tests		Original	After Stability Tests	
		Top	Bottom		Top	Bottom
E50	47.0	41.0	41.5	53.0	54.1	53.0
EP50	35.7	42.0	27.7	64.4	64.2	64.0
ER50	32.3	33.5	34.5	65.6	66.3	67.4
ES50	34.2	70.0	24.0	88.6	103.7	65.0
FR100	68.5	57.0	56.0	51.7	55.0	56.7
FS100	71.5	63.0	62.0	86.3	72.0	73.3

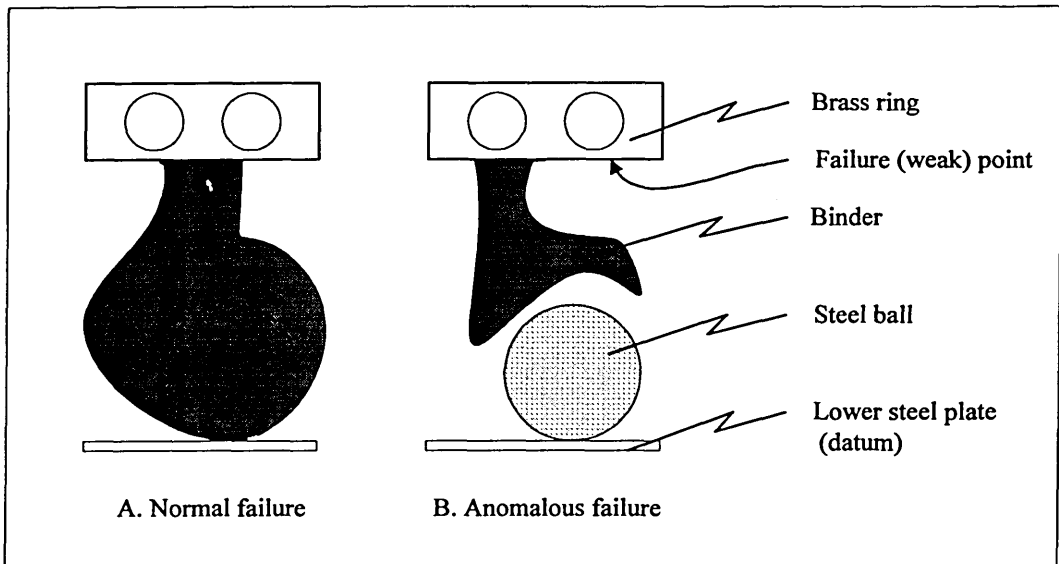


Figure 6.3 Deformation failure in a ring and ball softening point test

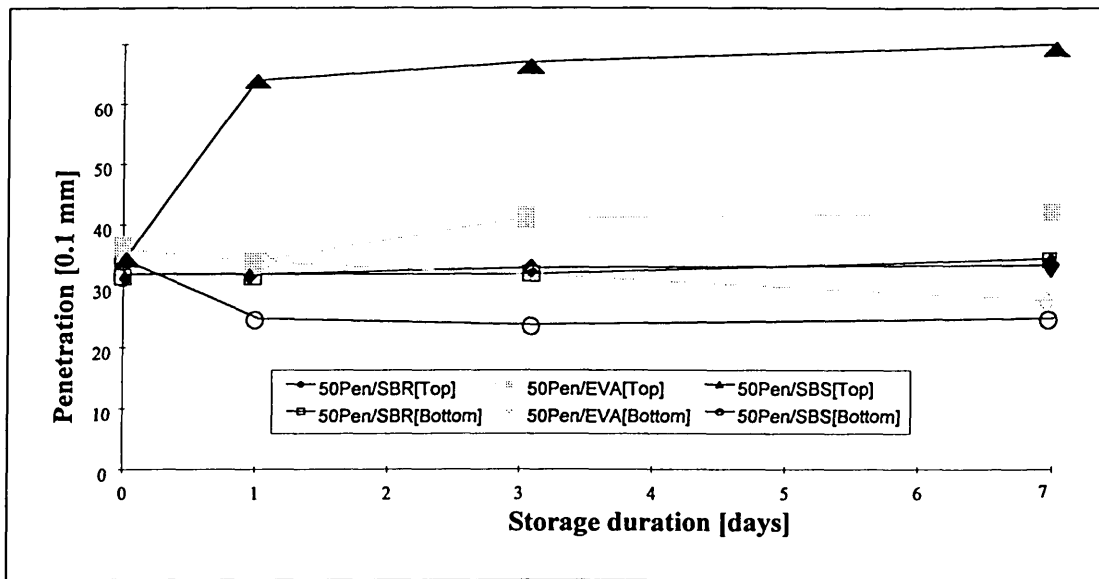


Figure 6.4 Penetration values of polymer modified binders during the storage stability test at top and bottom sections

### Analyses and Discussions

The lower penetration value at the bottom part of ES50 (SBS) binder after storage indicated that after separation from the SBS the base binder hardened and left the heavier components at the bottom. On the other hand, the higher penetration value at the top may be caused by the characteristics of SBS, i.e. it tends to swell, hence, it may

have a lower density than that of the base bitumen and consequently it may be more easily penetrated.

The anomalous tendency in the relationship between the penetration and softening point values, i.e. the higher penetration value with the higher softening point value, indicated that the behaviour of the blend has completely different patterns to that normally expected for bituminous binders, i.e. the normal rule of thumb is that the higher the penetration value, the lower the softening point value. Vonk and Bull [8] had also reported the same tendency on the study of blends of an elastomeric copolymer with different base bitumens.

The application of storage stability indices ( $SS_{pen}$  mm/10 and  $SS_{SP}^{0C}$ ) to the data showed that changes in the  $SS_{SP}$ , when an instability occurred, was not as sensitive as the changes in  $SS_{pen}$  mm/10 (Table 6.4). According to the  $SS_{SP}$  index, deviation within 2°C is within the permissible range, hence, the EP50 blend can be regarded as a stable blend. However, the analyses based on the  $SS_{pen}$  index indicated that the penetration values changed quite dramatically. Hence, care should be taken when using these indices.

Further analyses based on penetration indices reported that the bottom sections of the unstable ES50 (SBS) binder seems to have similar characteristics to the original base bitumen. Table 6.4 indicates that the PI values of the original 50 pen (before stability test) and the bottom section of ES50 (SBS) after stability test were similar. Hence, it seems that the SBS copolymer has been completely separated from the base bitumen, leaving the polymer rich phase at the top and the bitumen rich phase at the bottom.

Table 6.4 Penetration Indices (PIs) and Stability Indices (SSs) calculated from Penetration values and Softening Points of Binders before (Original) and after storage stability (Top & Bottom) by using Equations 5.3 and 5.4 Chapter Five. The penetration indices calculated were based on Equation 5.2. These results are after 7 days of storage.

Binder	Penetration Indices [0.1 mm]			Stability Indices	
	Original	After Stability		SSpen	SSsp
		Top	Bottom	[0.1 mm]	[°C]
E50	-0.29	-0.35	-0.54	-0.50	1.10
EP50 (EVA)	1.26	1.63	0.72	14.33	0.17
ER50(SBR)	1.34	1.53	1.77	-1.00	-1.10
ES50 (SBS)	4.66	8.08	0.58	46.00	38.67
FR100(SBR)	0.46	0.63	0.95	1.00	-1.70
FS100(SBS)	6.34	4.03	4.19	1.00	-1.30

### State of Dispersion

The state of dispersion of polymer within the bitumen solvent was observed under an Ultra Violet Fluorescent Microscope. The observations from this work confirm previous reports [4, 6, 7, 8] that there are basically two phases present in the polymer-bitumen blends, i.e. a continuous bitumen rich phase and a polymer rich phase.

The observations show that binders modified with SBR and EVA copolymers demonstrate fine dispersion whilst it was coarser for the SBS modified binder. The storage stability test on the unstable binder, ES50 (SBS), showed that the SBS copolymer was almost completely separated from the base bitumen. The top part of the blend appeared to be highly modified by the SBS copolymer whereas there was almost no polymer present in the bottom part. A similar situation was found for the EP50 blend but at a less significant level. The ER50 (SBR), FR100 (SBR), and FS100 (SBS) showed good stability as there were no significant changes in the state of dispersion. The photomicrographs of these binders are presented in *Appendix A*.

### Characteristics of Unstable Binders

Previous investigations [8] reported that incompatible blends of bitumen and styrene butadiene based elastomers could be separated completely into two phases, i.e. an asphaltene rich phase and a polymer rich phase, by using a hot centrifuge. The asphaltene rich phase was hard, brittle, non-elastic and had a relatively low melt

viscosity. The other phase, rich in polymer was soft, flexible, elastic, and had a high melt viscosity.

Similar conditions have been found in the storage stability tests carried out in this work, particularly in the case of the ES50 (SBS) binder as presented previously. Figure 6.5 shows this schematically.

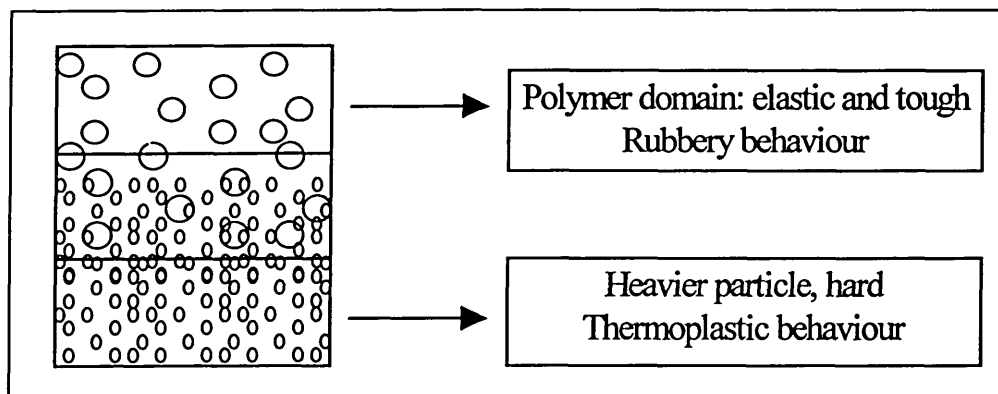


Figure 6.5 Schematic representation of unstable specimen after storage stability test.

## 6.2 Dynamic Mechanical (Rheological) Analyses on Properties of Bituminous Binders

Conventional empirical test methods are not always applicable to polymer modified bitumen, whereas fundamental rheological test methods should be equally applicable to both unmodified and modified binders. Although there is no agreement at present on the correlation of rheological tests with performance in an asphalt mixture, rheological measures on bituminous binders can be used to provide comparative information for predicting failure behaviour, and for quality control (not necessarily in all areas e.g. fatigue). Dynamic rheometers (dynamic mechanical tests) might play a more active role in specifying fundamental properties of bituminous binders. They are used frequently in research and development at present, however, their adaptation for specifications are still in development (*Section 3.2.2*).

In this study, the test was carried out following the procedures presented in *Chapter Five*. There are three ways of representing the rheological data:

1. By drawing Black curves (complex modulus against phase angle).

Advantages:

- ◆ simple
- ◆ fast
- ◆ no data modification is required
- ◆ provide general information on characteristics of binders
- ◆ reliable for quality control purposes

Disadvantages:

- ◆ no information on the test temperature
- ◆ no information on the rate of loading (frequency)
- ◆ cannot be used for design purposes

2. By developing master curves for complex modulus and phase angle at selected temperature.

Advantages:

- ◆ a reliable method for data extrapolation
- ◆ reference temperature (or frequency) can be flexibly selected
- ◆ provide information on the performance related properties
- ◆ can be used for design purposes

Disadvantages:

- ◆ needs a lot of data at various temperatures and frequencies
- ◆ need special techniques to develop a master curve, i.e. time-temperature superposition techniques (*Section 3.2.3*)
- ◆ more time consuming

3. By plotting dynamic (complex) viscosity against test frequency.

In general, dynamic viscosity has similar characteristics to the complex modulus function that it can be used to observe viscoelastic behaviour of bituminous binders. By plotting dynamic viscosities against temperature, there will be a stage where viscosities of different frequencies come into a single line, this viscosity can be related to a Newtonian viscosity, where the viscosity is independent of frequency (shear rate) (Figure 6.6).

As previously described in *Chapter Three*, there are two popular procedures for time-temperature superposition i.e. by using Arrhenius or WLF equations. The Arrhenius equation is usually associated with absolute rate theory where the chemical reactions (molecular mobility) are influenced by rate of diffusional (activation) energy and/or temperature changes [9]. It assumes that the two generalised empirical constants ( $K=0.4347 \Delta H/R$  and  $R=8.31$  Joule per Kelvin per mole) are applicable for bituminous binders, and the activation energy ( $\Delta H$ ) needs to be determined.

On the other hand, the WLF method is associated with the free-volume theory where the molecular mobility at any temperature, and hence changes in viscosity, is primarily dependent on the free-volume remaining [9]. The WLF time-temperature superposition procedure can be done by determining the coefficients  $C_1$  and  $C_2$  after selecting the reference temperature. The coefficients  $C_1$  and  $C_2$  for calculating the shift factors of the WLF equation were determined by two stages. Firstly, they were determined from a series of measurements at temperatures above the reference temperature ( $25^\circ\text{C}$ ). Secondly, they were determined from a series of measurements at temperatures below the reference temperature. The procedure of generating the master curves has been presented in *Chapter Three*.

Master curves in this study were developed by using WLF equation for the time-temperature superposition procedure. The Author prefers the use of WLF equation as opposed to the Arrhenius because most of the specimens were tested at temperatures above  $-5^\circ\text{C}$  where these temperatures were presumably above the glass transition temperatures of the specimens. Furthermore, Cheung [9] suggests that WLF equation is best applied at temperatures above the glass transition temperatures.

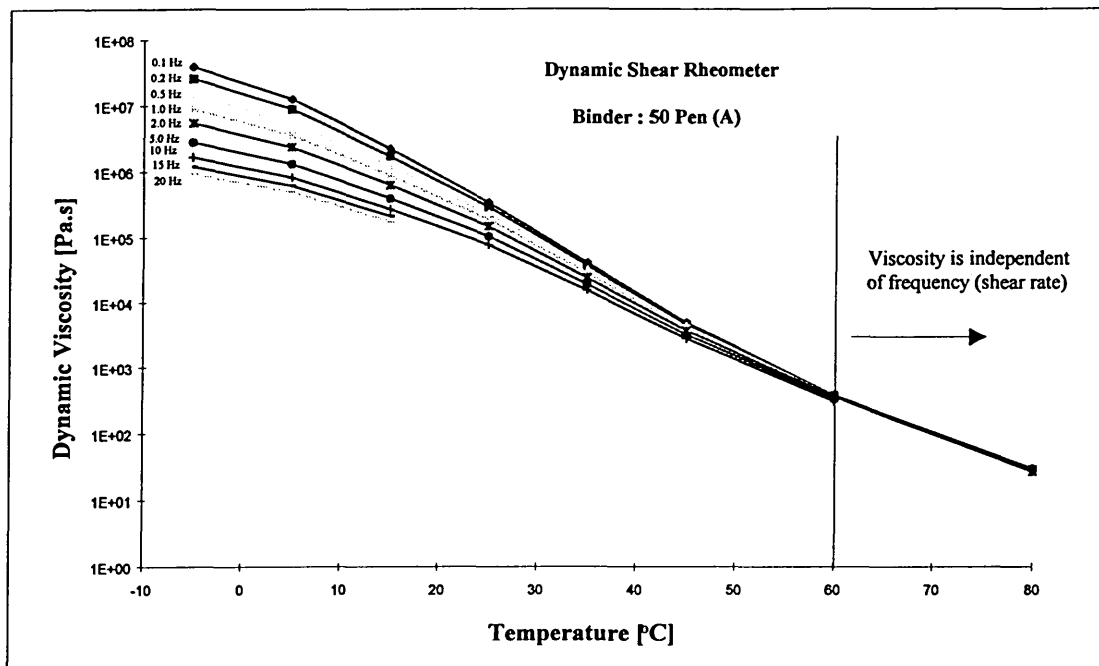


Figure 6.6 Dependency of the binder's dynamic viscosity on temperature and frequency (shear rate). Binder reference number: A50

### 6.2.1 Storage Stability of Polymer Modified Binders

Rheological measurements were undertaken on a dynamic shear rheometer. Temperature sweeps ranging from 0 to 80°C were conducted at a frequency of 1 Hz. The modified binders subjected to this test were those obtained from 7 day storage, to ensure that there was no further significant change in the phase separation.

Figure 6.7 and Figure 6.8 present the Black curves of the binders before and after storage stability tests. The black curves are a plot of complex modulus  $G^*$  against phase angle  $\delta$  in which a series of bitumens differing in penetration but not temperature susceptibility (penetration index) should give a single black curve. Therefore deviations from this curve indicate changes in composition or variation in structure caused by processing, ageing, or polymer addition.

Results show that the black curves before and after storage stability tests were close to each other for stable binders such as ER50 (SBR), EP50 (EVA), FR100 (SBR), and FS100 (SBS) (an example is presented in Figure 6.7 but the complete results can be

found in *Appendix A*). However, significant deviation from original curves was observed on the unstable binder, i.e. ES50 (SBS) blend (Figure 6.8).

In Figure 6.8, the black curve for the bottom section of ES50 (SBS) binder (after stability test) was shifted towards the curves of the original 50 pen binder (before stability test). This also indicates that the original binder and the bottom phase may have had similar properties which conforms with the analyses based on PI values (Table 6.4). Discrepancy was observed on the top section of ES50 (SBS) after stability test, that the complex modulus decreases as the phase angle decreases. Normally, complex modulus increases as phase angle decreases, or *vice versa*. This may indicate that the binder in that regime possess good elasticity but low stiffness. These properties may be responsible for the high softening point value with high penetration as well.

Dynamic viscosity was measured by a dynamic shear rheometer. The results from all binders studied (Figure 6.9) show that the viscosity changed after the stability test. The results for the bottom sections after the stability test tend to be higher than their original values whereas the top sections tend to be lower. Bigger deviations from the line of equality are found mostly on the top sections of unstable SBS modified binders after the stability test. The lower viscosity of the top sections of SBS modified binders after stability test may explain the high penetration value obtained on this section.

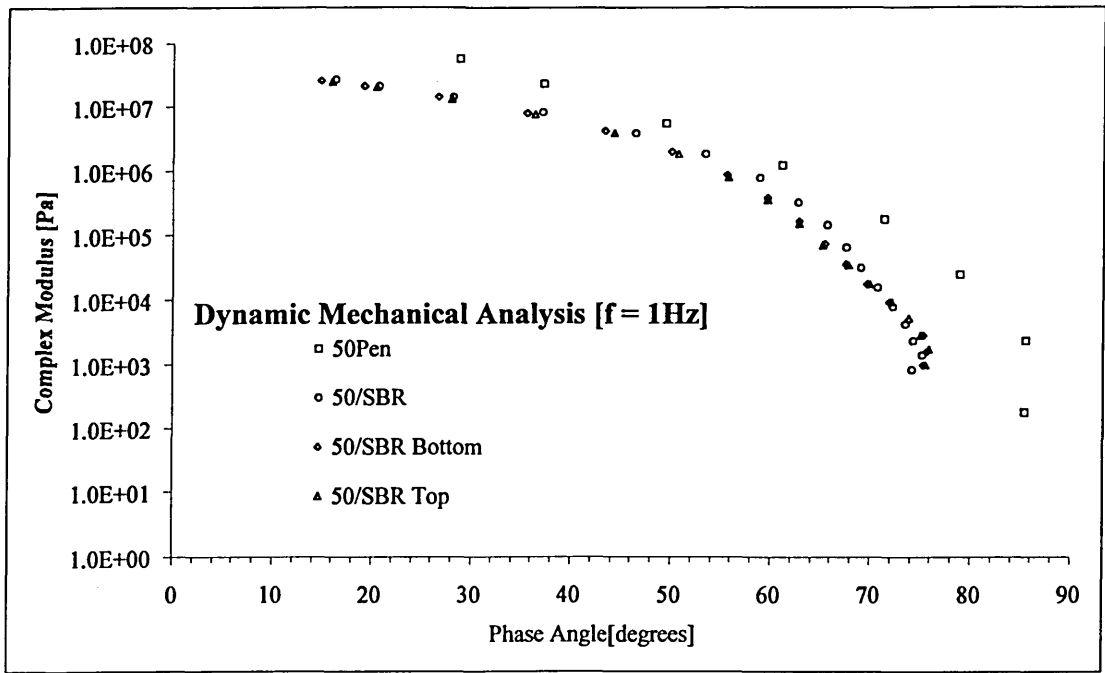


Figure 6.7 Black curves showing comparison of SBR modified binder (50 pen + 5% SBR), before and after seven day-storage stability test.

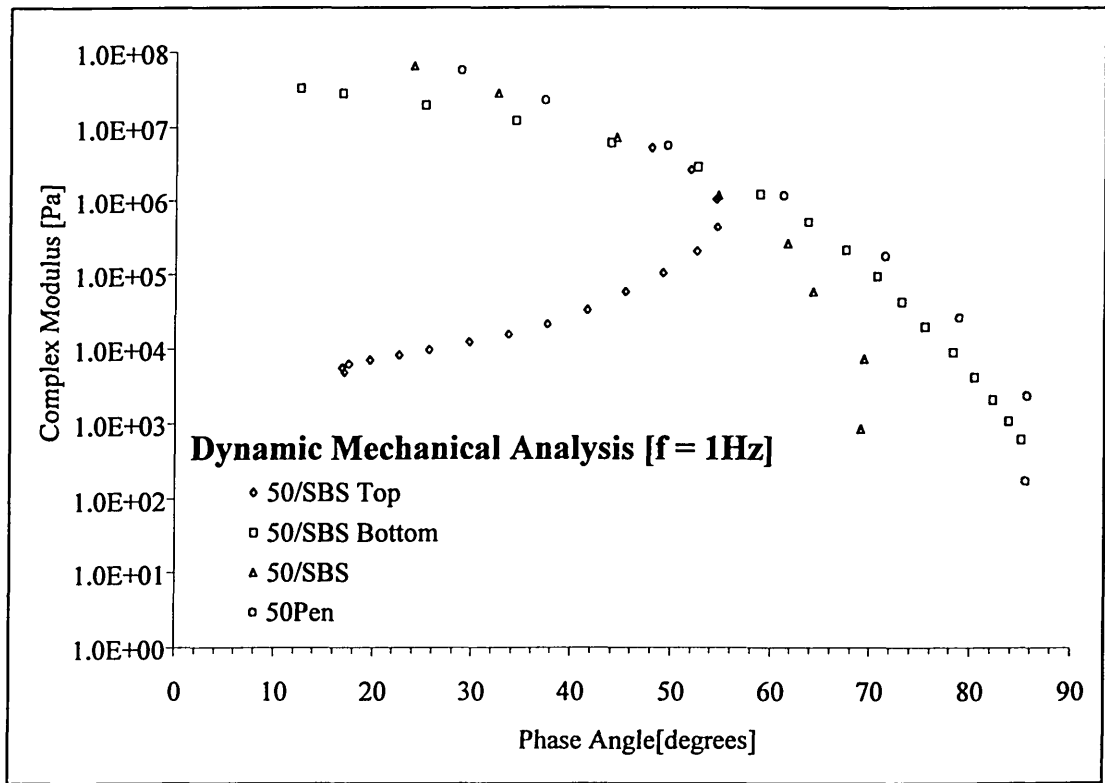


Figure 6.8 Black curves showing comparison of SBS modified binder (50 pen + 5% SBS), before and after seven day-storage stability test.

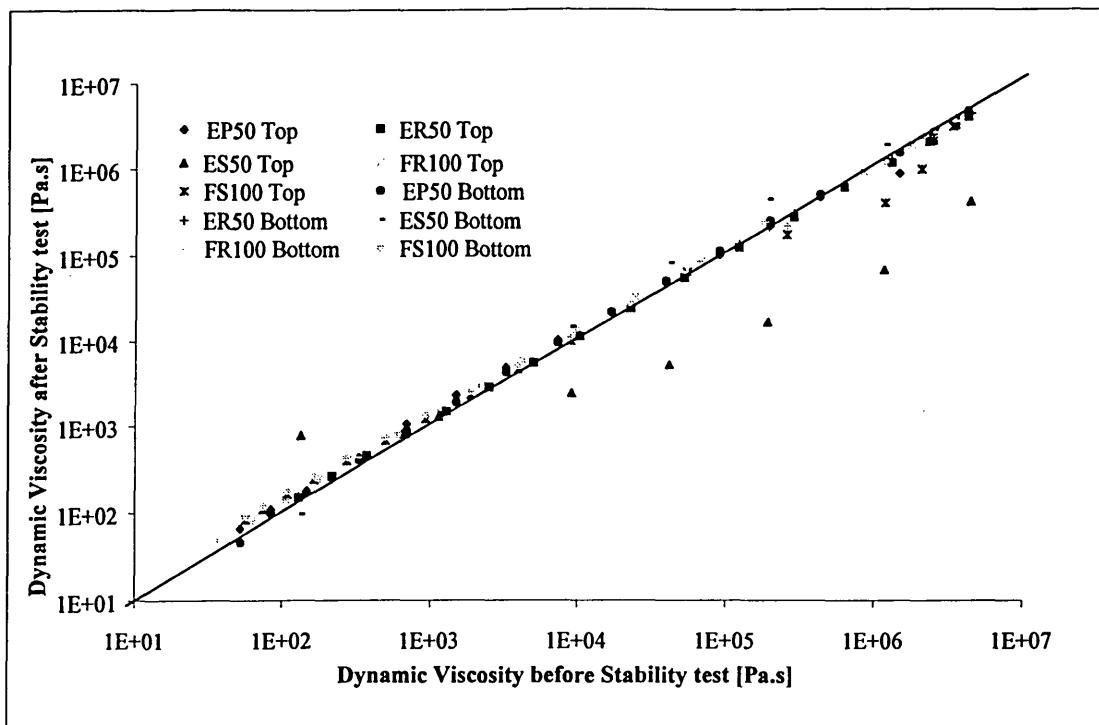


Figure 6.9 Dynamic viscosity before and after stability test as measured by a dynamic shear rheometer at several service temperatures. Temperature sweeps from 0°C to 80°C at a frequency of 1 Hz

### 6.2.2 Bituminous binders from different manufactures

Results from the dynamic mechanical test on 50 pen bitumens from different manufacturers indicate that these binders, plotted as Black curves, show no significant difference in their properties. All lines seem to come into a single curve (Figure 6.10).

These results are also consistent with the results on PI values (Figure 6.1), that these binders also show similar PI values.

### 6.2.3 Addition of EVA into 50 Pen bitumen from different manufactures

As a consequence of the previous results (6.2.2), there is also no significant difference when EVA was added as the modifier to these bitumens (Figure 6.11). Again, these results are also consistent with the results on PI values (Figure 6.1), that these binders also show similar PI values.

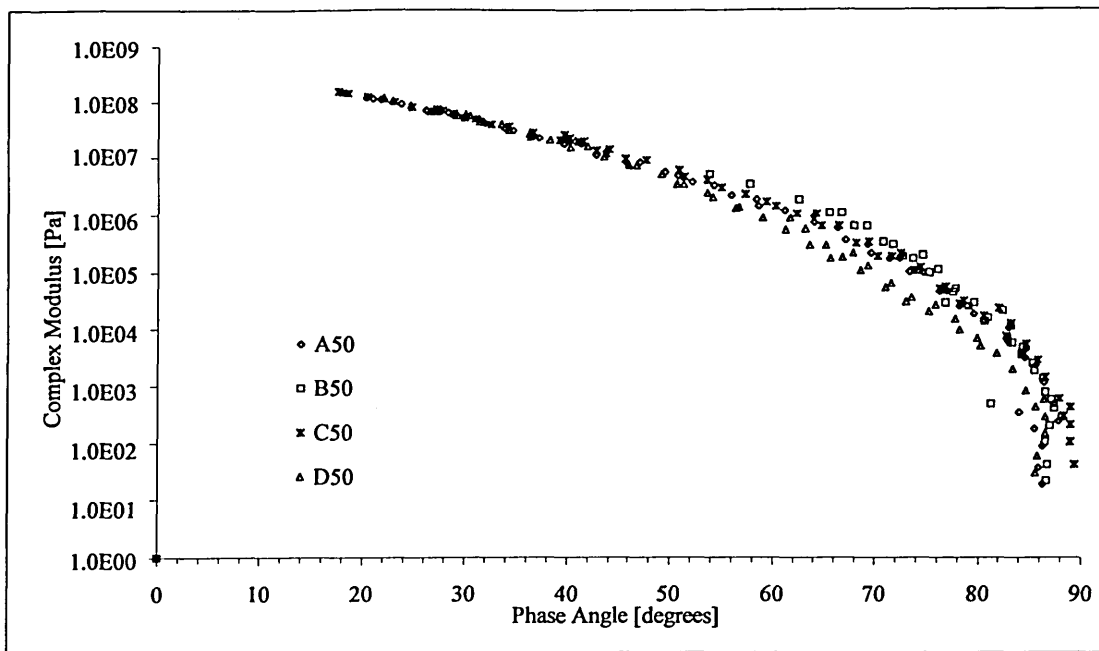


Figure 6.10 Black curves of 50 pen bitumens from different suppliers

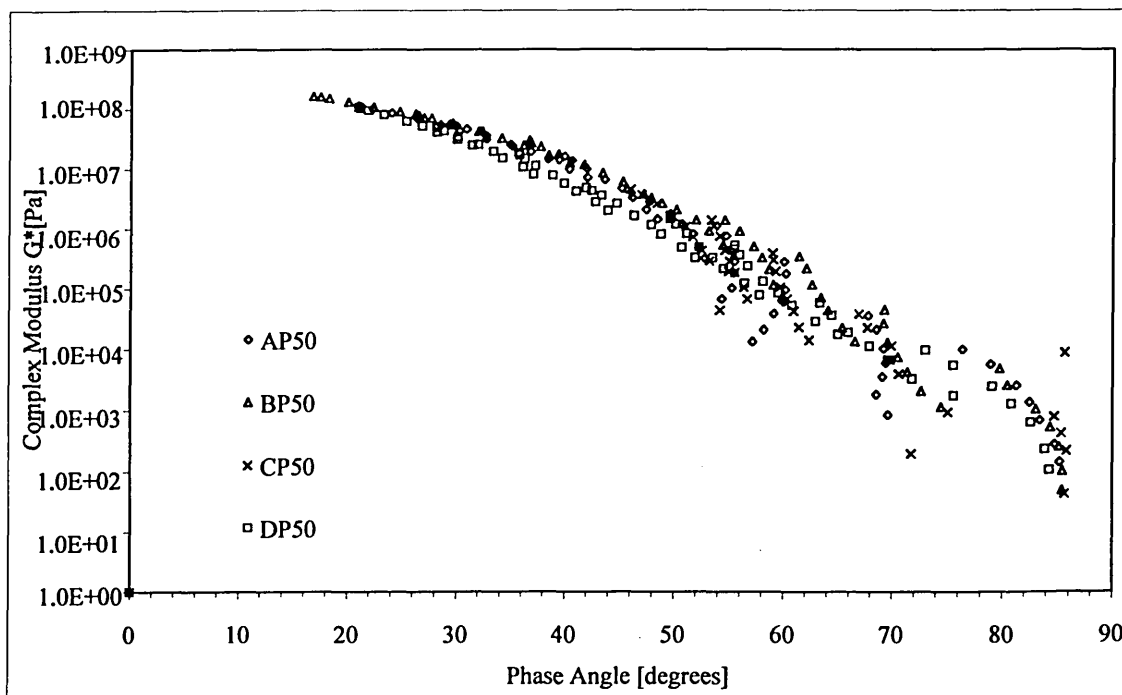


Figure 6.11 Black curves of EVA modified 50 pen binders with the base binder from different suppliers

#### 6.2.4 Addition of polymer modifiers into bitumen with different penetration grades

Figure 6.12 shows that different polymers modify the same bitumen in different ways. However, they all tend to increase the complex modulus and reduce the phase angle at high temperature (low frequency), which implies a better resistance to deformation. The complex modulus of all binders (unmodified and modified) come towards a unity, termed the glassy modulus ( $G_g$ ) [10], at high frequencies (low temperatures) where the binders should behave as an elastic solid (phase angle approaching  $0^\circ$ ). The average glassy (shear) modulus obtained from this study is 0.85 GPa which is close to the value reported by Christensen and Anderson [10], i.e. 1GPa<sup>a</sup>.

The glassy modulus of 0.85 GPa in this study was obtained by doing a regression analysis on the Black curves (Figure 6.10, Figure 6.11, Figure 6.13) and determined at a phase angle of  $0^\circ$  (fully elastic condition):

$$y = C_6 \delta^6 + C_5 \delta^5 - C_4 \delta^4 + C_3 \delta^3 - C_2 \delta^2 - C_1 \delta + C_0$$

*Equation 6.5*

where  $y$  = complex modulus [Pa]

$\delta$  = phase angle [degree]

$C_0 \dots C_6$  = regression coefficients (Table 6.5)

---

<sup>a</sup> In the same paper, Christensen and Anderson reported that the  $G_g$  values for paving grade bitumens are between 0.6 to 1.5 GPa. The value of 1 GPa can be used for engineering purposes.

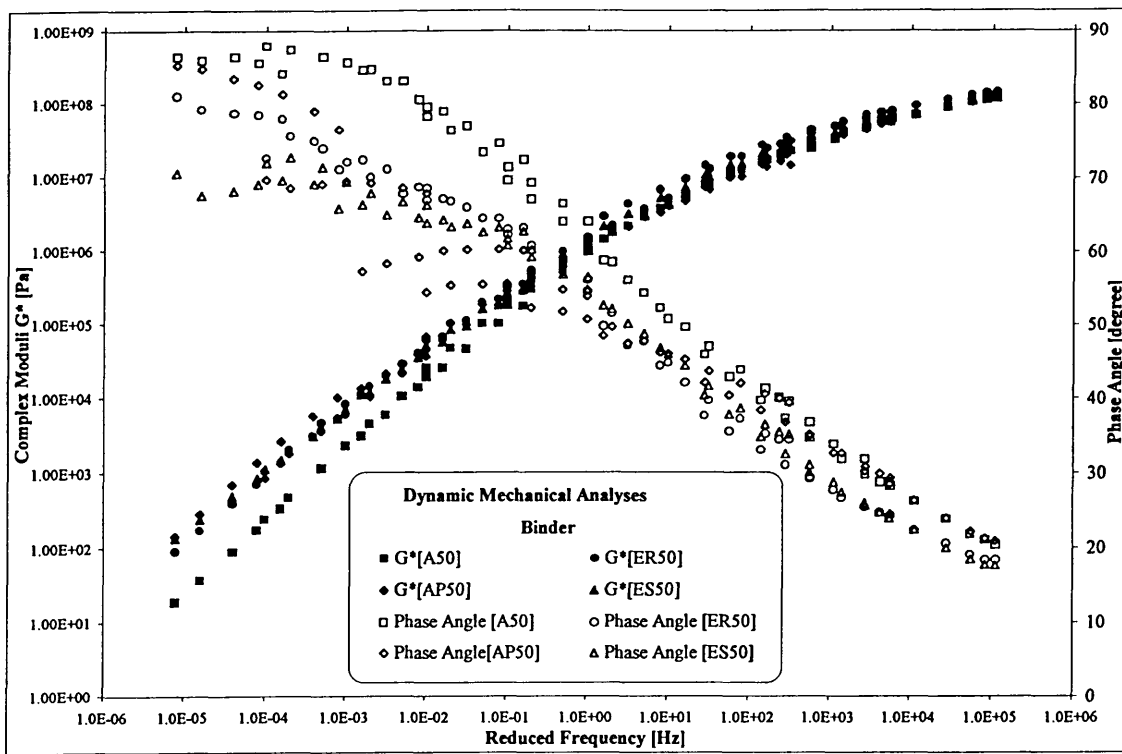


Figure 6.12 Master curves of complex modulus and phase angle. (Temperature : -5 to 80°C and frequency: 0.1 to 20 Hz. WLF time-temperature superimposition.)

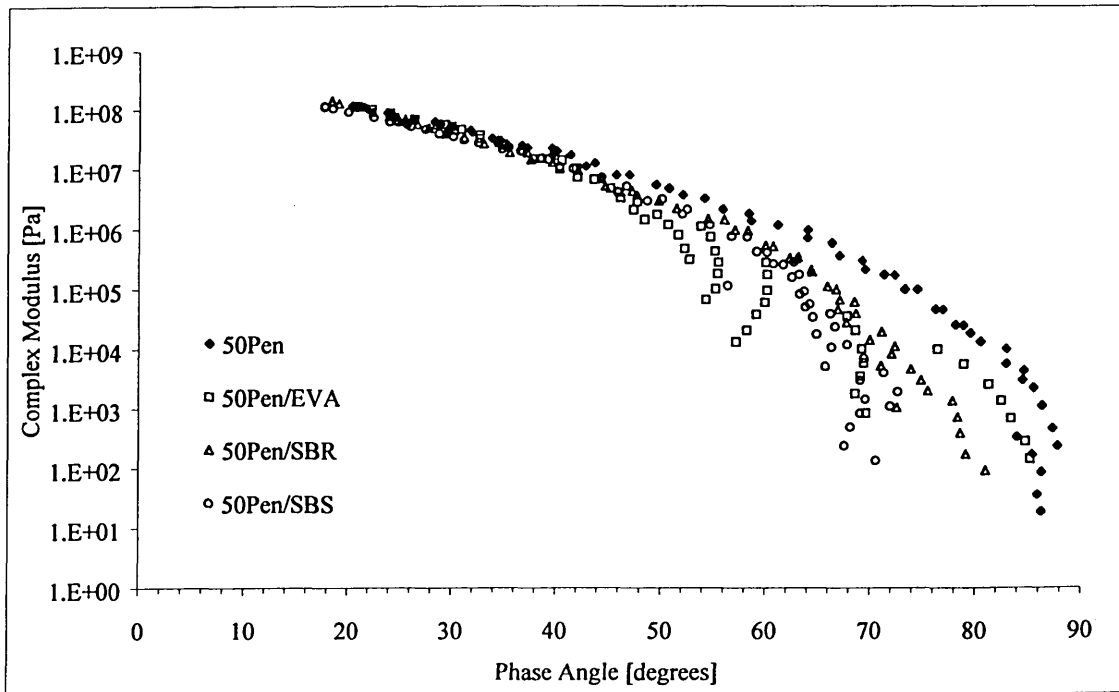


Figure 6.13 Black curves of polymer modified binders (50 pen based).

Table 6.5 Regression coefficients for Black curves of studied binders

Binder	$C_0$	$C_1$	$C_2$	$C_3$	$C_4$	$C_5$	$C_6$	$R^2$
A50	5.00E+08	-3.00E+07	5.87E+05	-4.45E+03	-1.72E+01	4.38E-01	-1.80E-03	0.999
B50	1.00E+09	-1.00E+08	4.00E+06	-7.59E+04	8.14E+02	-4.63E+00	1.09E-02	0.998
C50	6.00E+08	-4.00E+07	1.00E+06	2.17E+04	2.35E+02	-1.43E+00	3.70E-03	0.998
D50	7.00E+08	5.00E+07	2.00E+06	-3.13E+04	3.46E+02	2.13E+00	5.60E-03	0.997
AP50	4.00E+08	-2.00E+07	-1.32E+05	1.49E+04	-2.84E+02	2.27E+00	-6.80E-03	0.998
BP50	4.00E+08	-1.00E+07	-3.85E+05	2.04E+04	-3.45E+02	2.59E+00	-7.40E-03	0.991
CP50	3.00E+09	-2.00E+03	7.00E+06	1.37E+05	1.41E+04	-7.71E+00	1.75E-02	0.954
DP50	6.00E+08	-4.00E+07	6.88E+04	1.99E+03	-2.15E+02	2.51E+00	9.50E-03	0.996
ER50	8.00E+08	-7.00E+07	3.00E+06	-6.29E+04	7.91E+02	-5.39E+00	1.54E-02	0.998
ES50	5.00E+08	-3.00E+07	1.00E+06	-1.76E+04	1.61E+02	-6.92E-01	7.00E-04	0.999

The results indicate that there was no significant difference in the modification by different polymers as seen in the shape of the complex modulus vs. reduced frequency but their mechanisms take place in different ways, e.g. as seen from the shape of the phase angle vs. reduced frequency (Figure 6.12). The lowest maximum phase angle ( $70^\circ$ ) at the low frequency (high temperature) regime was found on the addition of SBS, and followed by SBR ( $80^\circ$ ), and EVA ( $85^\circ$ ). It is noticed that the shape of the phase angle vs. reduced frequency of EVA modified binder is not as continuous as the other binders, i.e. there are some flat areas (plateau) in the curve of phase angle which may indicate some sort of mechanisms such as molecular entanglements, where the phase angle is no longer dependent on frequency. As EVA copolymer does not have a network-like structure, this entanglement may be due to the crystallisation of polyethylene segments within the EVA which provide the stiffness and strength of the binder. This kind of mechanism can be beneficial to the resistance to deformation of the binder.

At the higher end of the test frequency, the difference between the polymer modified binders with regard to complex modulus and phase angle is less obvious. Furthermore, the complex modulus curves of the polymer modified binders converging towards the curve of the unmodified one and their phase angle curves are lower than the unmodified one. This may be an indication that the addition of polymer into 50 pen grade bitumen

does not improve the high frequency (low temperature) properties of the binder. The same condition applies to the modification of 100 pen based binder that the addition of polymers only improves high temperature properties of the base binder (Figure 6.14).

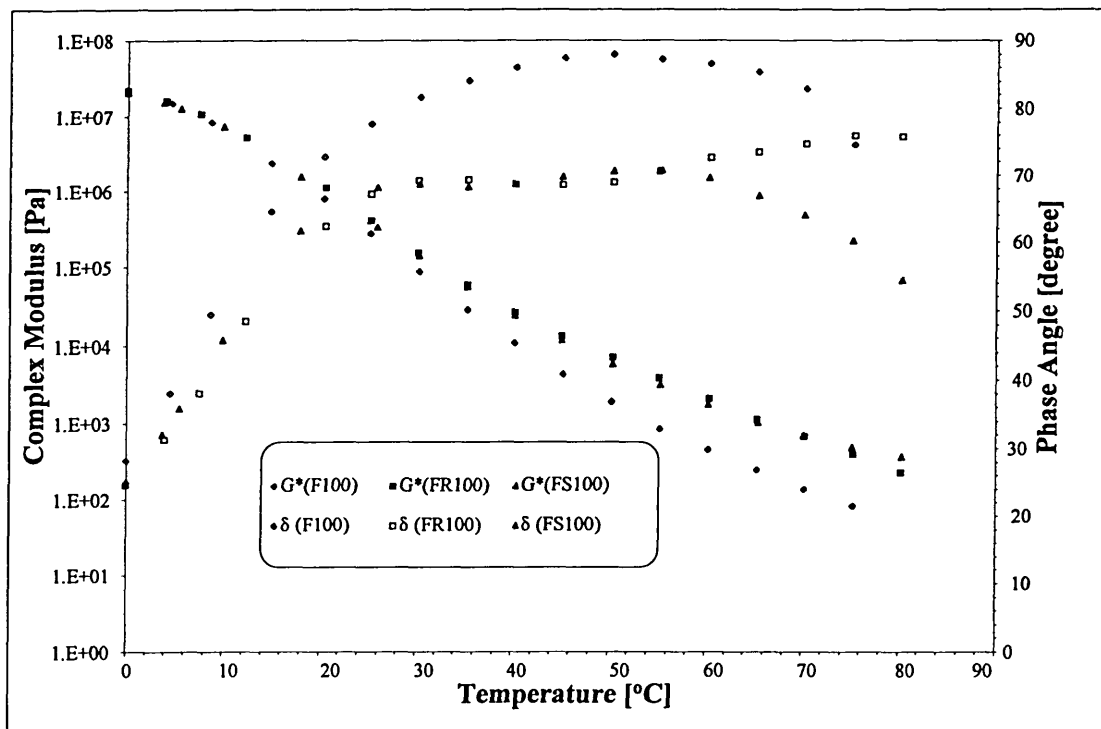


Figure 6.14 Dynamic mechanical tests on 100 pen based binders. Frequency sweeps of 1 Hz at temperatures 0 to 80°C

### 6.2.5 Repeatability

As previously mentioned in *Chapter Five*, DMA on binder were carried out at two strain levels to ensure that measurements were always in the linear viscoelastic region. The results suggest no significant difference between different target strain levels which indicated that the measurements were within the linear viscoelastic region. Consequently to this, the tests were not repeated due to time limitations. Furthermore, the selection of gap setting and plate size, which was adopted for this research, complied with the recommendation for complex modulus range based upon three independent laboratories in the UK, as presented in Table 6.6 [11].

The accuracy of measurement of dynamic shear rheometer (DSR) is dependent on the gap setting and plate size as presented in Table 6.7 [11]. The test temperature is also

tightly controlled as the DSR equipment used in this study, i.e. Bohlin instrument, has capability to maintain water bath temperature to within 0.1<sup>0</sup>C of the set point. The effect of temperature to the complex modulus is given in Figure 6.15 [12]. The Author has a strong confidence that the results presented in this thesis are within acceptable level of accuracy as the specimens were carefully prepared and the testing arrangements and procedures followed the recommendations in Table 6.6 and 6.7.

Other research work involving 33 laboratories reported that DMA by dynamic shear rheometer (DSR) has a good reproducibility, i.e. variations of 15.1% and 0.4% for multilaboratory measurements of complex modulus and phase angle, respectively; whereas if the measurements were only carried out by single operator these variations can be smaller, i.e 4.9% and 0.3% for complex modulus and phase angle, respectively[13].

*Table 6.6 DSR Compliance to ensure linearity response of 50 pen bitumen [11].*

Plate size (mm)	Gap setting (mm)	Complex Modulus [Pa]		
		Laboratory A	Laboratory B	Laboratory C
8	2	10 <sup>4</sup> -10 <sup>8</sup>	10 <sup>3.8</sup> -10 <sup>8</sup>	10 <sup>4.6</sup> -10 <sup>7.7</sup>
25	1	10 <sup>3</sup> -10 <sup>5.5</sup>	10 <sup>2.8</sup> -10 <sup>5.6</sup>	-

*Table 6.7 Accuracy of measurement of DSR [11].*

Gap setting (mm)	Actual Stiffness (Pa)	25 mm plate		8 mm plate	
		Measured (Pa)	Accuracy (%)	Measured (Pa)	Accuracy (%)
2	10 <sup>9</sup>	8.35*10 <sup>6</sup>	0.84	4.10*10 <sup>8</sup>	40.98
2	10 <sup>8</sup>	7.77*10 <sup>6</sup>	7.77	8.74*10 <sup>7</sup>	87.41
2	10 <sup>7</sup>	4.57*10 <sup>6</sup>	45.71	9.86*10 <sup>6</sup>	98.58
2	10 <sup>6</sup>	8.94*10 <sup>5</sup>	89.39	9.99*10 <sup>5</sup>	99.86
2	10 <sup>5</sup>	9.88*10 <sup>4</sup>	98.83	10 <sup>5</sup>	99.99

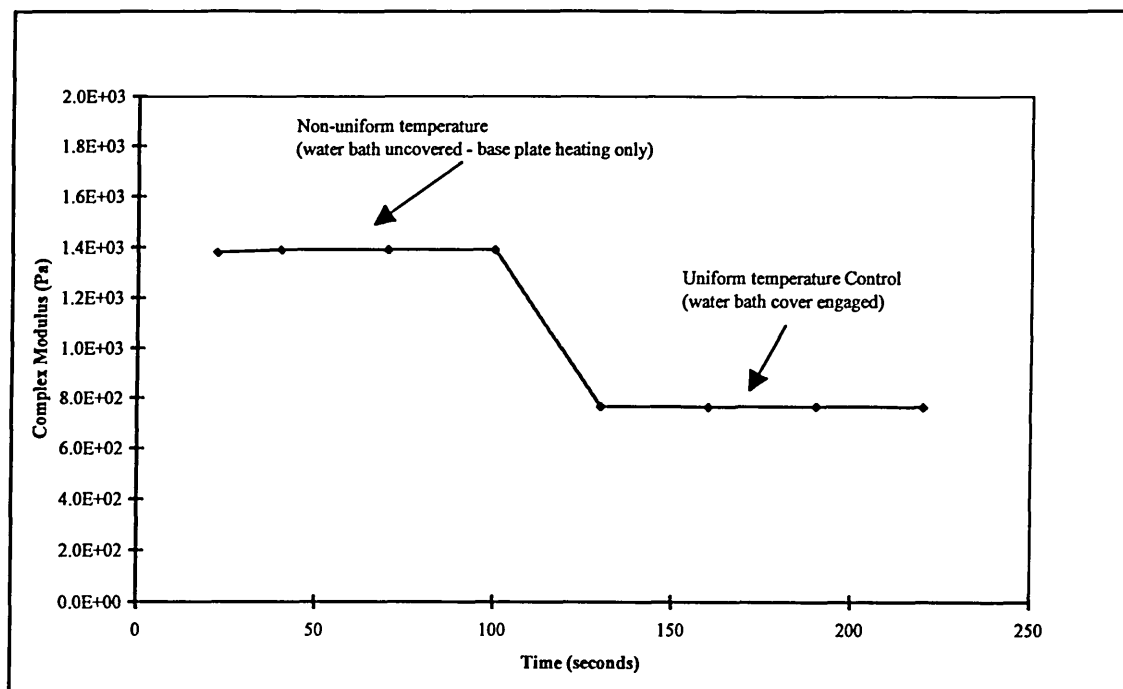


Figure 6.15 The effect of temperature control on the measured complex modulus in DSR [reproduce from Bohlin Rheology Workshop 1997].

### 6.3 Dynamic Mechanical Analyses on Properties of Bituminous Mixtures

Dynamic mechanical analyses (DMA) for HRA mixtures were carried out in the same manner as for the binder. However, the test procedure is different. The DMA tests for binders were carried out by dynamic shear test mode whereas the test for the mixtures was on the dynamic flexural test mode.

The interconversion factor to correlate between the two test modes are presented in Equation 6.6 where  $E^*(\omega)$  is the flexural or extensional complex modulus at frequency  $\omega$  and  $G^*(\omega)$  is the shear modulus at frequency  $\omega$ . The assumption that extensional and flexural moduli are equivalent is only a simplification for engineering use which is based on the condition that the extensional properties of the material are equivalent in tension and compression. Therefore, this assumption is valid as long as the strain levels resulting in the flexural test are maintained less than one percent [14]. It is understood that the behaviour of materials under small strain will predominantly be either fully

elastic or viscoelastic and, therefore the effect of plasticity is regarded to be insignificant.

The maximum permissible deformation in the flexural test carried out in this study is 50 micron and the average depth of the sample is 60 mm. Therefore, the resulting strain will be less than one percent. Hence, the assumption in Equation 6.6 can be adopted.

$$|E^*(\omega)| = 3 |G^*(\omega)|$$

Equation 6.6

The specimens used for this test were 30/14 type HRA wearing course and the volumetric properties of the mixture are presented in Table 6.8. The figures demonstrated in this table seem to be unrealistic. The target volumetric proportions aimed by the Author was initially between 4-6% for air voids, 21-24% for VMA, and 75-80% for VFB. However, this condition could not be achieved due to the limited capacity of the compactor. Therefore, these specimens (Table 6.6) were adopted for this exercise. The specimens were assumed to have similar volumetric proportions as their variability are still within the 95% confidence interval.

Table 6.8 Volumetric measurements for bending beam specimens.

No	Mixes Type	Max Density (Mg/m3)	Bulk Density (Mg/m3)	Air Voids	VMA	VFB
1	E	2.370	2.028	14.42%	28.14%	48.77%
2	EP	2.320	2.047	11.78%	27.49%	57.15%
3	ER	2.367	2.049	13.45%	27.41%	50.91%
4	ES	2.297	2.045	10.96%	27.54%	60.22%
Mean		2.339	2.042	12.65%	27.64%	54.26%
Standard deviation <sup>1</sup>		0.0361	0.0094	1.57%	0.33%	5.33%
95% Confidence Interval (CI) <sup>2</sup> (+/-)		0.0574	0.0150	2.50%	0.53%	8.48%

Note : <sup>(1)</sup>Standard deviation,  $s = \sqrt{\frac{\sum(x_i - \bar{x})^2}{n-1}}$

where:  $x_i$  is the observed data,  
 $\bar{x}$  is the mean values  
 $n$  is the sample size

<sup>(2)</sup>95% C.I. =  $t_c (s/\sqrt{n})$  where  $t_c = 3.18$  for  $n = 4$

### 6.3.1 High Temperature Properties

The findings on the DMA for HRA mixtures conform with the results for the binders, as shown in Figure 6.16 and Figure 6.17, that the addition of polymers always improves the low frequencies and/or high temperature properties by increasing the stiffness (complex modulus) and reducing the phase angle. The best properties at low frequency and/or high temperature regime are provided by EVA modification (mixture EP50) which shows the lowest phase angle and the highest mixture stiffness, then followed by SBS and SBR modification. Further evidence was demonstrated in Figure 6.18 and Figure 6.19 where frequency sweep tests were conducted at 45°C.

### 6.3.2 Medium Temperature Properties

Figures 6.19 and 6.20 demonstrated that EVA and SBR modified mixtures have the highest stiffness value and the lowest phase angles at 20°C. The high stiffness value of EVA modified HRA can help improving the resistance to permanent deformation at high service temperature [15] and also extending fatigue life of thick pavements at medium service temperatures (10-20°C). However, cracks may propagate more rapidly on stiff bituminous mixtures once crack initiation have taken place as Read [16] stated that *“the lower the stiffness of a bituminous mixture the better its resistance to crack propagation”*.

### 6.3.3 Low Temperature Properties

At high frequencies and/or low temperatures, the Black curves (Figure 6.15) of mixtures ES50 (SBS) and ER50 (SBR) merge with the curve of mixture E50 whereas the curve of mixture EP50 (EVA) was shifted to a higher stiffness values. This indicates that the addition of SBS and SBR into 50 pen bitumen in the mixtures does not affect the low temperature properties, in comparison to the unmodified mixture (50 pen). However, the addition of EVA into 50 pen bitumen has a detrimental effect on the mixture in that it has higher stiffness compared with the unmodified one which may lead to lower resistance to cracking.

The glassy modulus for these mixtures was calculated and the values lay within the range of 13 to 18 GPa (Figure 6.15). These values were obtained by correcting the Black curves of the mixtures so that instead of having the asymptotic tail at the high frequency-end of the curves, they were regressed linearly up to the point where the phase angle equal to  $0^\circ$ , i.e. at the fully elastic condition.

Closer observation from frequency sweep tests at  $-10^\circ\text{C}$  (Figure 6.22 and Figure 6.23) also indicates that some polymers, i.e. SBS and EVA, have detrimental effects at low temperature whereas the addition of SBR improve the low temperature response if compared with the unmodified 50 pen mixture. The improvement on the low temperature performance of SBR modified mixture (ER50) may be due to its low glass transition temperature (typically  $-75^\circ\text{C}$ ) which prevent it from crystallisation.

From these temperature regions, it can be concluded that the addition of polymer does not always improve the properties at both high and low temperatures. However, some polymers may improve the high temperature properties without sacrificing the low temperature properties of modified mixture, or *vice versa*.

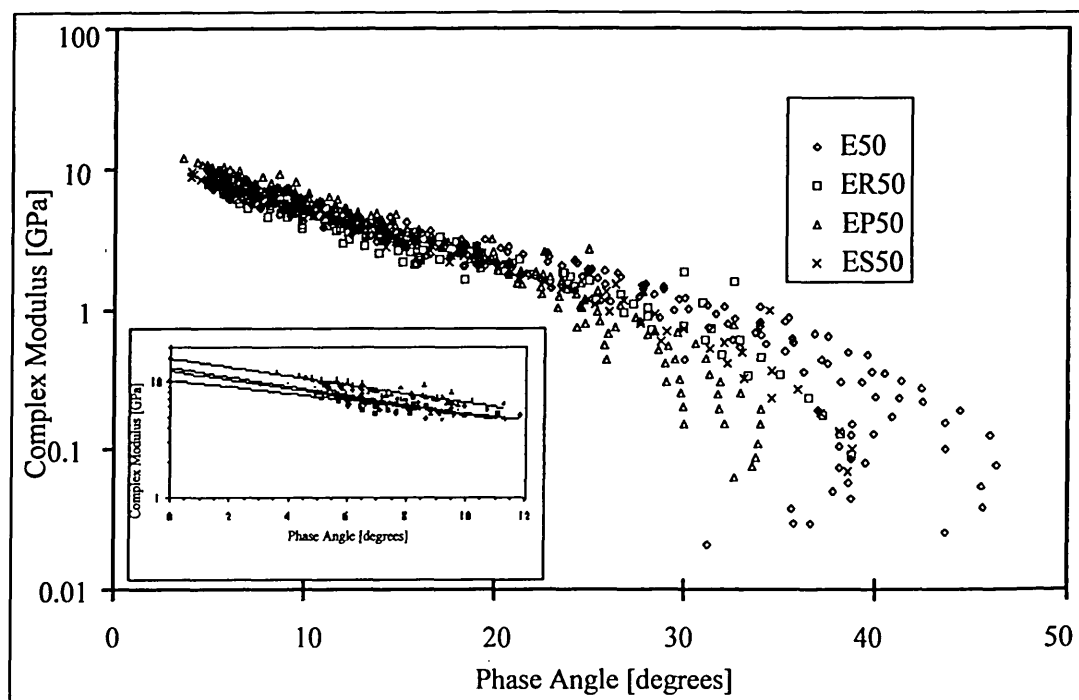


Figure 6.16 Black curves of bituminous mixtures obtained from the dynamic bending tests ( $T=-15$  to  $45^\circ\text{C}$  and frequency = 0.2 to 30 Hz)

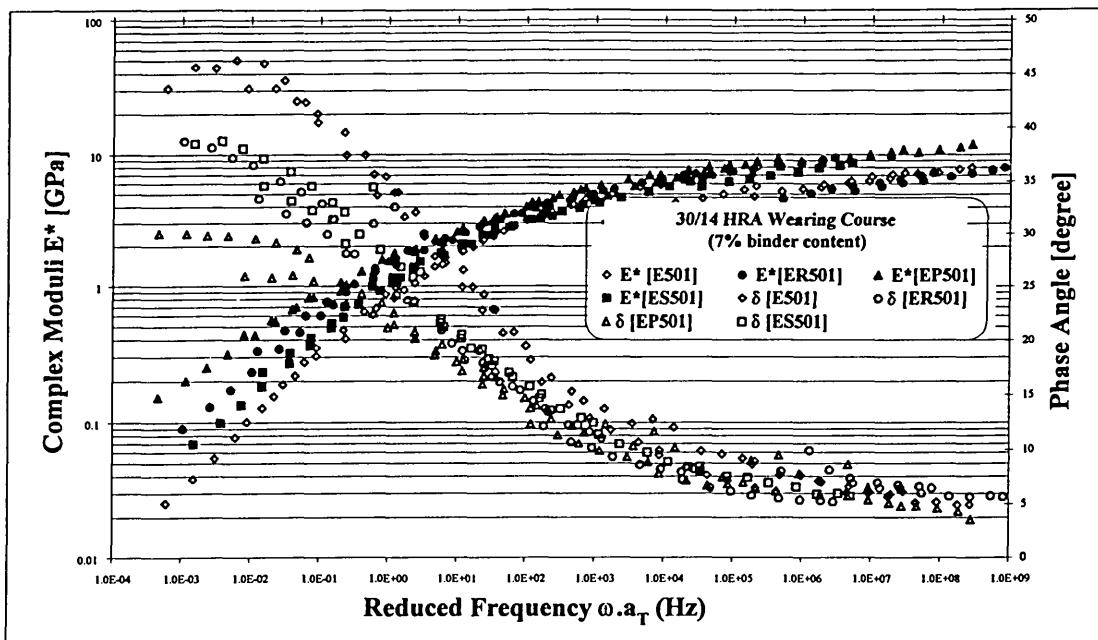


Figure 6.17 Master curves of bituminous mixtures ( $T = -15$  to  $45^\circ\text{C}$  and frequency = 0.2 to 30 Hz).

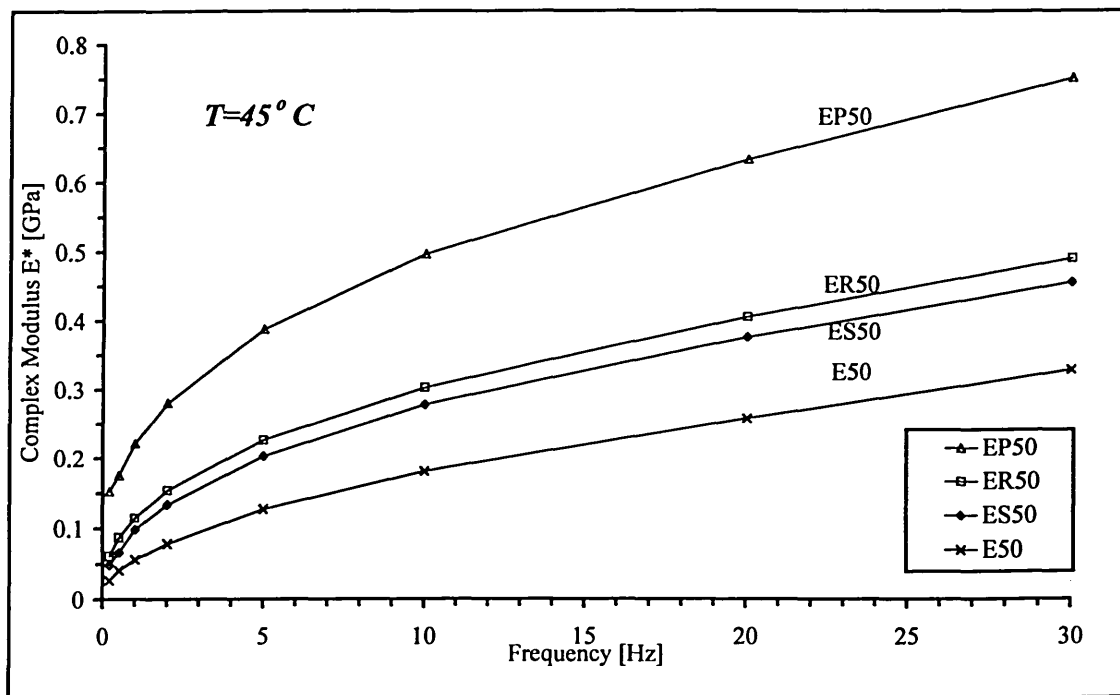


Figure 6.18 DMA of HRA mixtures at  $45^\circ\text{C}$  showing relationships between complex stiffness modulus and test frequency.

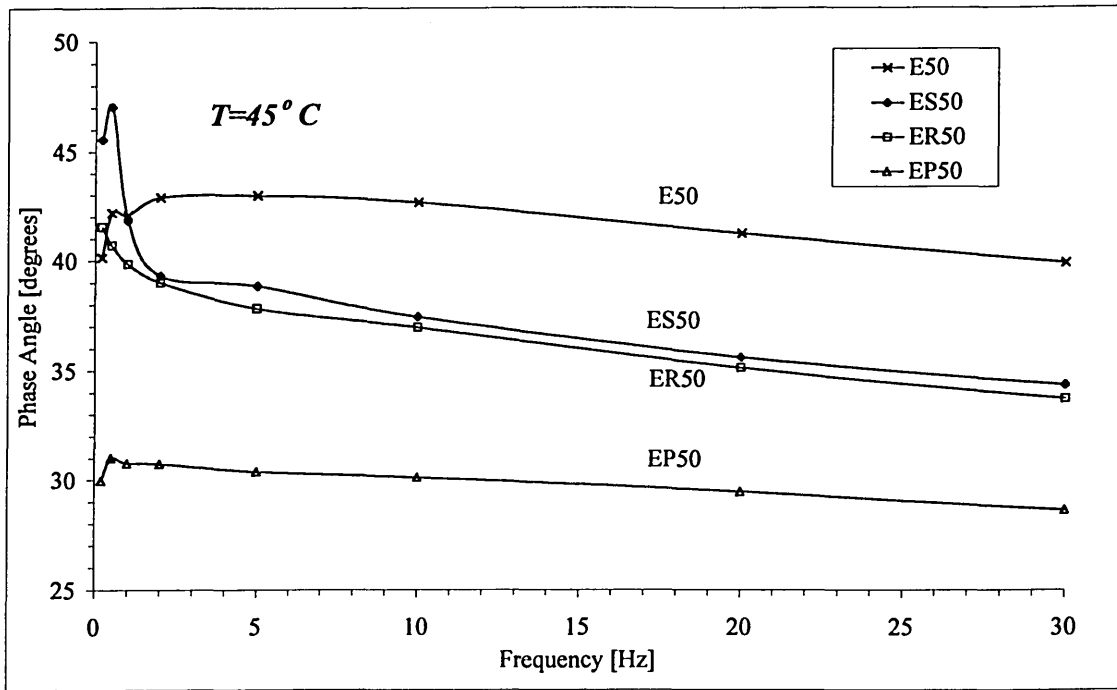


Figure 6.19 DMA of HRA mixtures at 45°C showing relationships between phase angle and test frequency.

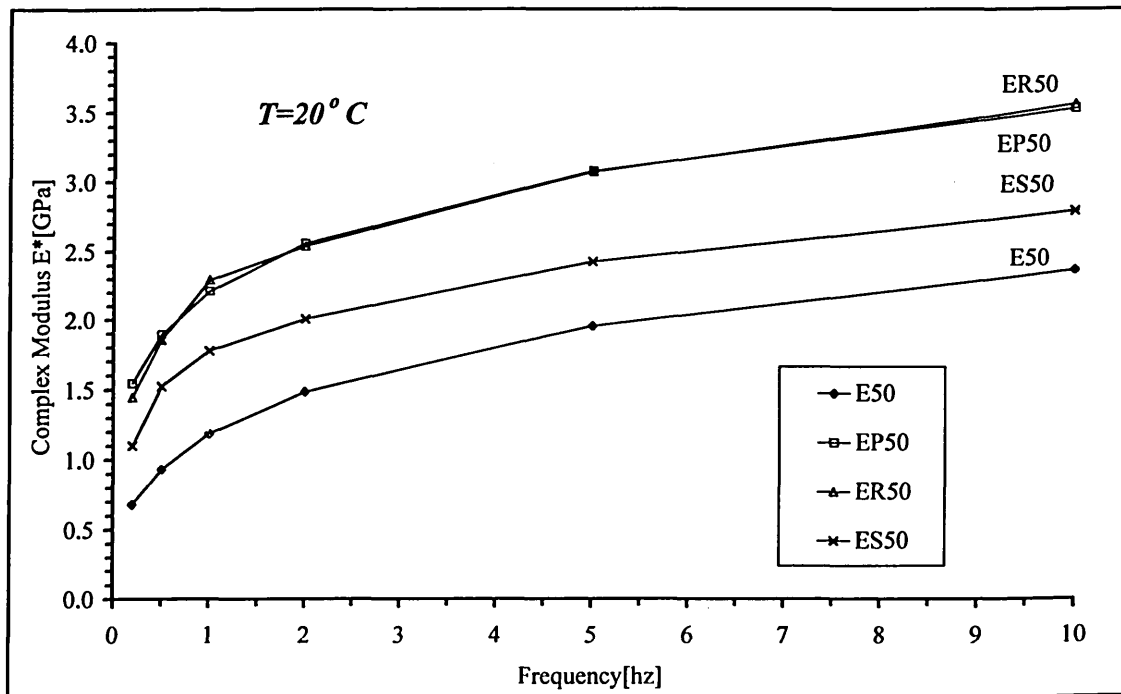


Figure 6.20 DMA of HRA mixtures at 20°C showing relationships between complex stiffness modulus and test frequency.

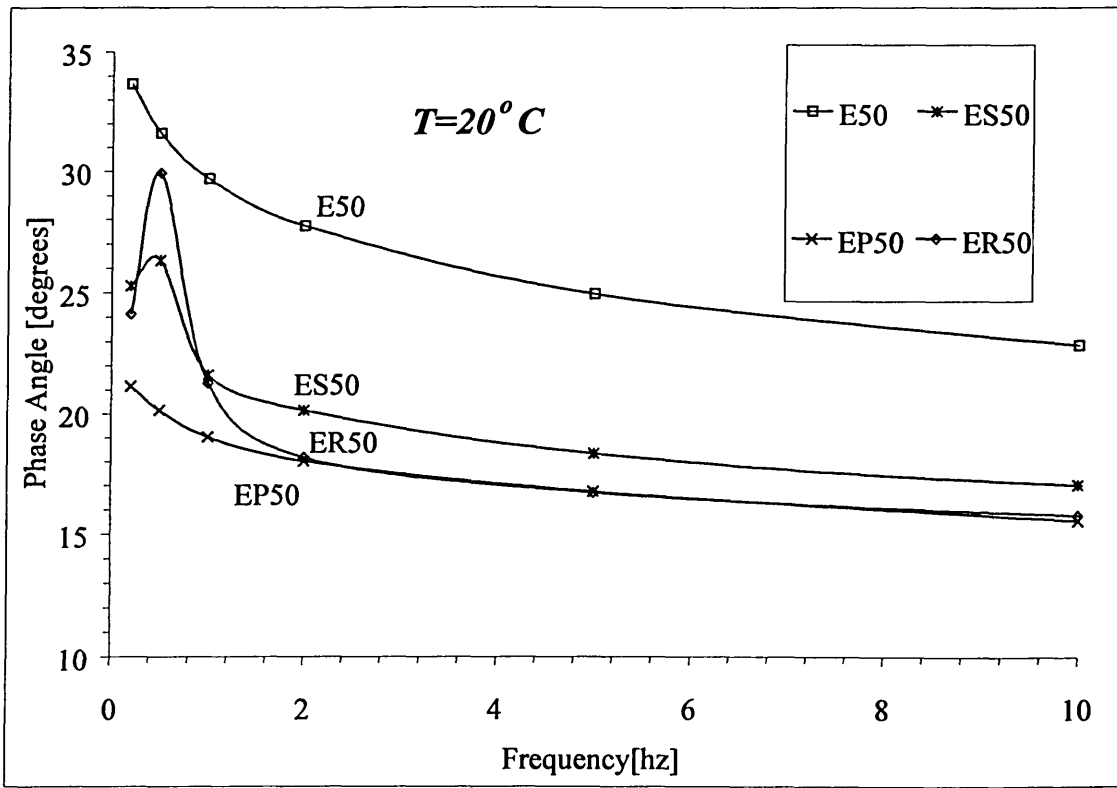


Figure 6.21 DMA of HRA mixtures at  $20^{\circ}C$  showing relationships between phase angle and test frequency.

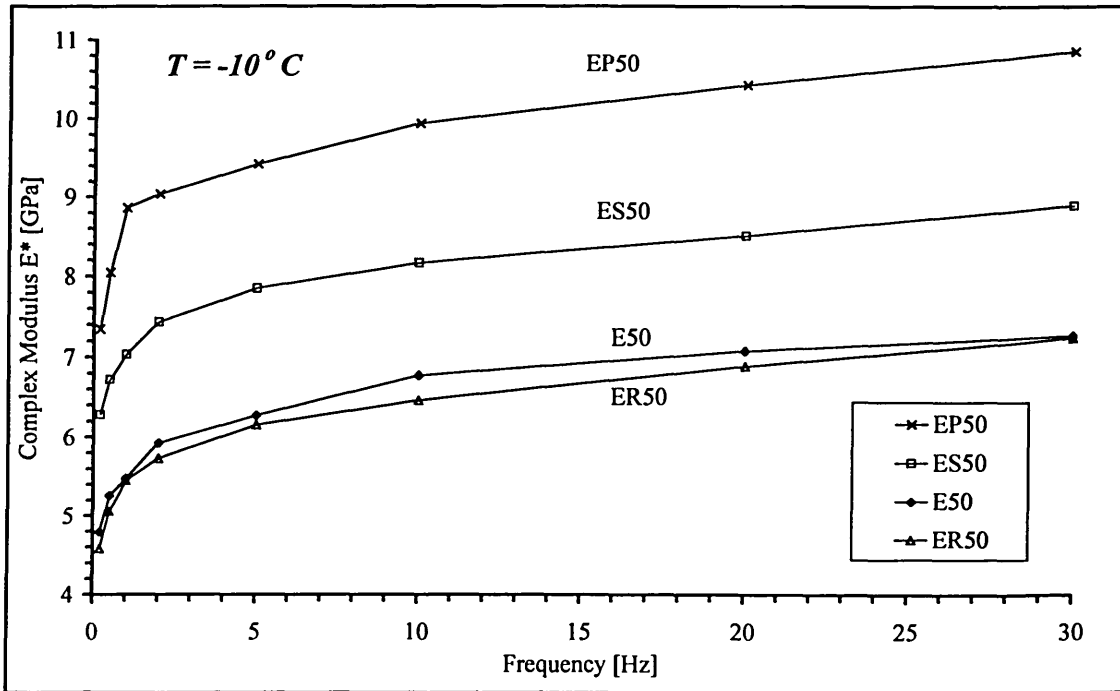


Figure 6.22 DMA of HRA mixtures at  $-10^{\circ}C$  showing relationships between complex stiffness modulus and test frequency.

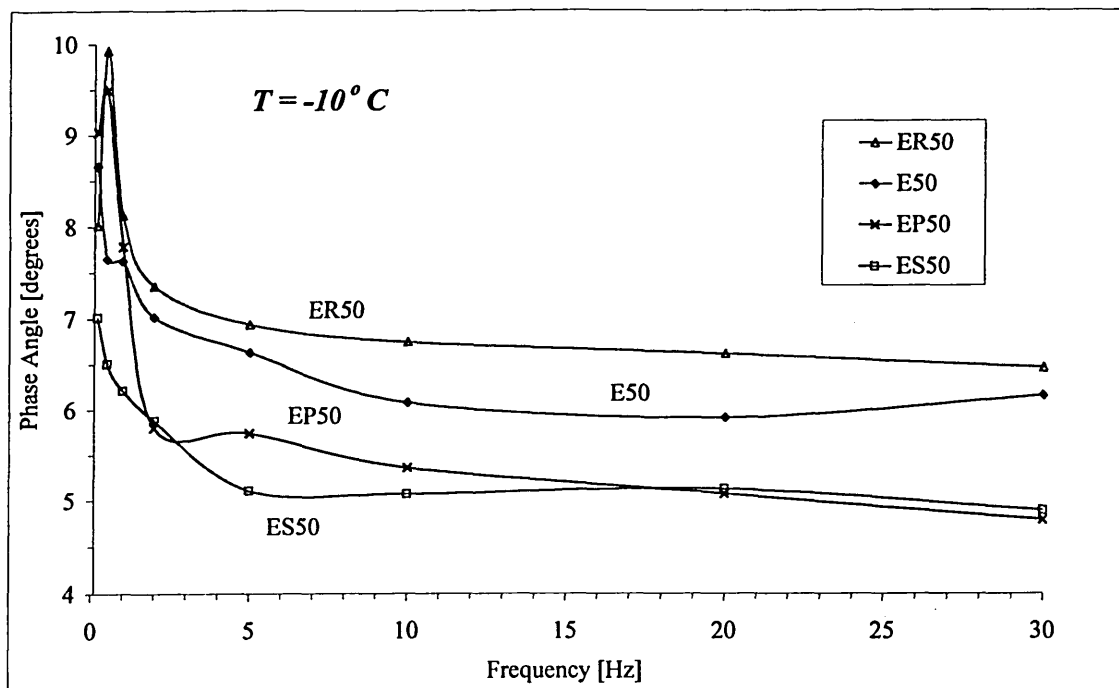


Figure 6.23 DMA of HRA mixtures at  $-10^{\circ}C$  showing relationships between phase angle and test frequency.

### 6.3.4 Repeatability

Repeatability of the measurements is presented by using the coefficient of variation from each set of data with four number of readings for each data point (each temperature and frequency). The summary results as presented in Table 6.9 shows that the variations are relatively low (details are presented in *Appendix E*). The wide range between the minimum and the maximum variations has been observed. However, this condition was primarily caused by some outliers.

Analyses on these variations indicates that at least 93.1% of the data lay within the 95% confidence interval, as demonstrated in Figures 6.24 to 6.27. Therefore, the mean variations can satisfactorily represent the overall variations of all test temperatures and frequencies.

Table 6.9 Repeatability of the dynamic mechanical testing for all test temperatures and frequencies.

	Variations of Complex Modulus (%)				Variations of Phase Angle (%)			
	E50	EP50	ER50	ES50	E50	EP50	ER50	ES50
Mixture type	E50	EP50	ER50	ES50	E50	EP50	ER50	ES50
Mean variation	1.91	2.68	1.91	2.10	3.15	7.44	3.24	3.72
Minimum variation	0.00	0.06	0.03	0.11	0.29	0.25	0.07	0.15
Maximum variation	13.98	25.32	18.05	12.63	20.61	54.54	35.27	21.01

Interlaboratory test programme, which was conducted by RILEM and incorporated 15 participant laboratories, reported that the variations on the value of complex modulus and phase angle were around 40% and 15%, respectively [17]. This study involved different geometries and shape of samples, which were tested by using different test equipments and mode of loadings at test temperatures of 0 and 20<sup>0</sup>C and frequencies of 1 and 10 Hz. Therefore, the variations obtained in this thesis were well below the finding by RILEM.

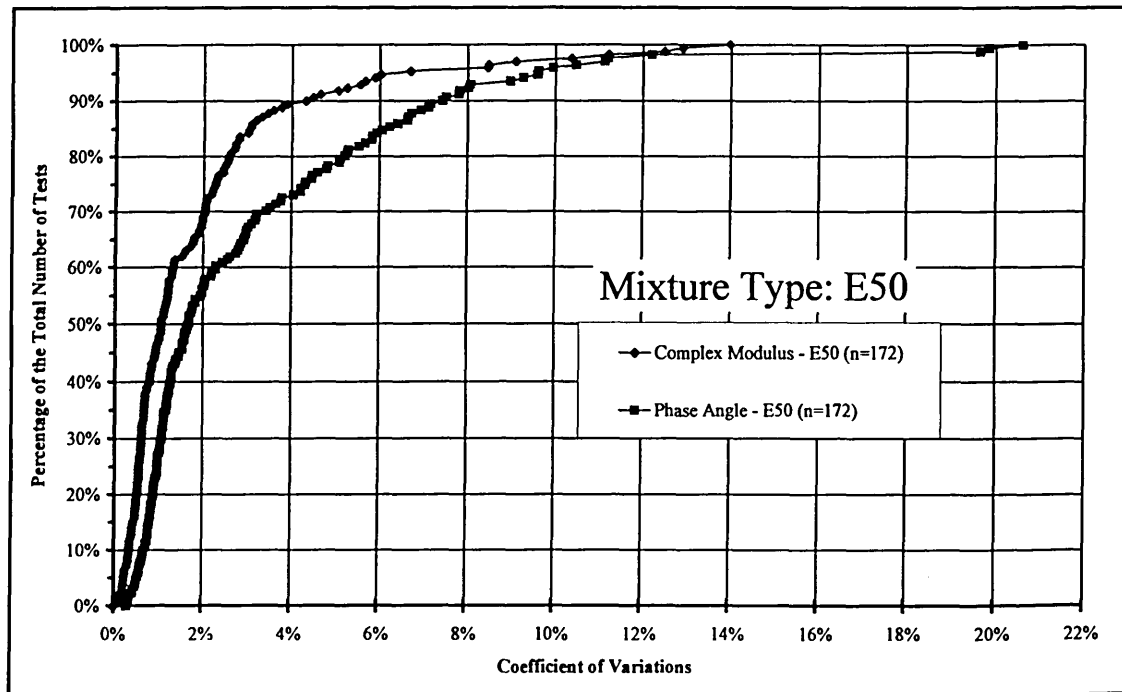


Figure 6.24 Test variability as indicated by the coefficient of variations for mixture E50.

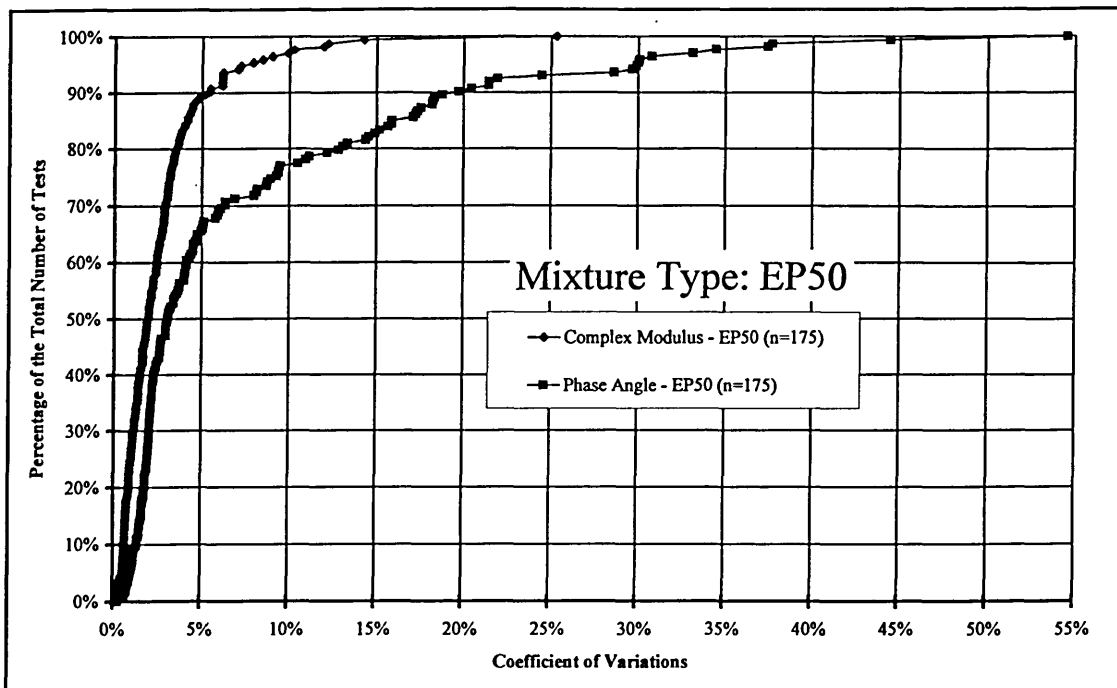


Figure 6.25 Test variability as indicated by the coefficient of variations for mixture EP50.

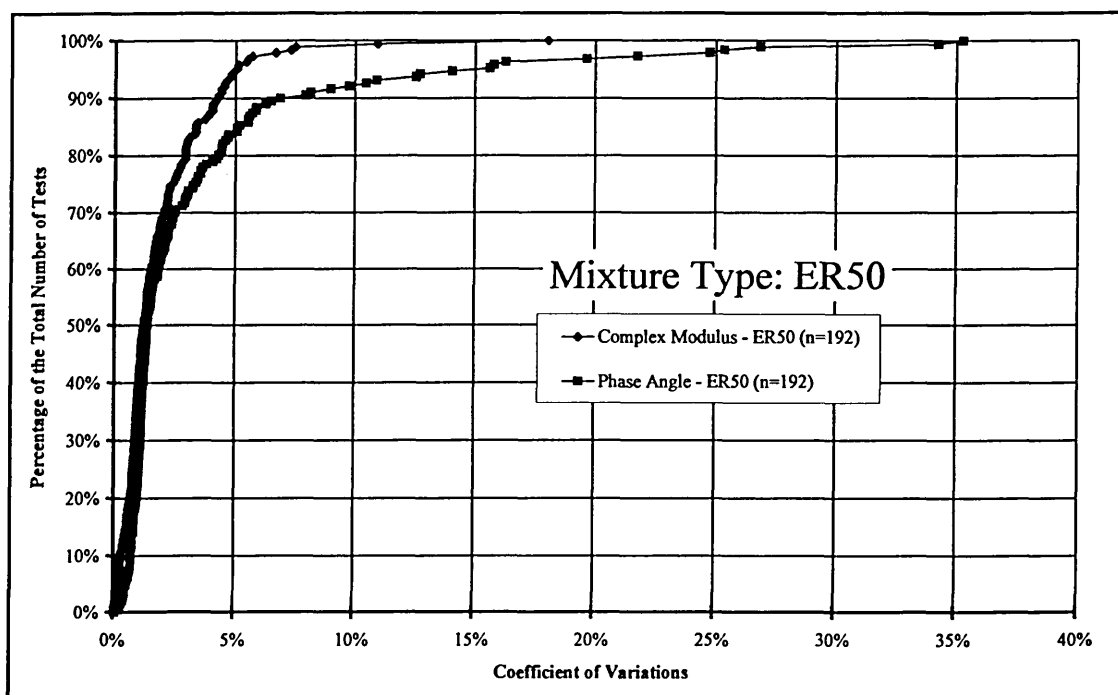


Figure 6.26 Test variability as indicated by the coefficient of variations for mixture ER50.

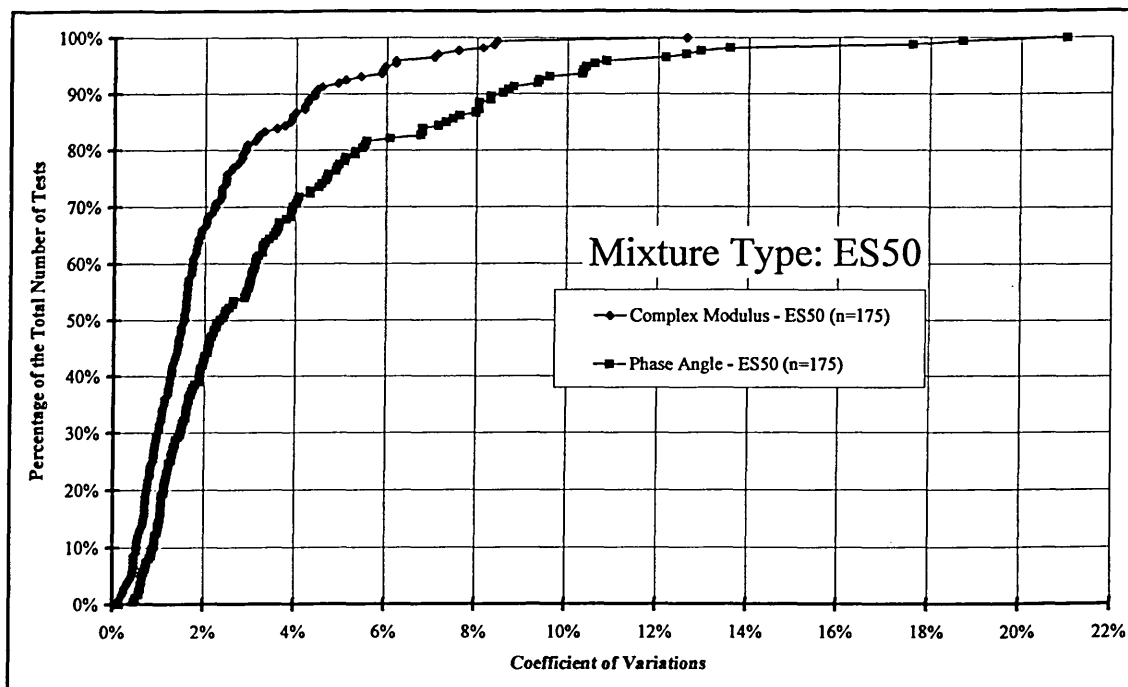


Figure 6.27 Test variability as indicated by the coefficient of variations for mixture ES50.

### 6.3.5 Effect of Binder-Aggregate Interactions to the Viscoelastic Properties of Bituminous Mixtures

The phase angle observed on the mixtures are less than (about a half of) those observed on the binder. The phase angles of the mixtures are between 30 to 40° but they are between 70 to 90° for the binders. This condition can be due to the difference in the deformation mechanism. The deformation of binders is purely due to viscous flow. However, the presence of aggregate in the mixture (about 93 percent of the total mass of mixture) contributes a significant amount of elasticity which discount the domination of viscous flow.

The contribution of binder-aggregate interaction to increase elasticity of HRA mixtures can be well observed by plotting phase angle of both binder and mixture versus frequency, as demonstrated in Figure 6.28 to Figure 6.31.

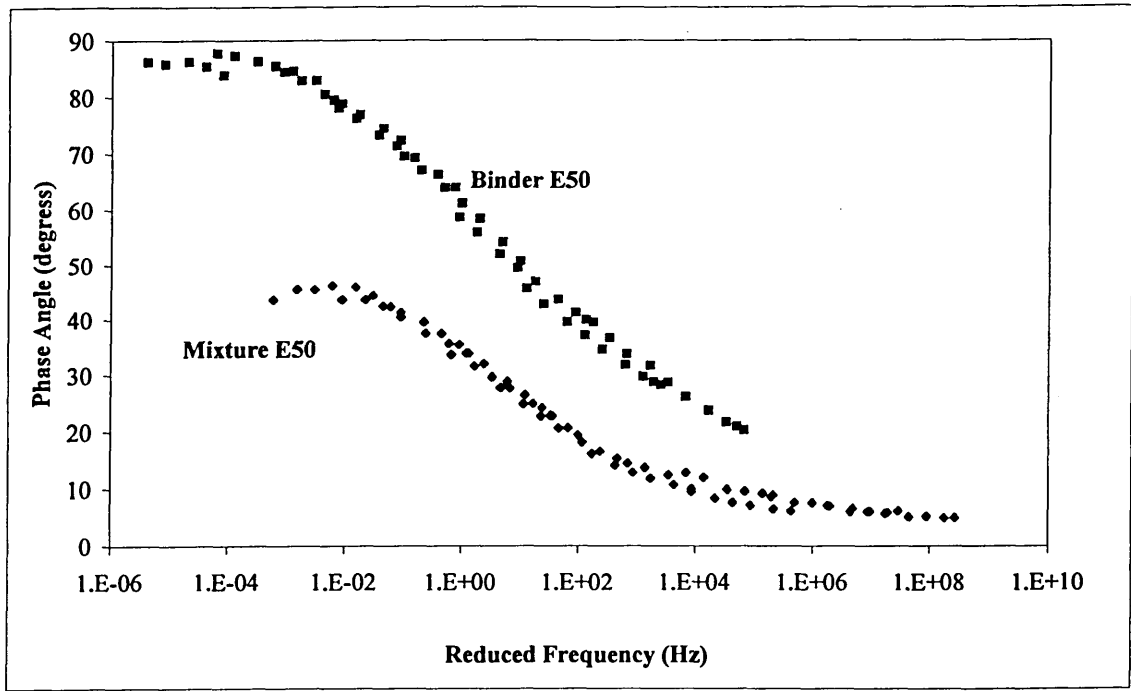


Figure 6.28 Master curves of the phase angle of mixture E50 (50 Pen) and binder E50 (50 Pen) versus the reduced frequency.

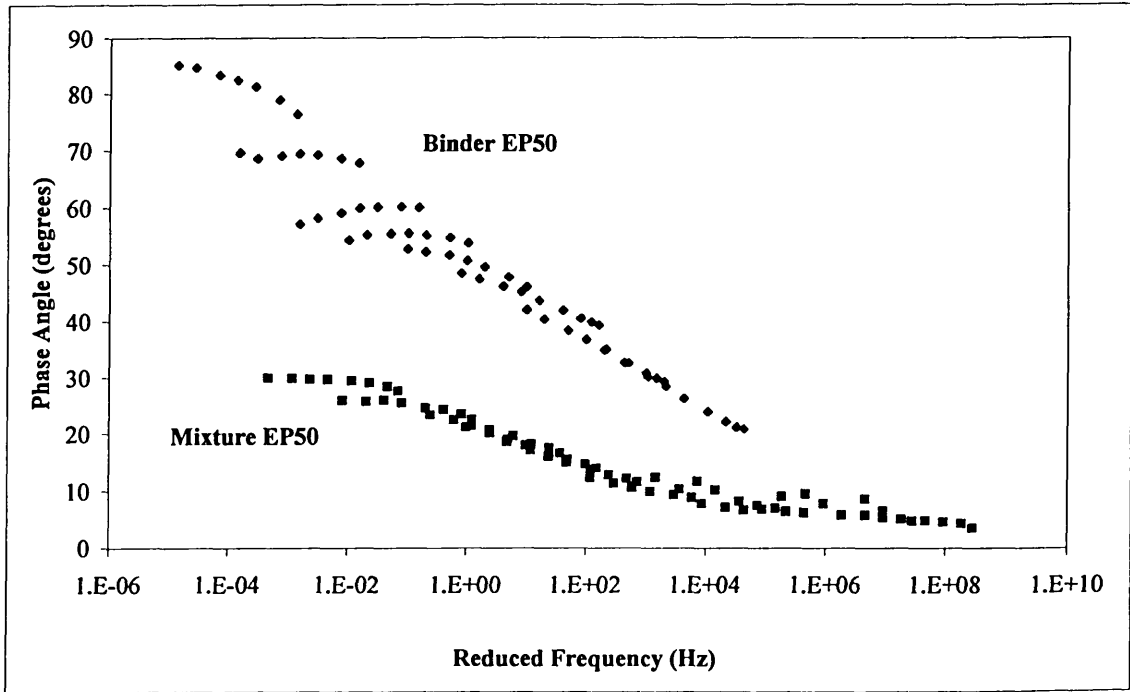


Figure 6.29 Master curves of the phase angle of mixture EP50 (EVA) and binder EP50 (EVA) versus the reduced frequency.

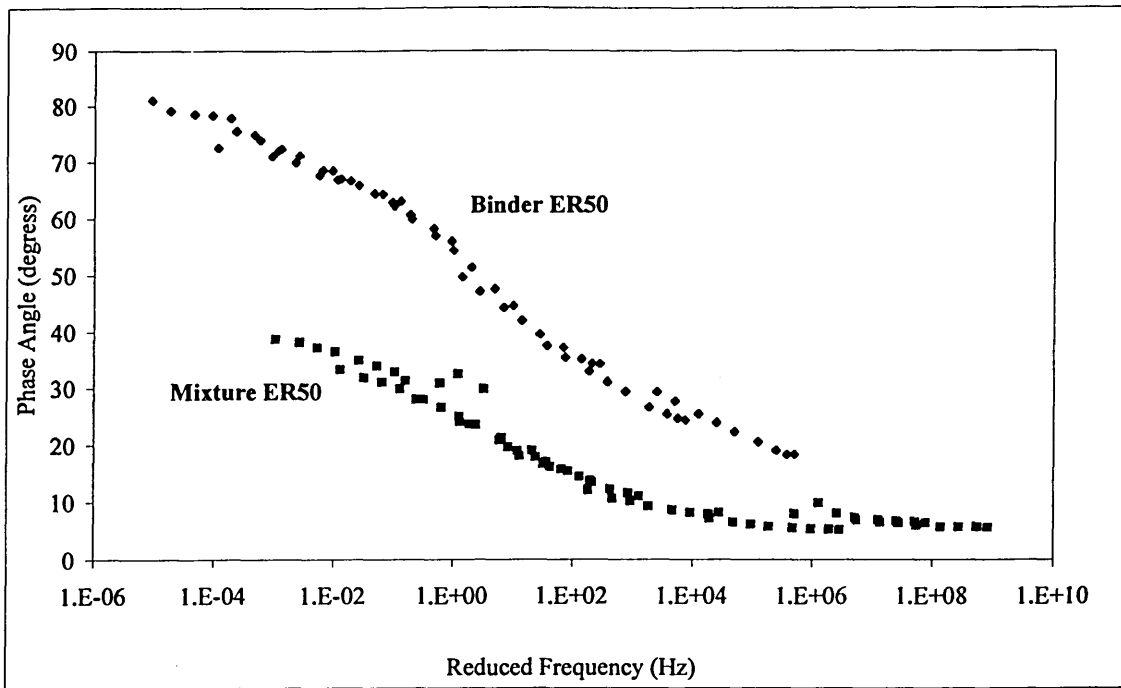


Figure 6.30 Master curves of the phase angle of mixture ER50 (SBR) and binder ER50 (SBR) versus the reduced frequency.

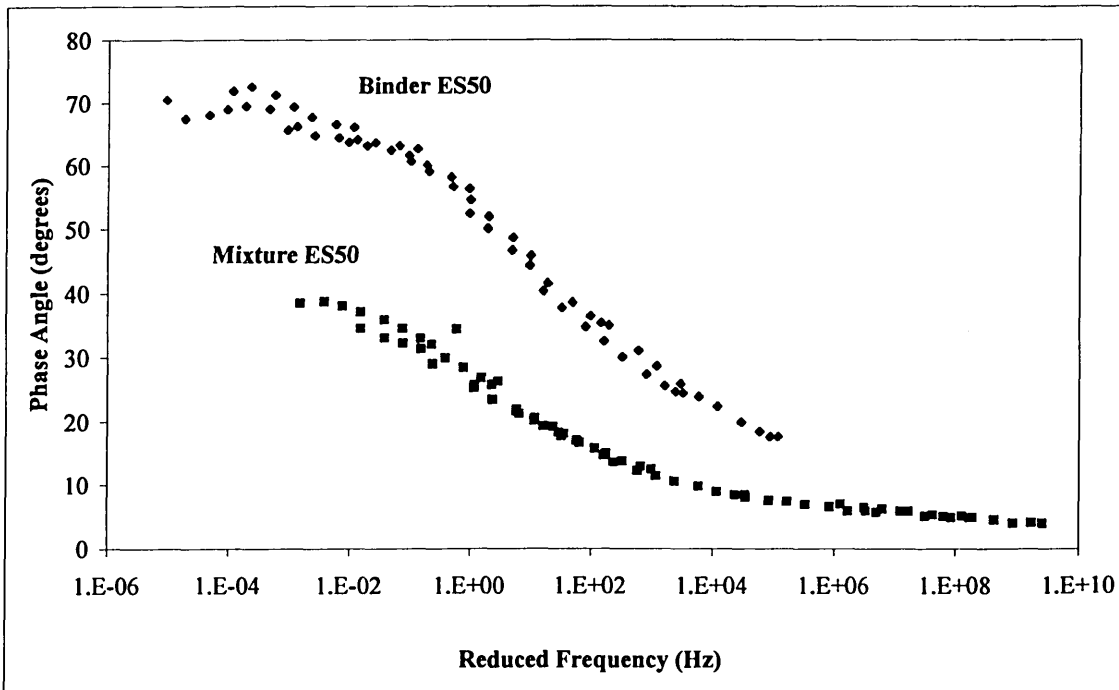


Figure 6.31 Master curves of the phase angle of mixture ES50 (SBS) and binder ES50 (SBS) versus the reduced frequency.

### 6.3.6 Correlation Between DMA of Binders and HRA Mixtures

Correlation between the complex (flexural) stiffness modulus of the binders and their mixture can be developed by converting the values complex shear modulus of the binder into complex flexural modulus using the Equation 6.6, as demonstrated in Figure 6.32. The relationship is only valid within the assumed condition that the test should be within the linear viscoelastic region but applies for any temperature or loading time. The curves of complex stiffness modulus of the binders versus the values of their corresponding mixtures are well fit by Equation 6.7.

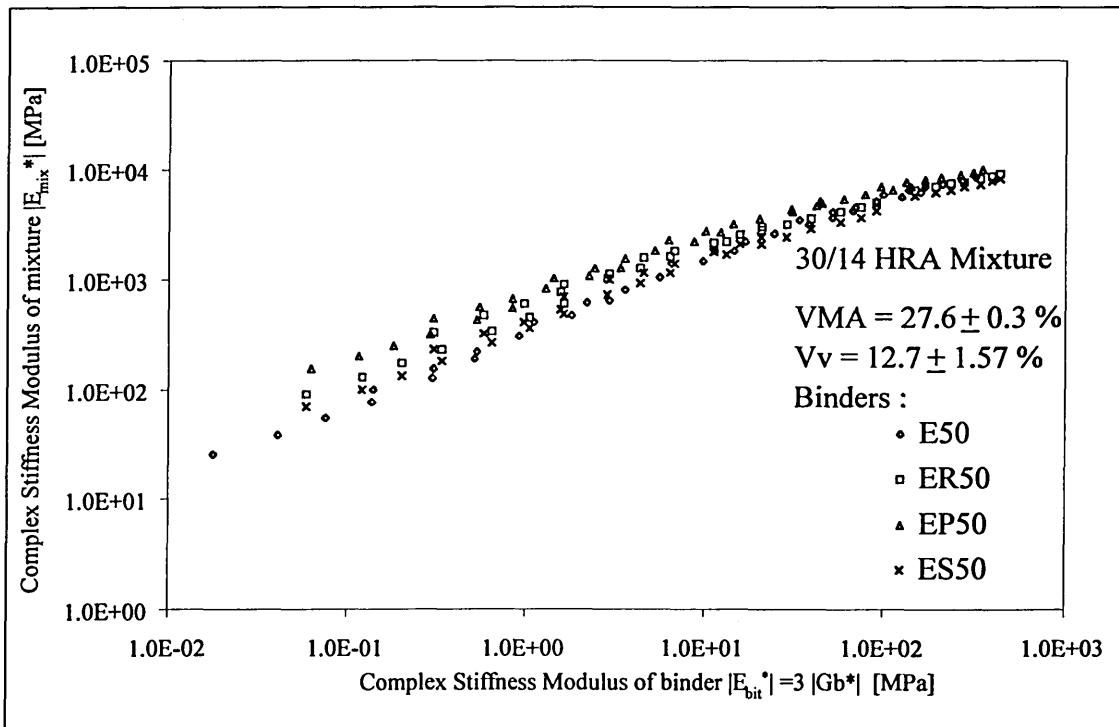


Figure 6.32 Correlations between the stiffness of binders and their mixtures.

$$|E_{mix}^*| = k (|E_{bit}^*|)^n$$

Equation 6.7

where  $|E_{mix}^*|$  and  $|E_{bit}^*|$  are the flexural complex (stiffness) modulus (in MPa) of the mixture and the binder, respectively. The stiffness modulus of the binder  $|E_{bit}^*|$  was calculated from the dynamic shear modulus of the binder ( $|G_b^*|$ ) multiplied by a factor of three. Rearrangement of Equation 6.7 into a double logarithms relationship is as follows:

$$\log |E_{mix}^*| = \log k + n \log |E_{bit}^*|$$

Equation 6.8

The constant  $k$  can be determined at  $|E_{bit}^*|$  equal to 1 MPa, as demonstrated in Table 6.10.

Table 6.10 Constants  $k$  and  $n$  obtained from the dynamic mechanical tests.

Mixture	$k$	$n$	$R^2$
E50 (50Pen)	323.61	0.6182	0.9927
EP50 (EVA)	710.64	0.4891	0.9856
ER50 (SBR)	532.89	0.5074	0.9769
ES50 (SBS)	401.75	0.5304	0.9852

The above results indicate that a strong correlation exists between the binders and their mixtures. The relationship can be used as a predictor to determine the mixture stiffness if the value of the binder stiffness is known, or *vice versa*, but so far, it should only be limited to the above volumetric composition.

The current understanding [18], based upon bituminous materials with unmodified bitumens, describes the relationship between stiffness modulus of binders  $|E_{bit}^*|$  and their mixtures  $|E_{mix}^*|$  as follows:

1. The minimum value of binder stiffness for elastic behaviour is 5 MPa.
2. For  $|E_{bit}^*| \geq 5$  MPa; the  $|E_{mix}^*|$  has the same value for different type of mixtures with the same binder stiffness, as the mixtures are approaching their glassy moduli. The mixture stiffness moduli only depend upon the binder stiffness and volumetric compositions.
3. For  $|E_{bit}^*| < 5$  MPa; a large number of parameters related to the properties of the aggregate become significant as the binder influence decreases. Furthermore, Hills [19] reported that the mixture stiffness at low binder stiffness depends upon: quality of aggregate grading, aggregate shape, state of material compaction, and confining condition; in addition to the mixture composition.

Nevertheless, this work incorporating the use of polymer modified binders on one type of mixture, i.e. HRA, suggests a new phenomenon. The condition at  $|E_{bit}^*| \geq 5 \text{ MPa}$  still applies, i.e. the  $|E_{mix}^*|$  has the same value for different mixture properties at the same binder stiffness, and are approaching their glassy moduli. However, the condition at which  $|E_{bit}^*| < 5 \text{ MPa}$  no longer applies, i.e. the  $|E_{mix}^*|$  varies with the type of binders. The latter condition may be caused by the effect of using polymer modified binders. The Author believes that the different mechanisms and structures (such as network structure, crosslinking behaviour and degree of crystallisations) exhibited by different polymer modified binders have an important role. It is generally understood that the characteristics and proportions of aggregates in bituminous mixtures hold the primary role in the resistance to permanent deformation at high service temperatures, especially when the binder stiffness is low [19]. This finding suggests that polymer modified binders also give significant contribution to the mixture performance, even at low binder stiffness. Some works on wheeltracking and dynamic creep tests confirmed the benefit of using polymer modified binders in improving the mixture resistance to permanent deformation at high temperatures (see *Chapter Seven*).

Figure 6.33 demonstrates the relationship between phase angle of the binders  $\delta_{bit}$  and their mixtures  $\delta_{mix}$ . A consistent trend on binder-aggregate interaction can be seen clearly at  $\delta_{bit}$  between  $25^\circ$  and  $45^\circ$ , i.e. that the phase angle of their mixtures are shifted by about  $30^\circ$  into the more elastic-behaviour (rigid/brittle) sides. However, there seems to be a minimum value for phase angle of the mixtures, i.e. the  $\delta_{mix}$  values became asymptotic towards  $5^\circ$  as the  $\delta_{bit}$  became less than  $20^\circ$ . This condition suggests that a fully-elastic behaviour ( $\delta=0^\circ$ ) may not be found in the mixtures and a small amount of plasticity would still be exist. This phenomenon may be explained as the presence of voids in the mixtures contributing to a certain degree of plasticity and enabling a small aggregate movement within the mixtures at very high frequencies or very low temperatures, where the binder starts behaving as elastic-solid (glassy) materials. This phenomenon was found on both unmodified and polymer modified mixtures.

In general, the results suggest that the relationships between  $\delta_{bit}$  and  $\delta_{mix}$  were not affected by the properties of the binders i.e. whether it is unmodified or polymer

modified binder. However, further investigations would have to be conducted to establish whether this relationship can be more generally applied to mixtures of other types and volumetric composition.

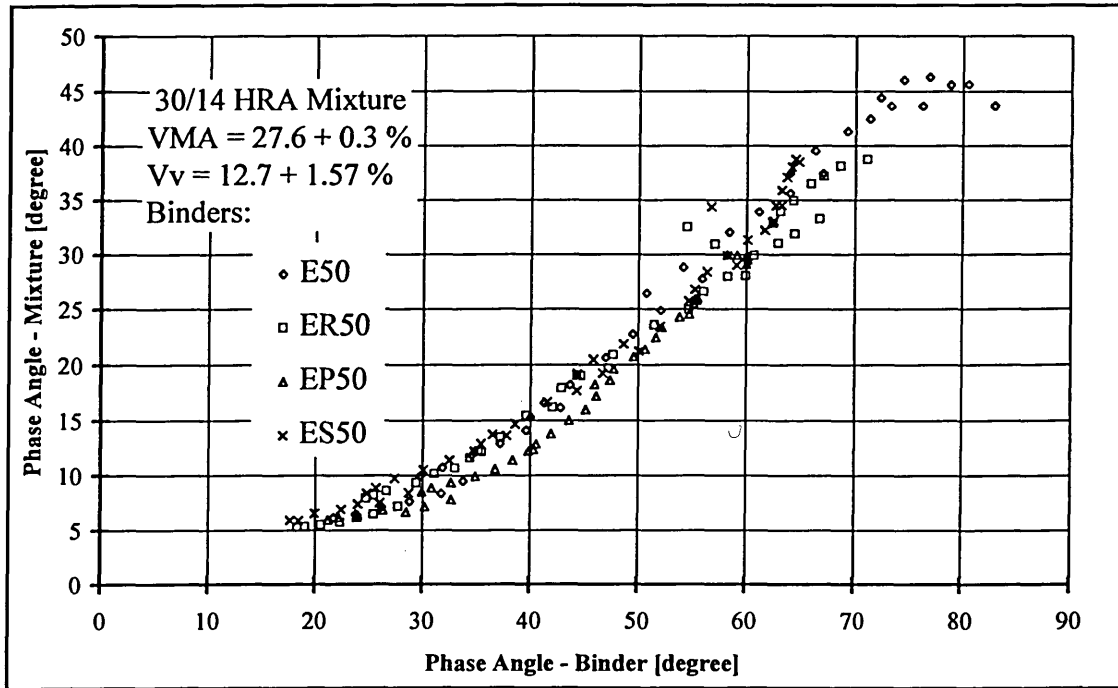


Figure 6.33 Correlations between the phase angles of binders and their mixtures

#### 6.4 Concluding Remarks

The use of empirical tests, such as penetration and softening point tests, may not always be a bad practice as long as the tests are carried out on materials within the limitation of the tests, e.g. the materials should have the same characteristics as the unmodified binder (thermoplastic material).

The storage stability test is essential for polymer modified binders, and the suitability of the analysis of the binder's stability based on empirical tests needs to be reassessed. The Author found that the use of Black curves from the dynamic mechanical data can be a promising solution due to their simplicity and reliability. Assessment on the storage stability of polymer modified binders should be carried out at different storage duration, e.g. 1, 3, and 7 days.

Dynamic mechanical analysis is a useful tool for the assessment of properties of bituminous materials. The method is applicable to both binders and mixtures and could be used for enabling a direct comparison between them. Furthermore, the assessment technique is flexible to fit in the purpose of the exercise whether it is for quality control or design. This technique also has a very good repeatability and reproducibility on the measurements.

The general understanding that the addition of polymers enhances the properties of the modified mixtures, and hence the performance, needs to be interpreted carefully as the improvement on a particular property may sometimes be followed by a detrimental effect on another. For example, the use of EVA to modify some 50 pen bitumens improves the high temperature properties, i.e. they demonstrated high stiffness which generally implies a good resistance to permanent deformation. However, they may have degraded the temperature properties by possessing high stiffness which generally implies higher susceptibility to fatigue cracking as opposed to their original (unmodified) 50 pen bitumens.

A new interpretation on the relationships between the mechanical properties of bituminous binders and their mixtures has been established incorporating the effect of using polymer modified binders. Therefore, the current understanding on these relationships may need to be revised. However, further works incorporating different type of bituminous mixtures should be conducted before any firm conclusion can be made for a wider range of mixtures.

## ***6.5 References***

- 1 Pfeiffer, J. Ph, and Van Doormaal, P.M., Journal Institute of Petroleum Technology, Vol. 22, 1936, p.414.
- 2 Siegmann, M.C., "Methods of Routine Investigation", The Properties of Asphaltic Bitumen, edited by J. Ph. Pfeiffer, Elsevier Publishing Company, Inc., 1950, pp. 155-188.

- 3 Anon, "Bituminous Materials in Road Construction", Department of Scientific and Industrial Research, Road Research Laboratory, Her Majesty's Stationery Office, 1962.
- 4 Morgan, P., and Mulder, A., "The Shell Bitumen Industrial Handbook", Shell Bitumen Ltd., 1995.
- 5 Anon, "DD ABE Method For The Determination Of The Storage Stability Of Modified Binder", British Standard Draft of Development (Second Draft) released on 17th November 1995, BSI London
- 6 Daly, W. H., Qui, Z. and Negulescu, I., "Preparation and Characterisation of Asphalt-Modified Polyethylene Blends", TRR1391, pp 56-64.
- 7 Brule, B. , Brion, Y. and Tanguy, A., "Paving Asphalt Polymer Blends: Relationships between, Structure and Properties", Proceedings of AAPT, Vol 55, 1986, pp 41-64.
- 8 Vonk, W.C., and Bull, A.L., "Phase Phenomena and Concentration Effects in Blends of Kraton D and Bitumen", VIIth International Roofing Congress, Munchen, Germany, 30 May-1 June 1989.
- 9 Cheung, C.Y., "Mechanical Behaviour of Bitumens and Bituminous Mixes", PhD Thesis, University of Cambridge, 1995.
- 10 Christensen, D.W., and Anderson, D.A., "Interpretation of Dynamic Mechanical Test Data for Paving Grade Asphalt Cements", Proceedings of AAPT, Vol. 61, 1992, pp. 67-116.
- 11 *Private Communication* with Mr L. Cowley of Croda Bitumen Ltd.
- 12 Lecture note from Bitumen Rheology Workshop by Dr B Hayton, 1997.
- 13 Anon, *Table 1. Precision Estimates for PG 64-22 Asphalt Binder Using AASHTO MP1. Performance Graded Binder Samples 155&156*, Strategic Highway Research Program, Washington D.C.
- 14 Anon, "Binder Characterization and Evaluation. Volume 3: Physical Characterization", SHRP-A-369, Strategic Highway Research Program, Washington D.C., 1994.

- 15 Anon, "Heavy Duty Pavements. The Arguments for Asphalt". European Asphalt Pavement Association. The Netherlands 1995.
- 16 Read, J.M., "Fatigue Cracking of Bituminous Paving Mixtures", PhD Thesis, University of Nottingham, 1996.
- 17 Francken, L., Hopman, P., Partl, M.N., and de la Roche, C, "RILEM Interlaboratory Tests on Bituminous Mixes in Repeated Loading. Teachings and Recommendations", Euroasphalt and Eurobitume Congress, 1996.
- 18 Brown, S.F., and Brunton, J.M., "An Introduction to the Analytical Design of Bituminous Pavements", 2<sup>nd</sup> Edition, University of Nottingham, 1980.
- 19 Hills, J.F., "Creep of Asphalt Mixes", Journal of Institute of Petroleum, London, England, Vol 59, No. 570, 1973, pp. 242-262.

# *Chapter Seven*

## **7. Analyses on the Resistance to Permanent Deformation of Bituminous Mixtures**

### ***7.1 Introduction***

Permanent deformation in bituminous layers is caused by the accumulation of plastic deformation in the mixture resulting from dynamic loading of traffic. This is a combined result of mixture compaction and displacement, and arises from binder permanent deformation and particle slip. Permanent deformation of a bituminous mixture is, therefore, affected by mixture composition. A wearing course hot rolled asphalt (HRA) type of mixture was selected for this study as it is a high quality material which is used especially on heavily trafficked roads, e.g. motorways, trunk roads and others in the UK.

HRA mixtures, in general, have lower resistance to permanent deformation when compared to more continuously graded mixtures, such as macadams, but have higher fatigue resistance and durability. Additionally, the popular 30% stone-content wearing course HRA has poor skid resistance if used as a surfacing material, and therefore, coated chippings are usually applied to the laid surface prior to compaction. However, wearing course mixtures containing 55% coarse aggregate do not require surface chippings to achieve adequate surface characteristic. Most of the discussions presented in this chapter will be focused on the properties and performance related to HRA mixtures, however, the performance of mixtures other than HRA may also be quoted wherever necessary.

Mixture variables, such as composition, compaction, and volumetric properties, contribute to the performance of HRA mixtures whereas different assessment techniques

may give different ranking of performance. Ranking performance of laboratory based testing which is close to the field performance can be obtained by conducting tests on a small scale wheel-tracking device. A simpler technique by using repeated load axial test (RLAT) on the NAT tester is presented here together with a novel analysis technique for extending the use of RLAT on the NAT tester by using a dissipated energy method.

## ***7.2 Effect of Mixture Variables on the Resistance to Permanent Deformation***

Four main constituents of HRA are presented in Figure 7.1, and the characteristics can be summarised as follows [1]:

1. Lower coarse aggregate content can be used in HRA means that the mixture is more expensive due to the very high binder content.
2. Fine aggregate forms the major proportion of the mortar and is probably the most important component affecting the performance of the material both during application and in service.
3. Filler fraction has two roles, firstly, it modifies the grading of the fine aggregate leading to a denser mixture with more contact points between aggregate particles and secondly, together with bitumen (binder) they lubricate and bind the fine aggregate to form the mortar. Therefore, the properties of the mortar will depend on the characteristics of the fine aggregate and on the amount and viscosity of the binder.
4. Bitumen (binder) acts as a lubricant during compaction and as a viscoelastic binder of high viscosity in service.

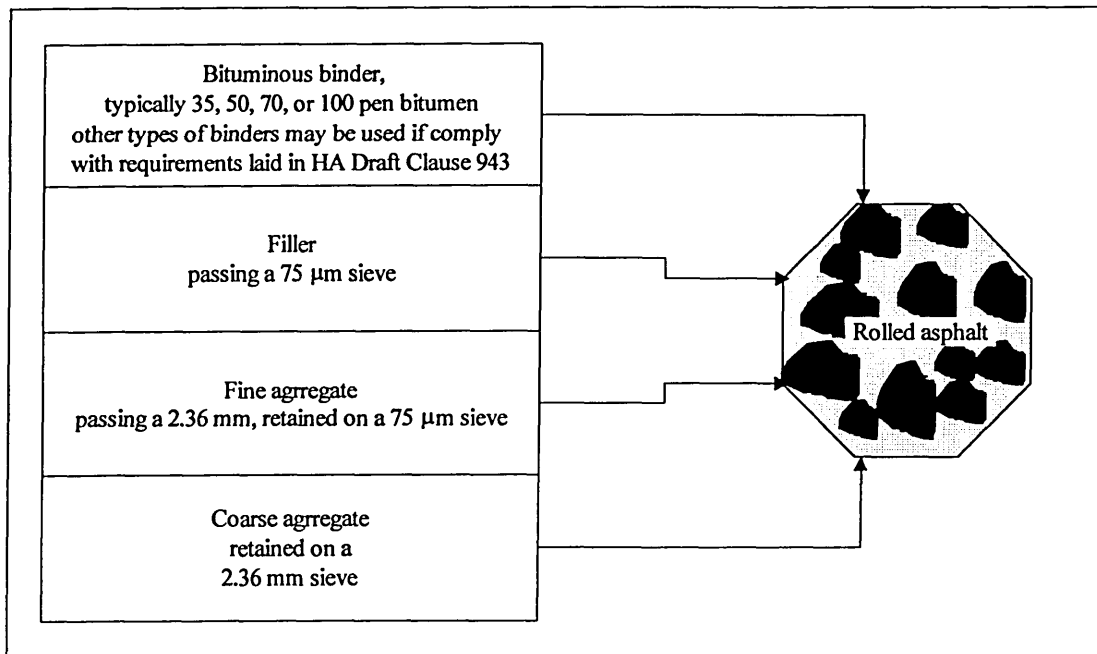


Figure 7.1 Constituents of a rolled asphalt

Traditionally, the requirements for the quality and proportions of aggregate and bitumen (binder) to be used in HRA have been specified by recipes [2], or alternatively, by Marshall design procedure [3]. However, the UK Highway Agency is developing a new design procedure towards performance related design for HRA wearing course mixtures [4].

### 7.2.1 Aggregate

Fine aggregates, mostly sand type, contribute the biggest proportion to the HRA mixtures, e.g. about 55% by mass of total mixture. Therefore, properties of selected sand used in a HRA mixture are usually considered to be the main variables which influence performance of the mixture both during application and in service. Szatkowski [5] reported a study on the effect of different sands to the wheel-tracking rate and the permissible binder content (Figure 7.2).

The quality of the sands governs the reorientation of aggregates and binder during the compaction process and leads to the final air voids level. Two sand fraction sizes, i.e. the 600 micron and the 212 micron fraction sizes, have been reported by Fordyce [6] to

be critical parameters to compaction performance of HRA. Sand and filler may form a good interlocked structure leading to low residual air voids when the ratio of 600 micron fraction size to the 212 micron fraction size is high. Problems in the mixing and laying process may occur if the mixtures have a high percentage of 212 micron fraction size of sand.

The effects of particle shapes and textures of sands (fine aggregates) are also an important factor in the performance of HRA mixtures. The more angular shape and rougher surface texture are preferred to form a good interlocking system between the aggregate particles.

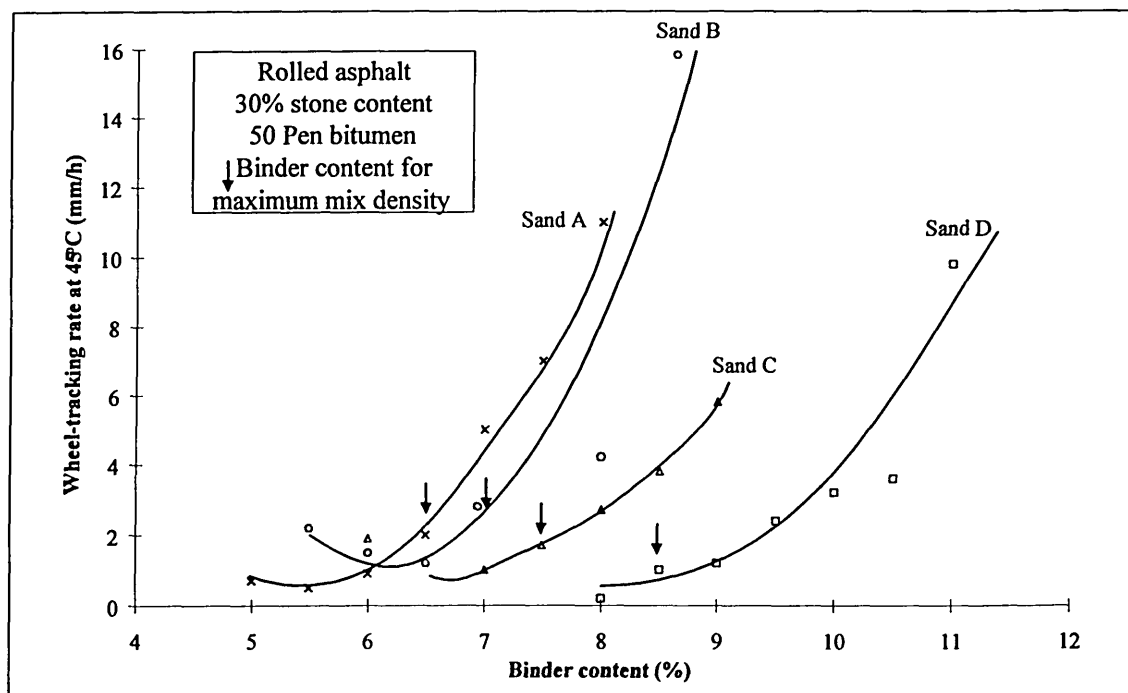


Figure 7.2 Effect of binder content on resistance to deformation. After Szatkowski [5].

### 7.2.2 Compaction

Different compaction techniques may produce specimens which have quite different engineering properties, even though they have the same volumetric composition. Gibb [7] reported three aspects which are significant in selecting a method of compaction:

1. The internal structure developed in the material and its influence on measured resistance to permanent deformation.

2. The limitations on the maximum aggregate size due to the limitations of the compaction mould.
3. The level of compacted density (volumetric properties) which is achieved.

Sousa, Deacon, and Monismith [8] reported an investigation into the effect of different methods of specimen preparation on permanent deformation characteristics of bituminous mixtures. The test for permanent deformation was carried out by compression and shear creep test. The mixtures were of one aggregate gradation but varied in binder source, aggregate type, binder content, and air void content. Three compaction procedures were selected, i.e. the Texas gyratory, kneading, and rolling wheel apparatus. Their results are summarised in Table 7.1.

*Table 7.1 Comparison between three compaction techniques. Summarised from Sousa, Deacon, and Monismith [8].*

Gyratory compactor	Kneading compactor	Rolling-wheel compactor
<ol style="list-style-type: none"> <li>1. Shape and size of specimens are limited</li> <li>2. Gyratory specimens are more sensitive to asphalt type than are kneading specimens</li> </ol>	<ol style="list-style-type: none"> <li>1. Adaptable for variety sizes and shapes of specimens</li> <li>2. Kneading specimens are more sensitive to aggregate type than are gyratory specimens</li> <li>3. Produce the stiffest mixtures</li> <li>4. Create more stable aggregate matrix than is commonly developed by conventional construction practise</li> </ol>	<ol style="list-style-type: none"> <li>1. Can produce specimens of necessarily sizes and shapes</li> <li>2. Specimens are cored from the mould and have good finish which are beneficial for volumetric measurement</li> <li>3. Comparisons with specimens extracted from in-service pavements are more valid</li> </ol>

Percentage refusal density (PRD) method was developed in the UK [9], incorporating the use of vibrating hammer to compact specimens down to the refusal density. In this procedure, samples, usually macadam type mixtures, with the same composition but having a wide range of density before conducting the test are compacted to the same refusal density and samples made with the same aggregate but vary in bitumen contents are compacted to the same voids in mineral aggregate (VMA). The test is insensitive to material variables other than compactive effort. A target level of compaction can be

specified in terms of percentage refusal density (PRD) at three levels: 100%, 96%, 93% termed 100 PRD, 96 PRD and 93 PRD respectively [10]. The level 2 (96 PRD) is a representative of good site compaction and level 3 (93 PRD) is regarded as the minimum acceptable based on UK practice. The use of the PRD compaction level is intended to ensure adequate properties, resistance to permanent deformation in particular, at very high density.

The Marshall compactor may be the simplest way for sample preparation. This method has been used in many parts of the world. This procedure incorporates the use of an impact hammer having a flat circular tamping face of  $3\frac{7}{8}$  inches (98.4 mm) diameter and a mass of 10 lb (4.5 kg) from a drop height of 18 inches (457 mm). It is of a common practice that different compactive efforts (number of hammer blows) may be adopted dependent upon the traffic category, as presented in Table 7.2 [11]. Despite its simplicity, however, it has been found that permanent deformation in Marshall designed pavements is a frequent occurrence due to low air void contents (less than 3%) as a result of in situ density being higher than the value which was used in the design [7]. For the reasons of simplicity and availability of the equipment, however, the Marshall compaction was adopted in this study.

*Table 7.2 The Asphalt Institute design criteria for roads [11]*

Marshall method mixture criteria	Traffic category		
	Light	Medium	Heavy
Number of traffic (equivalent standard axles)	less than $10^4$	between $10^4$ and $10^6$	higher than $10^6$
Compaction (number of blows each end of specimen)	35	50	75

### 7.2.3 Volumetric Properties

Volumetric proportions are important as they influence the mechanical performance of bituminous mixtures. The volumetric proportions of bituminous mixtures are usually represented by voids in mineral aggregate (VMA), air voids ( $V_v$ ), and voids filled with binder (VFB)<sup>a</sup>.

The procedure to determine these parameters is shown in Equations 7.1, 7.2, and 7.3, and the schematic representation of these variables can be found in *Chapter One* (Figure 1.1). Ranges of these parameters are generally specified as part of the mixture design process and as a preliminary step before mechanical testing. A summary on the use of volumetric composition for these purposes can be found in Gibb's thesis [7] which recommends a minimum air void content of 3% to ensure stability. Fordyce [6] reported that the mixture will be in danger of instability under loading due to pore pressure build-up or bleeding of the binder at high temperatures if the air void goes below 2% and there is a danger of loss of durability resulting from the voids being interconnected and having access to the layer surface if the void is greater than 6%.

$$VMA = 100 - \frac{G_{mb} P_s}{G_{sb}}$$

*Equation 7.1*

$$V_v = 100 \left( \frac{\rho_{mm} - \rho_{mb}}{\rho_{mm}} \right)$$

*Equation 7.2*

$$VFB = 100 \left( \frac{VMA - V_v}{VMA} \right)$$

*Equation 7.3*

where:

VMA : Voids in mineral aggregate (%).

$V_v$  : Air voids in compacted mixture (%).

VFB : Voids filled with binder (%).

---

<sup>a</sup> See *Glossary* for definitions.

- $G_{mb}$  : Bulk specific gravity<sup>b</sup> of compacted mixture.  
 $G_{sb}$  : Bulk specific gravity<sup>b</sup> of aggregate.  
 $\rho_{mb}$  : Bulk density of compacted mixture ( $\text{kg/m}^3$ ).  
 $\rho_{mm}$  : Maximum density of compacted mixture ( $\text{kg/m}^3$ ).

The procedure for conducting volumetric measurements in this study were in accordance with Draft for Development DD 228: 1996<sup>c</sup> [12] and the Asphalt Institute procedure [11]. Table 7.3 to Table 7.5 present the volumetric measurements of dynamic creep and wheel-tracking specimens with a notice that the densities are presented based on the recommendation of HA Draft Clause 943 [4], i.e. in units of  $\text{Mg/m}^3$  instead of  $\text{kg/m}^3$ .

There are two procedures carried out in this study:

1. To evaluate the changes in binder properties (by using polymer modifiers) by maintaining the volumetric properties of the mixtures.

The results presented in Tables 7.3 (A, B, C) indicate variations on the volumetric properties of different set of specimens for the dynamic creep test. Sets A and B demonstrate low variations within the 95% confidence interval and, therefore, they are regarded as having similar volumetric proportions. However, the variations in the VFB data of the set C are quite high. The minimum and maximum VFB are 79.88% and 85.29%, and the difference is 5.41% which is greater than the maximum allowable difference within 95% confidence interval i.e. 3.70%. High variations were also found on wheel-tracking specimens (Table 7.5). Therefore, ER (SBR50), and FS (SBS100) should not be regarded as having similar volumetric properties with the rest of the set and the same consideration is also applied for wheeltracking specimens. However, they may still be included during the discussion part of this thesis but, with a consent of their differences.

2. To observe the effect of change in volumetric properties upon the performance of the mixtures due to variations of compactive effort on Marshall size specimens.

---

<sup>b</sup> Often referred to as *Relative Density*

<sup>c</sup> This procedure is similar to the ASTM D2041-91: Standard Test Method for Theoretical Maximum Specific Gravity and Density of Bituminous Paving Mixtures

This procedure is particularly important to assess the sensitivity of the mixtures to variations of volumetric properties ( $V_v$  and VMA) due to changes in compactive effort when the mixture composition (binder and aggregate content) is constant. Table 7.4 shows the effect of compactive efforts upon the volumetric properties of HRA mixtures.

The binder content of these mixtures is constant at 7% by weight (an average of 16% by volume) of the total mixture. This condition complies with the Clause 943 [4] which requires that “*the binder content shall constitute not less than 15.5% by volume of the mixture at the target binder content*”<sup>d</sup>.

*Table 7.3 Volumetric measurements on Marshall size specimens for dynamic creep test. Names designated to the mixture types refer to the binder types as presented in Table 5.2 (Chapter Five).*

A. Specimens made with 50 Pen bitumens from different manufacturers

No	Mixture Type	Average Max Density (kg/m <sup>3</sup> )	Average Bulk Density (kg/m <sup>3</sup> )	Average Air Voids $V_v$	Average VMA	Average VFB
1	A	2.311	2.236	3.26%	20.78%	84.32%
2	B	2.366	2.254	4.73%	20.14%	76.52%
3	C	2.354	2.269	3.63%	19.61%	81.50%
4	D	2.358	2.247	4.70%	20.39%	76.93%
Standard Deviation		0.025	0.014	0.75%	0.49%	3.75%
95%Confident Interval		0.039	0.022	1.19%	0.78%	5.97%
Mean		2.347	2.252	4.08%	20.23%	79.82%

---

<sup>d</sup> Having said that, the stone content used in this study was not 35% as specified by the Clause 943, but 30% stone content was adopted instead.

B. Specimens made with EVA modified 50 Pen binders from different manufacturers

No	Mixture Type	Average Max Density (kg/m <sup>3</sup> )	Average Bulk Density (kg/m <sup>3</sup> )	Average Air Voids Vv	Average VMA	Average VFB
1	AP	2.346	2.258	3.76%	20.00%	81.21%
2	BP	2.355	2.248	4.54%	20.36%	77.68%
3	CP	2.328	2.257	3.06%	20.04%	84.73%
4	DP	2.335	2.254	3.47%	20.14%	82.78%
Standard Deviation		0.012	0.005	0.63%	0.16%	2.98%
95%Confident Interval		0.019	0.007	1.00%	0.25%	4.74%
Mean		2.341	2.254	3.71%	20.14%	81.60%

C. Specimens made with different polymer modified binders.

No	Mixture Type	Average Max Density (kg/m <sup>3</sup> )	Average Bulk Density (kg/m <sup>3</sup> )	Average Air Voids Vv	Average VMA	Average VFB
1	E (50Pen)	2.329	2.255	3.18%	20.11%	84.20%
2	EP (EVA50)	2.356	2.271	3.61%	19.54%	81.54%
3	ER (SBR50)	2.341	2.244	4.12%	20.50%	79.88%
4	ES (SBS50)	2.347	2.259	3.75%	19.97%	81.21%
5	F (100 Pen)	2.323	2.246	3.31%	20.43%	83.77%
6	FR (SBR100)	2.338	2.254	3.59%	20.14%	82.16%
7	FS (SBS100)	2.332	2.264	2.91%	19.79%	85.29%
Standard Deviation		0.011	0.010	0.40%	0.34%	1.91%
95%Confident Interval		0.011	0.009	0.39%	0.33%	1.85%
Mean		2.338	2.256	3.50%	20.07%	82.58%

*Table 7.4 Volumetric measurements of specimens with different Marshall compaction efforts. Names designated to the mixture types refer to the binder types as presented in Table 5.2 (Chapter Five).*

Mixture Type	Compaction Effort (no of blows)	Max Density (Mg/m <sup>3</sup> )	Bulk Density (Mg/m <sup>3</sup> )	Air Voids (V <sub>v</sub> )	VMA	VFB
E10	10	2.329	2.123	8.85%	24.79%	64.30%
E20	20	2.329	2.188	6.05%	22.48%	73.09%
E30	30	2.329	2.227	4.39%	21.11%	79.21%
E40	40	2.329	2.246	3.54%	20.41%	82.64%
E50	50	2.329	2.255	3.18%	20.11%	84.20%
E75	75	2.329	2.273	2.42%	19.48%	87.60%
ER10	10	2.341	2.097	10.42%	25.71%	59.46%
ER20	20	2.341	2.176	7.05%	22.91%	69.23%
ER30	30	2.341	2.206	5.75%	21.83%	73.67%
ER40	40	2.341	2.233	4.63%	20.90%	77.84%
ER50	50	2.341	2.244	4.14%	20.50%	79.79%
ER75	75	2.341	2.271	2.99%	19.54%	84.70%
EP10	10	2.356	2.136	9.33%	24.32%	61.62%
EP20	20	2.356	2.201	6.60%	22.04%	70.06%
EP30	30	2.356	2.242	4.86%	20.58%	76.40%
EP40	40	2.356	2.258	4.17%	20.01%	79.18%
EP50	50	2.356	2.271	3.61%	19.54%	81.54%
EP75	75	2.356	2.280	3.25%	19.24%	83.13%
ES10	10	2.347	2.144	8.67%	24.05%	63.97%
ES20	20	2.347	2.196	6.43%	22.20%	71.02%
ES30	30	2.347	2.239	4.59%	20.67%	77.77%
ES40	40	2.347	2.262	3.63%	19.86%	81.74%
ES50	50	2.347	2.259	3.75%	19.97%	81.21%
ES75	75	2.347	2.272	3.20%	19.51%	83.61%

*Table 7.5 Volumetric measurements of wheel-tracking specimens. Names designated to the mixture types refer to the binder types as presented in Table 5.2 (Chapter Five).*

No	Mixture Type	Average Max Density (kg/m <sup>3</sup> )	Average Bulk Density (kg/m <sup>3</sup> )	Average Air Voids Vv	Average VMA	Average VFB
1	E (50 Pen)	2.373	2.206	7.04%	21.86%	67.79%
2	EP (EVA50)	2.357	2.211	6.18%	21.67%	71.47%
3	ER (SBR50)	2.371	2.180	8.03%	22.75%	64.72%
4	ES (SBS50)	2.382	2.195	7.84%	22.22%	64.72%
5	F (100 Pen)	2.372	2.197	7.38%	22.17%	66.73%
6	FR (SBR100)	2.357	2.214	6.10%	21.58%	71.73%
7	FS (SBS100)	2.360	2.213	6.21%	21.59%	71.24%
Mean		2.367	2.202	6.97%	21.98%	68.34%
95%Confident Interval		0.010	0.012	0.82%	0.43%	3.13%
Standard Deviation		0.009	0.012	0.79%	0.42%	3.03%

#### 7.2.4 Binder

Many authors [5, 13] have reported close correlation between permanent deformation of bituminous mixture and properties of the bituminous binder, in the case of unmodified bitumens. The ring and ball softening point of bitumen has been widely adopted as an empirical parameter to represent viscosity and been used to predict resistance to permanent deformation of bituminous mixtures [5] while others use a relationship based on viscosity at 60°C of aged bitumen [15]. However, the lack of relationship between these conventional properties on polymer modified binders and their resistance to permanent deformation of bituminous mixtures has also been reported [14,15].

Phillips and Robertus [16] reported that the binder contribution to the permanent deformation arises solely from a dissipative process and described by a viscosity whereas the corresponding particle (aggregate) contribution arises through friction and slip which is described by a friction coefficient. As the temperature condition greatly affects the viscosity of bituminous binders, selection of a representative viscosity is important. Pavement design is commonly based on the assumption that wheel loading occurs in the linear viscoelastic regime and the viscosity in the linear viscoelastic regime is the so-called zero-shear-viscosity,  $\eta_0$ . Researchers in Europe [15, 16] have been proposing the zero shear-rate viscosity concept for predicting the binders' contribution

to the mixture performance whereas the SHRP work represents viscosity in a different way by extending the use of the viscoelastic approach by using dynamic mechanical analysis, e.g. in term of complex modulus and phase angle, and establishing relationships between these properties and the performance of their mixtures [14].

The binder's contribution to permanent deformation of bituminous mixtures can be illustrated as in Figure 7.3. The deformation of the binder and mixture during wheel loading is related to the viscoelastic (creep ) compliance,  $J(t)$ , which is inversely proportional to the stiffness modulus,  $S(t)$ . However, “*this is not the final quantity of interest for rutting and neither is it the period directly following loading when delayed elastic deformation is occurring gradually*” [16]. Therefore, the permanent deformation which remains should be regarded as that after both processes (loading and delayed elastic recovery) are completed.

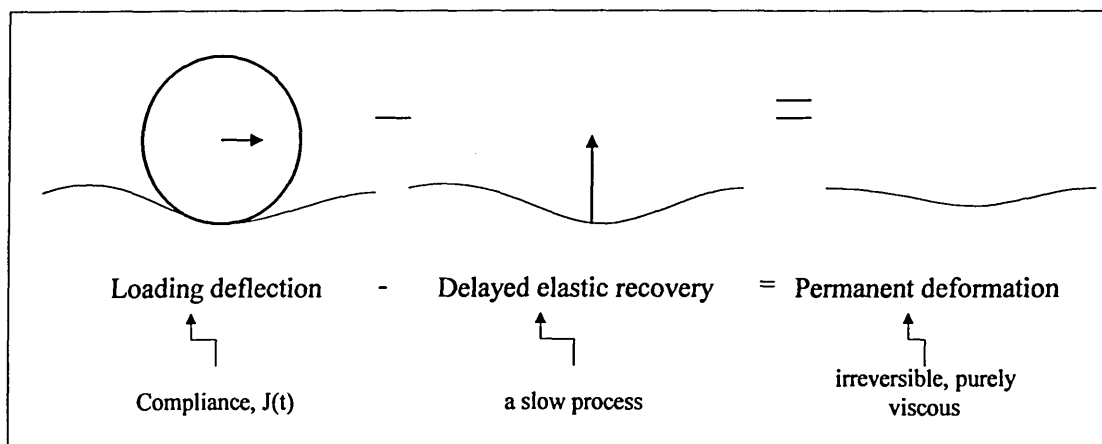


Figure 7.3 Deflection of Bituminous Pavement Under Traffic Loading and Binder Rheology. Reproduced after Phillips and Robertus [16]

#### 7.2.4.1 Ring and Ball Softening Point

The softening point test was originally used for straight-run (unmodified) and oxidised bitumens . The test has been widely used in practice, as one of the test standard tests to characterise the properties of the binder (BS 2000: Part 58, ASTM D36, IP 58).

The softening point temperature is not the melting point temperature of a bituminous binder because bitumen does not melt but gradually changes from a semi-solid (high viscosity) liquid to a low viscosity liquid on the application of heat. To some extent, softening point is regarded as the temperature at which the penetration at a standard temperature and rate of loading is 800 (0.1 mm). However, researchers reported that this relationship should not be necessarily applied for polymer modified binders due to its empirical nature.

The softening point has long been accepted as having a correlation with the mixture resistance to permanent deformation as the simple test to empirically represent the viscosity of bituminous binders, as reported by Szatkowski [5]. Further, he stated that the resistance to permanent deformation of bituminous mixtures can be improved by using binders with high softening point values. The linear relationship developed by Szatkowski [5] was based on some unmodified bitumens, a heavy duty bitumen (40 pen), a plastomeric binder, and a Trinidad Lake Epuré binder (Figure 7.4). Jacob [17] also reported correlation between wheel-tracking rut rate and softening point of binders (unmodified binders), as presented in Figure 7.5. However, recent research incorporating the use of polymer modified binders revealed that binders with high softening points do not necessarily give higher resistance to permanent deformation. Figure 7.6 indicates that binder E6 which has a high softening point is more susceptible to permanent deformation in comparison with the other binders which have lower softening points (E4, E5, P1, P2, HSB). Therefore some polymer modified binders may not have a linear relationship with the wheel-tracking rate, as also presented from this study (Figure 7.5 and Figure 7.7). Deviation from the linear relationship between softening point of the binders and the wheel-tracking rate was mostly found in elastomeric binders (see Figure 7.5 to Figure 7.7).

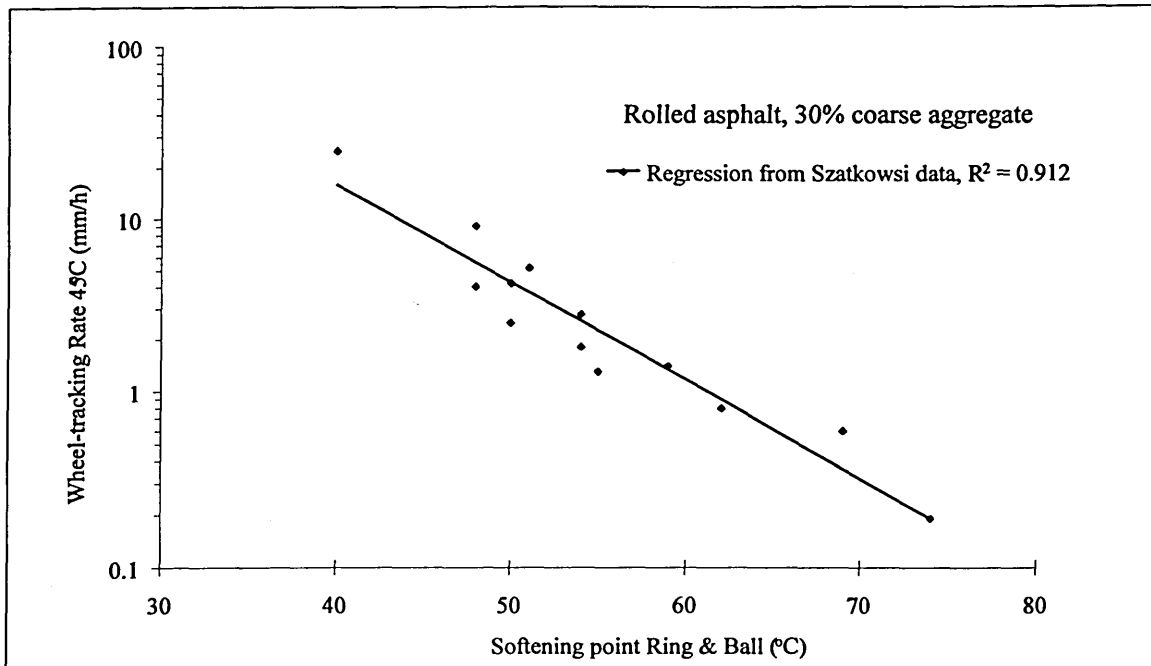


Figure 7.4 The effect of softening point of binders to the resistance to permanent deformation of hot rolled asphalt. Data for regression analysis were obtained from Szatkowski [5].

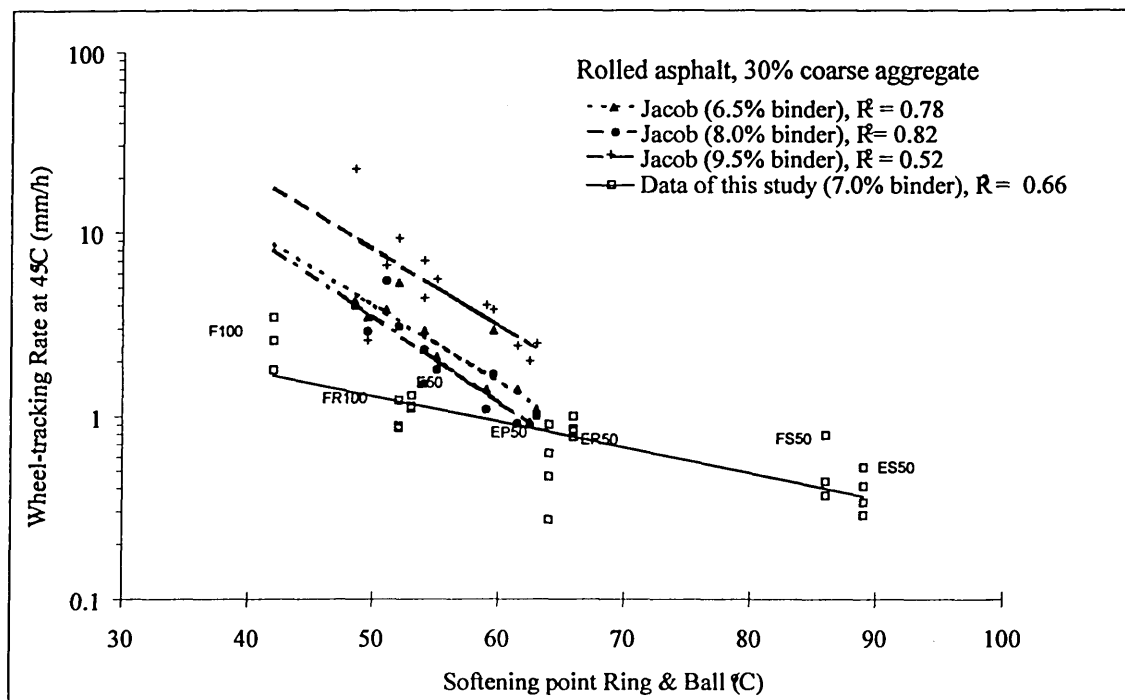


Figure 7.5 Effect of the softening point of binder on wheel-tracking rate at 45°C showing Jacobs' work [17] and this study.

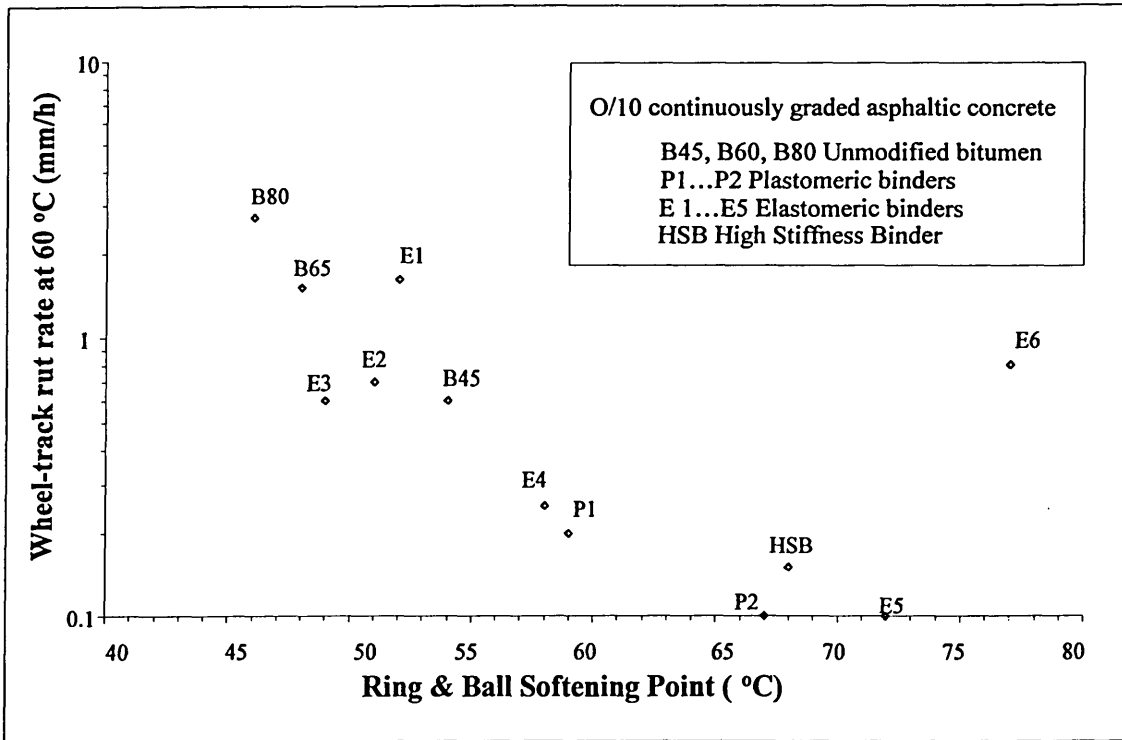


Figure 7.6 Effect of the softening point of binder on the wheel-tracking rate at 60°C. After Claxton, Lesage, and Planque [13]. Mixture type: 0/10 continuously graded asphaltic concrete. Binder content: 5.3%.

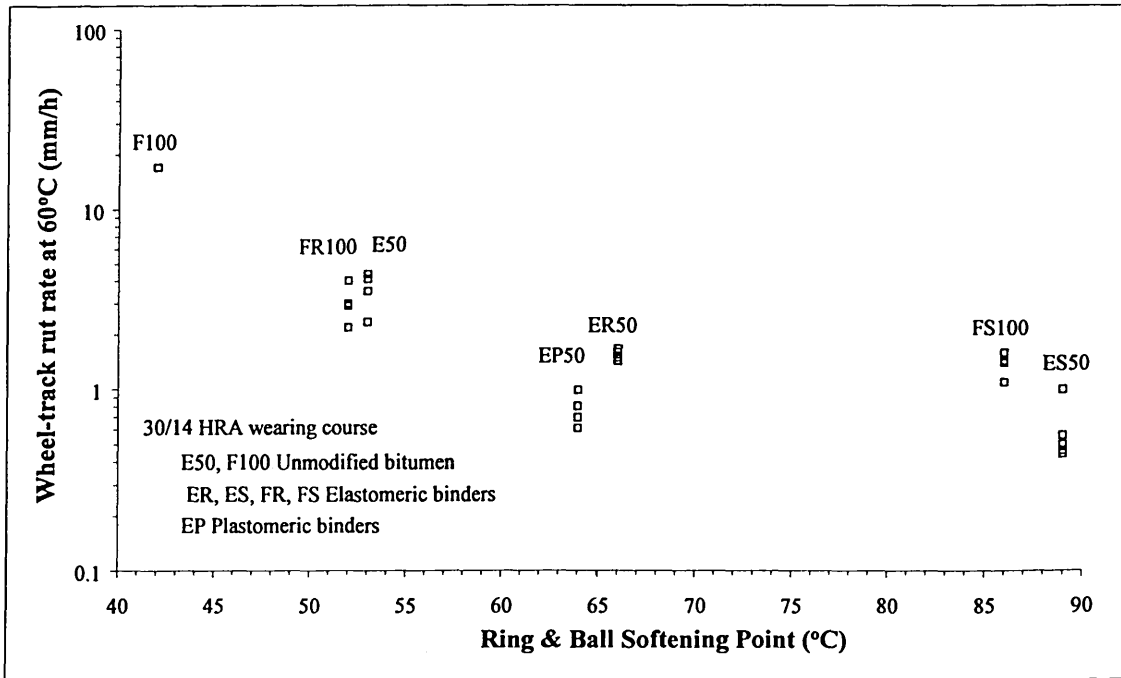


Figure 7.7 Effect of the softening point of the studied binders on the wheel-tracking rate at 60°C.

King *et al.* [18] also reported that the addition of polymer modified styrene butadiene block copolymer into a soft bitumen can increase the softening point value, but the rate of the improvement of the resistance to permanent deformation does not necessarily vary as much as that implied by the increase of softening point. Furthermore, Ellis, Widyatmoko, and Read [19] also reported that the softening point test procedure may not be suitable for some polymer modified binders if the materials are unstable in storage, due to the different behaviour in the deformation-mechanism during the transformation from semi-solid state to liquid during heat application (see *Chapter Six*).

#### 7.2.4.2 Viscosity

Theoretically, the binder contribution to permanent deformation can be described solely by a viscosity. Viscosity was originally a measure of the resistance to flow of liquids, which is basically synonymous with internal friction.

Viscosity is usually represented by:

$$\eta = \frac{\tau}{d\gamma/dt}$$

*Equation 7.4*

where  $\eta$  is the coefficient of dynamic viscosity or simply called as viscosity,  $\tau$  is the shear stress, and the  $d\gamma/dt$  is the strain rate. Liquids exhibiting Newtonian flow at a constant temperature and under a constant pressure comply with the following condition:

1. The only stress generated in simple shear flow is the shear stress  $\tau$ , the normal stress difference being zero.
2. The shear viscosity does not vary with shear rate.
3. The viscosity is constant with respect to time of shearing
4. The viscosities measured in different types of deformation are always in simple proportion to one another, e.g. the viscosity measured in uniaxial extensional flow is always three times the value measured in simple shear flow.

A liquid showing any deviation from the above behaviour is non-Newtonian, in which they are often classified as (see also Figure 7.8):

1. Shear-thinning (pseudoplastic) liquids
2. Shear-thickening (dilatancy) liquids
3. Bingham plastics

Non-Newtonian liquids are mostly of the shear thinning type. A shear-thinning pseudoplastic liquid exhibits a decrease in viscosity with increasing shear rate. In the limits of very low shear rates or stresses and very high shear rates or stresses the viscosity is constant. Those two extremes are the lower and the upper Newtonian regions. The terms “lower” and “upper” here refer to the shear rate or shear stress, not to the viscosity. Sometimes, the terms “first” and “second” Newtonian region are used instead. The viscosity of the first Newtonian region termed the “zero shear-rate viscosity” is the highest viscosity value for shear thinning liquids [20].

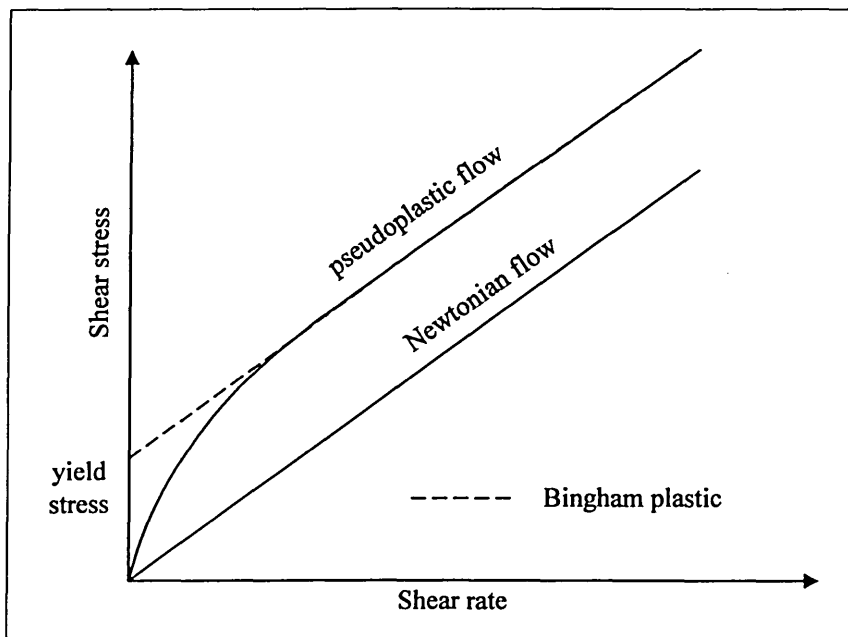


*Figure 7.8 Shear stress versus shear rate for a Newtonian liquid, a pseudoplastic liquid, and a Bingham plastic. After Sybilski [20].*

Bitumen, as a thermoplastic material, experiences change in consistency and rheological properties with changes in temperature. Under some conditions it may behave as a Newtonian liquid, but under others as non-Newtonian. In general, bitumen behaves as

Newtonian liquid at temperatures above 60°C. However, deviations from the Newtonian behaviour may be observed at this temperature for harder bitumens.

Polymer modifications usually tend to make binders harder, and therefore, the higher the polymer content of the modified binder, the greater the probability of deviation of the material behaviour from Newtonian and the lower the shear rate at the limit of the first Newtonian range. This phenomenon shows the need to measure properties of such materials at a low shear rate as close to zero-shear as possible. Sybilsky [15] presents an example of different polymer modified binders tested at 90°C showing test results and zero-shear viscosity (Figure 7.9).

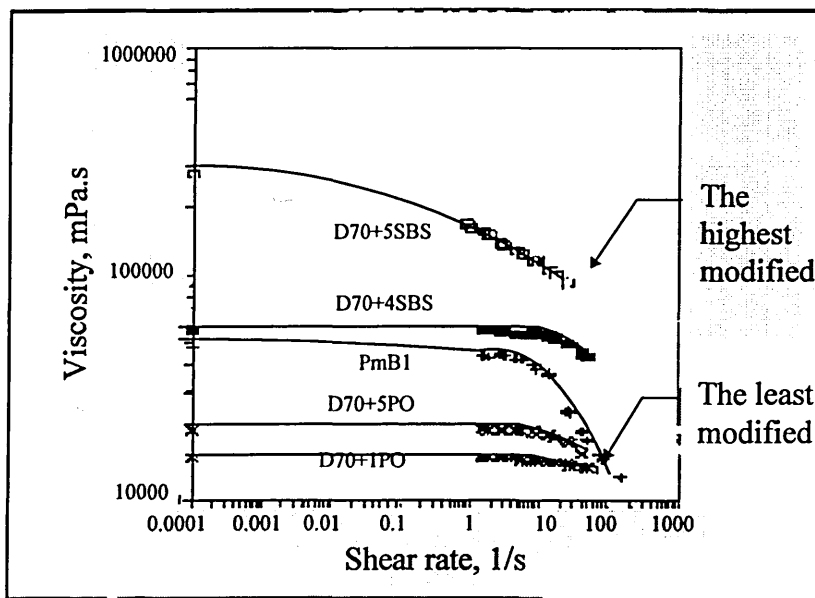


Figure 7.9 Viscosity test results and calculated zero-shear viscosity of different polymer-bitumen systems. After Sybilsky [15]

#### 7.2.4.3 SHRP Permanent Deformation Parameter $|G^*|/\sin \delta$

The SHRP studies [14, 21] proposed the inverse loss compliance,  $J''$ , of binder to be adopted as the specification criterion for permanent deformation of bituminous mixtures (Equation 7.5).

$$\frac{1}{J''} = \frac{|G^*|^2}{G'} = \frac{|G^*|^2}{|G^*| \sin \delta} = \frac{|G^*|}{\sin \delta}$$

*Equation 7.5*

These parameters were obtained from dynamic mechanical tests at a loading time of 0.1 seconds, to represent the loading time within a pavement that results from a pass of a truck tyre travelling at 80 km/h. The 0.1 second loading time also corresponds to 10 rad/s (1.6 Hz) of sinusoidal loading.

In order to protect against the possibility that the binder would contribute tenderness during mixing and laying, the  $|G^*|/\sin\delta$  should be greater than 1 kPa and 2.2 kPa for tank and aged materials. High values of  $|G^*|$  and low values of  $\delta$  are considered desirable attributes from the standpoint of permanent deformation resistance.

However, a study reported by Leahy, Monismith and Lundy [22] suggested that the parameter  $|G^*|/\sin\delta$  is not a reliable predictor of potential rutting. Their study presented a poor correlation between this parameter and the wheel-tracking rate ( $R^2 = 0.18$ ). Figure 7.10 also shows that the parameter of  $|G^*|/\sin\delta$  for polymer modified binders deviates far from the groups of unmodified bitumens of which the correlation factor is very poor ( $R^2=0.3156$ ). The explanation of the unsuitability of this parameter on some polymer modified binders is presented below.

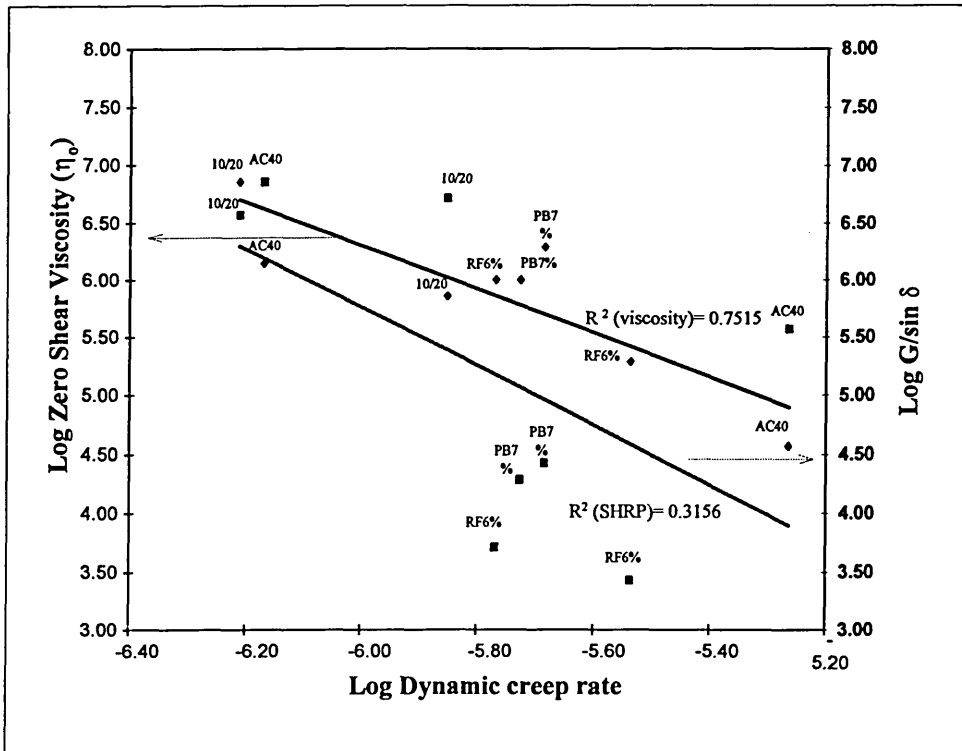


Figure 7.10 Comparison between the SHRP permanent deformation parameter ( $G^*/\sin \delta$ ) and the zero shear viscosity ( $\eta_0$ ). After Phillips [23].

The main difference between the SHRP quantity  $|G^*|/\sin \delta$  and the zero shear rate viscosity  $\eta_0$  arises from delayed-elastic recovery. The deformation during wheel loading is related to the viscoelastic compliance at the time scale of loading.  $|G^*|/\sin \delta$  is measured at short loading times representative of traffic loading, whereas recovery can be a slow process with certain binders. The delayed-elastic recovery occurs relatively fast and is limited with unmodified bitumen but conversely sometimes very slow and large with modified binders [23]. Neglecting the recovery process underestimates binder performance, i.e. permanent deformation. Therefore,  $|G^*|/\sin \delta$  presents a pessimistic view of performance.

Equation 7.6 shows the time dependent response during and after wheel loading [24] where  $J''$  is the shear loss compliance,  $J_{d.e.}$  is the delayed elastic creep compliance,  $\delta$  is the phase angle, and  $\omega$  is the radian frequency ( $\omega = 2\pi f$  where  $f$  is frequency in Hertz). The equation implies that binders with the same viscosity,  $\eta_0$ , but with more delayed

elasticity have larger values of  $J''$ , and hence lower values of  $|G^*|/\sin\delta$  [23]. Consequently, these binders are ranked lower in terms of  $|G^*|/\sin\delta$ .

$$J''(\omega) = \int_0^{\infty} \omega [J_{d.e.}(\infty) - J_{d.e.}(t)] \cos \omega t \, dt = \frac{1}{\omega \eta_0}$$

*Equation 7.6*

The parameters  $|G^*|/\sin\delta$  and  $\eta_0$  will give a similar ranking at purely viscous condition,  $\delta=90^\circ$  (Equation 7.7), and therefore  $|G^*|/\sin\delta$  should only be used at very low frequencies so the binder will behave as true a Newtonian fluid and the effect of delayed elasticity is negligible. It should be noted again here that the viscosity  $\eta_0$  is viscosity in the linear viscoelastic regime.

$$\frac{G^*}{\sin \delta} \equiv |G^*| \sin \delta = G'' = \omega \eta_0$$

*Equation 7.7*

### **7.3 Laboratory Wheel-tracking Test**

The wheel-tracking test has been recognised to be a robust and reliable procedure for small laboratory scale assessment especially for assessing the resistance to permanent deformation. The dynamic action imposed by the rolling wheel to the specimen adequately reflects the traffic loading on bituminous pavements. The wheel-tracking apparatus used in this study incorporated the use of a steel wheel coated with a thick solid rubber which complies with the BS 598: Part 110: 1996 [25]. The tyre contact (imprint) is 850mm<sup>2</sup> and an applied load of 520N which gives a corresponding contact stress of 612 kPa. Plots of wheel-tracking test results are presented in Figure 7.11 to Figure 7.17.

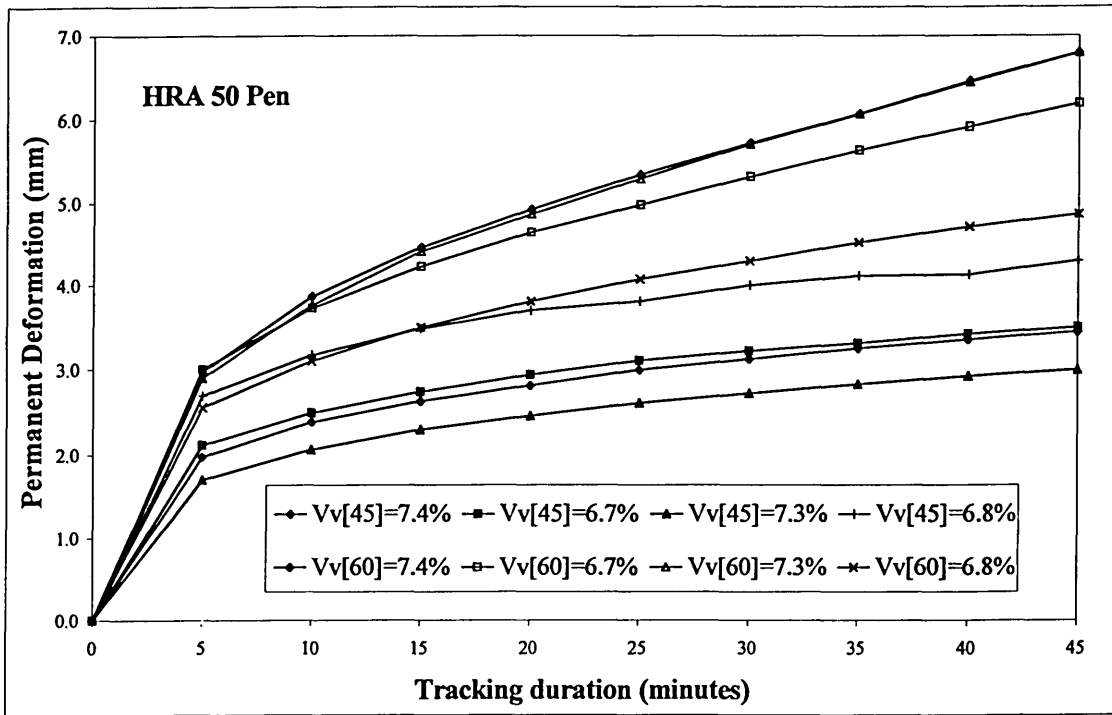


Figure 7.11 Wheel-tracking results at 45°C and 60°C for 50 pen HRA mixtures.

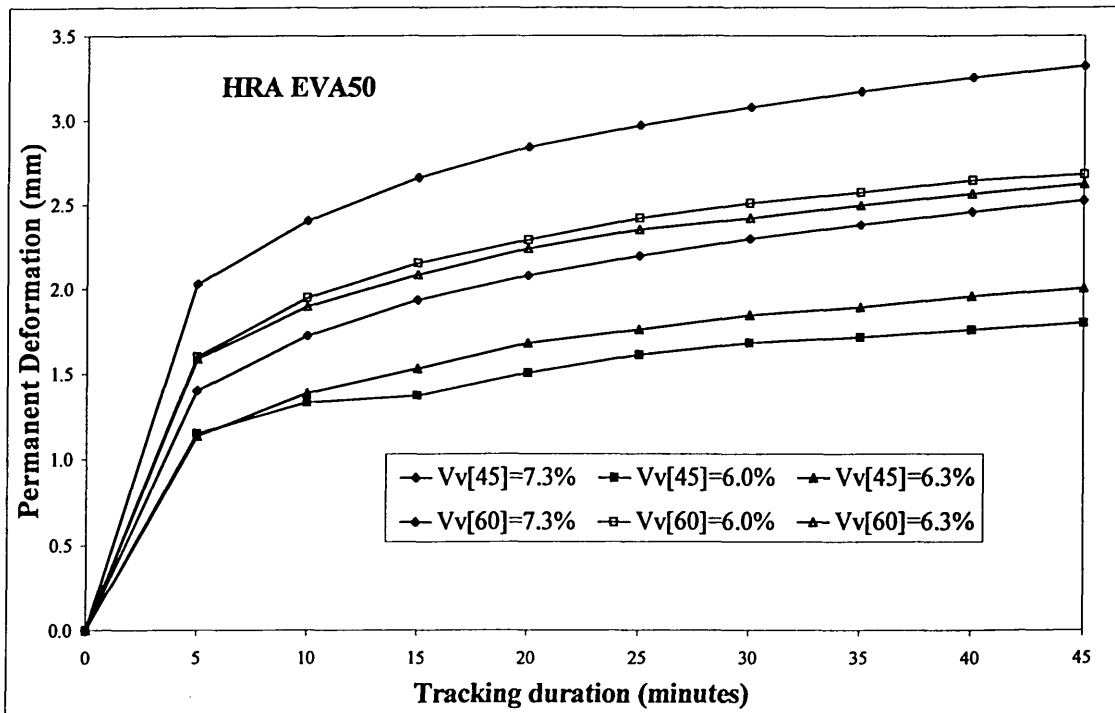


Figure 7.12 Wheel-tracking results at 45°C and 60°C for EVA modified HRA mixtures with 50 pen bitumen as the base binder.

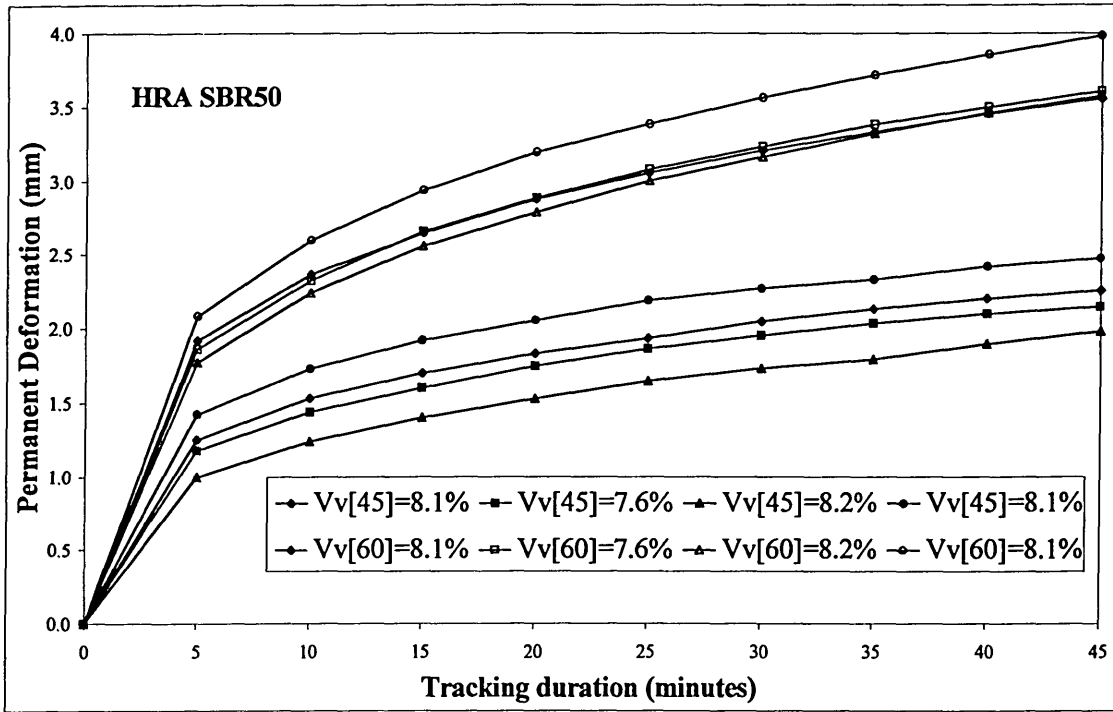


Figure 7.13 Wheel-tracking results at 45°C and 60°C for SBR modified HRA mixtures with 50 pen bitumen as the base binder.

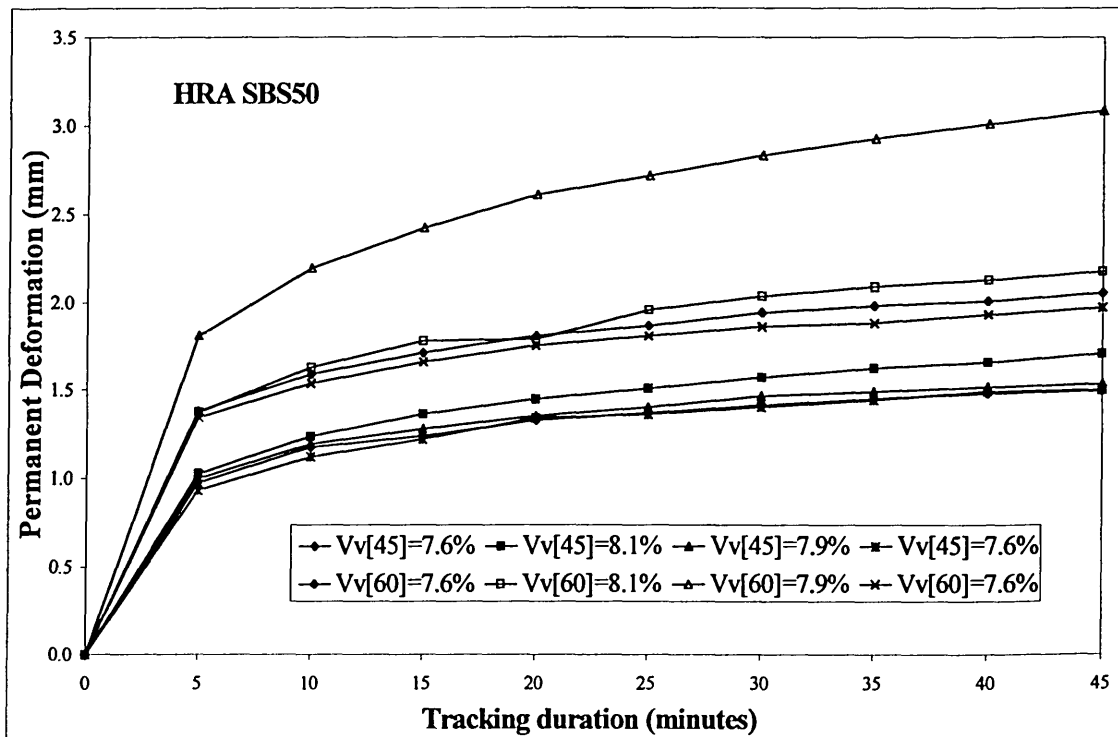


Figure 7.14 Wheel-tracking results at 45°C and 60°C for SBS modified HRA mixtures with 50 pen bitumen as the base binder.

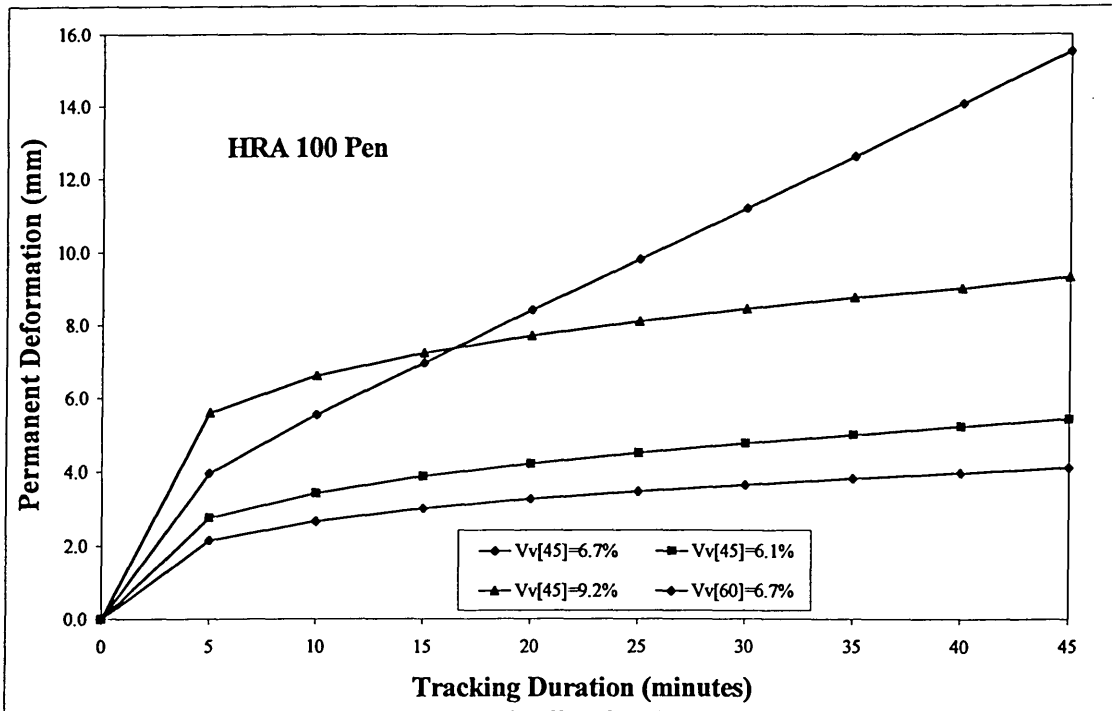


Figure 7.15 Wheel-tracking results at 45°C and 60°C for 100 Pen HRA mixtures.

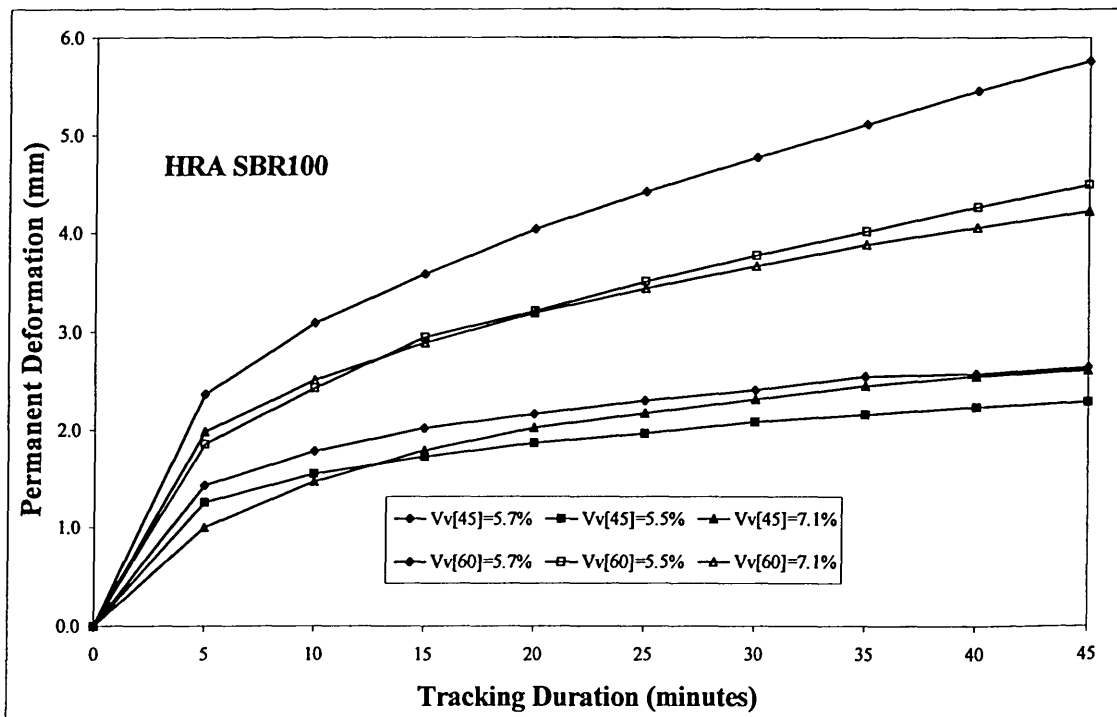


Figure 7.16 Wheel-tracking results at 45°C and 60°C for SBR modified HRA mixtures with 100 pen bitumen as the base binder.

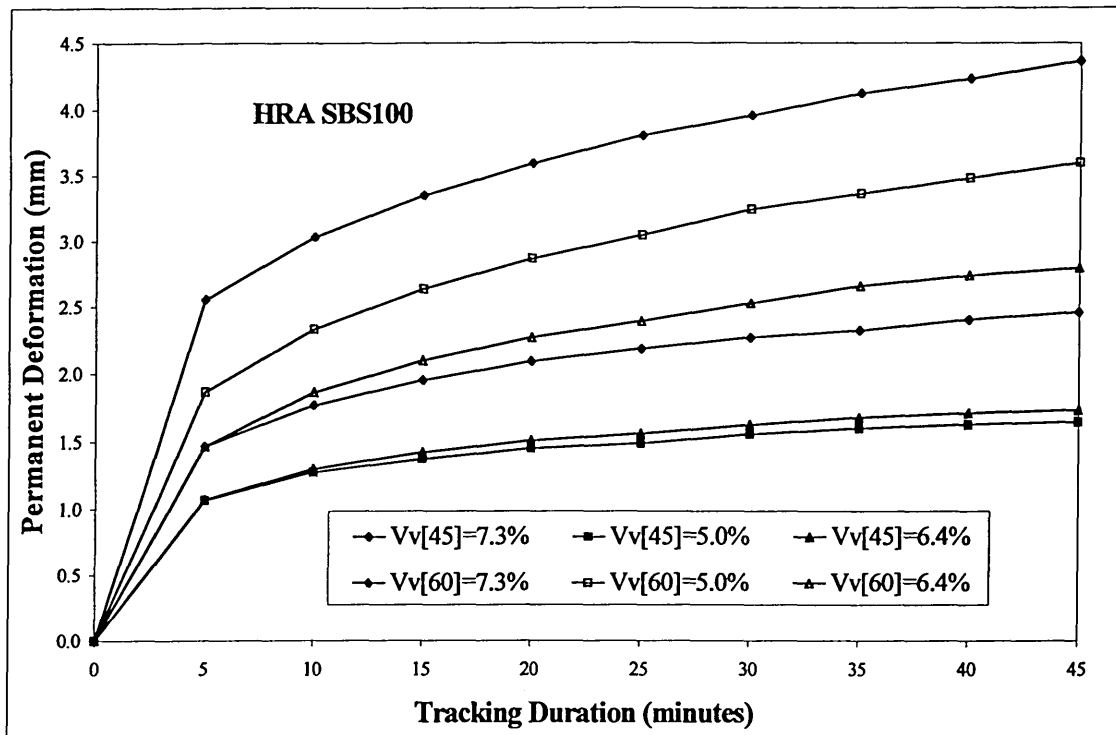


Figure 7.17 Wheel-tracking results at 45°C and 60°C for SBS modified HRA mixtures with 100 pen bitumen as the base binder.

Results presented in Figure 7.18 and Figure 7.19 were calculated based on Equations 4.1, 4.2, and 4.3 (see *Chapter Four*) for the average deformation rate, the minimum deformation rate, and the ultimate deformation whereas the calculation for the deformation rate based on BS 598:Part 110:1996 (Table 7.6 to Table 7.9) is presented in Equation 7.8, where  $T_R$  is the wheel-tracking rate (in mm/h),  $n$  is the total number of readings taken at 5 minute intervals for up to 45 minutes excluding the initial reading, and  $\Delta r_i$  is the change in vertical displacement from the initial value,  $r_o$ , to the  $i$ th reading (in mm). This equation requires a minimum of eight number of readings.

$$T_R = -3.6\Delta r_{n-3} - 1.2\Delta r_{n-2} + 1.2\Delta r_{n-1} - 3.6\Delta r_n$$

Equation 7.8

Even though the calculation and test procedure were conducted in accordance with the BS598:Part 110:1996, there are some exceptions:

1. The number of specimens used here are of four or three replicates per type of mixture instead of six replicates. Consequently to this, the mean wheeltracking rate values

were calculated as the average value from a number of specimens (three or four) rather than following the restriction prescribed by the BS method (i.e. the maximum wheeltracking rate from six determinations shall be less than 1.1 times their mean. The complete procedure refers to the specification [25]).

2. The specimens were double-tracked, instead of single-tracked, with a loading arrangement as presented in *Chapter Five*.

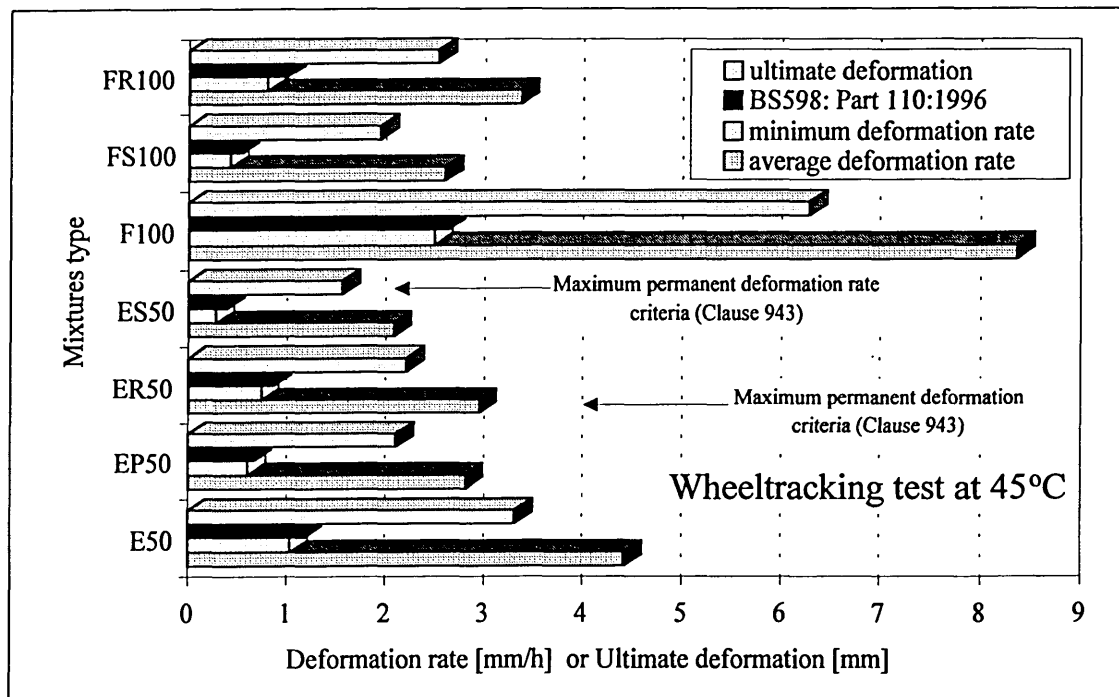


Figure 7.18 Results of wheel-tracking test at 45°C on different mixtures. These results shown are the average values from a number of replicates (see Table 7.6).

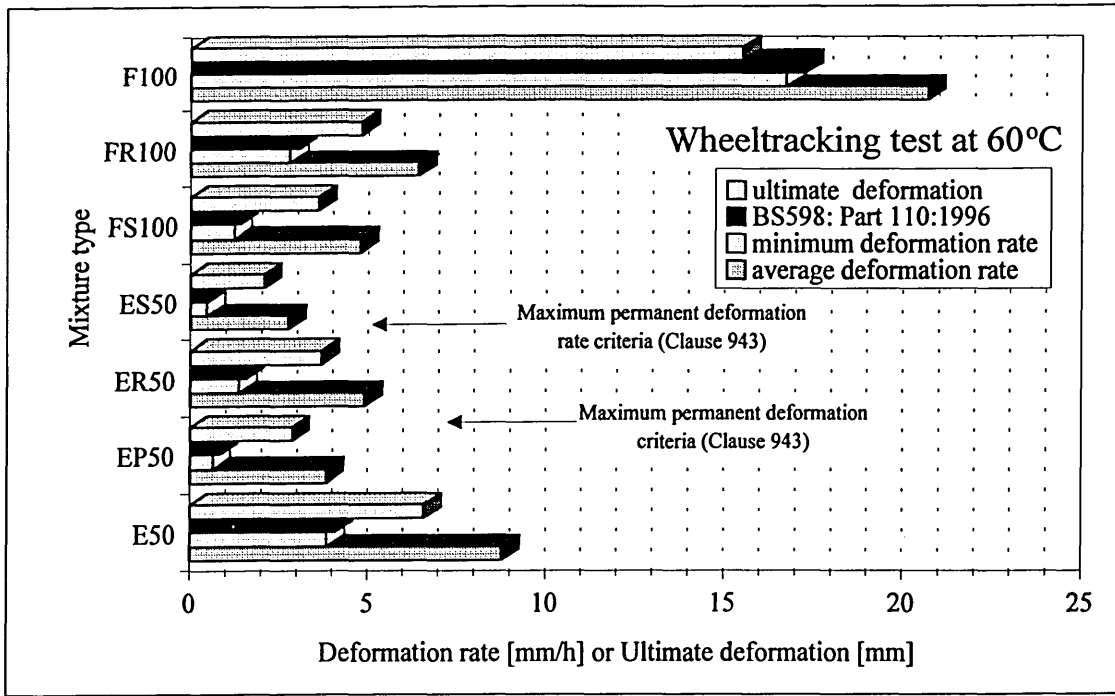


Figure 7.19 Results of wheel-tracking test at 60°C on different mixtures. These results shown are the average values from a number of replicates (see Table 7.6).

Table 7.6 Results from wheel-tracking tests. Rut depth at 45°C. (C.I.= confidence interval)

Test no. Mixture	Rut Depth at 45°C				Statistical Analyses		
	1	2	3	4	Mean	Standard Deviation	95%C.I. (+/-)
E (50 Pen)	3.45	3.50	2.99	4.30	3.31	0.54	0.87
EP (EVA50)	2.52	1.80	1.17	2.00	1.83	0.56	0.89
ER (SBR50)	2.26	2.14	1.98	2.48	2.13	0.21	0.33
ES (SBS50)	1.50	1.71	1.54	1.50	1.58	0.10	0.16
F (100 Pen)	4.10	5.41	9.32	n/a	6.28	2.72	4.32
FR (SBR100)	2.65	2.30	2.62	n/a	2.53	0.20	0.31
FS (SBS100)	2.46	1.65	1.73	n/a	1.95	0.45	0.71

Table 7.7 Results from wheel-tracking tests. Wheeltracking rate at 45°C. (C.I.= confidence interval)

Test no. Mixture	Wheeltracking Rate at 45°C				Statistical Analyses		
	1	2	3	4	Mean	Standard Deviation	95%C.I. (+/-)
E (50 Pen)	1.30	1.14	1.11	1.13	1.19	0.09	0.14
EP (EVA50)	0.91	0.47	0.27	0.63	0.55	0.27	0.43
ER (SBR50)	0.83	0.77	1.00	0.85	0.87	0.10	0.16
ES (SBS50)	0.33	0.52	0.29	0.41	0.38	0.10	0.16
F (100 Pen)	1.80	2.60	3.47	n/a	2.62	0.83	1.33
FR (SBR100)	0.89	0.86	1.22	n/a	0.99	0.20	0.32
FS (SBS100)	0.79	0.37	0.44	n/a	0.53	0.23	0.36

Table 7.8 Results from wheel-tracking tests. Rut depth at 60°C. (C.I.= confidence interval)

Test no. Mixture	Rut Depth at 60°C				Statistical Analyses		
	1	2	3	4	Mean	Standard Deviation	95%C.I. (+/-)
E (50 Pen)	6.80	6.20	6.80	4.88	6.60	0.91	1.44
EP (EVA50)	3.32	2.68	2.10	2.62	2.70	0.50	0.80
ER (SBR50)	3.56	3.61	3.58	3.98	3.58	0.20	0.32
ES (SBS50)	2.06	2.18	3.09	1.97	2.44	0.52	0.82
F (100 Pen)	15.51	n/a	n/a	n/a	15.51	n/a	n/a
FR (SBR100)	5.76	4.49	4.22	n/a	4.82	0.82	1.31
FS (SBS100)	4.37	3.61	2.80	n/a	3.59	0.78	1.25

Table 7.9 Results from wheel-tracking tests. Wheeltracking rate at 60°C. (C.I.= confidence interval)

Test no. Mixture	Wheeltracking Rate at 60°C				Statistical Analyses		
	1	2	3	4	Mean	Standard Deviation	95%C.I. (+/-)
E (50 Pen)	4.34	3.50	4.38	2.36	4.07	0.95	1.51
EP (EVA50)	0.99	0.69	0.61	0.80	0.76	0.16	0.26
ER (SBR50)	1.41	1.49	1.67	1.67	1.52	0.13	0.21
ES (SBS50)	0.44	0.56	1.00	0.46	0.67	0.26	0.42
F (100 Pen)	17.25	n/a	n/a	n/a	17.25	n/a	n/a
FR (SBR100)	3.98	2.90	2.20	n/a	3.03	0.89	1.42
FS (SBS100)	1.60	1.44	1.09	n/a	1.38	0.26	0.42

These results (Figure 7.18 and Figure 7.19) indicate that the minimum deformation rate values were similar to the values obtained by the BS method. The average deformation rate values were higher than either the minimum deformation rate or BS procedure. The higher values on average deformation rate were due to the initial deformation. The highest deformation at the first five minutes reported from this study was found on the mixture F100 tested at 60°C, i.e. the deformation was as high as 3.96 mm or corresponding to wheel-tracking rate of 47.5 mm/h at the first five minutes of tracking.

The effect of initial deformation has also been reported by Gibb [7] where he recommended the use of minimum strain (deformation) rate instead. Despite the differences amongst these methods, however, all methods provide the same order on the ranking of performance of bituminous mixtures at each test temperature. Nevertheless, the ranking of performance of the mixtures obtained at 45°C test was not in the same order as obtained at 60°C test. The FS100 provides better resistance to deformation at 45°C than the EP50, but, the ranking changed at 60°C where the EP50 shows better

performance than the FS100. Furthermore, the wheel-tracking rate for FS100 at 60°C test condition was almost three times of that at the 45°C test condition, whereas only slight increase on wheel-tracking rate was found on the EP50 mixture. This condition may be explained as follows:

1. The ring and ball softening point temperatures of EP50 and FS100 binders are 64 and 86°C respectively. If the softening point temperature of the polymer modified binders can be a predictor of the mixture resistance to permanent deformation, the wheel-tracking test should have always shown that the FS100 mixture has a better resistance to permanent deformation through out the temperature range than the EP50 or *vice versa*. A similar condition has been reported by King *et al.* [18] where a soft bitumen modified with a high concentration of polymer showed a very high softening point temperature but the mixture was susceptible to permanent deformation.
2. The base binder has a significant effect on the performance after polymer modification. The FS100 and EP50 were based on 100 pen and 50 pen bitumen, and therefore, at a temperature where the base binder alone would behave as a Newtonian liquid the performance of polymer modified binder may be reversed, e.g. most bitumens (unmodified) behaves as a Newtonian liquid at temperatures above 60°C and the temperature at which 100 pen bitumen behaves as a Newtonian liquid is lower than the 50 pen bitumen's. Figure 7.20 demonstrate that the temperature at which 100 pen bitumen is almost in purely viscous state ( $\delta = 88^\circ$ ) is 50°C as opposed to 60°C ( $\delta = 86^\circ$ ) for 50 pen bitumen.

The overall performance of polymer modified mixtures was satisfactory. These mixtures passed the permanent deformation criteria set by HA Draft Clause 943[4] at both test temperatures (45 and 60°C).

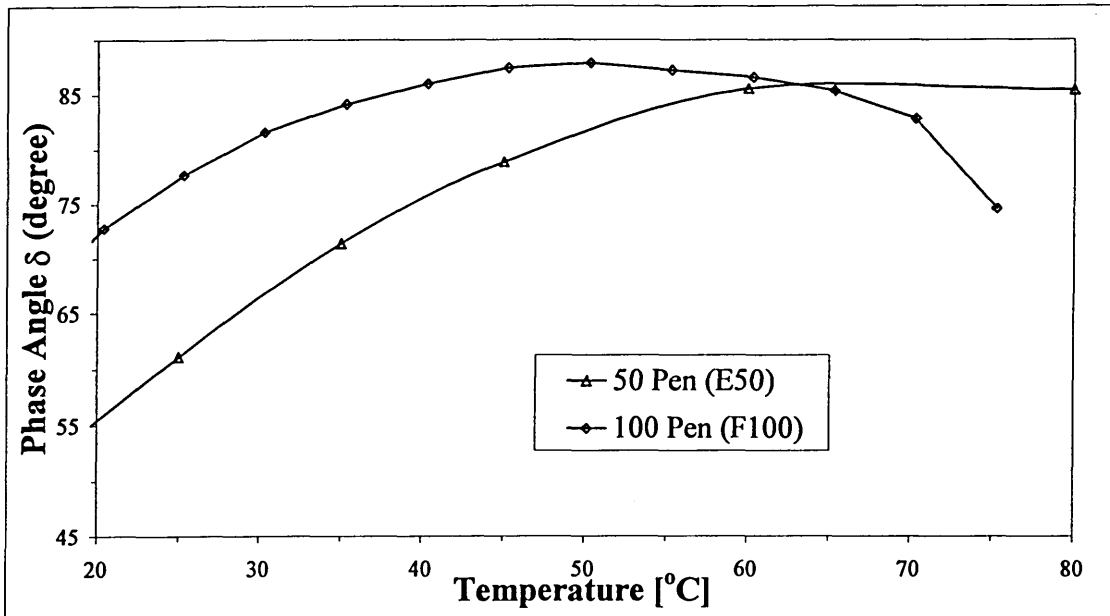


Figure 7.20 Phase Angle versus temperature for 50 pen and 100 pen bitumens (dynamic mechanical test by using temperature sweeps from 0 to 80°C at frequency 1 Hz).

#### 7.4 Marshall Test

Marshall test and analyses were carried out in accordance with BS 598: Part 107: 1990 at a test temperature of 60°C and loading rate of  $50 \pm 3$  mm per minute. The results shown in Table 7.10 indicate that the addition of polymer always increases the stability of the mixtures which usually means an increase in the resistance to permanent deformation. However, the stability values seem to be insensitive to different types of polymers. For example, the difference between the addition of EVA, SBR, or SBS is very small. The analyses of variance on mixtures EP50(EVA), ER50(SBR), and ES50(SBS) indicated that the difference between these mixtures are not significant at 5 per cent level. This condition supports the previous investigations reported by Tayebali *et al.* [26] that the test is insensitive to the permanent deformation characteristics of polymer modified mixtures.

Table 7.10 Marshall test results. Names designated to the mixture types refer to the binder types as presented in Table 5.2 (Chapter Five).

Code of Mixtures	Density g/ml	Compacted Aggregate Density g/ml	Marshall Stability kN	Marshall Flow mm
A50	2.261	2.110	10.805	2.560
B50	2.263	2.105	10.797	2.495
C50	2.266	2.107	10.880	2.897
D50	2.239	2.082	10.818	2.257
AP50	2.255	2.097	11.145	2.459
BP50	2.259	2.101	12.411	2.292
CP50	2.270	2.112	12.734	2.591
DP50	2.250	2.093	13.433	2.960
EP50	2.270	2.111	12.230	2.357
ES50	2.261	2.103	12.886	2.300
ER50	2.260	2.102	13.177	2.343
F100	2.248	2.091	8.067	1.820
FS100	2.264	2.105	8.713	2.113
FR100	2.254	2.096	9.110	2.353

Table 7.11 Individual data of mixtures EP50(EVA), ER50(SBR), and ES50(SBS).

Mixture type	EP50	ER50	ES50
Specimen 1	11.84	13.24	12.79
Specimen 2	13.57	13.28	13.91
Specimen 3	11.28	13.01	11.95
Analyses for 1 to 3			
Sum	36.69	39.53	38.66
Average	12.23	13.18	12.89
Variance	1.42	0.02	0.97

Table 7.12 Analyses of variance for testing whether there is a difference at 5 per cent level of significant ( $\alpha=5\%$ ) between mixtures EP50(EVA), ER50(SBR), and ES50(SBS).

Source of Variation	SS	df	MS	F	F crit
Between Groups	1.41293	2	0.70647	0.88181	5.14325
Within Groups	4.80691	6	0.80115		
Total	6.21984	8			

### 7.5 Dynamic Creep Test

The procedure for determining the dissipated energy per cycle and the total dissipated energy to failure point  $N_1$  have been presented in *Chapter Four*. On this repetitive constant load arrangement, the energy is dissipated at a constant level until the mixture is losing the stability and leads to a rapid increase in dissipated energy per cycle (Figure 7.21). Detailed illustrations and results can be found in the *Appendix C*.

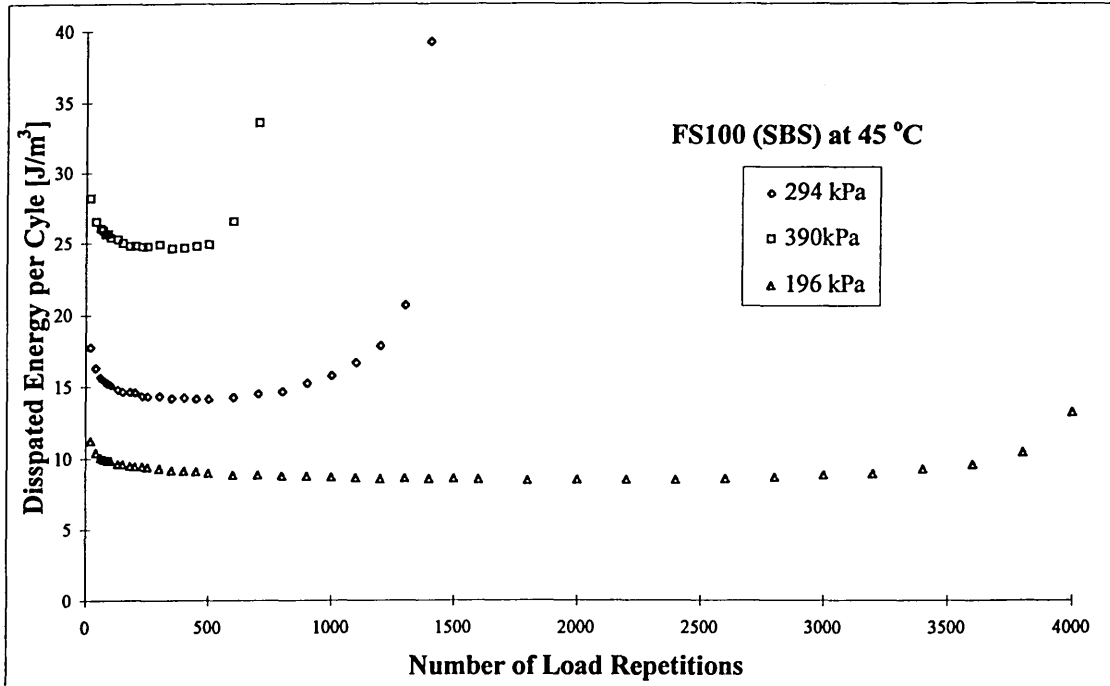


Figure 7.21 Typical relationship between dissipated energy per cycle and the number of load repetitions for SBS modified HRA (FS100) mixtures.

#### 7.5.1 Effect of the applied stress level and the repetitive loading

The energy dissipated by the bituminous materials during each loading cycle is dependent upon the test temperature and the applied stress level. The results presented in Figure 7.22 and Figure 7.23 show that the mixtures dissipate more energy at higher stress levels and/or at higher temperature. Furthermore, the higher dissipated energy per cycle leads to a shorter number of cycles to  $N_1$  (Figure 7.24). Therefore, to eliminate the effect of different stress levels upon the load repetition to failure, the average dissipated energy per cycle ( $w_o$ ) was normalised by the total dissipated energy up to the point  $N_1$  ( $W_{N1}$ ), or as shown in Equation 7.9., where  $w_{norm}$  is the normalised dissipated energy.

$$w_{norm} = \frac{w_o}{W_{N1}}$$

Equation 7.9

The polymer modified mixtures, as expected, dissipate less energy than the unmodified mixtures. The EVA modified mixture dissipates the least energy followed by the SBS modified mixture (Figure 7.25 and Figure 7.26).

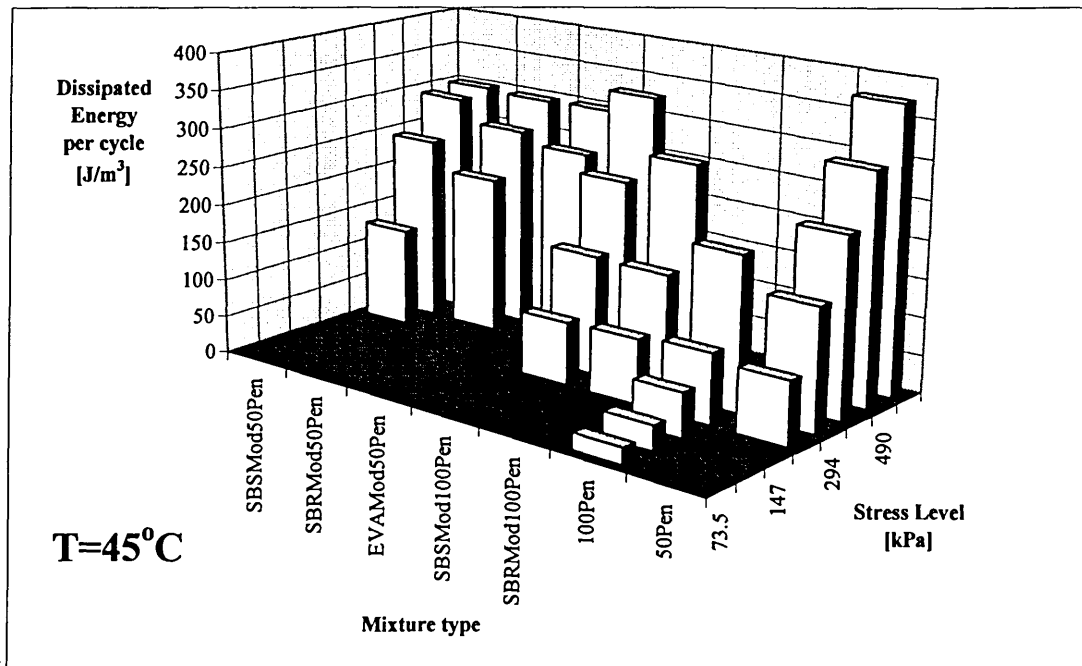


Figure 7.22 The effect of stress level upon the dissipated energy per cycle of the mixtures at test temperature of 45°C.

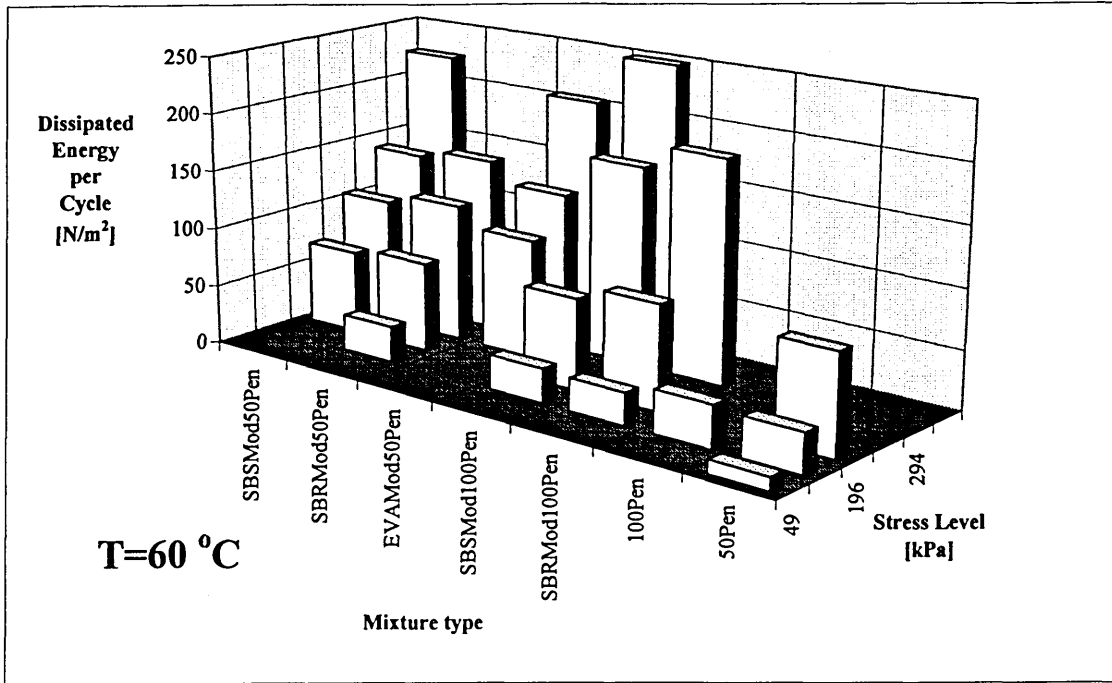


Figure 7.23 The effect of stress level upon the dissipated energy per cycle of the mixtures at test temperature of 60°C

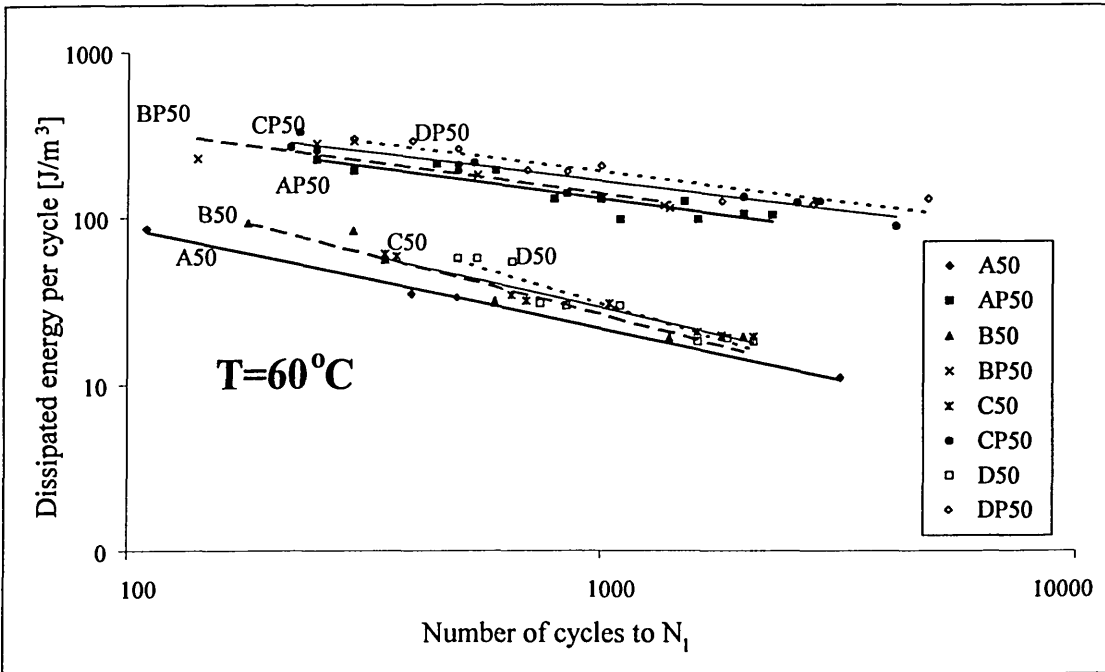


Figure 7.24 Typical relationships between dissipated energy per cycle and the number of cycles to N<sub>1</sub>. Mixtures 50 Pen and EVA Modified 50 Pen HRA. Test temperature 60°C.

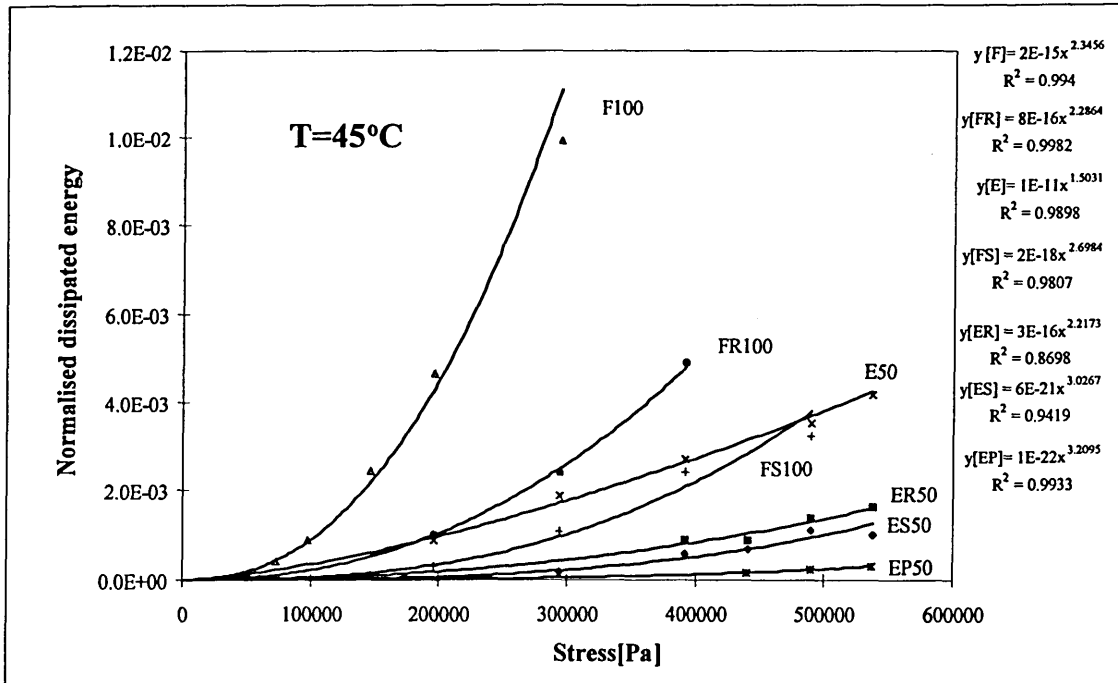


Figure 7.25 Relationship between the normalised dissipated energy and the stress level at a test temperature of 45°C.

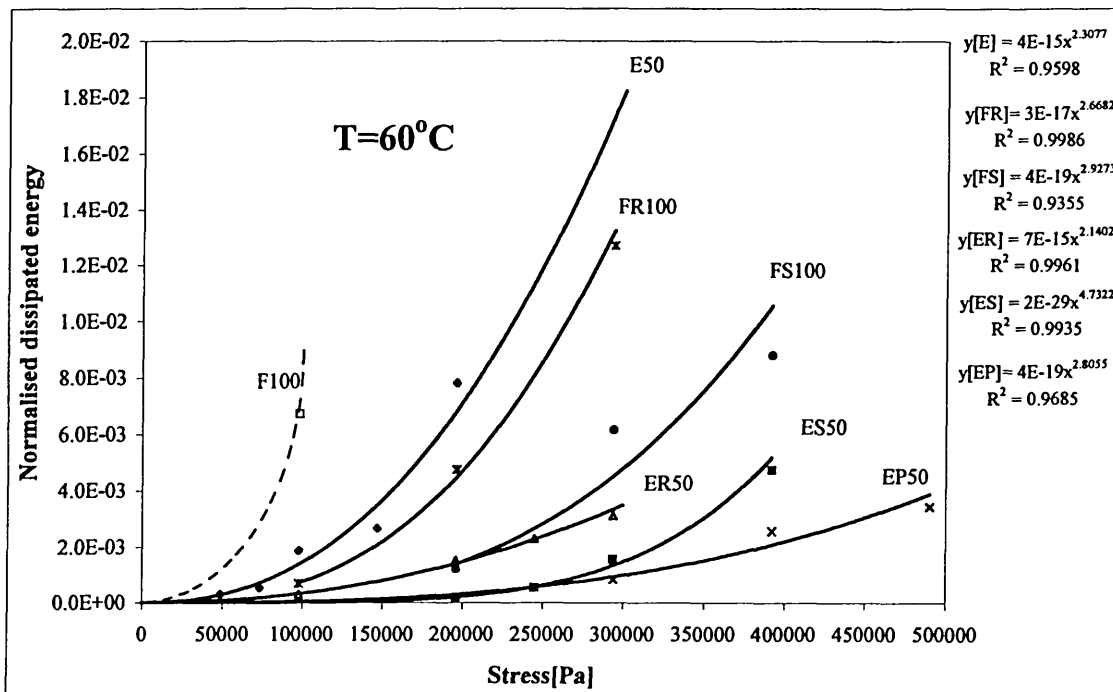


Figure 7.26 Relationship between the normalised dissipated energy and the stress level at a test temperature of 60°C.

### 7.5.2 Repeatability of Dynamic Creep Testing

Assessments on the repeatability of the dynamic creep testing, as shown in Table 7.13 and 7.14, suggest that the mean repeatability of all measurements at different stress levels and temperatures is around 20%. This variation seems to be relatively high. However, these tables show no sign of stress-dependent variation. This condition may be due to the variability in the properties of the individual specimens (such as volumetric condition and changes in mixture properties during preparation and manufacturing) and the number of cycles to  $N_1$ .

Table 7.13 Repeatability of dynamic creep testing at temperature 45°C.

Mixture - temperature	Average stress [kPa]	Normalised dissipated energy		
		average [J/m <sup>3</sup> ]	standard deviation [J/m <sup>3</sup> ]	coefficient of variation
E - 45°C	196	0.00104	0.00026	25.09%
	294	0.00217	0.00033	14.98%
	392	0.00289	0.00061	21.08%
EP - 45°C	490	0.00030	0.00007	23.50%
	538	0.00028	0.00001	4.40%
ER - 45°C	441	0.00088	0.00016	18.30%
	539	0.00163	0.00002	1.45%
ES - 45°C	392	0.00061	0.00020	33.45%
	440	0.00067	0.00004	5.45%
	490	0.00110	0.00003	2.82%
F - 45°C	73.5	0.00039	0.00015	37.45%
	98	0.00087	0.00025	28.81%
	147	0.00242	0.00042	17.54%
	196	0.00465	0.00031	6.76%
	294	0.00991	0.00118	11.95%
FR - 45°C	196	0.00100	0.00034	34.47%
	294	0.00239	0.00023	9.77%
	392	0.00491	0.00084	17.12%
FS - 45°C	294	0.00107	0.00019	18.12%
	392	0.00240	0.00109	45.39%
	490	0.00324	0.00019	5.88%
Maximum coefficient of variation				45.39%
Minimum coefficient of variation				1.45%
Mean coefficient of variation				18.28%

Table 7.14 Repeatability of dynamic creep testing at temperature 60°C.

Mixture - temperature	Average stress [kPa]	Normalised dissipated energy		
		average [J/m <sup>3</sup> ]	standard deviation [J/m <sup>3</sup> ]	coefficient of variation
E - 60°C	98	0.00220	0.00036	16.17%
EP - 60°C	245	0.00061	0.00020	33.14%
	294	0.00101	0.00025	24.95%
	392	0.00270	0.00104	38.44%
ER - 60°C	196	0.00154	0.00014	9.07%
	245	0.00231	0.00020	8.75%
	294	0.00320	0.00051	15.88%
ES - 60°C	294	0.00165	0.00049	29.43%
FR - 60°C	98	0.00069	0.00005	6.64%
	196	0.00478	0.00153	31.94%
	294	0.01272	0.00246	19.37%
FS - 60°C	196	0.00122	0.00001	0.67%
	294	0.00618	0.00290	46.89%
Maximum coefficient of variation				46.89%
Minimum coefficient of variation				0.67%
Mean coefficient of variation				21.64%

Interlaboratory studies on the assessment of stone mastic asphalts (SMAs) by using dynamic creep testing on the NAT machine reported variations as high as 22.8%, with a mean variation of around 16.3% [27].

Further analyses to assess the effect of the maximum variations in the data, i.e. around 45% , are presented in Figure 7.27 and also Figure 7.28. These examples confirm that most of the results fall within the 95% confident interval and demonstrate the independency of high variations with regard to stress level. Therefore, the use of mean values for further analyses seems to be reasonable and representative, as previously presented in Figure 7.25 and Figure 7.26, with a mean variation of around 20%. The Author also feels that these results are still within the reproducibility of the dynamic creep testing, with reservations on some values which show high variations.

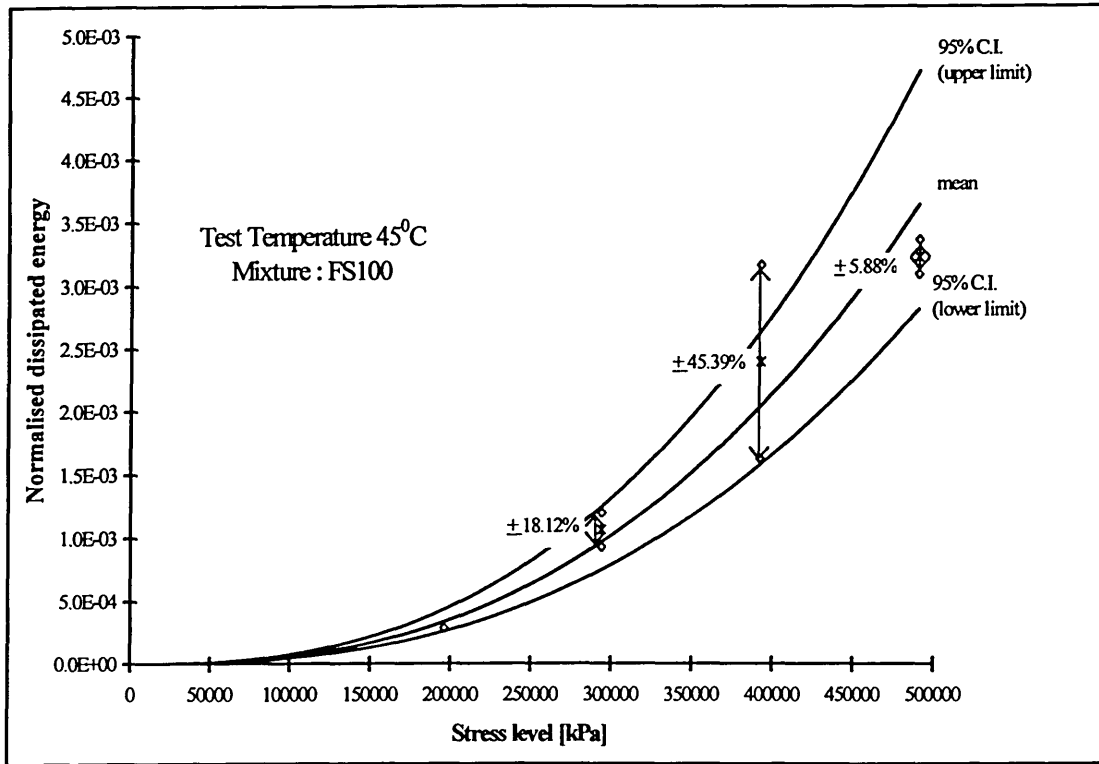


Figure 7.27 Variability of the normalised dissipated energy, showing the percentage variations, 95% Confidence Interval, and mean values, for mixture FS100 at 45°C.

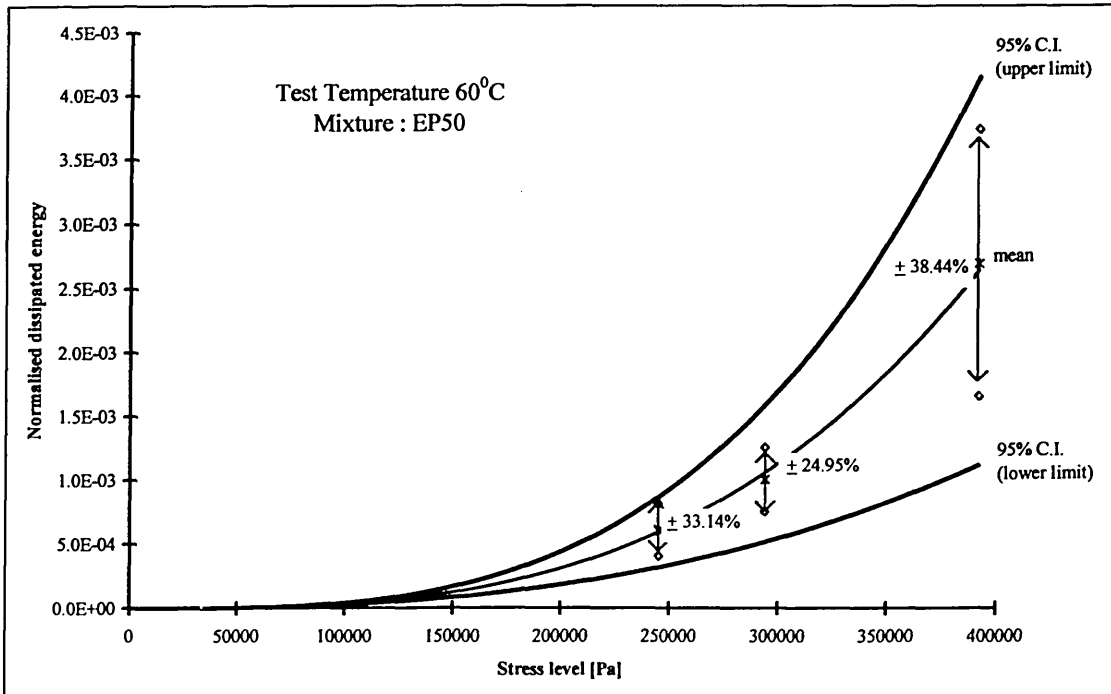


Figure 7.28 Variability of the normalised dissipated energy, showing the percentage variations, 95% Confidence Interval, and mean values, for mixture EP50 at 60°C.

### 7.5.3 Dissipated energy and the resistance to permanent deformation

Good correlations have been found between the normalised dissipated energy and the strain rate at different test temperatures ( $R^2 = 0.9371$  and  $0.9481$  at  $45$  and  $60^\circ\text{C}$  respectively). Figure 7.29 shows that there is no significant difference in the relationships between the normalised dissipated energy and the strain rate measured at  $45^\circ\text{C}$  and  $60^\circ\text{C}$ . The strain rate is produced from the accumulation of irrecoverable strain after load removal each cycle. The dissipated energy per cycle is derived from the total stress and strain developed during each load application, and therefore, represent the complete viscoelastic behaviour of the material under loading. The dissipated energy analysis is certainly more complicated. The good correlation between the strain rate and the normalised dissipated energy will support the current usage of strain rate method as a parameter of resistance to permanent deformation. Thus the strain rate can adequately represent the viscoelastic behaviour of bituminous materials under repetitive loading.

The permanent strain rates are determined in the region where the dissipated energy per cycle is constant, i.e. up to  $N_1$  cycles. The average linear regression coefficient obtained for the permanent strain rate, on the slopes of permanent strain and the number of load repetitions, is  $0.9950 \pm 0.0064$ . This condition brings some advantages that:

1. The end of the linear (constant rate of deformation) region, i.e. at  $N_1$  cycles, can be accurately defined.
2. A guarantee that the analysis is always performed in the linear region.

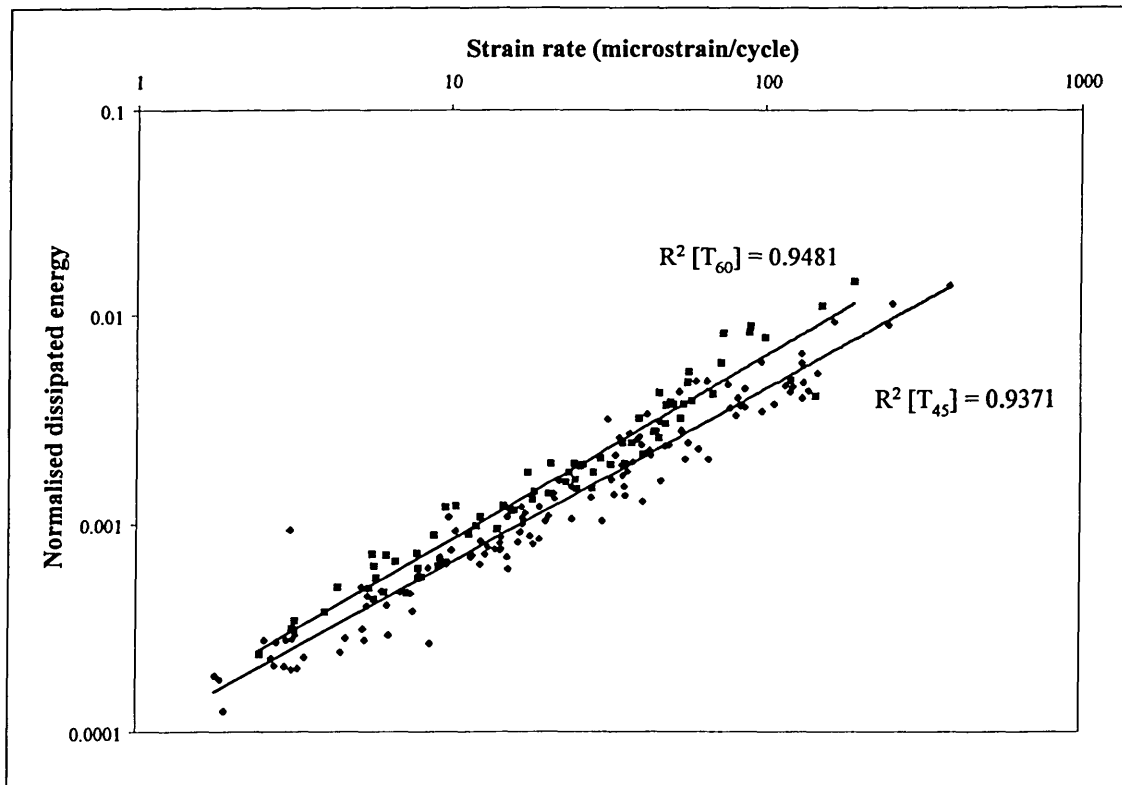


Figure 7.29 Correlation between normalised dissipated energy and strain rate in dynamic creep tests for all mixtures at two test temperatures.

The air void in the mixtures also significantly affect the normalised dissipated energy (Figure 7.30 and Figure 7.31). The higher the air void level, the higher the normalised dissipated energy. This also implies the higher the strain rate, and hence, lower resistance to permanent deformation. The ranking performance given by these figures indicate that the EVA modified mixture has the highest resistance to permanent deformation, then followed by SBS and SBR modified mixtures. Results also show that the polymer modified mixtures are not so sensitive to changes as unmodified binders in the strain rate and/or in the normalised dissipated energy at air void content between 3% to 5%. It is usually difficult in the field construction/compaction work to achieve a certain air void level, especially if the permissible range of target air void level is too tight. Therefore, the polymer modification can provide greater flexibility and tolerance in the permissible range of target air void level during construction.

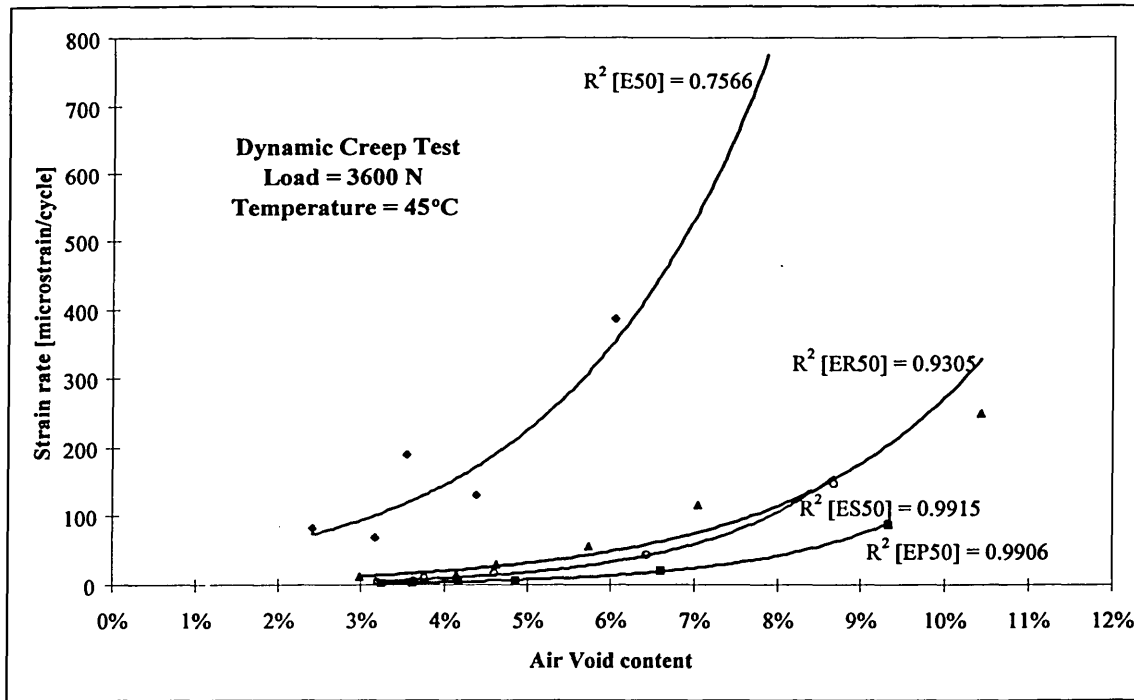


Figure 7.30 Effect of air void content on the strain rate in dynamic creep tests for mixtures with 50 pen bitumen as the base binder.

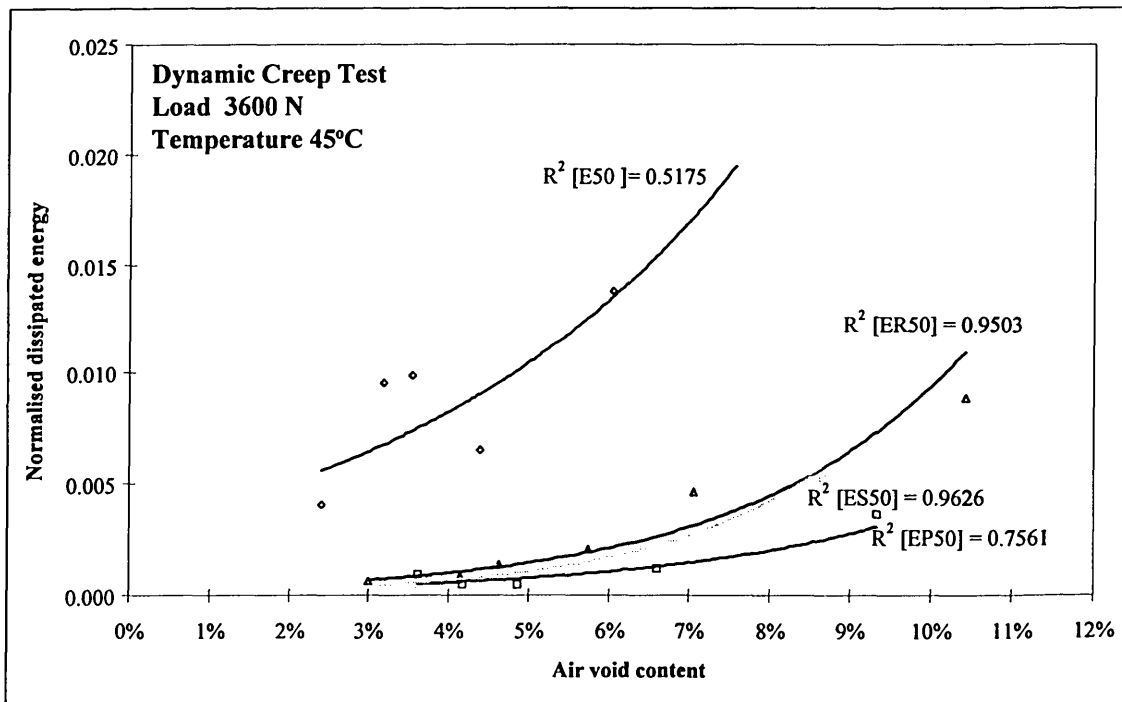


Figure 7.31 Effect of air void content on the normalised dissipated energy on dynamic creep testing for mixtures with 50 pen bitumen as the base binder.

#### 7.5.4 Dissipated energy and the wheel-tracking test

Good to fair correlations have been observed between the normalised dissipated energy obtained from the dynamic creep test and the wheel-tracking test results. The best correlation between wheel-tracking results and the normalised dissipated energy at both test temperatures (45 and 60°C) were obtained by dynamic creep specimens tested at a stress level of 196 kPa (Figure 7.32 and Figure 7.33). The correlations dropped if the specimens in dynamic creep tests were subjected to stress levels higher than 196 kPa, as observed from experiments at two test temperatures. Similar conditions are also observed in the relationship between the normalised dissipated energy and the wheel-tracking rut depth (Figure 7.34 and Figure 7.35). A possible explanation of this condition is that the dynamic creep test was conducted in an unconfined condition. A high applied stress in the dynamic creep testing may produce load-response behaviour which is very different from the wheeltracking. This may be due to the viscoelastic response of the unconfined specimen in which this can lead to a higher value of Poisson's ratio. On the other hand, the wheeltracking specimen has fixed boundaries which create a confined condition, and therefore the Poisson's ratio can be lower than that in unconfined condition. The effect of confining pressure towards the Poisson's ratio has been reported by Snaith [28]. Therefore, if the Poisson's ratio developed during the dynamic creep test is too much higher than that of the wheeltracking test, then the result may not be well correlated. Even though there was a possibility that the correlations between wheel-tracking results and the normalised dissipated energy could be higher at stress levels lower than 196 kPa, this procedure could not be applied at 45°C test temperature. The main difficulty when applied stress levels lower than 196 kPa was due to the limitation of the software, i.e. some specimens have not failed up to the maximum number of load applications available by the dynamic creep software (10000 pulses). Therefore, modification of the software may be required and for the analyses purpose, a stress level of 196 kPa is adopted by the Author as the standard stress level. Furthermore, running a test for longer than 10000 load applications is so time consuming (more than 5.6 hours).

The ranking performance given by the normalised dissipated energy and the wheel-tracking rate given in Table 7.15. The results indicate that the ranking performance

provided by the two tests are more or less similar. However, the wheel-tracking test seems to be more sensitive to changes in mixture properties and can differentiate the relative performance of mixtures with different binder types more accurately. This is shown by the consistency of results obtained at both test temperatures.

*Table 7.15 Ranking performance to the resistance to permanent deformation of the dynamic creep (at stress level of 196 kPa) and the wheel-tracking specimens.*

Ranking Performance	Normalised dissipated energy		Wheel-tracking rate	
	T=45°C	T=60°C	T=45°C	T=60°C
Better  Worse	EP50	EP50, ES50	ES50	ES50
	ES50	ER50, FS100	FS100	EP50
	ER50	FR100	EP50	FS100
	FS100	E50	ER50	ER50
	E50, FR100	F100	FR100	FR100
	F100		E50	E50
		F100	F100	

Figure 7.36 indicates that test temperature may not affect the relationship between the normalised dissipated energy and the wheel-tracking rate. However with wheel-tracking rut depth (Figure 7.37), more variability was found in the analyses on wheel-tracking rut depth which may mean that the rut depth is more sensitive to certain factors. Nevertheless, the overall results suggest that higher dissipated energy is correlated with lower resistance to permanent deformation as indicated by the wheel-tracking rate.

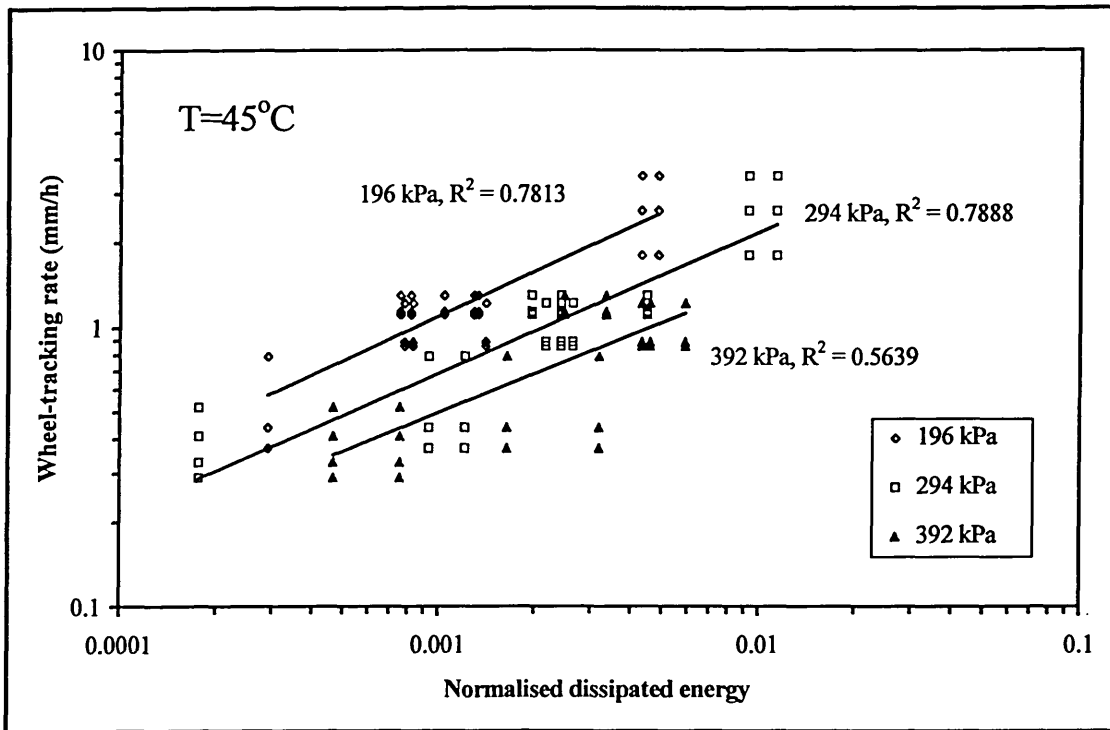


Figure 7.32 Relationship between the normalised dissipated energy from the dynamic creep test and the wheel-tracking rate for all mixtures. Test temperature  $45^{\circ}\text{C}$ .

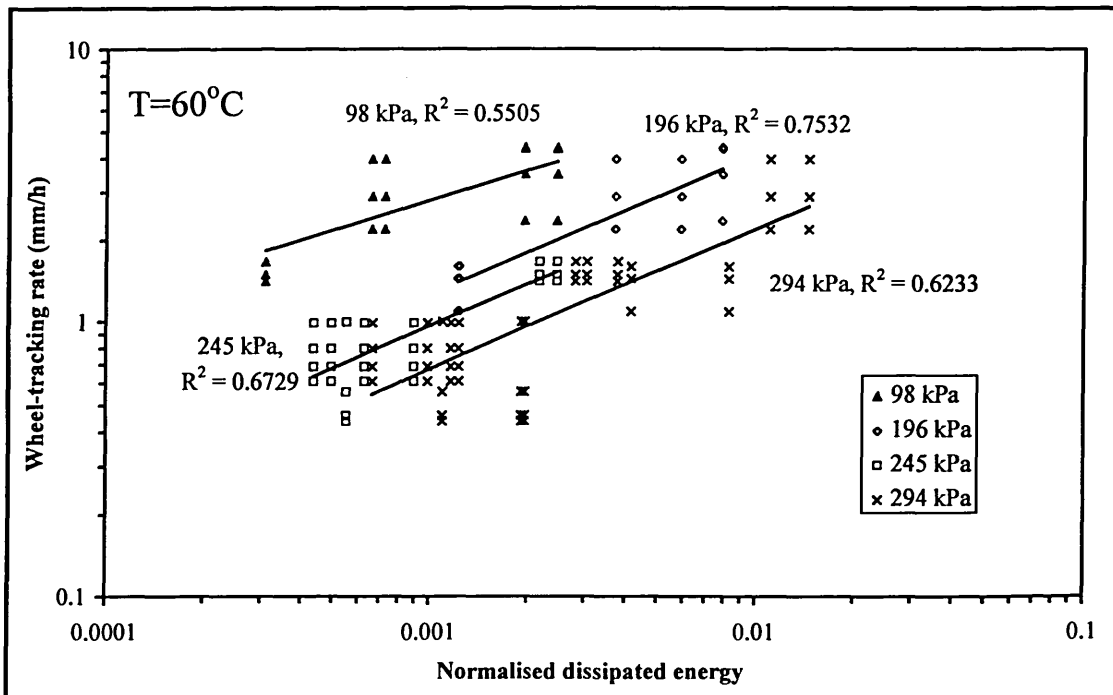


Figure 7.33 Relationship between the normalised dissipated energy from the dynamic creep test and the wheel-tracking rate for all mixtures. Test temperature  $60^{\circ}\text{C}$ .

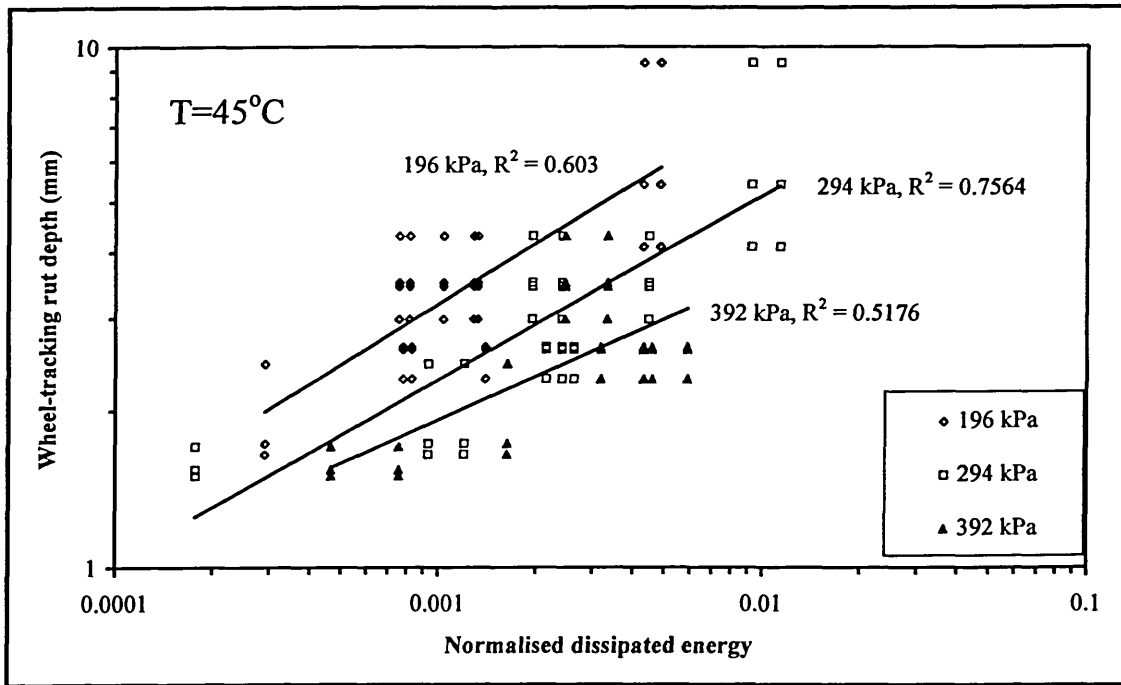


Figure 7.34 Relationship between the normalised dissipated energy from the dynamic creep test and the wheel-tracking rut depth for all mixtures. Test temperature 45°C.

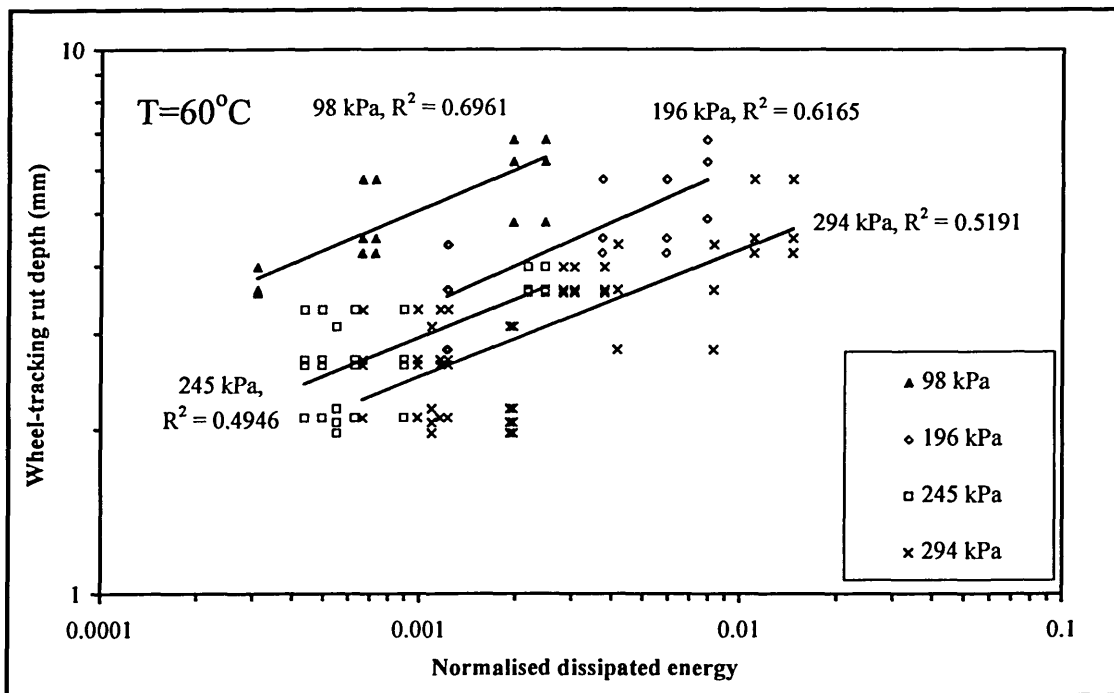


Figure 7.35 Relationship between the normalised dissipated energy from the dynamic creep test and the wheel-tracking rut depth for all mixtures. Test temperature 60°C.

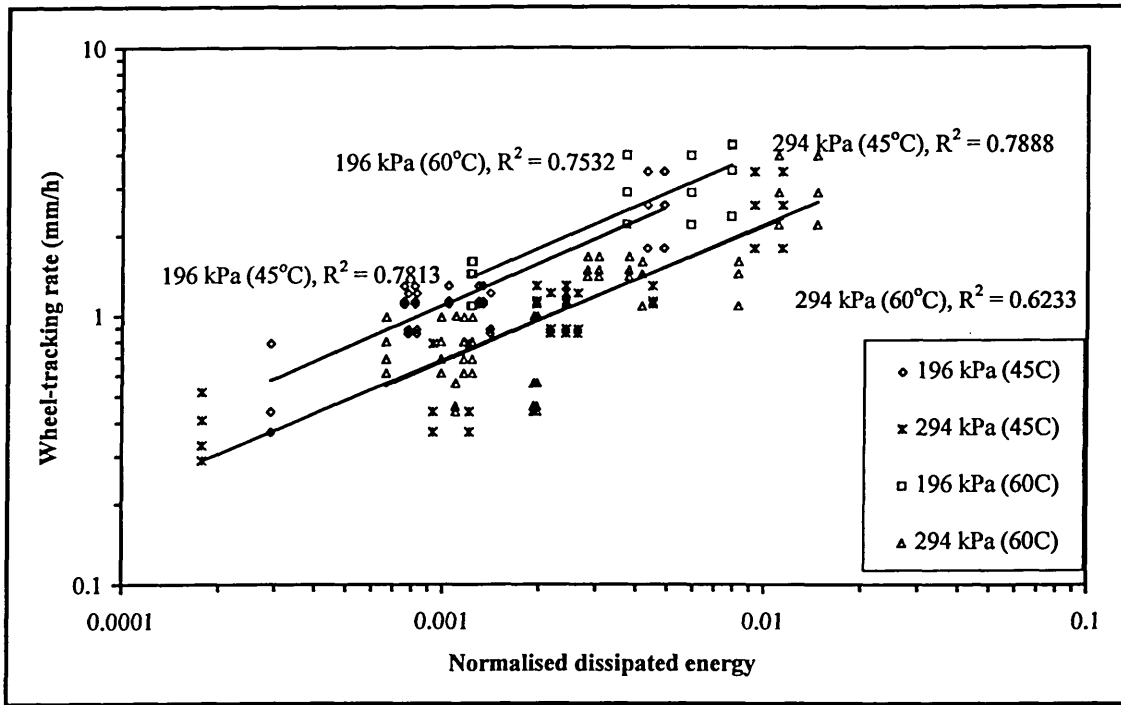


Figure 7.36 Relationship between the normalised dissipated energy from the dynamic creep test and the wheel-tracking rate, showing the effect of test temperature and applied stress.

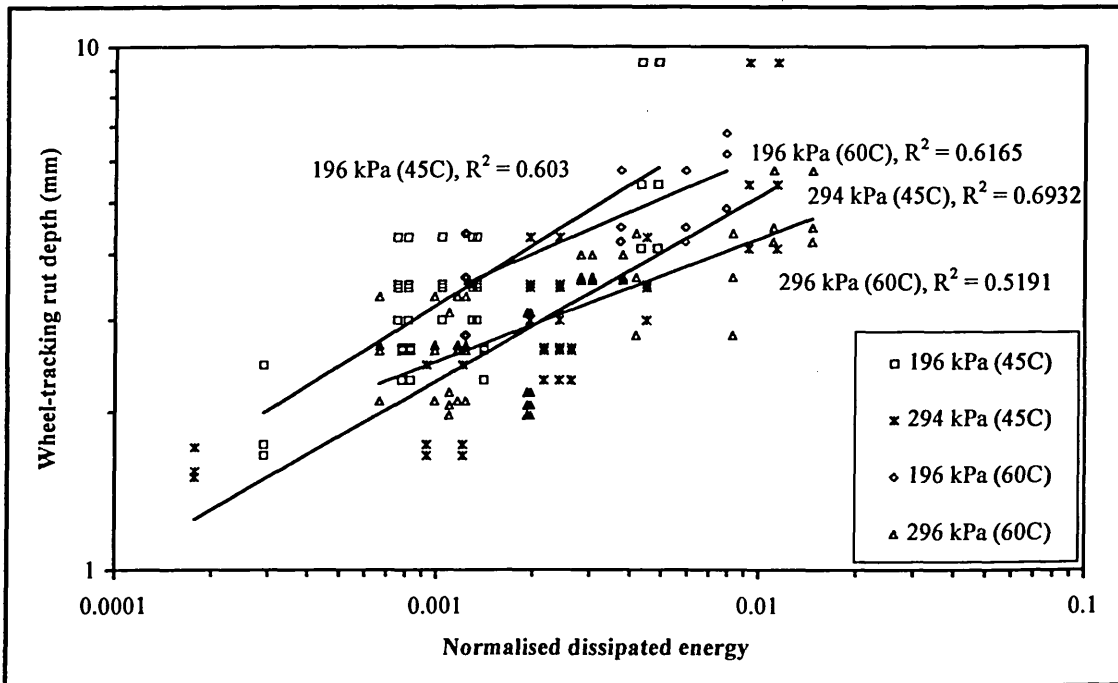


Figure 7.37 Relationship between the normalised dissipated energy from the dynamic creep test and the wheel-tracking rut depth for all mixtures, showing the effect of test temperature and the applied stress.

## ***7.6 Dilational Behaviour, Volumetric Deviatoric and Pavement Condition***

The exercise in this chapter has demonstrated the relationships between the resistance to permanent deformation and the dissipated energy. However, the major reservation on this exercise is the lack of confinement on the specimen during the dynamic creep testing. As reported in *Section 7.5.4*, viscoelastic response can be affected by the level of confinement. During traffic loading, a confining effect surrounding the wheelpath is developed and supports the traffic. Furthermore, the energy may not be dissipated uniformly through out the whole pavement structure under traffic loading. Therefore, it is necessary to know how the dissipated energy could be distributed in the pavement and contributes to development of pavement distress.

### **7.6.1 Dilational Behaviour and Volumetric Deviatoric Dissipated Energy**

Dilational characteristics of bituminous materials is a strain-related response, which usually occur under applied axisymmetric loading [29]. Its effect on permanent deformation is more pronounced at high temperatures as the bituminous materials become less elastic and are more compliant to generate a sufficient magnitude of strains to mobilise the dilational component of the materials. The deformation behaviour also depends upon the confining pressure as well as the deviatoric stress. The deviatoric stress produces an anisotropic distribution of bitumen film thickness which may lead to anisotropic behaviour on the mixtures where dilational behaviour can occur.

This dilational behaviour contributes a significant difference in the amount of energy dissipated by different types of loading, e.g. the energy dissipated in pure shear loading is greater than that of pure axial loading [30]. An analytical study by Cheung on the thin film behaviour of pure bitumens suggests a similar tendency, i.e. the bitumen stiffness is larger in compression than that in shear which leads to the greater creep dissipated energy rate in shear [29]. He also reported idealised micromechanical models on bituminous mixtures as demonstrated in Figure 7.38 and Figure 7.39, showing the effect of dilational rate at different bitumen film aspect ratio<sup>c</sup>, which suggest that there is no significant effect on creep dissipation rate contributed by shear components at film

---

<sup>c</sup> Bitumen film aspect ratio  $A_R$  is the ratio between the diameter and the thickness of the bitumen film [30].

aspect ratio more than 10. Therefore, Cheung claims that the estimation of creep surface can still be satisfactorily achieved by ignoring the shear components of the contact strains, provided that the bitumen film is very thin.

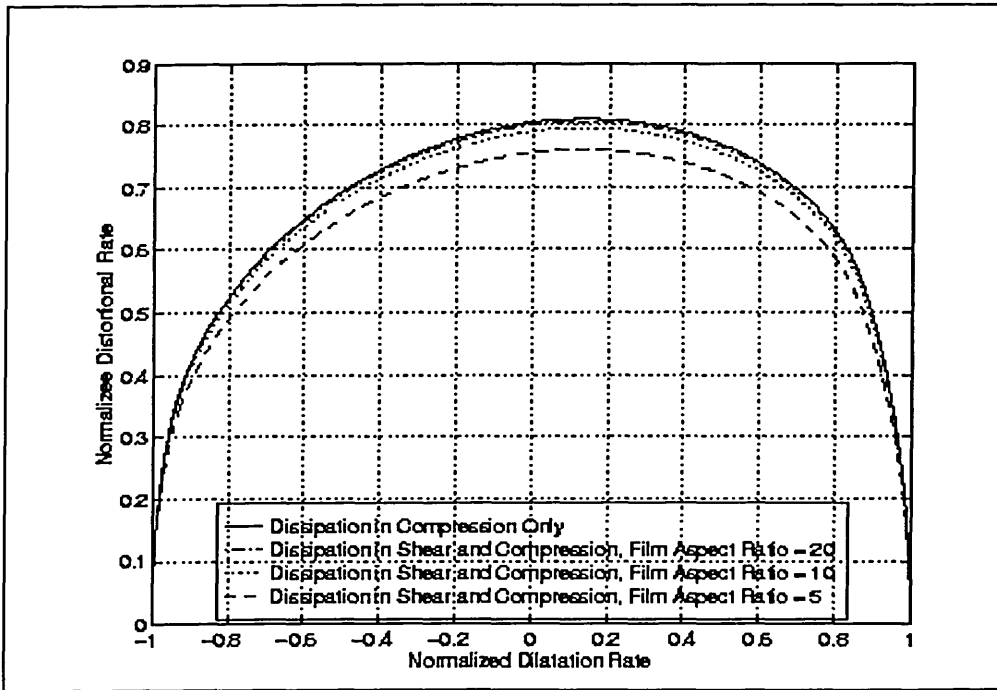


Figure 7.38 The normalised distorsional rate plotted against the normalised dilational rate at different bitumen film aspect ratio. After Cheung [29].

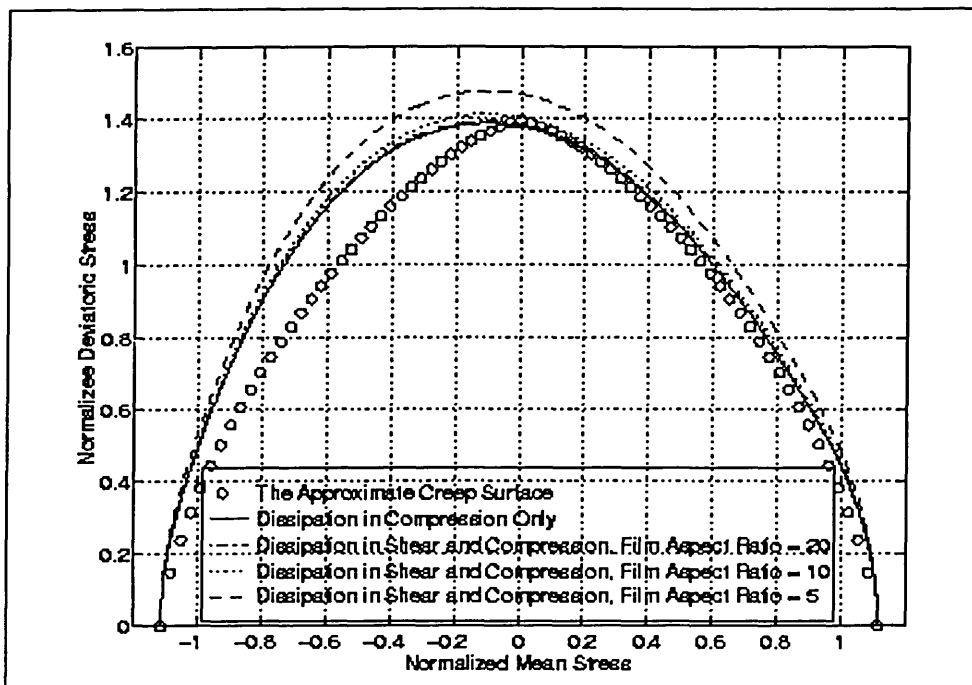


Figure 7.39 The normalised deviatoric stress plotted against the normalised mean stress at different bitumen film aspect ratio. After Cheung [29]

In the Author's work, the equivalent film thickness was estimated by Hveem method [1,31] as approximately  $8.454\mu\text{m}$ . However, it was not possible to determine an equivalent (representative) bitumen diameter to determine bitumen film aspect ratio ( $A_R$ ) -as suggested by Cheung- due to the variations of aggregate size (only single size aggregate was adopted in the Cheung's model) and hence, it is difficult to estimate the representative contact area of the aggregates. Therefore, if it was assumed that the film thickness is very thin, then the effect of shear would be negligible. However, this topic awaits further fundamental investigation.

### 7.6.2 Pavement Condition

There is, unfortunately, no information currently available on the measurement of energy dissipated by traffic loading on bituminous pavements which correlated with the pavement performance. On a smaller scale, however, laboratory pavement testing facilities (simulation) have been utilised to observe the energy developed under the wheel loading and viscoelastic analyses were utilised to generate dissipated energy plots in the pavement [32, 33]. These studies commonly agreed that the highest energy was dissipated at the bottom of bituminous layers, but a significant amount of energy is also dissipated at the pavement surface (Figure 7.40). This implies that the distortion distress can occur at both sides of the bituminous layers.

Previous reports [32, 33] suggest that this distress is manifested by the occurrence of surface cracking and/or cracks which initiate from the bottom of bituminous layers and propagate in form of fatigue cracking. However, it should be noted here that their experiments were conducted at ambient or lower temperatures where fatigue cracking is usually regarded as the major distress which leads to pavement damage. Nevertheless, an analytical approach developed by Cheung [29] and the results presented in this thesis (in which tests were undertaken at high temperatures) suggest that energy is also dissipated during the process of deformation (creep) of bituminous materials.

There are some currently available measurement techniques which can be adapted to measure the energy dissipated in bituminous pavements, such as wave propagation (e.g.

COLIBRI system, SASW method) and deflection tests (e.g. Falling Weight Deflectometer) [34]. The dissipated energy can be expressed by the material damping<sup>f</sup> as stated by Mamlouk [35] that “*material damping refers to the internal energy dissipation (viscous effect) which occurs in real materials subjected to dynamic loading*”. Mamlouk also reported that typical damping ratios of pavement materials range from 2 to 10%. Therefore, further assessments on bituminous pavements with known performance, or at a smaller scale (e.g. laboratory pavement testing facility), may need to be undertaken to take into account the permanent deformation in relation with the energy dissipated during the traffic loading.

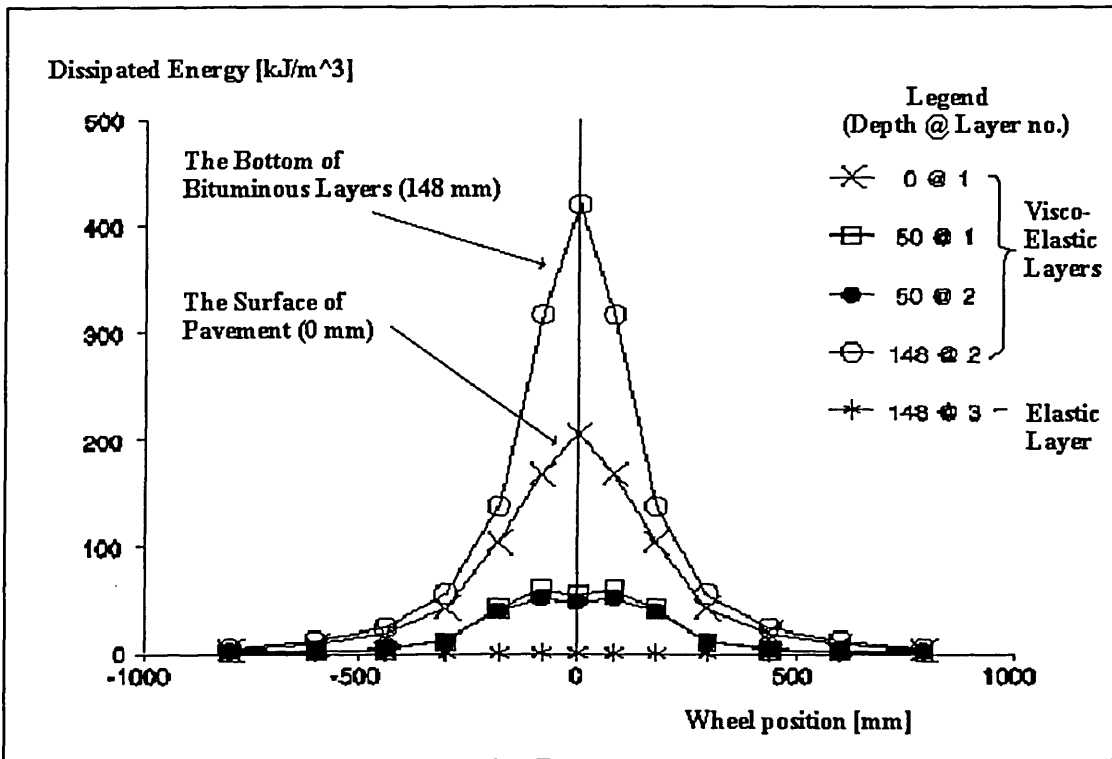


Figure 7.40 Dissipated energy versus transversal distance, for several depths. After Hopman [33].

### 7.7 Concluding remarks

The use of softening point as a binder predictor to permanent deformation of bituminous mixtures, especially when using polymer modified binder, should be avoided. The SHRP binder parameter of  $|G^*|/\sin\delta$  may not be suitable for predicting performance of

<sup>f</sup> Material damping is the ratio between the energy dissipated and the energy recovered during deformation process.

some polymer modified bituminous mixtures with regard to the resistance to permanent deformation. The zero shear-rate viscosity of the binder seems to be a reliable tool as a performance predictor to permanent deformation of bituminous mixtures, and may be applied for both unmodified and polymer modified materials.

Despite its complexity, the dissipated energy method could provide a wide range of information on the fundamental properties of viscoelastic materials, not only for an assessment of crack propagation or fatigue cracking but can also be adopted to assess the resistance to permanent deformation. Furthermore, the use of the dissipated energy method is capable of determining the point at which the deformation starts to deteriorate (point  $N_{1,}$ ), and supports the analysis based upon the strain rate technique for characterisation of the resistance to permanent deformation of bituminous mixtures.

Further work is necessary to investigate the phenomena of energy dissipation in the bituminous pavements, and to correlate them with the pavement performance. Currently available measurement techniques which are commonly used for monitoring pavement performance can be adapted for this purpose.

## ***7.8 References***

- 1 Whiteoak, D., "The Shell Bitumen Handbook", Shell Bitumen UK, 1990.
- 2 Anon, "Hot Rolled Asphalt for Roads and Other Paved Areas. Part 1. Specification for Constituent Materials and Asphalt Mixtures", British Standard 594: Part 1, 1992.
- 3 Anon, "Sampling and Examination of Bituminous Mixtures for Roads and Other Paved Areas. Part 107. Method of Test for the Determination of the Composition of Design Wearing Course Rolled Asphalt", British Standard 598: Part 107: 1990.
- 4 Anon, "Hot Rolled Asphalt Wearing Course. Performance-related Design Mix", UK Highways Agency Clause 943, Draft No. 4.0, 5 July 1996.
- 5 Szatkowski, W.S., "Rolled Asphalt Wearing Courses with High Resistance to Deformation", Proceedings of the Conference on the Performance of Rolled Asphalt Surfacing, London, 16 October 1979.

- 6 Fordyce, D., "The Compaction Mechanism of Rolled Asphalt and Its Influence on Material Design", Euroasphalt & Eurobitume Congress, 1996.
- 7 Gibb, J.M., "Evaluation of Resistance to Permanent Deformation in the Design of Bituminous Paving Mixtures" PhD Thesis, University of Nottingham, 1996.
- 8 Sousa, J.B., Deacon, J.A., and Monismith, C.L., "Effect of Laboratory Compaction Method on Permanent Deformation Characteristics of Asphalt-Aggregate Mixtures", Proceedings of AAPT, Vol. 60, 1991, pp. 533-585.
- 9 Anon, "The Percentage Refusal Density Test", Transport and Road Research Laboratory, TRRL Contractor Report No 1, Department of Transport, 1987.
- 10 Brown, S.F., Preston, J.N., and Cooper, K.E., "Application of New Concepts in Asphalt Mix Design", Proceedings of AAPT, Vol. 60, 1991, pp. 264-286.
- 11 Anon, "The Asphalt Handbook", Asphalt Institute Manual Series No.4, 1989.
- 12 Anon, "Methods for Determination of Maximum Density of Bituminous Mixtures", British Standard Draft for Development 228: 1996.
- 13 Claxton, M., Lesage, J., Planque, L., "When Can Bitumen Rheological Properties Be Used Successfully to Predict Asphalt Mix Performance?", Euroasphalt & Eurobitume Congress, 1996.
- 14 Bahia, H.U., and Anderson, D.A., "The New Proposed Rheological Properties of Asphalt Binders: Why Are They Required and How Do They Compare to Conventional Properties", Physical Properties of Asphalt Cement Binders, ASTM STP 1241, John C. Hardin, Ed., ASTM, Philadelphia, 1995, pp. 1-66.
- 15 Sybilsky, D., "Zero-shear viscosity Phenomenons at Measurement, Intrepretation, and Relation to Permanent Deformation", Eurobitume & Euroasphalt Congress, 1996.
- 16 Phillips, M.C., and Robertus, C., "Binder Rheology and Asphaltic Pavement Permanent Deformation, The Zero-shear Viscosity", Eurobitume & Euroasphalt Congress, 1996.

- 17 Jacobs, F.A., "Hot Rolled Asphalt: Effect of Binder Properties on Resistance to Deformation", TRRL LR 1003, 1981.
- 18 King, G.N., King, H.W., Harders, O., Chavenot, P., and Planche, J.P., "Influence of Asphalt Grade and Polymer Concentration on the High Temperature Performance of Polymer Modified Asphalts", Proceedings of AAPT, Vol. 61, 1992, pp. 29-66.
- 19 Ellis, C., Widyatmoko, I., and Read, J.M., "The Storage Stability and Behaviour of Polymer Modified Binders", Proceedings of the 2<sup>nd</sup> European Symposium on the Performance and Durability of Bituminous Mixtures, J.G. Cabrera (Editor), Leeds, April 1997, pp. 133-148.
- 20 Sybilski, D., "Non-Newtonian viscosity of polymer modified bitumens", Materials and Structures, Vol. 26, 1993, pp. 15-23.
- 21 Petersen, J.C., Robertson, R.E., Branthaver, J.F., Harsberger, P.M., Duvall, J.J., Kim, S.S., Anderson, D.A., Christiansen, D.W., Bahia, H.U., "Binder Characterization and Evaluation", Volume 1, SHRP-A-367, Strategic Highway Research Program, National Research Council, Washington, D.C., 1994.
- 22 Leahy, R.B., Monismith, C.L., and Lundy, J.L., "Performance-Based Properties of Asphalt Concrete Mixes", Engineering Properties of Asphalt Mixtures and the Relationship to their Performance, ASTM STP 1265, Gerard A. Huber and Dale S. Decker, Eds., American Society for Testing and Materials, Philadelphia, 1995.
- 23 Phillips, M.C., "Developments in Specifications for Bitumens and Polymer-Modified Binders, Mainly from a Rheological Point of View", Proceedings of the 2<sup>nd</sup> European Symposium on the Performance and Durability of Bituminous Mixtures, J.G. Cabrera (Editor), Leeds, April 1997, pp. 3-18.
- 24 Ferry, J.D., "Viscoelastic Properties of Polymers", 3<sup>rd</sup> Edition, John Wiley and Sons, 1980.
- 25 Anon, "Methods of Test for The Determination of Wheel-tracking Rate", British Standard 598: Part 110: 1996, BSI London.

- 26 Tayebali, A.A., Goodrich, J.L., Sousa, J.B., Monismith, C.L., "Relationship Between Modified Asphalt Binders Rheology and Binder-Aggregate Mixture Permanent Deformation Response", Proceedings of AAPT, Vol. 60, 1991, pp. 121-158.
- 27 Ulmgren, N., "Functional Testing of Asphalt Mixes for Permanent Deformation by Dynamic Creep Test. Modification Method and Round Robin Test", Euroasphalt & Eurobitume Congress, 1996.
- 28 Snaith, M.S., "Deformation Characteristics of Dense Bitumen Macadam Subjected To Dynamic Loading", PhD Thesis, University of Nottingham, 1973.
- 29 Cheung, C.Y., "Mechanical Behaviour of Bitumens and Bituminous Mixes", PhD Thesis, University of Cambridge, 1995.
- 30 Alavi, S.H., and Monismith, C.L., "Time and Temperature Dependent Properties of Asphalt Concrete Mixes Tested as Hollow Cylinders and Subjected to Dynamic Axial and Shear Loads", Proceedings of the Association of Asphalt Paving Technologists, Vol. 63, 1994, pp. 152-181.
- 31 Anon, "The Asphalt Handbook", Asphalt Institute Manual Series No.4 (MS-4), 1989.
- 32 Rowe, G.M., "Application of The Dissipated Energy Concept to Fatigue Cracking in Asphalt Pavements", PhD Thesis, University of Nottingham.
- 33 Hopman, P.C., "A Visco-elastic Analysis of Asphalt Pavements UsingVEROAD", Euroasphalt & Eurobitume Congress, 1996.
- 34 Von Quintas, H.L., Bush, A.J., and Baladi, G.Y., "Nondestructive Testing of Pavements and Backcalculation of Moduli", Second Volume, ASTM STP 1198, 1994.
- 35 Mamlouk, M.S., "Dynamic Analysis of Multilayered Pavement Structures - Theory, Significance, and Verification", Six International Conference on Structural Design of Asphalt Pavements, 1987, pp. 466-474.

# *Chapter Eight*

## **8. Discussions**

### ***8.1 Problems With Binder Characterisation***

The previous chapters have presented some of the factors affecting the performance of bituminous mixtures, where the performance can be enhanced by addition of polymer modifiers. Some conventional assessment techniques for bitumen are not applicable for some polymer modified binders. The reasons have been explained by the fact that the addition of polymer changes the microstructure of bitumens and consequently affects the mechanical properties and performance of the modified binders. Presentations and the discussion in *Chapter Three* demonstrate that the characteristics of polymer modified binders vary according to the characteristics of the polymer and the base binder (the unmodified bitumen). Bitumens have properties close to thermoplastic polymers (plastomers), i.e. they soften on heating and stiffen on cooling. Therefore, most of the established bitumen testing procedures (such as penetration and softening point tests) are applicable for assessing modified binders with thermoplastic polymers but problems with their applicability may be found with modified binders with polymers other than thermoplastics, such as those with elastomers.

#### **8.1.1 Limitations of Empirical Tests**

Anomalous behaviour of some modified binders can be observed when undertaking tests for empirically determining temperature susceptibility on elastomeric modified binders, e.g. based on penetration and ring and ball softening point tests. Application of these tests to unmodified bitumens usually results in a condition in which an increase of penetration value is followed by a reduction in softening point temperature. However,

this condition may not be found in some elastomeric modified binders. This study revealed that binders with high penetration values may also possess high softening point temperatures as in the case of top sections of an unstable SBS modified 50 pen after storage stability testing where the polymer phase in the binder becomes more dominant (*Chapter Six*). This phenomenon can also be demonstrated by using dynamic mechanical testing in that the increase of elasticity as shown by the phase angle of the binder leads to the increase of the softening point temperatures whereas at the same time the binder exhibits a reduction in the stiffness value as shown by the complex stiffness modulus which leads to the high penetration value. A three dimensional network structure which is normally found on SBS modified binders may be responsible for this behaviour. This structure resists the binder deformation by increasing molecular entanglement leads to a higher elasticity (if the binder is rolled like a ball and is let to free fall from a certain distance, it will bounce back) and cohesivity (the binder will not stick on glass, metal or wooden surface). Therefore, the binder will remain very elastic as long as the structure has not been broken. However, it loses its strength rapidly if the structure is broken (e.g. by tearing off the binder or by needle during a penetration test).

Based on these facts, therefore, there is a possibility that either one of these tests or both of them is no longer suitable for assessing polymer modified binders. The Author believes that both tests should be used very carefully when dealing with polymer modified binder by the following considerations:

1. The ring and ball softening point test which was originally developed for pure bitumen, as a thermoplastic material, to observe gradual changes from a semi-solid (high viscosity) liquid to a low viscosity liquid on the application of heat, may no longer be applicable if the modified binder does no longer behave as a thermoplastic material.
2. Theoretically, penetration test also empirically represents viscosity of bitumens for bitumens showing pure viscous flow (Newtonian liquids) when subjected to deformation [1]. The higher the penetration, the lower the viscosity. However, some polymer modified binders demonstrate non-Newtonian behaviour at high service temperature. Therefore, this correlation may not be valid when dealing with some polymer modified binders which do not behave as Newtonian liquid under deformation.

Limitations on the use of ring and ball softening point or penetration test are due to its empirical nature in representing the viscosity of bitumen. Consequently, why was a new technique proposed using more complicated rheological terms, e.g. complex modulus and phase angle, rather than promoting assessment based on viscosity? Furthermore, this new technique has been found unreliable in correlating the performance of some polymer modified binders to their mixture performance. The Author believes that the use of viscosity, the zero shear viscosity in particular, is a better way to predict mixture resistance to permanent deformation from the binder characteristics (Figure 7.10) [2,3,4]. Nevertheless, the analysis using dynamic mechanical analysis (DMA), *even though the parameter  $|G^*|/\sin\delta$  cannot be used a reliable binder predictor to resistance to permanent deformation of bituminous mixture*, still provides wide range of information on the viscoelastic properties of bituminous materials which is beneficial in studying the response behaviour of polymer modified materials.

### **8.1.2 Dynamic Mechanical Analysis (DMA)**

The simplest assessment technique using DMA is by developing Black curves. A Black curve can be used as a fast, simple and reliable technique for quality control purposes. Change of composition or variation in the structure of a bituminous binder caused by processing, ageing, or polymer addition can be demonstrated by plotting Black curves of observed samples against their reference binders.

A more comprehensive analysis using DMA can be carried out by developing master curves of complex modulus and/or phase angle as a reliable data extrapolation technique. Response and behaviour of bituminous mixtures under different temperature and loading times can be monitored, and to a certain extent be correlated to mixture performance. Accordingly, temperature susceptibility of bituminous binders can be better represented using this technique.

Complex modulus  $|G^*|$  may be a good representative of the viscoelastic behaviour of bituminous materials. However, it should be well understood that the analysis of binders using  $|G^*|$  alone is not sufficient and can be misleading as some materials may have the

same  $|G^*|$  value but exhibits different elasticity (or viscosity). Therefore, the additional information of phase angle as a measure of viscoelasticity is also necessary.

The main obstacles anticipated in promoting the use of such a rheological approach for industrial practices are the availability of the equipment, knowledge of the assessment technique, simplicity and practicability. Unlike the established penetration and ring and ball softening point tests, a dedicated laboratory with appropriate technical support is required. Therefore, this technique will be very costly and this may be the price that should be met by the industry and their clients for obtaining more reliable and precise performance related information.

## ***8.2 Mechanism Interaction of Polymer-Bitumen Blends***

In most cases, a two-phase system is found in a polymer modified binders where the polymer is dispersed in the bitumen. Observation under UV Fluorescent microscope indicates that the state of dispersion has a significant influence on the level of storage stability of the polymer modified binders. Polymer modified binders with a coarser state of dispersion tend to experience instability in hot storage and consequently, affect the physical properties of the binders. Therefore, the storage stability test becomes essential for polymer modified binders.

### **8.2.1 Molecular Entanglements**

Several possibilities about the role of the polymer in the mechanisms and interaction of polymer bitumen blends were presented in *Chapter Three*. Unfortunately, the observation under UV Fluorescent microscope was not able to reveal any information that supports or rejects any of these possibilities. However, the existence of a "network structure" can be recognised by carrying out DMA tests.

Molecular entanglements, as manifested by an existence of a plateau region in the complex modulus or phase angle, have been observed in the polymer modified binders. The molecular entanglements are generally attributed to the existence of a "network

structure” which is normally observed in polymeric materials, e.g. a more pronounced plateau region can be attributed to a stronger form of polymer “network”.

### 8.2.2 Role of the Base Binder

Even though, to a certain extent, the polymer plays a significant role in enhancing the performance of a modified binder, the base binder also has a significant influence on the end performance of the binder. Higher level of improvement was observed on the modification of a softer bitumen as opposed to the harder one. For example, the improvements on the wheeltracking rate (WTR) at 60°C due to the addition of the same level of SBS modifier (5% level) into two different base binders are as follows:

- (a). WTR of 100 Pen mixture (F100) = 17.25 mm/h  
WTR of SBS modified 100 Pen mixture (FS100) = 1.38 mm/h  
Level of improvement =  $17.25/1.38 = 12.53$  times
- (b). WTR of 50 Pen mixture (E50) = 4.07 mm/h  
WTR of SBS modified 50 Pen mixture (ES50) = 0.67 mm/h  
Level of improvement =  $4.07/0.67 = 6.10$  times

Others [5, 6] have also reported that the SBS copolymers were sensitive to the properties and source of the base binders (e.g. Venezuela, Middle East, Russia, *etc.*). These phenomena indicate the characteristics of the base binder is also accountable to the performance of polymer modified HRA mixtures.

### 8.2.3 Viscoelastic Behaviour of Modified Binders

Figure 8.1 demonstrates that there are three viscoelastic regions that can be observed from the Black curves of the studied binders. Binders in the zone I exhibit strong elasticity and the difference in the stiffness of different binders is very small. The different ranking of properties of different binders can be observed in the zones II and III where viscoelastic and viscous behaviour play the main roles in binder performance. The Author differentiates between zone II and III based upon the mechanisms of interaction of the polymers and their base binders. In zone II, the properties of both elements, i.e. the polymer and the base binder, have a mutual influence and contribute to

the enhanced performance of the blends. The contribution of the base binder reduces in the zone III where the polymer plays a dominant role in the properties of modified binders. Molecular entanglements, and hence the formation of a polymeric network to promote a better resistance to deformation is normally found or developed in zones II and III.

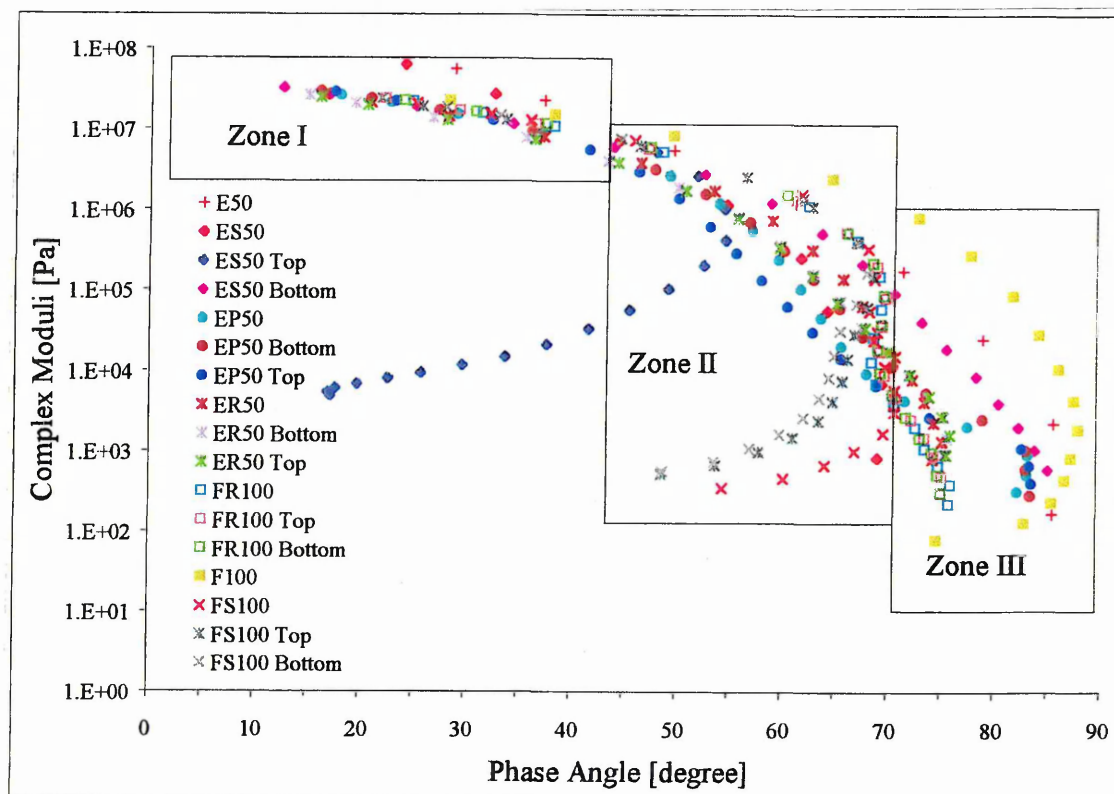


Figure 8.1 Black curves showing three zones of viscoelastic regimes. Temperature sweeps from 0 to 80°C at frequency of 1 Hz.

Table 8.1 demonstrates the properties of the viscoelastic zones observed from the studied binders. The Author named the third zone (zone III) as the “extended viscoelastic zone” as the viscoelastic behaviour of the binder can be maintained by the addition of polymer, i.e. by reducing the phase angle (and, hence, improving elasticity) of the modified binder, whilst unmodified binders start losing their elasticity and approach the viscous state when entering this zone. A clearer picture is demonstrated in

Figure 8.2 where some binders with similar PI values<sup>a</sup> exhibit different behaviour in the third zone.

*Table 8.1 Properties of the viscoelastic zones.*

Zone	Complex modulus G* (Pa)	Phase angle $\delta$ (degrees)	Predominant material behaviour
I	higher than $4 \times 10^6$	0 - 45	Elasticity
II	$10^2 - 10^7$	45 - 70	Viscoelasticity
III	less than $10^6$	70 - 90	Extended viscoelasticity

There are some phenomena that can be deduced from Figures 8.1 and 8.2, i.e.:

1. Black curves of different binders but with similar temperature susceptibility (PI value) are superimposed each other in zones I and II.
2. Polymers improve the viscoelasticity of the binders in zone III by lowering the phase angle.
3. The viscoelastic zones are predominantly affected by the phase angle. Nevertheless, the complex modulus (together with the phase angle) has also significant role for monitoring some changes in the consistency of the binders.

This classification of the viscoelastic zones should, however, be limited only for the studied binders. Further works on other types of bitumens or modified binders are necessary to obtain a wider applicability of the classification.

Binder ES50 obtained from the bottom section after stability test has a Black curve which is very close to the Black curve of the unmodified 50 pen (E50), even in zone III. This was due to the almost complete disassociation of polymer from the binder after the storage stability test leaving the base bitumen as dominant in this section. The evidence and discussion on this matter have been presented in *Chapter Six*.

---

<sup>a</sup> The PI values were determined based upon the standard penetration at 25°C and ring and ball softening point in accordance with the procedure laid down in *Chapter Six*.

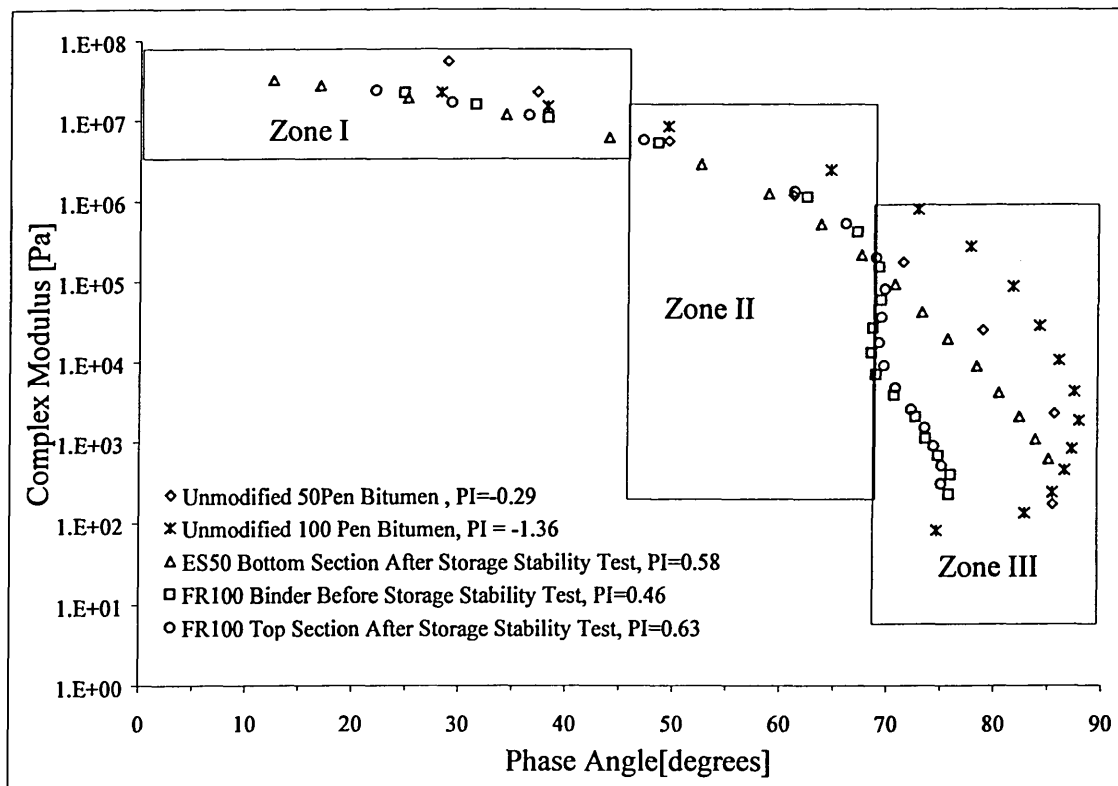


Figure 8.2 Black curves of binders with similar PI values (except for the unmodified 100 pen bitumen).

Finally, the DMA provides an indication that the addition of polymers always improve high temperature properties by increasing viscosity and complex stiffness modulus and reducing the maximum phase angle. However, The addition of polymers do not always benefit the low temperature properties of the modified binders as the polymers tend to increase the viscosity of the modified binders. An example has been presented that the addition of EVA copolymers into some 50 pen bitumens always results in the increase of stiffness throughout the temperature range as opposed to the unmodified 50 pen bitumens. However, the addition of polymers allow the use of softer bitumens to produce modified binders with higher stiffness at high temperature whilst maintaining the low stiffness at low temperatures. Hence, harder penetration grade bitumens can be replaced by softer modified binders to retain the advantages of high stiffness at high temperature but extending the low temperature properties by having lower stiffness at low temperatures (due to the use of softer bitumen as the base binder).

### 8.3 Performance of Polymer Modified Mixtures

The addition of polymers has no doubt contributed to the significant improvement of the performance of bituminous mixtures. Information provided in Chapters *Three*, *Six*, and *Seven* demonstrate that selection of appropriate polymer-bitumen blends increases the temperature range (or frequency range) where polymer modified mixtures perform satisfactorily as compared to the unmodified ones.

The ranking of phase angles obtained from the DMA of polymer modified binders shows good agreement with the ranking of the resistance to permanent deformation of the modified HRA mixtures, as demonstrated in Table 8.2. The binder-aggregate interaction contributes to improving the elasticity of the mixture. This can be observed by the lower value of the maximum phase angle of the mixture than the ones obtained from binder tests.

*Table 8.2 Comparison between the ranking performance obtained from the maximum phase angle and the resistance to permanent deformation of the binders and the mixtures.*

Binder or Mixture Code	Maximum Phase Angle (degrees)		Wheel-tracking rate of mixture at temperature 45°C (mm/h)
	Binder	Mixture	
ES50	70	35	0.4
FS100	70	N/A	0.5
EP50	85	31	0.7
ER50	80	33	0.9
FR100	76	N/A	1.0
E50	88	40	1.2
F100	88	N/A	2.6

*Note: N/A means that data are not available*

#### 8.3.1 Stiffness Modulus of Modified HRA Mixtures

Direct correlation between indirect tensile tests (ITSM) in the NAT machine and the DMA test cannot be carried out due to the difference in volumetric properties between ITSM and DMA specimens. Therefore, comparative analysis was conducted based upon two techniques:

1. Ranking of mixture stiffness from the both techniques indicates that the addition of polymer increases the stiffness of HRA mixtures with different level of improvements are found. The improvements from using polymer as obtained from ITSM test are summarised in Table 8.3 with the complete results presented in *Appendix D*, whereas DMA results as demonstrated by Figures 6.19 and 6.20 (*Chapter Six*) show that the addition of EVA and SBR on the 50 pen based mixtures increase the stiffness by 66% and the addition of SBS increases the stiffness by 34%, as compared with the unmodified 50 pen mixtures.
2. Adopting the Nottingham technique [7] to shift the value of elastic modulus (DMA) from the measured volumetric condition into the similar condition as ITSM specimens. The following relationship is adopted to accommodate the risetime of 120 milliseconds from the ITSM to its frequency equivalent of the DMA [8]:

$$f = \frac{1}{2 \pi t} = \frac{1}{2\pi(0.12)} = 1.3 \text{ Hz}$$

*Equation 8.1*

where :

$t$  = the loading time for ITSM (NAT) is 120 milliseconds (0.12 seconds)

$f$  = the equivalent frequency of the DMA

Van der Poel [9] was also suggested relationship similar to Equation 8.1 when he compared static loading and dynamic loading, i.e. the dynamic stiffness was found to be equal to the static one when he substituted the inverse value of angular frequency,  $1/\omega$ , ( $\omega = 2\pi \times \text{frequency}$ ), for the loading time,  $t$ .

The best agreement for the ITSM was found with testing from TRL when it was recalculated (1.35 Hz), whereas the uniaxial tension compression testing gave results from 0.8 - 1.4 Hz and the trapezoidal cantilever testing gave a value of 1.2 Hz [10], whereas RILEM reported that it was in a good agreement with a bending test at a frequency of 1 Hz [11]. These results gave fairly high confidence that the value of 1.3 Hz is correct (as given by Equation 8.1). Therefore, an equivalent frequency of 1.3 Hz was adopted.

The values of complex modulus  $E^*$  at 1.3 Hz were plotted on the charts of bitumen stiffness versus mixture stiffness provided in the Nottingham method (Figure 7 of Reference 7) at the corresponding volumetric values and then projected to the volumetric values of ITSM samples to get the estimated elastic modulus values. The comparison of the overall results between the ITSM and the “adjusted” DMA values ( $E^*_{\text{estimate}}$ ), as demonstrated in Table 8.4, indicates that the results from both testing arrangements are not significantly different at 5 per cent level. It must be noted here that these empirical relationships were only derived from unmodified bitumens. It is, therefore, very surprising. The detailed calculations are as follows:

*Method of analyses: t-test applied to paired comparison [12]*

Null hypothesis : there is no significant different in the results between the two testing procedure. If the null hypothesis is true than the distribution of t will be t-distribution with  $(k-1)$  degrees of freedom, as the estimated standard deviation  $s_d$  is calculated from  $k$  differences.

$$\text{Average difference } \bar{d} = 305$$

$$s_d^2 = \frac{\sum_{i=1}^k (d_i - \bar{d})^2}{k - 1} = 23706955$$

$$s_d = 4868.979$$

$$t_o = \frac{\bar{d}}{\frac{s_d}{\sqrt{k}}} = 0.125$$

The alternative hypothesis is that the pair results from the two procedures are not equal. Therefore, a two-tailed test is required. From the statistics table [12], it is found that  $t_{0.025,3} = 3.182$ . Thus,  $P(|t| > 3.182) = 0.05$ . As  $t_o$  is less than 3.182, the result is not significant at the 5 per cent level, and so there is a reasonable evidence that the null hypothesis is true. Therefore, there is no difference at 5% level of significant between the stiffness modulus measured by ITSM and DMA testing.

The overall results, however, show that the “adjusted” stiffness modulus ( $E^*_{\text{estimate}}$ ) values obtained from DMA testing are higher than those obtained from ITSM testing.

The procedure for DMA testing may be responsible for the higher stiffness modulus (as compared to the ITSM values) as the specimen was subjected to continuous frequency and temperature sweeps. This condition may cause the development of residual stress within the specimens caused by incomplete release of stress from previous loading leading to the high stiffness value.

Higher stiffness values for polymer modified mixtures indicate the improvement in the ability of the materials to distributing stresses occurring in bituminous pavements and therefore may contribute to increasing the crack initiation time of bituminous pavements at the particular loading and temperature condition.

*Table 8.3 Summary of improvements by the addition of polymer modifiers obtained from ITSM test.*

Base binder	Polymer modifier	Percentage increase of stiffness (refers to the stiffness of the base binder)
50 Pen	-	(reference for 50 pen based modified binders)
100 Pen	-	(reference for 100 pen based modified binders)
50 Pen	EVA	32%
50 Pen	SBR	55%
50 Pen	SBS	36%
100 Pen	SBR	48%
100 Pen	SBS	40%

*Table 8.4 Comparisons between ITSM results and the estimated elastic modulus ( $E'_{estimate}$ )*

Mixture	Reference	Measured value		Estimated value	
	ITSM [MPa]	VMA <sub>measured</sub>	E* <sub>measured</sub> [MPa]	VMA <sub>target</sub>	E* <sub>estimate</sub> [MPa]
E50	3200	28.14%	1650	20.11%	3500
EP50	4039	27.49%	2750	19.54%	5200
ER50	4744	27.41%	2750	20.50%	5000
ES50	4697	27.54%	2200	19.97%	4200

### 8.3.2 Performance of Polymer Modified Mixtures

Assessment of the performance of polymeric mixtures using the Marshall test procedure demonstrated that the addition of polymer into bituminous mixtures also always

improved the performance of the HRA mixtures. However, the test, as presented in *Chapter Seven*, failed to differentiate the benefits from using different polymers. Therefore, the Marshall test is not suitable for ranking performance of polymer modified HRA mixtures.

The sensitivity of the mixtures to the volumetric proportions, i.e. at air voids between 3-5%, their resistance to deformation, as measured by dynamic creep test, can be reduced by the addition of polymers (*Chapter Seven*). This condition can be beneficial during road construction where the variability of the final compaction is greater than in the laboratory. However, difficulties may still be expected during laying and compaction of polymer modified materials due to the viscosity being higher than for unmodified bitumen. Therefore, higher operational temperatures are required and specialised equipment may be necessary to prevent storage instability.

#### ***8.4 Application of The Dissipated Energy Method***

This study has proven that a certain amount of energy is dissipated during deformation of bituminous materials. The current understanding that dissipated energy method is beneficial for the determination of fatigue life has been extended to assessing the resistance to permanent deformation of bituminous mixtures. Factors that govern the level of dissipated energy in permanent deformation testing are different from those in fatigue testing. In fatigue testing, the dissipated energy is due to the parallel system of the dashpot and spring in a Burger's model. To the contrary, the dashpot in series with the spring of the model is the element which is responsible for dissipating energy during deformation.

It has also been presented that the energy method, by plotting hysteretic loops, can demonstrate that permanent deformation is influenced by repetitive loading and stress level. The repetitive loading governs the accumulation of damage towards the failure point, whereas the higher stress level leads to the higher dissipated energy per load cycle and accelerates the damage accumulation. Two key points have been observed,, i.e. repetitive loading and stress level. In summary, accumulation of damage can be retarded by decreasing stress level and/or reducing the number of load repetitions.

The normalised dissipated energy is well correlated with the strain rate in the region where the dissipated energy per cycle is constant, which indicates that the strain rate technique adequately represents viscoelastic response. Good correlation has also been found between the normalised energy and the wheel-tracking rate. However, the same good correlation can also be observed between the strain rate and the wheel-tracking rate, as demonstrated in Figure 8.3. This also indicates that the strain rate method, as a simple technique, is good enough as a performance parameter of resistance to permanent deformation of HRA mixtures.

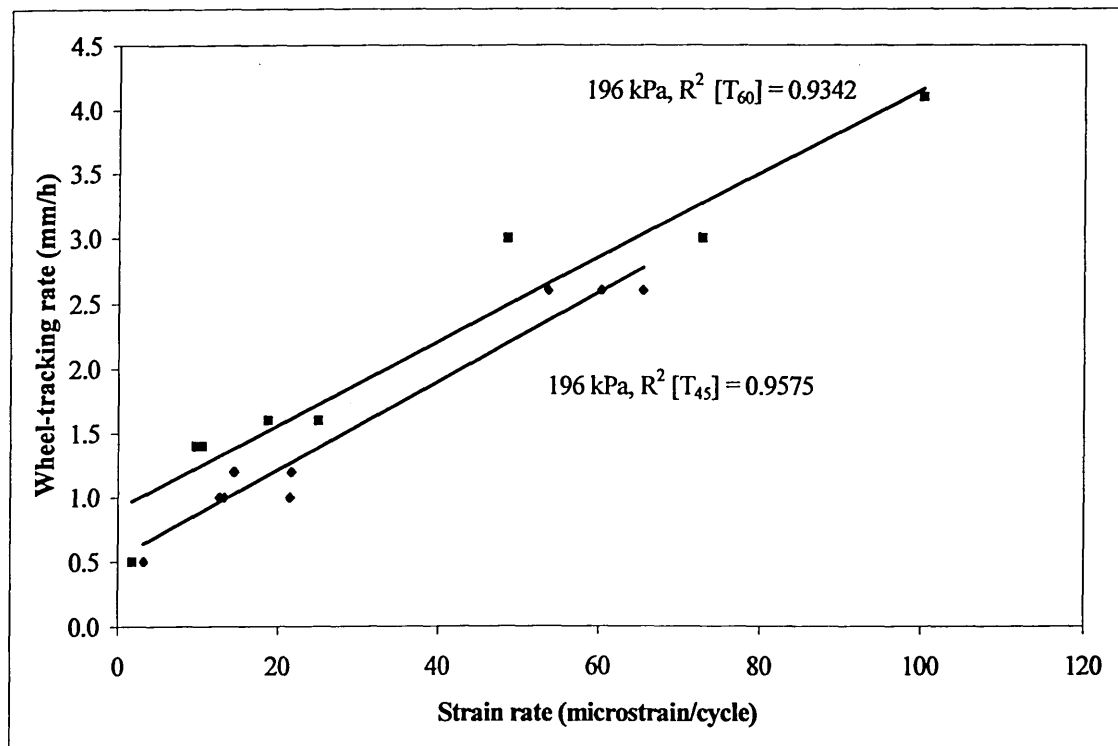


Figure 8.3 Relationship between strain rate and wheel-tracking rate at stress level of 196 kPa. Test temperatures are 45 and 60 °C.

Nevertheless, this study reveals important findings that:

- (i) *The point at which the permanent deformation starts to deteriorate, i.e. the point  $N_1$ , can be accurately defined by the dissipated energy method.*
- (ii) *A technique has been developed to identify the state of stability of a specimen whilst a test is progressing.*

This accurate definition of  $N_1$  ensures that the analysis is within the linear region where the specimen is mechanically stable and dissipated energy (or strain rate ) at a constant

rate. The analysis, which was presented in *Chapter Seven*, has shown that the strain rate can straightforwardly be determined in the linear region with a good accuracy, i.e. the coefficient of correlation of linearity ( $R^2$ ) is  $0.9950 \pm 0.00064$ . Therefore, a combined technique based upon the two methods can be developed. A routine for automatic analysis is described in Figure 8.4. Determination of some parameters in this routine follow the procedures developed by the Author which have been presented in *Chapter Four* but are rewritten for convenience. Description of the symbols refers to the definitions given in *Chapter Four*.

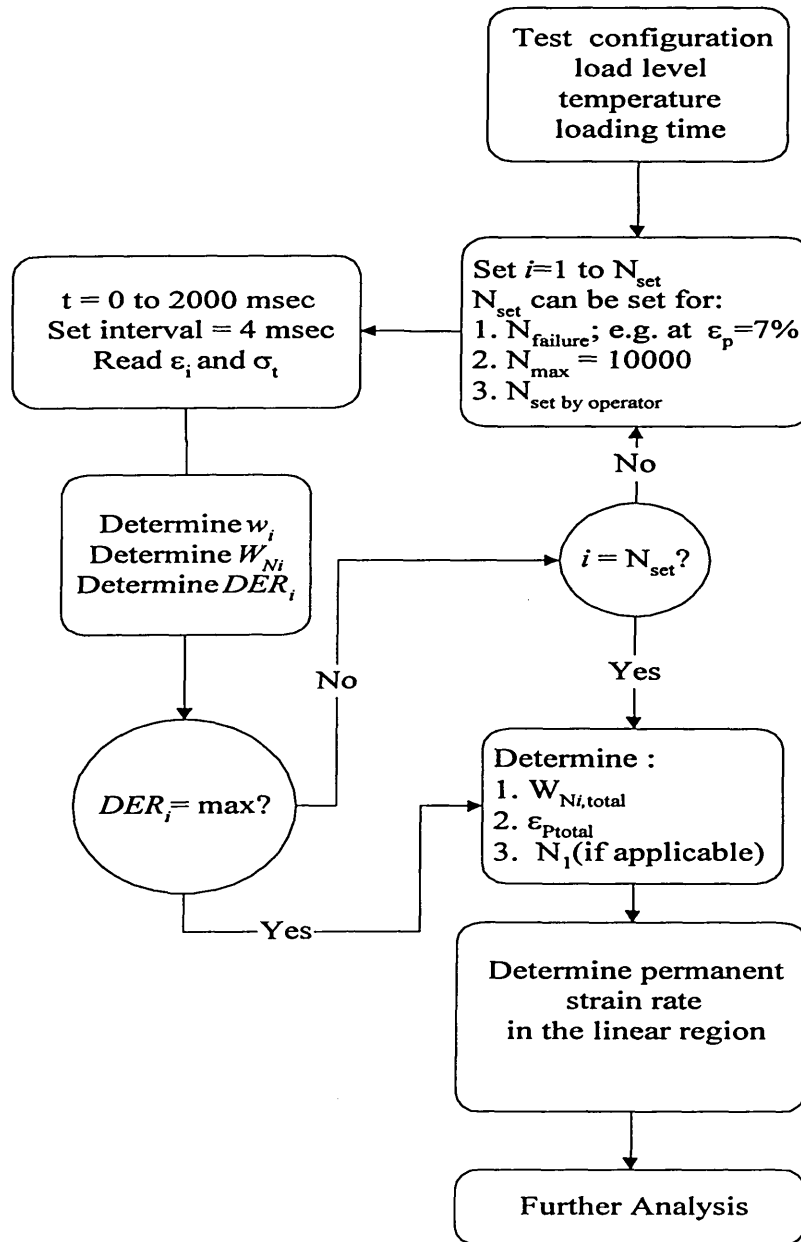


Figure 8.4 Flowchart for the analysis of permanent deformation.

Assessment procedure:

1. Determination of dissipated energy per cycle ( $w_i$ ):

$$w_i = \sum_{t=1}^{2000} \frac{(\sigma_t + \sigma_{t-1})}{2} (|\varepsilon_t| - |\varepsilon_{t-1}|)$$

*Equation 8.2*

2. Determination of cumulative dissipated energy ( $W_N$ ):

$$W_N = \sum_{i=1}^N w_i * n_i$$

*Equation 8.3*

3. Determination of dissipated energy ratio per cycle ( $DER_i$ ):

$$DER_i = W_N/w_i$$

*Equation 8.4*

4. Determination of  $N_i$  at the maximum  $DER_i$  (if applicable) or otherwise examination of whether  $DER_i/N_i \leq 1$  is conducted to ensure that the specimen is within linear region ( $N_i \leq N_I$ ).

*- see Chapter Four for details -*

5. Determination of permanent strain rate at the linear region ( $N_i \leq N_I$ ) by assuming that the first 100 load repetitions to be the compaction region (zone I):

$$\text{strain rate} = \frac{\varepsilon_{N_i} - \varepsilon_{100}}{N_i - 100}$$

*Equation 8.5*

6. Determination of permanent strain at the end of test where the specimen is still in the linear region ( $N_i \leq N_I$ ):

$$\varepsilon_p = \sum_{i=1}^N \varepsilon_{p,i}$$

*Equation 8.6*

In this procedure, the tests do not have to be carried out up to failure point ( $N_1$ ) but the number of repetitive loading cycles can be set by the operator. The routine can identify whether or not a specimen is still within the linear region as the test is progressing ( $DER_i/N_i \leq 1$ ).

Limitations of the procedure:

1. Maximum number of load repetition is 10000 cycles (5 hours 33 minutes) which is due to the limitation of the software.
2. Stress levels can be applied between 49 to 539 kPa but it is recommended to use stress levels between 98 to 196 kPa.
3. The compaction region (zone I) is assumed to end at 100 cycles of load repetition which is generally true at the recommended stress levels and at test temperatures between 45 and 60°C. However, the end of this compaction region is material specific and is affected by the applied stress level and the test temperature. The end of this region is shorter for lower stiffness materials or if the specimen is subjected to higher stress or higher test temperature. Therefore, a wider variety of materials and different testing conditions need to be assessed to see whether this assumption may be accepted for general purposes.

Possible applications of the dissipated energy method for performance assessment of bituminous pavements have been mentioned in *Chapter Seven*. Further works to follow up this possibility can be developed.

## 8.5 Reference

- 1 Siegmann, M.C., "Methods of Routine Investigation", The Properties of Asphaltic Bitumen, J. Ph. Pfeiffer ed., Elsevier, 1950, pp.121-154.
- 2 Sybilsky, D., "Zero-shear viscosity Phenomenons at Measurement, Intrepretation, and Relation to Permanent Deformation", Eurobitume & Euroasphalt Congress, 1996.

- 3 Phillips, M.C., and Robertus, C., "Binder Rheology and Asphaltic Pavement Permanent Deformation, The Zero-shear Viscosity", Eurobitume & Euroasphalt Congress, 1996.
- 4 Phillips, M.C., "Developments in Specifications for Bitumens and Polymer-Modified Binders, Mainly from a Rheological Point of View", Proceedings of the 2<sup>nd</sup> European Symposium on the Performance and Durability of Bituminous Mixtures, J.G. Cabrera (Editor), Leeds, April 1997, pp. 3-18.
- 5 Lu, X, and Isacson, U., "Rheological Characterization of Styrene-Buradiene-Styrene copolymer Modified Bitumens", Construction and Building Materials, Vol 11, No. 1, 1997, pp. 23-32.
- 6 Morgan, P., and Mulder, A., "The Shell Bitumen Industrial Handbook", Shell Bitumen, 1995.
- 7 Brown, S.F., and Brunton, J.M., "An Introduction to the Analytical Design of Bituminous Pavements", 2<sup>nd</sup> Edition, University of Nottingham, 1980.
- 8 Read, J.M., "Fatigue Cracking of Bituminous Paving Mictures", PhD Thesis, University of Nottingham, 1996.
- 9 Van der Poel, C., "A General System Describing The Viscoelastic properties of Bitumens and Its Relation to Routine Test Data", Journal of Applied Chemistry, No.4, May, 1954, pp. 221-236.
- 10 *Private Communication* with Dr J.M. Read.
- 11 Francken, L, Hopman, P., Partl, M.N, and de la Roche, C., "RILEM Interlaboratory Tests on Bituminous Mixes in Repeated Loading. Teachings and Recommendations", Euroasphalt & Eurobitume Congress, 1996.
- 12 Chatfield, C, "Statistics for Technology", 3<sup>rd</sup> Edition, Chapman and Hall, 1983.

## *Chapter Nine*

### **9. Conclusions**

The conclusions presented herein were drawn based upon literature and experimental works undertaken in this study. Limitations and applicability of these conclusions refer to the work's boundary set by the Author.

#### ***9.1 Binder characterisation***

Mechanisms of interactions of polymer modified binders have been observed in this study. The polymers modify the properties of bitumens by changing their physical (mechanical) and chemical properties. In some cases, the polymer modification results in a new binder with properties that are completely different from those commonly found in unmodified bitumens. Consequently, some empirical testing which was derived for unmodified bitumens may not be applicable for polymer modified binders.

There are some facts that need to be considered when dealing with polymer modified binders, i.e.:

1. Bitumens are complex viscoelastic materials with indefinite chemical compositions but predominantly consisting of hydrocarbons and their derivatives. They have been well understood to be a colloidal system and the main chemical components are asphaltenes, saturates, resins and aromatics.
2. Polymers are classified by the overall composition (i.e. homopolymer and copolymer) and the structural consideration (i.e. linear, branched, and block polymers).

3. Properties of polymer modified binders are affected by:

- ◆ Characteristics of the polymer, e.g. polymer concentration, chemical structure, and molecular weight distribution.
- ◆ Characteristics of the base binder (bitumen), e.g. bitumen source, chemical components, structure (colloidal state), and rheology (viscoelasticity).
- ◆ Compatibility of the blend, e.g. phase structure, thermal/mechanical history, and storage stability.

4. Storage stability testing is essential as a routine assessment technique for polymer modified binders. For polymer modified binder, storage stability can be assessed by plotting Black curves.

5. Fundamental testing such as dynamic mechanical tests for polymer modified binders is preferred to empirical bitumen testing. Even though it involves a new set of testing devices and assessment techniques, plotting Black curves from the rheological data can be a simple technique but provides sufficient information. Furthermore, the measurement offers a flexible and reliable data extrapolation facility by generating master curves.

6. Viscosity-temperature relationship charts can be developed from viscosity testing by a rotational viscometer. The information is beneficial for determining mixing, laying, and compaction temperature.

## ***9.2 Mixture Characteristics***

Polymer modified binders contribute to the improvements in mechanical properties of bituminous mixtures. Some testings on some rolled asphalts indicated that:

1. Rheological properties of bituminous binders strongly reflect the properties of their rolled asphalt mixtures.
2. Binder-aggregates interactions in bituminous mixtures have a significant role in contributing elasticity to the rolled asphalts as demonstrated from dynamic mechanical analysis (DMA) testing.
3. Indirect tensile stiffness modulus (ITSM) testing can be an alternative test to the DMA testing for the determination of the stiffness modulus of rolled asphalts.

4. DMA testing has shown low variability, i.e. the mean variations for phase angle and complex modulus were respectively below 8% and 3%. However, these figures vary with the type of material, test temperatures and frequencies.
5. The Marshall test is capable of demonstrating the enhanced performance when using polymers but cannot differentiate the benefits from using different polymers. Therefore, it is not suitable for ranking the performance of different polymer modified rolled asphalts.
6. In ranking performance of rolled asphalts, the wheeltracking test is more sensitive to mixture characteristics than the dynamic creep test.

### ***9.3 Effect of Binder Properties to Mixture Performance***

1. The use of ring and ball softening point on polymer modified binders has been reassessed and found unsuitable. Therefore, alternative tests were introduced because the softening point test cannot represent the resistance to permanent deformation of their mixtures.
2. SHRP introduces a binder parameter  $|G^*|/\sin\delta$  for representing the resistance to permanent deformation of bituminous mixtures. However, the technique does not appear to be accurate for some polymer modified binders.
3. Zero shear viscosity of bituminous binder can be a reliable parameter to represent the resistance to permanent deformation of unmodified and polymer modified bituminous mixtures.
4. The addition of polymers increases binder stiffness in the high temperature regime that to a great extent helps to increase the resistance to permanent deformation of bituminous mixtures.
5. The effect of polymer modification can be less effective, if not detrimental, at low temperatures when compared to the properties of the base binder. Therefore, the use of high penetration grade (soft) bitumen is preferable to obtain a better high temperature performance, to a certain extent, without sacrificing the low temperature performance.
6. Assessment of 50 pen bitumens from different bitumen manufacturers suggests that they have no significant difference with respect to their mechanical properties.

Addition of EVA copolymers into these bitumens also suggests no significant difference in the mechanical properties of the modified binders.

#### ***9.4 Resistance to Permanent Deformation***

A modification in the dynamic creep testing for analysing the resistance to permanent deformation of bituminous mixtures has been developed. Variability of the dynamic creep testing is relatively high, i.e. the mean variations were up to 20%, which may primarily be due to the variability in the properties of the individual specimens (such as volumetric condition and changes in mixture properties during preparation and manufacturing). The application of the dissipated energy method has been extended to assessing resistance to permanent deformation of rolled asphalts.

1. This new approach offers some advantages that:

- ◆ The use of the dissipated energy method enables accurate determination of the end of the linear region on the curves of permanent strain vs. number of repetitive loading cycles.
- ◆ Stability of rolled asphalts under load application can be identified simultaneously as the test progresses using the dissipated energy method.

2. Characteristics of the new approach:

- ◆ Higher dissipated energy per cycle indicates lower resistance to permanent deformation with higher strain rate, the sooner the point  $N_1$  is achieved.
- ◆ Higher applied stress and/or higher test temperature lead(s) to higher dissipated energy per cycle.

3. Correlation with the commonly adopted technique for assessing the resistance to permanent deformation of bituminous mixtures:

- ◆ The strain rate method correlates well with the dissipated energy method.
- ◆ The strain rate method is sufficient to be used as a routine assessment technique for the resistance to permanent deformation of rolled asphalts.
- ◆ Terminal strain method (final rut depth) also correlates well with the dissipated energy method but suggests more variability in their measurements.
- ◆ A combined technique incorporating strain rate and dissipated energy method provides greater accuracy in assessing resistance to permanent deformation of rolled asphalts.

# Chapter Ten

## 10. Recommendations and Future Works

### 10.1 Recommendations

Based on the study undertaken in this research several recommendations for future work are presented in this section. However, the recommendations are based upon the following observations.

1. Addition of polymers into hard binders, such as 50 pen bitumen, is not always beneficial in terms of low temperature performance. Similarly, the addition of polymers into soft binder can be beneficial for low temperature performance but there may be problems at high temperature. Modification of soft bitumen with high polymer concentrations may solve the problems at high temperature but may also bring new problems with instability of the blend during storage or transportation.
2. The use of minimum strain rate in the linear zone (zone II) is sufficient for assessing the resistance to permanent deformation of HRA mixtures. The dissipated energy method can be used for determining the linear zone. Therefore, a combination of the two methods provides a reliable assessment technique for the resistance to permanent deformation of HRA mixtures.
3. The use of high stress level, especially at high temperature, under repetitive loading in an unconfined condition, such as the dynamic creep in NAT, should be avoided. The maximum recommended stress level is 196 kPa.

## 10.2 Future Works

Due to time limitations, some areas of works which would be beneficial in studying the binder-aggregate interactions and the performance of bituminous mixtures were left for further investigations:

1. Analysis based on the chemical properties of polymer modified binders are necessary as the chemistry of the binder also influences the physical and/or mechanical properties.
2. Detailed information on the microstructure of the polymer modified binder has not been elaborated on in this study. Works using an electron microscope would be beneficial.
3. The effect of loading time which is also an important factor affecting the resistance to permanent deformation of bituminous mixtures has not been assessed in this study, as only one fixed loading time i.e. 200/1800 milliseconds of loading/unloading was adopted. Furthermore, the loading time affects the shape of the hysteretic loops and consequently variations in the dissipated energy. Therefore, it is recommended to perform further tests by varying the loading time, e.g. between 100/1900 and 300/1700 milliseconds of loading/unloading.
4. Determination of the dissipated energy under wheel tracking may help reduce the effect of specimen boundary conditions if the results are to be compared with the repetitive load axial (unconfined) testing. Therefore, the currently available wheel-tracking device at SHU needs to be modified to accommodate more detailed data acquisition as required for analysis based on dissipated energy.
5. The strain rate and dissipated energy techniques have only been validated on the wheel-tracking test due to the lack of access to field tests or laboratory pavement simulation tests. Therefore, further validation is necessary:
  - Field assessments on bituminous pavements with known performance, or at a smaller scale (e.g. laboratory pavement testing facility) may need to be undertaken to take into account the permanent deformation in relation with the energy dissipated during the traffic loading.
  - The energy dissipated in bituminous pavements can be measured by adapting currently available techniques, such as wave propagation (e.g. COLIBRI system, SASW method) and deflection tests (e.g. Falling Weight Deflectometer).

6. The assessment of the permanent deformation reported in this thesis was only undertaken on HRA mixtures at a testing condition set by the Author. Therefore, the applicability of the proposed technique combining the use of strain rate and dissipated method needs to be assessed on a wider range of materials (binders and mixtures) and testing conditions. Effect of confinement on this technique also needs to be investigated.
7. The use of a rheological model, such as Burger's or generalised Kelvin's model, may differentiate the effect of viscous and plastic components in the deformation behaviour of bituminous mixtures and may be able to be related back to the dissipated energy. If the model can successfully differentiate these effects, then there may be a chance for identification of which element is dominant in the binder-aggregate interactions at a given temperature and loading condition and consequently extending the use of the dynamic creep mode in the NAT to be a simple testing device to study the fundamental (rheological) properties of binder-aggregate interactions.

# *Appendix A*

## Storage Stability

### List of Symbols and Abbreviations:

$\delta$	Phase angle, units: degree
$G^*$	Complex Modulus, units: Pa or MPa
E50	50 Pen bitumen
F100	100 Pen bitumen
50/EVA or EP50	50 Pen bitumen + 5% Ethylene Vinyl Acetate
50/SBR or ER50	50 Pen bitumen + 5% Styrene Butadiene Rubber
50/SBS or ES50	50 Pen bitumen + 5% Styrene Butadiene Styrene
100/SBR or FR100	100 Pen bitumen + 5% Styrene Butadiene Rubber
100/SBS or FS50	100 Pen bitumen + 5% Styrene Butadiene Styrene

### A.1. Binders before storage stability test:

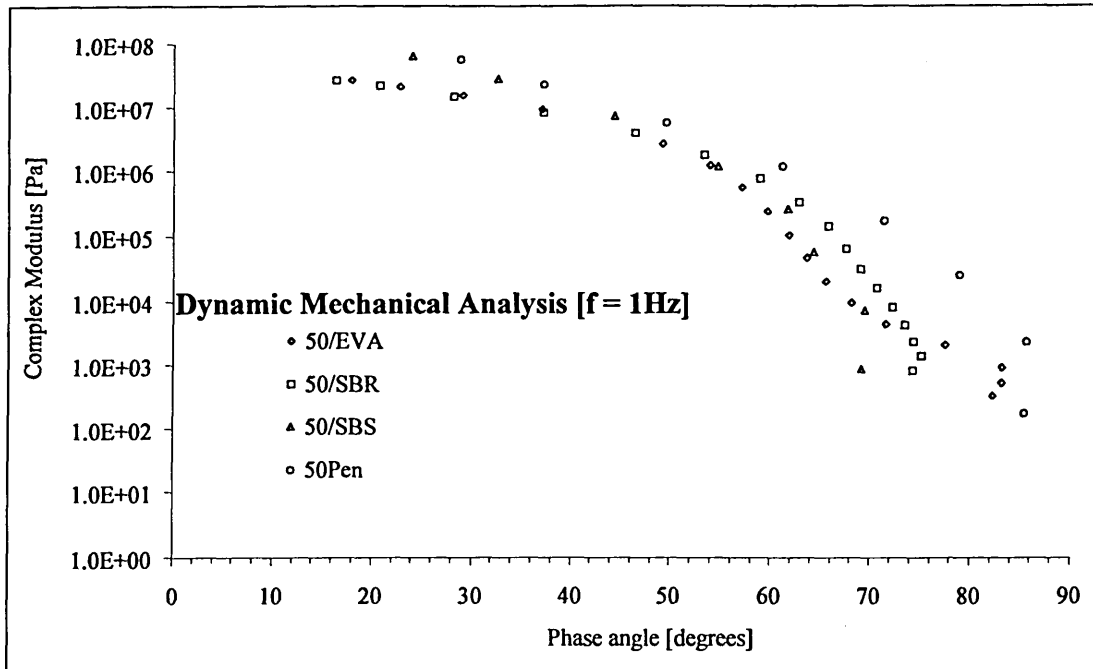


Figure A.1 Black curves showing comparison of modified binders with a 50 pen bitumen as the base binder.

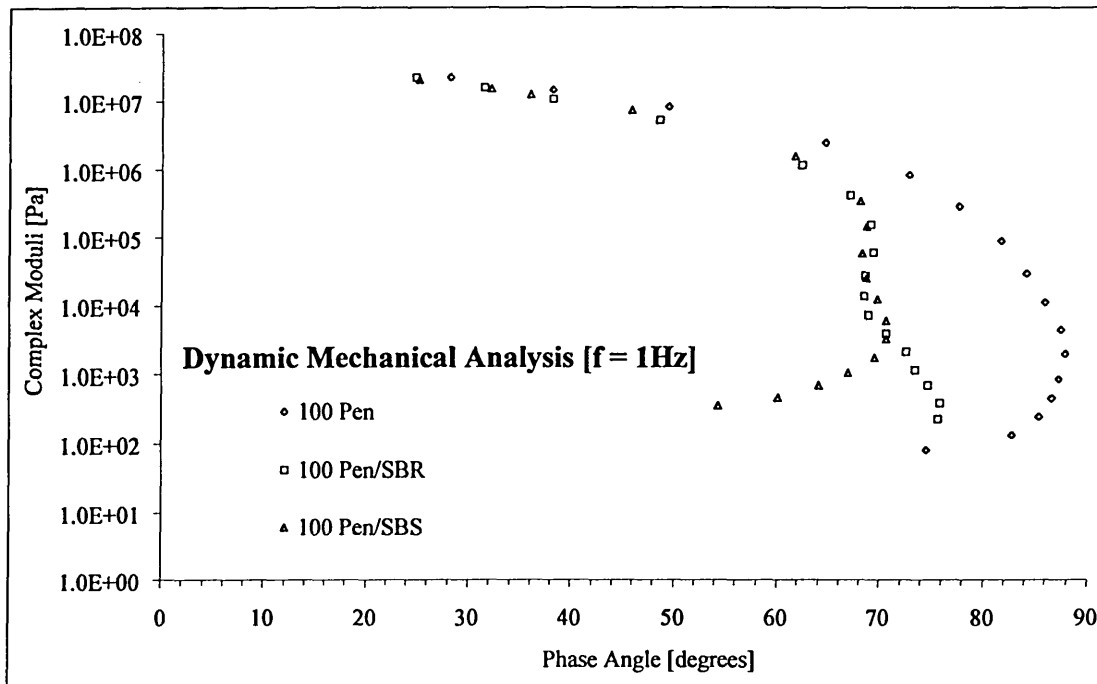


Figure A.2 Black curves showing comparison of modified binders with a 100 pen bitumen as the base binder.

## A.2. Binders after seven-day storage stability test

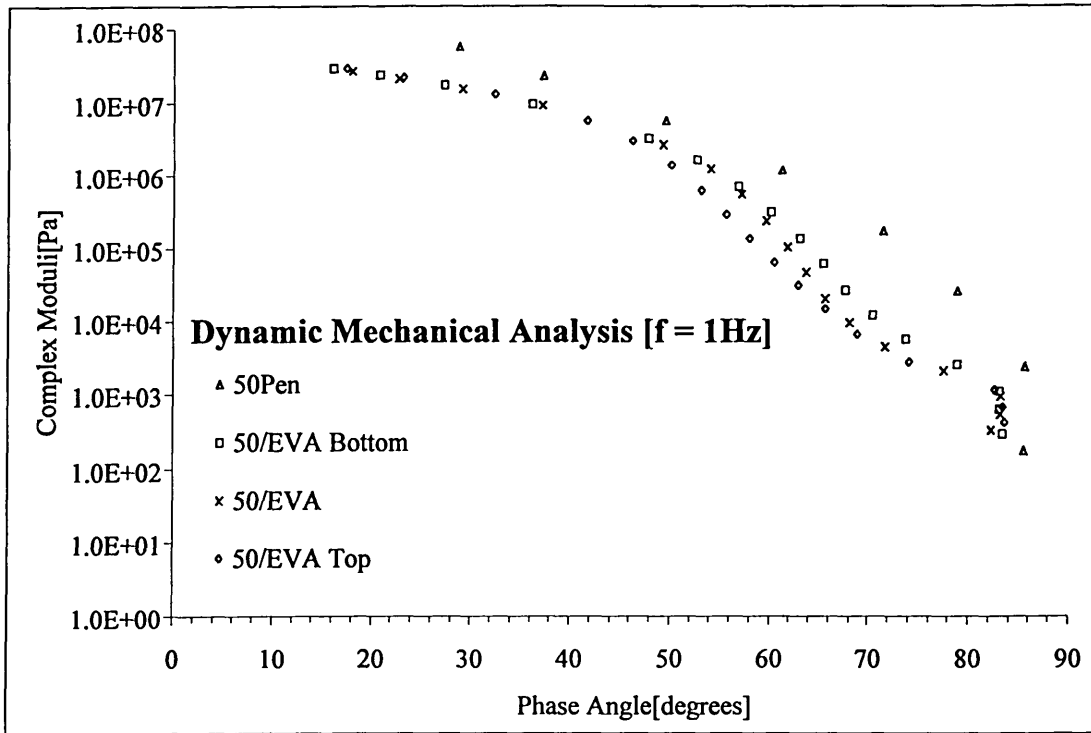


Figure A.3 Black curves showing comparison of EVA modified binder (50 pen + 5%EVA), before and after seven day-storage stability test.

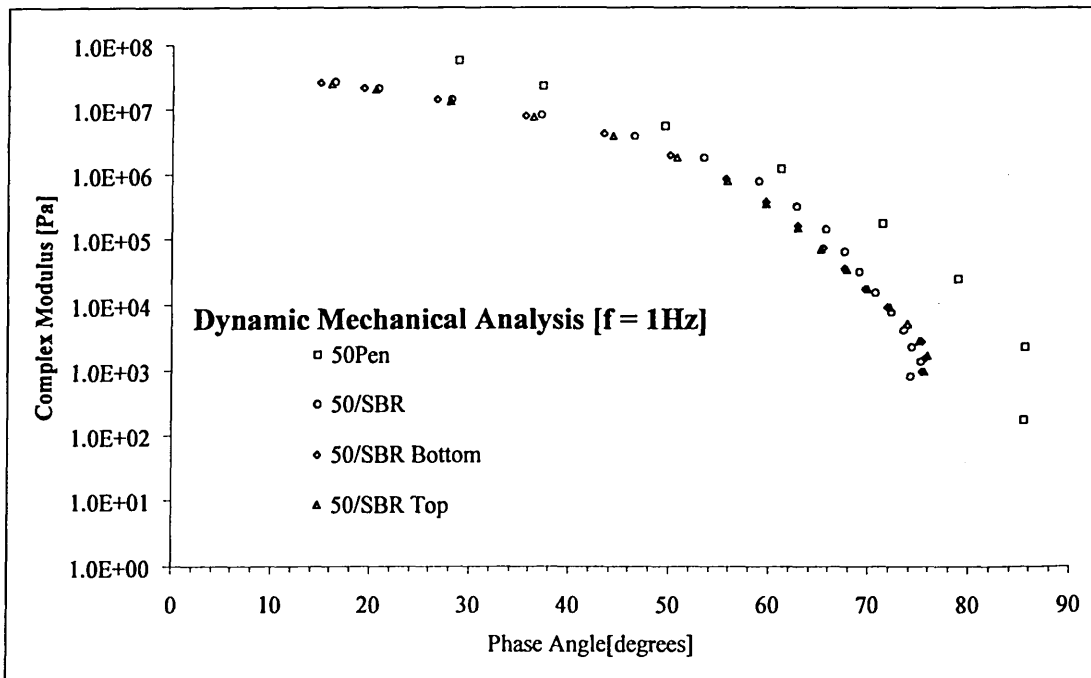


Figure A.4 Black curves showing comparison of SBR modified binder (50 pen + 5%SBR), before and after seven day-storage stability test.

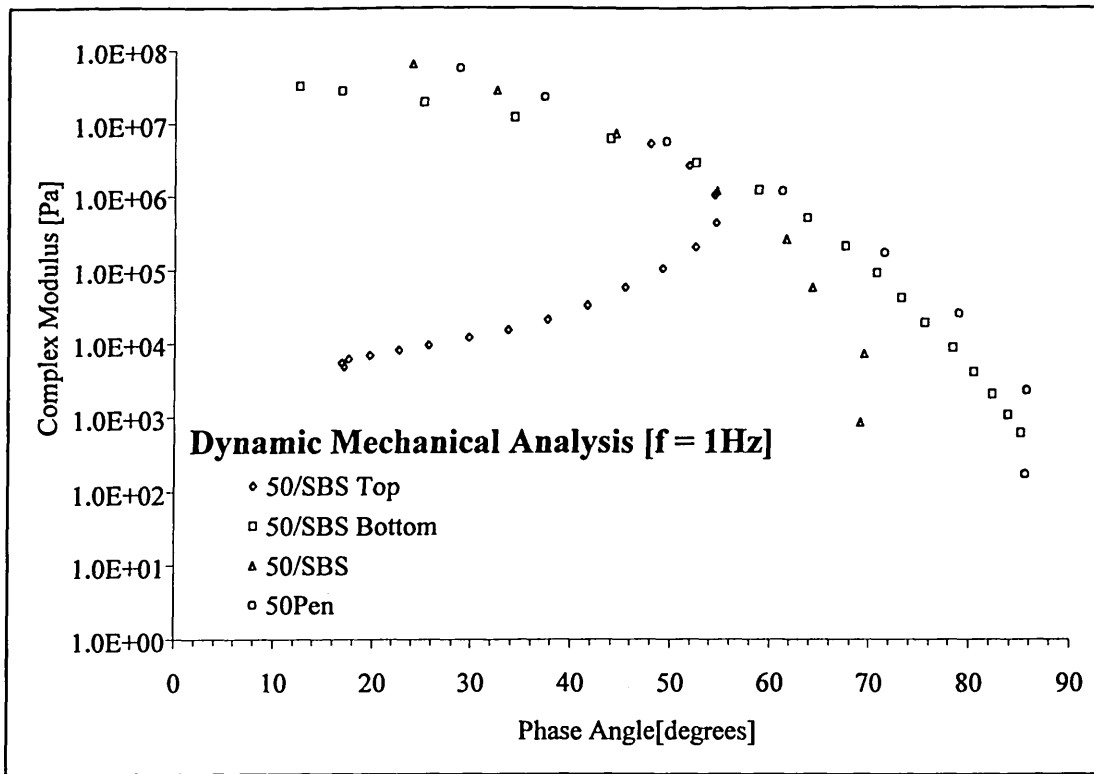


Figure A.5 Black curves showing comparison of SBS modified binder (50 pen + 5%SBS), before and after seven day-storage stability test.

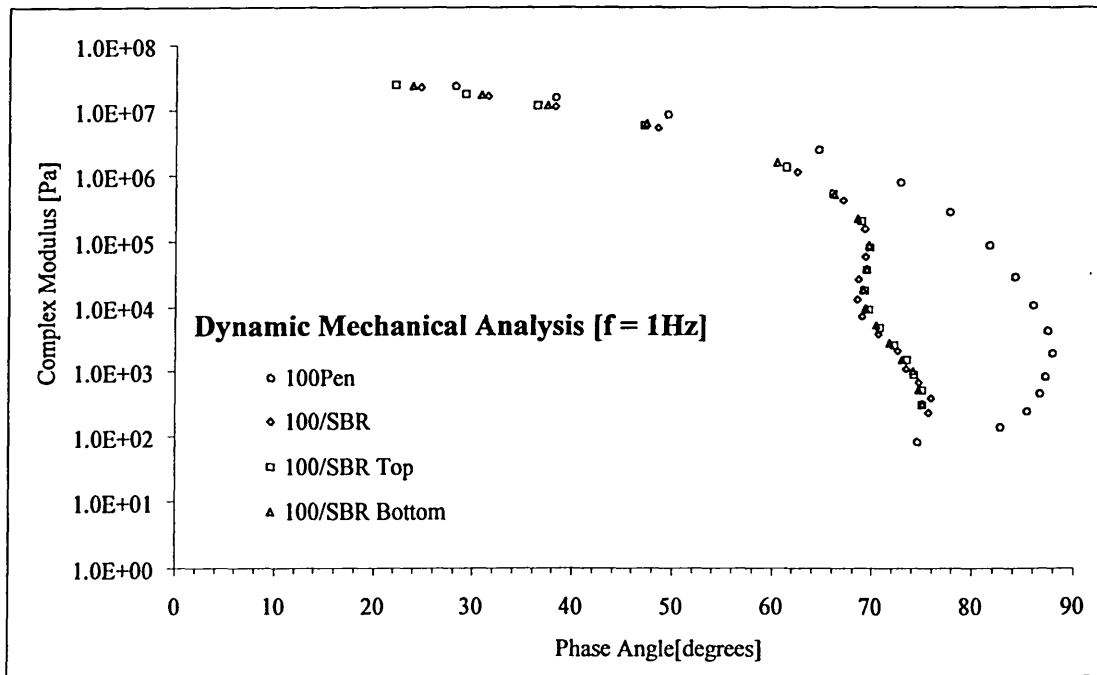


Figure A.6 Black curves showing comparison of SBR modified binder (100 pen + 5%SBR), before and after seven day-storage stability test.

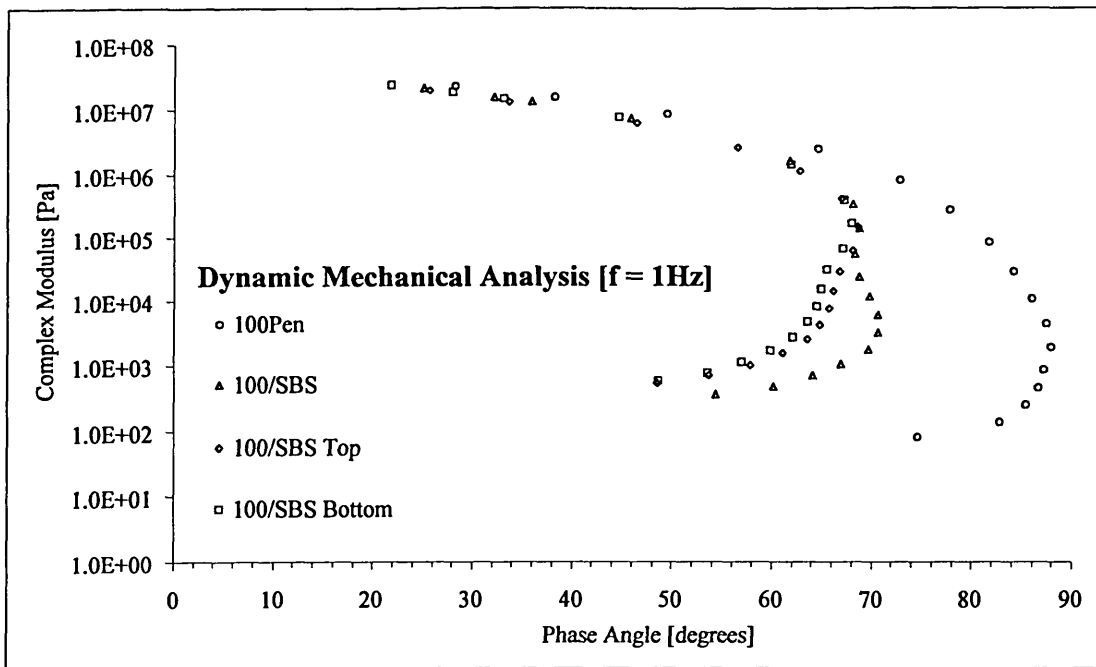


Figure A.7 Black curves showing comparison of SBS modified binder (100 pen + 5%SBS), before and after seven day-storage stability test.

### A.3. Raw Data

Measurements were carried out by temperature sweep from 0 to 80 °C at frequency of 1 Hz with exceptions that data were extracted from oscillation tests for 50 Pen bitumen (E50) and 50 Pen + 5%SBS binder (ES50) before stability test at test frequency of 1 Hz.

Gap setting: 2 mm. Plate diameter : 15 mm. Measurement interval 120 s. Thermal equilibrium time : 120 s.

Engineering units :

Temp (temperature) in centigrade (°C)

Phase angle ( $\delta$ ) in degree

Viscosity in Pa.s

Complex Moduli ( $G^*$ ) in Pa

**A.3.1.1. Unmodified bitumens : 50 Pen (E50) and 100 Pen (F100). Before Stability test.**

50 Pen Bitumen (E50)						100 Pen Bitumen (F100)					
Temp	$\delta$	Viscosity	G*	Temp	$\delta$	Viscosity	G*				
-5	28.76	8.93E+06	5.61E+07	0	28.18	3.61E+06	2.27E+07				
5	37.17	3.61E+06	2.27E+07	4.5	38.13	2.41E+06	1.51E+07				
15	49.49	8.81E+05	5.53E+06	8.7	49.43	1.34E+06	8.45E+06				
25	61.14	1.89E+05	1.19E+06	14.9	64.56	3.87E+05	2.43E+06				
35	71.36	2.82E+04	1.77E+05	20.4	72.76	1.28E+05	8.06E+05				
45	78.86	4.03E+03	2.53E+04	25.3	77.68	4.40E+04	2.77E+05				
60	85.56	3.65E+02	2.29E+03	30.3	81.64	1.40E+04	8.78E+04				
80	85.44	2.76E+01	1.73E+02	35.3	84.15	4.59E+03	2.88E+04				
				40.3	85.98	1.70E+03	1.07E+04				
				45.3	87.43	6.87E+02	4.31E+03				
				50.3	87.88	2.98E+02	1.87E+03				
				55.3	87.22	1.32E+02	8.30E+02				
				60.3	86.57	7.18E+01	4.51E+02				
				65.3	85.39	3.83E+01	2.41E+02				
				70.3	82.81	2.14E+01	1.34E+02				
				75.3	74.58	1.29E+01	8.11E+01				

**A.3.2. 50 Pen + 5% EVA Binder (EP50)**

Before Stability test				Top Part After Stability test				Bottom Part After Stability test			
Temp	$\delta$	Viscosity	G*	Temp	$\delta$	Viscosity	G*	Temp	$\delta$	Viscosity	G*
0	17.87	4.20E+06	2.64E+07	0	17.34	4.58E+06	2.88E+07	0	16	4.66E+06	2.93E+07
3.8	22.68	3.40E+06	2.14E+07	4.6	23.09	3.51E+06	2.21E+07	4.1	20.71	3.78E+06	2.37E+07
7.6	29.04	2.45E+06	1.54E+07	10	32.32	2.06E+06	1.30E+07	8.3	27.24	2.70E+06	1.70E+07
12.5	37.02	1.46E+06	9.15E+06	16	41.56	8.87E+05	5.57E+06	13.6	36.04	1.53E+06	9.63E+06
20.4	49.2	4.22E+05	2.65E+06	20.2	46.21	4.73E+05	2.97E+06	20.8	47.71	5.07E+05	3.18E+06
25.5	53.94	1.94E+05	1.22E+06	25.2	50.01	2.22E+05	1.40E+06	25.1	52.56	2.55E+05	1.61E+06
30.3	57.08	8.93E+04	5.61E+05	30.3	53.02	1.01E+05	6.32E+05	30.3	56.79	1.14E+05	7.16E+05
35.3	59.58	3.89E+04	2.44E+05	35.3	55.58	4.67E+04	2.94E+05	35.3	60.07	5.06E+04	3.18E+05
40.3	61.72	1.67E+04	1.05E+05	40.3	57.93	2.17E+04	1.36E+05	40.5	62.91	2.19E+04	1.38E+05
45.4	63.59	7.33E+03	4.61E+04	45.3	60.42	1.02E+04	6.42E+04	45.2	65.38	9.62E+03	6.05E+04
50.3	65.51	3.26E+03	2.05E+04	50.2	62.83	4.88E+03	3.07E+04	50.4	67.61	4.27E+03	2.68E+04
55.2	68.01	1.49E+03	9.37E+03	55.2	65.55	2.29E+03	1.44E+04	55.3	70.45	1.89E+03	1.19E+04
60.3	71.6	6.92E+02	4.35E+03	60.2	68.87	1.05E+03	6.62E+03	60.3	73.62	8.76E+02	5.50E+03
65.2	77.5	3.31E+02	2.08E+03	65.2	73.98	4.29E+02	2.70E+03	65.3	78.85	4.06E+02	2.55E+03
70.3	83.14	1.47E+02	9.25E+02	70.2	82.6	1.79E+02	1.12E+03	70.3	82.96	1.71E+02	1.07E+03
75.3	83.1	8.46E+01	5.32E+02	75.3	83.35	1.09E+02	6.83E+02	75.3	82.98	9.91E+01	6.23E+02
80.3	82.21	5.24E+01	3.29E+02	80.2	83.53	6.65E+01	4.18E+02	80.2	83.39	4.65E+01	2.92E+02

**A.3.3. 50 Pen + 5% SBR Binder (ER50)**

Before Stability test				Top Part After Stability test				Bottom Part After Stability test			
Temp	$\delta$	Viscosity	G*	Temp	$\delta$	Viscosity	G*	Temp	$\delta$	Viscosity	G*
0	16.29	4.22E+06	2.65E+07	0	16.00	3.97E+06	2.49E+07	-0.1	14.87	4.16E+06	2.61E+07
4.5	20.71	3.43E+06	2.15E+07	4.7	20.46	3.16E+06	1.99E+07	4.6	19.23	3.36E+06	2.11E+07
9.7	28.13	2.30E+06	1.44E+07	10.5	28.00	2.06E+06	1.30E+07	10.2	26.65	2.24E+06	1.41E+07
15.6	37.13	1.29E+06	8.07E+06	15.9	36.31	1.18E+06	7.44E+06	16.2	35.47	1.26E+06	7.91E+06
20.3	46.38	6.15E+05	3.86E+06	20.3	44.27	6.12E+05	3.85E+06	20.3	43.32	6.53E+05	4.10E+06
25.3	53.38	2.82E+05	1.77E+06	25.3	50.70	2.81E+05	1.77E+06	25.2	49.95	3.05E+05	1.92E+06
30.3	58.89	1.21E+05	7.60E+05	30.3	55.68	1.24E+05	7.81E+05	30.2	55.67	1.34E+05	8.40E+05
35.3	62.73	5.18E+04	3.26E+05	35.2	59.68	5.47E+04	3.44E+05	35.3	59.71	5.89E+04	3.70E+05
40.3	65.67	2.25E+04	1.42E+05	40.4	62.77	2.44E+04	1.53E+05	40.3	62.81	2.58E+04	1.62E+05
45.3	67.51	1.03E+04	6.50E+04	45.3	65.17	1.14E+04	7.15E+04	45.3	65.43	1.18E+04	7.40E+04
50.3	68.95	4.99E+03	3.14E+04	50.2	67.80	5.54E+03	3.48E+04	50.3	67.48	5.64E+03	3.54E+04
55.3	70.64	2.50E+03	1.57E+04	55.3	69.92	2.81E+03	1.77E+04	55.4	69.7	2.81E+03	1.77E+04
60.3	72.26	1.28E+03	8.01E+03	60.3	72.08	1.47E+03	9.23E+03	60.3	71.91	1.46E+03	9.18E+03
65.3	73.44	6.74E+02	4.23E+03	65.3	73.87	7.95E+02	5.00E+03	65.3	73.78	7.78E+02	4.89E+03
70.3	74.32	3.70E+02	2.32E+03	70.3	75.11	4.49E+02	2.82E+03	70.3	75.25	4.41E+02	2.77E+03
75.2	75.12	2.17E+02	1.37E+03	75.3	75.87	2.61E+02	1.64E+03	75.3	75.57	2.42E+02	1.52E+03
80.2	74.2	1.30E+02	8.18E+02	80.3	75.51	1.49E+02	9.39E+02	80.3	75.33	1.53E+02	9.59E+02

**A.3.4. 50 Pen + 5% SBS Binder (ES50)**

Before Stability test			Top Part After Stability test				Bottom Part After Stability test				
Temp	$\delta$	Viscosity	G*	Temp	$\delta$	Viscosity	G*	Temp	$\delta$	Viscosity	G*
-5	23.95	1.01E+07	6.35E+07	0	47.88	8.41E+05	5.28E+06	0	12.45	5.15E+06	3.23E+07
5	32.49	4.40E+06	2.77E+07	5	51.81	4.21E+05	2.65E+06	5	16.83	4.34E+06	2.73E+07
15	44.33	1.16E+06	7.30E+06	10.6	54.44	1.68E+05	1.05E+06	10.5	25.07	3.04E+06	1.91E+07
25	54.63	1.90E+05	1.19E+06	15.7	54.54	6.80E+04	4.28E+05	15.9	34.23	1.88E+06	1.18E+07
35	61.67	4.12E+04	2.59E+05	20.2	52.47	3.28E+04	2.06E+05	20.3	43.86	9.80E+05	6.16E+06
45	64.19	9.06E+03	5.69E+04	25.3	49.12	1.67E+04	1.05E+05	25.4	52.5	4.51E+05	2.84E+06
60	69.39	1.14E+03	7.13E+03	30.3	45.44	9.07E+03	5.70E+04	30.4	58.79	1.99E+05	1.25E+06
80	69.02	1.34E+02	8.43E+02	35.3	41.57	5.26E+03	3.31E+04	35.3	63.63	8.25E+04	5.19E+05
				40.4	37.63	3.37E+03	2.12E+04	40.2	67.49	3.43E+04	2.16E+05
				45.3	33.71	2.41E+03	1.51E+04	45.3	70.58	1.48E+04	9.33E+04
				50.4	29.69	1.87E+03	1.18E+04	50.3	73.13	6.68E+03	4.20E+04
				55.3	25.73	1.51E+03	9.48E+03	55.3	75.5	3.07E+03	1.93E+04
				60.2	22.59	1.28E+03	8.03E+03	60.3	78.26	1.41E+03	8.84E+03
				65.2	19.68	1.09E+03	6.87E+03	65.3	80.38	6.49E+02	4.08E+03
				70.3	17.61	9.60E+02	6.03E+03	70.3	82.28	3.30E+02	2.07E+03
				75.2	16.91	8.58E+02	5.39E+03	75.3	83.8	1.73E+02	1.08E+03
				80.3	17.15	7.75E+02	4.87E+03	80.2	85.05	9.80E+01	6.16E+02

**A.3.5. 100 Pen + 5% SBR Binder (FR100)**

Before Stability test			Top Part After Stability test			Bottom Part After Stability test					
Temp	$\delta$	Viscosity	G*	Temp	$\delta$	Viscosity	G*	Temp	$\delta$	Viscosity	G*
0	24.70	3.54E+06	2.22E+07	0	22.05	3.77E+06	2.37E+07	0	23.91	3.56E+06	2.24E+07
4	31.39	2.55E+06	1.60E+07	4.3	29.17	2.73E+06	1.71E+07	4.1	30.72	2.62E+06	1.65E+07
7.5	38.15	1.74E+06	1.09E+07	8	36.37	1.86E+06	1.17E+07	7.3	37.39	1.86E+06	1.17E+07
12.3	48.47	8.39E+05	5.27E+06	12.7	47.09	9.10E+05	5.72E+06	11.9	47.28	9.55E+05	6.00E+06
20.6	62.35	1.81E+05	1.14E+06	20.7	61.23	2.12E+05	1.33E+06	19.9	60.33	2.47E+05	1.55E+06
25.3	67.06	6.63E+04	4.16E+05	25.2	65.98	8.40E+04	5.28E+05	25.5	66.12	8.31E+04	5.22E+05
30.2	69.14	2.43E+04	1.53E+05	30.2	68.87	3.19E+04	2.01E+05	30.1	68.54	3.53E+04	2.21E+05
35.3	69.33	9.51E+03	5.97E+04	35.4	69.67	1.30E+04	8.15E+04	35.3	69.58	1.39E+04	8.71E+04
40.3	68.59	4.24E+03	2.66E+04	40.3	69.40	5.78E+03	3.63E+04	40.4	69.35	6.14E+03	3.86E+04
45.2	68.45	2.11E+03	1.32E+04	45.2	69.16	2.80E+03	1.76E+04	45.3	69.01	2.96E+03	1.86E+04
50.4	68.89	1.12E+03	7.02E+03	50.4	69.61	1.43E+03	9.02E+03	50.3	69.28	1.52E+03	9.57E+03
55.2	70.59	6.05E+02	3.80E+03	55.3	70.71	7.52E+02	4.73E+03	55.3	70.39	8.21E+02	5.16E+03
60.4	72.56	3.25E+02	2.04E+03	60.3	72.17	4.02E+02	2.52E+03	60.3	71.7	4.29E+02	2.70E+03
65.3	73.48	1.75E+02	1.10E+03	65.2	73.41	2.38E+02	1.50E+03	65.3	73	2.36E+02	1.48E+03
70.3	74.72	1.07E+02	6.75E+02	70.3	74.27	1.42E+02	8.90E+02	70.2	74.14	1.43E+02	9.89E+02
75.3	75.87	6.21E+01	3.90E+02	75.3	75.03	8.01E+01	5.03E+02	75.2	74.69	8.22E+01	5.17E+02
80.2	75.69	3.62E+01	2.27E+02	80.3	74.99	4.79E+01	3.01E+02	80.3	74.98	4.99E+01	3.14E+02

**A.3.6. 100 Pen + 5% SBS Binder (FS100)**

Before Stability test				Top Part After Stability test				Bottom Part After Stability test			
Temp	$\delta$	Viscosity	G*	Temp	$\delta$	Viscosity	G*	Temp	$\delta$	Viscosity	G*
0	25.04	3.31E+06	2.08E+07	0	25.61	3.06E+06	1.92E+07	0	21.75	3.82E+06	2.40E+07
3.8	32.11	2.46E+06	1.55E+07	5	33.60	2.11E+06	1.33E+07	3.5	27.92	2.95E+06	1.86E+07
5.5	35.89	2.06E+06	1.29E+07	10.5	46.30	9.91E+05	6.23E+06	5.9	33.01	2.34E+06	1.48E+07
10	45.77	1.17E+06	7.34E+06	15.9	56.46	4.09E+05	2.57E+06	11.2	44.52	1.21E+06	7.60E+06
18	61.66	2.53E+05	1.59E+06	20.3	62.73	1.75E+05	1.10E+06	19.3	61.84	2.23E+05	1.40E+06
25.9	68.04	5.38E+04	3.38E+05	25.3	66.90	6.39E+04	4.02E+05	25.7	67.06	6.27E+04	3.94E+05
30.3	68.68	2.24E+04	1.41E+05	30.3	68.55	2.41E+04	1.52E+05	30.2	67.94	2.67E+04	1.68E+05
35.3	68.21	8.98E+03	5.64E+04	35.2	67.97	1.00E+04	6.31E+04	35.3	66.97	1.09E+04	6.87E+04
40.3	68.64	3.91E+03	2.45E+04	40.3	66.78	4.59E+03	2.88E+04	40.3	65.45	5.05E+03	3.17E+04
45.2	69.69	1.86E+03	1.17E+04	45.3	66.13	2.28E+03	1.43E+04	45.3	64.89	2.52E+03	1.58E+04
50.4	70.59	9.29E+02	5.84E+03	50.3	65.69	1.20E+03	7.57E+03	50.3	64.38	1.33E+03	8.35E+03
55.4	70.62	4.98E+02	3.13E+03	55.3	64.78	6.71E+02	4.22E+03	55.3	63.52	7.34E+02	4.61E+03
60.3	69.57	2.73E+02	1.72E+03	60.2	63.45	3.91E+02	2.45E+03	60.3	62.02	4.27E+02	2.68E+03
65.4	66.87	1.64E+02	1.03E+03	65.3	61.03	2.40E+02	1.51E+03	65.2	59.73	2.62E+02	1.65E+03
70.2	64.01	1.09E+02	6.84E+02	70.2	57.81	1.61E+02	1.01E+03	70.3	56.92	1.75E+02	1.10E+03
75.2	60.15	7.49E+01	4.71E+02	75.2	53.69	1.09E+02	6.85E+02	75.2	53.59	1.19E+02	7.48E+02
80.3	54.34	5.68E+01	3.57E+02	80.3	48.52	8.38E+01	5.26E+02	80.2	48.61	9.07E+01	5.70E+02

**A.4. Photomicrographs of polymer modified binders, before and after a seven-day storage stability test.**



*Plate A.1. Photomicrographs (500 x magnifications) of EP50 binders (50 Pen + 5%EVA), before and after storage stability testing.*



*Plate A.2. Photomicrographs (500 x magnifications) of ER50 binders (50 Pen + 5%SBR), before and after storage stability testing.*

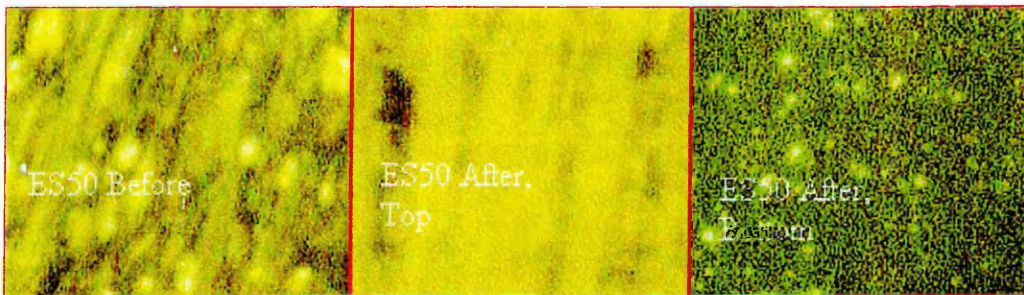


*Plate A.3. Photomicrographs (500 x magnifications) of ES50 binders (50 Pen + 5%SBS), before and after storage stability testing.*

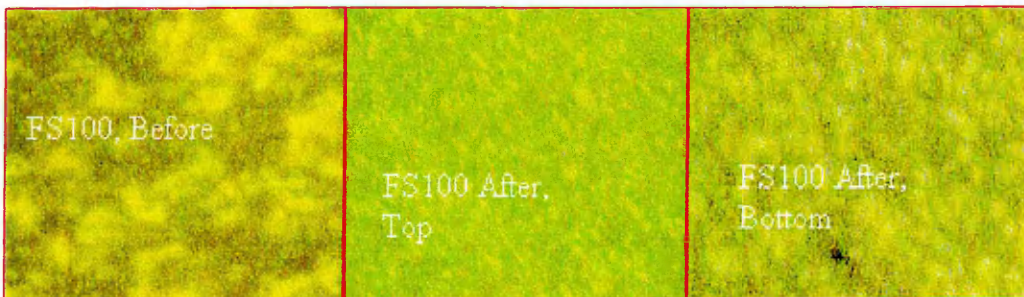


*Plate A.4. Photomicrographs (500 x magnifications) of FS100 binders (100 Pen + 5%SBS), before and after storage stability testing.*

# *Appendix B*

## Dynamic Mechanical Analyses

### List of Symbols and Abbreviations:

$\delta$	Phase angle, units: degree
$G^*$	Complex Modulus (binder), units: Pa
$E^*$	Complex Modulus (mixture), units: GPa
$E'$	Elastic Modulus (mixture), units: GPa
$E''$	Loss Modulus (mixture), units: GPa
WLF	William, Landell, and Ferry
$a_T$	Temperature shift factor
Avg	Average
Temp	Temperature
Log	Logarithm
A50, B50, C50, D50, E50	50 Pen bitumen from different manufacturers
F100	100 Pen bitumen
AP50, BP50, CP50, DP50, EP50	50 Pen bitumen (from different manufacturers) + 5% Ethylene Vinyl Acetate
ER50	50 Pen bitumen + 5% Styrene Butadiene Rubber
ES50	50 Pen bitumen + 5% Styrene Butadiene Styrene
FR100	100 Pen bitumen + 5% Styrene Butadiene Rubber
FS50	100 Pen bitumen + 5% Styrene Butadiene Styrene

# 1. Binder test

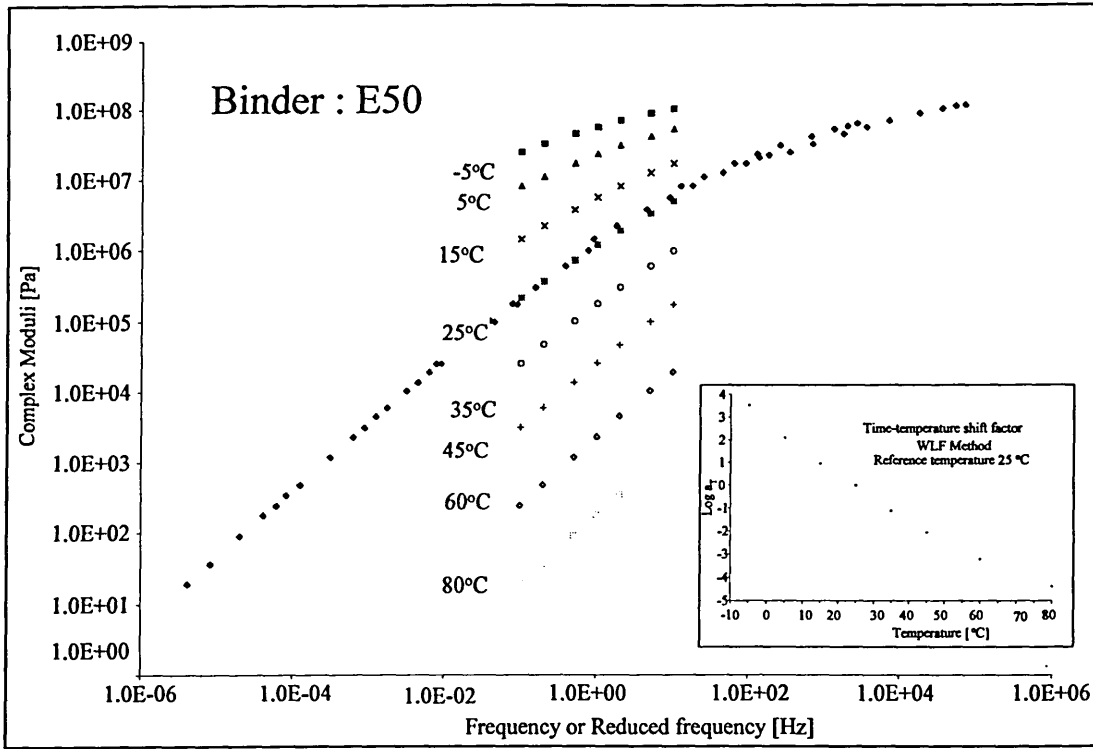


Figure B.1 Typical results of 50 pen bitumen showing dependency of complex (shear) moduli at different test temperatures to loading frequency and the master curve of complex (shear) modulus at reference temperature of 25°C as a function of reduced frequency. Binder reference: E50

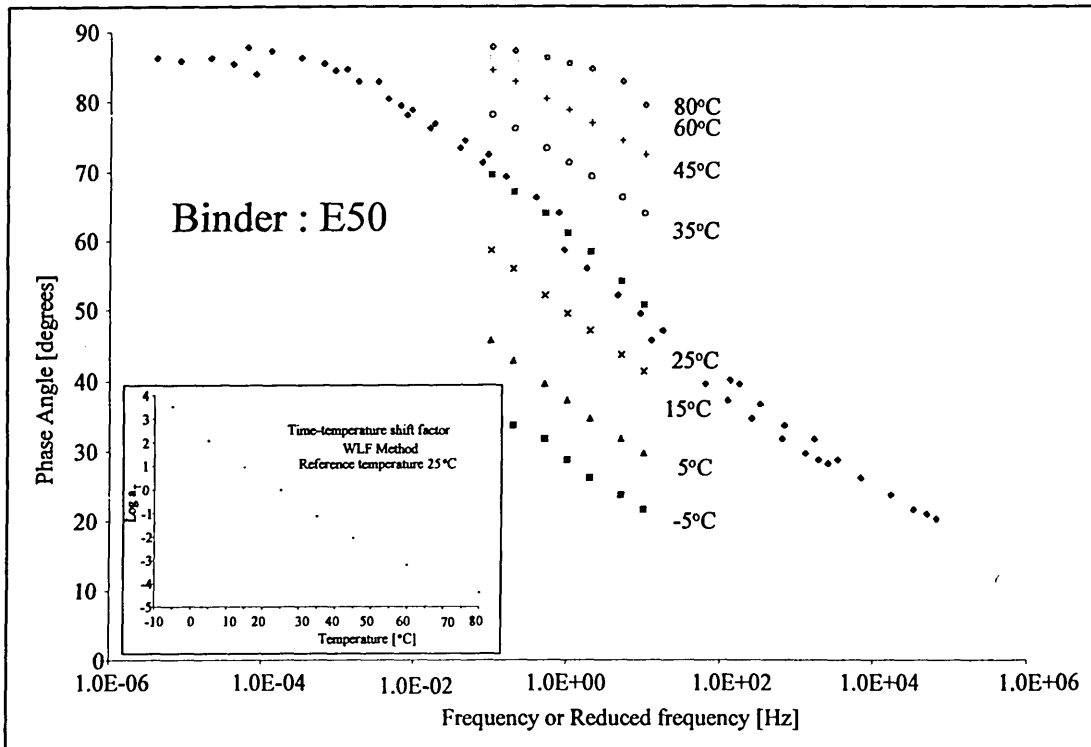


Figure B.2 Typical results of 50 pen bitumen showing dependency of phase angles at different test temperatures to loading frequency and the master curve of phase angle at reference temperature of 25°C as a function of reduced frequency. Binder reference: E50

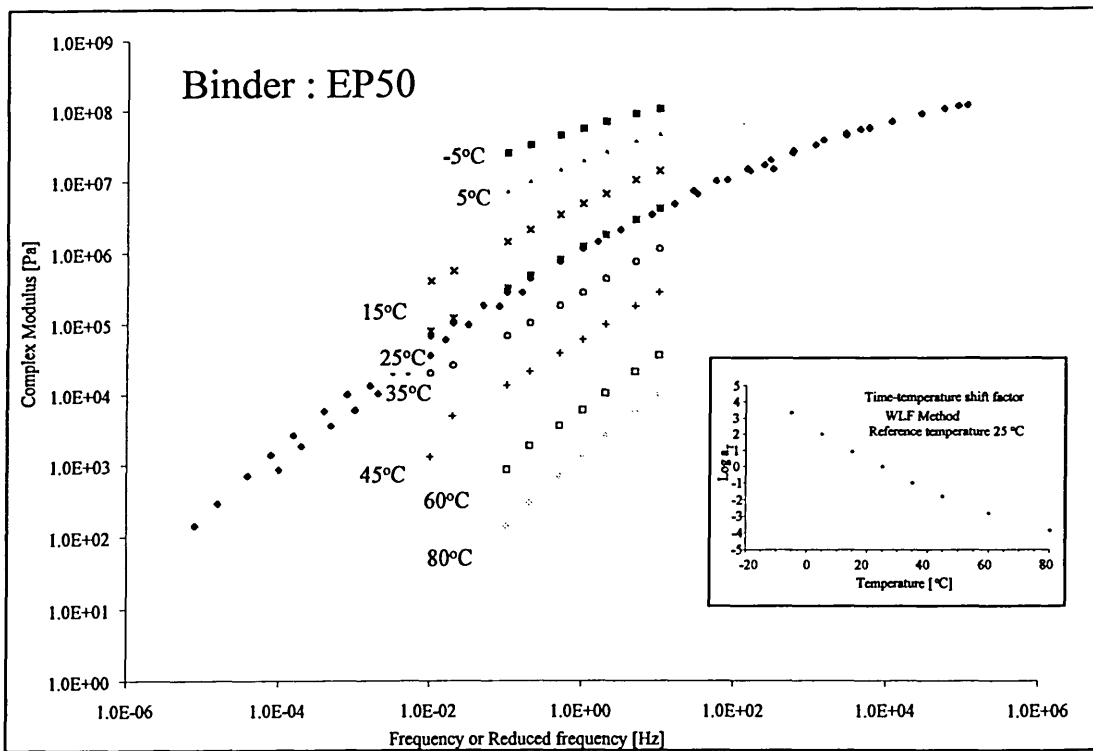


Figure B.3 Typical results of EVA modified 50 pen binder showing dependency of complex (shear) moduli at different test temperatures to loading frequency and the master curve of complex (shear) modulus at reference temperature of 25°C as a function of reduced frequency. Binder reference: EP50

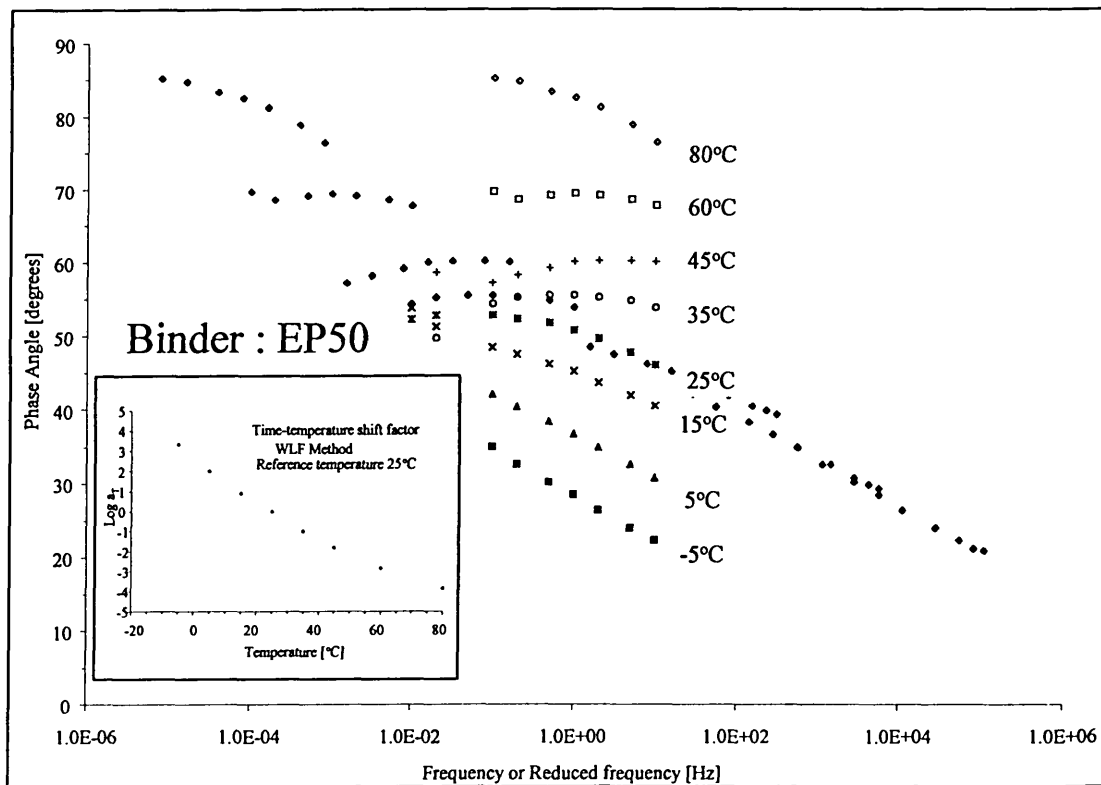


Figure B.4 Typical results of EVA modified 50 pen binder showing dependency of phase angles at different test temperatures to loading frequency and the master curve of phase angle at reference temperature of 25°C as a function of reduced frequency. Binder reference: EP50

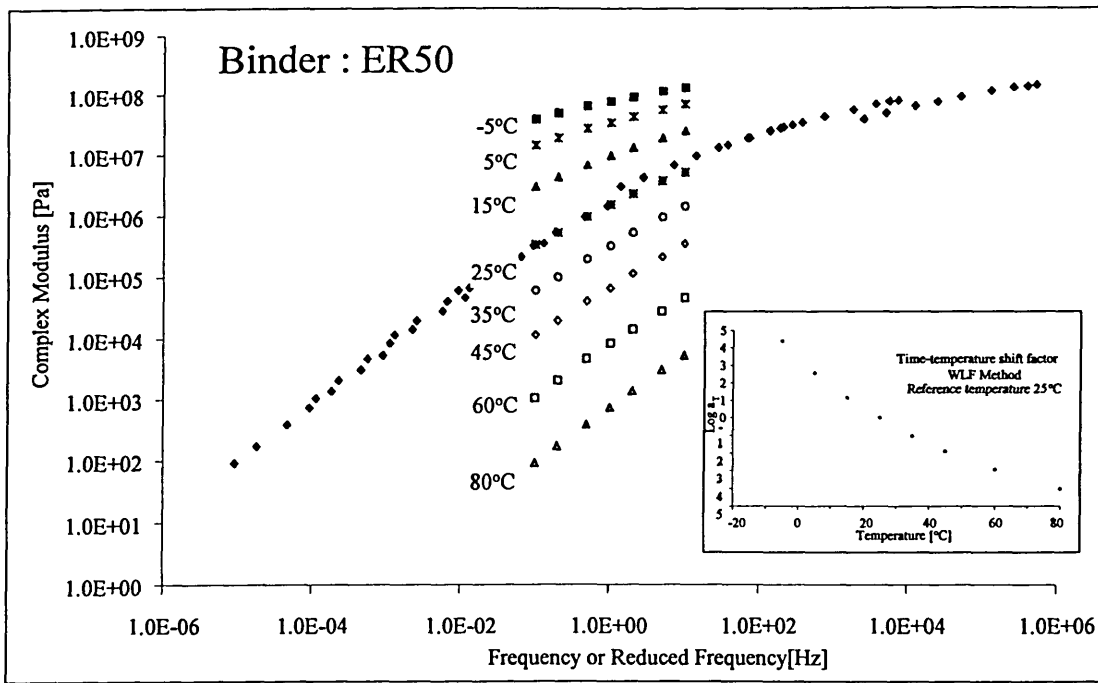


Figure B.5 Results of SBR modified 50 pen binder showing dependency of complex (shear) moduli at different test temperatures to loading frequency and the master curve of complex (shear) modulus at reference temperature of 25°C as a function of reduced frequency. Binder reference: ER50

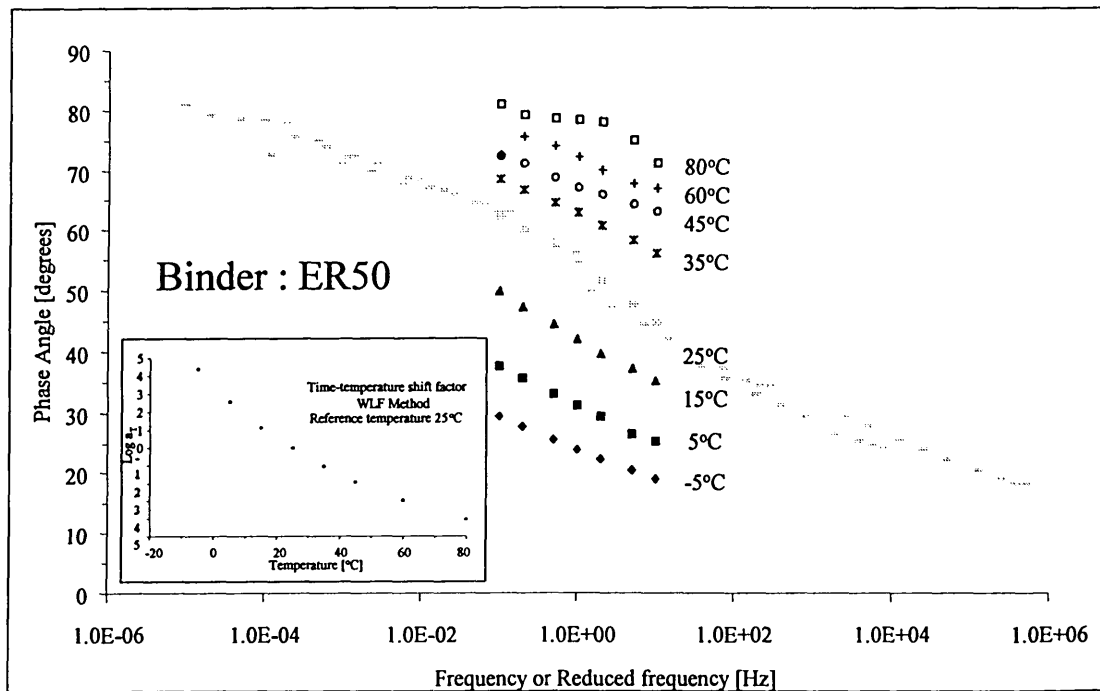


Figure B.6 Results of SBR modified 50 pen binder showing dependency of phase angles at different test temperatures to loading frequency and the master curve of phase angle at reference temperature of 25°C as a function of reduced frequency. Binder reference: ER50

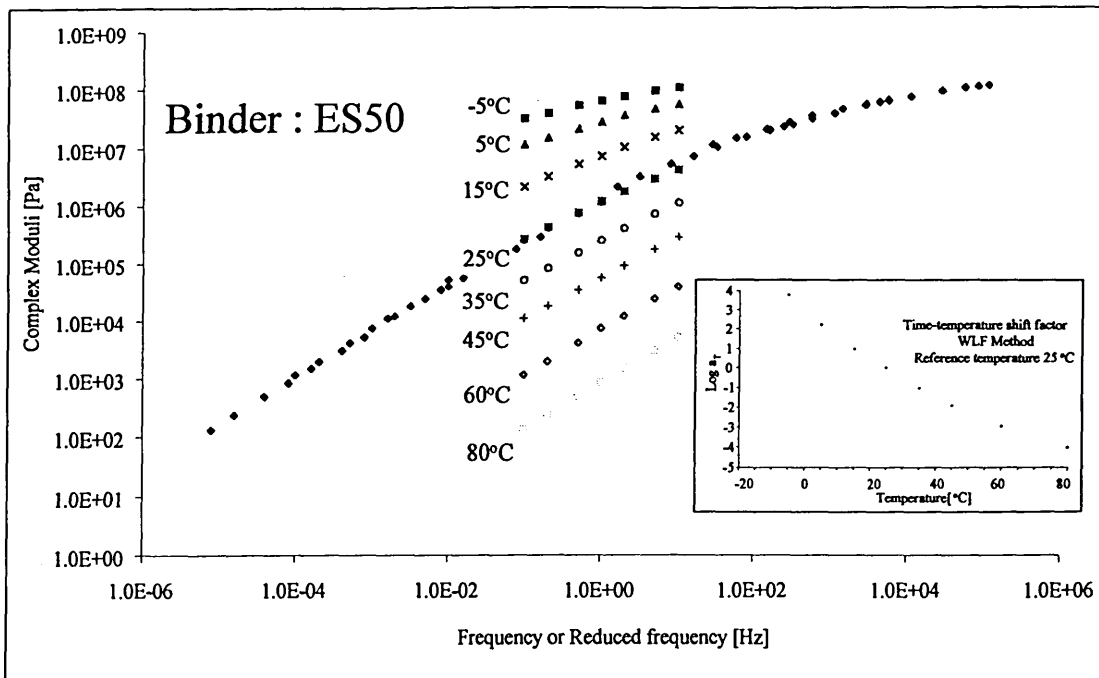


Figure B.7 Results of SBS modified 50 pen binder showing dependency of complex (shear) moduli at different test temperatures to loading frequency and the master curve of complex (shear) modulus at reference temperature of 25°C as a function of reduced frequency. Binder reference: ES50

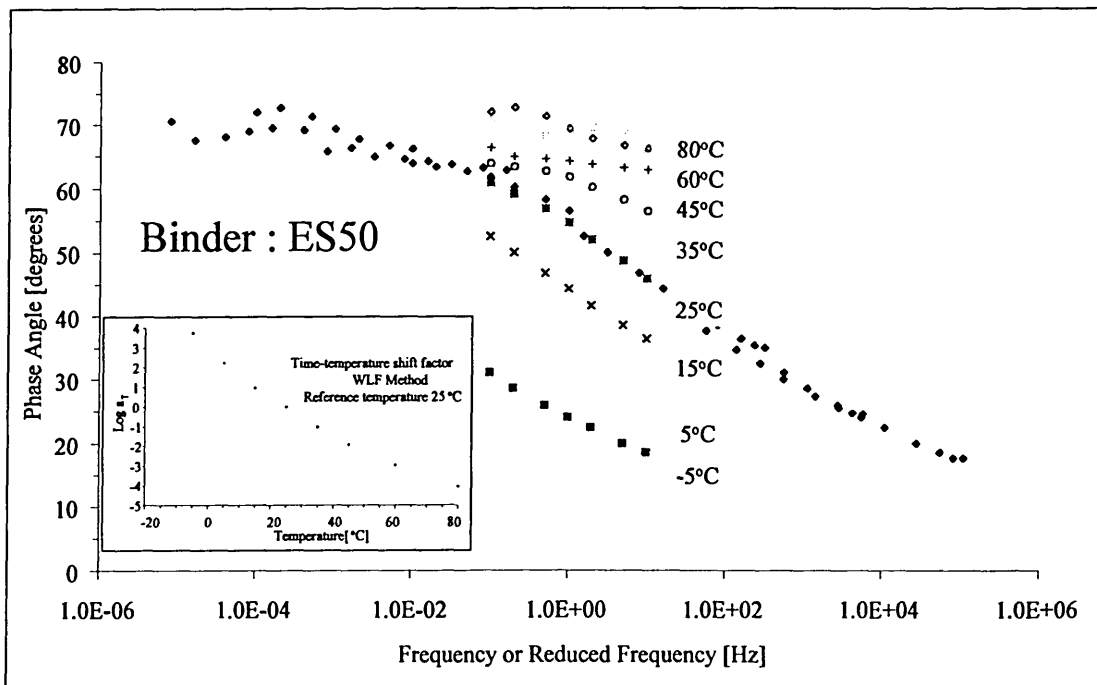


Figure B.8 Results of SBS modified 50 pen binder showing dependency of phase angles at different test temperatures to loading frequency and the master curve of phase angle at reference temperature of 25°C as a function of reduced frequency. Binder reference: ES50

## 2. Mixture test

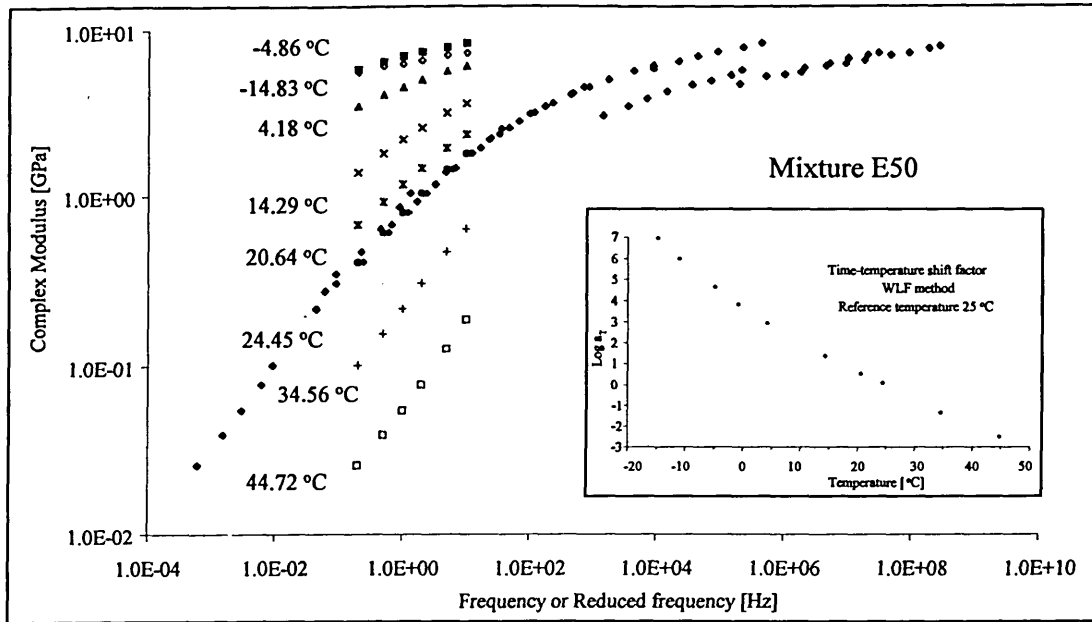


Figure B.9 Results of HRA with 50 pen bitumen showing dependency of complex (flexural) moduli at different test temperatures to loading frequency and the master curve of complex (flexural) modulus at reference temperature of 25°C as a function of reduced frequency. Mixture reference: E50

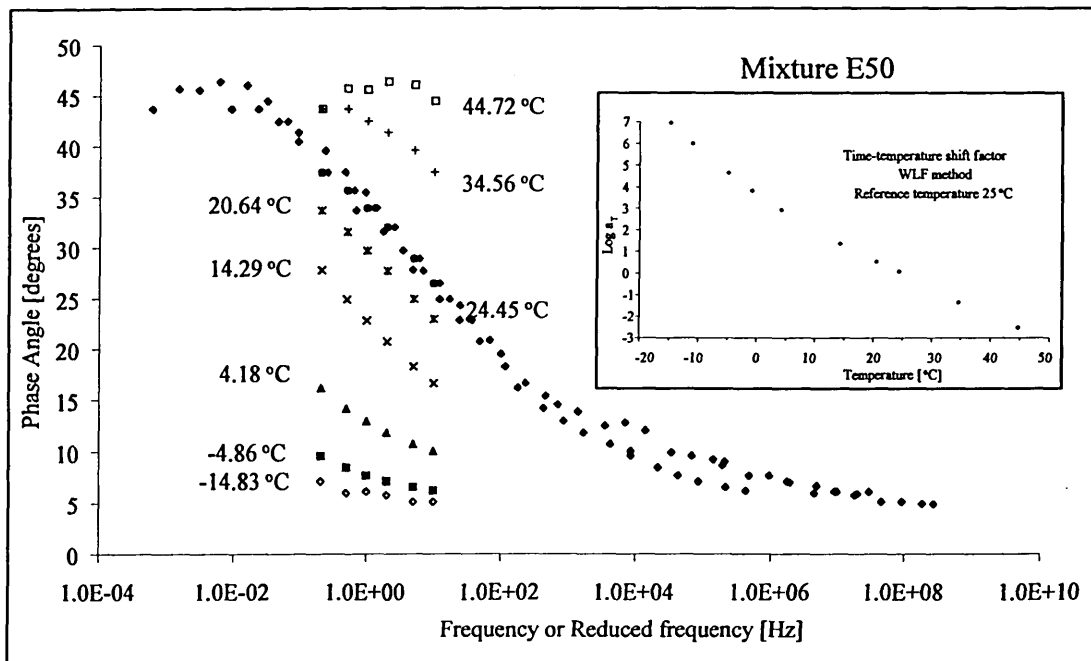


Figure B.10 Results of HRA with 50 pen bitumen showing dependency of phase angles at different test temperatures to loading frequency and the master curve of phase angle at reference temperature of 25°C as a function of reduced frequency. Mixture reference: E50

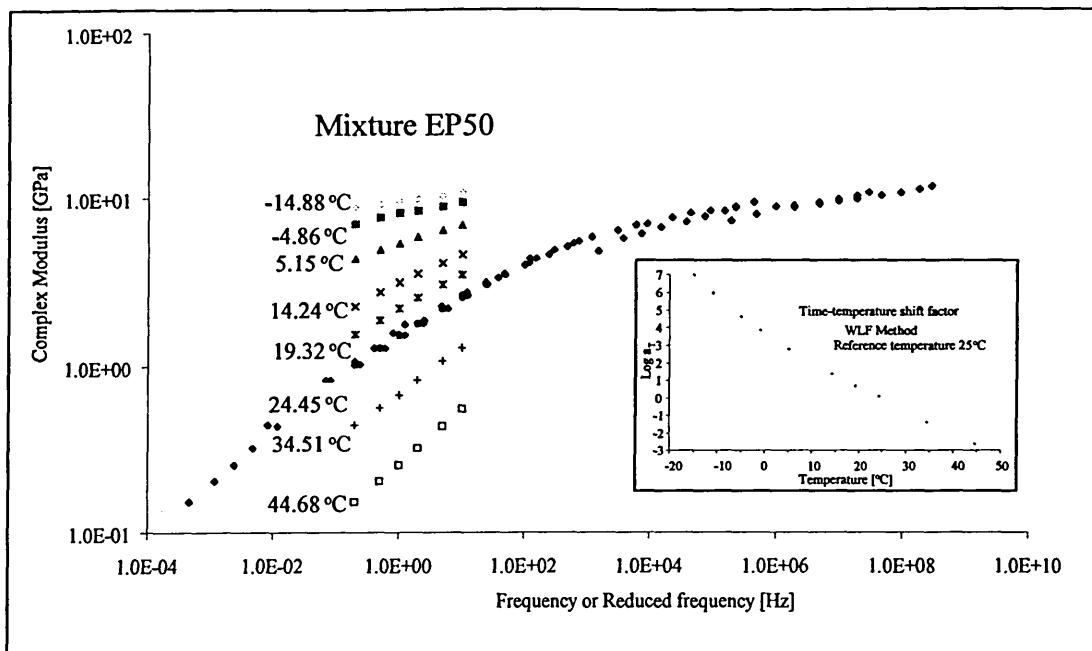


Figure B.11 Results of HRA with EVA modified 50 pen binder showing dependency of complex (flexural) moduli at different test temperatures to loading frequency and the master curve of complex (flexural) modulus at reference temperature of 25°C as a function of reduced frequency. Mixture reference: EP50

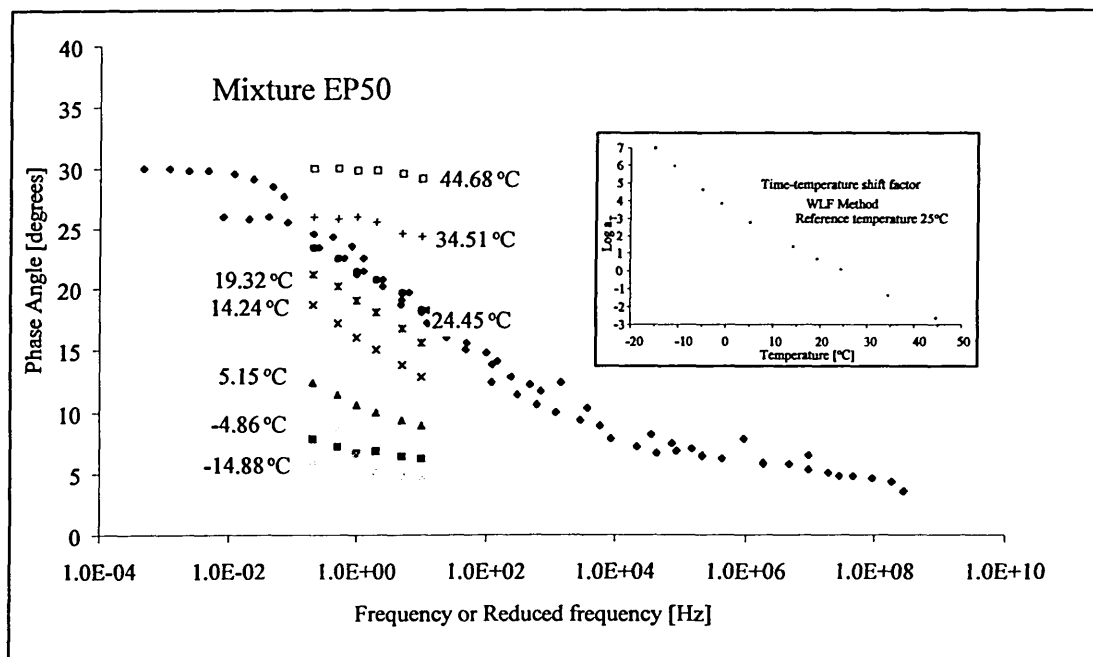


Figure B.12 Results of HRA with EVA modified 50 pen binder showing dependency of phase angles at different test temperatures to loading frequency and the master curve of phase angle at reference temperature of 25°C as a function of reduced frequency. Mixture reference: EP50

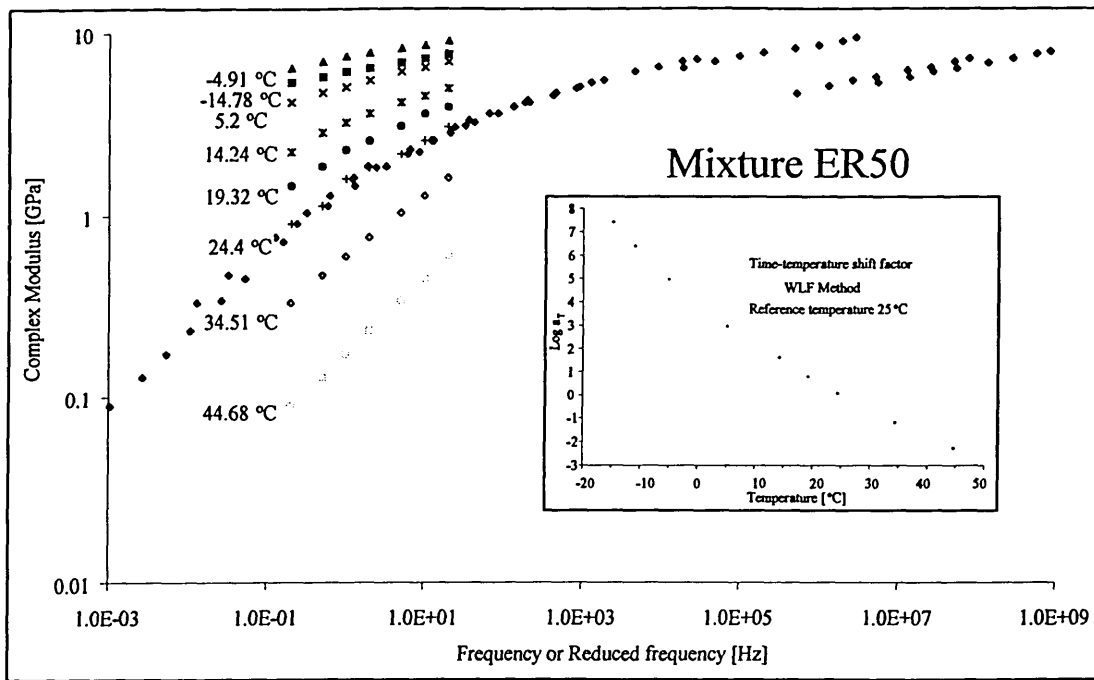


Figure B.13 Results of HRA with SBR modified 50 pen binder showing dependency of complex (flexural) moduli at different test temperatures to loading frequency and the master curve of complex (flexural) modulus at reference temperature of 25°C as a function of reduced frequency. Mixture reference: ER50

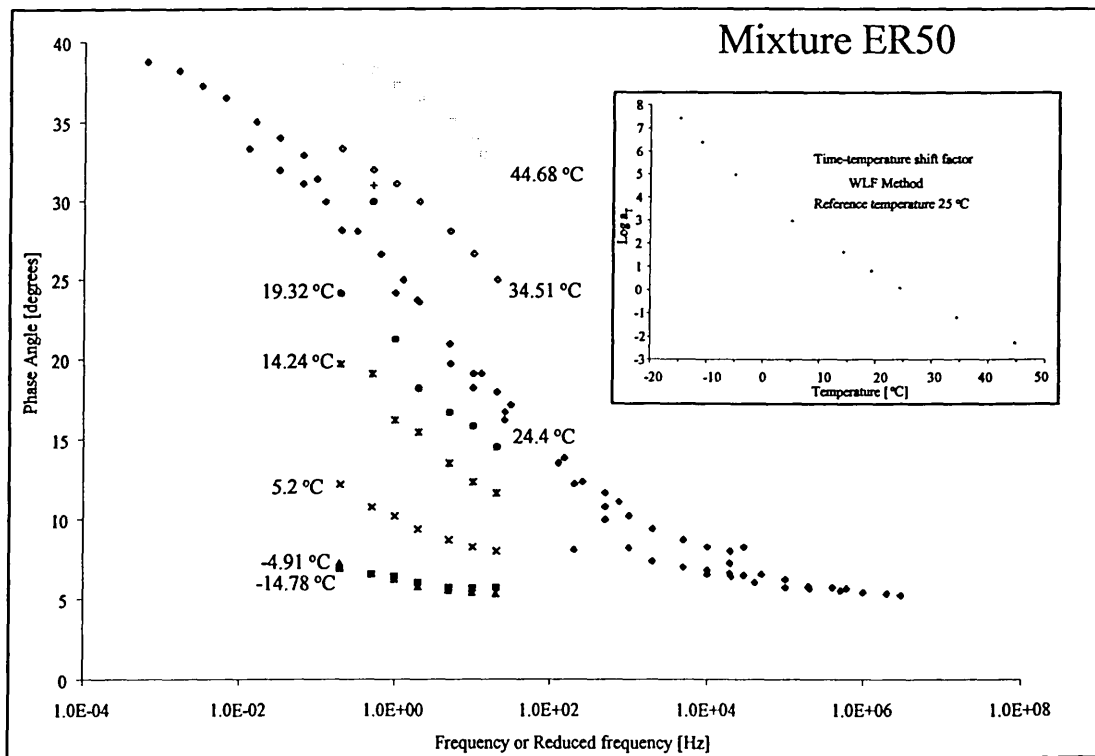


Figure B.14 Results of HRA with SBR modified 50 pen binder showing dependency of phase angles at different test temperatures to loading frequency and the master curve of phase angle at reference temperature of 25°C as a function of reduced frequency. Mixture reference: ER50

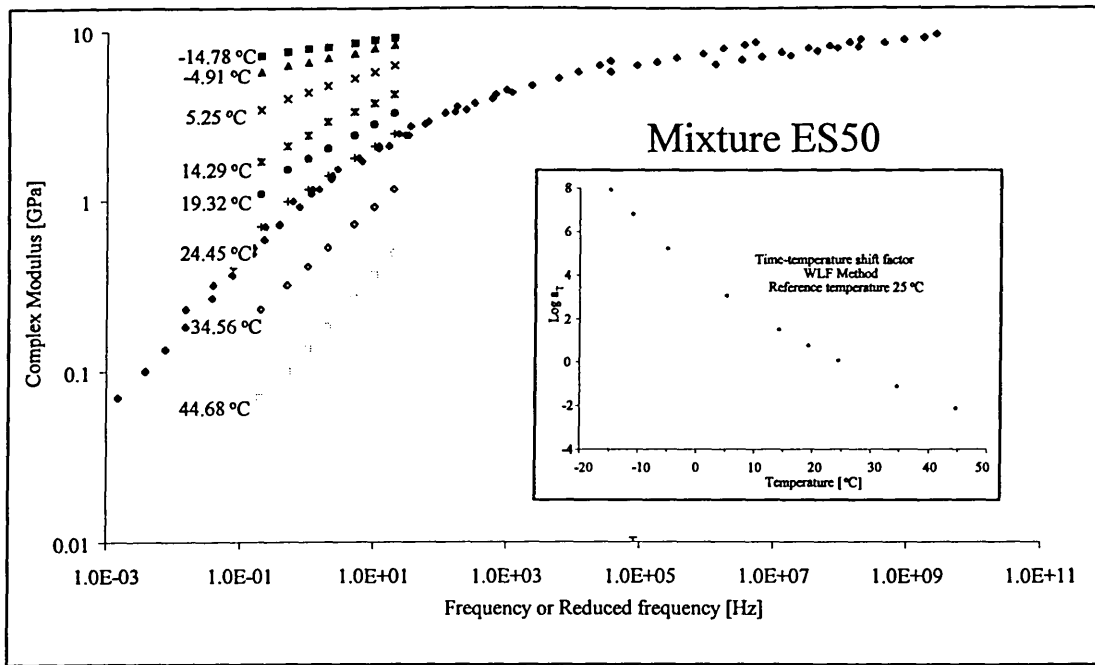


Figure B.15 Results of HRA with SBS modified 50 pen binder showing dependency of complex (flexural) moduli at different test temperatures to loading frequency and the master curve of complex (flexural) modulus at reference temperature of 25°C as a function of reduced frequency. Mixture reference: ES50

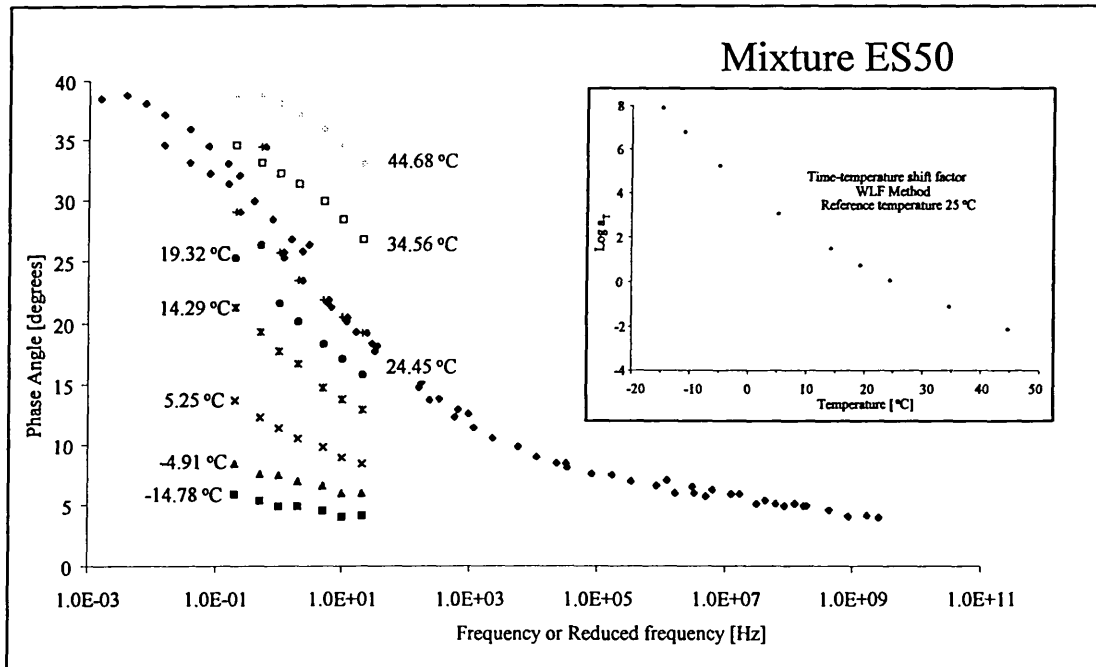


Figure B.16 Results of HRA with SBS modified 50 pen binder showing dependency of phase angles at different test temperatures to loading frequency and the master curve of phase angle at reference temperature of 25°C as a function of reduced frequency. Mixture reference: ES50

### 3. Raw data from oscillation tests on bituminous binders

#### 3.1. Binder 50 Pen (A50)

##### Phase Angle $\delta$ (degree)

Freq[Hz]	Temperature [°C]							
	-5	5	15	25	35	45	60	80
0.1	36.65	45.74	58.6	69.56	78.13	84.5	87.79	86.29
0.2	33.75	42.81	55.9	67.04	76.25	82.94	87.33	85.91
0.5	31.71	39.6	52.06	63.98	73.31	80.49	86.35	86.32
1	28.76	37.17	49.49	61.14	71.36	78.86	85.56	85.44
2	26.19	34.59	46.98	58.38	69.24	76.92	84.64	83.95
5	23.77	31.84	43.68	54.16	66.31	74.51	82.94	
10	21.74	29.78	41.32	50.73	63.99	72.36	79.53	
15	21	28.83	40.03					
20	20.33	28.28	39.56					

##### Viscosity (Pa.s)

Freq[Hz]	Temperature [°C]							
	-5	5	15	25	35	45	60	80
0.1	3.94E+07	1.26E+07	2.23E+06	3.46E+05	4.10E+04	4.95E+03	3.82E+02	3.01E+01
0.2	2.60E+07	8.87E+06	1.72E+06	2.96E+05	3.72E+04	4.67E+03	3.78E+02	2.91E+01
0.5	1.44E+07	5.42E+06	1.19E+06	2.32E+05	3.21E+04	4.34E+03	3.66E+02	2.80E+01
1	8.93E+06	3.61E+06	8.81E+05	1.89E+05	2.82E+04	4.03E+03	3.65E+02	2.76E+01
2	5.49E+06	2.39E+06	6.35E+05	1.47E+05	2.42E+04	3.67E+03	3.57E+02	2.69E+01
5	2.84E+06	1.33E+06	3.99E+05	1.04E+05	1.91E+04	3.18E+03	3.31E+02	
10	1.68E+06	8.31E+05	2.73E+05	7.67E+04	1.56E+04	2.76E+03	3.03E+02	
15	1.21E+06	6.22E+05	2.14E+05					
20	9.41E+05	5.00E+05	1.76E+05					

##### Complex Modulus $G^*$ (Pa)

Freq[Hz]	Temperature [°C]							
	-5	5	15	25	35	45	60	80
0.1	2.48E+07	7.91E+06	1.40E+06	2.17E+05	2.58E+04	3.11E+03	2.40E+02	1.89E+01
0.2	3.27E+07	1.11E+07	2.16E+06	3.67E+05	4.67E+04	5.87E+03	4.75E+02	3.66E+01
0.5	4.52E+07	1.70E+07	3.75E+06	7.30E+05	1.01E+05	1.36E+04	1.15E+03	8.81E+01
1	5.61E+07	2.27E+07	5.53E+06	1.19E+06	1.77E+05	2.53E+04	2.29E+03	1.73E+02
2	6.90E+07	3.00E+07	7.98E+06	1.85E+06	3.04E+05	4.62E+04	4.48E+03	3.38E+02
5	8.92E+07	4.17E+07	1.25E+07	3.26E+06	6.00E+05	1.00E+05	1.04E+04	
10	1.06E+08	5.22E+07	1.71E+07	4.82E+06	9.78E+05	1.73E+05	1.90E+04	
15	1.14E+08	5.87E+07	2.01E+07					
20	1.18E+08	6.29E+07	2.22E+07					

### 3.2. Binder 50 Pen (B50)

#### Phase Angle $\delta$ (degree)

Freq[Hz]	Temperature [°C]				
	25	35	45	60	80
0.01	76.77	84.14	81.22		
0.02	76.5	83.23	86.49		
0.05	74.09	80.59	85.44		
0.1	72.67	79.03	84.16	88.11	86.66
0.2	70.77	77.52	82.82	87.15	86.67
0.5	67.89	75.19	80.92	86.34	86.55
1	65.45	73.61	79.49	85.23	86.9
2	62.45	71.68	77.74	84.32	87.31
5	57.7	69.14	76.03	83.15	
10	53.74	66.62	74.51	82.27	

#### Viscosity (Pa.s)

Freq[Hz]	Temperature [°C]				
	25	35	45	60	80
0.01	4.55E+05	5.96E+04	7.73E+03		
0.02	3.92E+05	4.64E+04	6.02E+03		
0.05	3.39E+05	4.39E+04	5.78E+03		
0.1	2.99E+05	3.98E+04	5.59E+03	4.39E+02	3.34E+01
0.2	2.61E+05	3.62E+04	5.34E+03	4.46E+02	3.30E+01
0.5	2.10E+05	3.17E+04	4.94E+03	4.29E+02	3.22E+01
1	1.76E+05	2.81E+04	4.52E+03	4.02E+02	3.17E+01
2	1.45E+05	2.49E+04	4.14E+03	3.85E+02	3.13E+01
5	1.08E+05	2.05E+04	3.61E+03	3.59E+02	
10	8.19E+04	1.71E+04	3.12E+03	3.35E+02	

#### Complex Modulus $G^*$ (Pa)

Freq[Hz]	Temperature [°C]				
	25	35	45	60	80
0.01	2.86E+04	3.74E+03	4.85E+02		
0.02	4.93E+04	5.83E+03	7.57E+02		
0.05	1.06E+05	1.38E+04	1.82E+03		
0.1	1.88E+05	2.50E+04	3.51E+03	2.76E+02	2.10E+01
0.2	3.28E+05	4.55E+04	6.71E+03	5.61E+02	4.14E+01
0.5	6.60E+05	9.97E+04	1.55E+04	1.35E+03	1.01E+02
1	1.11E+06	1.77E+05	2.84E+04	2.52E+03	1.99E+02
2	1.82E+06	3.13E+05	5.20E+04	4.83E+03	3.93E+02
5	3.39E+06	6.43E+05	1.13E+05	1.13E+04	
10	5.15E+06	1.08E+06	1.96E+05	2.11E+04	

### 3.3. Binder : 50 Pen (C50)

#### Phase Angle $\delta$ (degree)

Freq[Hz]	Temperature [°C]							
	-5	5	15	25	35	45	60	80
0.01				78.27	64.2			
0.02				75.52	82.86			
0.05				72.15	80.25			
0.1	32.55	45.65	60.24	70.2	78.14	84.26	88.31	
0.2	29.89	42.8	57.29	68.11	76.19	82.7	87.86	89.34
0.5	26.62	39.19	53.62	64.7	73.7	80.52	86.54	88.92
1	24.82	36.51	50.79	62.21	71.55	78.52	85.8	88.99
2	23.08	34.25	47.66	59.31	69.38	76.75	84.63	88.96
5	20.47	30.95	44.09	54.99	66.39	74.37	83.08	
10	18.53	28.78	41.54	51.38	64.16	72.45	81.93	
15	17.96	27.78	40.12					
20	17.55	27.24	39.58					

#### Viscosity (Pa.s)

Freq[Hz]	Temperature [°C]							
	-5	5	15	25	35	45	60	80
0.01				4.37E+05	3.45E+04			
0.02				4.07E+05	5.25E+04			
0.05				3.49E+05	4.85E+04			
0.1	6.31E+07	1.51E+07	2.28E+06	3.02E+05	4.44E+04	6.17E+03	4.68E+02	
0.2	4.06E+07	1.07E+07	1.81E+06	2.58E+05	4.02E+04	5.84E+03	4.63E+02	3.33E+01
0.5	2.12E+07	6.51E+06	1.28E+06	2.06E+05	3.46E+04	5.33E+03	4.59E+02	3.32E+01
1	1.29E+07	4.38E+06	9.60E+05	1.68E+05	3.04E+04	4.95E+03	4.48E+02	3.32E+01
2	7.80E+06	2.85E+06	6.97E+05	1.34E+05	2.61E+04	4.52E+03	4.32E+02	3.32E+01
5	3.85E+06	1.59E+06	4.44E+05	9.64E+04	2.06E+04	3.90E+03	4.02E+02	
10	2.22E+06	9.85E+05	3.05E+05	7.19E+04	1.67E+04	3.38E+03	3.71E+02	
15	1.57E+06	7.33E+05	2.41E+05					
20	1.21E+06	5.86E+05	2.00E+05					

*Complex Modulus G\* (Pa)*

Freq[Hz]	Temperature [°C]							
	-5	5	15	25	35	45	60	80
0.01				2.74E+04	2.17E+03			
0.02				5.12E+04	6.60E+03			
0.05				1.10E+05	1.52E+04			
0.1	3.96E+07	9.50E+06	1.43E+06	1.90E+05	2.79E+04	3.88E+03	2.94E+02	
0.2	5.10E+07	1.34E+07	2.28E+06	3.25E+05	5.06E+04	7.34E+03	5.82E+02	4.19E+01
0.5	6.67E+07	2.05E+07	4.01E+06	6.46E+05	1.09E+05	1.68E+04	1.44E+03	1.04E+02
1	8.08E+07	2.75E+07	6.03E+06	1.05E+06	1.91E+05	3.11E+04	2.81E+03	2.09E+02
2	9.80E+07	3.58E+07	8.76E+06	1.68E+06	3.28E+05	5.68E+04	5.42E+03	4.17E+02
5	1.21E+08	4.98E+07	1.40E+07	3.03E+06	6.47E+05	1.22E+05	1.26E+04	
10	1.39E+08	6.19E+07	1.92E+07	4.52E+06	1.05E+06	2.12E+05	2.33E+04	
15	1.48E+08	6.91E+07	2.27E+07					
20	1.52E+08	7.37E+07	2.51E+07					

3.4. Binder : 50 Pen (D50)

*Phase Angle  $\delta$  (degree)*

Freq[Hz]	Temperature [°C]							
	-5	5	15	25	35	45	60	80
0.01					80.08	86.78		
0.02				69.64	78.48	84.58		
0.05				67.37	75.29	81.91		
0.1	36.36	45.99	56.33	65.57	72.91	80.16	85.55	85.5
0.2	34.19	43.54	54.1	63.51	70.94	78.16	84.59	85.8
0.5	31.34	40.25	51.29	61.15	68.51	75.2	83.32	86.53
1	29.23	38.2	49.17	58.98	66.75	73.47	81.72	86.53
2	27.34	36.17	46.72	56.61	65.15	71.44	79.84	86.39
5	24.67	33.41	43.68	53.55	63.11	69.26	77.73	86.05
10	22.9	31.34	41.94	50.66	61.67	67.8	75.78	
15	22.03	30.38	40.97					
20	22	29.94	40.7					

Viscosity (Pa.s)

Freq[Hz]	Temperature [°C]							
	-5	5	15	25	35	45	60	80
0.01				4.83E+05	6.45E+04	1.63E+04		
0.02				4.10E+05	6.35E+04	9.23E+03		
0.05				3.31E+05	5.56E+04	8.55E+03		
0.1	3.70E+07	1.11E+07	2.09E+06	2.78E+05	4.93E+04	8.15E+03	6.61E+02	4.71E+01
0.2	2.45E+07	7.94E+06	1.59E+06	2.29E+05	4.21E+04	7.64E+03	6.44E+02	4.70E+01
0.5	1.37E+07	4.81E+06	1.09E+06	1.73E+05	3.42E+04	6.62E+03	6.16E+02	4.63E+01
1	8.71E+06	3.27E+06	8.06E+05	1.37E+05	2.86E+04	5.77E+03	5.87E+02	4.54E+01
2	5.35E+06	2.15E+06	5.81E+05	1.07E+05	2.35E+04	5.00E+03	5.46E+02	4.46E+01
5	2.78E+06	1.23E+06	3.65E+05	7.48E+04	1.77E+04	4.06E+03	4.83E+02	
10	1.65E+06	7.76E+05	2.49E+05	5.49E+04	1.39E+04	3.40E+03	4.26E+02	
15	1.19E+06	5.80E+05	1.97E+05					
20	9.30E+06	4.70E+05	1.64E+05					

Complex Modulus G\* (Pa)

Freq[Hz]	Temperature [°C]							
	-5	5	15	25	35	45	60	80
0.01				3.04E+04	4.05E+03	1.03E+03		
0.02				5.15E+04	7.98E+03	1.16E+03		
0.05				1.04E+05	1.75E+04	2.69E+03		
0.1	2.32E+07	7.00E+06	1.31E+06	1.75E+05	3.09E+04	5.12E+03	4.15E+02	2.96E+01
0.2	3.07E+07	9.97E+06	2.00E+06	2.88E+05	5.29E+04	9.60E+03	8.09E+02	5.90E+01
0.5	4.30E+07	1.51E+07	3.43E+06	5.43E+05	1.07E+05	2.08E+04	1.94E+03	1.46E+02
1	5.47E+07	2.05E+07	5.07E+06	8.64E+05	1.80E+05	3.62E+04	3.69E+03	2.85E+02
2	6.72E+07	2.70E+07	7.31E+06	1.35E+06	2.95E+05	6.28E+04	6.86E+03	5.60E+02
5	8.74E+07	3.85E+07	1.15E+07	2.35E+06	5.55E+05	1.27E+05	1.52E+04	
10	1.04E+08	4.87E+07	1.56E+07	3.45E+06	8.74E+05	2.14E+05	2.68E+04	
15	1.12E+08	5.47E+07	1.85E+07					
20	1.17E+08	5.90E+07	2.06E+07					

3.5. Binder : 50 Pen + 5% EVA (AP50)

Phase Angle  $\delta$  (degree)

Freq[Hz]	Temperature [°C]							
	-5	5	15	25	35	45	60	70
0.01			53.79	52.23				
0.02			51.23	52.7	49.71	58.53		
0.1	35.02	42	48.4	52.72	54.3	57.16	69.62	85.2
0.2	32.63	40.32	47.37	52.19	55.22	58.18	68.56	84.74
0.5	30.18	38.38	46.12	51.62	55.41	59.09	69.09	83.4
1	28.46	36.73	45.16	50.63	55.49	59.93	69.42	82.49
2	26.32	34.87	43.6	49.56	55.11	60.12	69.19	81.27
5	23.97	32.62	41.93	47.7	54.68	60.16	68.56	78.92
10	22.22	30.82	40.52	45.99	53.78	60.01	67.78	76.4
15	21.2	29.9	39.86				67.23	72.41
20	20.89	29.29	39.34					

Viscosity (Pa.s)

Freq[Hz]	Temperature [°C]							
	-5	5	15	25	35	45	60	70
0.01			6.45E+06	1.27E+06	3.23E+05	2.09E+04		
0.02			4.50E+06	9.75E+05	2.06E+05	3.92E+04		
0.1	3.91E+07	1.15E+07	2.29E+06	5.03E+05	1.07E+05	2.14E+04	1.35E+03	2.29E+02
0.2	2.55E+07	7.92E+06	1.67E+06	3.78E+05	8.14E+04	1.66E+04	1.44E+03	2.26E+02
0.5	1.39E+07	4.73E+06	1.07E+06	2.56E+05	5.80E+04	1.22E+04	1.13E+03	2.22E+02
1	8.81E+06	3.16E+06	7.57E+05	1.91E+05	4.47E+04	9.67E+03	9.53E+02	2.20E+02
2	5.46E+06	2.08E+06	5.31E+05	1.40E+05	3.42E+04	7.69E+03	8.22E+02	2.06E+02
5	2.79E+06	1.17E+06	3.26E+05	9.11E+04	2.39E+04	5.66E+03	6.73E+02	1.82E+02
10	1.64E+06	7.41E+05	2.22E+05	6.46E+04	1.78E+04	4.47E+03	5.71E+02	1.61E+02
15	1.19E+06	5.54E+05	1.75E+05				5.14E+02	1.44E+02
20	9.23E+05	4.46E+05	1.45E+05					

Complex Modulus  $G^*$  (Pa)

Freq[Hz]	Temperature [°C]							
	-5	5	15	25	35	45	60	80
0.01			4.06E+05	7.96E+04	2.03E+04	1.31E+03		
0.02			5.65E+05	1.22E+05	2.59E+04	4.93E+03		
0.1	2.46E+07	7.25E+06	1.44E+06	3.16E+05	6.73E+04	1.34E+04	8.47E+02	1.44E+02
0.2	3.21E+07	9.95E+06	2.10E+06	4.75E+05	1.02E+05	2.09E+04	1.81E+03	2.83E+02
0.5	4.38E+07	1.48E+07	3.35E+06	8.04E+05	1.82E+05	3.85E+04	3.56E+03	6.99E+02
1	5.53E+07	1.98E+07	4.76E+06	1.20E+06	2.81E+05	6.07E+04	5.99E+03	1.38E+03
2	6.86E+07	2.61E+07	6.67E+06	1.76E+06	4.30E+05	9.67E+04	1.03E+04	2.59E+03
5	8.77E+07	3.68E+07	1.02E+07	2.86E+06	7.50E+05	1.78E+05	2.11E+04	5720
10	1.03E+08	4.66E+07	1.39E+07	4.06E+06	1.12E+06	2.81E+05	3.59E+04	10100
15	1.12E+08	5.22E+07	1.65E+07				48400	13600
20	1.16E+08	5.61E+07	1.45E+07					

3.6. Binder : 50 Pen + 5% EVA (BP50)

Phase Angle  $\delta$  (degree)

Freq[Hz]	Temperature [°C]							
	-5	5	15	25	35	45	60	80
0.05				56.9	61.3			
0.1	32.26	40.37	48.8	55.39	59.8	66.52	74.45	85.42
0.2	29.69	38.39	47.16	54.43	58.99	65.36	72.64	85.47
0.5	26.95	36.1	45.27	53.08	58.62	64.02	71.35	85.14
1	24.71	34.05	43.39	51.9	57.97	63.37	70.5	84.35
2	22.32	31.95	41.68	50.13	57.23	62.55	69.57	83.04
5	19.98	29.54	39.27	47.82	55.87	62.06	69.22	80.44
10	18.21	27.6	37.64	45.63	54.55	61.37	69.26	79.75
15	17.43	26.49	36.78	44.48	54.06	60.97	69.25	
20	16.76	26.17	36.6	43.61	53.61	60.81	67.51	

Viscosity (Pa.s)

Freq[Hz]	Temperature [°C]							
	-5	5	15	25	35	45	60	80
0.05				7.36E+05	1.41E+05			
0.1	6.97E+07	2.02E+07	4.20E+06	5.55E+05	1.15E+05	2.14E+04	1.81E+03	7.89E+01
0.2	4.35E+07	1.38E+07	3.03E+06	4.23E+05	9.11E+04	1.79E+04	1.66E+03	8.19E+01
0.5	2.33E+07	8.01E+06	1.94E+06	2.90E+05	6.60E+04	1.38E+04	1.36E+03	8.24E+01
1	1.45E+07	5.24E+06	1.37E+06	2.20E+05	5.14E+04	1.13E+04	1.18E+03	8.48E+01
2	8.64E+06	3.39E+06	9.51E+05	1.64E+05	3.99E+04	9.20E+03	1.03E+03	8.54E+01
5	4.28E+06	1.85E+06	5.69E+05	1.07E+05	2.87E+04	6.86E+03	8.44E+02	8.27E+01
10	2.45E+06	1.14E+06	3.79E+05	7.56E+04	2.19E+04	5.44E+03	7.12E+02	7.75E+01
15	1.73E+06	8.42E+05	2.92E+05	6.05E+04	1.82E+04	4.73E+03	6.30E+02	
20	1.33E+06	6.71E+05	2.40E+05	5.14E+04	1.57E+04	4.21E+03	5.73E+02	

Complex Modulus  $G^*$  (Pa)

Freq[Hz]	Temperature [°C]							
	-5	5	15	25	35	45	60	80
0.05				2.31E+05	4.43E+04			
0.1	4.38E+07	1.27E+07	2.64E+06	3.49E+05	7.26E+04	1.35E+04	1.14E+03	4.96E+01
0.2	5.47E+07	1.73E+07	3.81E+06	5.31E+05	1.15E+05	2.24E+04	2.08E+03	1.03E+02
0.5	7.32E+07	2.52E+07	6.09E+06	9.12E+05	2.07E+05	4.35E+04	4.26E+03	2.59E+02
1	9.10E+07	3.29E+07	8.61E+06	1.38E+06	3.23E+05	7.10E+04	7.40E+03	5.33E+02
2	1.09E+08	4.26E+07	1.19E+07	2.06E+06	5.01E+05	1.16E+05	1.30E+04	1.07E+03
5	1.34E+08	5.82E+07	1.79E+07	3.36E+06	9.00E+05	2.15E+05	2.65E+04	2600
10	1.54E+08	7.18E+07	2.38E+07	4.75E+06	1.38E+06	3.42E+05	4.47E+04	4870
15	1.63E+08	7.93E+07	2.75E+07	5.71E+06	1.71E+06	4.46E+05	5.94E+04	
20	1.67E+08	8.43E+07	3.01E+07	6.46E+06	1.98E+06	5.29E+05	7.21E+04	

3.7. Binder : 50 Pen + 5% EVA (CP50)

Phase Angle  $\delta$  (degree)

Freq[Hz]	Temperature [°C]				
	25	35	45	60	80
0.05	54.91	54.14			
0.1	53.15	56.62	62.3	75.06	85.64
0.2	52.47	56.3	61.39	71.71	85.66
0.5	51.62	55.48	60.89	70.58	85.82
1	50.97	55.01	60.26	69.8	85.34
2	49.86	54.58	59.64	69.91	84.71
5	48.34	54.1	59.23	67.71	
10	46.96	53.55	59.02	66.88	
15	45.93	53.33	58.95		
20	45.6	53.05	58.78		

Viscosity (Pa.s)

Freq[Hz]	Temperature [°C]				
	25	35	45	60	80
0.05	6.13E+05	1.40E+05			
0.1	4.55E+05	1.08E+05	2.25E+04	1.53E+03	6.86E+01
0.2	3.43E+05	8.33E+04	1.82E+04	1.55E+03	7.09E+01
0.5	2.31E+05	5.90E+04	1.35E+04	1.26E+03	7.06E+01
1	1.71E+05	4.52E+04	1.08E+04	1.07E+03	6.77E+01
2	1.27E+05	3.44E+04	8.45E+03	9.08E+02	6.35E+01
5	8.38E+04	2.40E+04	6.15E+03	7.24E+02	
10	5.97E+04	1.78E+04	4.78E+03	6.03E+02	
15	4.85E+04	1.48E+04	4.07E+03	5.11E+02	
20	4.10E+04	1.28E+04	3.60E+03		

Complex Modulus  $G^*$  (Pa)

Freq[Hz]	Temperature [°C]				
	25	35	45	60	80
0.05	1.93E+05	4.40E+04			
0.1	2.86E+05	6.77E+04	1.41E+04	9.42E+02	4.31E+01
0.2	4.31E+05	1.05E+05	2.28E+04	1.95E+02	8.90E+03
0.5	7.25E+05	1.85E+05	4.25E+04	3.94E+03	2.22E+02
1	1.08E+06	2.84E+05	6.78E+04	6.72E+03	4.25E+02
2	1.60E+06	4.32E+05	1.06E+05	1.14E+04	7.98E+02
5	2.63E+06	7.52E+05	1.93E+05	2.27E+04	
10	3.75E+06	1.12E+06	3.00E+05	3.79E+04	
15	4.57E+06	1.39E+06	3.84E+05	4.82E+04	
20	5.15E+06	1.61E+06	4.52E+05	1.54E+04	

3.8. Binder : 50 Pen + 5% EVA (DP50)

Phase Angle  $\delta$  (degree)

Freq[Hz]	Temperature [°C]							
	-5	5	15	25	35	45	60	80
0.1	31.35	37	43.87	51.85	57.73	64.95	75.59	84.3
0.2	29.97	36.04	42.72	50.62	56.37	62.9	71.77	83.86
0.5	28.12	34.12	40.94	48.72	54.45	60.69	69.6	82.59
1	26.78	33.27	39.84	47.81	53.47	59.44	67.89	80.81
2	25.32	31.88	38.79	46.27	52.22	58.06	65.9	79.08
5	23.24	30.04	37.16	44.68	51.06	56.66	64.39	75.56
10	21.83	28.72	36.17	43.27	50.04	55.91	63.25	73.01
15	21.11	28.17	35.71	42.37	49.56	55.46		
20	20.88	28.1	35.61	41.86	49.56	55.47		

Viscosity (Pa.s)

Freq[Hz]	Temperature [°C]							
	-5	5	15	25	35	45	60	80
0.1	4.00E+07	1.30E+07	3.18E+06	5.14E+05	1.25E+05	2.76E+04	2.76E+03	1.68E+02
0.2	2.50E+07	8.56E+06	2.22E+06	3.84E+05	9.73E+04	2.27E+04	2.61E+03	1.86E+02
0.5	1.33E+07	4.90E+06	1.35E+06	2.54E+05	6.81E+04	1.70E+04	2.13E+03	2.03E+02
1	8.31E+06	3.17E+06	9.17E+05	1.84E+05	5.16E+04	1.35E+04	1.80E+03	2.07E+02
2	5.01E+06	2.04E+06	6.21E+05	1.32E+05	3.89E+04	1.05E+04	1.50E+03	1.96E+02
5	2.61E+06	1.11E+06	3.63E+05	8.33E+04	2.61E+04	7.51E+03	1.15E+03	1.75E+02
10	1.52E+06	6.95E+05	2.37E+05	5.78E+04	1.88E+04	5.72E+03	9.18E+02	1.54E+02
15	1.10E+06	5.17E+05	1.83E+05	4.61E+04	1.55E+04	4.80E+03		
20	8.71E+05	4.14E+05	1.50E+05	3.84E+04	1.33E+04	4.18E+03		

Complex Modulus  $G^*$  (Pa)

Freq[Hz]	Temperature [°C]							
	-5	5	15	25	35	45	60	80
0.1	2.51E+07	8.17E+06	2.00E+06	3.23E+05	7.87E+04	1.74E+04	1.73E+03	1.06E+02
0.2	3.14E+07	1.08E+07	2.79E+06	4.82E+05	1.22E+05	2.85E+04	3.27E+03	2.34E+02
0.5	4.18E+07	1.54E+07	4.24E+06	7.99E+05	2.14E+05	5.33E+04	6.70E+03	6.39E+02
1	5.22E+07	1.99E+07	5.76E+06	1.16E+06	3.24E+05	8.46E+04	1.13E+04	1.30E+03
2	6.29E+07	2.56E+07	7.80E+06	1.66E+06	4.89E+05	1.32E+05	1.88E+04	2.47E+03
5	8.21E+07	3.50E+07	1.14E+07	2.62E+06	8.19E+05	2.36E+05	3.61E+04	5.49E+03
10	9.58E+07	4.37E+07	1.49E+07	3.63E+06	1.18E+06	3.59E+05	5.77E+04	9.68E+03
15	1.04E+08	4.88E+07	1.72E+07	4.34E+06	1.46E+06	4.52E+05		
20	1.09E+08	5.20E+07	1.89E+07	4.83E+06	1.67E+06	5.25E+05		

#### 4. Raw data from dynamic bending machine on bituminous mixtures

Engineering units :

- Temp (temperature) in centigrade (°C)
- Avg E' (average elastic modulus) in GPa
- Avg E'' (average loss modulus) in GPa
- Avg E\* (average complex modulus) in GPa
- Avg Phase Angle (average phase angle) in degree

##### 4.1. 50 Pen HRA Mixture (E50)

Temp (C)	Frequency (Hz.)	Avg E'	Avg E''	Avg E*	Avg Phase Angle
20.64	0.2	0.567	0.378	0.681	33.66
20.64	0.5	0.795	0.489	0.933	31.59
20.64	1	1.032	0.588	1.188	29.68
20.64	2	1.315	0.690	1.485	27.72
20.64	5	1.768	0.822	1.950	24.93
20.64	10	2.180	0.918	2.366	22.84
20.64	20	2.650	1.003	2.833	20.73
20.64	30	2.982	1.053	3.162	19.46
-4.86	0.2	5.789	0.971	5.870	9.52
-4.86	0.5	6.446	0.951	6.516	8.39
-4.86	1	6.907	0.929	6.969	7.66
-4.86	2	7.323	0.920	7.380	7.16
-4.86	5	7.890	0.899	7.941	6.50
-4.86	10	8.329	0.900	8.377	6.17
4.18	0.2	3.349	0.970	3.487	16.16
4.18	0.5	3.997	1.004	4.122	14.10
4.18	1	4.462	1.020	4.577	12.89
4.18	2	4.945	1.035	5.052	11.82
4.18	5	5.553	1.050	5.652	10.72
4.18	10	6.055	1.062	6.148	9.96
14.29	0.2	1.237	0.651	1.397	27.77
14.29	0.5	1.656	0.768	1.825	24.88
14.29	1	2.027	0.850	2.198	22.75
14.29	2	2.437	0.919	2.605	20.67
14.29	5	3.029	0.996	3.189	18.20
14.29	10	3.518	1.047	3.670	16.58
14.29	20	4.040	1.106	4.189	15.31
14.29	30	4.414	1.139	4.558	14.47
24.45	0.2	0.326	0.250	0.411	37.47
24.45	0.5	0.500	0.358	0.615	35.63
24.45	1	0.673	0.452	0.811	33.92

Temp (C)	Frequency (Hz.)	Avg E'	Avg E''	Avg E*	Avg Phase Angle
24.45	2	0.896	0.560	1.057	32.05
24.45	5	1.273	0.701	1.454	28.84
24.45	10	1.630	0.811	1.820	26.48
24.45	20	2.046	0.920	2.244	24.21
24.45	30	2.348	0.986	2.547	22.78
34.56	0.2	0.073	0.069	0.101	43.67
34.56	0.5	0.112	0.107	0.155	43.67
34.56	1	0.161	0.148	0.219	42.48
34.56	2	0.230	0.202	0.307	41.33
34.56	5	0.363	0.300	0.471	39.56
34.56	10	0.513	0.393	0.646	37.47
34.56	20	0.707	0.503	0.867	35.43
34.56	30	0.869	0.585	1.048	33.92
44.72	0.2	0.018	0.018	0.026	43.67
44.72	0.5	0.027	0.027	0.038	45.64
44.72	1	0.038	0.039	0.055	45.57
44.72	2	0.054	0.056	0.078	46.28
44.72	5	0.088	0.091	0.127	46.01
44.72	10	0.135	0.132	0.189	44.42
44.72	20	0.204	0.185	0.275	42.40
44.72	30	0.268	0.228	0.352	40.48
25.43	0.2	0.286	0.210	0.355	36.26
25.43	0.5	0.413	0.292	0.506	35.26
25.43	1	0.550	0.371	0.664	33.97
25.43	2	0.729	0.466	0.866	32.60
25.43	5	1.042	0.601	1.203	29.99
25.43	10	1.342	0.711	1.519	27.92
25.43	20	1.706	0.823	1.894	25.77
25.43	30	1.974	0.893	2.167	24.36
19.37	0.2	0.470	0.320	0.568	34.25
19.37	0.5	0.675	0.426	0.798	32.21
19.37	1	0.879	0.510	1.017	30.14
19.37	2	1.126	0.607	1.280	28.33
19.37	5	1.528	0.726	1.692	25.44
19.37	10	1.883	0.820	2.054	23.53
19.37	20	2.306	0.906	2.478	21.44
19.37	30	2.603	0.961	2.774	20.26
24.4	0.2	0.238	0.187	0.303	38.20
24.4	0.5	0.351	0.266	0.441	37.17
24.4	1	0.474	0.340	0.583	35.64
24.4	2	0.633	0.425	0.763	33.90
24.4	5	0.916	0.553	1.070	31.14
24.4	10	1.223	0.673	1.396	28.84
24.4	20	1.529	0.764	1.709	26.57

Temp (C)	Frequency (Hz.)	Avg E'	Avg E''	Avg E*	Avg Phase Angle
24.4	30	1.774	0.832	1.959	25.12
34.56	0.2	0.066	0.053	0.086	38.72
34.56	0.5	0.099	0.079	0.127	38.74
34.56	1	0.130	0.112	0.171	40.87
34.56	2	0.176	0.154	0.234	41.26
34.56	5	0.275	0.229	0.359	39.80
34.56	10	0.388	0.309	0.496	38.53
34.56	20	0.539	0.403	0.673	36.79
34.56	30	0.674	0.476	0.826	35.24
44.68	0.2	0.024	0.017	0.030	36.62
44.68	0.5	0.035	0.028	0.045	38.74
44.68	1	0.046	0.037	0.059	38.59
44.68	2	0.062	0.051	0.080	39.49
44.68	5	0.098	0.082	0.128	39.92
44.68	10	0.130	0.112	0.172	40.84
44.68	20	0.183	0.154	0.239	40.02
44.68	30	0.236	0.193	0.306	39.31
49.76	0.2	0.018	0.011	0.021	31.24
49.76	0.5	0.024	0.017	0.030	35.71
49.76	1	0.031	0.022	0.038	35.59
49.76	2	0.039	0.030	0.050	37.78
49.76	5	0.059	0.046	0.075	38.10
49.76	10	0.083	0.065	0.105	38.11
49.76	20	0.117	0.094	0.150	38.81
49.76	30	0.150	0.113	0.189	36.99
20.4	0.2	0.376	0.221	0.438	29.95
20.4	0.5	0.453	0.292	0.539	32.86
20.4	1	0.516	0.328	0.612	32.48
20.4	2	0.641	0.389	0.750	31.25
20.4	5	0.868	0.489	0.996	29.39
20.4	10	1.102	0.576	1.243	27.61
20.4	20	1.366	0.661	1.518	25.81
20.4	30	1.570	0.718	1.727	24.57
5.2	0.2	1.960	0.652	2.065	18.41
5.2	0.5	2.384	0.709	2.487	16.56
5.2	1	2.727	0.744	2.827	15.28
5.2	2	3.077	0.782	3.175	14.28
5.2	5	3.564	0.830	3.659	13.11
5.2	10	3.966	0.864	4.060	12.30
5.2	20	4.395	0.916	4.489	11.79
5.2	30	4.720	0.941	4.813	11.28
-14.83	0.2	5.576	0.694	5.619	7.11
-14.83	0.5	6.067	0.641	6.101	6.03
-14.83	1	6.285	0.667	6.321	6.07

Temp (C)	Frequency (Hz.)	Avg E'	Avg E''	Avg E*	Avg Phase Angle
-14.83	2	6.579	0.658	6.612	5.72
-14.83	5	7.094	0.634	7.122	5.11
-14.83	10	7.272	0.656	7.302	5.17
-14.83	20	7.723	0.663	7.751	4.91
-14.83	30	7.960	0.687	7.990	4.93
-10.97	0.2	4.743	0.721	4.798	8.66
-10.97	0.5	5.217	0.700	5.264	7.65
-10.97	1	5.434	0.727	5.483	7.63
-10.97	2	5.885	0.724	5.929	7.02
-10.97	5	6.233	0.722	6.276	6.63
-10.97	10	6.738	0.717	6.777	6.08
-10.97	20	7.046	0.729	7.083	5.91
-10.97	30	7.233	0.778	7.275	6.16
-5.94	0.2	3.827	0.742	3.898	10.98
-5.94	0.5	4.270	0.744	4.335	9.90
-5.94	1	4.643	0.752	4.703	9.21
-5.94	2	5.116	0.795	5.177	8.82
-5.94	5	5.490	0.738	5.540	7.66
-5.94	10	5.713	0.799	5.769	7.98
-5.94	20	6.243	0.800	6.294	7.30
-5.94	30	6.490	0.840	6.545	7.39
-0.86	0.2	2.950	0.722	3.037	13.76
-0.86	0.5	3.390	0.746	3.472	12.42
-0.86	1	3.800	0.868	3.901	12.81
-0.86	2	4.186	0.895	4.284	12.05
-0.86	5	4.593	0.800	4.662	9.90
-0.86	10	4.941	0.833	5.010	9.59
-0.86	20	5.335	0.866	5.405	9.23
-0.86	30	5.674	0.893	5.744	8.97
9.21	0.2	1.325	0.561	1.439	22.97
9.21	0.5	1.676	0.631	1.792	20.64
9.21	1	1.977	0.682	2.092	19.03
9.21	2	2.294	0.729	2.407	17.63
9.21	5	2.766	0.788	2.876	15.91
9.21	10	3.159	0.831	3.266	14.75
9.21	20	3.559	0.881	3.667	13.91
9.21	30	3.856	0.918	3.964	13.40
14.24	0.2	0.765	0.417	0.871	28.64
14.24	0.5	1.024	0.501	1.140	26.09
14.24	1	1.262	0.567	1.383	24.21
14.24	2	1.531	0.632	1.657	22.43
14.24	5	1.950	0.713	2.076	20.09
14.24	10	2.302	0.773	2.429	18.57
14.24	20	2.674	0.836	2.802	17.36

Temp (C)	Frequency (Hz.)	Avg E'	Avg E''	Avg E*	Avg Phase Angle
14.24	30	2.944	0.877	3.073	16.60
5.2	0.2	1.943	0.643	2.046	18.32
5.2	0.5	2.354	0.694	2.454	16.42
5.2	1	2.693	0.733	2.791	15.22
5.2	2	3.028	0.762	3.123	14.14
5.2	5	3.531	0.801	3.621	12.79
5.2	10	3.904	0.839	3.993	12.13
5.2	20	4.306	0.884	4.396	11.62
5.2	30	4.609	0.922	4.701	11.32

#### 4.2. 50 Pen + 5%EVA HRA Mixture (EP50)

Temp (C)	Frequency (Hz.)	Avg E'	Avg E''	Avg E*	Avg Phase Angle
5.15	0.2	4.250	0.929	4.350	12.34
5.15	0.5	4.831	0.969	4.927	11.36
5.15	1	5.304	0.989	5.396	10.58
5.15	2	5.774	1.008	5.861	9.91
5.15	5	6.361	1.046	6.447	9.36
5.15	10	6.859	1.069	6.942	8.88
5.15	20	7.377	1.102	7.459	8.52
5.15	30	7.803	1.118	7.883	8.17
-4.86	0.2	6.990	0.958	7.055	7.81
-4.86	0.5	7.602	0.955	7.662	7.17
-4.86	1	8.063	0.945	8.118	6.69
-4.86	2	8.315	0.998	8.376	6.87
-4.86	5	8.884	0.997	8.940	6.43
-4.86	10	9.350	1.010	9.405	6.20
-4.86	20	9.896	1.034	9.952	5.99
-4.86	30	10.397	1.026	10.449	5.66
14.24	0.2	2.162	0.729	2.282	18.63
14.24	0.5	2.625	0.811	2.748	17.18
14.24	1	3.021	0.865	3.143	15.98
14.24	2	3.442	0.921	3.564	14.99
14.24	5	4.029	0.988	4.148	13.78
14.24	10	4.521	1.030	4.637	12.84
14.24	20	5.049	1.091	5.166	12.20
14.24	30	5.449	1.118	5.562	11.60
19.32	0.2	1.441	0.558	1.546	21.16
19.32	0.5	1.778	0.652	1.894	20.15
19.32	1	2.090	0.720	2.211	19.02
19.32	2	2.435	0.791	2.560	18.02
19.32	5	2.948	0.886	3.078	16.73
19.32	10	3.400	0.946	3.529	15.55

Temp (C)	Frequency (Hz.)	Avg E'	Avg E''	Avg E*	Avg Phase Angle
19.32	20	3.884	1.020	4.016	14.72
19.32	30	4.259	1.062	4.390	14.01
24.45	0.2	0.941	0.406	1.025	23.37
24.45	0.5	1.188	0.491	1.286	22.47
24.45	1	1.429	0.561	1.535	21.42
24.45	2	1.686	0.638	1.803	20.73
24.45	5	2.101	0.748	2.230	19.61
24.45	10	2.510	0.827	2.643	18.24
24.45	20	2.908	0.916	3.049	17.49
24.45	30	3.222	0.962	3.363	16.63
34.51	0.2	0.393	0.191	0.437	25.93
34.51	0.5	0.501	0.241	0.556	25.77
34.51	1	0.604	0.294	0.672	26.00
34.51	2	0.742	0.354	0.823	25.50
34.51	5	0.971	0.443	1.068	24.55
34.51	10	1.172	0.529	1.286	24.29
34.51	20	1.444	0.626	1.574	23.47
34.51	30	1.646	0.682	1.782	22.51
44.68	0.2	0.132	0.076	0.153	29.97
44.68	0.5	0.173	0.100	0.200	29.94
44.68	1	0.218	0.124	0.251	29.77
44.68	2	0.275	0.157	0.317	29.75
44.68	5	0.378	0.213	0.434	29.47
44.68	10	0.480	0.267	0.549	29.09
44.68	20	0.610	0.330	0.693	28.40
44.68	30	0.727	0.380	0.821	27.65
25.43	0.2	0.715	0.331	0.789	24.80
25.43	0.5	0.939	0.430	1.033	24.58
25.43	1	1.175	0.622	1.332	27.78
25.43	2	1.474	0.642	1.608	23.50
25.43	5	1.781	0.696	1.912	21.34
25.43	10	2.125	0.777	2.263	20.09
25.43	20	2.573	0.890	2.723	19.08
25.43	30	2.844	0.931	2.992	18.13
5.5	0.2	3.549	0.902	3.662	14.27
5.5	0.5	4.079	0.956	4.190	13.20
5.5	1	4.528	1.000	4.637	12.46
5.5	2	5.118	1.031	5.221	11.40
5.5	5	5.758	1.022	5.848	10.06
5.5	10	6.235	1.070	6.327	9.74
5.5	20	6.812	1.129	6.905	9.42
5.5	30	7.106	1.152	7.199	9.23
-14.88	0.2	8.710	0.890	8.755	5.84
-14.88	0.5	9.099	1.382	9.208	8.62

Temp (C)	Frequency (Hz.)	Avg E'	Avg E''	Avg E*	Avg Phase Angle
-14.88	1	9.583	1.087	9.659	6.52
-14.88	2	9.922	0.879	9.962	5.09
-14.88	5	10.338	0.863	10.375	4.80
-14.88	10	10.762	0.859	10.798	4.58
-14.88	20	11.268	0.851	11.302	4.34
-14.88	30	11.838	0.740	11.861	3.58
-10.87	0.2	7.258	1.147	7.350	9.03
-10.87	0.5	7.933	1.307	8.052	9.49
-10.87	1	8.780	1.200	8.866	7.78
-10.87	2	8.994	0.911	9.041	5.80
-10.87	5	9.378	0.940	9.426	5.74
-10.87	10	9.898	0.925	9.942	5.36
-10.87	20	10.385	0.917	10.426	5.07
-10.87	30	10.821	0.903	10.860	4.79
-5.94	0.2	6.273	1.235	6.402	11.26
-5.94	0.5	7.179	1.161	7.274	9.17
-5.94	1	7.562	0.970	7.624	7.31
-5.94	2	7.841	1.004	7.905	7.29
-5.94	5	8.435	1.000	8.495	6.76
-5.94	10	8.802	0.996	8.859	6.47
-5.94	20	9.452	0.947	9.500	5.73
-5.94	30	9.845	0.951	9.892	5.53
-0.95	0.2	4.725	1.046	4.855	12.37
-0.95	0.5	5.685	1.039	5.780	10.35
-0.95	1	5.991	1.240	6.132	11.69
-0.95	2	6.595	1.189	6.708	10.19
-0.95	5	7.136	1.028	7.210	8.21
-0.95	10	7.752	1.015	7.818	7.47
-0.95	20	8.298	1.016	8.360	6.98
-0.95	30	8.744	0.995	8.801	6.50
9.21	0.2	2.424	1.125	2.690	25.00
9.21	0.5	2.973	1.045	3.162	19.82
9.21	1	3.648	1.003	3.785	15.35
9.21	2	3.978	0.988	4.099	13.95
9.21	5	4.689	1.063	4.809	12.77
9.21	10	5.200	1.067	5.308	11.60
9.21	20	5.745	1.103	5.850	10.87
9.21	30	6.172	1.112	6.271	10.21
14.19	0.2	1.591	0.662	1.725	22.89
14.19	0.5	2.188	0.750	2.313	18.93
14.19	1	2.390	0.969	2.595	22.59
14.19	2	2.947	0.921	3.088	17.35
14.19	5	3.578	1.025	3.723	15.97
14.19	10	3.944	1.018	4.073	14.47

Temp (C)	Frequency (Hz.)	Avg E'	Avg E''	Avg E*	Avg Phase Angle
14.19	20	4.510	1.077	4.637	13.43
14.19	30	4.893	1.110	5.018	12.78
5.2	0.2	3.482	0.888	3.594	14.31
5.2	0.5	4.064	0.952	4.173	13.19
5.2	1	4.633	1.218	4.803	14.75
5.2	2	5.148	1.110	5.269	12.11
5.2	5	5.836	1.108	5.941	10.74
5.2	10	6.283	1.048	6.370	9.48
5.2	20	6.818	1.081	6.903	9.01
5.2	30	7.132	1.115	7.219	8.90
5.25	0.2	3.474	0.890	3.586	14.37
5.25	0.5	4.119	1.083	4.264	14.65
5.25	1	4.751	1.169	4.895	13.78
5.25	2	5.200	1.119	5.321	12.12
5.25	5	5.801	1.081	5.902	10.55
5.25	10	6.353	1.073	6.443	9.59
5.25	20	6.835	1.086	6.921	9.03
5.25	30	7.242	1.102	7.325	8.66
24.45	0.2	0.665	0.329	0.742	26.35
24.45	0.5	0.868	0.412	0.961	25.43
24.45	1	1.061	0.489	1.168	24.75
24.45	2	1.288	0.567	1.408	23.77
24.45	5	1.712	0.698	1.848	22.18
24.45	10	2.029	0.772	2.171	20.83
24.45	20	2.410	0.873	2.563	19.93
24.45	30	2.706	0.931	2.861	18.99
34.56	0.2	0.267	0.148	0.306	29.06
34.56	0.5	0.363	0.201	0.415	28.97
34.56	1	0.455	0.247	0.518	28.58
34.56	2	0.576	0.306	0.653	28.01
34.56	5	0.772	0.399	0.869	27.39
34.56	10	0.969	0.485	1.084	26.59
34.56	20	1.231	0.585	1.363	25.42
34.56	30	1.425	0.650	1.566	24.53
44.72	0.5	0.128	0.080	0.151	32.09
44.72	1	0.163	0.101	0.192	31.78
44.72	2	0.208	0.128	0.245	31.75
44.72	5	0.293	0.178	0.343	31.29
44.72	10	0.380	0.229	0.444	31.12
44.72	20	0.493	0.291	0.573	30.52
44.72	30	0.594	0.336	0.682	29.57
49.76	0.2	0.052	0.034	0.062	32.63
49.76	0.5	0.063	0.041	0.075	33.52
49.76	1	0.074	0.049	0.088	33.75

Temp (C)	Frequency (Hz.)	Avg E'	Avg E''	Avg E*	Avg Phase Angle
49.76	2	0.091	0.061	0.110	33.88
49.76	5	0.125	0.084	0.150	33.99
49.76	10	0.161	0.108	0.194	34.01
49.76	20	0.214	0.138	0.255	32.94
49.76	30	0.258	0.160	0.304	31.86
20.3	0.2	0.652	0.411	0.780	32.54
20.3	0.5	0.679	0.306	0.745	24.35
20.3	1	1.144	0.495	1.246	23.43
20.3	2	1.355	0.557	1.465	22.38
20.3	5	1.719	0.670	1.845	21.32
20.3	10	2.068	0.781	2.211	20.68
20.3	20	2.463	0.865	2.611	19.37
20.3	30	2.751	0.923	2.902	18.54

#### 4.3. 50 Pen + 5%SBR HRA Mixture (ER50)

Temp (C)	Frequency (Hz.)	Avg E'	Avg E''	Avg E*	Avg Phase Angle
5.2	0.2	4.008	0.862	4.099	12.15
5.2	0.5	4.591	0.867	4.672	10.70
5.2	1	4.941	0.886	5.020	10.18
5.2	2	5.390	0.886	5.463	9.35
5.2	5	6.055	0.920	6.125	8.64
5.2	10	6.366	0.919	6.433	8.22
5.2	20	6.872	0.959	6.939	7.96
5.2	30	7.078	1.020	7.151	8.22
-4.91	0.2	6.367	0.807	6.418	7.22
-4.91	0.5	6.916	0.788	6.960	6.51
-4.91	1	7.403	0.802	7.447	6.18
-4.91	2	7.700	0.780	7.739	5.78
-4.91	5	8.172	0.791	8.210	5.53
-4.91	10	8.575	0.806	8.613	5.37
-4.91	20	9.016	0.838	9.054	5.31
-4.91	30	9.397	0.855	9.436	5.20
14.24	0.2	2.090	0.749	2.220	19.71
14.24	0.5	2.662	0.923	2.820	19.04
14.24	1	3.067	0.892	3.194	16.21
14.24	2	3.431	0.951	3.562	15.45
14.24	5	3.995	0.956	4.108	13.45
14.24	10	4.410	0.960	4.514	12.28
14.24	20	4.843	0.994	4.944	11.60
14.24	30	5.213	1.018	5.312	11.06
19.32	0.2	1.322	0.592	1.449	24.14

Temp (C)	Frequency (Hz.)	Avg E'	Avg E''	Avg E*	Avg Phase Angle
19.32	0.5	1.602	0.908	1.853	29.93
19.32	1	2.136	0.832	2.293	21.27
19.32	2	2.412	0.791	2.539	18.17
19.32	5	2.944	0.882	3.073	16.69
19.32	10	3.423	0.969	3.558	15.78
19.32	20	3.784	0.976	3.908	14.47
19.32	30	4.128	1.011	4.250	13.77
24.4	0.2	0.792	0.422	0.898	28.06
24.4	0.5	0.966	0.572	1.127	30.94
24.4	1	1.339	0.854	1.592	32.54
24.4	2	1.678	0.734	1.833	23.59
24.4	5	2.024	0.774	2.167	20.92
24.4	10	2.406	0.830	2.545	19.03
24.4	20	2.870	0.929	3.017	17.94
24.4	30	3.128	0.961	3.273	17.09
34.51	0.2	0.278	0.182	0.333	33.30
34.51	0.5	0.399	0.248	0.470	31.89
34.51	1	0.517	0.311	0.604	31.04
34.51	2	0.664	0.382	0.766	29.91
34.51	5	0.914	0.486	1.035	28.01
34.51	10	1.150	0.576	1.286	26.61
34.51	20	1.462	0.680	1.613	24.96
34.51	30	1.687	0.740	1.842	23.68
44.68	0.2	0.070	0.056	0.090	38.75
44.68	0.5	0.102	0.080	0.130	38.17
44.68	1	0.138	0.105	0.173	37.23
44.68	2	0.188	0.139	0.234	36.51
44.68	5	0.281	0.196	0.343	34.96
44.68	10	0.377	0.254	0.455	33.96
44.68	20	0.508	0.328	0.605	32.87
44.68	30	0.619	0.377	0.725	31.34
25.48	0.2	0.627	0.337	0.712	28.24
25.48	0.5	0.845	0.426	0.946	26.77
25.48	1	1.049	0.497	1.161	25.37
25.48	2	1.287	0.568	1.407	23.83
25.48	5	1.663	0.672	1.794	22.01
25.48	10	1.992	0.749	2.128	20.62
25.48	20	2.376	0.830	2.517	19.26
25.48	30	2.666	0.883	2.809	18.33
5.2	0.2	2.022	0.570	2.101	15.76
5.2	0.5	2.083	0.594	2.166	15.92
5.2	1	2.135	0.615	2.222	16.09
5.2	2	2.249	0.645	2.340	16.01
5.2	5	2.513	0.697	2.608	15.50

Temp (C)	Frequency (Hz.)	Avg E'	Avg E''	Avg E*	Avg Phase Angle
5.2	10	2.719	0.742	2.819	15.28
5.2	20	2.967	0.796	3.072	15.03
5.2	30	3.106	0.832	3.216	15.00
-14.78	0.2	5.255	0.637	5.293	6.92
-14.78	0.5	5.680	0.647	5.716	6.50
-14.78	1	6.093	0.685	6.132	6.41
-14.78	2	6.309	0.663	6.344	6.01
-14.78	5	6.774	0.675	6.808	5.69
-14.78	10	7.183	0.710	7.217	5.65
-14.78	20	7.579	0.761	7.618	5.74
-14.78	30	7.871	0.777	7.909	5.64
-10.92	0.2	4.539	0.639	4.584	8.01
-10.92	0.5	4.983	0.875	5.063	9.93
-10.92	1	5.401	0.772	5.457	8.12
-10.92	2	5.687	0.734	5.734	7.35
-10.92	5	6.114	0.744	6.159	6.94
-10.92	10	6.415	0.758	6.460	6.74
-10.92	20	6.847	0.793	6.893	6.61
-10.92	30	7.201	0.815	7.247	6.46
-5.94	0.2	3.719	0.643	3.774	9.82
-5.94	0.5	4.034	0.895	4.142	12.62
-5.94	1	4.514	0.716	4.570	8.99
-5.94	2	4.858	0.744	4.914	8.71
-5.94	5	5.217	0.744	5.270	8.12
-5.94	10	5.732	0.834	5.793	8.27
-5.94	20	6.026	0.834	6.084	7.89
-5.94	30	6.394	0.849	6.451	7.57
-0.95	0.2	2.940	0.624	3.005	11.99
-0.95	0.5	3.483	0.757	3.565	12.25
-0.95	1	3.763	0.789	3.848	11.80
-0.95	2	4.000	0.693	4.060	9.83
-0.95	5	4.528	0.784	4.595	9.82
-0.95	10	4.827	0.790	4.891	9.29
-0.95	20	5.244	0.840	5.311	9.10
-0.95	30	5.569	0.865	5.636	8.83
9.26	0.2	1.571	0.523	1.656	18.42
9.26	0.5	1.978	0.699	2.101	19.37
9.26	1	2.302	0.659	2.395	15.98
9.26	2	2.534	0.674	2.622	14.89
9.26	5	3.018	0.759	3.112	14.11
9.26	10	3.292	0.771	3.381	13.19
9.26	20	3.739	0.843	3.833	12.71
9.26	30	4.010	0.856	4.101	12.05
14.24	0.2	0.964	0.489	1.091	27.31

Temp (C)	Frequency (Hz.)	Avg E'	Avg E''	Avg E*	Avg Phase Angle
14.24	0.5	1.382	0.612	1.512	23.83
14.24	1	1.548	0.694	1.704	23.96
14.24	2	1.876	0.654	1.988	19.21
14.24	5	2.172	0.668	2.272	17.10
14.24	10	2.509	0.728	2.613	16.19
14.24	20	2.875	0.783	2.980	15.23
14.24	30	3.154	0.824	3.260	14.65
5.15	0.2	2.101	0.569	2.176	15.15
5.15	0.5	2.473	0.611	2.547	13.90
5.15	1	2.765	0.646	2.840	13.14
5.15	2	3.099	0.676	3.172	12.31
5.15	5	3.555	0.733	3.630	11.66
5.15	10	3.897	0.767	3.972	11.13
5.15	20	4.283	0.834	4.363	11.02
5.15	30	4.608	0.872	4.690	10.71
5.2	0.2	1.725	0.526	1.803	16.95
5.2	0.5	2.056	0.576	2.136	15.64
5.2	1	2.333	0.610	2.412	14.66
5.2	2	2.627	0.651	2.707	13.92
5.2	5	3.021	0.706	3.102	13.16
5.2	10	3.393	0.741	3.473	12.32
5.2	20	3.759	0.795	3.842	11.94
5.2	30	4.041	0.829	4.125	11.59
24.4	0.2	0.326	0.199	0.382	31.51
24.4	0.5	0.452	0.257	0.521	29.66
24.4	1	0.571	0.308	0.649	28.39
24.4	2	0.714	0.367	0.803	27.20
24.4	5	0.946	0.454	1.049	25.67
24.4	10	1.167	0.528	1.280	24.33
24.4	20	1.439	0.610	1.563	22.97
24.4	30	1.638	0.664	1.768	22.08
34.51	0.2	0.097	0.080	0.126	39.37
34.51	0.5	0.144	0.110	0.182	37.51
34.51	1	0.195	0.142	0.242	36.14
34.51	2	0.261	0.184	0.319	35.18
34.51	5	0.381	0.249	0.455	33.16
34.51	10	0.502	0.311	0.590	31.82
34.51	20	0.659	0.385	0.763	30.31
34.51	30	0.789	0.435	0.901	28.89
44.72	0.2	0.023	0.023	0.033	44.32
44.72	0.5	0.032	0.030	0.044	43.22
44.72	1	0.042	0.038	0.056	42.45
44.72	2	0.055	0.049	0.074	41.48
44.72	5	0.083	0.071	0.110	40.66

Temp (C)	Frequency (Hz.)	Avg E'	Avg E''	Avg E*	Avg Phase Angle
44.72	10	0.115	0.096	0.150	39.93
44.72	20	0.164	0.125	0.207	37.37
44.72	30	0.207	0.150	0.256	36.05
49.71	0.2	0.014	0.014	0.020	44.38
49.71	0.5	0.018	0.018	0.026	43.82
49.71	1	0.024	0.022	0.033	43.54
49.71	2	0.031	0.029	0.043	42.98
49.71	5	0.049	0.044	0.066	41.60
49.71	10	0.068	0.058	0.090	40.68
49.71	20	0.098	0.076	0.124	37.77
49.71	30	0.132	0.093	0.162	35.13
25.48	0.2	0.240	0.140	0.278	30.19
25.48	0.5	0.332	0.181	0.378	28.62
25.48	1	0.419	0.220	0.473	27.76
25.48	2	0.520	0.260	0.582	26.58
25.48	5	0.690	0.326	0.763	25.33
25.48	10	0.843	0.384	0.926	24.49
25.48	20	1.040	0.451	1.134	23.43
25.48	30	1.194	0.495	1.293	22.54
20.44	0.2	0.407	0.203	0.455	26.51
20.44	0.5	0.536	0.251	0.592	25.06
20.44	1	0.653	0.293	0.716	24.17
20.44	2	0.788	0.337	0.857	23.22
20.44	5	1.002	0.403	1.081	21.94
20.44	10	1.197	0.462	1.283	21.10
20.44	20	1.435	0.524	1.528	20.08
20.44	30	1.611	0.569	1.709	19.46
10.28	0.2	0.942	0.332	0.999	19.38
10.28	0.5	1.055	0.372	1.118	19.43
10.28	1	1.146	0.398	1.213	19.18
10.28	2	1.259	0.430	1.331	18.86
10.28	5	1.473	0.483	1.551	18.17
10.28	10	1.646	0.528	1.729	17.78
10.28	20	1.863	0.581	1.952	17.32
10.28	30	1.998	0.616	2.090	17.15

4.4. 50 Pen + 5%SBS HRA Mixture (ES50)

Temp (C)	Frequency (Hz.)	Avg E'	Avg E''	Avg E*	Av Phase Angle
5.25	0.2	3.307	0.801	3.403	13.63
5.25	0.5	3.829	0.829	3.918	12.22
5.25	1	4.228	0.851	4.314	11.39
5.25	2	4.635	0.860	4.714	10.52
5.25	5	5.162	0.889	5.239	9.78
5.25	10	5.631	0.881	5.700	8.90
5.25	20	6.158	0.910	6.225	8.41
5.25	30	6.550	0.923	6.614	8.02
-4.91	0.2	5.630	0.835	5.692	8.44
-4.91	0.5	6.150	0.813	6.204	7.53
-4.91	1	6.462	0.840	6.516	7.42
-4.91	2	6.848	0.831	6.899	6.93
-4.91	5	7.292	0.839	7.340	6.58
-4.91	10	7.806	0.808	7.848	5.91
-4.91	20	8.181	0.852	8.226	5.96
-4.91	30	8.597	0.859	8.640	5.72
14.29	0.2	1.576	0.612	1.691	21.23
14.29	0.5	1.965	0.687	2.081	19.28
14.29	1	2.309	0.737	2.424	17.70
14.29	2	2.758	0.826	2.879	16.67
14.29	5	3.175	0.830	3.282	14.67
14.29	10	3.586	0.877	3.691	13.75
14.29	20	4.079	0.933	4.185	12.89
14.29	30	4.341	0.960	4.445	12.48
19.32	0.2	0.997	0.471	1.102	25.29
19.32	0.5	1.365	0.677	1.525	26.33
19.32	1	1.653	0.655	1.778	21.62
19.32	2	1.885	0.691	2.007	20.14
19.32	5	2.300	0.762	2.423	18.33
19.32	10	2.670	0.818	2.793	17.04
19.32	20	3.100	0.876	3.222	15.78
19.32	30	3.399	0.912	3.519	15.02
24.45	0.2	0.614	0.340	0.703	29.02
24.45	0.5	0.819	0.562	0.997	34.40
24.45	1	1.044	0.504	1.160	25.76
24.45	2	1.273	0.552	1.388	23.44
24.45	5	1.634	0.656	1.761	21.89
24.45	10	1.956	0.731	2.088	20.50
24.45	20	2.306	0.803	2.442	19.21
24.45	30	2.581	0.844	2.715	18.11
34.56	0.2	0.192	0.131	0.233	34.54

Temp (C)	Frequency (Hz.)	Avg E'	Avg E''	Avg E*	Avg Phase Angle
34.56	0.5	0.269	0.175	0.321	33.09
34.56	1	0.351	0.221	0.415	32.23
34.56	2	0.454	0.276	0.531	31.32
34.56	5	0.632	0.363	0.730	29.90
34.56	10	0.812	0.439	0.923	28.41
34.56	20	1.034	0.522	1.159	26.80
34.56	30	1.203	0.582	1.336	25.83
44.68	0.2	0.055	0.043	0.070	38.54
44.68	0.5	0.078	0.062	0.100	38.77
44.68	1	0.106	0.083	0.134	38.08
44.68	2	0.145	0.110	0.182	37.12
44.68	5	0.219	0.158	0.270	35.90
44.68	10	0.302	0.207	0.366	34.51
44.68	20	0.412	0.267	0.491	32.96
44.68	30	0.499	0.311	0.588	32.04
25.48	0.2	0.525	0.287	0.598	28.74
25.48	0.5	0.699	0.367	0.790	27.66
25.48	1	0.878	0.428	0.978	26.02
25.48	2	1.086	0.503	1.197	24.89
25.48	5	1.453	0.605	1.574	22.62
25.48	10	1.717	0.675	1.845	21.45
25.48	20	2.073	0.750	2.205	19.91
25.48	30	2.320	0.802	2.455	19.08
5.3	0.2	2.944	0.783	3.047	14.91
5.3	0.5	3.371	0.821	3.470	13.69
5.3	1	3.730	0.847	3.825	12.79
5.3	2	4.131	0.865	4.221	11.83
5.3	5	4.652	0.900	4.739	10.95
5.3	10	5.084	0.916	5.166	10.22
5.3	20	5.549	0.953	5.631	9.76
5.3	30	5.902	0.981	5.983	9.45
-14.78	0.2	7.065	0.725	7.102	5.86
-14.78	0.5	7.486	0.699	7.518	5.34
-14.78	1	7.808	0.668	7.837	4.89
-14.78	2	8.031	0.684	8.060	4.88
-14.78	5	8.453	0.669	8.479	4.53
-14.78	10	8.839	0.618	8.861	4.01
-14.78	20	9.144	0.660	9.168	4.13
-14.78	30	9.498	0.659	9.522	3.98
-10.97	0.2	6.241	0.768	6.288	7.01
-10.97	0.5	6.683	0.762	6.726	6.51
-10.97	1	6.995	0.761	7.037	6.21
-10.97	2	7.398	0.762	7.438	5.88

Temp (C)	Frequency (Hz.)	Avg E'	Avg E''	Avg E*	Avg Phase Angle
-10.97	5	7.821	0.698	7.852	5.10
-10.97	10	8.135	0.720	8.167	5.07
-10.97	20	8.476	0.758	8.510	5.12
-10.97	30	8.865	0.756	8.898	4.89
-5.89	0.2	5.154	0.820	5.219	9.04
-5.89	0.5	5.654	0.818	5.713	8.24
-5.89	1	6.050	0.799	6.102	7.53
-5.89	2	6.489	0.801	6.539	7.05
-5.89	5	6.792	0.802	6.840	6.75
-5.89	10	7.334	0.792	7.377	6.17
-5.89	20	7.656	0.796	7.697	5.94
-5.89	30	7.963	0.828	8.006	5.95
-0.9	0.2	4.114	0.835	4.198	11.48
-0.9	0.5	4.625	0.849	4.702	10.41
-0.9	1	4.976	0.858	5.049	9.80
-0.9	2	5.470	0.893	5.543	9.26
-0.9	5	5.941	0.855	6.002	8.19
-0.9	10	6.401	0.848	6.458	7.56
-0.9	20	6.746	0.874	6.802	7.40
-0.9	30	7.060	0.886	7.116	7.16
9.26	0.2	2.099	0.667	2.203	17.58
9.26	0.5	2.554	0.761	2.665	16.60
9.26	1	2.904	0.797	3.011	15.35
9.26	2	3.286	0.827	3.388	14.14
9.26	5	3.791	0.861	3.888	12.81
9.26	10	4.254	0.877	4.343	11.66
9.26	20	4.682	0.921	4.772	11.13
9.26	30	4.993	0.947	5.082	10.74
14.29	0.2	1.371	0.579	1.489	22.88
14.29	0.5	1.727	0.657	1.848	20.83
14.29	1	2.043	0.712	2.164	19.23
14.29	2	2.449	0.803	2.578	18.13
14.29	5	2.951	0.830	3.066	15.72
14.29	10	3.310	0.857	3.419	14.52
14.29	20	3.794	0.947	3.911	13.99
14.29	30	4.066	0.935	4.172	12.96
5.2	0.2	2.727	0.694	2.815	14.27
5.2	0.5	2.902	0.772	3.003	14.92
5.2	1	2.939	0.773	3.039	14.74
5.2	2	3.008	0.758	3.102	14.14
5.2	5	3.250	0.765	3.339	13.24
5.2	10	3.574	0.826	3.668	13.02
5.2	20	4.017	0.894	4.115	12.55

Temp (C)	Frequency (Hz.)	Avg E'	Avg E''	Avg E*	Avg Phase Angle
5.2	30	4.294	0.933	4.395	12.26
19.32	0.2	0.656	0.357	0.747	28.59
19.32	0.5	0.880	0.444	0.985	26.81
19.32	1	1.087	0.512	1.201	25.25
19.32	2	1.388	0.627	1.524	24.26
19.32	5	1.734	0.677	1.862	21.33
19.32	10	2.057	0.742	2.187	19.84
19.32	20	2.410	0.802	2.540	18.42
19.32	30	2.707	0.852	2.838	17.48
24.4	0.2	0.385	0.241	0.454	32.09
24.4	0.5	0.534	0.312	0.619	30.35
24.4	1	0.686	0.440	0.819	32.60
24.4	2	0.892	0.516	1.032	29.93
24.4	5	1.198	0.563	1.323	25.18
24.4	10	1.465	0.631	1.595	23.33
24.4	20	1.789	0.738	1.936	22.41
24.4	30	2.000	0.768	2.142	21.01
34.51	0.2	0.114	0.087	0.144	37.53
34.51	0.5	0.168	0.126	0.211	36.90
34.51	1	0.229	0.178	0.291	37.85
34.51	2	0.313	0.221	0.384	35.27
34.51	5	0.444	0.291	0.531	33.27
34.51	10	0.590	0.364	0.693	31.70
34.51	20	0.776	0.449	0.897	30.03
34.51	30	0.926	0.504	1.054	28.55
44.72	0.5	0.052	0.044	0.069	40.37
44.72	1	0.068	0.058	0.090	40.48
44.72	2	0.091	0.077	0.120	40.05
44.72	5	0.137	0.112	0.178	39.28
44.72	10	0.189	0.148	0.241	38.17
44.72	20	0.262	0.193	0.326	36.32
44.72	30	0.325	0.224	0.394	34.56
49.76	0.2	0.022	0.018	0.028	39.28
49.76	0.5	0.031	0.026	0.040	40.52
49.76	1	0.042	0.036	0.055	40.54
49.76	2	0.057	0.050	0.076	41.01
49.76	5	0.089	0.076	0.118	40.67
49.76	10	0.128	0.106	0.167	39.73
49.76	20	0.184	0.142	0.232	37.70
49.76	30	0.238	0.172	0.294	35.80
20.4	0.2	0.596	0.311	0.672	27.58
20.4	0.5	0.795	0.390	0.886	26.16
20.4	1	0.979	0.451	1.079	24.75

Temp (C)	Frequency (Hz.)	Avg E'	Avg E''	Avg E*	Avg Phase Angle
20.4	2	1.191	0.514	1.297	23.35
20.4	5	1.544	0.608	1.660	21.50
20.4	10	1.822	0.655	1.937	19.78
20.4	20	2.102	0.704	2.216	18.52
20.4	30	2.297	0.745	2.415	17.98
5.2	0.2	2.223	0.885	2.401	21.66
5.2	0.5	2.660	0.829	2.786	17.26
5.2	1	2.838	0.863	2.967	16.90
5.2	2	3.063	0.883	3.188	16.08
5.2	5	3.163	0.815	3.266	14.45
5.2	10	3.549	0.880	3.656	13.91
5.2	20	3.605	0.837	3.701	13.08
5.2	30	3.646	0.838	3.741	12.94
-4.91	0.2	4.438	0.828	4.514	10.57
-4.91	0.5	4.951	1.080	5.079	12.45
-4.91	1	5.397	0.828	5.460	8.73
-4.91	2	5.843	0.953	5.922	9.25
-4.91	5	6.235	0.823	6.290	7.53
-4.91	10	6.661	0.819	6.712	7.01
-4.91	20	7.138	0.816	7.185	6.53
-4.91	30	7.398	0.858	7.448	6.62
14.24	0.2	1.139	0.500	1.245	23.62
14.24	0.5	1.261	0.775	1.491	32.04
14.24	1	1.462	0.605	1.582	22.48
14.24	2	1.672	0.685	1.808	22.26
14.24	5	2.000	0.762	2.141	20.81
14.24	10	2.218	0.777	2.350	19.32
14.24	20	2.482	0.818	2.613	18.24
14.24	30	2.670	0.864	2.807	17.93
20.4	0.2	0.554	0.489	0.741	41.38
20.4	0.5	0.939	0.485	1.057	27.31
20.4	1	1.209	0.625	1.362	27.23
20.4	2	1.458	0.729	1.636	26.44
20.4	5	1.872	0.708	2.001	20.72
20.4	10	2.208	0.780	2.342	19.47
20.4	20	2.593	0.828	2.722	17.72
20.4	30	2.870	0.867	2.998	16.81
24.45	0.2	0.412	0.333	0.534	39.08
24.45	0.5	0.395	0.401	0.564	44.89
24.45	1	0.811	0.475	0.940	30.34
24.45	2	0.979	0.512	1.105	27.60
24.45	5	1.317	0.639	1.465	25.79
24.45	10	1.626	0.695	1.768	23.13

Temp (C)	Frequency (Hz.)	Avg E'	Avg E''	Avg E*	Avg Phase Angle
24.45	20	1.947	0.745	2.084	20.96
24.45	30	2.193	0.793	2.332	19.88
34.51	0.2	0.106	0.120	0.161	48.37
34.51	0.5	0.203	0.189	0.279	43.14
34.51	1	0.270	0.186	0.328	34.61
34.51	2	0.361	0.243	0.436	33.94
34.51	5	0.514	0.320	0.605	31.97
34.51	10	0.684	0.421	0.804	31.53
34.51	20	0.881	0.488	1.007	28.94
34.51	30	1.041	0.546	1.175	27.68
44.68	0.2	0.033	0.043	0.055	52.55
44.68	0.5	0.036	0.032	0.048	42.61
44.68	1	0.037	0.079	0.087	64.75
44.68	2	0.093	0.108	0.144	49.55
44.68	5	0.168	0.155	0.229	42.54
44.68	10	0.236	0.187	0.301	38.41
44.68	20	0.326	0.236	0.402	35.90
44.68	30	0.403	0.281	0.491	34.83
25.48	0.2	0.349	0.259	0.437	37.42
25.48	0.5	0.352	0.339	0.494	42.37
25.48	1	0.592	0.483	0.775	39.82
25.48	2	0.861	0.527	1.016	31.34
25.48	5	1.157	0.569	1.290	26.10
25.48	10	1.419	0.627	1.551	23.82
25.48	20	1.731	0.694	1.865	21.87
25.48	30	1.967	0.743	2.103	20.70
5.25	0.2	2.13225	0.65825	2.2315	17.17
5.25	0.5	2.54175	0.721	2.64225	15.84
5.25	1	2.855	0.75725	2.954	14.86
5.25	2	3.22775	0.78775	3.32275	13.72
5.25	5	3.75475	0.81525	3.84225	12.26
5.25	10	4.01425	0.86125	4.106	12.12
5.25	20	4.53925	0.88125	4.6245	11.02
5.25	30	4.6055	0.9325	4.69975	11.49
-14.83	0.2	5.64125	0.732	5.6885	7.39
-14.83	0.5	6.2475	1.09475	6.34525	9.97
-14.83	1	6.503	0.76775	6.54875	6.74
-14.83	2	6.84975	0.723	6.888	6.03
-14.83	5	7.23775	0.74075	7.2755	5.85
-14.83	10	7.5525	0.70425	7.5855	5.34
-14.83	20	7.93825	0.7265	7.972	5.24
-14.83	30	8.2585	0.71875	8.29	4.98
-10.97	0.2	5.07575	1.05075	5.187	11.69

Temp (C)	Frequency (Hz.)	Avg E'	Avg E''	Avg E*	Avg Phase Angle
-10.97	0.5	5.02075	0.8865	5.1	10.15
-10.97	1	5.89525	0.913	5.96725	8.79
-10.97	2	6.09825	0.755	6.14475	7.06
-10.97	5	6.63575	0.8205	6.68675	7.05
-10.97	10	6.8715	0.7465	6.91225	6.21
-10.97	20	7.2315	0.7675	7.273	6.07
-10.97	30	7.573	0.764	7.61175	5.77
-5.94	0.2	3.514	0.643	3.57525	10.19
-5.94	0.5	3.695	0.93325	3.82025	14.28
-5.94	1	3.80825	0.80925	3.89375	12.03
-5.94	2	3.8415	1.1665	4.0305	16.94
-5.94	5	4.35675	0.82975	4.4355	10.84
-5.94	10	4.192	0.828	4.2735	11.18
-5.94	20	4.3165	0.88275	4.40625	11.53
-5.94	30	4.4135	0.923	4.5095	11.81
0.12	0.2	2.858	0.8135	2.97475	15.90
0.12	0.5	3.05825	1.1815	3.28925	21.34
0.12	1	3.17425	0.77525	3.26775	13.75
0.12	2	3.32225	0.8515	3.43025	14.40
0.12	5	3.63375	0.8605	3.735	13.36
0.12	10	3.78475	0.84175	3.8775	12.56
0.12	20	3.9335	0.8645	4.028	12.43
0.12	30	4.0305	0.88375	4.127	12.39
9.21	0.2	1.45925	0.76025	1.6595	27.35
9.21	0.5	1.68475	0.72925	1.841	23.32
9.21	1	1.7725	0.589	1.86825	18.38
9.21	2	1.89225	0.641	1.99825	18.72
9.21	5	2.2625	0.72525	2.37625	17.78
9.21	10	2.53425	0.775	2.6505	17.01
9.21	20	2.8665	0.83475	2.98575	16.24
9.21	30	3.00925	0.8705	3.133	16.14
15.31	0.2	0.70025	0.47375	0.86575	35.86
15.31	0.5	1.09325	0.6095	1.25575	29.08
15.31	1	1.25575	0.60275	1.39425	25.56
15.31	2	1.37625	0.60125	1.50175	23.59
15.31	5	1.6775	0.658	1.802	21.43
15.31	10	1.9115	0.71625	2.04175	20.54
15.31	20	2.2295	0.78175	2.36275	19.33
15.31	30	2.3885	0.81175	2.5225	18.77
5.1	0.2	1.90225	0.77625	2.06225	22.09
5.1	0.5	2.50475	0.79125	2.6295	17.45
5.1	1	2.855	0.76375	2.9555	14.99
5.1	2	3.22375	0.87675	3.34425	15.14

Temp (C)	Frequency (Hz.)	Avg E'	Avg E''	Avg E*	Avg Phase Angle
5.1	5	3.662	0.81425	3.75175	12.56
5.1	10	4.08825	0.84775	4.17525	11.74
5.1	20	4.5155	0.857	4.59675	10.79
5.1	30	4.65625	0.9045	4.74425	11.04
5.15	0.2	2.1185	0.6565	2.21775	17.23
5.15	0.5	2.52075	0.7105	2.619	15.75
5.15	1	2.8315	0.744	2.92775	14.73
5.15	2	3.2775	0.79875	3.37375	13.72
5.15	5	3.68225	0.79875	3.76775	12.25
5.15	10	3.93375	0.84225	4.02325	12.10
5.15	20	4.28125	0.9045	4.37675	11.95
5.15	30	4.537	0.96575	4.64	12.07
-4.91	0.2	3.762	0.75725	3.83775	11.39
-4.91	0.5	4.214	0.79325	4.28825	10.67
-4.91	1	4.5195	0.8065	4.5915	10.14
-4.91	2	4.97275	0.98625	5.0765	11.17
-4.91	5	5.54075	0.78825	5.59675	8.11
-4.91	10	5.827	0.8185	5.88475	8.01
-4.91	20	6.12075	0.851	6.18	7.95
-4.91	30	6.415	0.8785	6.476	7.86
14.24	0.2	0.93475	0.4205	1.02575	24.14
14.24	0.5	1.08075	0.4965	1.18925	24.69
14.24	1	1.19975	0.5385	1.31525	24.19
14.24	2	1.3635	0.5845	1.484	23.21
14.24	5	1.654	0.66075	1.78125	21.78
14.24	10	1.8855	0.72025	2.0185	20.92
14.24	20	2.2045	0.79225	2.3425	19.77
14.24	30	2.33125	0.816	2.47025	19.30
20.35	0.2	0.4885	0.2925	0.57075	31.65
20.35	0.5	0.74575	0.4505	0.8775	31.17
20.35	1	0.88975	0.562	1.06225	32.44
20.35	2	1.13	0.65775	1.316	30.14
20.35	5	1.5415	0.6985	1.6935	24.29
20.35	10	1.825	0.701	1.95525	21.02
20.35	20	2.15725	0.772	2.29125	19.70
20.35	30	2.40475	0.81975	2.54075	18.83
24.35	0.2	0.28525	0.1995	0.35375	34.38
24.35	0.5	0.47925	0.37025	0.60925	37.52
24.35	1	0.47225	0.438	0.651	43.20
24.35	2	0.779	0.417	0.8835	28.18
24.35	5	1.058	0.53225	1.18425	26.69
24.35	10	1.3075	0.60175	1.4395	24.73
24.35	20	1.61125	0.6805	1.749	22.91

Temp (C)	Frequency (Hz.)	Avg E'	Avg E''	Avg E*	Avg Phase Angle
24.35	30	1.8385	0.73325	1.9795	21.75
34.51	0.2	0.07	0.08775	0.11275	52.15
34.51	0.5	0.15625	0.1315	0.20475	40.01
34.51	1	0.19975	0.14775	0.24875	36.49
34.51	2	0.2675	0.18925	0.328	35.31
34.51	5	0.3925	0.265	0.474	34.06
34.51	10	0.522	0.3315	0.61825	32.43
34.51	20	0.6935	0.412	0.807	30.73
34.51	30	0.82825	0.4665	0.9505	29.41
44.68	0.5	0.0465	0.039	0.061	40.18
44.68	1	0.06175	0.053	0.0815	40.72
44.68	2	0.087	0.074	0.1145	40.43
44.68	5	0.136	0.1135	0.177	39.85
44.68	10	0.18775	0.1495	0.24025	38.58
44.68	20	0.2675	0.19825	0.333	36.58
44.68	30	0.3385	0.23475	0.4115	34.76
25.33	0.2	0.27575	0.175	0.327	32.76
25.33	0.5	0.4675	0.27775	0.544	30.70
25.33	1	0.5155	0.35725	0.63475	35.10
25.33	2	0.69925	0.38475	0.79875	28.84
25.33	5	0.972	0.50225	1.0945	27.29
25.33	10	1.219	0.565	1.3435	24.89
25.33	20	1.485	0.64375	1.6185	23.44
25.33	30	1.678	0.686	1.81275	22.25
5.2	0.2	1.47275	0.51125	1.559	19.15625
5.2	0.5	1.9215	0.70475	2.04775	20.1025
5.2	1	2.00225	0.7255	2.14425	20.31325
5.2	2	2.33625	0.78375	2.47225	18.38525
5.2	5	2.656	0.68575	2.74325	14.4705
5.2	10	3.03225	0.759	3.1255	14.05825
5.2	20	3.175	0.768	3.267	13.635
5.2	30	3.11325	0.84825	3.22775	15.37475
-4.91	0.2	2.77575	0.65525	2.85225	13.2945
-4.91	0.5	3.174	0.96875	3.329	17.08075
-4.91	1	3.508	0.7045	3.57825	11.3795
-4.91	2	3.75125	0.7285	3.8215	10.99875
-4.91	5	4.251	0.77	4.32025	10.264
-4.91	10	4.56	0.7635	4.6235	9.5315
-4.91	20	4.77575	0.8275	4.8475	9.87125
-4.91	30	4.63925	0.85925	4.71975	10.62275
14.19	0.2	0.6205	0.36	0.71925	30.476
14.19	0.5	0.55025	0.461	0.721	39.07825
14.19	1	0.964	0.486	1.08025	26.69825

Temp (C)	Frequency (Hz.)	Avg E'	Avg E''	Avg E*	Avg Phase Angle
14.19	2	1.064	0.488	1.171	24.65325
14.19	5	1.312	0.57225	1.43125	23.579
14.19	10	1.5575	0.63625	1.6825	22.22475
14.19	20	1.8135	0.70025	1.94425	21.117
14.19	30	2.003	0.7545	2.141	20.6305
20.88	0.2	0.3315	0.265	0.4285	39.395
20.88	0.5	0.4305	0.267	0.51225	30.08575
20.88	1	0.60775	0.44075	0.758	36.2895
20.88	2	0.86225	0.5545	1.0275	32.639
20.88	5	1.13375	0.56125	1.266	26.24475
20.88	10	1.39275	0.61925	1.5245	23.96525
20.88	20	1.7195	0.6795	1.84925	21.57475
20.88	30	1.918	0.724	2.05025	20.6885
24.4	0.2	0.2265	0.2135	0.31375	43.45825
24.4	0.5	0.19425	0.1175	0.231	30.94375
24.4	1	0.28675	0.24825	0.383	43.352
24.4	2	0.43925	0.36575	0.57875	39.7425
24.4	5	0.65725	0.4125	0.777	32.00275
24.4	10	0.79575	0.43325	0.90625	28.5685
24.4	20	0.98275	0.5015	1.1035	27.05625
24.4	30	1.1205	0.54525	1.24625	25.95675
34.51	0.2	0.06725	0.0745	0.10175	49.0245
34.51	0.5	0.09875	0.08475	0.13075	41.34775
34.51	1	0.143	0.1305	0.19575	42.64
34.51	2	0.202	0.18325	0.27425	41.915
34.51	5	0.30825	0.21475	0.37575	34.88375
34.51	10	0.413	0.2755	0.497	33.72
34.51	20	0.5595	0.34875	0.6595	31.9625
34.51	30	0.679	0.3995	0.78775	30.482
44.72	0.2	0.01725	0.02125	0.028	52.597
44.72	0.5	0.01875	0.026	0.0325	55.3325
44.72	1	0.04375	0.045	0.06325	45.5685
44.72	2	0.06425	0.05625	0.0855	41.49975
44.72	5	0.10125	0.09	0.13575	41.75825
44.72	10	0.1435	0.1215	0.18825	40.32825
44.72	20	0.205	0.16125	0.2615	38.23875
44.72	30	0.25925	0.19275	0.32325	36.6205
25.48	0.2	0.195	0.15	0.24775	38.3815
25.48	0.5	0.2905	0.21275	0.36425	36.67825
25.48	1	0.41125	0.24325	0.47775	30.61425
25.48	2	0.53775	0.3365	0.6355	31.94075
25.48	5	0.741	0.40025	0.8425	28.386
25.48	10	0.9225	0.473	1.03675	27.16475

Temp (C)	Frequency (Hz.)	Avg E'	Avg E''	Avg E*	Avg Phase Angle
25.48	20	1.139	0.5415	1.2615	25.439
25.48	30	1.33325	0.59875	1.4615	24.1995

# *Appendix C*

## Dynamic Creep

### List of Symbols and Abbreviations:

$V_v$	Air void content of the mixture, units: %
$N_1$	Number of cycles to end of linear region
$w_i$	Dissipated energy per cycle, units: $J/m^3$
$w_{NI}$	Cumulative dissipated energy up to $N_1$ , units: $J/m^3$
$w_{norm}$	Normalised dissipated energy
A50, B50, C50, D50, E50	50 Pen bitumen from different manufacturers
F100	100 Pen bitumen
AP50, BP50, CP50, DP50, EP50	50 Pen bitumen (from different manufacturers) + 5% Ethylene Vinyl Acetate
ER50	50 Pen bitumen + 5% Styrene Butadiene Rubber
ES50	50 Pen bitumen + 5% Styrene Butadiene Styrene
FR100	100 Pen bitumen + 5% Styrene Butadiene Rubber
FS50	100 Pen bitumen + 5% Styrene Butadiene Styrene

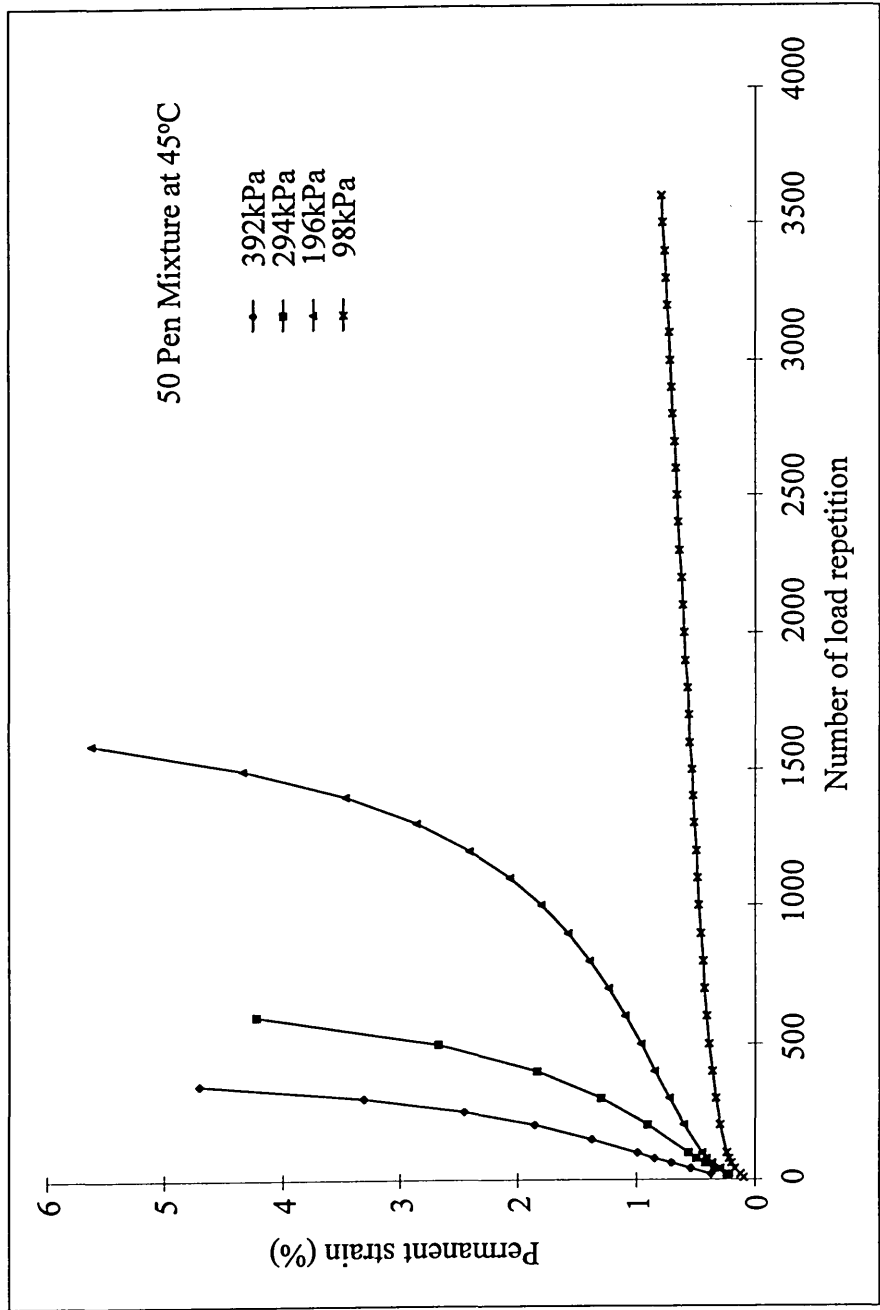


Figure C.1 Typical plots of permanent strain and number of load repetition showing the effect of applied stress levels for HRA mixtures with 50 pen binder. Test temperature at 45°C.

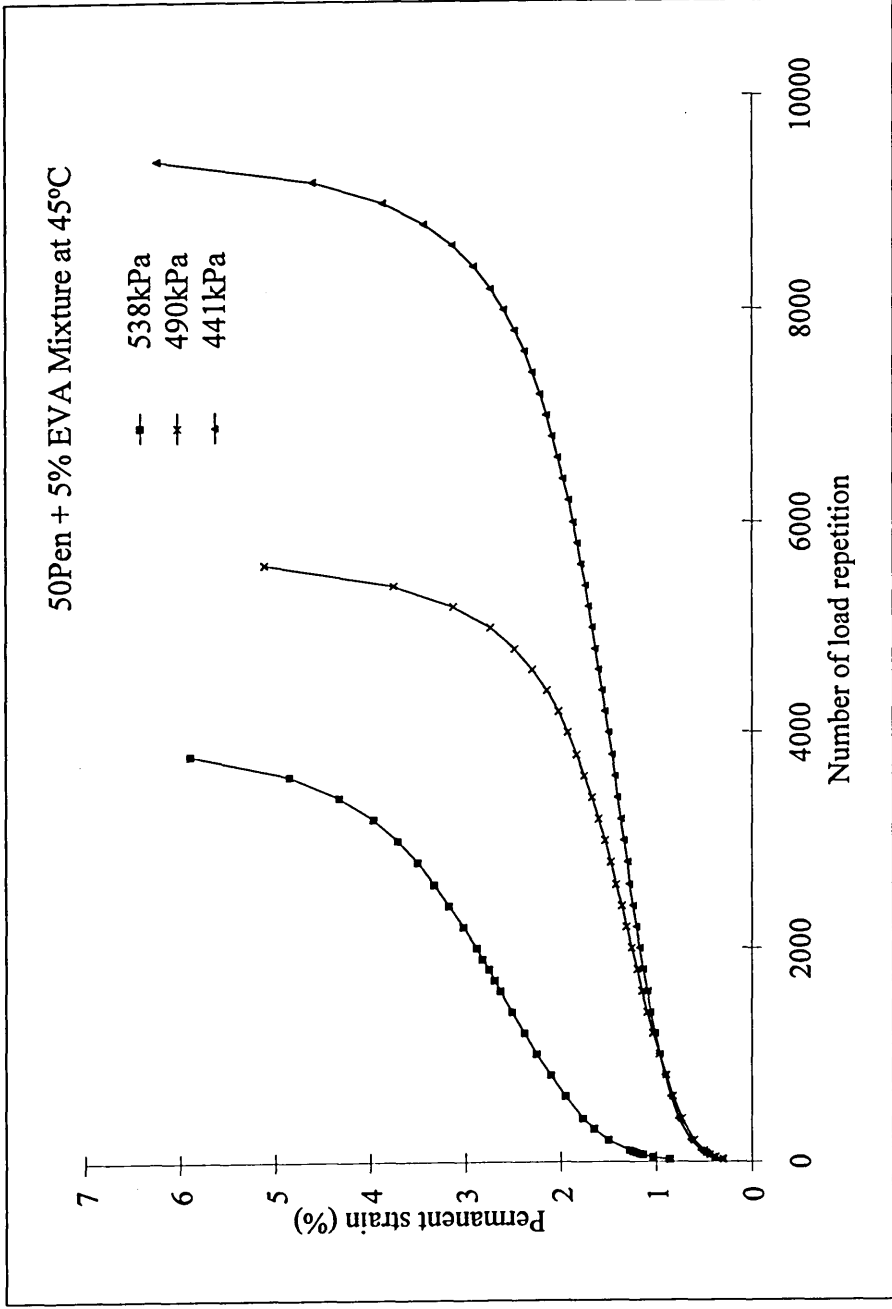


Figure C.2 Typical plots of permanent strain and number of load repetition showing the effect of applied stress levels for HRA mixtures with EVA modified 50 pen binder. Test temperature at 45°C.

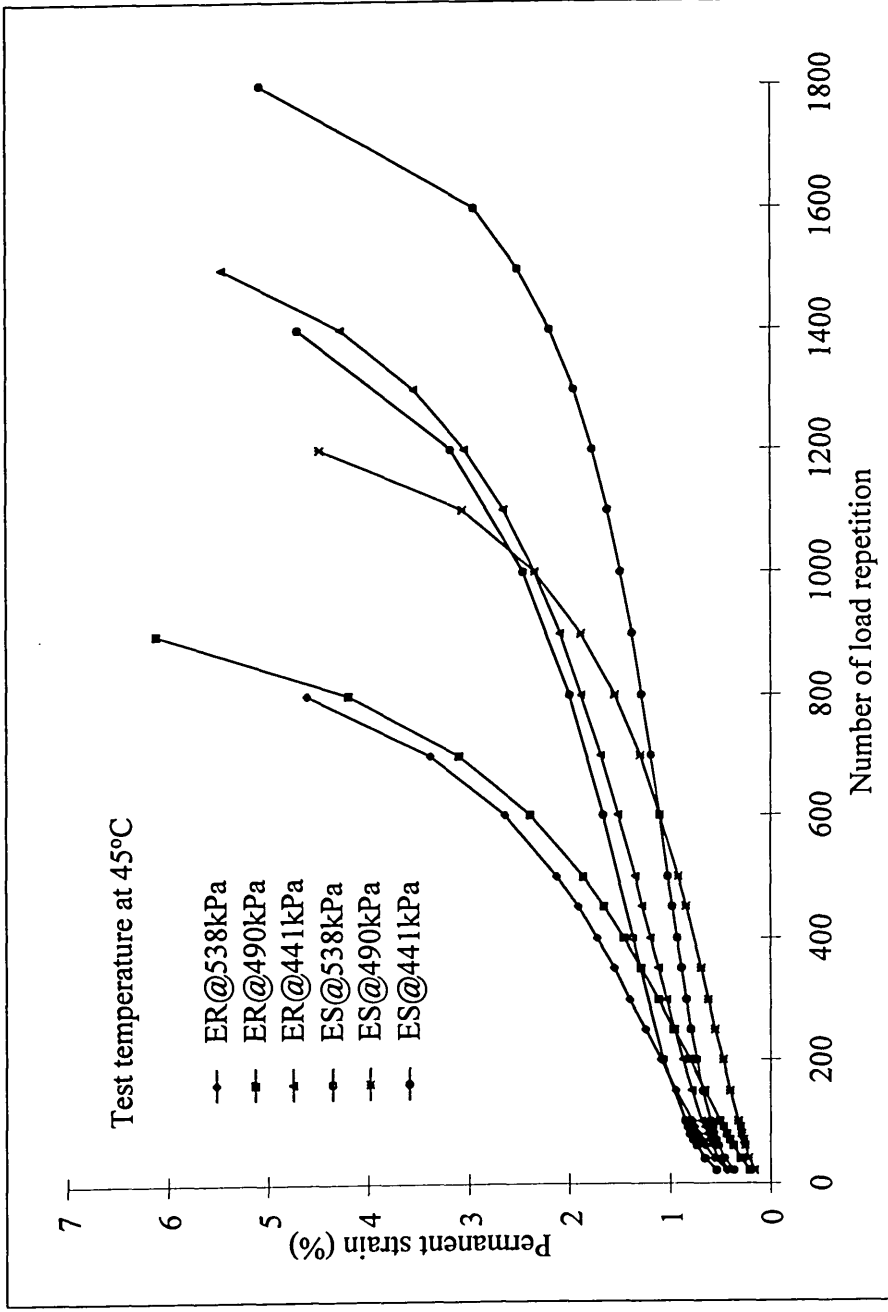


Figure C.3 Typical plots of permanent strain and number of load repetition showing the effect of applied stress levels for HRA mixtures with SBR and SBS modified 50 pen binders. Test temperature at 45°C

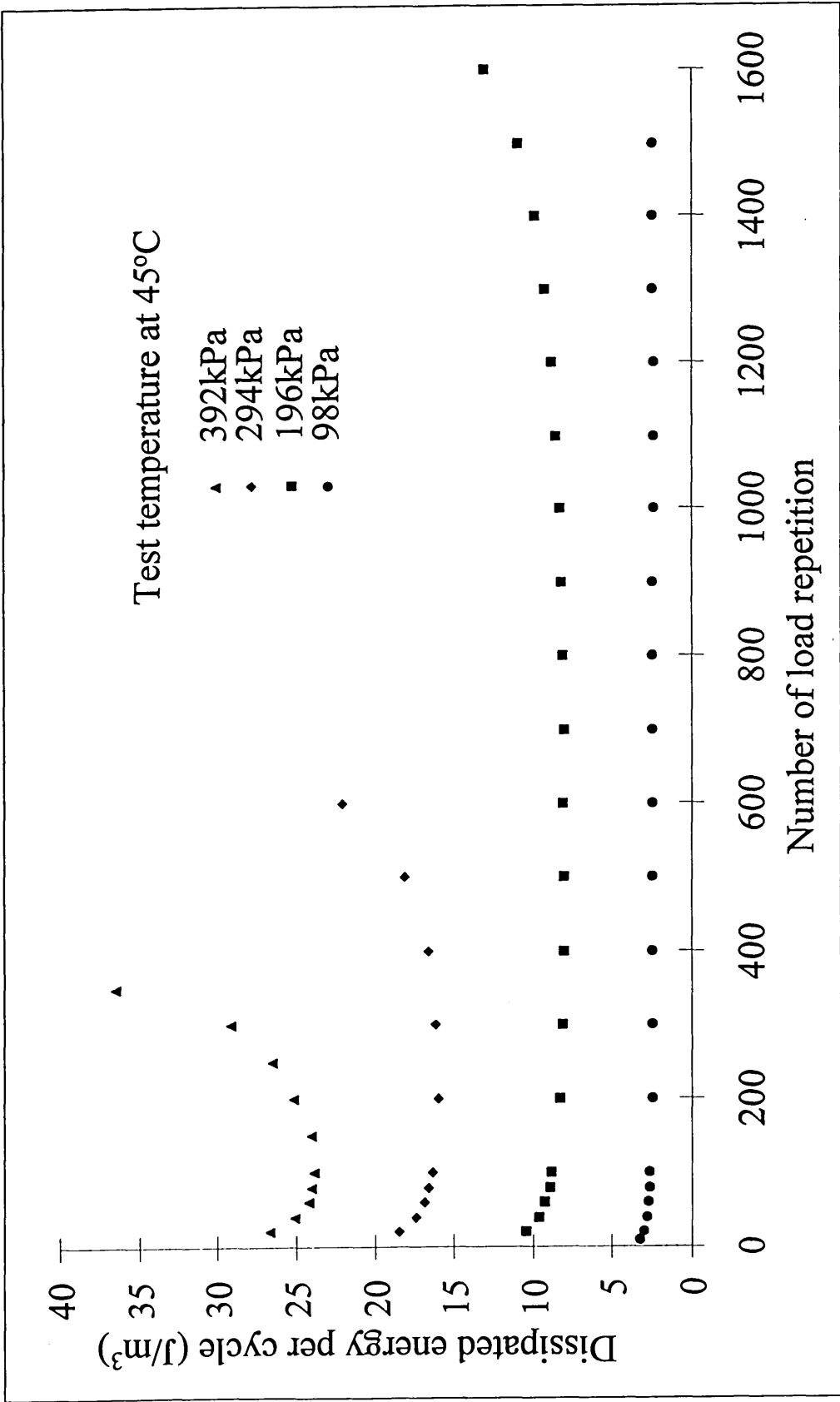


Figure C.4 Typical plots of dissipated energy per cycle to the number of load repetition showing the effect of different stress levels. Test temperature 45°C. Mixture 50 Pen HRA.

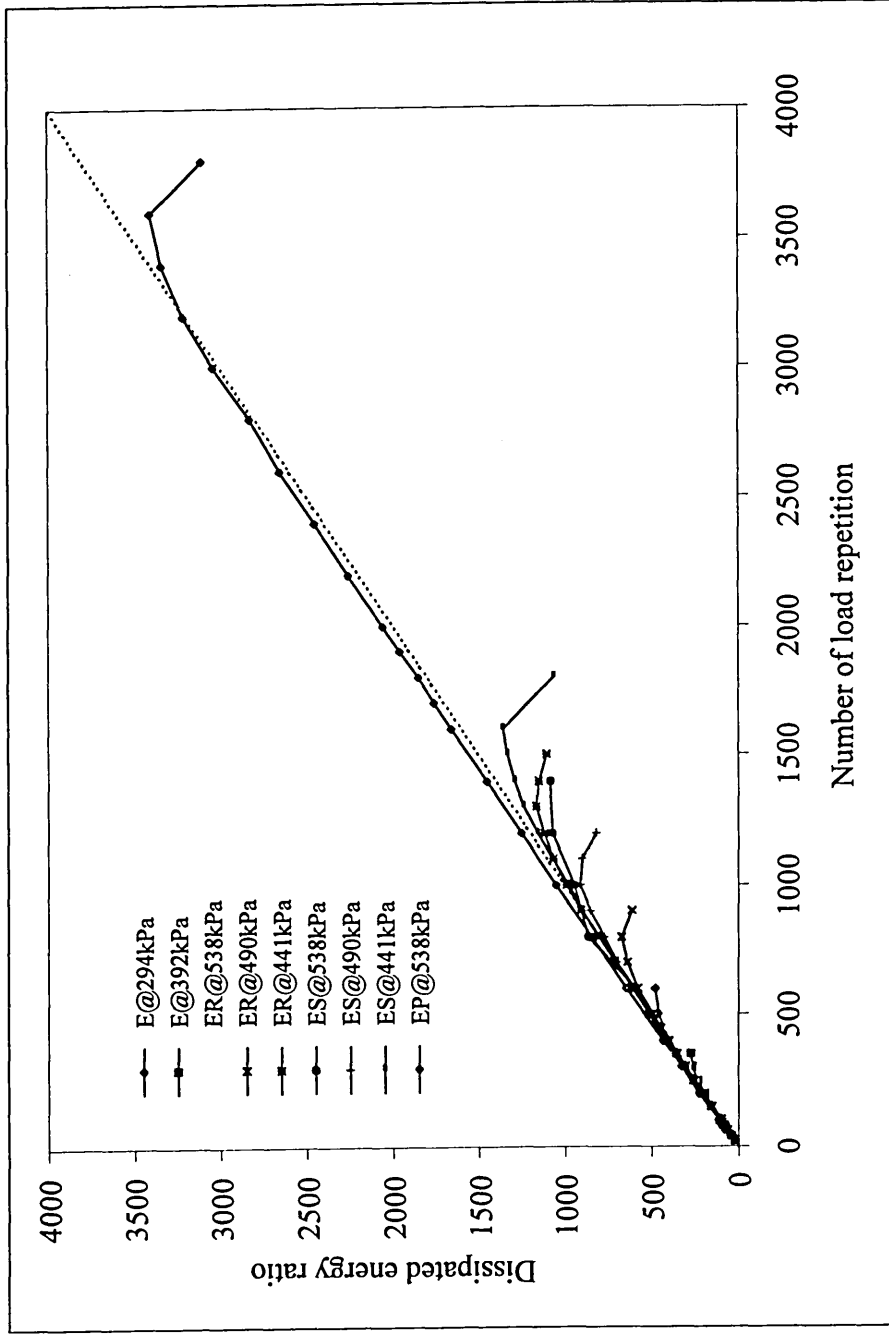


Figure C.5 Typical plots of dissipated energy ratio and number of load repetition showing the effect of applied stress levels for HRA mixtures. Test temperature at 45°C

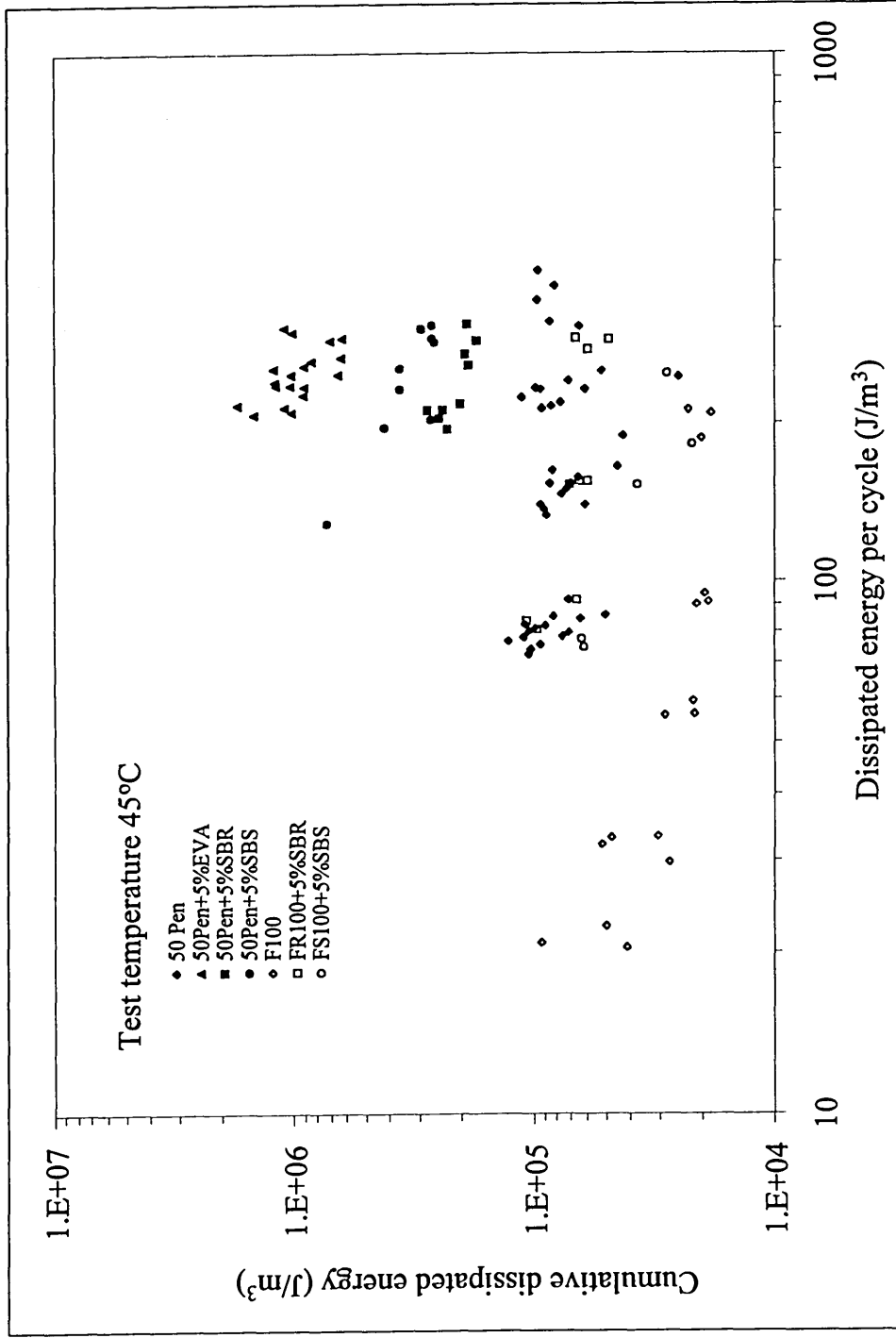


Figure C.6 Plots of dissipated energy per cycle and the cumulative dissipated energy for HRA mixtures. Test temperature at 45°C

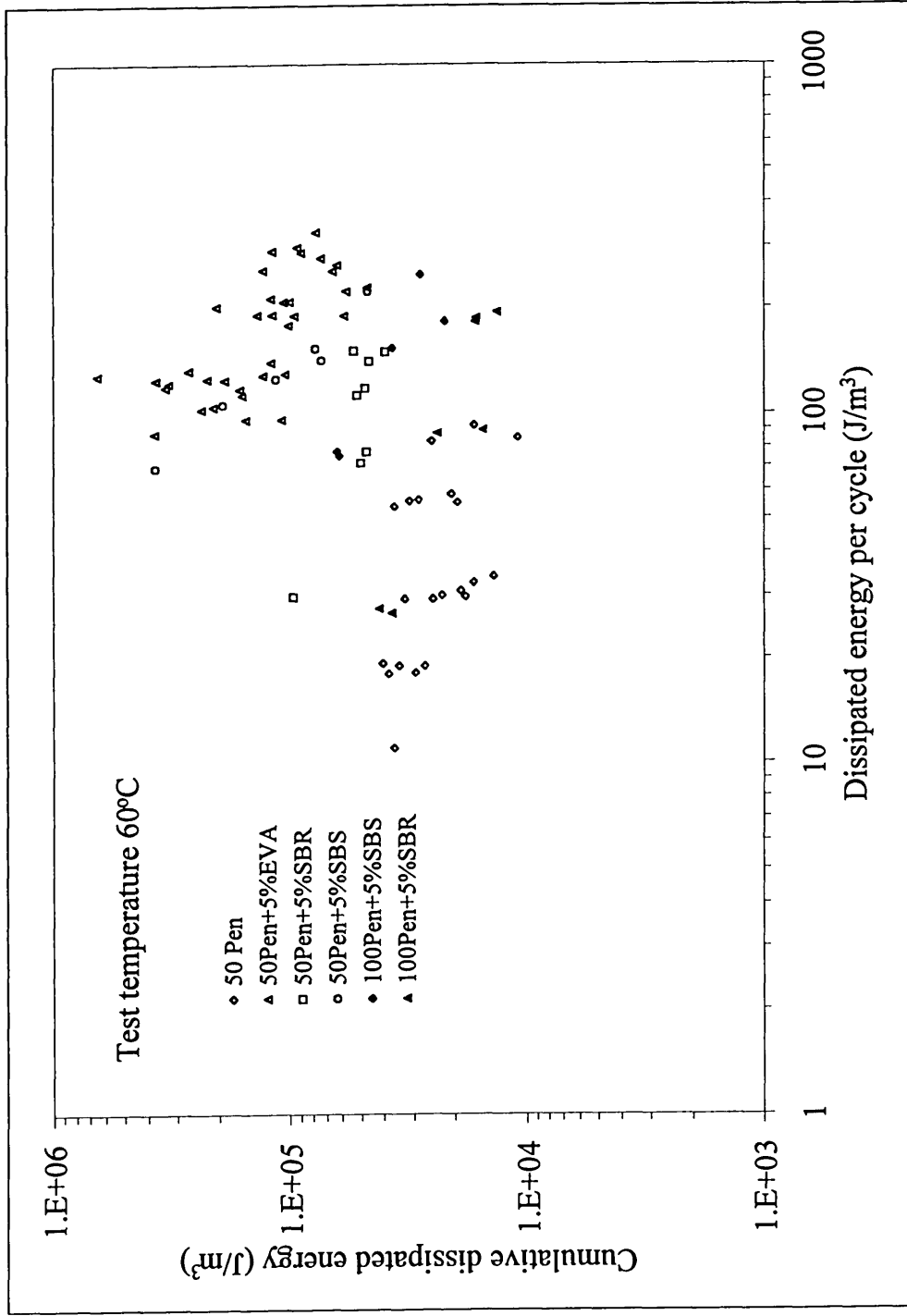


Figure C.7 Plots of dissipated energy per cycle and the cumulative dissipated energy for HRA mixtures. Test temperature at 60°C

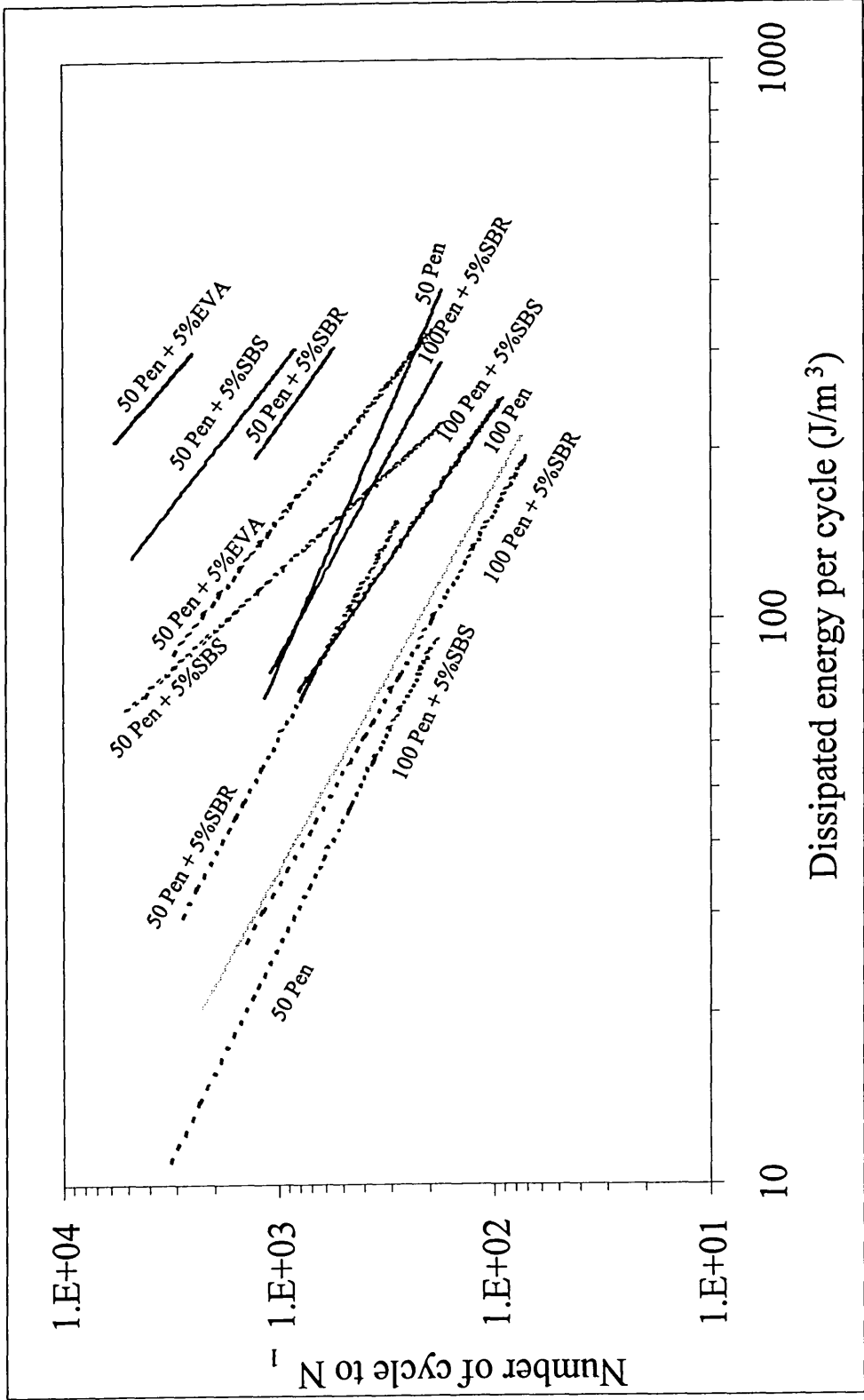


Figure C.8 The effect of dissipated energy per cycle to the number of cycles to NI. Solid lines indicate test at 45°C and dashed lines indicate test at 60°C.

Table C.1 Summary results from dynamic creep test

Mixtures type	V <sub>v</sub> %	Temperature °C	Load N	Stress Pa	N1 cycles	Strain rate		w <sub>i</sub> J/m <sup>3</sup>	W <sub>N1</sub> J/m <sup>3</sup>	W <sub>norm</sub>
						microstrain/cycle	R <sup>2</sup>			
A507	3.40%	45	2449	300	200	86.56	1.0000	189.39	42473.0	0.00446
A508	3.60%	45	1633	200	720	41.25	0.9991	92.00	71700.0	0.00128
A509	3.55%	45	1633	200	900	30.69	0.9959	85.70	82800.0	0.00104
A525	3.79%	45	3200	392	380	57.27	0.9970	231.47	94136.6	0.00246
A526	3.57%	45	3200	392	280	80.98	0.9976	239.45	72118.7	0.00332
A521	3.31%	45	2400	294	480	36.81	0.9984	163.18	83955.3	0.00194
A527	2.95%	45	2400	294	400	49.88	0.9975	158.21	65806.3	0.00240
A522A	3.11%	45	1600	196	700	21.64	0.9949	84.82	64042.2	0.00132
A523	3.03%	45	1600	196	1200	14.55	0.9873	81.33	100025.8	0.00081
A524	3.02%	45	1600	196	1300	14.45	0.9812	82.65	109653.7	0.00075
A528	3.01%	60	1600	196	110	100.16	0.9981	85.05	10863.3	0.00783
A529	3.30%	60	800	98	500	32.50	0.9881	32.76	16841.9	0.00195
A531	3.11%	60	800	98	400	37.77	0.9937	34.03	13904.5	0.00245
A530	2.87%	60	400	49	3200	3.22	0.9950	11.02	36109.1	0.00031
AP545	3.78%	45	4400	538	3400	6.44	0.9990	295.34	1017466.0	0.00029
AP542	3.66%	45	4400	538	3600	5.41	0.9990	300.82	1102935.0	0.00027
AP543	3.79%	45	4000	490	3500	4.67	0.9990	255.97	909463.4	0.00028
AP544	3.74%	45	4000	490	2600	7.67	0.9976	246.04	651809.7	0.00038
AP546	3.61%	45	4000	490	4100	4.50	0.9990	245.91	1023628.7	0.00024
AP521	3.78%	60	3200	392	250	58.70	0.9979	224.13	57843.2	0.00387
AP524	3.94%	60	3200	392	300	39.77	0.9954	190.27	58967.5	0.00323
AP530	3.53%	60	3200	392	600	23.53	0.9953	191.90	119178.0	0.00161

Mixtures type	V <sub>v</sub> %	Temperature °C	Load N	Stress Pa	N1 cycles	Strain rate		W <sub>i</sub> J/m <sup>3</sup>	W <sub>NI</sub> J/m <sup>3</sup>	W <sub>norm</sub>
						microstrain/cycle	R <sup>2</sup>			
AP526	3.39%	60	3200	392	450	30.20	0.9983	208.69	100270.4	0.00208
AP531	3.55%	60	2400	294	800	14.88	0.9908	129.18	105518.5	0.00122
AP532	3.89%	60	2400	294	1000	12.14	0.9803	128.16	130544.7	0.00098
AP522	3.74%	60	2400	294	850	15.78	0.9912	139.41	120692.7	0.00116
AP525	4.09%	60	2400	294	1500	6.73	0.9995	124.99	188819.0	0.00066
AP527	3.80%	60	2000	245	2000	4.41	0.9977	104.42	211416.4	0.00049
AP533	3.90%	60	2000	245	1600	5.77	0.9883	96.02	153496.5	0.00063
AP535	3.93%	60	2000	245	2300	5.75	0.9904	102.84	236310.5	0.00044
AP534	3.79%	60	2000	245	1100	9.00	0.9970	96.26	108056.7	0.00089
B504	5.57%	45	4000	490	200	76.67	0.9994	302.50	64983.3	0.00466
B502	4.96%	45	3200	392	160	97.40	1.0000	243.83	24996.8	0.00975
B503	4.69%	45	2400	294	450	42.00	0.9916	153.89	70318.1	0.00219
B505	4.78%	45	2400	294	260	83.56	0.9967	165.64	44929.0	0.00369
B506	5.73%	45	2400	294	510	35.12	0.9944	147.15	76392.2	0.00193
B508	4.67%	45	1600	196	590	35.52	0.9832	86.19	50391.2	0.00171
B509	4.63%	45	1600	196	900	20.68	0.9709	79.54	72060.2	0.00110
B510	5.76%	45	1600	196	1370	12.98	0.9827	74.23	103111.8	0.00072
B512	5.05%	45	1600	196	940	20.17	0.9942	78.65	76080.7	0.00103
B507	4.55%	45	800	98	3600*	1.31	0.9887	24.64	not fail	not fail
B511	4.99%	45	800	98	3600*	2.66	0.9900	26.57	not fail	not fail
B527	4.93%	60	1600	196	180	78.33	0.9823	92.37	16834.2	0.00549
B529	4.14%	60	1600	196	300	41.64	0.9986	82.78	25207.0	0.00328

Mixtures type	V <sub>v</sub> %	Temperature °C	Load N	Stress Pa	N1 cycles	Strain rate		w <sub>i</sub> J/m <sup>3</sup>	W <sub>NI</sub> J/m <sup>3</sup>	W <sub>norm</sub>
						microstrain/cycle	R <sup>2</sup>			
B523	4.11%	60	1200	147	350	34.36	0.9963	55.38	19747.1	0.00280
B520	4.20%	60	800	98	600	21.67	0.9897	31.06	18922.4	0.00164
B521	4.61%	60	800	98	600	20.16	0.9928	29.92	18150.2	0.00165
B522	3.78%	60	600	73.5	1400	9.86	0.9867	19.04	27103.1	0.00070
B525	3.59%	60	600	73.5	2000	5.13	0.9959	19.21	40618.1	0.00047
BP505	4.33%	45	4400	538	3200	5.30	0.9860	260.37	843736.7	0.00031
BP506	4.53%	45	4000	490	5000	3.28	0.9789	239.05	1198754.1	0.00020
BP502	4.66%	45	4000	490	4800	3.13	0.9925	234.95	1185015.2	0.00020
BP501	4.21%	45	3600	440	8000	1.91	0.9877	216.91	1734342.9	0.00013
BP512	4.78%	45	3600	440	4800	2.98	0.9865	210.42	1022540.5	0.00021
BP510	4.54%	60	4000	490	300	54.23	0.9953	288.94	89611.3	0.00322
BP508	4.57%	60	4000	490	250	51.30	0.9959	277.86	74049.6	0.00375
BP509	4.64%	60	3200	392	550	17.65	0.9977	179.39	101477.3	0.00177
BP513	4.72%	60	3200	392	140	120.93	0.9996	228.27	47104.2	0.00485
BP511	4.64%	60	2400	294	1360	5.66	0.9977	117.32	164269.3	0.00071
BP515	4.11%	60	2400	294	1400	6.30	0.9760	112.58	159573.4	0.00071
BP507	4.79%	60	1600	196	6000*	0.62	0.9559	63.20	not fail	not fail
C530	3.86%	45	4400	538	240	132.41	0.9919	386.56	96258.5	0.00402
C531	3.62%	45	4400	538	220	138.47	0.9868	359.90	82273.5	0.00437
C532	3.88%	45	4000	490	280	98.55	0.9960	338.21	97074.9	0.00348
C504	3.59%	45	4000	490	270	77.72	0.9968	308.96	86181.3	0.00359
C501	3.56%	45	3200	392	360	39.43	0.9999	215.00	84562.2	0.00254

Mixtures type	V <sub>v</sub> %	Temperature °C	Load N	Stress Pa	N1 cycles	Strain rate		w <sub>i</sub> J/m <sup>3</sup>	W <sup>NI</sup> J/m <sup>3</sup>	w <sub>norm</sub>
						microstrain/cycle	R <sup>2</sup>			
C502	3.94%	45	3200	392	340	54.26	0.9976	218.89	77815.7	0.00281
C506	3.93%	45	3200	392	420	43.29	0.9976	213.12	93334.6	0.00228
C503	3.95%	45	2400	294	650	24.59	0.9917	134.26	88842.3	0.00151
C505	3.84%	45	2400	294	550	36.72	0.9905	154.22	86236.1	0.00179
C512	3.71%	45	2400	294	650	24.97	0.9957	140.37	94097.1	0.00149
C508	3.95%	45	1600	196	1100	16.85	0.9757	82.04	89560.6	0.00092
C509	3.73%	45	1600	196	1390	11.88	0.9809	78.19	110062.1	0.00071
C529	2.83%	45	1600	196	1300	13.98	0.9963	80.25	105338.2	0.00076
C507	2.98%	45	800	98	3600*	1.81	0.9945	27.61	not fail	not fail
C511	3.08%	45	800	98	3600*	2.56	0.9864	28.43	not fail	not fail
CP503	2.56%	45	4400	538	2500	6.34	0.9757	284.57	705701.6	0.00040
CP504	2.63%	45	4000	490	4800	2.78	0.9660	253.14	1216478.6	0.00021
CP506	2.77%	45	4000	490	4400	3.47	0.9958	235.68	1040614.2	0.00023
CP509	3.19%	60	4400	538	230	68.31	0.9984	327.64	77751.0	0.00421
CP510	3.36%	60	4000	490	220	46.41	0.9999	265.57	62768.0	0.00423
CP519	3.33%	60	4000	490	250	50.06	0.9975	255.35	66046.2	0.00387
CP505	3.45%	60	3200	392	500	20.94	0.9936	189.79	96356.3	0.00197
CP507	3.12%	60	3200	392	540	23.91	0.9958	213.61	120284.3	0.00178
CP511	3.38%	60	3200	392	500	26.50	0.9980	208.25	106711.0	0.00195
CP512	3.28%	60	2400	294	2000	5.55	0.9992	132.40	268993.6	0.00049
CP513	2.84%	60	2400	294	2900	3.22	0.9957	124.92	368195.7	0.00034
CP514	2.86%	60	2400	294	2600	4.02	0.9933	121.71	324505.5	0.00038

Mixtures type	V <sub>v</sub> %	Temperature °C	Load N	Stress Pa	N1 cycles	Strain rate		w <sub>i</sub> J/m <sup>3</sup>	W <sub>NI</sub> J/m <sup>3</sup>	W <sub>norm</sub>
						microstrain/cycle	R <sup>2</sup>			
CP521	3.00%	60	2000	245	4200	2.48	0.9824	87.68	375325.6	0.00023
D510	5.47%	45	3200	392	200	133.06	0.9988	249.66	52373.3	0.00477
D507	4.52%	45	3200	392	250	107.16	0.9967	232.07	61453.0	0.00378
D508	4.79%	45	3200	392	550	38.22	0.9979	223.19	112557.6	0.00198
D509	4.89%	45	3200	392	450	48.44	0.9973	232.52	98276.6	0.00237
D501	4.85%	45	2400	294	650	35.94	0.9980	137.69	90775.9	0.00152
D503	5.01%	45	2400	294	450	66.63	0.9987	150.60	73045.1	0.00206
D506	4.57%	45	2400	294	400	61.56	0.9984	140.29	61017.3	0.00230
D502	5.12%	45	1600	196	1400	15.23	0.9975	72.79	105353.1	0.00069
D504	4.85%	45	1600	196	1600	15.34	0.9969	76.77	127268.9	0.00060
D505	4.41%	45	1600	196	1200	18.45	0.9913	75.72	94011.5	0.00081
D521	4.58%	60	1200	147	650	25.48	0.9966	53.41	36096.8	0.00148
D522	4.30%	60	1200	147	550	28.52	0.9929	55.79	31274.0	0.00178
D523	4.62%	60	1200	147	500	36.09	0.9972	56.10	28706.1	0.00195
D524	4.19%	60	800	98	1100	11.50	0.9925	29.41	32814.1	0.00090
D525	4.64%	60	800	98	750	18.44	0.9934	30.14	22898.9	0.00132
D526	4.43%	60	800	98	850	16.03	0.9962	29.36	25023.7	0.00117
D527	4.79%	60	600	73.5	2100	6.22	0.9889	18.03	38504.3	0.00047
D528	4.52%	60	600	73.5	1600	7.97	0.9998	18.18	29504.8	0.00062
D529	4.82%	60	600	73.5	1850	8.00	0.9923	18.91	34452.1	0.00055
DP521	3.80%	45	3800	465.5	7000	1.88	0.9987	207.94	1481591.0	0.00014
DP520	3.30%	45	3800	465.5	5000	2.08	0.9974	214.48	1101845.0	0.00019

Mixtures type	V <sub>v</sub> %	Temperature °C	Load N	Stress Pa	N1 cycles	Strain rate		w <sub>i</sub> J/m <sup>3</sup>	W <sub>NI</sub> J/m <sup>3</sup>	W <sub>norm</sub>
						microstrain/cycle	R <sup>2</sup>			
DP518	3.49%	45	4000	490	4000	3.42	0.9983	226.01	916583.5	0.00025
DP515	2.99%	45	4000	490	3800	3.36	0.9970	234.50	908659.9	0.00026
DP514	3.64%	45	4200	514.5	2400	5.77	0.9993	265.24	637721.1	0.00042
DP513	3.36%	45	4400	539	2200	6.30	0.9997	288.02	634317.1	0.00045
DP505	3.43%	60	3200	392	850	14.59	0.9991	187.92	16365.0	0.01148
DP511	3.45%	60	2400	294	1800	6.17	0.9977	125.15	225111.1	0.00056
DP509	3.22%	60	4000	490	500	33.39	0.9992	256.98	130292.4	0.00197
DP508	3.86%	60	4000	490	300	58.28	0.9946	297.86	93102.5	0.00320
DP507	4.02%	60	4000	490	400	42.37	0.9995	290.02	118782.2	0.00244
DP506	3.32%	60	2400	294	4900	2.47	0.9995	128.97	646999.5	0.00020
DP512	3.36%	60	2400	294	2800	3.81	0.9985	119.00	337245.7	0.00035
DP510	3.14%	60	3200	392	700	18.31	0.9978	192.39	138585.1	0.00139
DP504	3.67%	60	3200	392	1000	14.46	0.9997	202.75	204921.1	0.00099
ER519	3.81%	45	3200	392	1200	18.08	0.9984	212.23	241352.2	0.00088
ER520	4.06%	45	3200	392	1150	19.30	0.9976	194.99	229846.8	0.00085
ER517	3.79%	45	3600	441	1300	14.56	0.9990	212.07	279442.9	0.00076
ER518	4.42%	45	3600	441	1200	16.56	0.9990	204.56	249228.4	0.00082
ER506	4.74%	45	3600	441	900	24.58	0.9980	217.38	204296.2	0.00106
ER516	4.30%	45	4000	490	700	33.47	0.9963	268.71	193570.8	0.00139
ER509	4.54%	45	4000	490	700	36.36	0.9999	256.89	187302.2	0.00137
ER515	4.01%	45	4400	539	600	32.67	0.9964	284.95	172615.1	0.00165
ER508	4.03%	45	4400	539	600	46.89	0.9905	306.43	189469.9	0.00162

Mixtures type	V <sub>v</sub> %	Temperature °C	Load N	Stress Pa	N1 cycles	Strain rate		w <sub>i</sub> J/m <sup>3</sup>	W <sub>N1</sub> J/m <sup>3</sup>	W <sub>norm</sub>
						microstrain/cycle	R <sup>2</sup>			
ER513	4.31%	60	800	98	3200	3.14	0.9971	29.86	96550.5	0.00031
ER510	4.22%	60	1600	196	700	18.70	0.9950	71.91	50031.3	0.00144
ER505	3.99%	60	1600	196	600	25.00	0.9934	77.41	47361.8	0.00163
ER511	4.10%	60	2000	245	400	35.36	0.9960	118.30	48240.2	0.00245
ER507	4.06%	60	2000	245	450	41.22	0.9902	112.76	52046.1	0.00217
ER512	3.65%	60	2400	294	350	44.73	0.9983	151.03	54060.5	0.00279
ER514	3.90%	60	2400	294	250	55.39	0.9994	149.82	39782.7	0.00377
ER504	4.16%	60	2400	294	300	48.53	0.9993	141.13	46616.7	0.00303
ES519	4.10%	45	2400	294	5600	1.86	0.9904	129.55	731970.6	0.00018
ES514	3.83%	45	3200	392	1300	10.19	0.9999	203.23	269661.1	0.00075
ES516	3.60%	45	3200	392	2100	7.56	0.9917	196.14	421487.4	0.00047
ES512	3.62%	45	3600	440	1500	9.78	0.9973	231.58	360331.4	0.00064
ES513	3.88%	45	3600	440	1400	9.38	0.9954	252.48	363686.4	0.00069
ES517	3.69%	45	4000	490	900	17.11	0.9986	287.19	266231.3	0.00108
ES518	3.75%	45	4000	490	900	17.42	0.9975	304.82	268158.8	0.00114
ES511	3.57%	45	4000	490	900	15.28	0.9985	283.45	260380.0	0.00109
ES507	3.51%	45	4400	538	1000	17.09	0.9912	299.09	296742.7	0.00101
ES505	3.72%	60	1600	196	5200	1.80	0.9985	69.42	373263.5	0.00019
ES504	4.12%	60	2000	245	1800	5.84	0.9947	105.82	192864.7	0.00055
ES506	3.48%	60	2400	294	900	12.55	0.9993	125.38	114912.8	0.00109
ES521	3.74%	60	2400	294	500	24.91	0.9961	153.23	78372.8	0.00196
ES522	3.77%	60	2400	294	450	26.09	0.9971	141.83	74306.2	0.00191

Mixtures type	V <sub>v</sub> %	Temperature °C	Load N	Stress Pa	N1 cycles	Strain rate		w <sub>1</sub> J/m <sup>3</sup>	W <sub>NI</sub> J/m <sup>3</sup>	W <sub>norm</sub>
						microstrain/cycle	R <sup>2</sup>			
ES520	3.90%	60	3200	392	200	56.95	0.9983	223.99	47012.6	0.00476
F114	3.12%	45	600	73.5	4400	2.70	0.9980	20.89	93330.2	0.00022
F115	2.92%	45	600	73.5	2000	5.27	0.9989	20.45	41095.4	0.00050
F116	3.04%	45	600	73.5	2200	5.52	0.9998	22.44	49984.0	0.00045
F113	3.05%	45	800	98	900	12.50	0.9996	33.17	30690.6	0.00108
F109	3.36%	45	800	98	900	9.95	0.9986	29.66	27295.9	0.00109
F111	3.59%	45	800	98	1600	8.59	0.9946	32.03	52192.7	0.00061
F112	3.47%	45	800	98	1400	11.67	0.9935	33.08	47665.1	0.00069
F106	2.82%	45	1200	147	500	25.92	0.9940	55.75	28814.6	0.00193
F105	2.96%	45	1200	147	370	34.78	0.9970	56.11	21480.6	0.00261
F110	3.99%	45	1200	147	350	37.30	0.9986	59.32	21835.4	0.00272
F104	3.23%	45	1600	196	220	53.63	0.9999	90.24	21056.7	0.00429
F107	3.76%	45	1600	196	200	65.38	0.9990	94.29	19560.4	0.00482
F108	3.58%	45	1600	196	200	60.22	0.9989	91.20	18846.4	0.00484
F118	3.74%	45	2400	294	90	254.17	0.9950	208.86	18512.2	0.01128
F119	3.33%	45	2400	294	110	165.95	0.9975	211.69	22938.6	0.00923
F117	3.29%	45	2400	294	105	166.02	0.9976	187.16	20273.0	0.00923
F120	3.22%	60	800	98	120	73.95	0.9996	34.63	4267.7	0.00811
F121	3.21%	60	800	98	180	57.33	0.9997	37.31	6973.4	0.00535
FR106	3.12%	45	1600	196	1300	13.23	0.9971	83.74	107835.9	0.00078
FR109	3.15%	45	1600	196	1200	12.63	0.9980	80.77	97782.0	0.00083
FR110	3.21%	45	1600	196	700	21.45	0.9991	92.11	65951.2	0.00140

Mixtures type	V <sub>v</sub> %	Temperature °C	Load N	Stress Pa	N1 cycles	Strain rate		w <sub>i</sub> J/m <sup>3</sup>	W <sub>N1</sub> J/m <sup>3</sup>	W <sub>norm</sub>
						microstrain/cycle	R <sup>2</sup>			
FR104	3.30%	45	2400	294	450	33.70	0.9985	153.04	71159.8	0.00215
FR107	3.26%	45	2400	294	370	40.20	0.9987	155.79	59528.5	0.00262
FR111	3.08%	45	2400	294	400	40.67	0.9987	156.10	64888.8	0.00241
FR105	3.32%	45	3200	392	165	131.02	0.9975	286.53	48827.0	0.00587
FR108	3.37%	45	3200	392	200	121.25	0.9876	287.30	66837.9	0.00430
FR112	3.14%	45	3200	392	200	123.59	0.9770	274.50	60171.8	0.00456
FR118	3.16%	60	800	98	1500	9.78	0.9950	27.59	41976.4	0.00066
FR115	3.25%	60	800	98	1400	7.92	0.9969	26.80	37114.2	0.00072
FR113	3.06%	60	1600	196	165	72.72	0.9993	89.29	15244.4	0.00586
FR117	3.21%	60	1600	196	270	48.55	0.9985	87.72	23714.4	0.00370
FR114	3.42%	60	2400	294	70	192.72	0.9950	194.03	13414.3	0.01446
FR116	2.91%	60	2400	294	90	152.20	0.9989	183.04	16671.9	0.01098
FS107	3.19%	45	1600	196	4000*	0.85	0.9956	80.14	not fail	not fail
FS112	2.99%	45	1600	196	5200*	0.26	0.9966	82.08	not fail	not fail
FS104	3.20%	45	1600	196	3400	3.23	0.9979	86.83	299023.4	0.00029
FS106	3.23%	45	2400	294	800	15.23	0.9996	167.94	139659.8	0.00120
FS105	2.67%	45	2400	294	1050	10.48	0.9998	145.21	156256.9	0.00093
FS108	2.63%	45	3200	392	300	31.77	0.9989	236.20	74521.9	0.00317
FS109	2.92%	45	3200	392	600	22.22	0.9924	247.90	152150.6	0.00163
FS110	2.94%	45	4000	490	300	42.44	0.9860	354.72	105256.4	0.00337
FS111	2.71%	45	4000	490	300	46.39	0.9964	327.15	105496.9	0.00310
FS113	2.95%	60	1600	196	800	10.45	0.9998	77.62	63303.7	0.00123

Mixtures type	V <sub>v</sub> %	Temperature °C	Load N	Stress Pa	N1 cycles	Strain rate		w <sub>i</sub> J/m <sup>3</sup>	W <sub>N1</sub> J/m <sup>3</sup>	w <sub>norm</sub>
						microstrain/cycle	R <sup>2</sup>			
FS117	3.12%	60	1600	196	800	9.72	0.9994	75.11	61841.9	0.00121
FS116	2.89%	60	2400	294	120	88.98	0.9977	182.68	22199.1	0.00823
FS114	3.23%	60	2400	294	230	145.13	0.9523	153.38	37128.2	0.00413
FS115	3.21%	60	3200	392	110	89.81	0.9999	247.96	28144.8	0.00881
E10	8.85%	45	3600	441	n/a	n/a	n/a	n/a	n/a	n/a
E20	6.05%	45	3600	441	68	386.02	0.9974	429.96	31287.6	0.01374
E30	4.39%	45	3600	441	150	131.56	0.9970	309.32	47762.0	0.00648
E75	2.42%	45	3600	441	240	82.12	0.9966	302.84	75028.5	0.00404
EP10	9.33%	45	3600	441	260	86.61	0.9991	304.55	84062.3	0.00362
EP20	6.60%	45	3600	441	800	19.29	0.9996	241.59	199851.5	0.00121
EP30	4.86%	45	3600	441	2100	6.99	0.9949	235.37	500216.2	0.00047
EP40	4.17%	45	3600	441	2100	6.13	0.9981	232.35	492732.0	0.00047
EP50	3.61%	45	3600	441	4700	3.10	0.9992	191.19	204000.0	0.00094
EP75	3.25%	45	3600	441	n/a	2.68	0.9960	232.69	n/a	n/a
ER10	10.42%	45	3600	441	110	247.82	0.9980	383.14	43226.9	0.00886
ER20	7.05%	45	3600	441	210	116.52	0.9994	331.75	71845.2	0.00462
ER30	5.75%	45	3600	441	490	56.06	0.9989	255.44	124357.3	0.00205
ER40	4.63%	45	3600	441	700	28.13	0.9993	230.56	171397.8	0.00135
ER50	4.14%	45	3600	441	1130	14.60	0.9990	211.00	244000.0	0.00086
ER75	2.99%	45	3600	441	1500	12.50	0.9992	227.61	354254.9	0.00064

Mixtures type	V <sub>v</sub> %	Temperature °C	Load N	Stress Pa	N1 cycles	Strain rate		w <sub>i</sub> J/m <sup>3</sup>	W <sub>NI</sub> J/m <sup>3</sup>	W <sub>norm</sub>
						microstrain/cycle	R <sup>2</sup>			
ES10	8.67%	45	3600	441	180	147.39	0.9998	358.81	68393.1	0.00525
ES20	6.43%	45	3600	441	450	43.53	0.9985	277.34	128919.5	0.00215
ES30	4.59%	45	3600	441	800	16.92	0.9997	250.77	205639.6	0.00122
ES40	3.63%	45	3600	441	2100	7.39	0.9942	248.87	530567.8	0.00047
ES50	3.75%	45	3600	441	1450	9.40	0.9901	242.03	362008.9	0.00067
ES75	3.20%	45	3600	441	2500	5.47	0.9939	250.49	625333.6	0.00040

note: n/a = data not available

## *Appendix D*

# Indirect Tensile Stiffness Modulus

### List of Symbols and Abbreviations:

ITSM	Indirect Tensile Stiffness Modulus, units: MPa
95% CI	95% Confidence Interval
A50, B50, C50, D50, E50	50 Pen bitumen from different manufacturers
F100	100 Pen bitumen
AP50, BP50, CP50, DP50, EP50	50 Pen bitumen (from different manufacturers) + 5% Ethylene Vinyl Acetate
ER50	50 Pen bitumen + 5% Styrene Butadiene Rubber
ES50	50 Pen bitumen + 5% Styrene Butadiene Styrene
FR100	100 Pen bitumen + 5% Styrene Butadiene Rubber
FS50	100 Pen bitumen + 5% Styrene Butadiene Styrene

*Table D.1 Indirect Tensile Stiffness Modulus at 20°C of HRA mixtures with 50 pen bitumen from different manufacturers.*

	ITSM [MPa] at 20°C			
Mixture type	A	B	C	D
Lower range (95%C.I.)	2801	2506	3320	2775
Mean values	3030	3009	3545	3020
Upper range(95%C.I.)	3260	3511	3770	3265
Coefficient of Variations	7.6%	16.7%	6.3%	8.1%

*Table D.2 Indirect Tensile Stiffness Modulus at 20°C of HRA mixtures with 50 pen bitumen from different manufacturers modified by 5% EVA.*

	ITSM [MPa] at 20°C			
Mixture type	AP	BP	CP	DP
Lower range(95%C.I.)	3654	3616	3716	3142
Mean values	3918	3845	4137	3433
Upper range(95%C.I.)	4182	4073	4558	3724
Coefficient of Variations	6.7%	5.9%	10.2%	8.5%

*Table D.3 Indirect Tensile Stiffness Modulus at 20°C of HRA mixtures showing relative improvement to the base binder, due to the modification by EVA copolymers.*

	ITSM [MPa] at 20°C			
Mixture type	A	B	C	D
Unmodified	3030	3009	3545	3020
EVA Modification	3918	3845	4137	3433
Improvement	29%	28%	17%	14%

*Table D.4 Indirect Tensile Stiffness Modulus at 20°C of HRA mixtures with 50 pen bitumen modified by different polymers, showing relative improvement to the base binder (50 pen bitumen).*

	ITSM [MPa] at 20°C			
Mixture type	E50	EP50	ER50	ES50
Lower range(95%C.I.)	2733	3624	3879	3110
Mean values	3067	4039	4744	4161
Upper range(95%C.I.)	3401	4454	5609	5212
Coefficient of Variations	5.6%	5.2%	9.3%	12.9%
Improvement	*	32%	55%	36%

Table D.5 Indirect Tensile Stiffness Modulus at 20°C of HRA mixtures with 100 pen bitumen modified by different polymers, showing relative improvement to the base binder (100 pen).

Mixture type	ITSM [MPa] at 20°C		
	F100	FS100	FR100
Lower range(95%C.I.)	1108	1730	1720
Mean values	1499	2224	2092
Upper range(95%C.I.)	1890	2718	2464
Coefficient of Variations	13.3%	11.3%	9.1%
Improvement	*	48%	40%

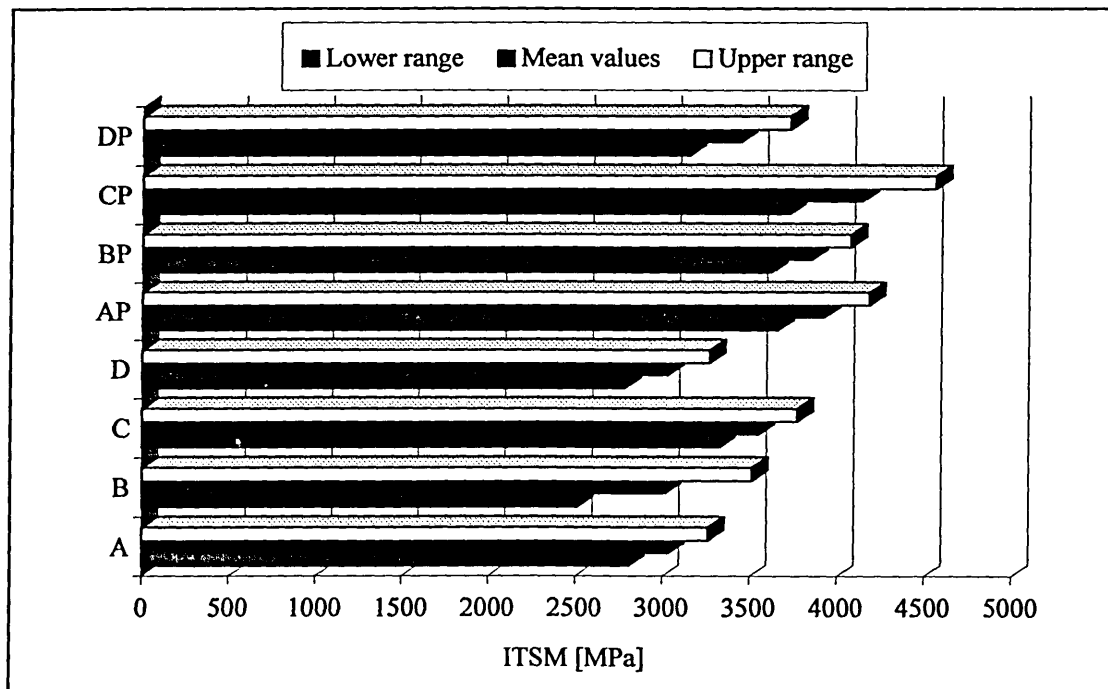


Figure D.1 ITSM results for HRA mixtures with 50 pen bitumen and EVA modified 50 pen binders. Test temperature : 20°C.

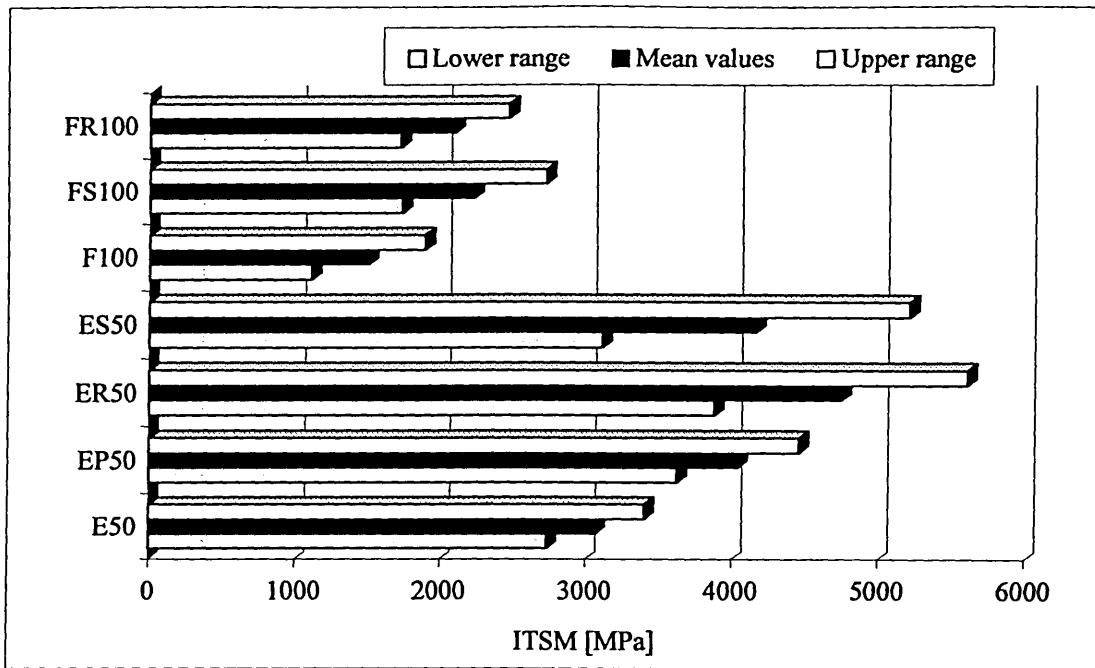


Figure D.2 ITSM results for HRA mixtures with different polymer modified binders (50 pen bitumen and 100 pen bitumen as the based binders). Test temperature : 20°C.

## *Appendix E*

### Analyses on The Repeatability of Dynamic Mechanical Testing on Bituminous Mixtures

## E.1. Mixture E50

Description of mixture : HRA with a straight run 50 pen bitumen.

Number of reading per test condition = 4.

Repeatability is expressed by coefficient of variation, i.e. the percentage of standard deviation by the sample mean.

Temperature (°C)	Frequency (Hz)	Variation in Complex Modulus	Variation in Phase Angle
20.64	0.2	2.62%	1.58%
20.64	0.5	1.22%	1.07%
20.64	1	1.06%	1.30%
20.64	2	0.68%	1.04%
20.64	5	0.51%	0.89%
20.64	10	0.67%	0.98%
20.64	20	0.30%	0.63%
20.64	30	0.36%	1.11%
-4.86	0.2	0.42%	1.20%
-4.86	0.5	0.25%	1.54%
-4.86	1	0.36%	1.94%
-4.86	2	0.88%	1.44%
-4.86	5	0.66%	1.66%
-4.86	10	0.67%	1.17%
4.18	0.2	1.01%	1.64%
4.18	0.5	1.04%	2.56%
4.18	1	1.56%	3.18%
4.18	2	1.61%	3.51%
4.18	5	2.28%	4.32%
4.18	10	2.31%	5.30%
14.29	0.2	0.92%	1.23%
14.29	0.5	0.52%	0.90%
14.29	1	0.40%	0.51%
14.29	2	0.34%	0.50%
14.29	5	0.43%	0.92%
14.29	10	0.38%	0.85%
14.29	20	0.62%	1.29%
14.29	30	0.54%	1.60%

Temperature (°C)	Frequency (Hz)	Variation in Complex Modulus	Variation in Phase Angle
24.45	0.2	3.19%	5.53%
24.45	0.5	1.29%	2.29%
24.45	1	1.19%	2.04%
24.45	2	1.00%	1.08%
24.45	5	0.55%	0.95%
24.45	10	0.46%	0.97%
24.45	20	0.21%	0.83%
24.45	30	0.29%	1.03%
34.56	0.2	6.70%	5.82%
34.56	0.5	4.49%	2.74%
34.56	1	3.76%	3.21%
34.56	2	1.97%	2.86%
34.56	5	1.89%	1.53%
34.56	10	1.15%	1.70%
34.56	20	0.69%	1.69%
34.56	30	0.49%	1.83%
44.72	0.2	5.06%	1.54%
44.72	0.5	1.31%	0.75%
44.72	1	1.06%	0.67%
44.72	2	8.46%	5.22%
44.72	5	5.89%	3.21%
44.72	10	5.67%	4.47%
44.72	20	3.31%	4.30%
44.72	30	2.80%	3.65%
25.43	0.2	1.99%	2.18%
25.43	0.5	1.80%	1.98%
25.43	1	1.33%	1.74%
25.43	2	1.12%	1.30%
25.43	5	0.69%	1.20%
25.43	10	0.62%	0.92%
25.43	20	0.33%	1.02%
25.43	30	0.34%	0.56%

Temperature (°C)	Frequency (Hz)	Variation in Complex Modulus	Variation in Phase Angle
19.37	0.2	1.12%	0.87%
19.37	0.5	1.23%	0.97%
19.37	1	0.73%	1.76%
19.37	2	0.60%	0.81%
19.37	5	0.47%	0.77%
19.37	10	0.24%	0.54%
19.37	20	0.22%	0.66%
19.37	30	0.07%	0.30%
24.4	0.2	2.49%	2.05%
24.4	0.5	1.37%	1.04%
24.4	1	0.80%	0.89%
24.4	2	0.94%	1.11%
24.4	5	0.54%	1.25%
24.4	10	2.06%	1.69%
24.4	20	0.60%	0.58%
24.4	30	0.22%	0.87%
34.56	0.2	3.09%	9.95%
34.56	0.5	2.69%	6.73%
34.56	1	2.45%	2.94%
34.56	2	1.76%	1.13%
34.56	5	1.30%	2.29%
34.56	10	1.05%	1.28%
34.56	20	0.81%	1.27%
34.56	30	0.56%	2.20%
44.68	0.2	1.96%	2.02%
44.68	0.5	12.91%	4.04%
44.68	1	9.10%	2.97%
44.68	2	5.26%	4.20%
44.68	5	10.37%	5.67%
44.68	10	4.32%	4.59%
44.68	20	2.03%	4.20%
44.68	30	2.57%	2.45%

Temperature (°C)	Frequency (Hz)	Variation in Complex Modulus	Variation in Phase Angle
49.76	0.2	0.00%	4.83%
49.76	0.5	13.98%	4.45%
49.76	1	12.50%	8.06%
49.76	2	8.49%	5.83%
49.76	5	6.02%	6.65%
49.76	10	5.56%	5.27%
49.76	20	4.65%	2.92%
49.76	30	3.58%	4.79%
20.4	0.2	11.22%	19.65%
20.4	0.5	3.89%	1.58%
20.4	1	2.33%	1.83%
20.4	2	0.97%	1.11%
20.4	5	0.94%	0.97%
20.4	10	1.05%	1.11%
20.4	20	0.67%	0.99%
20.4	30	0.83%	0.75%
5.2	0.2	0.53%	0.77%
5.2	0.5	0.55%	0.43%
5.2	1	0.40%	0.34%
5.2	2	0.59%	0.84%
5.2	5	0.83%	1.39%
5.2	10	0.78%	1.76%
5.2	20	1.24%	2.79%
5.2	30	1.17%	3.09%
-14.83	0.2	2.04%	7.52%
-14.83	0.5	0.53%	3.76%
-14.83	1	2.20%	9.27%
-14.83	2	2.08%	9.62%
-14.83	5	0.13%	7.81%
-14.83	10	1.99%	9.59%
-14.83	20	1.34%	7.44%
-14.83	30	1.11%	6.95%

Temperature (°C)	Frequency (Hz)	Variation in Complex Modulus	Variation in Phase Angle
-10.97	0.2	2.27%	6.41%
-10.97	0.5	0.61%	2.83%
-10.97	1	2.56%	7.17%
-10.97	2	2.05%	6.63%
-10.97	5	2.53%	11.12%
-10.97	10	2.09%	7.83%
-10.97	20	1.18%	5.93%
-10.97	30	2.99%	10.47%
-5.94	0.2	1.52%	3.02%
-5.94	0.5	1.21%	3.78%
-5.94	1	0.35%	2.98%
-5.94	2	2.73%	11.20%
-5.94	5	0.90%	2.61%
-5.94	10	2.79%	8.97%
-5.94	20	0.20%	3.43%
-5.94	30	3.07%	12.19%
-0.86	0.2	0.80%	1.18%
-0.86	0.5	0.61%	1.08%
-0.86	1	3.44%	19.85%
-0.86	2	2.45%	20.61%
-0.86	5	2.72%	7.12%
-0.86	10	2.17%	6.05%
-0.86	20	2.22%	6.22%
-0.86	30	3.02%	8.03%
9.21	0.2	0.48%	0.58%
9.21	0.5	0.47%	0.48%
9.21	1	0.65%	0.42%
9.21	2	0.63%	0.64%
9.21	5	0.20%	0.80%
9.21	10	0.08%	0.76%
9.21	20	0.73%	1.33%
9.21	30	0.84%	1.46%

Temperature (°C)	Frequency (Hz)	Variation in Complex Modulus	Variation in Phase Angle
14.24	0.2	1.21%	0.97%
14.24	0.5	0.50%	0.90%
14.24	1	0.57%	0.36%
14.24	2	0.49%	0.73%
14.24	5	0.70%	1.09%
14.24	10	1.71%	1.98%
14.24	20	0.54%	0.79%
14.24	30	0.58%	0.72%
5.2	0.2	0.62%	1.25%
5.2	0.5	0.54%	0.83%
5.2	1	0.32%	0.29%
5.2	2	0.61%	1.20%
5.2	5	0.15%	1.37%
5.2	10	0.39%	0.60%
5.2	20	1.91%	5.11%
5.2	30	1.79%	5.08%

## E.2. Mixture EP50

Description of mixture : HRA with EVA modified 50 pen binder.

Number of reading per test condition = 4.

Repeatability is expressed by coefficient of variation, i.e. the percentage of standard deviation by the sample mean.

Temperature (°C)	Frequency (Hz)	Variation in Complex Modulus	Variation in Phase Angle
5.15	0.2	1.51%	4.02%
5.15	0.5	1.99%	4.54%
5.15	1	1.82%	5.13%
5.15	2	1.75%	5.76%
5.15	5	2.95%	7.98%
5.15	10	2.95%	9.42%
5.15	20	3.21%	8.18%
5.15	30	3.30%	9.48%

Temperature (°C)	Frequency (Hz)	Variation in Complex Modulus	Variation in Phase Angle
-4.86	0.2	0.41%	3.42%
-4.86	0.5	0.87%	6.33%
-4.86	1	0.67%	4.96%
-4.86	2	3.74%	13.08%
-4.86	5	3.80%	14.90%
-4.86	10	3.69%	15.89%
-4.86	20	3.35%	17.57%
-4.86	30	3.49%	20.46%
14.24	0.2	0.79%	1.83%
14.24	0.5	0.75%	1.66%
14.24	1	0.57%	1.47%
14.24	2	0.67%	1.70%
14.24	5	0.93%	2.09%
14.24	10	0.71%	2.29%
14.24	20	1.31%	3.49%
14.24	30	1.18%	3.60%
19.32	0.2	1.03%	2.28%
19.32	0.5	1.12%	2.13%
19.32	1	0.76%	1.68%
19.32	2	0.64%	1.79%
19.32	5	0.70%	1.78%
19.32	10	0.22%	0.40%
19.32	20	0.69%	2.05%
19.32	30	0.61%	2.01%
24.45	0.2	1.86%	2.64%
24.45	0.5	1.65%	2.42%
24.45	1	0.84%	1.54%
24.45	2	0.89%	2.34%
24.45	5	0.92%	1.34%
24.45	10	1.25%	1.20%
24.45	20	0.58%	1.24%
24.45	30	0.63%	2.20%

Temperature (°C)	Frequency (Hz)	Variation in Complex Modulus	Variation in Phase Angle
34.51	0.2	2.70%	4.30%
34.51	0.5	2.66%	2.65%
34.51	1	2.27%	2.41%
34.51	2	1.72%	2.25%
34.51	5	1.40%	2.16%
34.51	10	1.43%	2.13%
34.51	20	1.66%	1.65%
34.51	30	1.29%	1.82%
44.68	0.2	7.91%	4.76%
44.68	0.5	6.16%	4.40%
44.68	1	4.79%	4.71%
44.68	2	3.60%	2.68%
44.68	5	3.05%	1.83%
44.68	10	3.12%	2.66%
44.68	20	2.40%	2.73%
44.68	30	2.77%	2.29%
25.43	0.2	2.25%	1.50%
25.43	0.5	1.51%	4.09%
25.43	1	4.00%	15.66%
25.43	2	4.32%	6.35%
25.43	5	1.22%	1.05%
25.43	10	0.74%	1.39%
25.43	20	0.95%	2.03%
25.43	30	0.55%	1.14%
5.5	0.2	1.04%	1.59%
5.5	0.5	0.91%	2.60%
5.5	1	0.89%	2.98%
5.5	2	2.46%	3.07%
5.5	5	1.09%	4.14%
5.5	10	1.01%	2.15%
5.5	20	1.40%	8.76%
5.5	30	2.75%	8.70%

Temperature ( <sup>0</sup> C)	Frequency (Hz)	Variation in Complex Modulus	Variation in Phase Angle
-14.88	0.2	0.26%	1.01%
-14.88	0.5	3.40%	24.49%
-14.88	1	1.67%	54.54%
-14.88	2	3.87%	17.13%
-14.88	5	3.27%	18.34%
-14.88	10	3.04%	19.72%
-14.88	20	2.81%	21.45%
-14.88	30	0.06%	0.25%
-10.87	0.2	9.01%	18.79%
-10.87	0.5	7.08%	37.40%
-10.87	1	2.88%	30.02%
-10.87	2	2.85%	15.86%
-10.87	5	3.11%	14.56%
-10.87	10	2.01%	18.20%
-10.87	20	2.60%	18.25%
-10.87	30	2.45%	21.47%
-5.94	0.2	6.19%	29.91%
-5.94	0.5	2.00%	15.18%
-5.94	1	1.20%	5.96%
-5.94	2	0.92%	9.28%
-5.94	5	0.70%	10.93%
-5.94	10	3.08%	12.17%
-5.94	20	1.54%	8.96%
-5.94	30	2.43%	17.39%
-0.95	0.2	12.22%	44.43%
-0.95	0.5	2.56%	11.14%
-0.95	1	0.45%	37.66%
-0.95	2	1.89%	28.62%
-0.95	5	1.64%	6.90%
-0.95	10	2.05%	3.75%
-0.95	20	1.11%	3.41%
-0.95	30	1.35%	6.10%

Temperature (°C)	Frequency (Hz)	Variation in Complex Modulus	Variation in Phase Angle
9.21	0.2	2.14%	30.07%
9.21	0.5	11.97%	29.67%
9.21	1	4.65%	10.47%
9.21	2	0.92%	2.23%
9.21	5	2.84%	1.82%
9.21	10	2.14%	1.94%
9.21	20	1.29%	1.90%
9.21	30	0.76%	1.51%
14.19	0.2	14.26%	12.82%
14.19	0.5	2.24%	1.16%
14.19	1	9.92%	34.45%
14.19	2	1.48%	4.14%
14.19	5	4.46%	4.50%
14.19	10	0.19%	1.09%
14.19	20	1.01%	1.84%
14.19	30	1.06%	1.75%
5.2	0.2	0.66%	1.95%
5.2	0.5	0.60%	1.54%
5.2	1	2.46%	33.10%
5.2	2	4.04%	17.29%
5.2	5	3.19%	5.07%
5.2	10	1.65%	3.19%
5.2	20	0.40%	2.06%
5.2	30	2.51%	9.40%
5.25	0.2	0.63%	1.97%
5.25	0.5	3.67%	21.94%
5.25	1	3.47%	13.34%
5.25	2	3.23%	14.38%
5.25	5	3.08%	5.90%
5.25	10	2.16%	1.90%
5.25	20	0.21%	0.93%
5.25	30	0.72%	4.00%

Temperature (°C)	Frequency (Hz)	Variation in Complex Modulus	Variation in Phase Angle
24.45	0.2	1.42%	1.63%
24.45	0.5	1.19%	1.91%
24.45	1	1.12%	1.39%
24.45	2	0.93%	1.98%
24.45	5	4.18%	0.85%
24.45	10	1.65%	2.49%
24.45	20	0.56%	0.67%
24.45	30	0.52%	1.18%
34.56	0.2	1.45%	0.77%
34.56	0.5	2.87%	1.66%
34.56	1	2.08%	2.59%
34.56	2	1.86%	2.07%
34.56	5	1.80%	2.21%
34.56	10	1.55%	2.09%
34.56	20	1.97%	1.99%
34.56	30	0.97%	2.04%
44.72	0.5	6.17%	4.07%
44.72	1	5.47%	3.76%
44.72	2	4.50%	3.27%
44.72	5	3.39%	2.97%
44.72	10	2.87%	2.96%
44.72	20	2.26%	2.03%
44.72	30	2.00%	2.11%
49.76	0.2	2.41%	0.79%
49.76	0.5	10.27%	5.05%
49.76	1	8.45%	4.52%
49.76	2	7.19%	4.09%
49.76	5	6.20%	4.63%
49.76	10	5.46%	3.12%
49.76	20	4.37%	3.04%
49.76	30	4.18%	3.68%
20.3	0.2	6.19%	30.76%
20.3	0.5	25.32%	8.16%
20.3	1	5.16%	2.02%
20.3	2	2.42%	2.97%
20.3	5	1.87%	3.11%
20.3	10	2.58%	2.20%
20.3	20	1.42%	1.00%
20.3	30	0.28%	0.94%

### E.3. Mixture ER50

Description of mixture : HRA with SBR modified 50 pen binder.

Number of reading per test condition = 4.

Repeatability is expressed by coefficient of variation, i.e. the percentage of standard deviation by the sample mean.

Temperature (°C)	Frequency (Hz)	Variation in Complex Modulus	Variation in Phase Angle
5.2	0.2	1.76%	2.91%
5.2	0.5	0.47%	1.09%
5.2	1	2.29%	4.29%
5.2	2	1.66%	5.88%
5.2	5	1.32%	8.99%
5.2	10	1.51%	5.55%
5.2	20	1.87%	8.15%
5.2	30	3.29%	6.87%
-4.91	0.2	0.27%	0.84%
-4.91	0.5	0.38%	1.02%
-4.91	1	1.71%	10.89%
-4.91	2	1.09%	6.50%
-4.91	5	0.27%	1.80%
-4.91	10	1.43%	2.42%
-4.91	20	0.50%	0.40%
-4.91	30	1.06%	3.78%
14.24	0.2	0.77%	0.96%
14.24	0.5	4.05%	15.61%
14.24	1	4.64%	4.40%
14.24	2	3.11%	12.55%
14.24	5	3.94%	3.64%
14.24	10	0.92%	1.80%
14.24	20	1.33%	2.51%
14.24	30	2.08%	4.44%
19.32	0.2	1.12%	1.14%
19.32	0.5	7.49%	24.74%
19.32	1	3.73%	6.26%
19.32	2	1.23%	2.12%
19.32	5	2.58%	1.03%
19.32	10	4.83%	5.53%
19.32	20	1.01%	1.86%
19.32	30	0.95%	2.04%

Temperature (°C)	Frequency (Hz)	Variation in Complex Modulus	Variation in Phase Angle
24.4	0.2	1.46%	1.27%
24.4	0.5	18.05%	19.65%
24.4	1	0.21%	12.70%
24.4	2	4.42%	5.59%
24.4	5	1.63%	1.21%
24.4	10	0.77%	0.87%
24.4	20	1.04%	1.55%
24.4	30	0.52%	1.17%
34.51	0.2	2.06%	1.41%
34.51	0.5	2.54%	2.16%
34.51	1	1.92%	1.43%
34.51	2	1.83%	1.12%
34.51	5	0.88%	1.33%
34.51	10	0.89%	1.42%
34.51	20	1.27%	1.14%
34.51	30	0.62%	1.62%
44.68	0.2	10.92%	5.71%
44.68	0.5	7.31%	4.59%
44.68	1	4.95%	4.04%
44.68	2	4.08%	3.45%
44.68	5	2.18%	3.26%
44.68	10	1.38%	2.35%
44.68	20	1.36%	1.51%
44.68	30	0.57%	2.09%
25.48	0.2	1.67%	2.44%
25.48	0.5	1.11%	1.19%
25.48	1	0.98%	1.25%
25.48	2	0.72%	1.40%
25.48	5	0.75%	1.07%
25.48	10	0.69%	1.03%
25.48	20	0.57%	1.24%
25.48	30	0.29%	0.29%
5.2	0.2	3.43%	2.81%
5.2	0.5	2.49%	1.91%
5.2	1	1.63%	1.19%
5.2	2	1.20%	0.69%
5.2	5	0.83%	0.57%
5.2	10	0.86%	0.71%
5.2	20	0.66%	0.47%
5.2	30	0.65%	0.74%

Temperature (°C)	Frequency (Hz)	Variation in Complex Modulus	Variation in Phase Angle
-14.78	0.2	0.24%	1.47%
-14.78	0.5	0.17%	1.32%
-14.78	1	1.87%	4.73%
-14.78	2	0.15%	0.77%
-14.78	5	0.26%	3.44%
-14.78	10	1.14%	1.00%
-14.78	20	0.73%	3.56%
-14.78	30	0.13%	2.98%
-10.92	0.2	0.18%	0.89%
-10.92	0.5	1.44%	26.84%
-10.92	1	2.04%	15.78%
-10.92	2	1.94%	5.85%
-10.92	5	2.30%	2.52%
-10.92	10	0.23%	1.25%
-10.92	20	0.13%	1.95%
-10.92	30	0.44%	2.93%
-5.94	0.2	0.30%	1.22%
-5.94	0.5	4.42%	35.27%
-5.94	1	2.83%	10.47%
-5.94	2	2.44%	5.19%
-5.94	5	0.09%	1.07%
-5.94	10	3.36%	7.94%
-5.94	20	0.22%	0.71%
-5.94	30	0.58%	1.96%
-0.95	0.2	0.12%	0.54%
-0.95	0.5	2.22%	14.05%
-0.95	1	2.64%	21.75%
-0.95	2	1.11%	3.04%
-0.95	5	2.94%	4.69%
-0.95	10	1.64%	1.54%
-0.95	20	0.76%	1.09%
-0.95	30	0.90%	1.31%
9.26	0.2	0.62%	1.35%
9.26	0.5	5.11%	16.26%
9.26	1	1.44%	5.06%
9.26	2	0.93%	1.04%
9.26	5	2.93%	3.37%
9.26	10	0.06%	0.78%
9.26	20	2.75%	1.81%
9.26	30	0.55%	1.14%

Temperature (°C)	Frequency (Hz)	Variation in Complex Modulus	Variation in Phase Angle
14.24	0.2	5.44%	34.24%
14.24	0.5	3.36%	9.76%
14.24	1	4.53%	25.33%
14.24	2	4.25%	4.42%
14.24	5	0.06%	1.24%
14.24	10	0.80%	0.94%
14.24	20	0.12%	0.07%
14.24	30	0.59%	0.64%
5.15	0.2	0.38%	1.58%
5.15	0.5	0.21%	1.43%
5.15	1	0.32%	1.36%
5.15	2	0.86%	1.65%
5.15	5	1.27%	1.34%
5.15	10	0.44%	1.36%
5.15	20	0.03%	0.45%
5.15	30	0.76%	0.75%
5.2	0.2	1.41%	1.34%
5.2	0.5	1.17%	0.77%
5.2	1	0.82%	1.14%
5.2	2	0.78%	0.73%
5.2	5	1.16%	1.21%
5.2	10	0.86%	0.84%
5.2	20	1.05%	1.31%
5.2	30	1.07%	2.10%
24.4	0.2	2.17%	0.92%
24.4	0.5	1.19%	0.99%
24.4	1	0.91%	1.06%
24.4	2	0.96%	1.24%
24.4	5	1.13%	1.07%
24.4	10	1.43%	1.60%
24.4	20	0.91%	1.05%
24.4	30	1.02%	1.17%
34.51	0.2	4.79%	2.23%
34.51	0.5	3.00%	1.37%
34.51	1	2.72%	1.76%
34.51	2	2.21%	1.08%
34.51	5	1.35%	1.52%
34.51	10	1.66%	1.16%
34.51	20	1.33%	1.13%
34.51	30	1.03%	1.57%

Temperature (°C)	Frequency (Hz)	Variation in Complex Modulus	Variation in Phase Angle
44.72	0.2	5.53%	0.34%
44.72	0.5	3.86%	0.49%
44.72	1	3.04%	0.84%
44.72	2	1.71%	0.22%
44.72	5	4.57%	4.21%
44.72	10	4.18%	2.38%
44.72	20	4.04%	3.55%
44.72	30	3.37%	2.25%
49.71	0.2	2.96%	2.24%
49.71	0.5	5.06%	0.96%
49.71	1	2.92%	0.48%
49.71	2	1.90%	1.03%
49.71	5	0.76%	0.78%
49.71	10	6.67%	4.46%
49.71	20	5.70%	3.07%
49.71	30	4.31%	3.24%
25.48	0.2	2.22%	1.84%
25.48	0.5	1.54%	2.27%
25.48	1	1.38%	0.85%
25.48	2	1.13%	1.26%
25.48	5	1.12%	1.21%
25.48	10	0.96%	0.67%
25.48	20	1.01%	1.12%
25.48	30	1.00%	1.20%
20.44	0.2	1.76%	1.30%
20.44	0.5	1.26%	1.18%
20.44	1	1.38%	0.52%
20.44	2	1.04%	0.71%
20.44	5	0.79%	0.84%
20.44	10	1.04%	0.64%
20.44	20	0.82%	1.15%
20.44	30	0.98%	1.53%
10.28	0.2	2.94%	5.08%
10.28	0.5	2.26%	1.36%
10.28	1	1.53%	1.14%
10.28	2	1.38%	1.03%
10.28	5	0.94%	0.74%
10.28	10	0.97%	0.86%
10.28	20	0.87%	1.00%
10.28	30	0.94%	1.12%

Temperature (°C)	Frequency (Hz)	Variation in Complex Modulus	Variation in Phase Angle
44.72	0.2	5.53%	0.34%
44.72	0.5	3.86%	0.49%
44.72	1	3.04%	0.84%
44.72	2	1.71%	0.22%
44.72	5	4.57%	4.21%
44.72	10	4.18%	2.38%
44.72	20	4.04%	3.55%
44.72	30	3.37%	2.25%
49.71	0.2	2.96%	2.24%
49.71	0.5	5.06%	0.96%
49.71	1	2.92%	0.48%
49.71	2	1.90%	1.03%
49.71	5	0.76%	0.78%
49.71	10	6.67%	4.46%
49.71	20	5.70%	3.07%
49.71	30	4.31%	3.24%
25.48	0.2	2.22%	1.84%
25.48	0.5	1.54%	2.27%
25.48	1	1.38%	0.85%
25.48	2	1.13%	1.26%
25.48	5	1.12%	1.21%
25.48	10	0.96%	0.67%
25.48	20	1.01%	1.12%
25.48	30	1.00%	1.20%
20.44	0.2	1.76%	1.30%
20.44	0.5	1.26%	1.18%
20.44	1	1.38%	0.52%
20.44	2	1.04%	0.71%
20.44	5	0.79%	0.84%
20.44	10	1.04%	0.64%
20.44	20	0.82%	1.15%
20.44	30	0.98%	1.53%
10.28	0.2	2.94%	5.08%
10.28	0.5	2.26%	1.36%
10.28	1	1.53%	1.14%
10.28	2	1.38%	1.03%
10.28	5	0.94%	0.74%
10.28	10	0.97%	0.86%
10.28	20	0.87%	1.00%
10.28	30	0.94%	1.12%

#### E.4. Mixture ES50

Description of mixture : HRA with SBS modified 50 pen binder.

Number of reading per test condition = 4.

Repeatability is expressed by coefficient of variation, i.e. the percentage of standard deviation by the sample mean.

Temperature (°C)	Frequency (Hz)	Variation in Complex Modulus	Variation in Phase Angle
5.25	0.2	1.01%	2.01%
5.25	0.5	0.72%	1.66%
5.25	1	1.06%	2.33%
5.25	2	0.84%	2.44%
5.25	5	1.48%	5.08%
5.25	10	0.57%	2.97%
5.25	20	0.53%	0.92%
5.25	30	1.47%	3.13%
-4.91	0.2	0.39%	4.03%
-4.91	0.5	0.47%	4.72%
-4.91	1	2.56%	8.30%
-4.91	2	2.45%	8.81%
-4.91	5	2.48%	7.47%
-4.91	10	1.13%	8.05%
-4.91	20	2.47%	10.60%
-4.91	30	2.15%	12.94%
14.29	0.2	0.82%	1.79%
14.29	0.5	0.70%	1.56%
14.29	1	0.17%	1.51%
14.29	2	2.77%	5.47%
14.29	5	1.21%	3.00%
14.29	10	1.20%	2.08%
14.29	20	0.59%	2.53%
14.29	30	1.23%	3.27%
19.32	0.2	1.09%	1.61%
19.32	0.5	3.93%	10.41%
19.32	1	2.37%	3.03%
19.32	2	2.88%	0.62%
19.32	5	1.77%	2.26%
19.32	10	0.42%	1.06%
19.32	20	0.23%	0.86%
19.32	30	0.34%	1.48%

Temperature (°C)	Frequency (Hz)	Variation in Complex Modulus	Variation in Phase Angle
24.45	0.2	2.37%	3.27%
24.45	0.5	1.92%	17.61%
24.45	1	4.19%	3.29%
24.45	2	2.36%	3.04%
24.45	5	1.45%	0.75%
24.45	10	1.65%	1.14%
24.45	20	1.52%	1.28%
24.45	30	0.72%	0.68%
34.56	0.2	5.42%	3.02%
34.56	0.5	3.09%	3.11%
34.56	1	2.32%	1.90%
34.56	2	2.06%	1.98%
34.56	5	1.30%	1.66%
34.56	10	0.79%	1.72%
34.56	20	0.96%	1.75%
34.56	30	0.69%	1.22%
44.68	0.2	12.63%	4.70%
44.68	0.5	8.44%	3.64%
44.68	1	7.13%	4.07%
44.68	2	5.88%	4.31%
44.68	5	3.74%	3.94%
44.68	10	3.29%	3.92%
44.68	20	2.22%	3.63%
44.68	30	1.94%	2.98%
25.48	0.2	1.81%	2.20%
25.48	0.5	1.64%	1.92%
25.48	1	1.02%	1.96%
25.48	2	1.08%	1.30%
25.48	5	1.83%	1.62%
25.48	10	0.31%	1.08%
25.48	20	0.47%	1.62%
25.48	30	0.52%	1.07%
5.3	0.2	1.48%	1.50%
5.3	0.5	0.53%	0.88%
5.3	1	0.91%	2.02%
5.3	2	0.88%	2.63%
5.3	5	1.56%	4.00%
5.3	10	1.40%	4.58%
5.3	20	1.72%	4.92%
5.3	30	1.74%	5.53%

Temperature (°C)	Frequency (Hz)	Variation in Complex Modulus	Variation in Phase Angle
-14.78	0.2	0.26%	0.99%
-14.78	0.5	0.78%	4.31%
-14.78	1	0.74%	4.89%
-14.78	2	1.29%	4.66%
-14.78	5	1.91%	6.08%
-14.78	10	1.25%	10.35%
-14.78	20	1.06%	8.05%
-14.78	30	0.96%	6.80%
-10.97	0.2	0.11%	0.51%
-10.97	0.5	0.82%	2.87%
-10.97	1	1.20%	5.32%
-10.97	2	0.55%	12.61%
-10.97	5	0.67%	6.79%
-10.97	10	1.44%	10.33%
-10.97	20	1.63%	13.58%
-10.97	30	2.04%	21.01%
-5.89	0.2	0.21%	0.72%
-5.89	0.5	0.44%	2.09%
-5.89	1	0.46%	2.19%
-5.89	2	1.86%	10.86%
-5.89	5	2.89%	9.37%
-5.89	10	1.58%	8.05%
-5.89	20	1.56%	9.60%
-5.89	30	2.02%	12.16%
-0.9	0.2	0.13%	1.03%
-0.9	0.5	0.64%	1.89%
-0.9	1	1.70%	5.32%
-0.9	2	1.43%	9.33%
-0.9	5	0.54%	5.56%
-0.9	10	3.14%	8.58%
-0.9	20	2.48%	7.32%
-0.9	30	2.19%	7.14%
9.26	0.2	6.20%	8.31%
9.26	0.5	0.72%	1.19%
9.26	1	0.82%	0.94%
9.26	2	0.81%	1.05%
9.26	5	1.01%	1.53%
9.26	10	0.76%	2.07%
9.26	20	1.82%	3.18%
9.26	30	1.28%	2.47%

Temperature (°C)	Frequency (Hz)	Variation in Complex Modulus	Variation in Phase Angle
14.29	0.2	0.95%	0.99%
14.29	0.5	0.67%	0.81%
14.29	1	0.46%	0.85%
14.29	2	5.09%	4.97%
14.29	5	2.71%	3.41%
14.29	10	0.47%	1.19%
14.29	20	3.99%	5.11%
14.29	30	0.75%	0.74%
5.2	0.2	4.19%	6.75%
5.2	0.5	3.18%	2.25%
5.2	1	3.86%	1.65%
5.2	2	2.22%	1.37%
5.2	5	1.36%	0.58%
5.2	10	0.71%	1.04%
5.2	20	1.62%	1.15%
5.2	30	1.13%	1.34%
19.32	0.2	1.28%	1.22%
19.32	0.5	1.12%	1.21%
19.32	1	1.08%	1.28%
19.32	2	4.41%	7.97%
19.32	5	0.92%	0.58%
19.32	10	0.71%	0.48%
19.32	20	1.41%	1.02%
19.32	30	1.44%	1.14%
24.4	0.2	1.60%	1.17%
24.4	0.5	1.72%	1.32%
24.4	1	2.05%	18.71%
24.4	2	7.05%	8.70%
24.4	5	2.61%	1.44%
24.4	10	1.60%	1.06%
24.4	20	4.27%	3.08%
24.4	30	0.61%	0.64%
34.51	0.2	4.93%	3.51%
34.51	0.5	4.26%	2.62%
34.51	1	5.97%	7.62%
34.51	2	1.86%	2.15%
34.51	5	1.70%	2.12%
34.51	10	0.89%	1.89%
34.51	20	1.61%	1.07%
34.51	30	0.90%	1.61%

Temperature (°C)	Frequency (Hz)	Variation in Complex Modulus	Variation in Phase Angle
44.72	0.5	8.13%	4.51%
44.72	1	7.59%	3.56%
44.72	2	6.21%	3.90%
44.72	5	4.47%	2.40%
44.72	10	3.57%	2.93%
44.72	20	2.82%	1.70%
44.72	30	2.36%	3.11%
49.76	0.2	2.92%	1.00%
49.76	0.5	1.24%	0.94%
49.76	1	0.90%	0.66%
49.76	2	8.38%	3.90%
49.76	5	5.92%	3.33%
49.76	10	4.42%	2.91%
49.76	20	4.58%	3.60%
49.76	30	3.91%	3.79%
20.4	0.2	1.37%	2.13%
20.4	0.5	1.33%	0.91%
20.4	1	1.59%	1.37%
20.4	2	1.74%	0.15%
20.4	5	2.82%	0.62%
20.4	10	1.61%	1.91%
20.4	20	1.63%	0.65%
20.4	30	1.56%	1.12%